



MIT
International Center for
Air Transportation

**UNDERSTANDING THE EFFECT OF COGNITIVE REFERENCE
FRAMES ON UNMANNED AIRCRAFT OPERATIONS**

Matthew R. Rabe and R. John Hansman

*This report is based on the Doctoral Dissertation of Matthew R. Rabe submitted to the
Department of Aeronautics and Astronautics in partial fulfillment of the requirements for the
degree of
Doctor of Philosophy at the Massachusetts Institute of Technology.*

*The work presented in this report was also conducted
in collaboration with the members of the Doctoral Committee:*

Prof. R. John Hansman (Chair)

Prof. David A. Mindell

Prof. Julie A. Shah

Report No. ICAT-2016-03

June 2016

MIT International Center for Air Transportation (ICAT)
Department of Aeronautics & Astronautics
Massachusetts Institute of Technology
Cambridge, MA 02139 USA

Distribution
Approved for public release; distribution is unlimited

UNDERSTANDING THE EFFECT OF COGNITIVE REFERENCE FRAMES ON UNMANNED AIRCRAFT OPERATIONS

by

Matthew R. Rabe and Prof. R. John Hansman

ABSTRACT

As an ever-greater share of our national military airborne resources transition from manned to unmanned aircraft (UA) the issues associated with unmanned aircraft operations become more and more important. This study seeks to understand the difficulties associated with controlling both the unmanned aircraft and an onboard video sensor.

Traditional unmanned aircraft involve multiple operators controlling multiple control displays that are often oriented on misaligned reference frames. One example unmanned aircraft mission includes a target described on a north-up reference frame, such as a map. The pilot plans a flight path, to this target, on a north-up map, but controls the aircraft along that flight path using an aircraft-view reference frame that offers a forward-looking cockpit view. Finally, the sensor operator controls the sensor to point at the target area using a sensor-view reference frame that offers a sensor viewfinder perspective. Any unmanned aircraft operator or team of operators is required to manage tasks across these multiple reference frames (north-up, aircraft-view, and sensor-view).

This study investigated several display design techniques that had the potential to reduce the cognitive burden associated with correlating information from multiple reference frames. Orientation aids, reference frame alignment, display integration, and reduced display redundancy were all evaluated with human subject simulator experiments. During four separate experiments, a total of 80 subjects were asked to complete a series of representative unmanned aircraft operational tasks involving target acquisition, imagery orientation, target tracking, and flight path control.

A simulator was developed to support this effort and allow for modification of display characteristics. Over all four experiments the reference frame alignment technique reduced basic orientation time and improved target acquisition time along with

other performance and workload measures. The currently accepted practice of placing an orientation aid, such as a north arrow, on the displayed sensor video was only significant on the basic imagery orientation task and did not have a significant impact on the more involved target acquisition task. This research introduced a potential benefit of reference frame alignment on unmanned aircraft operations

ACKNOWLEDGEMENTS

This material is based upon work supported by the Air Force Rapid Capabilities Office under Air Force Contract No. FA8721-05-C-0002. Any opinions, findings, and conclusions or recommendations expressed in this material are those of the author and do not necessarily reflect the views of the United States Air Force, Department of Defense, or the US Government.

This page intentionally left blank.

Table of Contents

Table of Contents.....	7
1. Introduction	11
1.1. Background	11
1.2. Motivation.....	11
1.2.1. Reference Frames and Display Techniques	15
1.2.2. Motivation Summary	28
1.3. Thesis Objectives.....	29
2. Related Work	31
2.1. Unmanned Aircraft	31
2.1.1. Single vs. Multiple Aircraft.....	31
2.1.2. Levels of Automation	31
2.1.3. Display Design	32
2.2. Cognitive Orientation.....	34
2.2.1. Reference Frame Rotation.....	34
2.2.2. Cognitive vs. Display Reference Frames	34
2.2.3. Object Rotation vs. Perspective-Taking	35
2.2.4. Aircraft Orientation Studies.....	36
2.3. Multitasking	38
2.3.1. Performance Operating Curves	38
2.3.2. Switch Cost.....	38
2.3.3. Training Effect.....	39
3. Experimental Methods.....	41
3.1. Overview	41
3.2. Simulator Description	42
3.2.1. Simulator Scenarios	42
3.2.2. Simulation Model.....	43
3.2.3. Simulator Displays.....	45
3.2.4. Simulator Controls	50
3.2.5. Simulator Hardware.....	53
3.2.6. Environment	54

3.2.7.	Timeline	54
3.3.	Simulator Required Tasks.....	54
3.3.1.	Target Preview	54
3.3.2.	Target Acquisition & Flight Path Tracking.....	55
3.3.3.	Dual-Tracking	55
3.3.4.	Reaction Time & Orientation Time	56
3.3.5.	Observations and Workload Rating	56
3.4.	Simulator Display Features	57
3.4.1.	Reference Frame Alignment	57
3.4.2.	Orientation Aids.....	59
3.4.3.	Display Integration.....	61
3.4.4.	Display Redundancy.....	61
3.4.5.	Target Movement	62
3.1.	Simulator Changes between Experiments	64
3.2.	Dependent Variables.....	65
3.2.1.	Target Acquisition Time	65
3.2.2.	Sensor Track Error.....	66
3.2.3.	Flight Path Error	67
3.2.4.	Orientation Time.....	68
3.2.5.	Bedford Workload Rating	68
3.2.6.	Secondary Task Reaction Time	70
3.2.7.	User Preferences.....	71
3.3.	Population.....	71
3.4.	Controlling for Unwanted Effects	71
3.4.1.	Training	71
3.4.2.	Display Order	73
3.4.3.	Image Difficulty	74
3.4.4.	Subject Variability	74
4.	Experiment 1: Orientation Aids and Reference Frame Alignment	75
4.1.	Experiment 1 Overview.....	75
4.1.1.	Experiment 1 Scenario and Tasks	75
4.1.2.	Experiment 1 Timeline	77

4.2.	Experiment 1 Hypotheses	77
4.3.	Experiment 1 Display Configurations (Independent Variables).....	77
4.4.	Experiment 1 Dependent Variables	80
4.5.	Experiment 1 Results	81
4.5.1.	Data Analysis Method	81
4.5.2.	Experiment 1 Performance Measures	82
4.5.3.	Experiment 1 Workload Measures	91
4.5.4.	Experiment 1 User Preferences	95
4.6.	Experiment 1 Limitations	95
4.7.	Experiment 1 Conclusions.....	96
5.	Experiment 2: Imagery Rotation Subtask	97
5.1.	Experiment 2 Overview.....	97
5.1.1.	Experiment 2 Scenario and Tasks	97
5.1.2.	Experiment 2 Timeline	97
5.2.	Experiment 2 Hypotheses	98
5.3.	Experiment 2 Display Configurations (Independent Variables).....	98
5.4.	Experiment 2 Dependent Variables	102
5.5.	Experiment 2 Results	103
5.5.1.	Data Analysis Method.....	103
5.5.2.	Experiment 2 Selection Answer Time Results.....	105
5.5.3.	Experiment 2 Selection Answer Error Results	108
5.6.	Experiment 2 Limitations	110
5.7.	Experiment 2 Conclusions.....	111
6.	Experiment 3: Display Integration and Reference Frame Alignment	113
6.1.	Experiment 3 Overview	113
6.1.1.	Experiment 3 Scenario and Tasks	113
6.1.2.	Experiment 3 Timeline	115
6.2.	Experiment 3 Hypotheses	115
6.3.	Experiment 3 Display Configurations (Independent Variables).....	116
6.4.	Experiment 3 Dependent Variables	120
6.5.	Experiment 3 Results	121
6.5.1.	Data Analysis Method.....	121

6.5.2.	Experiment 3 Performance Measures	122
6.5.3.	Experiment 3 Workload Measures	133
6.5.4.	Experiment 3 User Preferences	139
6.6.	Experiment 3 Limitations	140
6.7.	Experiment 3 Conclusions.....	140
7.	Experiment 4: Redundancy Reduction and Reference Frame Alignment	145
7.1.	Experiment 4 Overview.....	145
7.1.1.	Experiment 4 Scenario and Tasks	145
7.1.2.	Experiment 4 Timeline	147
7.2.	Experiment 4 Hypotheses	148
7.3.	Experiment 4 Display Configurations (Independent Variables).....	148
7.4.	Experiment 4 Dependent Variables	152
7.5.	Experiment 4 Results	153
7.5.1.	Data Analysis Method.....	153
7.5.2.	Experiment 4 Performance Measures	154
7.5.3.	Experiment 4 Workload Measures	167
7.5.4.	Experiment 4 User Preferences	173
7.6.	Experiment 4 Limitations	175
7.7.	Experiment 4 Conclusions.....	175
8.	Conclusions	179
	Bibliography	187
	List of Figures	197
	Appendix A: Display Configurations.....	205
	Appendix B: Subject Characteristics	221
	Appendix C: Experiment 1 Data Analysis	227
	Appendix D: Experiment 2 Data Analysis.....	253
	Appendix E: Experiment 3 Data Analysis	259
	Appendix F: Experiment 4 Data Analysis	287
	Appendix G: Subjective Response Data	319
	Appendix H: Imagery Rotation Cognitive Process Examination	325
	Appendix I: Imagery Feature Categories.....	333

1. Introduction

1.1. Background

Unmanned Aircraft (UA) have become an essential asset to the United States military and our international partners. They are now in routine use for the Intelligence Surveillance and Reconnaissance (ISR) mission. Despite the continued growth in their use among the US military services, like the rest of the Department of Defense (DOD), the unmanned aircraft budget is shrinking. In order to reduce overall costs and still increase operational flight hours, there is a need to reduce operating costs [1, 2]. Manpower expenses represent a large portion of these operating costs, and unmanned aircraft are typically controlled by multiple operators. If these aircraft could be controlled by a single operator, the Air Force would benefit from the reduced manpower cost and personnel need. To that end, this research investigated one particular challenge which has led to the dual-crew requirement for unmanned aircraft: the management of multiple tasks across multiple reference frames. This research identified this particular challenge, investigated the significance of this challenge and explored possible approaches to mitigate this multi-task multi-reference-frame problem through display design techniques. The results and findings described throughout this document relied on four human subject simulator experiments.

1.2. Motivation

This research was motivated by the possibility of single-operator control of the unmanned aircraft surveillance mission. Such a challenge involves multiple tasks currently displayed across multiple different reference frames. With that in mind, this research focused on the challenge of mentally transforming information between two different reference frames. With this single-operator control capability, the US military could reduce the manpower portion of unmanned aircraft operating costs. The study focused specifically on the military unmanned surveillance mission. In 2008, after 15 years in service, the MQ-1B Predator (Figure 1) and MQ-9 Reaper (Figure 2) aircraft reached 1 million flight hours; 2 years later that mark had doubled, and in 2014 another million was added [3, 4]. These numbers are unprecedented given that 90% of these missions are flown in combat. Only transport aircraft draw any comparison to these sorts of flying hours [5]. Considering that the total USAF budget request for fiscal year 2016 included an increase of up to 1.2 million flight hours, it is easy to see that the unmanned aircraft surveillance mission represents a large and increasing portion of the USAF flying-hour program [6]. This does not necessarily translate to an equal share of the flying-hour budget.



**Figure 1: USAF MQ-1B Predator Aircraft [9]
Sensor camera location highlighted.**



**Figure 2: USAF MQ-9 Reaper Aircraft [8]
Sensor camera location highlighted.**

Since the current fleet of unmanned aircraft are designed for low-cost, long-loiter surveillance, the costs per flying hour are significantly lower for unmanned aircraft [7]. These reduced flying hour costs have helped to enable the overwhelming increase in utilization of these systems. However, these costs have largely been reduced based on the airframe design and little effort has been focused on reducing the manpower costs associated with unmanned aircraft operations. The basic manpower requirement to operate an unmanned aircraft exceeds that of a typical F-16 fighter aircraft because the unmanned aircraft requires two crewmembers [8, 9, 10, 11, 12]. This does not include any consideration for other support personnel which support the unmanned aircraft throughout its mission, or the requirement for another 2 crewmembers available to land the aircraft at any given time. The basic minute-by-minute operations of the unmanned aircraft in the US Air Force, so often referred to as drones and thought of as robots, actually require two operators to continuously manage the flight path and sensor control at every point of the mission. Unfortunately for the Air Force budget, the unmanned aircraft pilot receives the same paycheck as a fighter pilot. So, given these staggering flight hours and the consistent need for two operators, this cost should be sufficient motivation to investigate the single-operator mission [13, 14]. However, the cost only represents a small portion of the need here.

A more significant consideration and motivation to develop single-operator control capability, is the manpower shortage [15, 16]. While the costs are important, the mere shortage of manpower has a greater impact on the day to day operations of the Air Force fleet. The Air Force struggled to keep pace with the ever-increasing need for unmanned aircraft surveillance during Operation Enduring Freedom (Afghanistan) and Operation Iraqi Freedom to an eventual peak of 65 Combat Air Patrols (CAPs). These were commitments to keep 65 aircraft airborne at all times to support ground personnel requirements. With the drawdown of these conflicts, the Air Force drew down to 55 CAPs and reduced manpower; however, the current surge in operations against ISIS has brought this number back to 65 [17, 18]. In response to this need, the Air Force has forcibly transitioned pilots from other aircraft, developed an accelerated path to Remotely Piloted Aircraft (RPA) pilot separate from the traditional pilot training, introduced bonus pay incentives for RPA pilots, transitioned navigators and other non-pilot aircrew to the RPA pilot role, and is now considering enlisted pilots for this role [19, 20, 21, 22, 23, 24, 25, 26, 27]. In the long term, the Air Force is betting on research efforts which promise manpower gains associated with multi-aircraft control [28, 29, 30, 31, 32, 33].



Figure 3: USAF MQ-1B Predator Control Station [55]

Displays are titled to match this research. The pilot, on the left, is responsible for the aircraft control task which brings together the navigation and aircraft displays. His control inputs directly influence response on the aircraft display and indirectly influence response on the navigation display. The sensor operator, on the right, is responsible for control of the aircraft sensor. His control inputs directly influence response on the sensor display; however, he must consider camera location on the navigation display to plan for or request different camera look angles of the target of interest.

As the Air Force trends in the two directions of increased responsibilities for individual operators or reduced qualifications for multiple operators, it was important to start with an understanding of why the dual-crew requirement developed. This investigation relies on an understanding of the requirements for an unmanned aircraft surveillance mission. These missions involve fixed-wing aircraft with some type of video sensor on board. The aircraft is maneuvered in the vicinity of the target and the camera gimbals are controlled to track some important features or personnel in the target area. At times this may require precise placement of the aircraft in order to set the proper camera angle, and precise control of the camera to maintain a quality image for intelligence gathering. All the while, continuous interpretation of the video is required in order to produce timely and actionable information to ground personnel or decision-makers.

These two primary tasks, aircraft and sensor control, are traditionally represented in two different reference frames and assigned to two different operators, as shown in Figure 3. Here, the pilot seated in the left of the MQ-1B control station is controlling the aircraft with the stick controller in his right hand and the throttle in his left hand. The pilot does this through the aircraft display located in his or her central field of view. The pilot must also reference the navigation display located above the aircraft display and coordinate his or her controls in order to manage the aircraft route of flight. Simultaneously, the sensor operator uses a similar stick controller to manage the camera pointing. He or she controls the pointing using the sensor display centrally positioned in front of him or her, but also must reference the top navigation display to plan requests for different camera angles, or to anticipate

changes to the scene as the aircraft maneuvers along its flight path. Both must reference a mission display, in this case centrally located, but more often independently available on both sides of the main displays, such as the mission display in Figure 4. As currently designed, this process requires a good deal of coordination between the two positions.

There are extensive efforts to provide systems which allow one pilot to control multiple aircraft; in fact the Air Force has already purchased one which allows one pilot to control four aircraft [34]. However, the design of that multi-aircraft control station highlights the current need for two operators. This design does allow control of four aircraft by one pilot; however, it retains the need for four sensor operators to control the camera on each of the four aircraft [35]. The need for one sensor operator per aircraft is interesting because the many efforts to address this problem have only focused on the pilot. This may be unique to surveillance missions, and the US military has stated its intent to explore broader areas of unmanned aircraft involvement. However, currently the most widespread use is in ISR operations so that is the focus here [1]. With the understanding that current missions with continuous video collection require one operator per camera, this research focused on how to fulfill that requirement and the necessary aircraft control need in one operator. Providing single-operator control could improve both the manpower shortage and the manpower costs associated with current arrangements. However, such a system would require a single operator to manage these multiple tasks across different reference frames. This situation is depicted in Figure 4, where an operator must understand the mission description provided on the mission display and execute control on the aircraft and sensor displays. The single operator would now take on both of the previously described control tasks and associated coordination with the navigation reference frame.

Development of a single-operator design would require optimization of the displays for both tasks rather than the combination of displays which were previously optimized for individual tasks. Although the aircraft and navigation displays have developed together to enable the aircraft control task, the addition of the sensor control may require a different design for the aircraft and navigation displays as well. A departure from the standard configuration of these displays may increase the operator's ability to control both the aircraft and sensor tasks even if it decreased the operator's ability to control the individual aircraft control task. An understanding of the multi-task requirements is essential to developing a suitable display configuration.



Figure 4: Single-Seat Reference Frame Requirements [55, 139]

This represents the multiple reference frames which a single operator would have to manage. An aircraft display has been added to the upper right screen of the MQ-1B control station.

It is interesting that current efforts have avoided focusing on single-operator control and instead investigated this multi-aircraft control and individual sensor control arrangement [36, 37, 38]. With an understanding of the dual-control coordination problem, imagine now that the pilot is coordinating aircraft movements and camera angle requirements with four different sensor operators. Any coordination requirements that existed between the sensor operator and pilot in the current architecture would increase significantly across the four simultaneous and possibly independent missions. It seems reasonable then to pursue a single-operator arrangement where each aircraft can be controlled by one person, to meet the needs of the sensor video requirements. This is the challenge addressed by this research.

1.2.1. Reference Frames and Display Techniques

As the term reference frame is used throughout this research, it refers to an established system of spatial representation to define a position and/or orientation for a specific task or purpose [39]. This is not an arbitrary understanding of relationships between objects, but rather, an established system to represent information which is important to some task. In contrast, a cognitive reference frame, as used throughout this research, is a mental representation of space to support operator decision-making. This may or may not represent an established system.

These mental points of view support decision-making but may not be useful for precise measurements, such as those afforded from an established reference frame [40]. However, for the

purposes of this research, it is important to understand that operators could mentally keep track of cognitive reference frames that are different from the established reference frames included in the display architecture. The designer has direct control over the reference frames used in the displays and controls, but only partial influence over the operator's cognitive reference frames. With this in mind, this study focused on adjusting the display and control reference frames and assumed that this manipulated the necessary cognitive reference frames of the operator.

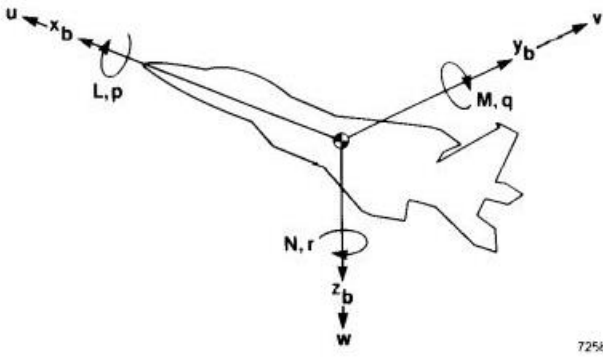


Figure 5: Aircraft Body Axis [140]
 This axis is oriented front, right and down on the aircraft.



Figure 6: Earth Axis System
 This axis is oriented north, east, and down into the earth.

In the realm of aerospace several key reference frames are considered during aircraft design. These include the body, and earth axes [41, 42, 43, 44]. Their use has also become commonplace during aircraft operations, and most, if not all, pilots rely on them during their operation of an aircraft. The body axis, shown in Figure 5, is fixed to the aircraft body in a standardized manner. The body axis is physically observed by a manned aircraft pilot. It is fixed to the aircraft and is the basis for a typical aircraft display.

The earth axis is fixed to the earth as shown in Figure 6. At any given point around the earth (usually taken at the aircraft location), the earth axis is oriented north, east, and down toward the center of the earth.

The traditional aircraft display is a two-dimensional projection of the aircraft axis but also includes orientation information relative to the earth axis. This traditional representation, shown in Figure 7, is organized with the aircraft front axis into the display, the aircraft right axis is oriented to the right, and the aircraft down axis is down in the display. The tilt of the horizon line represents the angle between the aircraft right axis and the earth north-east axes plane.

The traditional two-dimensional projection of the earth axis onto a navigation display is shown in Figure 8. This representation fixes the earth north axis up in the display, the earth east axis to the right and the earth down axis into the display. This navigation display is an example of the north-up reference frame used during this research. Other common representations of the navigation display could rotate the map data to fix the aircraft front axis (current heading) in the up direction. This type of navigation display, known as track-up, was not used in this research.

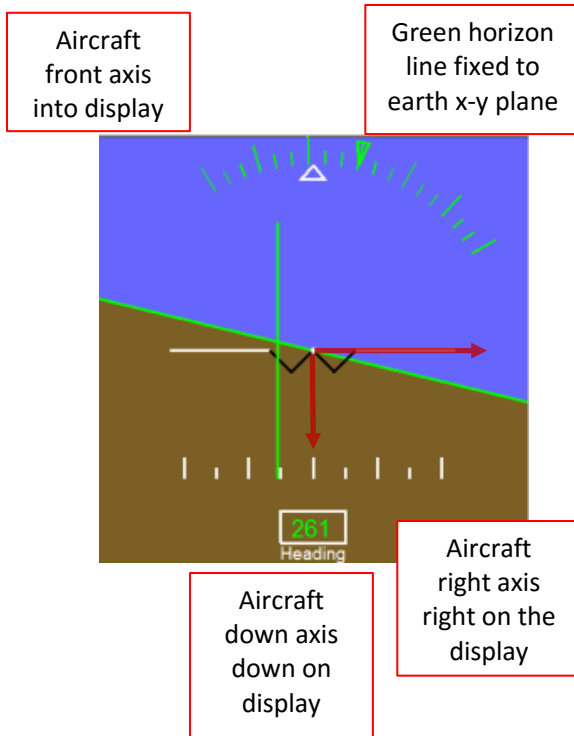


Figure 7: Aircraft-View Reference Frame

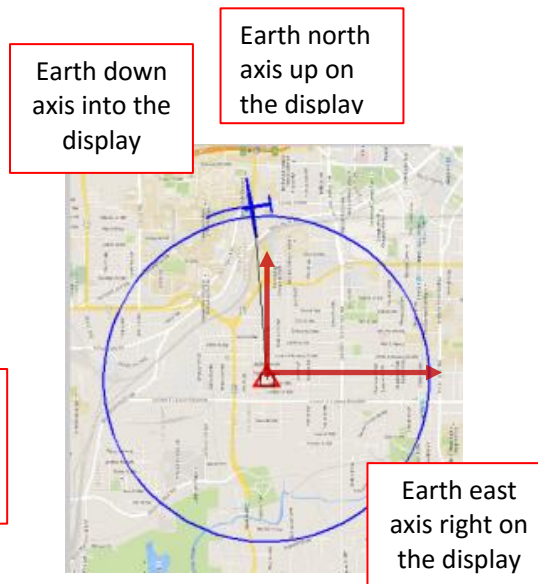


Figure 8: North-up Reference Frame

Currently, the pilot or pilots must consider information in the body axis to maintain safe flight, and then follow a plan developed in the earth axis in order to follow a route from one location to another. This coordination among the different axes is not a new aircraft control problem; however, the unmanned aircraft surveillance task adds a sensor display with its own physical and traditionally displayed reference frames.

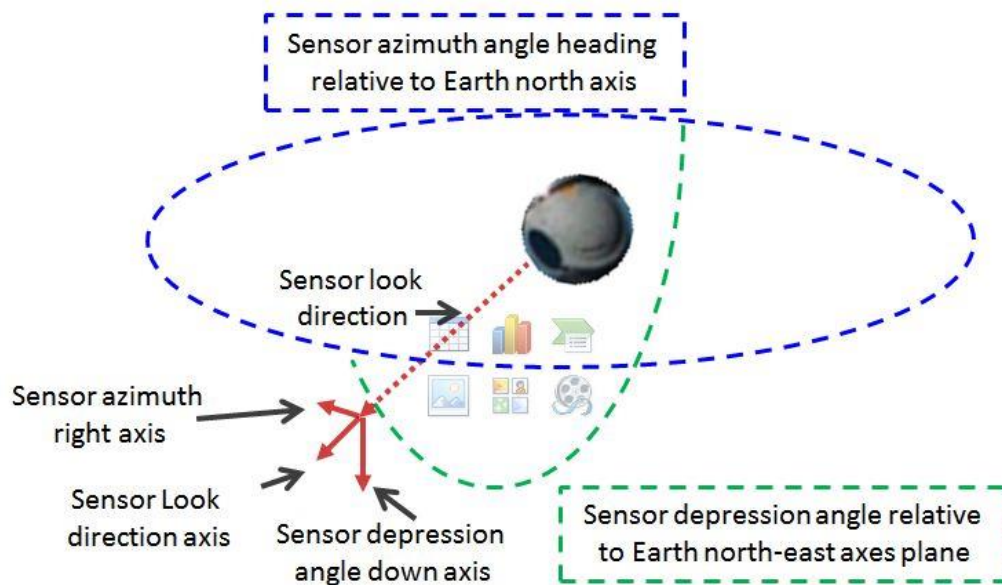


Figure 9: Sensor-View Axis

The physical sensor reference frame is oriented in the sensor pointing direction, azimuth right, and depression angle (also known as elevation angle) down.

The physical reference frame associated with a gimbaled aircraft sensor is displaced and rotated from the aircraft body axis. This reference frame, as shown in Figure 9 is oriented with the current sensor pointing direction, tangential to sensor azimuth changes, and tangential to sensor depression angle changes. The axis system is also translated from the aircraft center of gravity (the origin of the aircraft body axis) to the sensor center of rotation (origin for the physical sensor axis). Azimuth and depression angle (also known as elevation) are the control angles available with a gimbaled sensor so it is natural to organize a physical reference frame around these angles.

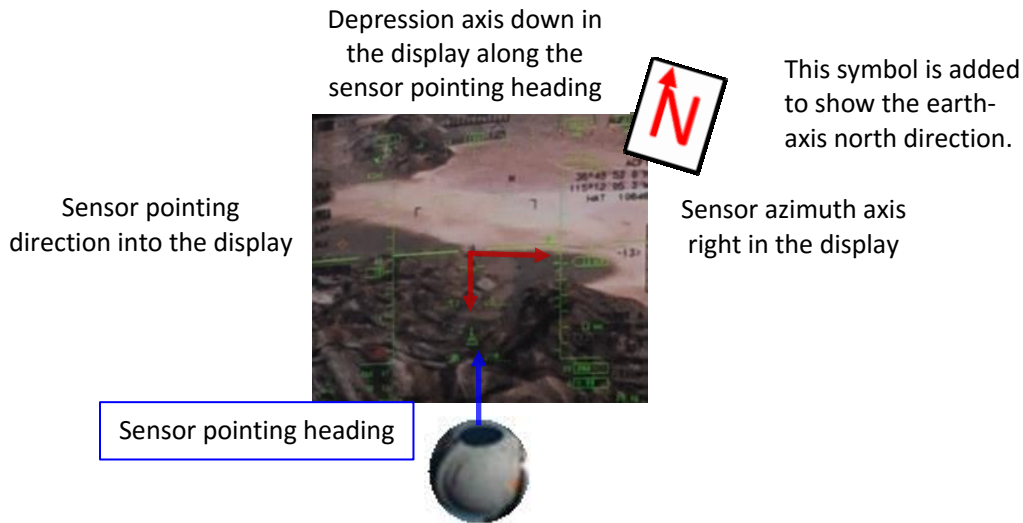


Figure 10: Sensor-View Reference Frame

This two-dimensional projection of the physical sensor reference frame shows the raw sensor video as it is collected by the video camera on the aircraft. It oriented along the current sensor pointing direction into the display, the depression axis down, and the azimuth axis to the right. This aligns the top of the display with current sensor pointing heading relative to the Earth north axis.

The sensor-view reference frame shown in Figure 10 is the two-dimensional projection of the sensor reference frame. The current sensor pointing direction is into the display. The sensor azimuth axis is right on the display and the depression angle axis is down on the display. Most medium to high-altitude aircraft operate at larger depression angles so that the azimuth and depression angle axes are similar dimensions, but at lower depression angles (lower altitude or further from the target) the depression axis will cover a longer distance on the ground. With the two-dimensional representation the up-down direction represents portions of the current sensor pointing heading and the depression axis.

In moments when the aircraft is south of the target then the sensor-view and north-up reference frame are aligned with north at the top of both displays. Although sensor pointing involves this azimuth and depression angle, only the azimuth is really depicted on the two-dimensional display orientation. The sensor video image dimensions are changed relative to depression angle as the x-axis is stretched at a lower depression angle (aircraft at a lower altitude), and when the aircraft is directly over the target (known as nadir), the x and y axis both have the same dimensions. With the sensor control task the operator must continually transform this sensor-view reference frame into the north-up reference frame in order to analyze and communicate information obtained from the sensor images.

Although the sensor reference frame transformations are relatively new, decades of research have provided techniques to assist the pilot with the multiple-reference-frame task as it involves navigation from one airport to the next. Six of these techniques will be included in this research: predictive aids, course guidance, orientation aids, reference frame alignment, redundancy reduction and integration. Most of these are widely available throughout modern aircraft to assist the pilot with this mental transformation of information from one reference frame to another. This is not an exhaustive list, but these are prominent techniques that were investigated during this research. Similar efforts have not been applied to the added difficulty of the sensor reference frame coordination. This research

sought to fill that void and provide some insight into the difficulty associated with simultaneously managing both of these coordination tasks, and which of these display techniques would benefit operators faced with such a challenge.

While all six of these techniques were included in this research, two of them were not directly tested for their effectiveness. Predictive aids and course guidance were used throughout experiments but no effort was made to directly measure their effect against a baseline display.

Since the current systems included orientation aids, this research focused on the effectiveness of that technique and the reference frame alignment technique as one potential alternative. Both of these techniques assisted the operator in correlating information on two separate displays. Additionally, the display integration and display redundancy reduction techniques addressed the physical workload of switching between displays. Through these four techniques both the mental and physical aspects of the multiple reference frame problem were examined.

1.2.1.1. Basic Displayed Reference Frames

Before applying these various display techniques, it is important to understand the basic reference frames associated with the unmanned aircraft surveillance mission. A basic understanding of the mission requires three reference frames across four separate displays, as shown in Figure 11.

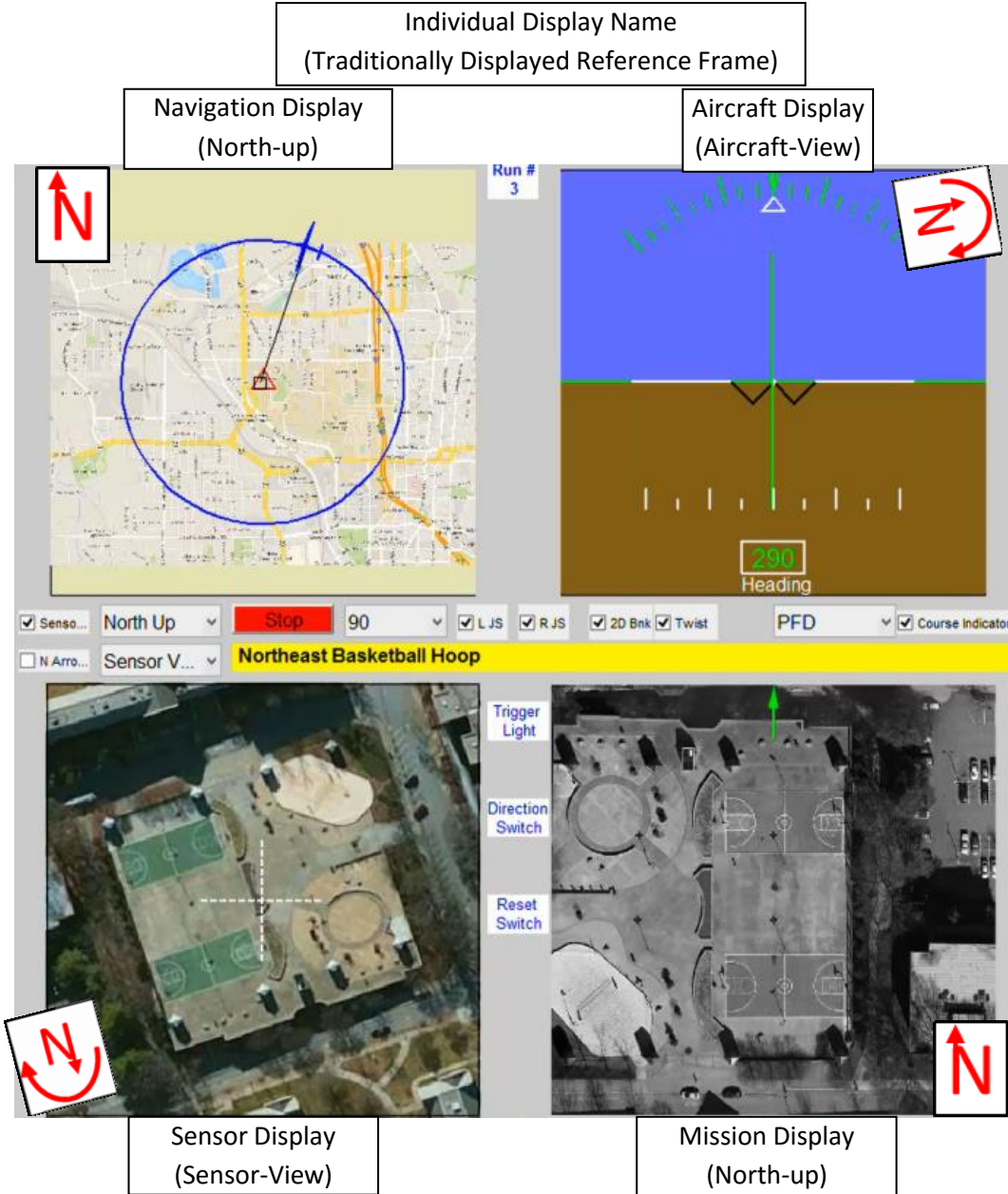


Figure 11: Multiple Reference Frames in Unmanned Aircraft Control
N symbols are added to show the north direction in each of the displays. The upper left and lower right displays are fixed at north-up while the north direction in the other two displays would change throughout the mission. [Map Data and Image ©Google]

1.2.1.1.1. Mission Display

On the bottom right of Figure 11, the **mission display** provides a description of the mission requirement. This is the primary purpose for flying the aircraft, and it is usually displayed or described in a north-up reference frame such as the earth-axis. Terms of description here often include cardinal directions such as that shown in the yellow field in the center of Figure 11 “Northeast Basketball Hoop”. For any given mission, the operator would take the information provided in the north-up mission description and plan a route of flight on the north-up navigation display.

1.2.1.1.2. Navigation Display

On the upper left of Figure 11, the **navigation display** provides a map of the target area and is traditionally presented in the north-up reference frame. The blue circle represents a defined flight plan and is a simple orbit around the target; however, more complex routes may be required if airspace restrictions or terrain limitations prevent the use of a simple orbit. This plan is developed on the navigation display to support the requirements described on the mission display; however, direct control of the aircraft is conducted on the aircraft display.

1.2.1.1.3. Aircraft Display

On the upper right of Figure 11, the **aircraft display** provides an aircraft bank indication and is traditionally presented in the aircraft-view reference frame as shown. This provides a perspective as if the operator were sitting in the cockpit and looking out the front of the aircraft. This reference frame is completely intuitive when the operator is sitting in the cockpit, given that this is the reference frame of their physical perception as well; however, the unmanned aircraft operator is disconnected from this physical reference frame and left solely with the aircraft-view display. The aircraft display is also aligned with the typical control axis since control stick tilt is often used to control bank angle or bank angle rate of change. However, the operator must determine if left or right bank is appropriate based on the aircraft location relative to the desired flight path on the navigation display. At the same time the single operator is controlling the aircraft via the aircraft display, he or she must also interpret the video on the sensor display and make control decisions there.

1.2.1.1.4. Sensor Display

On the lower left of Figure 11, the **sensor display** shows the sensor video in a sensor-view reference frame. This is oriented as if the operator were holding the video camera onboard the aircraft. For this reason, the video will rotate on the display as the aircraft completes an orbit around the aircraft. Additionally, as shown in Figure 11, the north direction in the video scene will move with respect to the display itself. In order to communicate in the north-up reference frame the operator must maintain awareness of the north direction in the video to explain events to ground personnel and other decision-makers.

Since the current position of the aircraft in Figure 11 is north of the target area, the sensor-view reference frame is inverted with respect to the north-up reference frame. The north, east, south and west direction are actually down, left, up, and right on the sensor-view sensor display. This is similar to the disconnect between the aircraft and navigation displays; however, the broader aircraft industry has long experienced the aircraft-view to north-up view transformation and has developed several techniques to address it. This research investigated those techniques as they apply to both transformations which would be required of a single-seat unmanned aircraft operator.

To support a single operator in performing these two separate transformations, required during unmanned aircraft surveillance operations, six different display design techniques were investigated during this research: predictive aids, course deviation indicators, reference frame alignment, orientation aids, redundancy reduction, and integration. Those techniques are described during the following sections. All of them were used on the displays which were evaluated during this research, but only four of them were evaluated as design variables during any given experiment. These were reference frame alignment, orientation aids, redundancy reduction, and display integration. The other techniques, predictive aids and course deviation indicators, were used across each display in a given experiment. In this way, their contribution was provided equally across all data.

1.2.1.2. Predictive Aids

Predictive aiding was initially developed in the 1950s and 60s, but the higher fidelity models and increased computation power available in current systems has increased its use [45]. This display technique not only shows the current status of the system, but also the predicted status at some future time [46]. This feature has been developed for aircraft, navigation and sensor displays [47, 48, 49, 50]. One common use for aircraft control is on the navigation display; however, this display technique has been investigated across several realms of remote vehicle operation. The use of predictive aids is often used to address time delay of control inputs and displayed response; however, these benefits could also help address the switch cost associated with multitask control.

Such a technique might appear like Figure 12 on the navigation display. Here a line (“noodle”) projects forward of the aircraft location to depict where the aircraft will be in 10 seconds with current turn rate. Here 10 seconds was chosen because it provided a future projection of the aircraft which could also be used as an indication of current aircraft bank angle. Shorter predictive times would not have allowed for enough line curvature to provide any significant indication of aircraft bank angle. Furthermore, with a 10 second predictive time, at maximum bank angle (45 degrees) the predictive aid did not complete a full 180 degree turn. Longer predictive times, used on displays for straighter flight paths [51], could create confusing displays when the aircraft is controlled at or near maximum turn performance because the predicted aid could wrap around onto the current aircraft location. A line was chosen over discrete predicted locations because it matched the task of following a desired orbit. The line also provides rate of change information which would be



Figure 12: Predictive Aid
This image highlights a sample predictive aid which displays the future aircraft position with current turn rate. [Map Data ©Google]

difficult to interpret from discrete aircraft symbols. Additionally, since the predictive aid is estimated information it is important that the operator can distinguish between the true state of the aircraft (aircraft symbol) and the estimated future projection (predictive aid). The relatively short line allows provides the predicted location while preserving the emphasis of the current aircraft location.

This technique provides the operator feedback in the navigation frame (earth axis) based on control actions in the aircraft reference frame (body axis). Otherwise, an operator can imagine themselves sitting in the aircraft of Figure 12 and planning to increase left turn to return to the large blue circular flight path. With the predictive aid, the operator will immediately notice an incorrect bank control. In this case, if the operator were to push the stick right because, on the navigation screen, it looks like the aircraft needs to move to the right, then the predictive aid would move left here to show a the proper movement to the right in the aircraft reference frame.

1.2.1.3. Course Deviation Indicators

Course guidance is another practice regularly used to assist with coordination between these two reference frames. As shown in the right image of Figure 13 as a course deviation indicator, this technique can provide information in the aircraft display to follow a plan developed in the navigation display [52]. Since the green line in the aircraft display is to the left of center, the aircraft needs to turn left to line up the green line with the central white dot on the display. The operator must determine how much left bank is required because this course deviation indicator is an instantaneous indication of course deviation and does not provide control input guidance. If the operator just commands left bank until the white dot aligns with the green line then then the aircraft will fly right through the desired flight path and never actually stabilize on course.

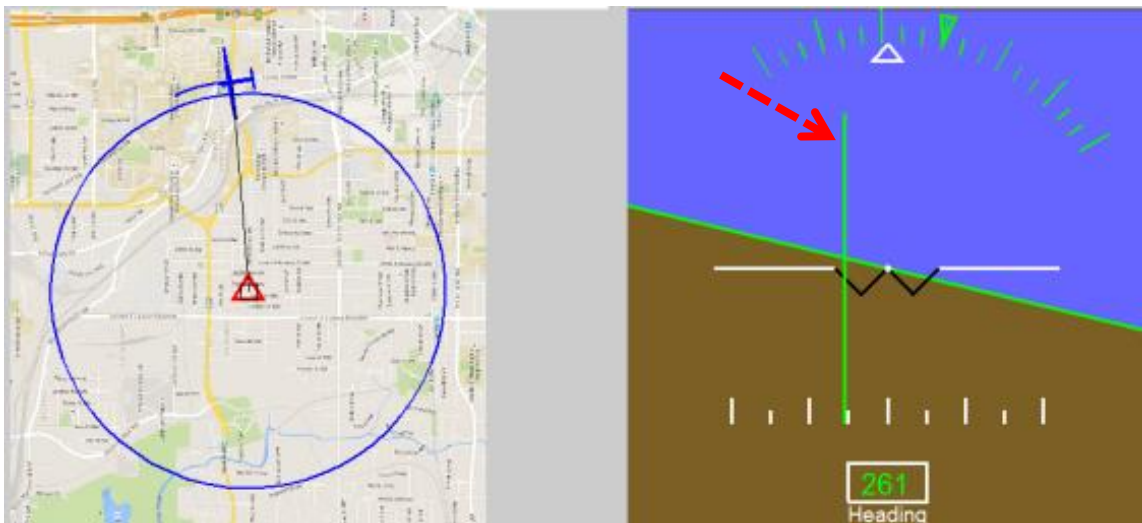


Figure 13: Course Deviation Indicator

The course deviation indicator, highlighted, provides an understanding, in the right aircraft display, of the location of the desired flight path in the left navigation display. Here the aircraft is right of course (north of the orbit in the left image), so the vertical line appears to the left of center in the right aircraft display. This indicates that the aircraft must turn left to get back on course. [Map Data ©Google]

1.2.1.4. Reference Frame Alignment

This same aircraft to navigation coordination could also be addressed with reference frame alignment. This would call for the alignment of these two displays so that the operator did not have to imagine sitting in the aircraft on the map display. In Figure 14 the navigation display, on the left, is rotated “track-up” so that the aircraft is traveling up on the display. This could allow the operator to quickly make decisions about left or right bank control because he or she would not need to imagine sitting in the aircraft on the navigation display. However, this could make it challenging for the operator to plan navigation tasks. As depicted, this display does not identify the north direction on the map, so this could be difficult for an operator to plan a route or request necessary airspace to complete a mission. It might even make it difficult to find a target. This research program focused aligning reference frames to the north-up reference frame which would reverse the alignment seen in Figure 14. Although reference frame alignment could be used with almost any underlying reference frame, the north-up orientation of the unmanned aircraft mission was used as the basis for reference frame alignment throughout this research. Previous efforts have focused on aligning navigation displays with the aircraft-view reference frame (Figure 14); however, the remote operator in an unmanned aircraft system does not directly perceive the aircraft-view reference frame so this presents an opportunity to focus the reference frame alignment on a different underlying reference frame, the north-up orientation.

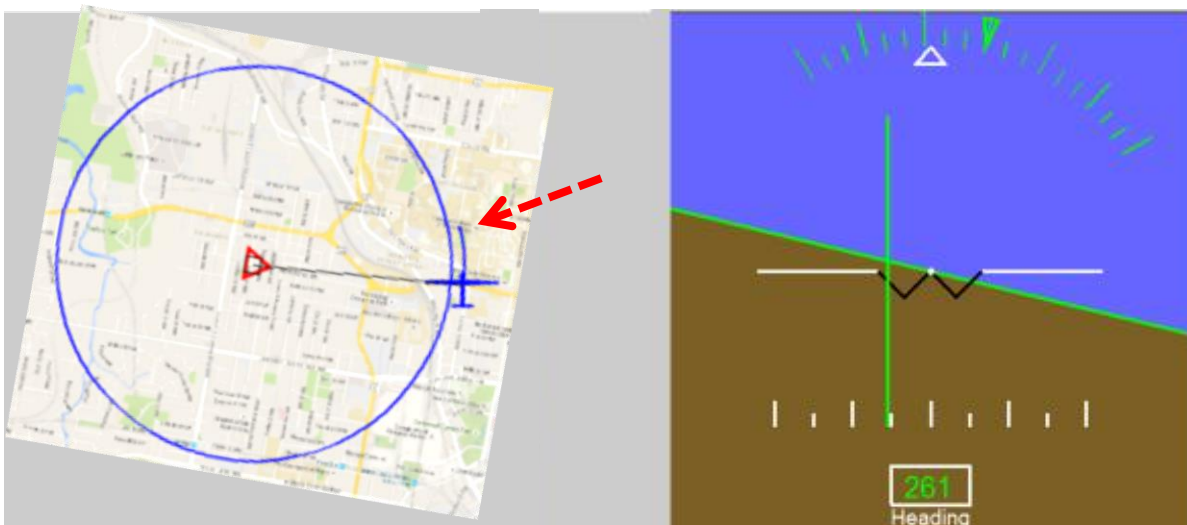


Figure 14: Navigation Display Reference Frame Alignment

The left navigation display from Figure 13 has been rotated so that the flight path direction of the vehicle is up on the display. This should assist with the transformation between the navigation and aircraft displays for the purpose of controlling the aircraft. [Map Data ©Google]

1.2.1.5. Orientation Aids

Another tool which could assist these transformations between different reference frames is the orientation aid. Understanding the various possible orientation aid configurations requires a shared understanding of some definitions for widely used terms. Here, *egocentric* will refer to a first-person point of view as if the operator was sitting in the aircraft or holding the video camera, while *exocentric*

will refer to a third-person top-down view aligned north-up. These two descriptive terms will be used to understand the different orientation aid configurations and may also be used to describe display characteristics. Both of these are visible in Figure 13, since the left half of that display represents an exocentric reference frame and the right half represents an egocentric reference frame.

An orientation aid guides the operator through a mental transformation from one reference frame to another by providing a cue in one reference frame which is defined in another reference frame. This can either be an egocentric or exocentric cue. One common example is the compass. In an aircraft or on the ground, a compass points a steady direction in the earth axis, so when held by a person, or mounted on the body axis of an aircraft, it provides a cue to translate one of the angles between the body axis and the earth axis. As one might imagine, the modern aircraft pilot has tools far beyond the compass to complete this transformation. However, the compass is still an essential piece of equipment in modern aircraft. As typically used, the compass represents an egocentric orientation aid because it informs the user of his or her current direction of travel or the direction that the compass is pointing.

All surveillance aircraft require coordination between the sensor video and the north-up navigation reference frames, and the most widely used technique to improve this coordination performance is an exocentric orientation aid such as a north arrow. This symbol is often overlaid on the sensor video or even static imagery and it provides a reference to the north direction of the north-up reference frame. Here this is referred to as an exocentric orientation aid because it provides a symbol aligned to the exocentric north-up reference frame. In contrast, an egocentric orientation aid is provided when the sensor-view heading is displayed at the top of the video imagery similar to how a compass would be read. This would represent an egocentric orientation aid because it would be aligned with the egocentric sensor-view, but would still offer information to align the two reference frames.

While exocentric orientation aids have widespread use in operational surveillance systems [53, 54, 55, 56, 57], only research examining egocentric orientation aids is available in the collected literature [58, 59]. This current project measured the effectiveness of the exocentric orientation aid and compared it to other possible display techniques for alleviating the cognitive orientation burden associated with switching between reference frames.

The heading reading in the right image of Figure 14 represents one possible use of an egocentric orientation aid like the compass. This provides a reference to the earth axis navigation display to let the pilot know which direction the aircraft is headed. In this case a heading of 261 is just south of west. The heading scale is anchored at north, just like the earth-axis system, and rotates clockwise through east counting each degree until returning to north at 360 heading. Pilots and navigators are very familiar with this system and regularly receive instructions of this form from air traffic control or other pilots. However, very few ground forces communicate with aircraft via heading references, and even fewer would be concerned about information relative to the aircraft's current flight path. For this reason, the surveillance problem and in particular the unmanned aircraft surveillance problem have introduced new challenges and opportunities to the transformation problem between reference frames.

While several studies have addressed the aircraft navigation transformation difficulty [60, 61, 62, 63], only three prior studies were found that have addressed the transformation associated with the sensor control [59, 58, 64]. Here, the operator must control the sensor gimbals in relation to the aircraft, in order to maneuver the video image on the ground. A good deal of investment has been made to ground stabilize the video so that the sensor operator can issue commands relative to a position on the ground. This sort of system would command autonomous gimbal movements to negate aircraft motions and keep the camera pointed at the same location despite aircraft rotations and translations. While this is surely valuable to enable the airborne surveillance mission, more can be done. To date, the primary means developed to assist operators with transforming from the sensor display to the navigation display for communication with ground forces, has been the orientation aid. As shown in Figure 3 and enlarged in Figure 15, the orientation aid provided in the sensor video is usually a north arrow or in this case a letter N representing the direction of north in the imagery. The current crew must interpret this symbol to quickly translate information observed in the video to the navigation reference frame for transmission to ground personnel. Simply telling the ground personnel that enemy fighters are off to the right of the house would not prove helpful. The common reference frame which is used for these methods of communication is the north-up reference frame. Therefore, as the surveillance mission focuses more and more of the operator's attention on mission tasks in the north-up reference frame, past efforts such as the reference frame alignment in Figure 14 may not be as productive.



Figure 15: Enlarged Image of MQ-1B Predator Display [55]
This image shows the current use of an orientation aid for transforming information between the sensor and navigation reference frames. The highlighted "N" depicts the north direction in this scene. The arrow was added, but is displayed to point in the north direction as well.

1.2.1.6. Redundancy Reduction

As different display design techniques are applied to a given control problem they can often result in a display with duplicated information. This is not to be confused research showing redundancy gains when the same information is presented in multiple modalities such as redundant aural and visual alarms [65]. Only a few studies have looked at this phenomenon, but most operational systems include visual display redundancy [66]. Operational systems often include this redundancy not for a performance benefit but for abnormal operations. The effect to normal operations is uncertain, but was evaluated in this research.

This display technique called for removing redundant information to eliminate potential distractions. While this technique may limit operator flexibility and narrow available control techniques, it could also provide for a less distracted operational environment and effectively mandate more effective control techniques. For instance, in the Figure 13 example, the predictive aid in the left navigation display offers a bank indication as well as a projected flight path. This information could be used to control the aircraft bank without the aircraft display. This effectively leverages the added information of a predictive aid, and eliminates the original aircraft reference frame which was presented from the cockpit point-of-view.

1.2.1.7. Integration

Display integration involves overlaying previously separately displayed information onto one combined display. Here the navigation, aircraft, and sensor displays were combined onto one larger integrated display. Benefits of display integration are documented to support their use in other systems [46, 67, 68, 69, 70]; however, there are also recognized drawbacks to this technique, which are discussed further in the literature review section of this document. With an integrated display, the operator could have access to higher-fidelity error reporting since the integrated display can occupy a much larger portion of the screen. This could allow the operator to observe and correct error signals earlier during tracking performance tasks.

Additionally, an integrated display could offer a shorter switching time between tasks since the information necessary for two tasks would be in closer proximity on the display. This proximity compatibility is the primary benefit cited for display integration in past efforts; however, this benefit is reserved for tasks where both pieces of integrated information are required to accomplish a single task [71, 72, 73]. Unlike those programs, the display integration in this research supported seemingly separate tasks that were both accomplished by the same operator.

Also, if displays were integrated with misaligned reference frames, this would present a cognitive dissonance on a single display. An example of such a technique is shown in Figure 15, and is currently in use by both the MQ-9 Reaper and the MQ-1B Predator. This display has the sensor video, previously discussed, with an aircraft display overlaid on top of it. In this image, the green lines are all associated with the aircraft control task, while the black information is connected to the sensor control task. This technique allowed the pilot to monitor activities in the sensor-view reference frame while controlling in the aircraft-view reference frame. This can create difficulty when the video scene is moving and creates a sense that the aircraft is turning. However, this technique and an alternate means of integration, in which the reference frames were aligned, were examined for potential interactions between display integration and reference frame alignment effects. For further details of how this technique was implemented during this research see section 3.4.3.

1.2.2. Motivation Summary

The general idea of this research is to shift the focus from one operator controlling several vehicles to one operator controlling several aspects of one vehicle. An added benefit of this approach is the retained flexibility of each vehicle. Several concepts outlined for the future use of unmanned aircraft

call for one pilot controlling several aircraft with the assistance of automation [31]. These plans can put forth manpower savings, at the pilot position, on the order of 64%; however, these do not account for the additional requirements of sensor control. A plan that could combine these positions into one would represent a real 50% operational manpower savings and may retain essential operational flexibility afforded by continuous control of each vehicle. This is not to say that increased automation has no place in this problem space. Multi-vehicle control opportunities could be explored within the single-operator realm; however, this research focuses on the initial phase of single-operator control of one vehicle. This would allow each vehicle to immediately maneuver in response to the needs of the surveillance task, rather than waiting in line for a pilot to respond to requests for repositioning.

This chapter described the reasoning behind a single-operator focus and the associated cognitive challenge of transforming information between reference frames to accomplish the two primary control tasks: aircraft and sensor. It also highlighted the possible need to focus on the north-up mission reference frame as the central purpose of surveillance tasks. With this possible shift in focus away from the aircraft axis and towards the navigation axis, each of the previously described techniques (predictive aiding, course guidance, reference frame alignment, orientation aids, redundancy reduction, and integration) could be leveraged to assist with this transformation. This research explored these possibilities and others based on a phased approach to lessons from literature and a responsive experimental approach.

1.3. Thesis Objectives

The purpose of this research was to gain a better understanding of the impact of multiple cognitive reference frames on unmanned aircraft operations. This research sought to characterize the challenge associated with multiple reference frames and evaluate the potential for several display techniques to address this problem. Reference frame alignment, orientation aids, display integration, and display redundancy reduction were all evaluated for their effectiveness at addressing the multiple reference frame difficulty involved with unmanned aircraft surveillance operations. Exocentric orientation aids are the currently accepted technique, while reference frame alignment represented a novel approach to reduce this cognitive burden during unmanned aircraft operations. Accordingly, the thesis objective was:

Characterize the impact of multiple reference frames on unmanned aircraft operations and evaluate the potential of reference frame alignment, orientation aids, display integration, and display redundancy reduction for addressing this problem.

This objective was analyzed through four separate experiments:

1. Experiment 1: This unmanned aircraft simulator experiment evaluated reference frame alignment and orientation aids in the multitask setting of unmanned aircraft control and found that both were effective at reducing basic orientation time between sensor video and the north-up reference frame, but only reference frame alignment was helpful with more complex tasks such as finding a target location in the sensor video.

2. Experiment 2: This imagery rotation subtask study evaluated reference frame alignment and orientation aids and found that both were effective at reducing the required time to find a target location in an image.
3. Experiment 3: This unmanned aircraft simulator experiment evaluated reference frame alignment and display integration in the multitask setting of unmanned aircraft control and found that reference frame alignment was effective at reducing basic orientation time and was helpful with more complex tasks such as finding a target location in the sensor video. However, display integration demonstrated no measurable benefit with either task.
4. Experiment 4: This unmanned aircraft simulator experiment evaluated reference frame alignment and display redundancy reduction in the multitask setting of unmanned aircraft control and found that both techniques were effective at reducing basic orientation time and helpful with more complex tasks such as finding a target location in the sensor video.

These experiments and their results are discussed in detail throughout this document, but the overall findings show that reference frame alignment and display redundancy reduction demonstrated positive effects across multiple measurements, but orientation aids and display integration were less effective at addressing the multiple reference frame impact on unmanned aircraft operations.

2. Related Work

This review of previous literature focused on three primary subjects: first, unmanned aircraft display design, which also required an understanding of different control architectures and levels of automation; second, the cognitive difficulty associated with switching reference frames or orientations; and finally, the current understanding of the challenges associated with multitasking and how that pertains to the multiple reference frames and control tasks of Unmanned Aircraft operations.

2.1. Unmanned Aircraft

The wealth of literature concerning Unmanned Aircraft covers several areas of interest. Several researchers are investigating means to increase the number of vehicles controlled by one operator, which usually relies on increasing the level of automation of each vehicle. Others have focused on different display designs that support single-vehicle control and either increase or decrease the operator's sense of remote presence on the vehicle.

2.1.1. *Single vs. Multiple Aircraft*

Many researchers are focused on leveraging increased levels of automation to enable one pilot to control several unmanned aircraft [38, 74, 75, 76, 30, 77, 78, 79]. There are areas of research seeking to identify just how many aircraft a single operator could control [80, 37, 81], and what level of automation is desirable in such multi-vehicle control scenarios [82, 83, 84, 85, 86, 87, 38, 88]. This emphasis on multi-vehicle control may have decreased efforts associated with holistic single-vehicle control.

Many see unmanned aircraft as a continuation of manned aircraft and therefore have focused largely on the aircraft control portion of the unmanned aircraft mission; however, the unmanned aircraft mission is far more than merely an aircraft control mission. The benefits and challenges of unmanned aircraft have a lot to do with increased station times, decreased risk to operator lives, and in some cases even their disposability [89]. Harnessing these advantages may require considering the entire surveillance mission and not just the pilot portion.

This should not be interpreted to discount the value of research into coordinated use of unmanned aircraft to facilitate swarm tactics or other large formations of vehicles; however, a focus on the larger surveillance mission may bring increased research back to the single-vehicle control.

2.1.2. *Levels of Automation*

The multi-vehicle control scenario is often reliant on increased levels of automation; this allows for intermittent operator control of each individual vehicle, but reduces the overall flexibility of any *one* vehicle to respond to a changing mission environment. The multi-vehicle control goal has often focused researchers' investigation of appropriate levels of automation in unmanned aircraft control [82, 83, 84, 85, 86, 87]; however, there are a few researchers who have investigated the advantages of increasing levels of automation in single-vehicle control [90, 91, 92].

Unfortunately, and perhaps because of the current division of tasks between two operators, there is little research seeking to increase levels of automation with an interest in enabling a single operator to share time between sensor and aircraft control [59, 58, 93, 75]. Despite the significant benefit in manpower savings, most of the research regarding unmanned aircraft leaves the imagery collection task to a second operator or simplifies the task to an automatic compensation system that perfectly fixes the camera on some geographic location. As demonstrated in programs such as the RQ-4 Global Hawk, when we attempt to fully automate such collection tasks we decrease one of the significant benefits of airborne surveillance: flexibility [38]. There is a need to retain flexibility of targeting and allow for increased control of the vehicle and sensor to respond to unforeseen circumstances.

2.1.3. Display Design

Without relying on increasing automation levels, we can still approach these control difficulties through display design. Which display features enhance a controller's ability to manage multiple tasks including image processing? Many researchers have developed display principles over years of Human Factors research; however, few have done so in the remote multitask control setting of unmanned aircraft operations. This added to a small but growing body of work that investigates display design for single unmanned aircraft control. Several experiments designed to inform manned aircraft displays and controls can also support this work because it was collected on simulators which, in effect, mirror the unmanned aircraft environment.

2.1.3.1. Exocentric vs. Egocentric

In a virtual transition from manned to unmanned aircraft control, the operator is removed from the egocentric (first-person) cockpit view to a set of remote displays. One underlying question is whether or not to provide the unmanned aircraft operator with an egocentric view with which to control the vehicle. This question has been posed in several studies with varying types of displays and missions, and results have highlighted variations in the results that were influenced by the required tasks of the mission scenarios [94, 95, 96]. For local guidance tasks the egocentric view was found to be more beneficial, but for global awareness tasks the exocentric view prevailed [97]. This represents a dilemma for unmanned aircraft display designers since the mission often requires both types of tasks. One potential route is to focus on the aircraft control or local guidance tasks and choose an egocentric display, but even in basic aircraft control, if the airspace is heavily restricted with keep-out zones then the global awareness may be important.

The question of perspective is not unique to unmanned aircraft, but has been debated across all of the unmanned vehicle domains. Multiple studies examining ground vehicles found that a tethered display from a point-of-view aft and above the ground vehicle was more beneficial in navigating remote ground vehicles [98, 99]. These results do not directly carry over to the three-dimensional control problem associated with aircraft, but given that many unmanned aircraft carry out their missions from a level flightpath it could represent an advantage of straying from the egocentric view to a more optimized remote control view.

2.1.3.2. Stimulus-Response Compatibility

Regardless of the display perspective, there is an important relationship between the displayed stimulus and the control input required to address that stimulus. During the multitask control of an unmanned aircraft, it would be necessary for the operator to manage the flight path of the unmanned aircraft and the pointing of the imagery sensor. This task would be much more difficult if the necessary control input was not in the same direction as any displayed error [46]. So, any technique such as Reference Frame Alignment would require additional information processing to allow for control inputs in the same direction as any displayed error.

2.1.3.3. Orientation Aids

Some researchers have investigated the benefit of different orientation aids to allow the unmanned aircraft operator to transfer information between different display reference frames. One study had subjects locate a target in an image displayed in the sensor-view reference frame and provide a location description in the exocentric north-up reference frame [100, 59, 58]. These researchers characterized this orientation burden and identified a cardinal direction benefit. In other words, the subjects were faster at the information transfer when the sensor was oriented with the north, south, east, or west direction up. Next, they attempted to lighten the cognitive burden by providing an egocentric orientation aid in the sensor image by displaying the sensor heading at the top of the image. They observed little benefit of such a reference. Most of the industry has chosen a different approach by displaying the north direction on the sensor image, but no research was published to describe the effectiveness of such an exocentric orientation aid.

2.1.3.4. Similarity Confusion vs. Cooperation

Research regarding the stimulus-response compatibility principle, described in 2.1.3.2, is well-established [101, 102, 103, 104], but less common is an understanding of how that might scale up to multitask control scenarios. There is some evidence that executing multiple tasks in a common direction, which requires control inputs in a common direction, can lead to similarity confusion [105]. Here, the operator would actuate the controller for task B when he or she actually intended to control task A. This could lead to a significant increase in operator workload and decrease in achieved performance. However, there are other bodies of evidence that indicate a cooperation effect [106]. Here the operator increases performance on the two tasks *because* he or she is controlling them both in the same sense. Perhaps the ability to assess and correct error is improved because the orientations are homogeneous. At any rate, these competing phenomena have not been investigated using the unmanned aircraft multitask scenario.

2.1.3.5. Predictive Aids

Many years of research have investigated the benefit of predictive aids for various control tasks. A predictive aid is a display technique which provides a signal for the current state of the system and a projected future state [46]. There are many factors to consider when adding such a display feature [107,

47]. The basic time step at which the future state should be predicted is a function of the task requirement and frequency of control inputs. Some displays provide multiple future state estimations, but this could also lead to display clutter. In the aircraft navigation and control domain, predictive aids are often included on the navigation display to provide some feedback of the current control actions of the operator; however, to the knowledge of this author, none have been used to replace the aircraft control display. Since the predictive aid is responsive to current control inputs, it is possible to provide a predicted flight path and an indication of control inputs.

Similarly to the previous use of reference frame alignment tailored to the aircraft-view reference frame, some use of predictive aiding has been applied to an egocentric point of view. These implementations are often included for tasks which require 3-dimensional flight path guidance [49]. Since this research investigated display techniques tailored to the surveillance portion of the unmanned aircraft mission, the vertical guidance was far less important than the lateral guidance, and therefore a navigation display predictive aid was investigated here.

2.2. Cognitive Orientation

2.2.1. Reference Frame Rotation

The basic difficulty associated with rotating information from one reference frame to another has been examined by multiple researchers [108, 98, 109, 59]. Some studies looked at the time required for a subject to determine whether or not a letter was displayed in the forward or reverse direction, or whether it matched a target letter [39, 110, 111]. They found that as the letter was rotated the subject's time to answer increased linearly. While letter rotation is different than imagery rotation in an unmanned aircraft task, this highlights a basic cognitive difficulty associated with reference frame rotation. Other studies observed similar difficulties associated with reference frame rotation across a wide variety of tasks and environments [112, 113, 114, 115, 112, 116].

2.2.2. Cognitive vs. Display Reference Frames

Another cognitive difficulty associated with multiple reference frames is the subject's ability to maintain cognitive reference frames that are not provided on a display. As opposed to manned aircraft operators, the unmanned aircraft operator has no ability to directly perceive reference frames associated with the aircraft. This gives the designer or designers a greater capability to control the cognitive reference frames associated with unmanned aircraft as opposed to manned aircraft control. However, the operator can still develop, and maintain, his or her own mental representation to support some decision-making process or simply for information storage [112]. This may pose a problem when researching the reference frame effects. Although the display configuration may be adjusted to reduce the number of reference frames, the operator may continue to maintain a mental representation of additional reference frames. This is of particular importance if our measure relies on the subject's cognitive reference frames to match those that are displayed in front of him or her.

When given the opportunity to investigate this effect, one researcher found no effect associated with those individuals who maintained an additional mental or cognitive reference frame [112]. These data were obtained using a virtual tunnel task where subjects observed an egocentric display of a tunnel passage that turned in one direction. After some degree of turn (egocentric reference frame rotation with respect to exocentric view), subjects were asked to identify the direction to the starting location of the tunnel. Some of the subjects referenced the starting location with respect to the exocentric frame while others referenced an additional mental reference frame that was centered on the current location but oriented in the same direction as the starting point. The authors referred to this as an allocentric reference frame and they saw no degradation in performance associated with this procedure [112].

While this result lessens some of the concern associated with cognitive reference frames independent of displayed reference frames, it was observed in a much simpler study of reference frame interactions. These researchers were not interested in controlling the number of reference frames, but rather understanding the difficulties associated with rotations between reference frames. As this current study examined the reference frame alignment effect during unmanned aircraft operations it is possible that a subject's decision to maintain an additional cognitive reference frame affected the experiment's ability to measure the reference frame alignment impact.

2.2.3. Object Rotation vs. Perspective-Taking

A good deal of cognitive literature has investigated the mental rotation or cognitive orientation capability of various subject populations. Some of this literature has provided evidence that there are two separate mental pathways in the brain that can be used for these sorts of tasks [117, 118, 119, 120]. These research efforts have split such mental rotation tasks into two categories: object rotation and perspective taking. Object rotation refers to the act of mentally rotating an image that appears as a 2D or 3D object (exocentric representation), while perspective taking involves imagining oneself in a scene (egocentric representation) and then visualizing one's relationship with other aspects of that scene.

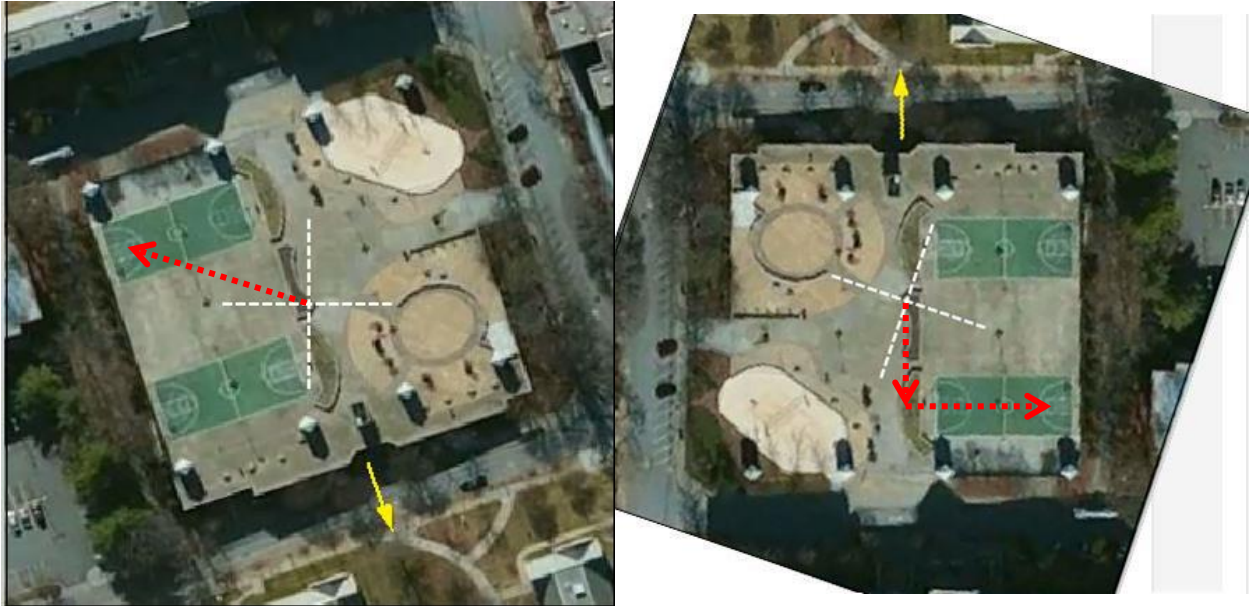


Figure 16: Target Acquisition Task Mental Process Differences

The left image depicts a perspective-taking task where the subject imagines themselves in the scene facing north in the image and then moves back and to the right towards the target. The right image depicts the object rotation task where the subject has already mentally rotated the image to north-up and then he or she moves south and east to the target. [Image ©Google]

Both of these could be applicable to the unmanned aircraft control problem. There are aspects that seem to require a perspective-taking task, such as imagining oneself in the aircraft to decide whether to bank left or right. The sensor-video orientation task could be accomplished with either perspective-taking or object rotation. When completing a target acquisition task and attempting to apply some instructions from the north-up reference frame, a subject could imagine moving through the video in the direction of the instructions, or the subject could imagine rotating the video and then deciding which way the target location would be. A visual depiction of this difference is provided in Figure 16. The main difference is whether or not the subjects attempt to mentally immerse themselves (egocentric) in the scene or they just consider the scene as an object to mentally rotate.

2.2.4. Aircraft Orientation Studies

Multiple studies have addressed the multiple reference frame environment of manned and unmanned aircraft. A particular body of research, from Clemson University, investigated cardinal direction judgments in a surveillance task [58, 59]. This research, in 2001 and 2004, included an aircraft and sensor representation similar to that of this current research [59, 58]. However, the operator's task was a simple cardinal direction judgment which did not include any multitask aircraft and sensor control. In the Clemson study subjects were shown an image with four rectangles around one central rectangle. This represented a building with four surrounding parking lots. One of these symbolic parking lots had vehicles in it, and the subject was to identify the cardinal direction from the building to this parking lot. This is similar to the orientation investigated in this current research; however, the Clemson study focused on an egocentric orientation aid to decrease the misalignment difficulty.

The Clemson research involved a static observation of the scene as the aircraft flew straight and level rather than orbiting the target. This limitation was focused on a scenario where the aircraft included a fixed nose camera rather than a gimbaled sensor. This allowed subjects to maintain a relatively constant angle of rotation throughout their decision process and is unrealistic of most current unmanned aircraft surveillance tasks. However, this may have contributed to the development of their egocentric orientation aid which consisted of a sensor-view heading at the top of the sensor display. Rather than indicate the direction of North (exocentric aid) the Clemson research informed the operator of the video camera's orientation heading. This did not improve the subject's accuracy or speed in completing the cardinal direction task.

In summary, the Clemson study highlighted the problem of reference frame misalignment between the sensor display and the mission display, but focused on shifting information to the egocentric point of view rather than the exocentric map view. This research was followed with an additional study that included navigation performance and further supported the concept of tailoring the unmanned aircraft control to an aircraft perspective rather than a north-up orientation [64]. However, this research did not lead to a suitable display aid to address the multiple reference frame issue. Furthermore, their study did not evaluate the current aids used for this process (exocentric orientation aids).

Other studies have focused on the difference in navigation performance based on a north-up or track-up map display [121]. A track-up display rotates the map so that the aircraft's flight path is always towards the top of the map. This is like a compensatory display because the map moves around the aircraft symbol rather than the aircraft moving over the map. The track-up vs. north-up debate has grown into a wide area of research involving personal, ground and air vehicle navigation performance, but when focused on manned aircraft these studies generally find that pilots prefer track-up while navigators or mission planners prefer north-up. This is intuitive since the pilot would continuously think of their physical reference frame in the cockpit which is oriented track-up, and the navigator might be more likely to think of the different north-up displays used in mission planning. These investigations have been dependent on the sets of tasks presented to the operator. When terminal area tasks are presented and involve complex arrival corridors, subjects have preferred more egocentric displays for finer flight path guidance [122]. However, when these studies have added more global awareness tasks the exocentric north-up map becomes more beneficial [123, 97]. Since the navigator is often more concerned with global awareness tasks with respect to geographic or airspace features and the pilot is often concerned with local guidance tasks like following the mission plan, these operator differences match other areas of research.

One unique aspect of the unmanned aircraft design space is that the pilot has no access to the physical reference frame of the aircraft. This is usually seen as a great hindrance and since most of this research has been to support manned aircraft or has grown from research programs which support manned aircraft, its focus is usually centered on the idea of providing the ground-based pilot with a sense of that aircraft-view reference frame. However, little has been done to investigate other more optimal control reference frames. The tethered perspective offered on several popular flight simulator video games highlights the potential benefits of stepping away from the egocentric-focused design. The best aircraft control interface for the unmanned aircraft mission might be presented in an entirely new reference frame not currently used in aircraft displays.

2.3. Multitasking

The single-vehicle unmanned aircraft control task requires multitasking between aircraft control functions and sensor video control. Few literature sources address the heterogeneity involved in this scenario, but there is ample information available regarding the difficulties of multitasking and the pitfalls associated with measuring such performance.

2.3.1. *Performance Operating Curves*

Norman and Bobrow of the University of California, San Diego and the Xerox Company respectively, were some of the first to model multitasking effects. They characterized the multitasking effect from a resource-limited perspective [124]. Today their approach is often displayed on performance operating characteristic (POC) curves as shown in Figure 17 [46]. The basic understanding here is that increasing performance of task A will decrease performance on task B because the operator has limited resources to accomplish both tasks. An increasing multitask efficiency is realized when the POC curve pushes outward toward the optimal performance. Such increases might be realized with tasks involving different types of resources. For instance, if an additional task is required in an auditory channel when the primary task is largely visual, this can increase the multitasking efficiency.

This objective characterization of the multitasking penalty is important for the unmanned aircraft mission scenario. Multi-vehicle control generally addresses this issue with intermittent control supported by increasing levels of automation. Similarly, single-vehicle control might benefit from some measure of automation in aircraft control and sensor pointing, but in order to maintain flexibility of action a higher switching frequency would be required between tasks. This research considered how these differences affect the multitasking performance penalty.

2.3.2. *Switch Cost*

Switch cost is incurred anytime an operator attempts to switch between multiple tasks. This is usually described as a cost of controlling multiple independent vehicles, but can also be applied to multiple tasks associated with one vehicle [125]. The switch cost associated with multitasking is highlighted in Figure 18. This description, from the left side of Figure 18, was developed by a research program studying multi-vehicle control, in which the multitasking switch was prompted by a performance threshold [37]. After the subject resumed control of the vehicle of interest, the switch cost time was observed as a continued period of decreasing performance as the subject oriented with the new task and determined an appropriate control action to improve performance. This switch cost is evident in all forms of sequential multitasking, but may be a more significant issue with higher-

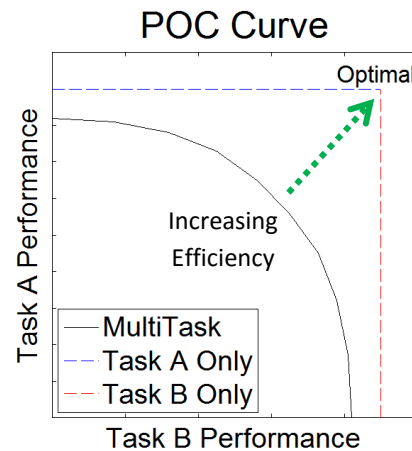


Figure 17: Performance Operating Characteristic [46]

frequency task switching. The right side of Figure 18 addresses this difference. Here the task switching is prospective and does not rely on a performance cue. This encourages higher frequency task switching and, perhaps, higher performance; however, such techniques require a higher proportion of time spent in switch cost. For this reason orientation time should have more impact on multitasking with higher frequency task switching.

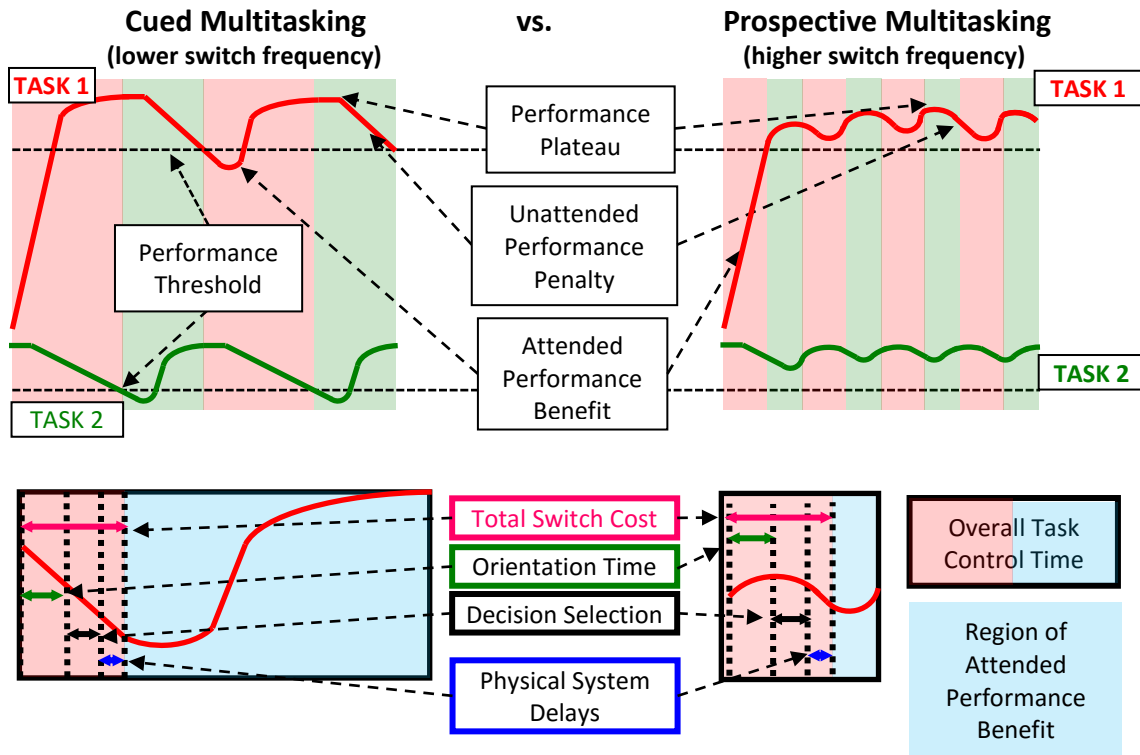


Figure 18: Multitasking Frequency Effect on Switch Cost

In the top figures, the red areas indicate regions of task 1 control, and the green regions indicate task 2 control. The images on the left depict an automated (cued) multitasking in which the operator switches tasks at a certain performance threshold. On the right, in a higher frequency prospective multitasking, a larger portion of control time is spent in switch cost. At even higher frequencies an operator could switch tasks before fully completing switch cost.

The bottom region of Figure 18 shows that a higher percentage of task control time is consumed by switch cost during multitasking with higher switch frequencies. One portion of that switch cost is the orientation time associated with the display, which could be influenced by the display reference frame. This research focuses on the orientation time cost and display techniques that can be used to decrease this orientation time and facilitate increased multitasking performance and decreased operator workload.

2.3.3. Training Effect

A previous study testing multitasking in response to visual and aural stimuli, training effect was observed over the course of multiple experimental sessions on multiple days [126]. That study included an fMRI measurement to observe changes in the cognitive processes as the subject became more

familiar with the task. Other research has highlighted that humans are “poor” multitaskers, or in other words humans pay a relatively large penalty in performance when completing multiple tasks simultaneously or near simultaneously [127]. However, some have also discovered that through practice and training with certain multitask scenarios, humans can increase their performance for both tasks [106]. This is akin to increasing their performance operating characteristic efficiency from Figure 17. This is particularly important when experimenting with multitasking scenarios. A proper study should attempt to mitigate this effect when evaluating different display design techniques.

3. Experimental Methods

This chapter provides an overview of the four experiments conducted as part of this research. It outlines the basic design of the simulator along with the performance and workload measures used for the three simulator experiments. These measures coincide with the set of tasks required of the unmanned aircraft operator. Each of the subsequent chapters provides a standalone account of each independent simulator experiment, including the specific methods and results from each experiment. Finally, chapter 8 summarizes the conclusions from all four experiments.

3.1. Overview

In order to investigate the multiple-reference-frame challenge associated with unmanned aircraft operations, a basic unmanned aircraft simulator was developed. This simulator was used to probe the effectiveness of several feasible display characteristics: orientation aids, reference frame alignment, display integration, and display redundancy reduction. Four experiments were included in this research: three involved the aircraft simulator with representative unmanned aircraft operator tasks; the fourth experiment (#2) closely examined the individual imagery rotation subtask. This imagery rotation is required by unmanned aircraft operators searching for targets in a sensor video image. Each experiment included a baseline display configuration and alternative display configurations which incorporated the display characteristics shown in Table 1.

Table 1: Display Characteristics by Experiment Number

This table describes the four experimental studies carried out during this research program and the corresponding display characteristics of each. Each experiment included some evaluation of reference frame alignment and one other display technique.

Experiment	Simulator	Reference Frame Alignment	Orientation Aids	Display Integration	Display Redundancy Reduction
1	X	X	X		
2		X	X		
3	X	X		X	
4	X	X			X

These display techniques were chosen for their potential influence on the cognitive orientation challenge, or for their potential interactions with the reference frame alignment technique. As shown in Table 1, reference frame alignment was evaluated in every experiment. Since this technique involved aligning displays, it served as both a measure of the significance of the multiple reference frame difficulty, and a possible mitigating technique.

Similarly to its use in aircraft navigation, reference frame alignment was applied by rotating the video image to north-up before displaying it to the operator. This would increase the level of information acquisition automation, and could also apply to information other than the sensor video [128]. An orientation aid is currently available on most sensor videos to assist with operator mental rotation requirements. As tested here, this feature involved a north arrow on the sensor video to provide a continuous indication of the north direction. Display integration combined the separate

displays onto one central display. Finally, display redundancy reduction evaluated the usefulness of separate displays with repeated information. An effort was made to reduce this redundancy and thereby simplify the multitask crosscheck of the operator. This was also evaluated for its interactions with the reference frame alignment technique.

These techniques address the problem of multiple cognitive reference frames with different approaches. First, the reference frame alignment and orientation aid techniques retain multiple displays of information, but assist the operator in switching between displays by either aligning the displays to a common reference frame or providing an alignment cue with the orientation aid. Conversely, the display integration and display redundancy reduction techniques both attempt to reduce the operator's visual scan by providing all necessary information on fewer displays. The integration technique provides all information on one central display while the display redundancy reduction technique eliminates one display which is not essential to the required tasks. In this way, the first two techniques (reference frame alignment and orientation aids) directly address the mental challenge of multiple cognitive reference frames, while the last two techniques (display integration and display redundancy reduction) address the physical challenge of visually scanning multiple displays. These techniques and their implementation in these experiments are described in detail in section 3.4.

3.2. Simulator Description

The unmanned aircraft simulator was designed as a tool to explore the multiple reference frame tasks associated with unmanned aircraft operations. During each experiment, the subject was asked to complete representative unmanned aircraft tasks that involved the control and navigation of the aircraft and control of the sensor video in order to accomplish a described surveillance mission. These tasks were designed to be representative and also include some measure of interaction between the different reference frames.

3.2.1. *Simulator Scenarios*

For the basic simulator scenario, the operator had to control an aircraft to follow a predesigned path around a target area, and control an onboard video sensor to continuously track a specific target. This was done to provide the operator with a multitask requirement for both aircraft and sensor control. Each of these scenarios began with a 15 second time period to observe the satellite image and textual description of a target, as if he or she were given a targeting request from a commander on the ground. After this 15 second period, the simulation began with the aircraft positioned along a defined circular orbit around the desired target. The operator was required to locate the predefined target and click on that target as if to employ a weapon. This was an attempt to provide a realistic unmanned aircraft task. Additionally, this was designed to provide a higher level of seriousness and reduce potential target acquisition errors which hinder the data analysis and understanding of the various display effects. After this initial target selection, the operator continued to track the target location and follow the predefined aircraft flight path.

To measure the time required for operators to orient information across reference frames, a representative orientation task was added to the sensor video tracking task. The subjects were told to observe the target area for personnel running away so that they could inform the team members on the ground to enable a pursuit of the suspected enemy fighters. Subjects were to notify ground personnel, via the control stick switch, as soon as they determined the direction of the suspect movement. However, they were also only allowed one transmission so if they transmitted incorrectly, the ground personnel would pursue in the wrong direction and have no hope of finding the suspect. On the other hand if their response was slow the suspect would get a larger head start and this would also hinder pursuit by the team members on the ground. While the single transmission is not indicative of realistic scenarios, it was added to encourage the subjects to complete reference frame transformation and produce an answer which they thought was correct. It also provided an easier measure of performance because the first response could be captured as the answer time for this task.

Since the operators were completing tasks on multiple screens it is entirely possible that they would be observing the aircraft display or navigation display while the suspect exited the target and fled in some direction. To prevent this confound, and to capture a secondary measure of workload, a reaction time test was added to the simulation scenario. Here operators were told that a light would blink on the simulator to warn them of activity at the target area. They were to respond to the light as quickly as possible and then visually observe the target for the fleeing suspect. This was to ensure the operator would not miss the suspect's movement, and it provided a reaction time measurement for how quickly the operator responded to the light. This reaction time task was described as a secondary task; however, the subjects were instructed to respond as quickly as possible and not wait for a break in their primary tasks. These instructions were confirmed by reviewing training results and ensuring reaction times less than the one second benchmark.

Each of these scenarios lasted for 3.2 minutes to allow for one full aircraft rotation around the target. This complete orbit was designed to address the angular effect on axis and object transformations, and corresponding influence on performance. By ensuring the operator or experimental subject continued the task through all 360 degrees of axis rotation, the angular effects could be observed. Furthermore, this ensured each experimental trial had some influence from every angle of rotation. The largest difference occurred at the beginning of the trial as the operator was first exposed to the target area through the simulator sensor video. This angle effect was manipulated from trial to trial in order to measure its effect.

This general scenario was used during each of the three simulator experiments.

3.2.2. Simulation Model

Since the simulator was designed to investigate an unmanned aircraft with a focus on reference frame transformation, the operator only controlled bank angle of the aircraft. This is reasonable for an unmanned aircraft simulator since these systems often rely on significant levels of stability augmentation so they are often equipped with airspeed and altitude hold modes. In order to understand the aircraft control reference frame transformation requirements, the bank angle task was still controlled by the operator. Here the operator could command an aircraft roll rate. Figure 19 demonstrates the bank angle measurement between the aircraft vertical axis and the earth vertical axis.

If this angle is increased, turn rate will increase. The operator was able to adjust this bank angle by controlling roll rate. This limited aircraft control input also enabled inexperienced operators to participate in these experiments, and it retained the transformation required between the aircraft-view and north-up reference frames.

It was important to maintain a continuous tracking task requirement so the simulator was developed with turbulence effects applied to aircraft bank angle. This was initially developed to ensure the operator had to stay actively engaged in the flying task and could not just set a

bank angle that would follow the orbit and then ignore the task. Additionally, a constant wind simulation was available so the aircraft would require different levels of bank at different points around the orbit. This could also increase the aircraft control difficulty on the operator.

To provide a realistic image scene, simulated sensor video was created from a single airborne photo that was cropped and zoomed to reveal the current sensor pointing area. The subject could control the pointing of the camera by commanding the image to move up, down, left or right in relation to the on-screen display. The simulation included sensor gimbal compensation that represented a geo-stabilization feature. This would prevent or minimize sensor oscillations despite aircraft movements. While this simulated sensor gimbal control on the aircraft, the subject never directly controlled any simulated gimbals since the image was controlled in relation to displayed orientation and pointing with respect to the ground, not with respect to gimbal angles. This capability was included because it is representative of actual systems; however, it does represent a degree of automation in sensor video control. Additionally, to avoid abrupt performance measures, the simulator did not model any gimbal limits. This is an artificiality compared with actual systems, but could have produced significant spikes in performance measurements given only minor differences in aircraft control.

The sensor video pointing had an injected turbulence presented during all simulator experiments. Once again, this was added to ensure a continuous tracking task requirement. This was simulated as a rotation around the x-axis direction of the aircraft as if it was induced by aircraft bank or bank turbulence; however, the magnitude and frequency of these oscillations were completely independent from the aircraft location or control. The oscillations were modeled as a sum of sines on the crosshair rate of movement. The sum of sines technique ensured repeatability of the oscillatory pattern from one subject to the next [129]. The cursor rate (rather than cursor displacement) turbulence provided a smooth oscillation of the crosshairs that could be controlled by the operator. Although not necessarily realistic with respect to an actual system, this allowed the operators to actively counter these oscillations. Abrupt turbulence would not have been controllable by the operator. With a smooth pattern, performance differences could be measured between trials.

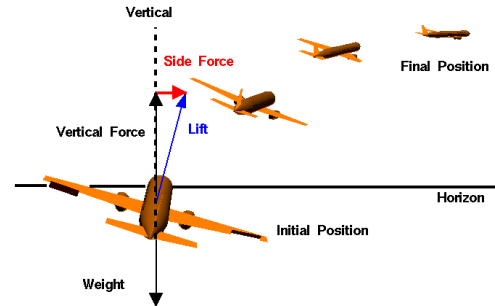


Figure 19: Bank Angle [141]
The bank angle is measured between the blue and black arrows.

3.2.3. Simulator Displays

The basic simulator display configuration, with the traditional representation of each reference frame, is shown in Figure 20.

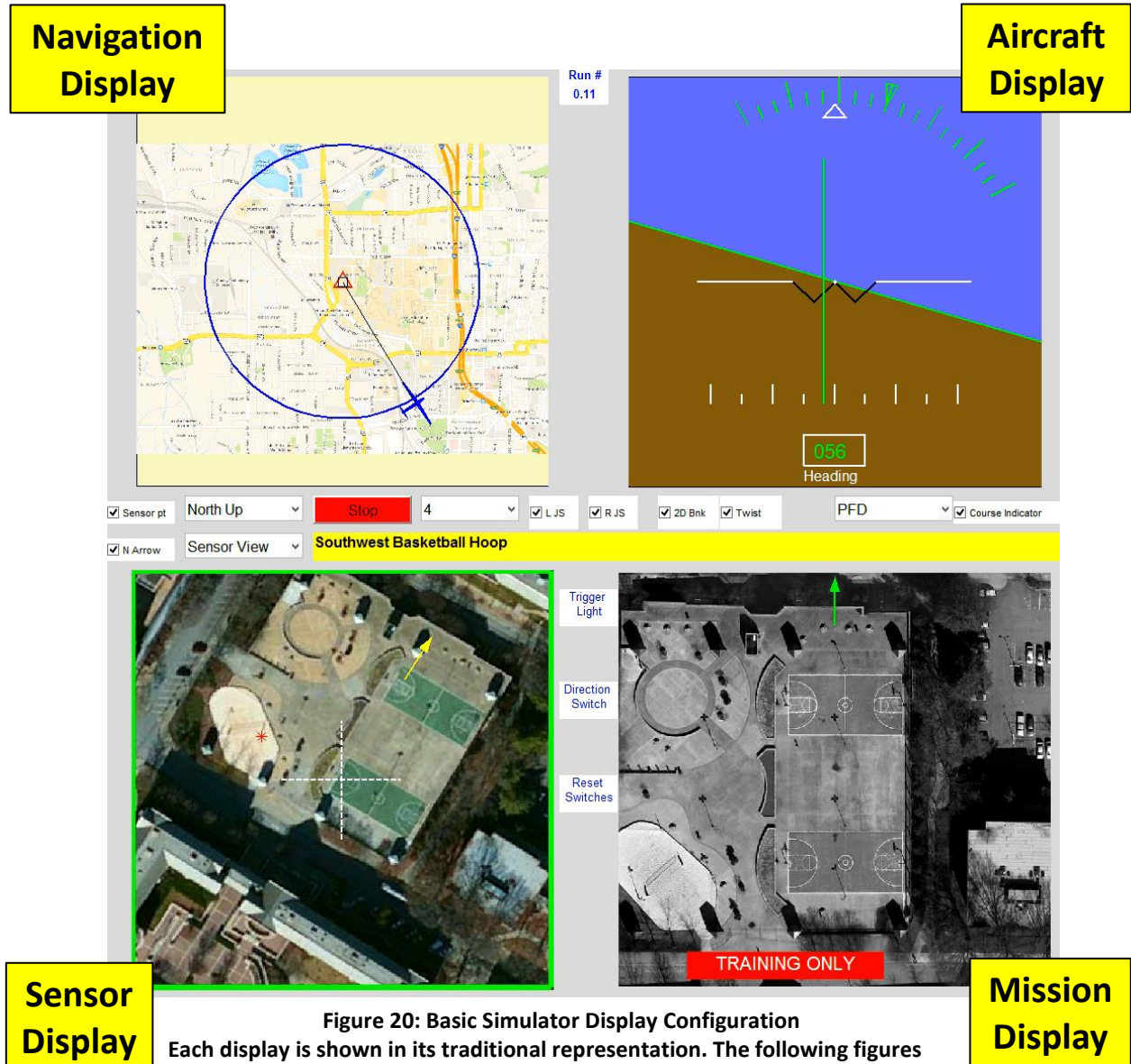


Figure 20: Basic Simulator Display Configuration
 Each display is shown in its traditional representation. The following figures describe each of the applicable symbols. [Map Data and Image ©Google]

3.2.3.1. Navigation Display

The navigation display in the upper left of Figure 20 provides a north-up map with the aircraft location indicated by an aircraft symbol. The desired aircraft flight path, target location, and current sensor pointing location are also displayed here. At times, this display also includes the predictive aid. These various features are labeled in Figure 21 which shows two examples of the navigation display. The left example was used during experiment 1, without the predictive aid, and the right example was used during experiments 3 and 4, with the predictive aid.

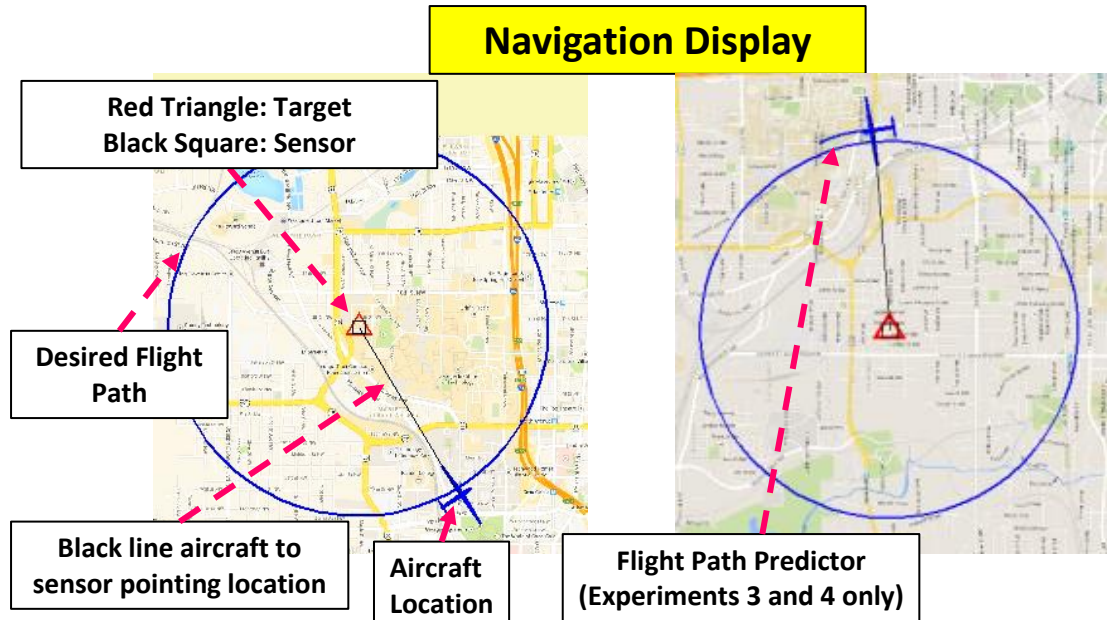


Figure 21: The Navigation Display

This figure shows two examples of the navigation display (experiment 1 on the left, and experiments 3 and 4 on the right) The display shows a north-up map, aircraft location symbol, sensor pointing location, target location, and desired flight path. [Map Data ©Google]

3.2.3.2. Aircraft Display

The aircraft display in the upper right of Figure 20 provides an interface for aircraft control. The aircraft bank angle is displayed via the traditional aircraft-view representation or the north-up representation. Examples of these are provided in Figure 22. In both representations the current bank angle, heading, and course deviation are visible on this display. The bank angle is indicated on the aircraft-view version with the white triangle location on the green bank scale. On the north-up version, the bank angle is indicated by the white line location on a similar green bank scale. Each version displayed the course deviation, displacement from the desired flight path on the navigation display, with the green line on a white course deviation scale below the aircraft symbol. The heading was displayed numerically in the aircraft-view version and graphically, via the aircraft symbol, on the north-up version. The north-up version shown in Figure 22 includes curvature in the bank indicator and course deviation indicator. These lines would have been straight in experiment 1 (right side of Figure 26) because these features were added with the predictive aid for experiments 3 and 4.

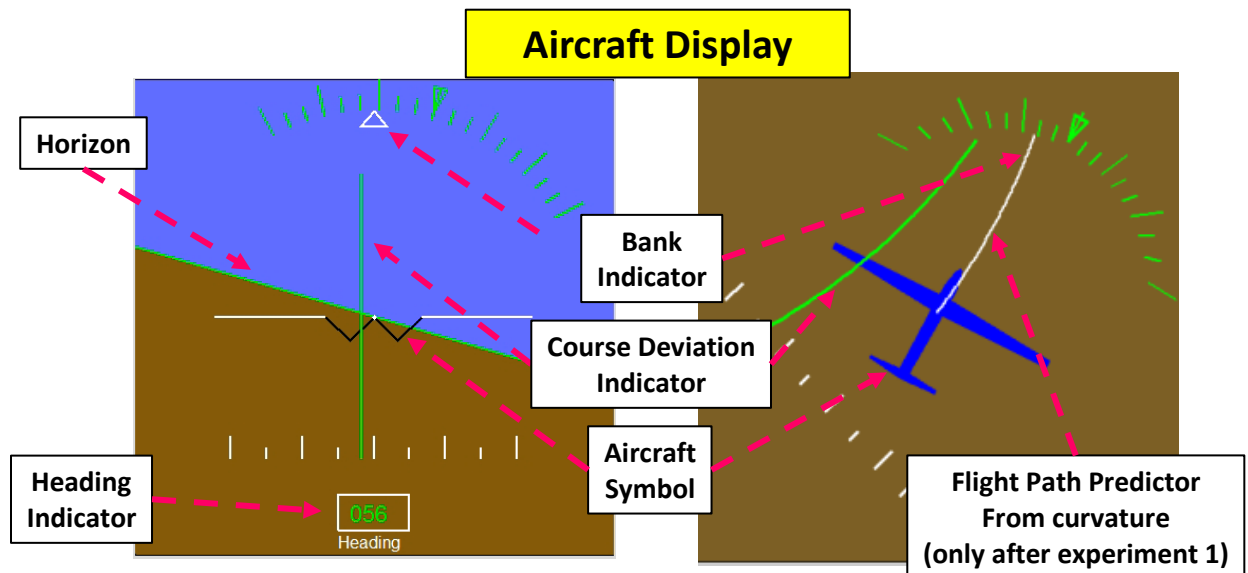


Figure 22: The Aircraft Display

This figure shows two examples of the aircraft display (aircraft-view on the left, and north-up on the right). The display shows an aircraft symbol, and current bank angle indication. The aircraft-view display shows the horizon as seen from the aircraft cockpit, and a heading indicator. Heading information is perceived via aircraft symbol pointing direction on the north-up version. Both displays show displacement from the desired orbit on navigation display with a course deviation indicator.

3.2.3.3. Sensor Display

The sensor display in the lower left of Figure 20 provides an interface for sensor control. The sensor pointing location displayed via the white crosshairs over the sensor video. The video was either displayed in its traditional sensor-view orientation or it was rotated to north-up. Examples of these are provided in Figure 23. In both representations the current pointing location was always visible with the white crosshairs; however, the orientation aid was only visible on some of the display configurations. Figure 23 also provides an example of the moving symbol. This was visible on either display during one of the specified tasks.

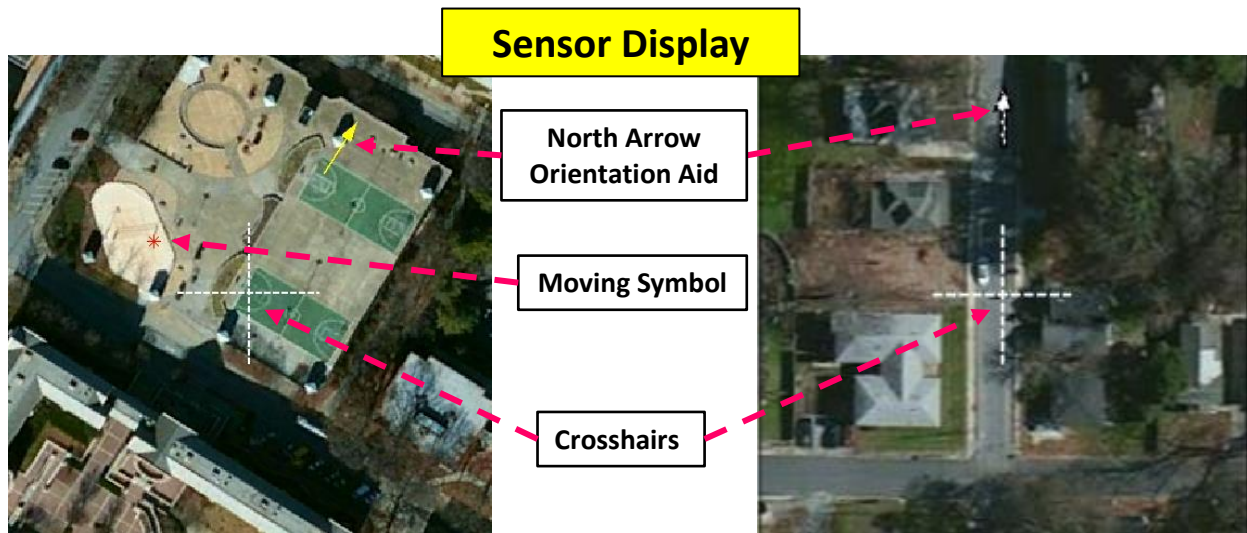


Figure 23: The Sensor Display

This figure shows two examples of the sensor display (sensor-view on the left, and north-up on the right). The display shows crosshairs to indicate the sensor pointing location. At times each of these showed the north arrow orientation aid as displayed here; however, some versions of this display did not include the north arrow. The same moving symbol was shown on either version, but here an example is visible on the sensor-view version. [Map Data ©Google]

3.2.3.4. Mission Display

The mission display in the lower right of Figure 20 provides a satellite image of the target location. This display is accompanied by a textual description of the target. An example of this is provided in Figure 24. This black and white image was always displayed north-up and always included the north arrow fixed pointer as a reminder that north was always up on this display. The textual description described the target location visible in the satellite image as shown in Figure 24.

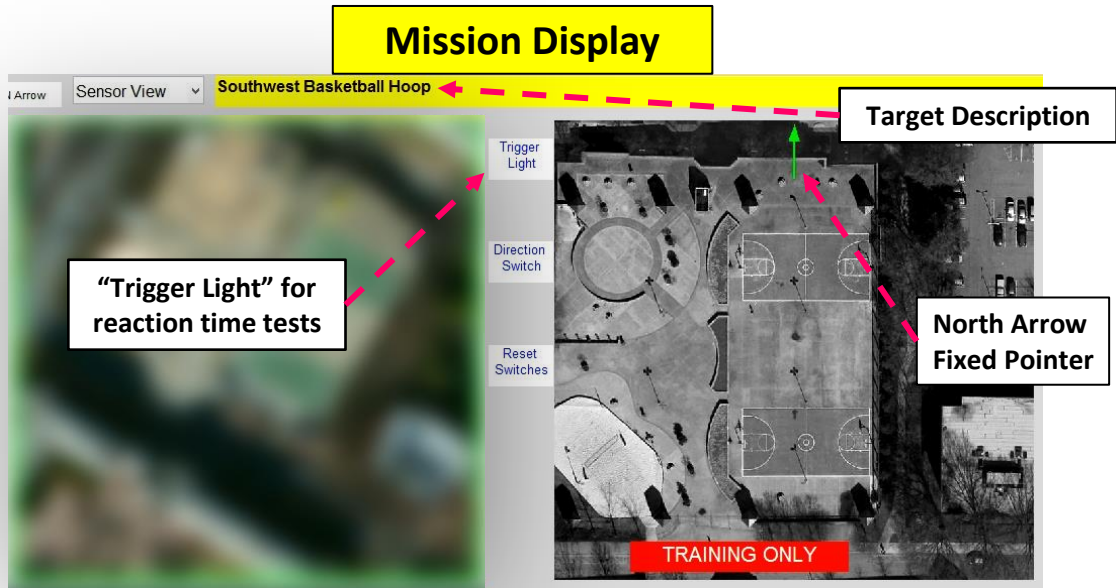


Figure 24: The Mission Display

This figure shows the mission display and accompanying textual target description. This display was always oriented north-up and always included the north arrow fixed pointer as a reminder. The "trigger light" is also shown here and was used for the visual reaction time test. [Image ©Google] (left, sensor display is blurred out because it is not the focus of this discussion)

3.2.4. Simulator Controls

Representative of current unmanned aircraft, the simulator provided an interface to control aircraft bank, which would in turn control aircraft heading and navigation. Altitude and airspeed were maintained without operator input. Simultaneous to the aircraft bank control, the operator also had to control sensor video pointing. Unlike an actual system, no camera zoom, focus, or other refinement was capable with the simulated video. So, the two continuous control tasks were the aircraft bank angle and the sensor left-right and up-down slew.

To allow for control of the simultaneous tracking tasks, two control sticks were used to interface with the simulator. In all cases, the left control stick was used for sensor pointing and sensor orientation tasks, while a right control stick was used for aircraft control. The simulator setup and display are shown in Figure 25.



Figure 25: Simulator Setup

In order to maintain control-display compatibility between different display configurations, the aircraft controls were changed to match the displays. When reference frame alignment was applied to the aircraft control display, the control action via the aircraft (right) control stick was changed. With the traditional aircraft display, bank angle was controlled via left or right tilt on the control stick. When the aircraft display was adjusted to the north-up representation, as shown in the right side of Figure 26, the bank control was switched to a twisting motion on the control stick. This change is depicted in Figure 27. The intention of this adjustment was to allow the subject to control the aircraft without using a mental point-of-view, or cognitive reference frame, in the aircraft perspective. No other control stick inputs were used for aircraft control.

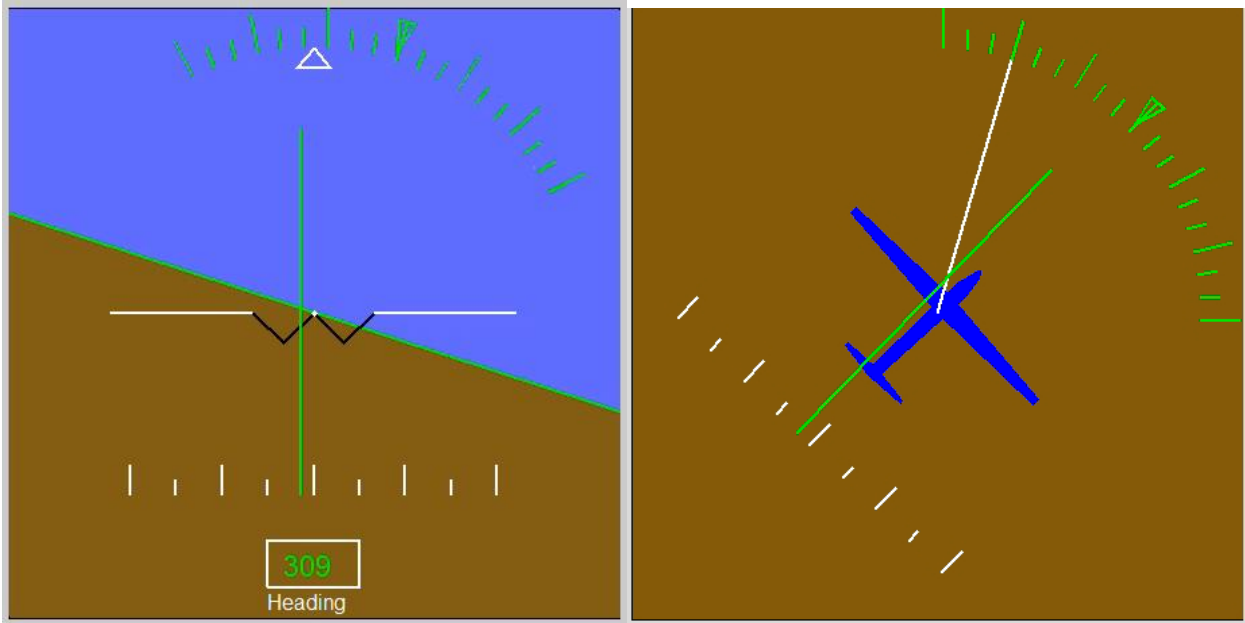


Figure 26: Aircraft Display Reference Frame Alignment

The left image is presented in the aircraft-view reference frame and bank was controlled via control stick tilt. The right image is presented north-up and was controlled via control stick twist. This difference in control maintained a sense of control-display compatibility because both motions were aligned with their respective bank angle indicators: the white triangle on the left, and the white line on the right.



Figure 27: Aircraft Control Stick Movement

Control stick tilt, on the left, was used to control bank on aircraft-view displays and control stick twist, on the right, was used to control bank angle on north-up aircraft displays.



Figure 28: Sensor Display Reference Frame Alignment

The left image is displayed in sensor-view, while the right is aligned to north-up. Since controls were relative to the displayed orientation, no difference was evident to the operator during reference frame alignment. [Image ©Google]

When the sensor display was rotated, and fixed in the north-up reference frame, the crosshair control remained the same as in the rotating sensor-view reference frame (Figure 28). The subject used the left control stick shown in Figure 29 to control the crosshair pointing location on the sensor video. The crosshair control was compensatory, so the symbol remained fixed in the center of the sensor video screen as shown in the left and right side of Figure 29. To move the crosshairs left, which actually moves the video image right, the subject would push the control stick to the left. This tilt control was mirrored to move the crosshairs right. The up/down control was set as if the bottom of the control stick were transposed onto the display, so tilting the control stick forward would move the crosshairs up in the video and tilting the control stick back would move them down in the video. This up/down control schema was a difficult decision because it did not match similar aircraft pointing tasks, where pulling back on the stick would move the aircraft nose up on a display. The decision was made because it provided a consistent mapping of the control stick movement which was explainable by transposing the base of the control stick on the crosshairs. The alternative technique would map the horizontal and vertical motions inconsistently.



Figure 29: Sensor Control Stick

This control stick was used for sensor pointing and the following switches. From left to right, reset switches are highlighted in green, trigger switch in blue, and orientation switch in red.

The subject was also required to use some of the hands on switches included with the left control stick. The black circle switch shown in the right portion of Figure 29 was used to provide an orientation answer for the orientation time measurement. Here, the subject would push the black circle forward to indicate north, right to indicate east, left to indicate west, and pull back to indicate south. This translation remained constant regardless of the current orientation of the sensor video image, but it was also consistent with the basic sensor control stick movements. The left control stick was also used to register the initial target acquisition location and to respond to reaction time stimuli. Both of these were input via the trigger switch shown in the middle of Figure 29. Finally, if the subject became disoriented and wished to return to the initial pointing location, any of the black switches on the left side of the control stick base would jump the video back to the original pointing location. During trials with a moving target this could also be used to find the moving vehicle during times of disorientation. Although this was used during training, it was never used during any of the experimental trials since it would have negated the requirement to track the target.

3.2.5. Simulator Hardware

These experiments were hosted on a laptop connected to a large flat screen display. The two control sticks were placed on the table in front of the display. The keyboard visible in Figure 25 was used for limited input between simulator trials, but was not used in direct control of the simulator. All subject control was available via one of the two control sticks. The simulator software was created in Matlab® release 2013b. The first experiment was run on a Hewlett Packard G17 laptop computer, with Windows 7 64-bit operating system, 2.2 GHz Intel® Core™ 2 Duo processor T6600, and 4 GB RAM. Experiments 3 and 4 were run on a Lenovo ThinkPad S1 Yoga, with Windows 10 64-bit operating system, 2.40 GHz Intel Core i7-4500U CPU, and 8 GB RAM.

A 55 or 65 inch display, one right-hand Logitech® Extreme 3D Pro control stick, and one right-hand Thrustmaster® T-Flight Stick X control stick were used for these experiments. Each of the simulator experiments were video recorded for data review.

3.2.6. Environment

All experiment trials were conducted in a confined room on the main MIT campus or at MIT Lincoln Laboratory. These rooms provided a secluded environment for efficient instruction and operations of the unmanned aircraft. Although an operationally representative environment may have included more outside interruptions or coordination with other participants, this setting allowed for a controlled environment for consistency from subject to subject and trial to trial.

3.2.7. Timeline

After signing the necessary consent form, each subject participated in a training session followed by a series of official trials, a post-experiment survey, and a video release form. Each trial lasted 3 minutes and 12 seconds with allowable breaks in between training or experimental trials. For each of the 80 participants, total experiment time was between 1.5 and 3 hours.

3.3. Simulator Required Tasks

Each experimental trial consisted of several required tasks that were completed sequentially or simultaneously. These tasks followed the scenario provided in 3.2.1. The subject was given an initial preview time to gain an understanding of the upcoming target, then the simulation began and the subject was required to control the sensor imagery to first find and then continuously track the defined target with the crosshair symbology. Simultaneously, the subject had to control the aircraft to maintain the desired flight path. For the remainder of the trial, the subject had to continue to keep the crosshairs on the target with his/her left hand and the aircraft on the circle with his/her right hand. During Experiment 3 and 4, at approximately halfway through each trial, the target vehicle would move through the imagery scene and the subject would have to continue tracking as the vehicle moved along the roadways. In all three simulator experiments, this dual task tracking continued while responding to secondary tasks. These secondary tasks included a visual reaction time test always followed by an orientation task. Finally, after each trial the subject was asked for a subjective workload rating using the Bedford workload scale. Each of these tasks is described in more detail throughout this section.

3.3.1. Target Preview

First, the subject previewed the target location with a satellite image and textual description using the north-up reference frame, while the other three control screens (sensor, navigation, and aircraft control) were not visible. After 15 seconds, the simulation began with the aircraft initially located along a designated orbit around the target and the sensor crosshairs pointed in the vicinity of,

but not on, the target. An example of the Target Preview display is shown in Figure 30 with the yellow highlighted textual description: “Northeast Basketball Hoop”.

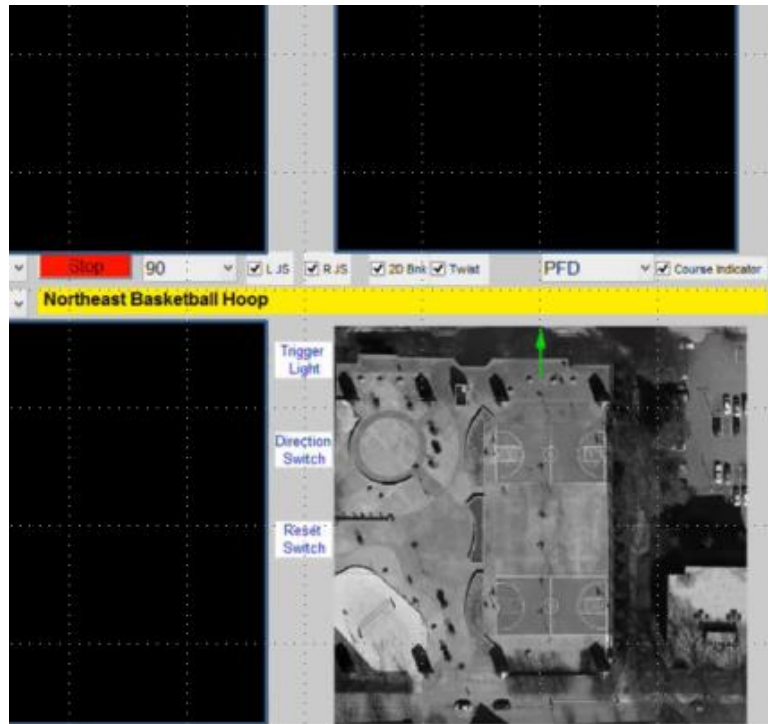


Figure 30: Target Preview Example

Only the bottom right display was visible for the first 15s of each trial. The target textual description is highlighted yellow. [Image ©Google]

3.3.2. Target Acquisition & Flight Path Tracking

As the simulation began, the subject was required to find the target from the satellite image and textual description provided during target preview and still visible in target acquisition. The subject would find the target in the sensor video display and maneuver the crosshairs to point at that target location. When tracking the target, the subject had to squeeze the left control stick trigger, while keeping the sensor crosshairs on the target. This simulated a weapon release on the target. The subject also had to control aircraft bank to keep the aircraft on the displayed orbit around the target. The instructions called for simultaneous execution of these two tasks.

3.3.3. Dual-Tracking

Once the target was identified, the subject continued to track the target with the sensor crosshairs and controlled the aircraft to continue following the displayed orbit around the target. For these experiments, the displayed orbit was always a simple circular orbit of constant distance from the target, as shown in Figure 31. For experiments 3 and 4, the target began moving approximately half-way through the trial. When the target was stationary the operator only had to correct for the oscillations in

geo-stabilization of the sensor, but with the moving target the operator had to continue correcting for the oscillations and move the crosshairs along with the target.

3.3.4. Reaction Time & Orientation Time

While continuing to track both the target and flight path, the subject was exposed to several reaction time and orientation time tasks. A reaction time was measured in response to a high frequency blinking light near the center of the simulator display. For experiments 3 and 4 the light was repositioned to the left side of the display to avoid placing it over the integrated display. This difference is discussed in section 3.1. This light alternated between red and yellow until the subject squeezed the left control stick trigger to respond to the stimulus. Reaction time was measured from the start of blinking to the trigger squeeze.

This was not directly representative of any specific unmanned aircraft task, but it was explained as an activity sensor at the target area. The requirement to immediately respond to this cue could parallel other potential urgent response requirements while flying unmanned aircraft, but its frequency throughout the simulator represented an invasive measurement.

After the subject responded with a trigger squeeze, a red asterisk symbol appeared on the sensor video. The symbol delayed momentarily and then moved in a cardinal direction off of the display. The subject was told to treat this symbol as a fleeing suspect and to indicate which direction the suspect had left the scene. This answer of north, south, east, or west was input via the control stick trim switch, as shown in Figure 32. If the cardinal directions in the sensor video were rotating, as they would when displayed in the traditional sensor-view reference frame, the subject's control input would not match the direction of symbol movement on the screen. For instance, if the aircraft were north of the target and the symbol moved to the right on the sensor video display, the movement would actually be to the west and the subject would indicate that by moving the trim switch to the left. Although this represented a control-display incompatibility, the intent was to simulate a communication event with the subjects notifying ground personnel of a fleeing subject and the direction he or she traveled.

The reaction time and orientation time stimuli continued at varying intervals (10-20s) until the end of the trial. This amounted to 9-11 orientation answers per trial, depending on how quickly the subject completed the initial target acquisition phase.

3.3.5. Observations and Workload Rating

After each trial the subject was asked to provide a workload rating and any comments regarding that specific trial. No specific questions were asked during this period, but the subject was asked for any

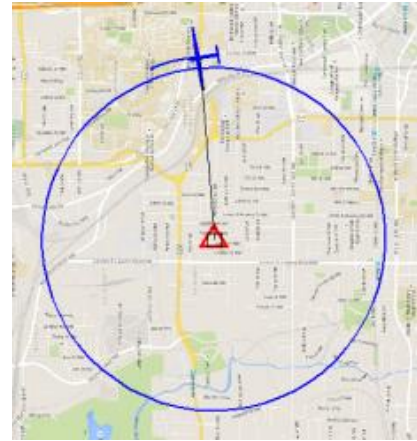


Figure 31: Displayed Orbit Example
The blue circle identified the desired flight path. [Map Data ©Google]

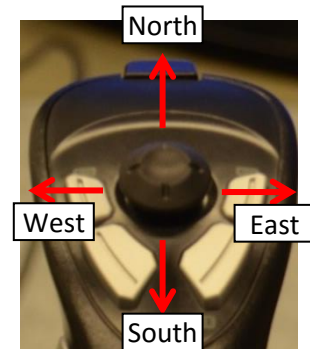


Figure 32: Trim Switch

comments so that he or she might have an opportunity to verbalize observations from that specific trial. Additionally, the subject was reminded of comments made during the trial and asked for any additional clarification.

At the conclusion of the subject's experimental period, he or she was asked a series of questions regarding their experience with the displays. At this time the subject described their ranking of the displays and described the techniques they were using to control the simulation. The subjects were also questioned about their awareness of the different experimental methods that were used during the simulation. This provided an understanding of their awareness of turbulence, winds, or the reuse of target areas during subsequent trials. This information provided a more complete understanding of the results. After the defined questions, the subjects were given the opportunity to express their assessment of the displays and simulation.

3.4. Simulator Display Features

With the exception of the moving target characteristic, all other independent variables tested with these experiments were based on display configuration. Four different display configurations were examined in each simulator experiment. Each of these is shown in Appendix A: Display Configurations; however, this section describes the display variables from each experiment and how they were adjusted via the display configuration. Each simulator experiment (1, 3, and 4) was designed to explore two display variables and their interaction.

3.4.1. Reference Frame Alignment

Each experiment examined the reference frame alignment effect in a similar manner. The sensor video alignment is evident in Figure 33 by comparing the bottom left display in both display configurations. In the misaligned example the imagery on the lower left appears upside down compared with the bottom right satellite imagery. On the aligned example (bottom half of Figure 33), this imagery appears right-side up, but the image is zoomed in and not centered with respect to the lower right satellite image. The white arrows in the bottom left image display the north direction in the given imagery. This also illustrates the difference between the misaligned and aligned displays. This imagery alignment effect was also tested in the experiment 2 cognitive study.

An examination of the upper-right display in Figure 33 reveals how reference frame alignment was applied to the aircraft display. Here, a novel display was developed to allow for aircraft bank control on a top-down image of the aircraft. The misaligned display, top half of Figure 33, shows a traditional aircraft display where bank is controlled by tilting the control stick (right hand) left or right to control the white triangle at the top of the display and adjust where this triangle lines up on the green bank scale. This display represents what an operator might observe looking out the front of a cockpit. On the aligned display, bottom half of Figure 33, the operator would control the white bank pointer protruding from the front of the aircraft symbol and change where it points on the same green bank scale. To prevent a requirement to maintain an aircraft reference frame to decide whether to tilt the stick left or right, here the bank control is actuated by twisting the stick counterclockwise or clockwise, which in turn

moves the tip of the white line counterclockwise or clockwise respectively. As applied here, this alignment was thought to reduce the required operator reference frames from 3 (misaligned) to 1 (aligned).

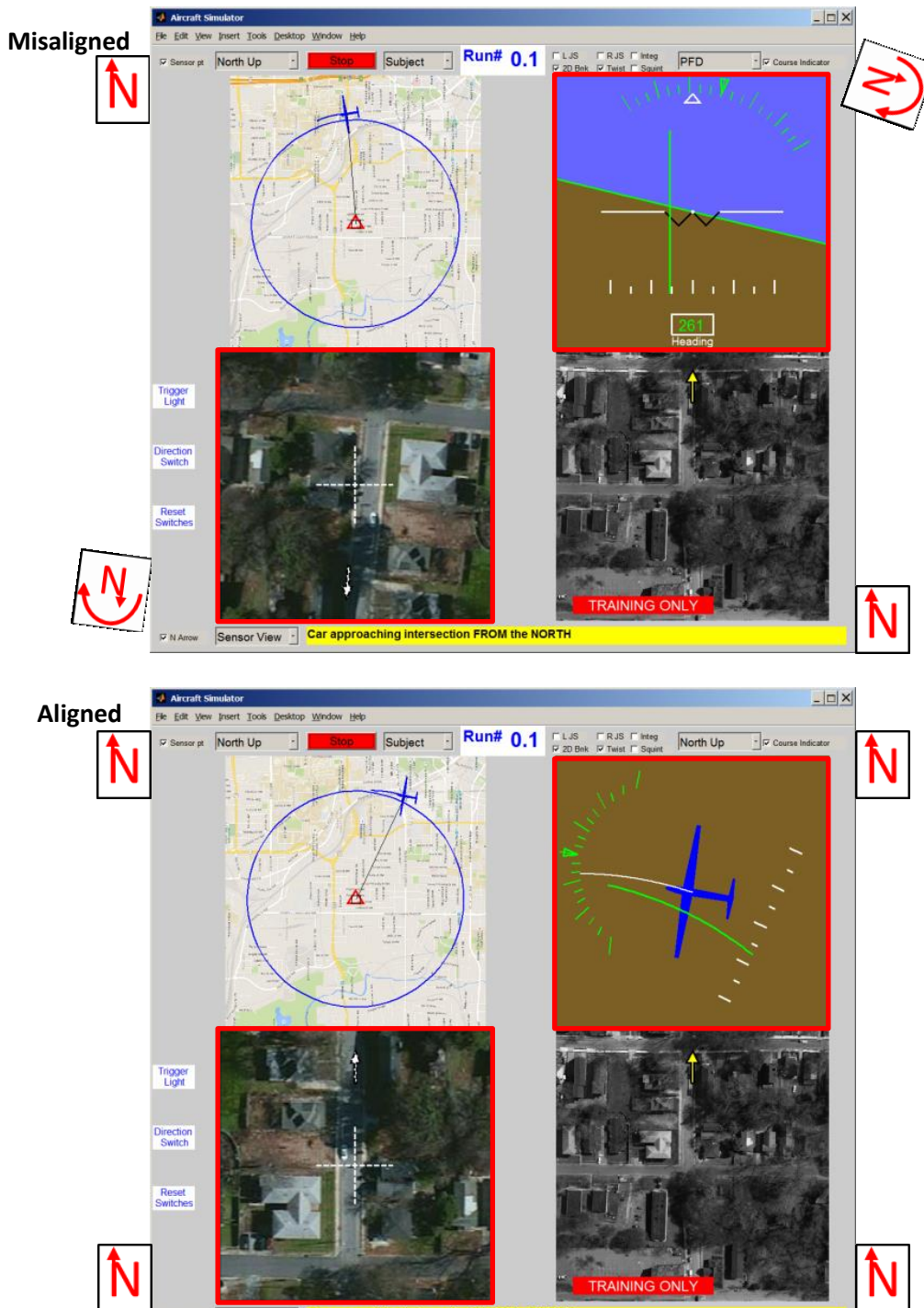


Figure 33: Reference Frame Alignment Example

N symbols were added to indicate the direction of north in each display. Red borders indicate displays that were aligned to north-up. The top display configuration includes two reference frames that were both aligned to north-up in the bottom display configuration. [Map Data and Image ©Google]

This display technique was examined across all three simulator experiments (1, 3, and 4). In each of these experiments a different secondary effect was tested. Experiment 1 was used to compare reference frame alignment with the current practice of exocentric orientation aids. This was further examined in the imagery rotation cognitive study conducted in experiment 2. In experiment 3 reference frame alignment was examined in combination with display integration to understand the potential interaction effects. Given that current systems integrate information with misaligned reference frames, this experiment sought to measure the potential benefits of first aligning reference frames and then integrating. Finally, experiment 4 examined reference frame alignment alongside display redundancy reduction. This approach again focused observations on the imagery rotation aspect of the unmanned aircraft operator's tasks. Rather than complete a reference frame alignment of the aircraft display, this display was removed to reduce display redundancy. This allowed the operator to focus only on the navigation display, and control aircraft bank using the flight path prediction aid protruding from the front of the aircraft symbol. This required the operator to maintain a cognitive representation of the aircraft-view reference frame in order to determine whether to turn the aircraft right (push stick to the right) or turn to the left (push stick to the left).

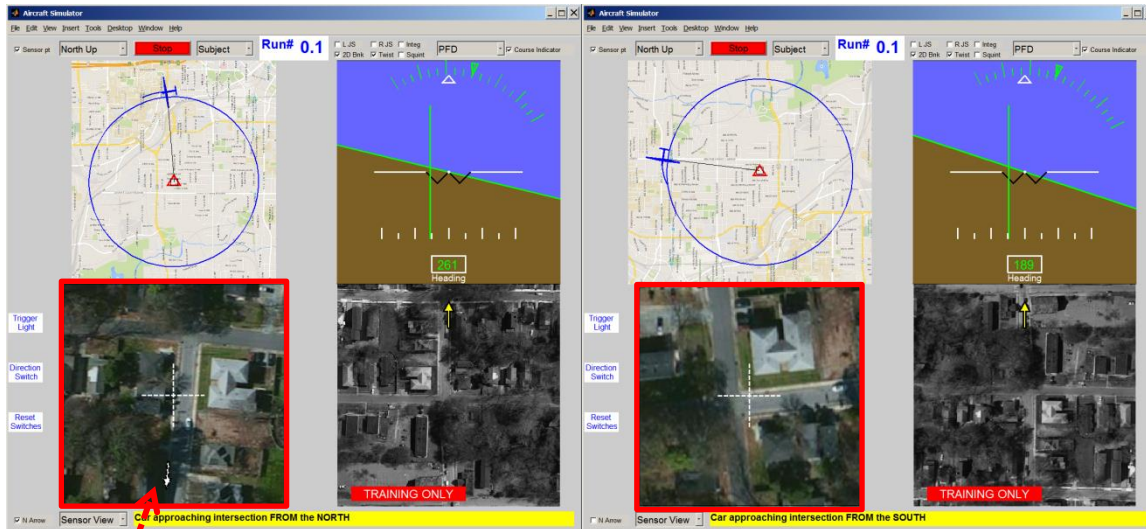
The following sections describe the secondary effects that were examined alongside the reference frame alignment effect.

3.4.2. Orientation Aids

The exocentric orientation aid was tested only on the sensor video display. As visible in the lower left display on the left side of Figure 34, the exocentric orientation aid in these experiments consisted of a single white arrow that always pointed in the north direction of the sensor video. The lower left display of the left half of shows this arrow pointing down on the image. In this case the aircraft is north of the target so the top of the video is actually the southern direction on the image. Consequently the north arrow is at the bottom of the image to indicate that north is in the direction towards the location of the video camera. The lower left display in the right half of Figure 34 demonstrates a display without the orientation aid. Here, if it were included, the north arrow would be to the left of the display since the aircraft position is actually to the west of the target. This is also evident by comparing the north-up satellite image (lower right display) with the sensor video. An operator could use the imagery features of the satellite image to establish personalized orientation aids. For instance, an odd-shaped building on one corner of an intersection could be used as a basis for orientation comparisons. This information could be used to mentally align these two reference frames without the use of an added orientation aid. Enlarged examples of sensor displays with and without this orientation aid are shown in Figure 35.

Display Configuration with Orientation Aid

Display Configuration without Orientation Aid



Orientation Aid

Figure 34: Orientation Aid Example

The left display configuration shows an orientation aid, white north arrow, on the bottom left display highlighted with the added red arrow. This is not present in the display on the right. [Map Data and Image ©Google]

Sensor Display with Orientation Aid

Sensor Display without Orientation Aid



Orientation Aid

Figure 35: Orientation Aid Example - Enlarged

These are enlarged examples of the sensor displays in Figure 34. The left display configuration shows an orientation aid, white north arrow, highlighted with the added red arrow. This is not present in the display on the right. [Image ©Google]

The exocentric orientation aid, as tested during these experiments, represents the common practice across systems in this industry. Although no evidence was found of controlled research documenting the effectiveness of this technique, it is used in nearly every known surveillance system to allow the operator to correlate observations with exocentric north-up navigation or map views. This

technique was examined to understand its effectiveness and also to compare to the reference frame alignment effect.

3.4.3. Display Integration

The display integration technique involved combing information, previously available on multiple displays, onto one display. Here, the aircraft, sensor, and navigation displays were combined into one larger display. This required a ratio scaling between the different information, and this integration required that the satellite image be occluded during the experimental trial. The target-preview time still provided the subject with time to observe the satellite image, but reference to that image after the start of a trial would require selecting a switch on the control stick to display the satellite image instead of the sensor video. This allowed for integration without losing access to any of the previously available information. The aircraft and sensor displays were overlaid on top of and in the middle of a larger navigation display. This covered a significant portion of the navigation display, which could also be shown through the activation of a control stick switch. This display integration, for the misaligned integration, is shown in the right side of Figure 36.

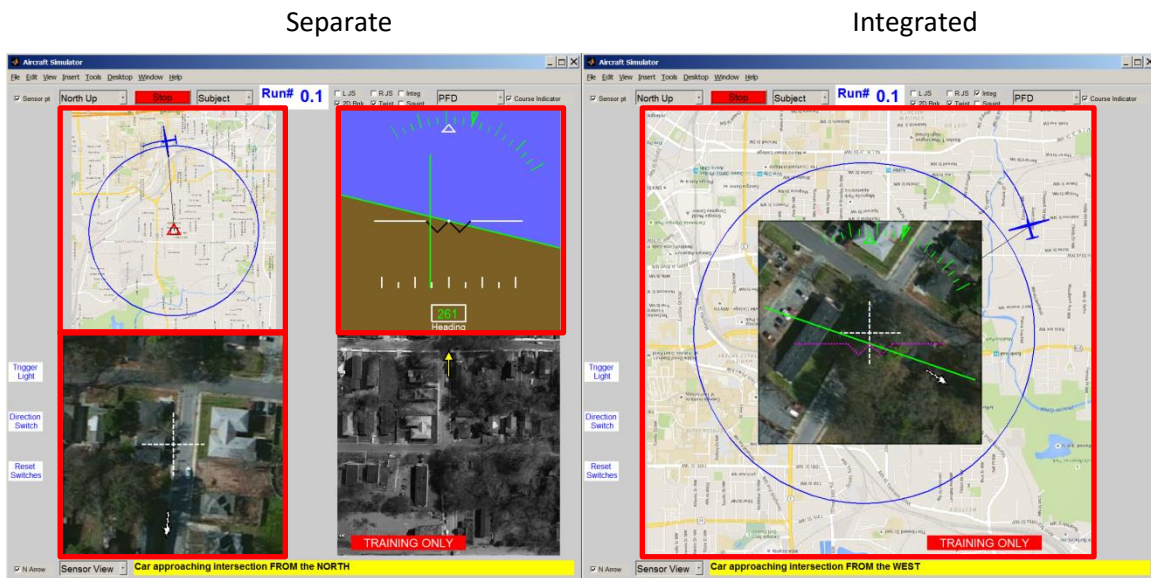


Figure 36: Display Integration Example

The three red displays on the left image are integrated into one larger display on the right image. [Map Data and Image ©Google]

3.4.4. Display Redundancy

Display redundancy was examined in experiment 4. After the inclusion of a flight path prediction aid on the navigation display (not available during experiment 1), it was possible to control aircraft bank angle by observing the movement of that flight path prediction tool. Although using the predictive aid as a bank indicator represents a degree of reference frame alignment, the subject would still have to consider the aircraft orientation to determine which way to control the bank. For instance, if the aircraft

were moving south on the navigation display and the subject wanted to maneuver the aircraft to the east or right on the display, the correct bank command would be to push the stick to the left. This orientation requirement remained regardless of the inclusion of the aircraft display, so this was considered as a separate display characteristic than reference frame alignment.

As shown in Figure 37, this modification included the simple removal of the aircraft display. This figure shows the misaligned example, but a case was also examined with the aligned displays. When active, this display technique decreased the resolution of the displayed error. The subject had to rely completely on the displacement between the aircraft and circular flight path on the navigation display. With the aircraft display visible, the subject could observe the same magnitude of error by examining the displacement between the vertical green line and the white dot in the center of the aircraft display. Additionally, without the aircraft display, there was no direct indication of bank angle. The subject had to rely on the perceived curvature of the predictive aid to determine the aircraft's current bank angle. With the aircraft display the bank angle was indicated by the white triangle and green bank scale across the top of the display.

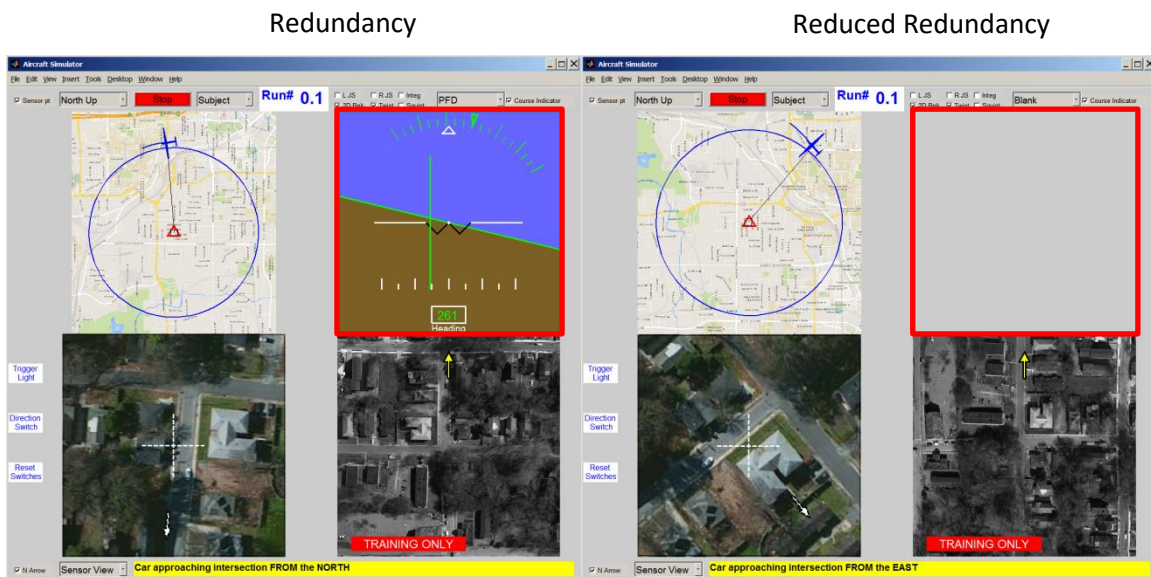


Figure 37: Display Redundancy Reduction Example
The red outline is highlighting the removal of the aircraft display which was present on the left display configuration, but not on the right configuration. [Map Data and Image ©Google]

3.4.5. Target Movement

Target movement was added to the simulator to increase realism and to address observations from experiment 1. Stationary targets allow the subject to observe salient features in the sensor video or satellite images and use them as improvised orientation aids. With a moving target, the sensor video scene continuously changes throughout a trial, so this should make it more challenging to orient oneself using imagery features. Following this reasoning, the inclusion of moving targets should increase the performance benefit of reference frame alignment and other orientation aids, since it would degrade performance of other orientation techniques.

Moving targets were included on every trial in experiments 3 and 4; however, each scenario began with a static target that initiated movement approximately half way through the trial. Once the target began moving, it maintained a constant speed throughout the remainder of the trial. This allowed moving target and stationary target analysis during each experimental trial. The left side of Figure 38 shows the static target during the initial phase of an experiment after the subject has located the target, and the right side of Figure 38 shows what the target would look like during the movement phase.

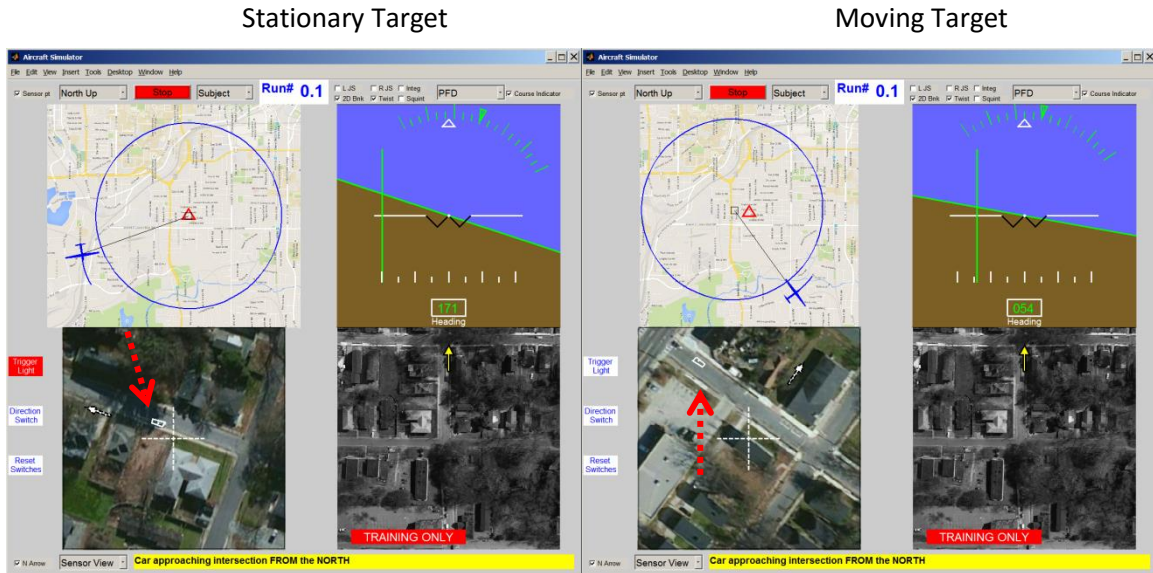


Figure 38: Moving Target Example

The red arrows indicate the location of the target vehicle (the white rectangle included in experiments 3 and 4). In the left image the vehicle is still at its starting location, while the right image vehicle is driving away from the starting location. The operator continued to track this white rectangular symbol while it moved along streets and turned at intersections. [Map Data and Image ©Google]

3.1. Simulator Changes between Experiments

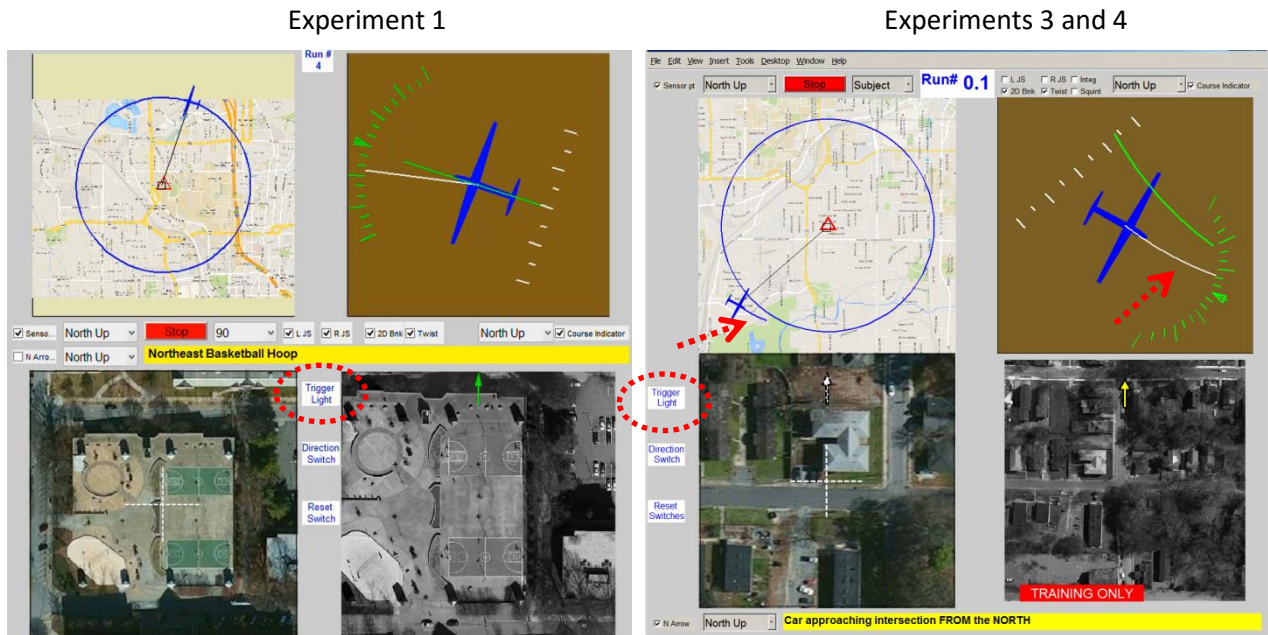


Figure 39: Simulator Differences between Experiments

The predictive aid symbol is shown on the navigation and aircraft displays during experiments 3 and 4. The “trigger light” (stimulus for the reaction time test) was moved to allow for integrated displays during experiments 3 and 4. The predictive aid and different trigger light locations are highlighted with red dashed symbols in this figure. [Map Data and Image ©Google]

Experiments 3 and 4 used a different version of the aircraft simulator than that used in experiment 1. The dependent performance and workload measures did not change, but some changes were made to the simulator itself. As noted, moving targets, display integration, and display redundancy reduction were all included in the second version of the simulator. This allowed measurement of these treatment effects. In addition, the flight path predictor was not included during experiment 1. This was added to both the navigation and north-up aircraft displays as shown in Figure 39. These changes are important when considering results across all the simulator experiments, but changes were not made during individual experiments, so this is not a factor when considering those results.

3.2. Dependent Variables

A variety of performance and workload measurements were used to analyze the effectiveness of these display techniques. With the exception of post-experiment questionnaire measurements, each of these measured performance and workload with one of the scenario-developed tasks.

1. **Target Acquisition Time:** this is the time from the start of the simulation until the subject selected the target location via the control stick.
2. **Sensor Track Error:** this is the distance from the sensor crosshairs to the target location normalized by the diagonal distance across the sensor display and analyzed as a cumulative Root Mean Sum Squared Error.
3. **Flight Path Error:** this is the orthogonal distance from the orbit circle to the aircraft location normalized by the radius of the planned aircraft orbit and analyzed as a cumulative Root Mean Sum Squared Error.
4. **Orientation Time:** this is the time from the movement of the symbol on the sensor video, to the subject's direction answer via the control stick.
5. **Bedford Workload Rating:** this is a subjective workload rating provided by the subject at the conclusion of each trial.
6. **Reaction Time:** this was the response time from the blinking of a light on the display, to the subject's response via the control stick.
7. **Subjective Rankings:** this is a subjective ranking of the four displays, provided by the subject at the conclusion of his or her entire experimental period.

Each of these measurements is described further in the following sections.

3.2.1. Target Acquisition Time

Target acquisition time was measured starting from the end of the initial target-preview time of 15 seconds, and then stopped when the subject selected the target location with the left control stick trigger. This represents how long the subject took to find the target location and maneuver the crosshairs to that location, once the sensor video was visible to the subject. The subject was told to envision this target selection with the seriousness of employing a weapon on the target. In this scenario acquisition errors would be catastrophic; however, if subjects faced uncertainty, they had no opportunity to ask clarifying questions. This left some operators to make the decision with some doubt, but more often the errors were made hastily with the opinion that he or she was selecting the correct target. If the target location was chosen incorrectly, the subject was given a display indication of the correct target location. This allowed the subject to locate and track the correct target following an error in acquisition. The target acquisition time data that resulted from errors of target identification were not included in the target acquisition time data analysis because they were not good indicators of the time required to perform the necessary transformation and find the target location. Throughout the three simulator experiments target acquisition times ranged from 1.7 to 48.4 seconds.

3.2.2. Sensor Track Error

This performance measurement represents the distance from the displayed crosshairs to the target location. This was measured as the straight line distance across the sensor video display (Euclidian distance between target and crosshairs). This measurement was collected continuously throughout the simulation, starting with the initial target acquisition. If the target was incorrectly selected, then the tracking error collection began after the crosshairs were moved to the actual target location. This removed the initial error associated with an incorrect target acquisition. Two examples of sensor track error measurement are shown in Figure 40. The dashed red double arrows show the measurement of sensor track error. This measurement was intended as a performance measurement because tracking a target represents a realistic task associated with unmanned aircraft operations. In order to account for the changing zoom of in the sensor video, sensor track error was normalized to the sensor display diagonal. This removed the zoom effect from the sensor track error measurement.

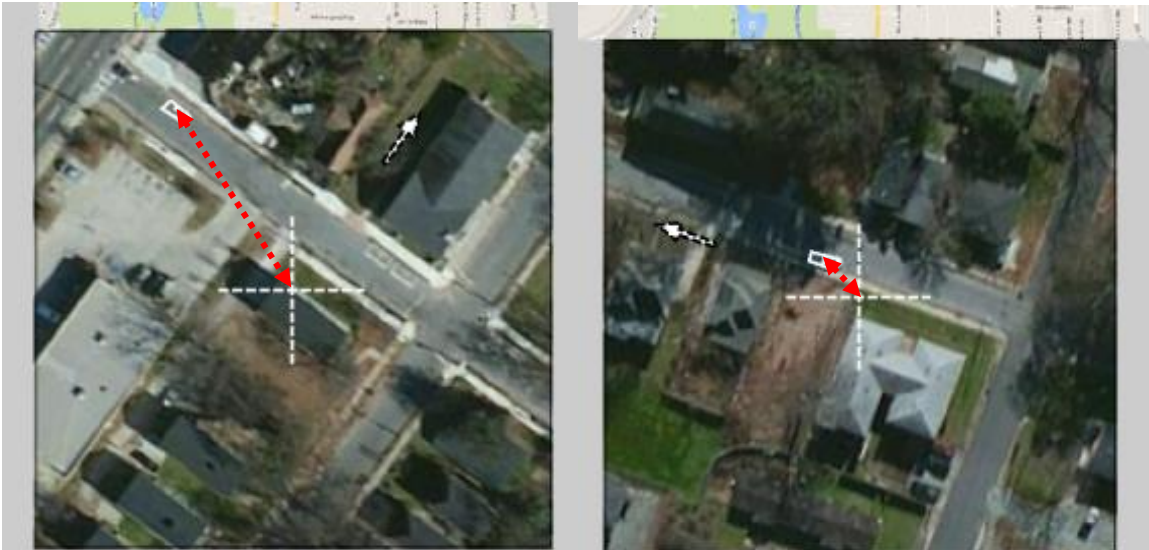


Figure 40: Sensor Track Error Example

This distance, shown here on two different sensor displays, was normalized with respect to the diagonal distance of the sensor display. [Image ©Google]

3.2.3. Flight Path Error

This performance measurement represents the orthogonal distance from the planned flight path to the aircraft location. A scaled version of this error was also visible on the aircraft display as the distance from the green course deviation indicator to the white dot in the center of the aircraft symbol. To prevent map zoom changes from influencing the measurement, this error was normalized with the radius of the flight path orbit.

This measurement was collected continuously throughout the simulation, starting with the initial target acquisition. Two examples of flight path error measurements are shown in the top of Figure 41 with the dashed red arrows. The aircraft display representation is shown in the bottom of Figure 41. This measurement was intended as a performance measurement because following a planned flight path represents a realistic task associated with unmanned aircraft operations.

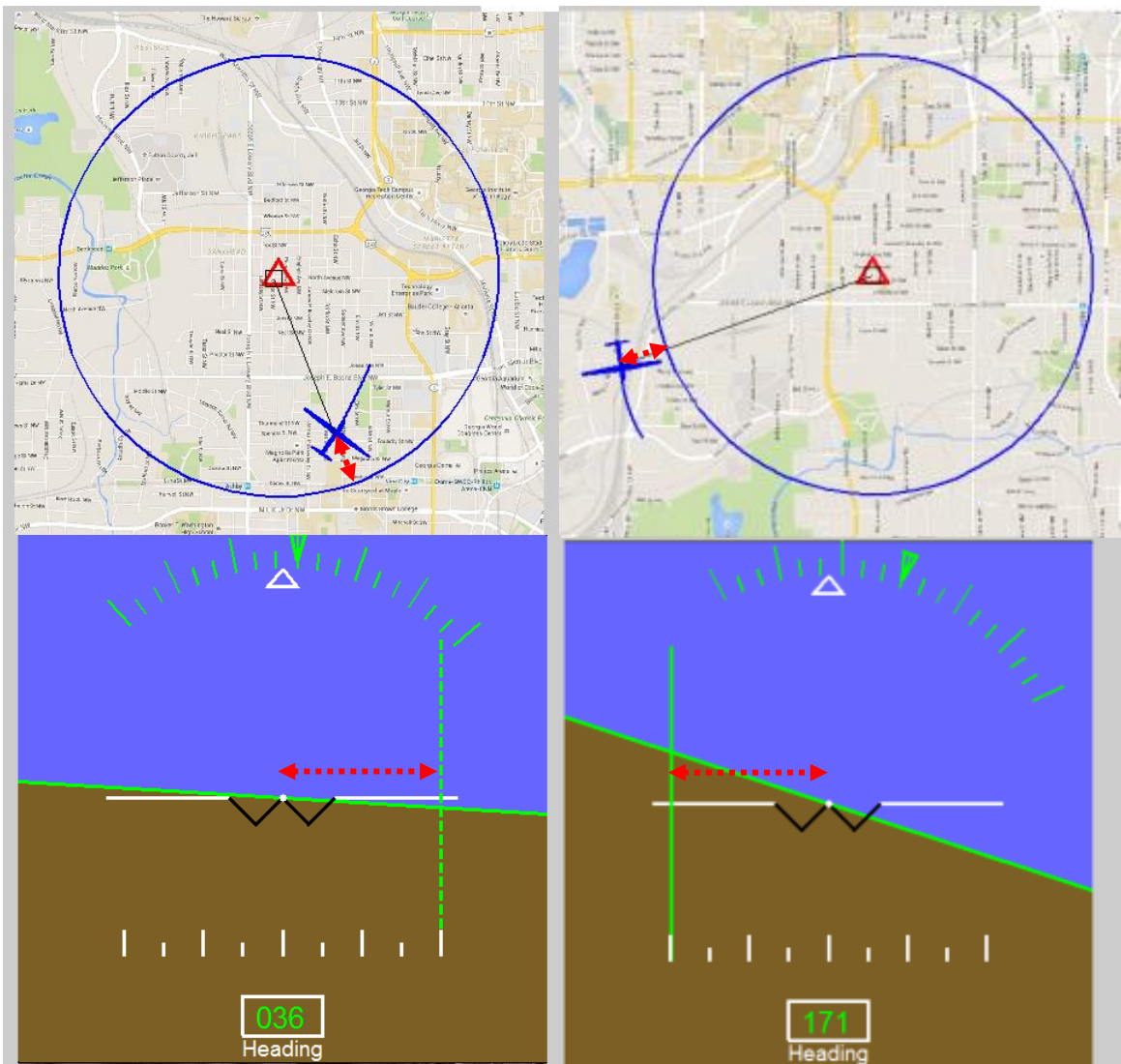


Figure 41: Flight Path Error Examples

This distance, indicated by the red dashed arrows, was normalized based on the radius of the planned flight path orbit - blue circle visible on the upper navigation display examples. [Map Data ©Google]

3.2.4. Orientation Time

Orientation time was a measurement of how quickly the subject could determine the direction of movement for a symbol in the sensor video, which represented a fleeing suspect. This measurement began when a symbol on the sensor video began moving across the image, and the time was stopped when the subject provided an answer to describe the direction of movement of the symbol. If the sensor video was presented in the sensor-view reference frame, this answer would require the subject to mentally align the sensor video to match the north-up reference frame. Each of these movements followed one of the four cardinal directions: north, south, east, or west. Answers were provided via the left control stick trim switch, as shown in Figure 32. Two examples of the moving symbol are shown in Figure 42. The red dashed arrows are added to this figure to show the direction of movement, west in the left image and east in the right image. Only the red asterisk symbol was visible during the simulation. The subjects were told to treat these symbols as fleeing suspects and inform the ground personnel that someone had fled north, south, east, or west as appropriate. With this scenario in mind, it was explained that a wrong answer would be catastrophic for ground personnel because they would pursue the suspect in the wrong direction, while a delayed correct answer would allow the suspect to get a larger head start in the pursuit. The subject was told to answer quickly but accurately. Similarly to target acquisition time, orientation times which were the result of incorrect answers were removed from the analysis.



Figure 42: Moving Orientation Task Symbol Example

Red asterisk was displayed as a moving symbol across the video. The red arrows are added here to highlight that symbol and show its direction of motion. [Image ©Google]

3.2.5. Bedford Workload Rating

Subjects were asked to evaluate their overall workload after each experimental trial using the Bedford Workload Scale (Figure 43). The subjects considered all of the required tasks during a trial. For experiments 3 and 4 which contained both stationary and moving target time during each trial, the subjects were asked to provide a separate rating for the stationary portion and the moving target portion. These values could be identical, but two numbers were recorded for each run. Since the

Bedford Workload Scale measures spare capacity for additional tasks, the subject was given a description of possible additional tasks (above and beyond the required tasks associated with the simulator). They were told to consider radio calls, additional displays of system information, chat messages, or other administrative functions as potential additional tasks. Given this information, subjects would begin with the Bedford Workload Scale in the bottom left of Figure 43 and progress through the decision tree until arriving at a rating on the right of the scale. Once there, they would read the rating and ensure that the description matched what they experienced during the trial. Subjects became familiar with the scale during the training portion of their experiment and could ask questions at that time. As presented in Figure 43 this scale produces an ordinal rather than ratio representation of workload.

Bedford Workload Scale

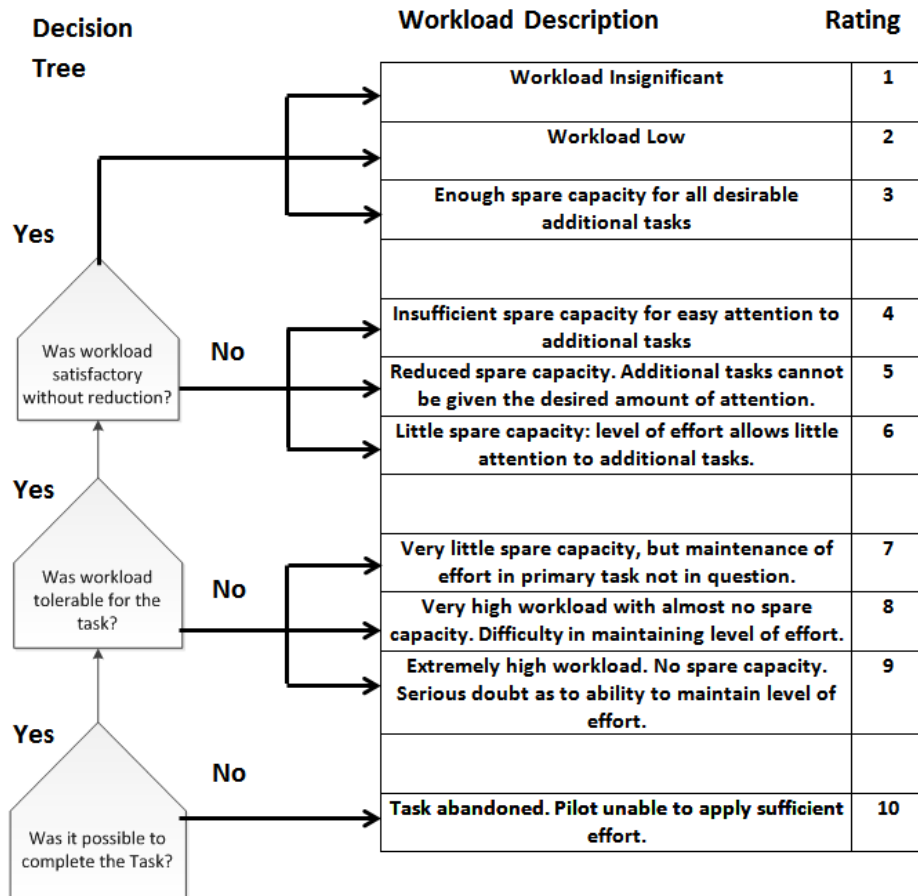


Figure 43: Bedford Workload Scale [130]

This scale is used as a flow chart starting in the bottom left and arriving at a numerical, ordinal, rating in the far right column.

3.2.6. Secondary Task Reaction Time

To measure workload throughout the experimental trials rather than relying on the subjective rating between trials, a secondary task was added to the simulator. Subjects responded to a blinking light in the middle (experiment 1) or on the side (experiments 3 and 4) of the simulator display (Figure 44). This light was labeled as the “trigger light” because the subject was to squeeze the trigger anytime this light was blinking. This light was relocated from the center of the display to the left of the display to allow for the integrated display option used during experiment 3. The red dashed ovals were added to Figure 44 to highlight the location of the light and were not visible during the simulation. When activated this light (white rectangle in the figure) alternated between yellow and red to provide a visual stimulus to the subject. The blinking continued indefinitely until the subject compressed the control stick trigger. The stimulus was replicated every 10-20 seconds throughout an experimental trial, and the blink frequency was approximately 10 Hertz.

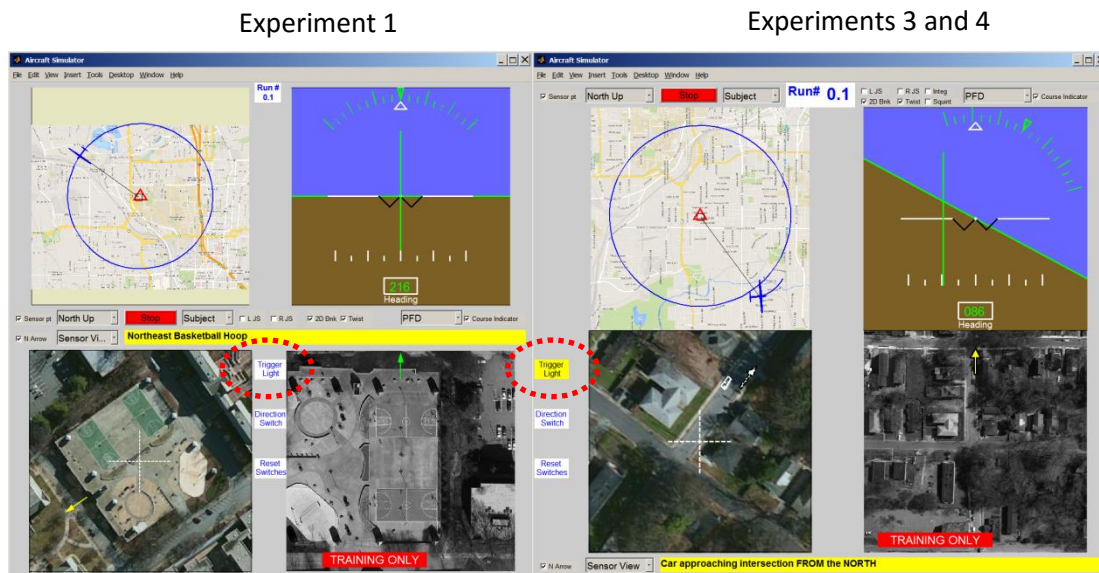


Figure 44: Trigger Light Example
Red ovals highlight the change in location for the “trigger light” which would initiate a reaction time test during simulator experiments. This location was adjusted in order to allow for the integrated display configurations in experiments 3 and 4. [Map Data and Image ©Google]

This reaction time was measured in response to a visual stimulus in order to remove potential effects of multiple sensory channels. As described by Wickens in multiple resources theory, providing an aural alarm could have allowed the subject to process information for this secondary task independently from the primary visual tasks [131]. This could have reduced the sensitivity of this workload measurement. By targeting the visual channel along with each of the other tasks, the secondary task workload measurement attempts to capture decreasing capability for additional tasks just as the Bedford Workload Scale attempts to measure this capacity subjectively. Although the two measurements do not focus on the same additional task, they are both attempting to measure additional capacity.

3.2.7. User Preferences

Subjects ranked the given display configurations from one to four, where 1 represented their favorite choice for the given tasks, and 4 represented their last choice. Additionally, for experiment 4, subjects rated each display configuration on a scale of 1 to 10 where 1 was their most favorable display configuration and 10 was their least favorable display configuration. This allowed subjects to rate multiple display options with an equal rating, but required them to delineate into separate rankings.

3.3. Population

Participants in these experiments included males and females ranging from 18 to 63 years old. They were mostly recent or current undergraduate or graduate students at MIT or Harvard. Flight experience among this group ranged from none to extensive. Two participants were USAF Test Pilots, but no participants had any unmanned aircraft flight experience. For a more detailed breakdown of subject characteristics and experience for each experiment refer to Appendix B: Subject Characteristics.

3.4. Controlling for Unwanted Effects

The experiment was designed to control for several confounding effects, and, when possible, these effects were also included in the regression analysis. This section outlines methods which were used to control for these confounding effects.

3.4.1. Training

A training plan was completed at the beginning of each subjects' experiment which was designed to plateau his or her performance before experimental trials began. All were able to complete the training requirements with satisfactory performance; however, time required for this portion of the experiment varied between 20 minutes to over one hour. Subjective observations during the experiment still showed performance improvements beyond the training phase of the experiment. This was also regularly reported from the subjects' perspectives in post experiment questionnaires. This continued influence of a learning effect was accounted for in the regression analyses by including the subject's trial number as an independent variable.

This training plan relied on hard performance benchmarks which were designed to ensure that the subject was completing the tasks with the desired urgency. The required benchmarks during the training phase were:

1. Less than 10 second Target Acquisition Time: time from initial simulator motion (after target-preview time) until the subject's trigger squeeze indicating the target location
2. Less than 2 second Orientation Time: time from initial symbol movement on the sensor video until the subject's cardinal direction response on the left control stick trim switch
3. Less than 1 second Reaction Time: response time from initiation of blinking light on the display panel until the subject's trigger squeeze reaction input

4. Flight path error: within approximately $2/3$ wingspan (full wingspan for moving target) of the displayed orbit
5. Sensor track error: within $1/2$ sensor crosshair (full crosshair for moving target) width of the current target

These benchmarks were evaluated individually using each of the four possible display configurations. While these benchmarks ensured that the subject was able to complete the required tasks, they did not measure a subject's training plateau. The subject and experiment facilitator both determined whether the subject was ready to proceed to the next display configuration during training and then on to the actual experiment. During the training period of the experiment performance feedback was visible after each trial. An example of this feedback is shown in Figure 45. Here, the plot areas have been reduced in order to enlarge the textual labels. The red and green outlines inform the subject and experimenter if the subject has passed the benchmark in that specific performance area. The green block to the right of the figure indicates that the sensor track error and flight path error benchmarks were met simultaneously.

Starting at the upper left and proceeding counterclockwise around Figure 45, each of these containers displays a different benchmark. The upper left container signifies that the subject did not meet the 10 second target acquisition benchmark since this time was almost 40 seconds during this training trial.

The middle left container assesses the subject's visual reaction time and here every attempt was greater than one second. This may have indicated that the subject would see the light and then perform a tracking correction before squeezing the trigger.

The lower left container shows the orientation time results for this training trial. Here the subject met the requirement because several of the results were below the 2 second benchmark. All of these represent correct answers because none of them are the red asterisk symbol, but the black circles indicate a correct answer that is provided after the 2 second benchmark.

The bottom right container shows the flight path error throughout the training trial, where positive values indicate a flight path outside the displayed circle and negative values indicate the aircraft was inside the displayed circle. The magenta line indicated an error of $2/3$ wingspan during experiment 1, which included only stationary targets, and slightly more than a full wingspan for experiments 3 and 4, which included moving targets. Here, the subject met the benchmark because he or she was able to control the aircraft between the magenta lines for greater than 20 seconds. Since the aircraft position was initialized on the displayed circle, indicated by the initial zero error in the bottom right plot, this 20 second performance period could not begin until after the vertical dashed magenta line.

Finally, the upper right container displays the sensor track error. The error drops near zero around 40 seconds which corresponds to the target acquisition time, and then oscillations persist throughout the training trial. Here, the horizontal magenta line represents $1/2$ crosshair width of error for experiment 1 with static targets and 1 full crosshair width of error for experiments 3 and 4 with moving targets.

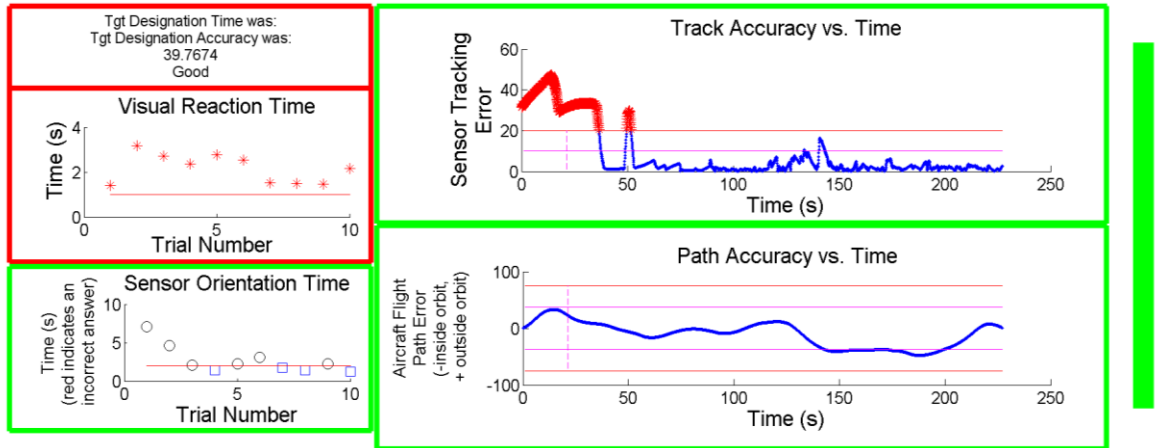


Figure 45: Training Performance Feedback Example

Green borders indicate a training benchmark has been passed for this training display configuration. Red outlines indicate that a benchmark was not passed, and the green bar to the right indicates that the flight path and sensor tracking performance benchmarks were met simultaneously.

As previously stated, each subject was able to meet these training benchmarks, but some subjects completed the training with only one or two trials per display configuration, while others required several trials with each display configuration. This was the largest variation in overall subject timeline.

3.4.2. Display Order

To prevent errors associated with learning a new display each trial during the experimentation, a subject completed all trials with one of the four configurations before moving onto another display configuration. This introduced a total of four display reconfigurations throughout each subject's experiment, counting the reconfiguration after the training period. This minimized reconfigurations to prevent subject errors, but this method increased the likelihood of a learning effect as subjects became more familiar with the simulator and its required tasks.

To mitigate this learning effect during the experiment, the display configuration order was counter-balanced across subjects using a repeated Latin Square method. Since each experiment involved four displays, there were four positions which a display configuration could be presented to the subject. Table 2 shows the display configuration order of the 16 subjects and four displays for experiment 4. This controlled how many times each display configuration was presented in the first, second, third, or fourth position during an experiment (left column), but also what display configuration preceded or followed another display configuration. This varied the potential learning effect which would be present with the display configurations in the later positions, and varied the potential learning effect of transitioning from one display configuration to another.

For example, over these 16 subjects display configuration G was seen in the same order position 4 times for each of the possible four positions. Display configuration G is in the first position for subjects 3, 7, 10, and 15. Additionally display configuration G follows each of the other display configurations 4 times. Display configuration G follows display configuration A for subjects 1, 5, 11, and 13.

Table 2: Counter-Balanced Display Order – Order and sequence were counter balanced to prevent learning effects. The four positions indicate in what order that subject experienced the four different display configurations (A, B, G, and H) during their experimental trials.

Experiment 4 Display Configuration Position																
Subject	1	2	3	4	5	6	7	8	9	10	11	12	13	14	15	16
Position 1	B	H	G	A	B	H	G	A	A	G	B	H	B	H	G	A
Position 2	H	G	A	B	H	G	A	B	B	A	H	G	H	G	A	B
Position 3	A	B	H	G	A	B	H	G	G	H	A	B	A	B	H	G
Position 4	G	A	B	D	G	A	B	H	H	B	G	A	G	A	B	H

3.4.3. Image Difficulty

Each experiment reused imagery throughout an experiment period. This meant that subjects viewed the same target scene more than once during their time with the simulator. This helped control the performance differences associated with images and provided an equal comparison between different display types, but it introduced a greater possibility for learning effects. For experiment 1, each image scene was repeated four times, but the target of interest was different each time the image was used in a scenario. Experiments 3 and 4 used the same moving vehicles four times during an experiment, but the entire world orientation was adjusted with each reuse of a target vehicle. This provided the same vehicle movements and scenery from one display configuration to the next, but the orientation of that movement was different each time it was used in a scenario. Subjects provided mixed feedback regarding imagery reuse. Some reported, in experiment 1, that it increased their ability to complete orientation tasks after they were already familiar with the scenery. No subject reported any benefit from the reuse of imagery in experiment 3 or 4. Since each subject saw each image area with every display, any learning effects would have applied to the later display configuration for any particular subject. As discussed, the order with which each subject saw the display configurations was altered to account for potential learning effects, but these imagery issues may have contributed to some of the observed learning effects observed during the simulations. When appropriate, learning effects were included in the regression model as a significant trial number coefficient.

3.4.4. Subject Variability

As observed during the training portion of each experiment, each subject had various degrees of experience or capability with these tasks. This variance was not eliminated with the relatively brief training time before each experiment; therefore, as is expected with human subject experiments, a subject effect would remain in the data analysis. To control for this subject variability, pairwise comparisons were analyzed within-subjects and regression analysis was conducted with a random subject effect term.

4. Experiment 1: Orientation Aids and Reference Frame Alignment

4.1. Experiment 1 Overview

This experiment sought to characterize the impact of multiple reference frames on the unmanned aircraft scenario. Possible display mitigation strategies of exocentric orientation aids and reference frame alignment were analyzed for their effectiveness in dealing with the sensor-view transformation and the aircraft-view transformation. The aircraft-view transformation required the operator to imagine sitting in the aircraft, visible on the north-up map, and then determine the desired direction of bank control to maneuver the aircraft toward the desired flight path. The sensor-view transformation required the operator to observe motion on the sensor display and determine the cardinal direction of that movement with respect to the north-up reference frame. This simulator experiment was conducted from November 2014 to February 2015 and involved 36 human subjects.

4.1.1. Experiment 1 Scenario and Tasks

This first human subjects experiment was conducted in the unmanned aircraft simulator. The scenario required the subject to control an aircraft with an onboard video sensor. As previously described in 3.2.1, the scenario started with a 15 second target-preview time where the subject had the opportunity to read the target description and observe the target area satellite image. One (out of four) of the target areas included a graphical depiction of the target over top of the satellite image, while the remaining three areas included only textual descriptions to accompany the target. An example of each of these cases, is shown in is shown in Figure 46. Black and white, rather than color, satellite images provided a sensor of realism and removed potential color cues present in both the satellite image and real-time imagery. Obvious color similarities between images would have added an alternative, and difficult to control, technique for comparing the images. The left image in Figure 46 provides an example of a cued target, where the subject could match the satellite image to the available sensor video, while the left image relied on the subject to use the textual description to find the target. All textual descriptions, which did not include a visual cue, relied on cardinal direction information. This was realistic because missions are typically described in relation to the standardized cardinal directions. Furthermore, it prepared the subjects for future tasks which would be communicated to ground personnel in the north-up reference frame.

“Indicated Ventilation Shaft”



“Building on Southeast
Corner of Intersection”



Figure 46: Example Target Images from Experiment 1

Visual cues (left image), or textual descriptions (right image) described the specific target location in each satellite image. [Image ©Google]

After the initial target-preview time, the aircraft simulation began. The aircraft location was initialized along the desired circular flight path surrounding the target. The aircraft was initialized at zero bank angle so subjects were required to add left bank to maintain the aircraft on the circle. All orbits were flown to the left, to avoid any directional confusion from trial to trial. Simultaneously, they were required to control the sensor video crosshairs to find and click on the target location. This click was accomplished with the trigger on the left control stick, as shown in Figure 29. After this initial selection, the subject received graphical feedback in the form of a box around the target. If the subject selected the correct target, the box was green, otherwise the box was red and positioned on the correct target. This allowed the subject to correct the mistake and then find and track the correct target. The target acquisition time was not included with an error in target identification, but this process preserved the collection of tracking data even after such errors. The tracking data were not collected until the subject first moved the crosshairs to the correct target.

After initial selection, the subject maintained the sensor display crosshairs on the target, and the aircraft on the flight path. Their tracking performance was recorded in both of these tasks. Throughout the remainder of each trial, at 10-20 seconds intervals, subjects responded to a reaction time light which was said to inform them of activity in the target area. They responded to this blinking light with the same trigger that was used to identify the target. After each reaction time test, subjects knew to observe the sensor video for movement near the target area. A red asterisk symbol, representing a person, departed the target area in a primary cardinal direction of north, south, east, or west. The subjects had to tell ground personnel which direction the suspect fled. They provided this input to ground personnel via the left control stick trim button, as shown in Figure 32. This represented a basic orientation task where the subject had to mentally align the sensor-view reference frame to north-up in order to provide an answer for the direction of travel. This provided the most accurate measurement of the orientation time cost associated with different reference frames, and it was representative of actual mission requirements during unmanned aircraft surveillance.

The subject continued with this scenario, and accompanying tasks, for 3 minutes and 12 seconds in order to allow an entire orbit around the target area. At the end of this time, the simulator froze and the subject was asked to provide an assessment of their mental workload during that particular trial. The Bedford Workload Scale, Figure 43, was used for this assessment.

4.1.2. Experiment 1 Timeline

During experiment 1, after initially completing the consent form, each subject underwent a training period with each of the possible display configurations. After reaching the required training performance, as described in section 3.4.1, each subject continued on to complete 13 experimental trials. The entire process, for a single subject, lasted 1.5 to 2.5 hours.

4.2. Experiment 1 Hypotheses

The objective of experiment 1 was to characterize the impact of different reference frames on unmanned aircraft operations, and evaluate the possible mitigation techniques of reference frame alignment and orientation aids. This produced two overall experiment 1 hypotheses.

Hypothesis 1: Reference frame alignment reduces the orientation time required to interpret a display, and consequently increases performance across tasks that require coordination between information usually provided in multiple reference frames.

Hypothesis 2: Orientation aids reduce the orientation time required to interpret a display, and consequently increase performance across tasks that require coordination between information usually provided in multiple reference frames.

Each of these hypotheses was investigated by modifying the display configurations that each subject used to control the simulator. These display configurations acted as the independent variables during this experiment and are discussed in the next section.

4.3. Experiment 1 Display Configurations (Independent Variables)

As previously discussed, each of the three simulator experiments (1, 3, and 4) examined a different display characteristic in combination with reference frame alignment. The following table describes how the experiment 1 displays were adjusted to investigate the reference frame alignment and orientation aid effects. The four display configurations used in experiment 1 are shown in the following figures. For enlarged versions of these images see Appendix A: Display Configurations.

In experiment 1, display configuration A (Figure 47) presented the traditional display representation. Here, each display maintained its original reference frame, which required the subject to transform information for the aircraft control and sensor interpretation tasks. The aircraft

transformation effect was only measured using flight path tracking performance, but the sensor transformation effect was directly measured via an orientation task within the sensor display. Display configuration B (Figure 48) added reference frame alignment to the sensor display only. This image was rotated to north-up, but the operator could still control the camera pointing in the same manner as the other display configurations. The aircraft display remained in the aircraft-view reference frame so the aircraft transformation was still required. Performance differences between display configuration A (Traditional) and B (Sensor Aligned) were attributed directly to the orientation requirement associated with the sensor-view reference frame. This offered one measurement of the reference frame alignment effect. In this case, any measurable effect represented an effect of reference frame alignment which was greater than the orientation aid effect because the orientation aid is present in both of these displays. A lack of measurable effect here would indicate that reference frame alignment offered no improvement over the orientation aid technique.

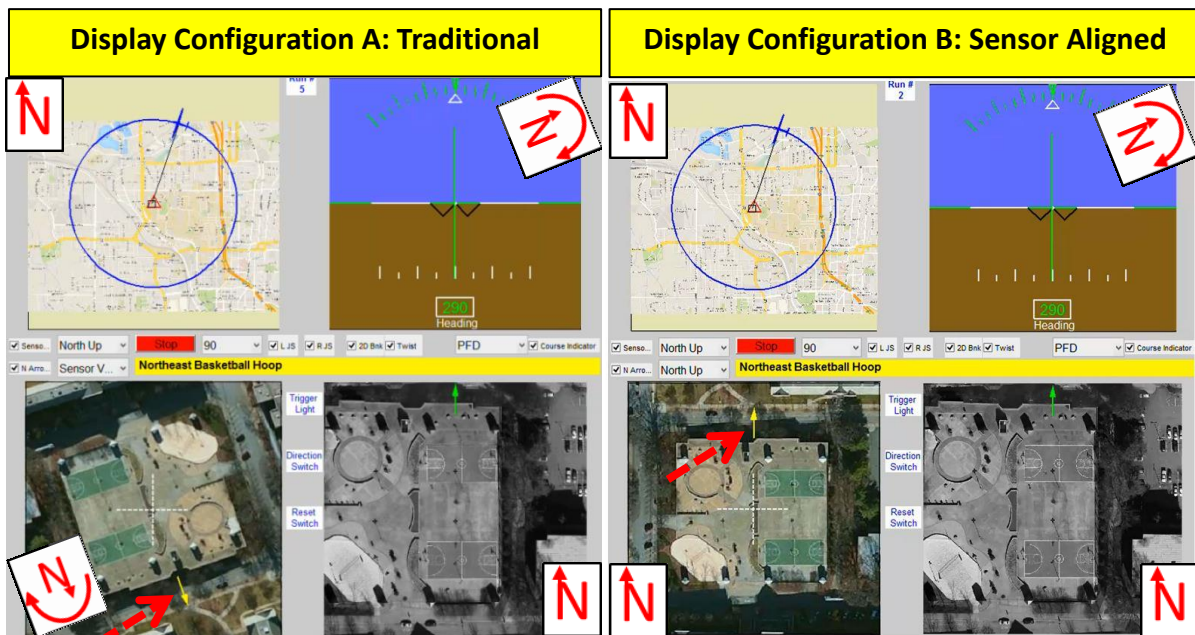


Figure 47: DISPLAY CONFIGURATION A: Traditional
N symbols indicate fixed or rotating north direction.

The red arrow highlights the orientation aid.

[Map Data and Image ©Google]

Figure 48: DISPLAY CONFIGURATION B: Sensor Aligned

N symbols indicate fixed or rotating north direction.

The red arrow highlights the orientation aid.

[Map Data and Image ©Google]

A second measure of reference frame alignment effectiveness, and the corresponding impact of multiple reference frames, was measured by comparing display configurations C and D, shown in Figure 49 and Figure 50 respectively. Display configuration C includes the traditional reference frames, but, unlike configuration A, it does not have an orientation aid. Display configuration D has reference frame alignment applied to both the sensor and aircraft displays which brings all four displays to the north-up orientation, but it also does not have an orientation aid. Comparing these two configurations provided the truest sense of the multiple reference frame effect because only the aircraft heading shown in the aircraft-view display (upper right of Figure 49) provided any assistance in transforming between reference frames. Here, without orientation aids, the benefit of reference frame alignment was

measured as directly as possible. This also represented a measurement of the combined reference frame transformation problem, as display configuration C required the subject to perform both transformations with virtually no assistance from the display design.

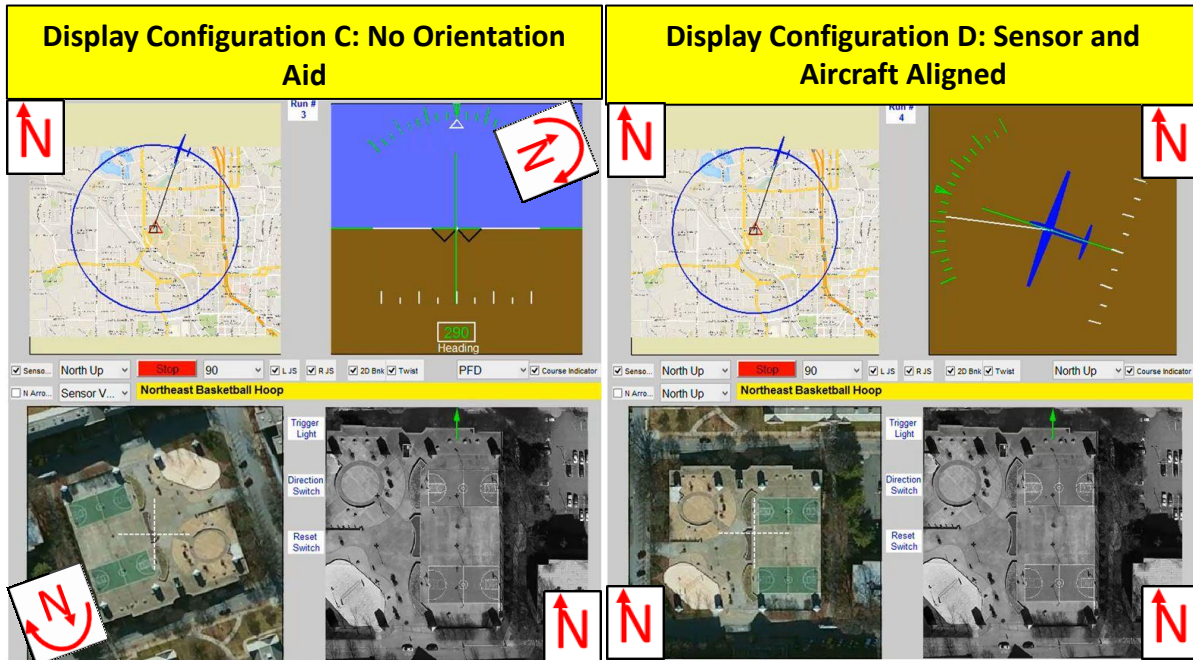


Figure 49: DISPLAY CONFIGURATION C: No Orientation Aid
N symbols indicate fixed or rotating north direction.
The north arrow orientation aid is not included.
[Map Data and Image ©Google]

Figure 50: DISPLAY CONFIGURATION D: Sensor and Aircraft Aligned
N symbols indicate fixed or rotating north direction.
The north arrow orientation aid is not included.
[Map Data and Image ©Google]

As these display configurations are understood in light of the rest of this research, it should be noted that experiment 1 did not include a predictive aid on the navigation or aircraft displays. The current aircraft position is shown, but no future projection is displayed. Additionally, the target description (yellow bar across the middle of each display configuration) and reaction time cue (top white box between the bottom two displays) are located centrally on these display configurations. The simulator was later reconfigured to move these switches to the periphery to allow for an integrated display configuration. As this experiment is compared with others in this research, it may be important to understand these differences in the simulator design.

Table 3: Experiment 1 Display Configurations
Gray indicates design variables that were explored during this experiment.

Display	A Traditional	B Sensor Aligned	C No Orientation Aid	D Sensor and Aircraft Aligned
Aircraft	Aircraft-View	Aircraft-View	Aircraft-View	North-up
Navigation	North-Up			
Sensor	Sensor-View	North-Up	Sensor-View	North-Up
Mission	North-Up			
# Reference Frames	3	2	3	1
Reference Frame Alignment	No	Yes	No	Yes
Orientation Aid	Yes	Yes	No	No

As shown in Table 3 and described earlier in this section, experiment 1 focused on reference frame alignment and exocentric orientation aids. These rows are highlighted to demonstrate the treatments across the four display configurations of experiment 1. Here, three levels of reference frame alignment and two levels of exocentric orientation aids were examined. Rows 2 through 5 of this table describe the reference frame of each of the individual displays: aircraft, navigation, sensor, and mission. These orientations are described as north-up, aircraft-view, or sensor-view.

Here, north-up indicates that the north direction is fixed at the top of the displayed information. A traditional map would usually be displayed in the north-up orientation.

The aircraft-view label indicates that the information was displayed with respect to the direction of aircraft travel. Here, the current aircraft heading would always be into the display as if the display represented the frontal view out of the aircraft cockpit.

Finally, the sensor-view description indicates that a display shows the representation which would be observed from the sensor location. Here, the top of the display always represents the heading from the aircraft to the sensor pointing location. For instance, if the aircraft were north of the target area, then south would be the direction at the top of a sensor-view image.

The orientations identified in rows 2-5 demonstrate how the number of reference frames was determined. Experiment 1 adjusted the number of reference frames from 1 to 3 because reference frame alignment was performed separately on the sensor display and the aircraft display. This provided three different levels of reference frame alignment treatment and only two levels of orientation aid treatment.

4.4. Experiment 1 Dependent Variables

The same performance and workload measurements were used during each simulator experiment. A short description of each is provided here. For a more in depth understanding of each measure, reference section 3.1. Each of these performance measurements evaluated the subject on one of the scenario-dependent tasks. The most direct measure of the transformation difficulty was the orientation time performance. This captured the difficulty of transforming from the sensor-view

reference frame to the north-up reference frame. However, each of these metrics could be used to demonstrate a difference between the display configurations.

The eight performance and workload measurements collected during experiment 1:

1. **Orientation Time:** this is the time from the movement of the symbol on the sensor video (representing a fleeing suspect), to the subject's direction answer via the left control stick.
2. **Target Acquisition Time:** this is the time from the start of the simulation until the subject selected the target location via the control stick.
3. **Sensor Track Error:** this is the distance from the sensor crosshairs to the target location normalized by the diagonal distance across the sensor display and analyzed as a cumulative Root Mean Sum Squared Error.
4. **Flight Path Error:** this is the orthogonal distance from the orbit circle to the aircraft location normalized by the radius of the planned aircraft orbit and was analyzed as a cumulative Root Mean Sum Squared Error.
5. **Bedford Workload Rating:** this is a subjective workload rating provided by the subject at the conclusion of each trial.
6. **Reaction Time:** this was the response time from the blinking of a light on the display, to the subject's response via the control stick.
7. **Subjective Rankings:** this is a subjective ranking of the four displays, provided by the subject at the conclusion of his or her entire experimental period.

4.5. Experiment 1 Results

4.5.1. Data Analysis Method

Each of the dependent variables measured during experiment 1 was analyzed independently of one another. When possible a linear regression analysis for the dependent variable as a function of reference frame alignment and orientation aids was conducted. This method accounted for several variables other than simply the display configuration. For each regression analysis, the following independent variables were considered.

Fixed Effects:

1. **Alignment (Xalign):** Categorical reference frame alignment setting of none, sensor display only, or sensor and aircraft displays aligned to north-up
2. **Orientation Aid (XorientAid) :** Categorical orientation aid setting describing whether or not the display included an orientation aid (yes or no)
3. **Initial Angle (XinitAngle):** Angle of rotation, in degrees, between the sensor display and north-up reference frame at the start of an experiment trial
4. **Subject Trial Number (XtrialNum):** Counted up from 1 to 13 as the experiment progressed

Random Effects:

5. **Image (Ximage):** Categorical image number 1 to 3

6. **Subject (Xsubject):** Categorical subject number from 1 to 36

As noted, the first four of these variables were considered as fixed effects, while the final two were considered as random effects. This required a mixed-effects linear regression analysis. The image and subject number were considered as random effects because no direct effect of any subject or image involved in this experiment was of interest to the objective. The experimental design minimized these random effects by controlling their presentation across the experimental trials, but it was still important to track the effects of these variables in order to build an appropriate model for the fixed effects. Each regression analysis considered the first four variables as potential predictor variables. With this approach a significant display design technique, such as reference frame alignment, would show up in multiple regression models to indicate its influence on the dependent variables measured during this experiment.

In addition to the regression analysis, pairwise comparisons were carried out between the specific displays. These were conducted for every dependent variable. For those suited to parametric analysis (1-4 and 6) a pairwise t-test comparison was conducted. Since the two subjective measures (5 and 7) collected during this experiment could not be analyzed with the regression method they were compared with a Kruskal-Wallis rank test to determine if a difference was measured between the different displays. The regression analysis offered a more complete interpretation of the results, so when possible those results are shown in this section and the pairwise comparisons are available in Appendix C: Experiment 1 Data Analysis. Since the subjective measures were not analyzed via a regression analysis, the Kruskal-Wallis rank test results are presented in this section. Each of the following sections discusses one of the dependent variables (1 through 8).

4.5.2. Experiment 1 Performance Measures

Each of the performance measurements and the secondary workload measurement (reaction time) were skewed distributions. This was an expected result since each of the measures represented a positive-only minimization for the subjects. For instance, while orientation time could never be negative, values as high as 9.2s (across all 3 experiments) were observed. Any attempt to directly fit these data using a regression analysis would be invalid. For this reason each of these variables were transformed using the Box-Cox transformation procedure. One example of the transformation's effect is shown in Figure 51. Here the top image shows the original skewed orientation time distribution for experiment 1, and the bottom image shows the distribution of the transformed orientation time. For details on any particular transformation used in experiment 1, see Appendix C: Experiment 1 Data Analysis. Since transformation was required for every parametric measure, it is important to understand the limitation on interpretation of results. Resulting effects

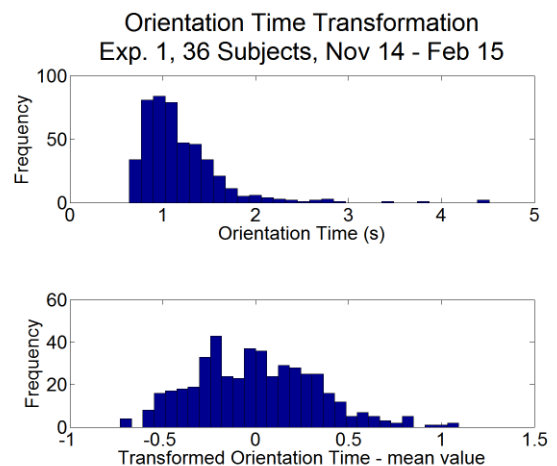


Figure 51: Experiment 1 Orientation Time Transformation Example

discovered in the regression analysis which are displayed in their original units should be interpreted as an effect on the median of the original distribution. For instance, if the reference frame alignment effect decreased orientation time by 0.5 seconds, this effect would increase on longer orientation times (those in the tail of the distribution), and decrease in magnitude on shorter orientation times (those close to zero). Although these transformations increase complexity at interpreting the results, they enable the detailed regression analyses which follow and provide a clear indication of whether or not a display technique impacted a particular dependent measure.

4.5.2.1. Experiment 1 Orientation Time Results

This dependent measure was the required time for a subject to determine a direction of movement in the sensor display. This was described as a suspect fleeing the target area and represented as a red asterisk over the sensor video (see Figure 42). The fitted regression model for orientation time, developed from experiment 1, is shown in Equation 1. This was the basic measurement of the multiple reference frame challenge. Estimates of these effects are shown in Table 4. Initial Angle and image had no significant effect on orientation time, so they do not show up in the regression model.

$$OT'_{e1} \approx \beta_0 + \beta_1 * XorientAid + \beta_2 * Xalign1 + \beta_3 * Xalign2 + \beta_4 * XtrialNum + \beta_{5i} * Xsubject_i + \beta_{6i} * XorientAid * Xsubject_i + \beta_{7i} * Xalign * Xsubject_i$$

$$i = 1:36 \text{ subjects}$$

Equation 1: Experiment 1 Orientation Time Regression Estimation

Table 4: Experiment 1 Orientation Time Predictor Variable Coefficients

Predictor Variable	Term	Transformed Regression Estimate	Lower 95% Conf. Interval	Upper 95% Conf. Interval	t-stat	p-value	Reverse Transformed Estimate (β')	Units
(Intercept)	β_0	0.45	0.35	0.55	8.91	<1E-10	0.32	S
XorientAid	β_1	-0.15	-0.20	-0.10	-6.03	3.35E-09	-0.16	S
Xalign1 Sensor Display Only	β_2	-0.26	-0.31	-0.21	-9.94	<1E-10	-0.30	S
Xalign2 Sensor and Aircraft Displays	β_3	-0.39	-0.46	-0.33	-11.97	<1E-10	-0.51	S
XtrialNum	β_4	-0.01	-0.02	-0.01	-7.00	<1E-10	-0.01	s/#

Initial Angle, image, and all interaction terms were tested, but they did not meet the 0.05 significance requirement for inclusion in this regression.

These results revealed several effects on orientation time. The orientation aid and reference frame alignment both demonstrated useful effects by reducing orientation time. As this experiment was designed, the Xalign (sensor display only) estimate represents a reference frame alignment impact beyond the orientation aid impact and this is confirmed with the regression analysis. The orientation aid impact was estimated as a reduction of 0.16 seconds on the median orientation time, and the alignment of sensor video decreased this by an additional 0.3 seconds. When compared to no orientation aid, and

including the aircraft display alignment, Xalign (sensor and aircraft displays) demonstrated at total of 0.5 second reduction in orientation time. These seem to agree with the fact that Xalign (sensor display only) included an orientation aid and sensor video alignment.

The learning effect recorded with the trial number term and the subject variations recorded with the subject number term were expected given the nature of human subject experiments. However, of additional interest was the interaction of orientation aid and alignment effects with the random subject effects. This indicates that these features did not benefit all subjects equally. Despite these interactions, this experiment captured the basic impact of multiple reference frames and demonstrated that reference frame alignment was more effective than orientation aids at addressing the difficulty of a basic orientation task.

Although the subject effect makes it difficult to display the overall orientation time results, the overall distributions provide insight into this effect. First, to understand the idea of a regression effect acting on the median of a distribution, reference the raw data shown in both Figure 52 and Figure 53. These charts show the shift in these skewed distributions when the design techniques are included. The effect is more noticeable with the alignment effect, but both reduced the skew on the distribution by eliminating much of the tail. This idea is not fully captured by the regression analysis because it only demonstrates the effect on the median of the distribution. For this reason, the benefit identified by the regression model could be interpreted as an underestimate of the potential impact of either reference frame alignment or orientation aids with respect to this basic orientation task.

Orientation Time vs. Alignment (Observed Data) Exp. 1, 36 Subjects, Nov 14 - Feb 15

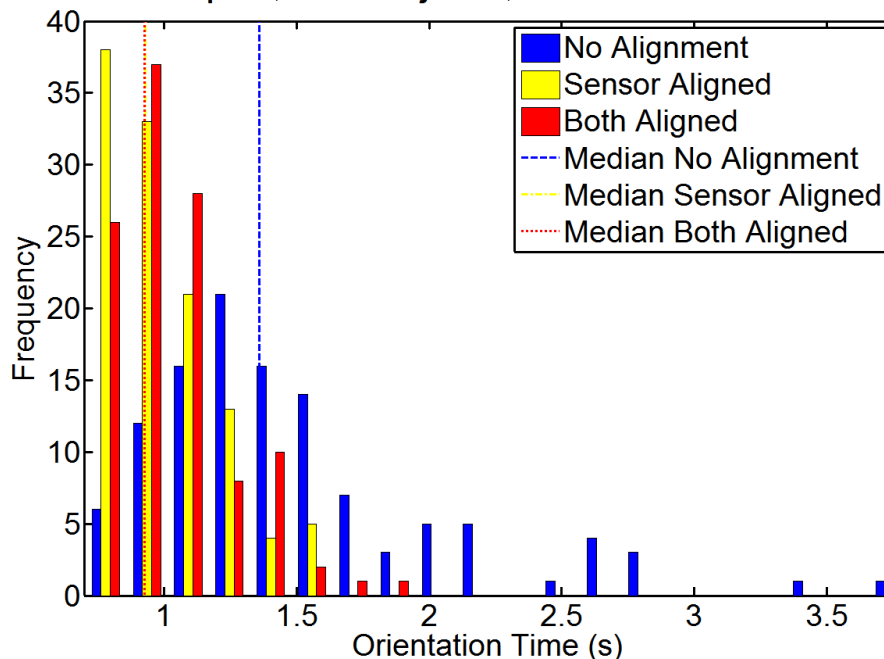


Figure 52: Orientation Time Alignment Effect

Blue distribution is observed data without alignment. Yellow distribution is alignment of the sensor video only, and red has alignment of sensor and aircraft displays.

Orientation Time vs. Orientation Aid (Observed Data)
Exp. 1, 36 Subjects, Nov 14 - Feb 15

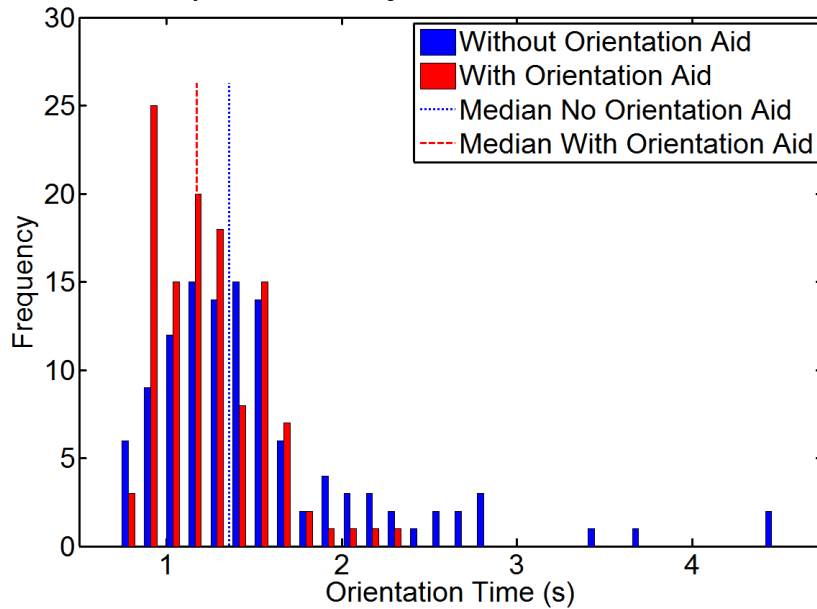


Figure 53: Orientation Time Orientation Aid Effect
Blue distribution is observed data without the orientation aid. Red distribution is observed data with the orientation aid and is shifted left of the blue data.

Another significant measure of the effectiveness of these two display techniques is their effect on error rate (percentage of orientation answers, for the entire experiment, which were wrong) of the orientation answer. Although the regression analysis did not include orientation times which resulted from incorrect answers, a qualitative observation of such data is revealing. The data shown in Figure 54 demonstrate this for both factors. There is a clear reduction in error rate (as a percentage of orientation answers) when the sensor display is aligned. As expected the aircraft display does not affect this error rate. Additionally, a smaller reduction is evident when the orientation aid is displayed. This increased accuracy should also be considered a benefit of these display techniques in addressing the multiple reference frame challenge.

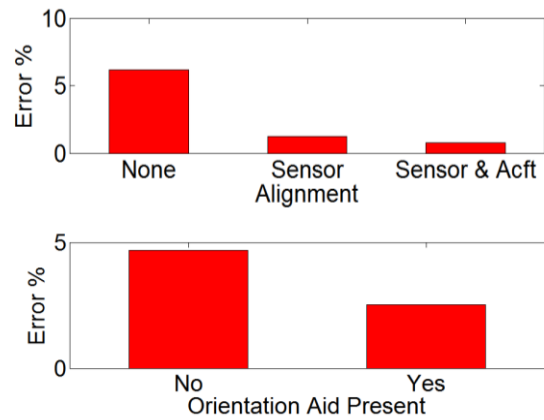


Figure 54: Orientation Errors vs. Orientation Aid and Alignment Settings

These orientation time results demonstrated a significant impact of the multiple reference frames on the basic orientation task, and they demonstrated a significant reduction of that effect with reference frame alignment, which supports the reference frame alignment hypothesis (#1) and the orientation aid, which supports the orientation aid hypothesis (#2).

4.5.2.2. Experiment 1 Target Acquisition Time Results

This target acquisition time was measured from the start of the simulation until the subject identified the target location. If the subject misidentified the target, that time was not included in this regression analysis. This process was described as a weapon release to encourage the subject to take the accuracy requirement seriously. The regression model for target acquisition time, developed from experiment 1, is shown in Equation 2. Estimates of these effects are shown in Table 5. While orientation time represented a basic measurement of the multiple reference frame challenge, target acquisition time measured a broader impact of that challenge. Here, more than a simple orientation task was required. Subjects had to follow descriptions of the target area or complete imagery rotations between the target satellite image and the observed sensor video in order to locate a target in the sensor video scenery. Since this task could require multiple transformations between the satellite image and the sensor video, any orientation time effect would be magnified in this target acquisition task. This was very representative of an actual unmanned aircraft surveillance task.

$$TAT'_{e1} \approx \beta_0 + \beta_1 * Xalign1 + \beta_2 * Xalign2 + \beta_3 * XinitAngle + \beta_4 * XtrialNum + \beta_5 * XinitAngle * XtrialNum + \beta_{6i} * Subject_i + \beta_{7m} * Ximage_m + \beta_{8m} * XinitAngle * Ximage_m$$

$$i = 1:36 \text{ subjects}, m = 1:3 \text{ images}$$

Equation 2: Experiment 1 Target Acquisition Time Regression Model

Table 5: Experiment 1 Target Acquisition Time Predictor Variable Coefficients

Predictor Variable	Term	Transformed Regression Estimate	Lower 95% Conf. Interval	Upper 95% Conf. Interval	t-stat	p-value	Reverse Transformed Estimate (β')	units
(Intercept)	β_0	10.255	9.563	10.947	29.15	<1E-10	3.753	s
Xalign1 Sensor Display Only	β_1	-0.333	-0.832	0.166	-1.31	0.190	-0.330	s
Xalign2 Sensor and Aircraft Display	β_2	-0.688	-1.183	-0.192	-2.73	6.68E-03	-0.714	s
XinitAngle	β_3	0.018	0.009	0.026	3.86	1.34E-04	0.017	s
XtrialNum	β_4	-0.080	-0.131	-0.028	-3.03	2.60E-03	-0.076	s/#
XinitAngle*XtrialNum	β_5	-8.95E-04	-0.002	-6.78E-05	-2.13	3.40E-02	-0.001	s/#
Orientation aid, and all other interaction terms were tested, but they did not meet the 0.05 significance requirement for inclusion in this regression.								

These results revealed a difference between the alignment treatments. While the orientation time readings found fairly equal impact of both alignments, the target acquisition time regression model only determined the second level of alignment to offer a significant impact. So just aligning the sensor display did not produce a significant effect on target acquisition time, but aligning both the sensor display and aircraft display decreased the target acquisition time. Further inspection of the model

reveals that the initial angle between sensor-view and the north-up reference frame is included in the model. This factor could have captured the effectiveness of aligning the sensor display because it represents the angular rotation involved with the reference frame alignment effect on sensor video. However, despite the inclusion of this initial angle, the align2 setting remained in the model because it also included the aircraft display rotation.

As a reminder, this aircraft display alignment is demonstrated in Figure 55. This effect represented a 0.4 second reduction on the median target acquisition time, independent of sensor display rotation or sensor-view rotation angle. This is interesting because most subjects had no familiarity with the north-up version of this display, and neither of these displays was directly involved with the target acquisition task. The alignment effect can be further understood by examining the initial angle impact. From Table 5 the 0.017 seconds/degree effect of initial angle could represent as much as 3.06 seconds of increased target acquisition time when the sensor display was rotated 180 degrees from the north-up reference frame. This multiplies the initial angle effect to reveal the maximum impact from this factor. Based on this combination of effects, the total alignment impact on the target acquisition time ranged from 0.7 to 4 seconds.

Unlike orientation time, the target acquisition time results show no measureable interaction effect with subject. This indicates that, here, alignment had a similar impact across all subjects who participated in this study. The usefulness of display alignment was felt equally across each subject in the target acquisition task. There were differences associated with subject, but they did not interact with other factors. The image, however, did have an effect on the alignment effectiveness through the observed angular effect. The significance of the angle of rotation was dependent on which image the subject was observing. Furthermore, a learning effect lessened the significance of the rotation angle as the experiment progressed. Although this lessens the significance of the overall alignment effect, the significance holds that alignment had a beneficial influence on target acquisition time.

The orientation aid did not show any measureable effect in this regression model, despite its benefits on the basic measure of orientation time. One theory for this lack of significance is that subjects reported the use of image characteristics in their mental rotation. Rather than relying on the orientation aid, they reported using features in the satellite image and then look for those corresponding features in the sensor video. This allowed them to locate the target without depending on the north arrow orientation aid. To investigate this phenomenon, this research included a secondary study, experiment 2, of the imagery rotation subtask and the effectiveness of orientation aids and reference frame alignment specifically applied to this singular task. Experiment 2 is discussed in section 5.

The overall target acquisition time results are displayed in Figure 56 and Figure 57 (larger versions are available in Appendix C: Experiment 1 Data Analysis). Figure 56 shows the similar shift

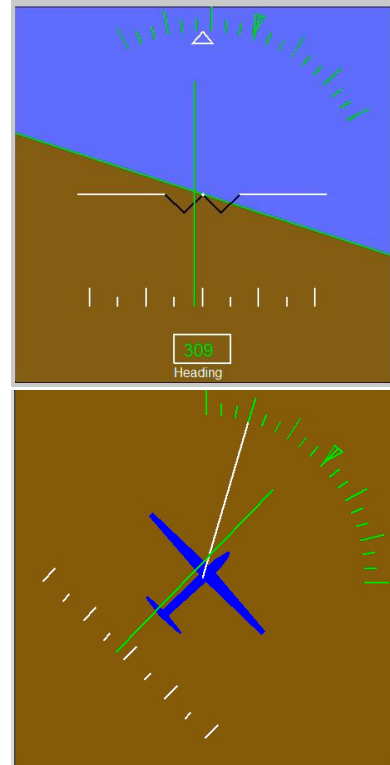


Figure 55: Aircraft Display Reference Frame Alignment
The top display is presented in the aircraft-view reference frame. The bottom display has been aligned to north-up.

associated with alignment levels 1 and 2; however, a more significant tail is still present with alignment level 1 and not with level 2. Most of this variation was captured with the angle of sensor-view rotation rather than the basic alignment category. Figure 57 shows the very similar distributions of target acquisition time with and without orientation aid. The similarity of these distributions matches the regression model because no orientation aid effect was included in the model.

Tgt Acquisition Time vs. Alignment (Observed Data)
Exp. 1, 36 Subjects, Nov 14 - Feb 15

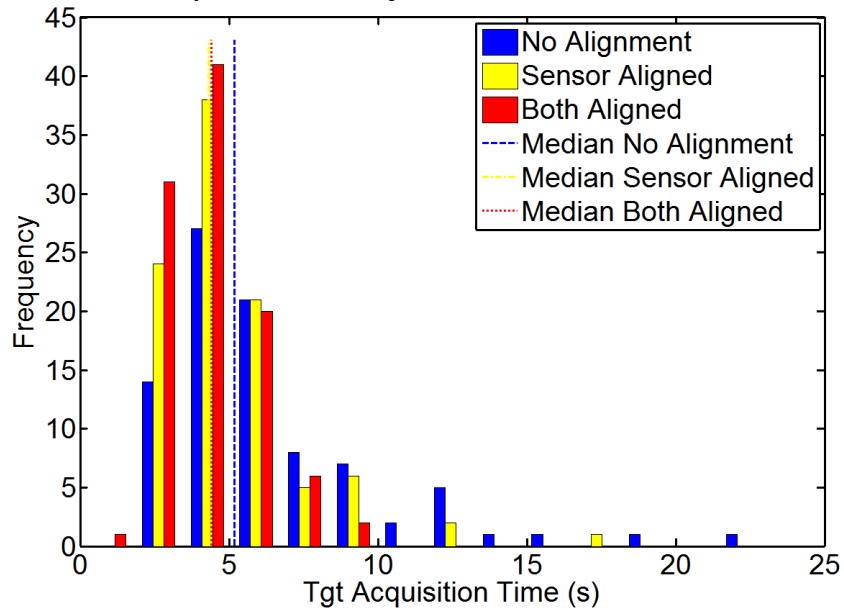


Figure 56: Target Acquisition Time Alignment Effect
Blue distribution is observed data without alignment. Yellow distribution is alignment of the sensor video only, and red has alignment of sensor and aircraft displays.

Tgt Acquisition Time vs. Orientation Aid (Observed Data)
 Exp. 1, 36 Subjects, Nov 14 - Feb 15

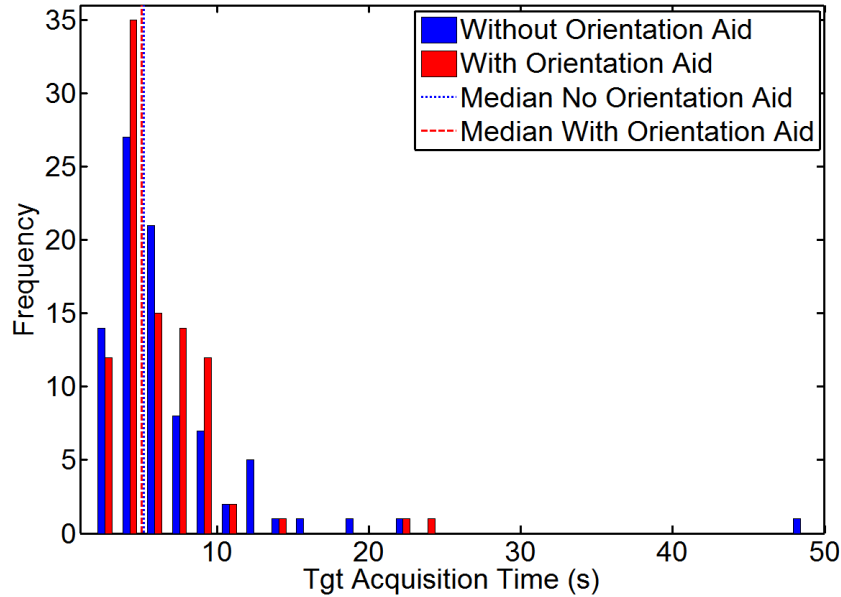


Figure 57: Target Acquisition Time Orientation Aid Effect
 Blue distribution is observed data without the orientation aid. Red distribution is observed data with the orientation aid.

Once again, another measure of the effectiveness of these two display techniques is their effect on error rate (percentage of target location answers, for the entire experiment, which were the wrong target) of the target acquisition task. Although the regression analysis did not include target acquisition times which resulted from errors in target selection, a qualitative observation of such data is revealing. The data shown in Figure 58 demonstrates this for both display techniques. There is a noticeable reduction in error rate when the sensor display is aligned. As expected, the aircraft display does not have as large an effect on this error rate. Unlike orientation time results, here no change is evident when the orientation aid is included. This increased accuracy associated with reference frame alignment should also be considered a benefit of this display technique in addressing the multiple reference frame challenge. However, the orientation aid showed no measurable effect on the target acquisition time or accuracy.

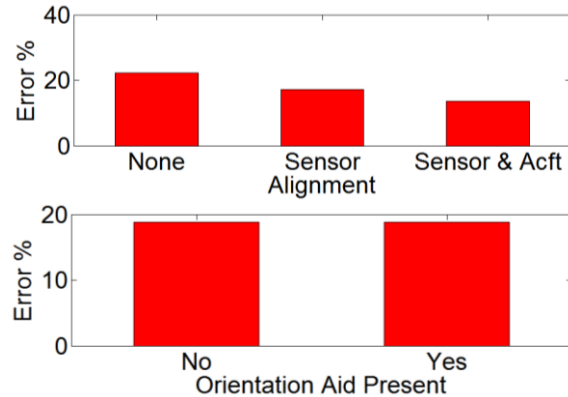


Figure 58: Target Acquisition Errors vs. Orientation Aid and Alignment Settings

These target acquisition time results demonstrated a significant impact of reference frame alignment on the target acquisition time and accuracy. This supported the reference frame alignment hypothesis (#1). However, the lack of a significant orientation aid effect on time or accuracy of target acquisition failed to support the orientation aid hypothesis (#2).

4.5.2.3. Experiment 1 Tracking Task Results

Since, the experiment 1 results showed no significant effects of interest for the flight path error or sensor track error the results are combined in this section. These terms were both analyzed as a root mean squared error for each individual run.

After transformation, the regression analysis resulted in the models shown in Equation 3 and Equation 4. Neither of these measures revealed any impact of reference frame alignment or orientation aids on tracking performance. Consequently, as measured in this experiment, they do not characterize any impact of multiple reference frames on these tracking tasks.

$$FPE'_{e1} \approx \beta_0$$

**Equation 3: Flight Path Error Regression Estimation
No terms remained in the model**

$$STE'_{e1} \approx \beta_0 + \beta_1 * X_{trialNum}$$

**Equation 4: Sensor Track Error Regression Estimation
Only the subject's trial number remained in the model.
This represented a learning effect in the video tracking task.**

These results were expected for the sensor track error because this task required no transformation of information from one reference frame to another. All the information required to control crosshair pointing was available in the sensor display, and the control movements were aligned with the display rather than any real-world axis. However, flight path error may have revealed the impact of the aircraft control transformation requirement. A lack of significant impact here either demonstrates that these tasks were not challenging enough to have revealed a primary task performance difference, or that the task of imagining oneself in the aircraft, for the purpose of determining required bank direction, is an insignificant portion of the tracking task difficulty.

It was also thought that aircraft and sensor track errors would grow as workload increased on other required tasks. As the orientation and target acquisition tasks changed in difficulty, they might have overwhelmed the subject enough to induce performance changes in tracking tasks; however, this was not observed during experiment 1.

One possible reason for this lack of an alignment effect in tracking tasks was the unique design of the north-up aircraft display. While most subjects had some form of experience with a traditional aircraft-view display, only one had experienced anything like the north-up display. These two variations are shown in Figure 55. The top aircraft-view display is recognized as a standard primary flight display with tilt bank control similar to most aircraft flight controls and video game simulations. The bottom north-up view was similar to a submarine navigation screen familiar to one subject, but required familiarization for every other subject in the study. However, despite this limitation, the bottom display showed no significant change in performance over the top. These results do not support the reference frame alignment or orientation aid hypotheses but they also demonstrated no disadvantage of either of these display techniques (reference frame alignment or orientation aid).

4.5.3. Experiment 1 Workload Measures

4.5.3.1. Experiment 1 Bedford Workload Rating Results

After each individual trial, subjects were asked to provide an assessment of the mental workload observed during that trial. The subjects provided a rating from 1-10 in accordance with the Bedford workload rating scale in Figure 43. This subjective workload was measured over the entire trial including target acquisition, tracking, orientation, and reaction time tasks. These results were analyzed with a Kruskal-Wallis rank test to evaluate a difference in the distribution of these ordinal data. The raw data are plotted in Figure 59 and Figure 60 with respect to the two display techniques. Figure 59 shows a fairly clear decrease in workload associated with the two alignment levels as compared to the blue distribution without alignment.

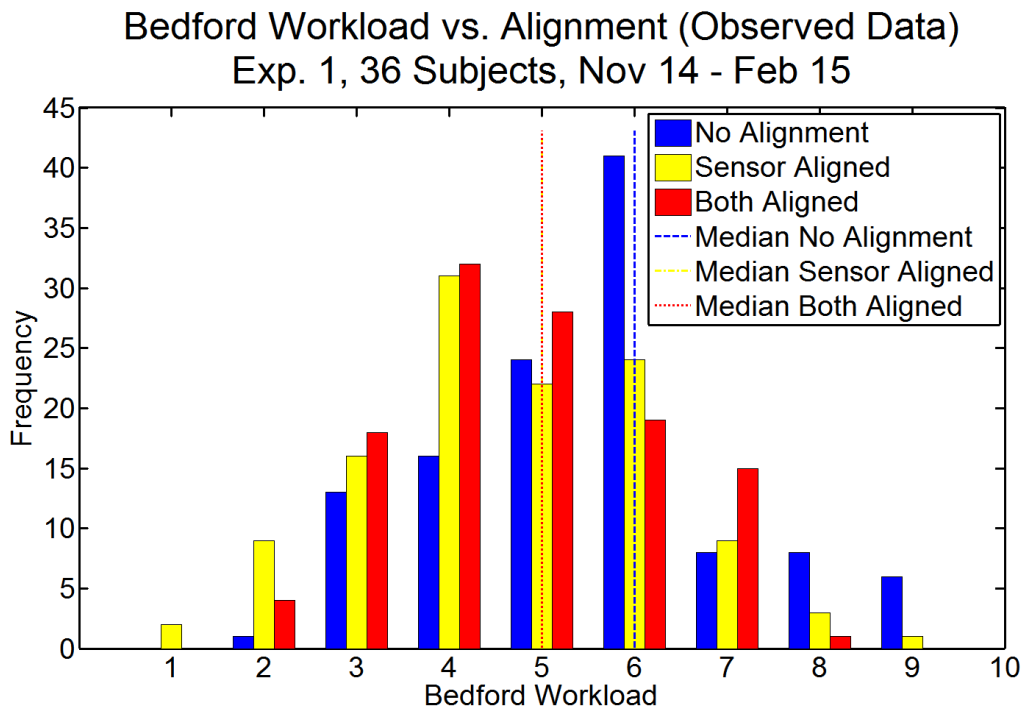


Figure 59: Bedford Workload Rating Alignment Effect
Blue distribution is observed data without alignment. Yellow distribution is alignment of the sensor video only, and red has alignment of sensor and aircraft displays.

Although this effect seems significant in the raw distribution, the Kruskal-Wallis test results in Table 6 demonstrate the reference frame alignment effect only in the absence of the orientation aid. In other words, based on these subjective workload ratings, subjects did not find the reference frame alignment particularly important if the display already had an orientation aid (display configuration B: Sensor Aligned).

Table 6: Experiment 1 Subjective Bedford Workload Results

These are the results of Kruskal-Wallis rank tests for pairwise comparisons of displays. Green indicates a significant difference with a family significance of 0.05 Bonferroni corrected to 0.008.

A – misaligned / orient aid B – aligned sensor / orient aid C – misaligned / no orient aid D – aligned sensor and aircraft / no orient aid	Adding Reference Frame Alignment		Including Orientation Aid		Interaction Effects		
	Display	Display	Display	Display	Display	Display	
	A ≠ B	C ≠ D	A ≠ C	B ≠ D	C ≠ B	A ≠ D	
Bedford Workload (1-10)	Chi-sqr	1.24	12.87	6.38	0.36	15.54	0.29
	p-value	0.27	3.34E-04	1.16E-02	0.55	8.09E-05	0.59

These results can also be observed for the orientation aid effect. Figure 60 demonstrates the distribution changes from blue to red when adding an orientation aid. However, this did not produce a significant result in Table 6. It is certainly trending toward significance when no alignment was present (comparing display configuration A: Traditional and C: No Orientation Aid in the third column of results) with a p-value of 0.0116; however, with the six pairwise comparisons, the Bonferroni corrected p-value would need to be less than 0.0042 for significance. Therefore, while there is a qualitative difference in orientation aid, our objective non-parametric evaluation did not find a significant difference in workload associated with orientation aid. The multiple reference frame impact and corresponding usefulness of reference frame alignment is demonstrated with these subjective workload ratings. This supports the reference frame alignment hypothesis (#1), but these results offered no support for the orientation aid hypothesis (#2).

Bedford Workload vs. Orientation Aid (Observed Data)
Exp. 1, 36 Subjects, Nov 14 - Feb 15

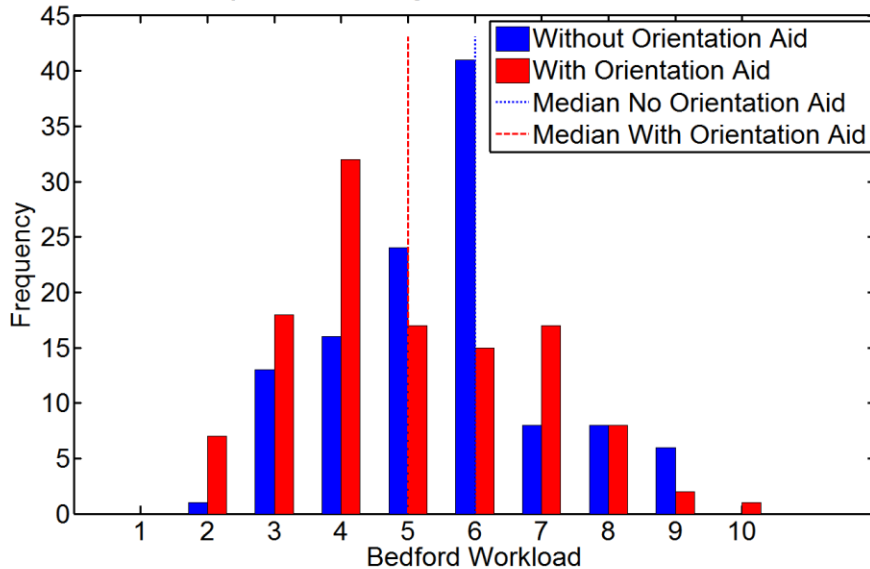


Figure 60: Bedford Workload Rating Orientation Aid Effect
Blue distribution is observed data without the orientation aid. Red distribution is observed data with the orientation aid and is shifted left of the blue data.

4.5.3.2. Experiment 1 Reaction Time Results

The reaction time test provided a secondary task workload measurement. Here subjects responded to a blinking visual light with a trigger squeeze. This was not directly representative of any specific unmanned aircraft task, but it was explained to the subject as an activity sensor at the target area. The requirement to immediately respond to this cue could represent several different urgent tasks required of an unmanned aircraft operator, such as emergency situations, weather or airspace changes, evasive maneuvering, and in-flight deconfliction with other aircraft. However, the frequency of this urgent stimulus throughout the simulator represented an invasive measurement. This invasiveness was accepted because it provided a more frequent measurement of workload over the subjective Bedford workload rating, and this technique provided an objective measure while the Bedford rating might have been influenced by subjects' opinions. Orientation aid, initial angle and image had no significant effect on reaction time, so they do not show up in the regression model.

$$RT'_{e1} \approx \beta_0 + \beta_1 * Xalign1 + \beta_2 * Xalign2 + \beta_3 * XtrialNum + \beta_{4i} * Xsubject_i + \beta_{5i} * XtrialNum * Xsubject_i$$

$$i = 1:36 \text{ subjects}$$

Equation 5: Experiment 1 Reaction Time Regression Estimation

Table 7: Experiment 1 Reaction Time Predictor Variable Coefficients

Predictor Variable	Term	Transformed Regression Estimate	Lower 95% Conf. Interval	Upper 95% Conf. Interval	t-stat	p-value	Reverse Transformed Estimate (β')	units
(Intercept)	β_0	-0.07	-0.12	-0.02	-2.95	3.35E-03	-0.07	s
Xalign1 Sensor Display Only	β_1	-0.04	-0.06	-0.02	-3.72	2.21E-04	-0.04	s
Xalign2 Sensor and Aircraft Display	β_2	-0.04	-0.06	-0.02	-3.83	1.44E-04	-0.04	s
XtrialNum	β_3	-3.73E-03	-0.01	-1.07E-03	-2.76	6.07E-03	-3.54E-03	s/#
Orientation aid, initial angle, image, and all interaction terms were tested, but they did not meet the 0.05 significance requirement for inclusion in this regression.								

The reaction time regression model, shown in Table 7 and Equation 5, shows the effect of reference frame alignment, but not any measureable impact of orientation aid. This parallels one portion of the Bedford workload ratings and is visible in the greater shift associated with Figure 61 than that shown in Figure 62. This model shows a significant impact from each level of alignment, a subject effect and then a learning effect which was different across subjects. This demonstrates an effect of the multiple reference frame tasks, and the effective influence of reference frame alignment to mitigate that effect which supports the reference frame alignment hypothesis (#1).

Reaction Time Alignment Effect(Observed Data)
Exp. 1, 36 Subjects, Nov 14 - Feb 15

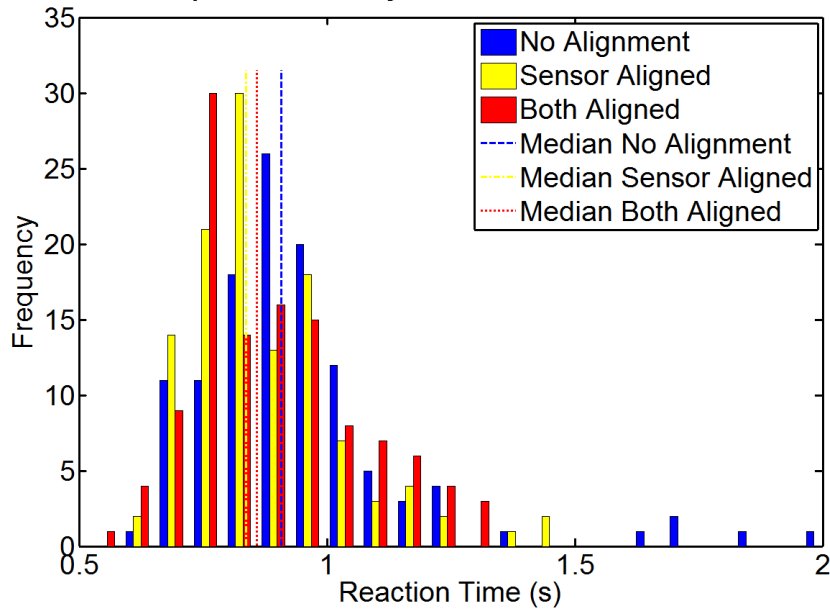


Figure 61: Reaction Time Alignment Effect

Blue distribution is observed data without alignment. Yellow distribution is alignment of the sensor video only, and red has alignment of sensor and aircraft displays.

Reaction Time Orientation Aid Effect (Observed)
Exp. 1, 36 Subjects, Nov 14 - Feb 15

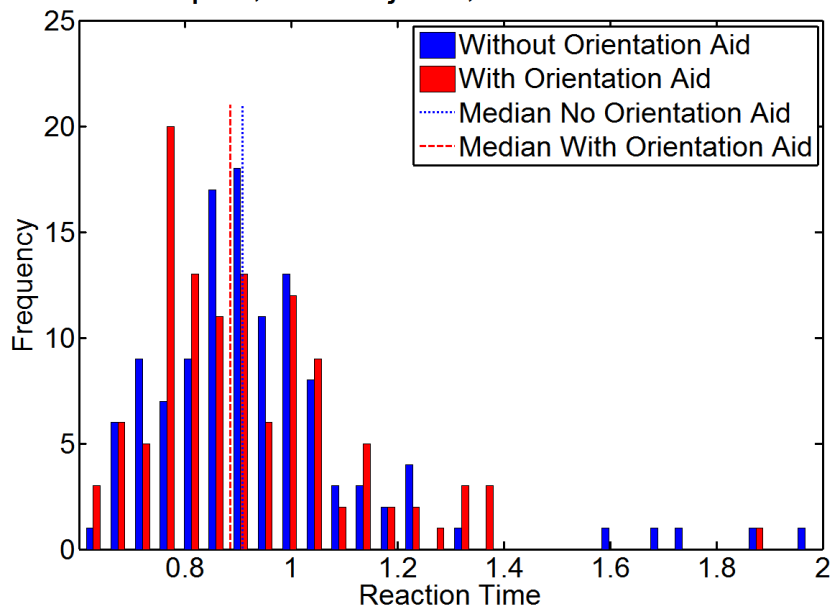


Figure 62: Reaction Time Orientation Aid Effect

Blue distribution is observed data without the orientation aid. Red distribution is observed data with the orientation aid and is shifted left of the blue data.

4.5.4. Experiment 1 User Preferences

4.5.4.1. Experiment 1 Subjective Ranking Results

After subjects completed their entire experiment, during the post-experiment questionnaire, they were asked to provide a ranking of the four displays from one to four, with one as the best and four as the worst. These results are all provided in Appendix G: Subjective Response Data.

These data were collected to capture the subject’s preference regarding the displays and does not necessarily represent a significant workload or performance benefit from any particular display. Here, as displayed in Table 8, they reinforce the rest of the findings from experiment 1. Based on these results, subjects clearly preferred reference frame alignment and also preferred orientation aids when reference frame alignment was not included.

Table 8: Experiment 1 Subjective Ranking Results

These are the results of Kruskal-Wallis rank tests for pairwise comparisons of displays. Green indicates a significant difference with a family significance of 0.05 Bonferroni corrected to 0.008.

A – misaligned / orient aid B – aligned sensor / orient aid C – misaligned / no orient aid D – aligned sensor and aircraft / no orient aid		Adding Reference Frame Alignment		Including Orientation Aid		Interaction Effects	
		Display	Display	Display	Display	Display	Display
		A ≠ B	C ≠ D	A ≠ C	B ≠ D	C ≠ B	A ≠ D
Rankings (1-4)	Chi-sqr	43.50	43.46	18.33	1.47	53.03	25.50
Kruskal-Wallis	p-value	<1E-10	<1E-10	1.86E-05	0.23	<1E-10	4.42E-07

4.6. Experiment 1 Limitations

These results have limitations based on the collection methods. The subjects population of this experiment (characteristics available in Appendix B: Subject Characteristics) were mostly graduate and undergraduate MIT students with no experience operating unmanned aircraft. These preferences might be different with a population of subjects more similar to unmanned aircraft operators.

Additionally, the short time associated with each individual run was not indicative of actual surveillance tasks, which could span hours tracking the same target. This could mask potential vigilance issues with the display techniques. If a display included features which a subject could manage for minutes at a time but would prove challenging or impossible for long periods, this would not be discovered with this experiment.

Finally, the simulator design was simplified to focus on the multiple reference frame aspect of unmanned aircraft control, and the results and conclusions should stay limited in kind. These results do not indicate a benefit to sweeping changes of unmanned aircraft displays in general, but apply directly to the on-station surveillance time. It would be inappropriate, for instance, to advocate display changes during takeoff and landing phases of a flight based on these results alone. While not an exhaustive list these were evaluated as the most applicable limitations to these data and corresponding results and conclusions.

4.7. Experiment 1 Conclusions

This experiment explored the impact of reference frames on unmanned aircraft operations, and evaluated two possible mitigation techniques to address this difficulty. Experiment 1 provided a wealth of data regarding the multiple reference frame challenge of unmanned aircraft surveillance. This highlights a potential design space to support operator control. Only two particular display techniques were addressed in this experiment: reference frame alignment and orientation aids.

The reference frame alignment hypothesis (#1) was supported because the reference frame alignment technique offered improved performance and workload across every measure except for the tracking tasks (flight path error and sensor track error). This was supported by objective and subjective results. Reference frame alignment improved median orientation time by 0.3 to 0.5 seconds when subjects were identifying the direction of movement in the sensor video. Furthermore reference frame alignment improved performance on the more complex target acquisition task. When subjects were asked to locate a target in the sensor video, their median target acquisition time was reduced by 0.7 to 4 seconds depending on the angle of image rotation. This demonstrates the additive effect of the orientation time benefit. When the task requires subjects to complete multiple orientations the basic orientation benefit becomes more amplified.

The alignment technique also showed a qualitative reduction in error rates (percentage of answers, for the entire experiment, which were wrong) on basic orientation tasks (demonstrated error rate reduction from 6 to 1%) and more complex target acquisition tasks (demonstrated error rate reduction from 22 to 15%). Given the severe consequences associated with these errors this may prove a more significant contribution than the accelerated response times. However, the orientation time and target acquisition time tasks represent a small sample of the potential benefits of this alignment technique. With increased response times, to the reaction time test, on the order of ½ second this effect would increase with more complex higher-frequency task switching. While these environments were not tested in this experiment, more complex surveillance tasks which require aggressive relocation of the aircraft may require higher-frequency task switching and consequently experience a greater benefit from the reference frame alignment technique.

In contrast to reference frame alignment, the orientation aid was only helpful in the most basic orientation task. During the basic orientation task where the subject identified a motion direction in the sensor video, the orientation aid (e.g. north arrow) reduced median orientation time by 0.16 seconds; however, this result did not carry forward to the more complex target acquisition task where the subject had to locate a specific target in the sensor video. This technique, which is uniformly applied throughout the industry, seemed to offer only superficial assistance with the more complex multiple reference frame tasks. This is important because it indicates an area for improvement.

Experiment 1 demonstrated that the reference frame alignment technique was able to reduce orientation time, and target acquisition time, during representative unmanned aircraft mission tasks, more effectively than the current practice of including an orientation aid (e.g. north arrow) on the sensor video.

5. Experiment 2: Imagery Rotation Subtask

5.1. Experiment 2 Overview

This experiment investigated the multiple-reference-frame effect on target acquisition. Experiment 2 was developed in order to examine specific findings from experiment 1. Experiment 1 found that both orientation aids and reference frame alignment had a measurable improvement on orientation time. It was thought that this decrease in orientation time would lead to a decrease in target acquisition time, or the time to locate a target within the sensor display. However, only reference frame alignment (aligning the sensor video to north-up) decreased this time. Feedback from participants suggested that subjects were not using the orientation aid during the initial target acquisition phase of the simulator experiments. Instead they were performing an imagery rotation task directly on the perceived features in the imagery. With this knowledge, experiment 2 was developed to test this imagery rotation task, between the sensor video and north-up satellite imagery, in a more controlled environment than the multitask simulator.

This study specifically measured the difficulty of finding a target in a rotating reference frame. This did not involve the unmanned aircraft simulator. This experiment only involved the single target acquisition task repeated with different display design techniques of reference frame alignment and orientation aids. These were the same techniques evaluated in experiment 1, but here they were presented in a single task environment without any of the additional workload present with the multiple tasks included in the unmanned aircraft simulator. An imagery rotation test interface was developed which displayed two identical images side by side. The left image included a target identification cue, and the right image did not. The subject was instructed to find the target location on the right image and select it with a computer mouse.

5.1.1. Experiment 2 Scenario and Tasks

This experiment only involved the target acquisition task. The subjects were told to select the target location as if they were employing a weapon. This was done to provide a sense of importance to the accuracy of the selection. While none of the subjects had any experience operating unmanned aircraft, all of them understood the theoretical significance of selecting the wrong target. At the same time, subjects were told to select the target as quick as possible to avoid missing a potential opportunity to find the target. Their goals were accuracy and speed.

5.1.2. Experiment 2 Timeline

During experiment 2, after initially completing the consent form, each subject participated in four different cognitive rotation studies. Each of these studies was obtained from the MIT Man Vehicle Laboratory. Two of these tests were designed to measure a subject's ability to perform object rotation and two were designed to measure perspective taking ability. These tests and their results are discussed in Appendix H: Imagery Rotation Cognitive Process Examination.

Next, each subject completed a brief training period with each of the possible display configurations on the imagery rotation test interface. After familiarity with each display configuration, and confirming the correct target location twice in a row with each display, each subject continued on to complete 72 experimental trials. The entire process, for a single subject, lasted approximately 1 hour.

5.2. Experiment 2 Hypotheses

This experiment was designed to take a closer look at the target acquisition task and the lack of orientation aid impact, observed in experiment 1. This study evaluated the orientation aid and alignment effectiveness at addressing the increased challenges of misaligned reference frames on two identical images. Consequently, two of these hypotheses match those of experiment 1, but they were evaluated in the imagery rotation test interface and not the unmanned aircraft simulator.

Hypothesis 1: Reference frame alignment reduces the orientation time required to interpret a display, and consequently increases performance across tasks that require coordination between information usually provided in multiple reference frames.

Hypothesis 2: Orientation aids reduce the orientation time required to interpret a display, and consequently increase performance across tasks that require coordination between information usually provided in multiple reference frames.

Hypothesis 3: Imagery features and lack of symmetry reduce the time required to interpret image orientation, and consequently increase performance across tasks that require image orientation.

5.3. Experiment 2 Display Configurations (Independent Variables)

Experiment 2 reexamined the display characteristics from experiment 1. However, these displays were only designed for a basic imagery rotation test. They represent the bottom two displays from the aircraft simulator, as shown in Figure 63. However, in experiment 2 the targeting task was conducted on the right still image (previous satellite image) in order to prevent a control confound from the subject selecting a target location on a rotating image. The two identical images represented the entire useful display.

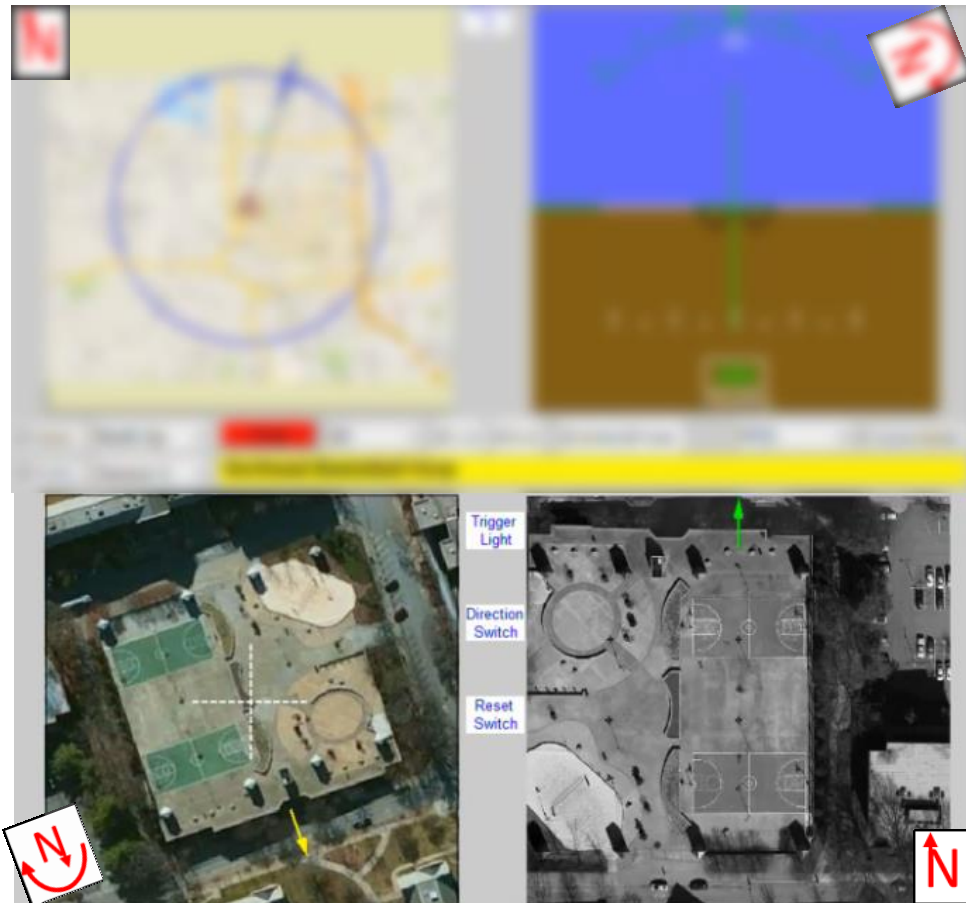


Figure 63: Imagery Task Display Development

For experiment 2, a separate interface was developed to focus on only the bottom two displays of this simulator. [Map Data and Image ©Google]

Table 9 describes how the experiment 2 displays were adjusted to investigate the reference frame alignment and orientation aid effects. The three display configurations used in experiment 2 are shown in the following figures. Only the left side of the figure changes between display configurations.

Table 9: Experiment 2 Display Configurations

Gray indicates design variables which were explored during this experiment.

Display Configuration	Traditional	Aligned	No Orientation Aid
Sensor	Sensor-View	North-Up	Sensor-View
Mission	North-Up		
# Reference Frames	2	1	2
Reference Frame Alignment	No	Yes	No
Orientation Aid	Yes	No	No

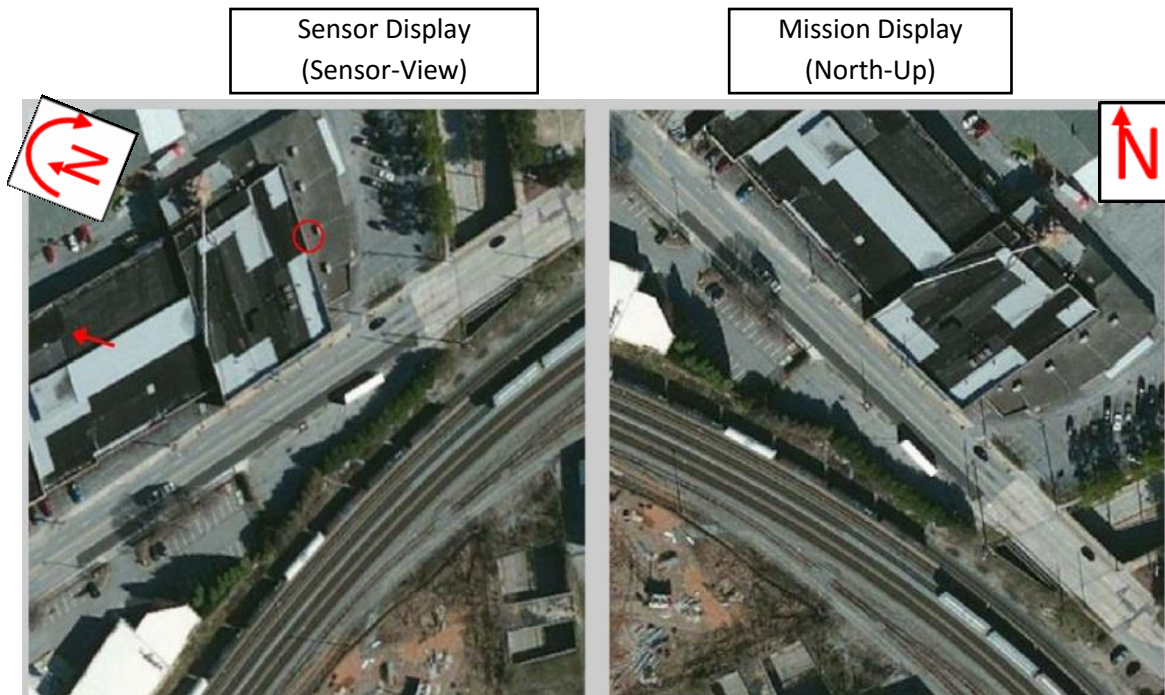


Figure 64: TRADITIONAL DISPLAY CONFIGURATION

N symbols were added here to indicate fixed or rotating north direction. On the left image, the red circle indicates the target location, and the red arrow is the orientation aid. The subject's task was to find the target location in the right image. [Image ©Google]

In the experiment 2 traditional display configuration (Figure 64) the left image was rotating as it would in the simulator sensor display. This represented the video from a sensor on an aircraft that is flying around the target. This configuration also included an orientation aid to inform the subject of the north direction. The right image was fixed north-up as it would be if it were a satellite image. The subject only made inputs on the right stationary image to avoid any control confounds during this imagery rotation test. This was different than the simulator experiments where the subject controlled the crosshairs on the sensor video, not the satellite image.

Performance with this baseline traditional configuration was compared to the aligned configuration and a configuration without the orientation aid. In this way, both techniques were evaluated, but no interaction effects were included in this experiment.

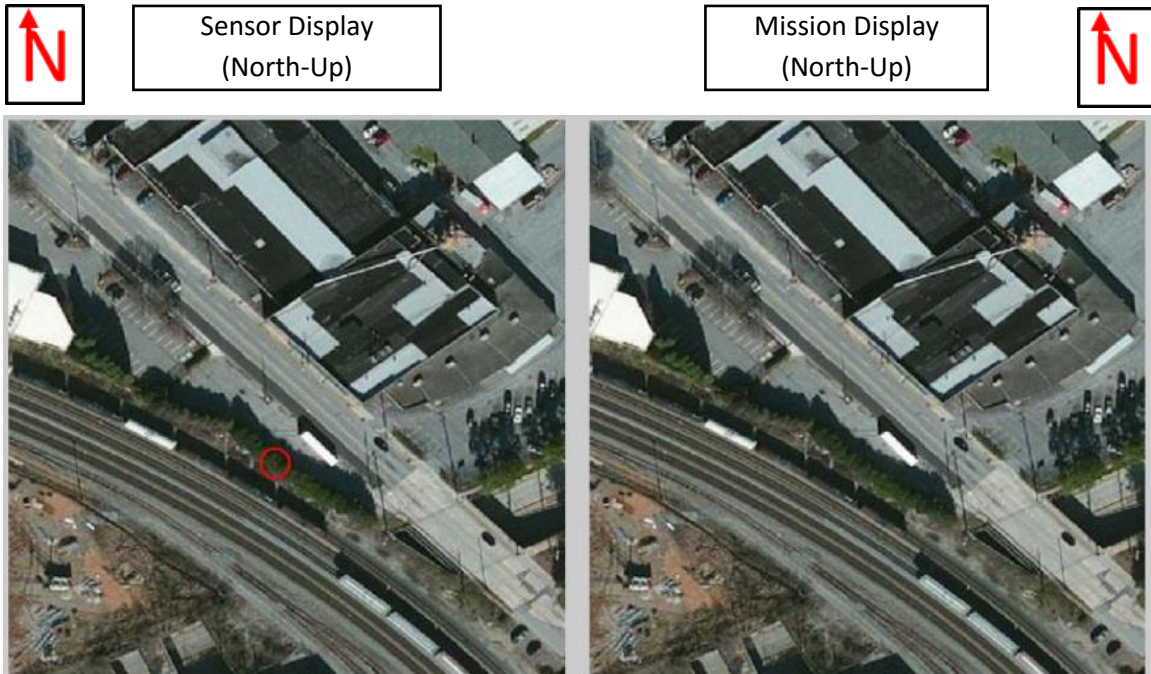


Figure 65: ALIGNED DISPLAY CONFIGURATION
 N symbols were added here to indicate fixed or rotating north direction. The red circle indicates the target location. The subject's task was to find the target location in the right image. [Image ©Google]

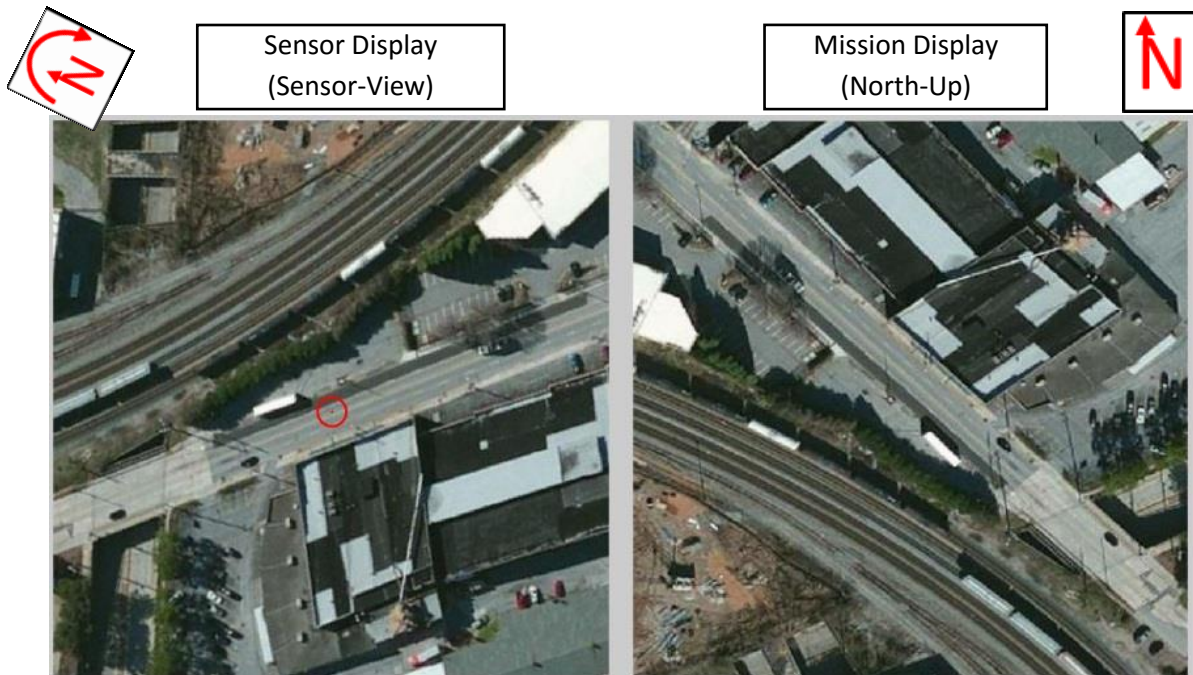


Figure 66: NO ORIENTATION AID DISPLAY CONFIGURATION
 N symbols were added here to indicate fixed or rotating north direction. The red circle indicates the target location. The subject's task was to find the target location in the right image. [Image ©Google]

Although the image shown in Figure 66 has many features available for orientation, some of the images were relatively featureless and still others included ambiguous features. These characteristics

were included to examine their effect on the reference frame alignment or orientation aid techniques. Past research has found that objects involved in object rotation may include features which don't require rotation for identification. This could be possible with target identification also and would prevent the need for image rotation during this study. If an image were to possess "orientation-free" information near the target area, then mental rotation would be less important. However, for this task, the targets were often chosen on the corner of or just off of small features. In this way, subjects might choose the wrong corner or wrong side if they relied solely on "orientation-free" features [132]. It was thought that a featureless or ambiguous image would increase orientation time and make the task more difficult (hypothesis 3). This should have increased the measured effectiveness of reference frame alignment and orientation aids. For all of the images used in this study see Appendix D: Experiment 2 Data Analysis. Figure 67 shows one example from each imagery category.

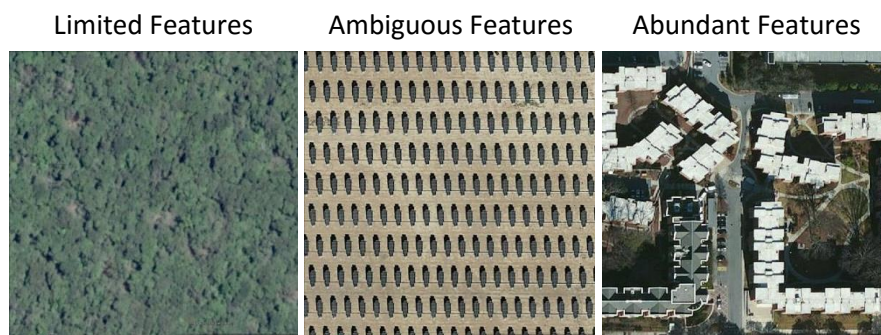


Figure 67: Image Feature Examples

These are examples from the three broad categories of images that were sampled during experiment 2. The full group is visible in Appendix I: Imagery Feature Categories [Map Data and Image ©Google]

5.4. Experiment 2 Dependent Variables

Only two dependent variables were recorded during this experiment. While this task was designed to replicate a simplified target acquisition task, the terms used here do not match the terms used with the unmanned aircraft simulator. Different terms are used to avoid any direct comparison of these data with the simulator data. Since the environment was significantly different between this target acquisition task and the similar task in the simulator, it would be inappropriate to directly compare results. For that reason, the following measures are used to evaluate target identification with the imagery rotation test interface. Each of these metrics could be used to demonstrate a difference between the display treatments.

The two performance measurements collected during experiment 2:

1. **Selection Answer Time:** this is the time from the start of the trial (when both images appeared) until the mouse button was depressed.
2. **Selection Answer Error:** this is the distance in % screen width between the target location and the location selected by the subject.

5.5. Experiment 2 Results

5.5.1. *Data Analysis Method*

Each of the two dependent variables measured during experiment 2 was analyzed independently using linear regression analysis as a function of reference frame alignment and orientation aid. For each regression analysis, the following independent variables were considered.

Fixed Effects:

1. **Alignment (Xalign):** Categorical reference frame alignment setting describing whether or not the left image was aligned to north-up like the right image (yes or no)
2. **Orientation Aid (XorientAid) :** Categorical orientation aid setting describing whether or not the display included an orientation aid (yes or no)
3. **Initial Angle (XinitAngle):** Angle of rotation, in degrees, between the left and right images at the start of a trial
4. **Subject Trial Number (XtrialNum):** Counted up from 4 to 75 as the experiment progressed
5. **Imagery Features (Xfeatures):** categorical feature categories: limited, ambiguous, or abundant (examples shown in Figure 67)

Random Effects:

6. **Image (Ximage):** Categorical image number 1 to 24
7. **Subject (Xsubject):** Categorical subject number from 1 to 12

Just as described in experiment 1, the first five of these variables were considered as fixed effects, while the final two were considered as random effects. This required a mixed-effects linear regression analysis. The image and subject number were considered as random effects because no direct effect of any subject or image involved in this experiment was of interest to the objective. The experimental design minimized these random effects by controlling their presentation across the experimental trials, but it was still important to track the effects of these variables in order to build an appropriate model for the fixed effects. Both regression analyses considered the first five variables as potential predictor variables.

Both of these performance measurements (selection answer time and selection answer error) were skewed distributions. This was an expected result since each of the measures represented a positive-only minimization for the subjects. For this reason each of these variables was transformed using the Box-Cox transformation procedure. One example of the transformation's effect is shown in Figure 68. Here the top image shows the original skewed selection answer time distribution for experiment 2, and the bottom image shows the distribution of the transformed selection answer time. For details on

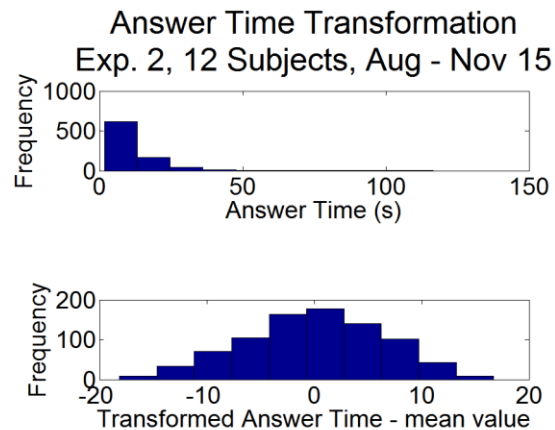


Figure 68: Experiment 2 Selection Answer Time Transformation Example

either transformation used in experiment 2, see Appendix D: Experiment 2 Data Analysis.

Since transformation was required for both dependent variables, it is important to reiterate the limitation on interpretation of results. The effects discovered in the regression analysis are then displayed in their original units, and should be interpreted as change in the median of the original distribution. For instance, if the reference frame alignment effect decreased selection answer time by 0.5 seconds, this effect would be amplified on longer selection answer times (those in the tail of the distribution), and decrease in magnitude on shorter selection answer times (those close to zero). Although these transformations increase complexity at interpreting the results, they enable the detailed regression analyses which follow and provide a clear indication of whether or not a display technique impacted a particular dependent measure.

To prepare for these regression analyses, certain data were removed from the results. The removed data are plotted in red on Figure 70. These points were removed because the error values were misleading due to imagery ambiguity. Two of the images were perfectly symmetric both vertically and horizontally. This provided two possible targets, and the red data points represent occasions where the subject selected the ambiguous target.

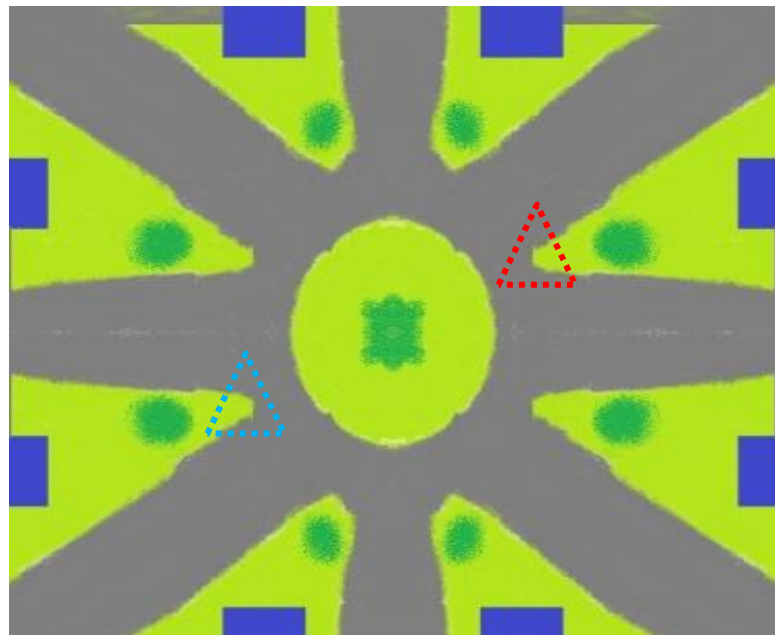


Figure 69: Experiment 2 Target Ambiguity Example
The blue dotted triangle highlights the correct target, and the red dashed triangle highlights the ambiguous incorrect target. If subjects selected the ambiguous location, their data was removed from the analysis.

The example in Figure 69 demonstrates the ambiguous target issue in one of the images. Pairs of colored triangles indicate the location of the three targets and their ambiguous alternative. This ambiguity was intentional to present a more challenging scenario; however, only two of these discarded results represent a subject guessing between two known alternatives. Each of the other eleven discarded results was an error of ignorance, where the subject did not realize there were two possible answers, but chose the first location that seemed to match the target location. This is reinforced by the generally low times associated with most of the red symbols in Figure 70. The two red symbols with higher values of answer time were the two instances where the subject realized there were two ambiguous locations. These two dependent variable performance measures were analyzed independently of one another through the regression analyses that follow.

Answer Time vs. Answer Error (NOT transformed) Exp. 2, 12 Subjects, Aug - Nov 15

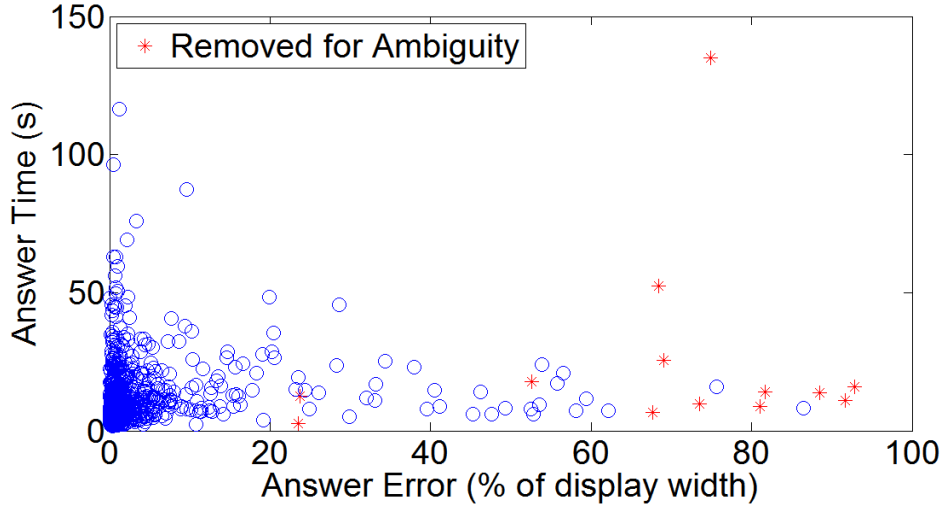


Figure 70: Imagery Rotation Results Error vs. Time

This graph shows the relationship between selection answer time and selection answer error. Red symbols are data points that were removed because the subject selected an ambiguous target on a symmetric image.

5.5.2. Experiment 2 Selection Answer Time Results

This regression measure represented the time from imagery appearance until the subject selected a target. Other than the ambiguous data, no other errors of target selection were removed from this regression analysis. As shown in Figure 70, this included some data with large selection errors, but also data with small error and large selection answer times. The selection answer time regression shown in Equation 6 includes ten independent variables that were found significant to the 0.05 level; however, this model includes a total of 112 estimated coefficients. The first four of these $\beta_0, \beta_1, \beta_2,$ and β_3 are the model intercept term and the fixed effects predictor variables: image alignment, orientation aid, and initial angle. Here initial angle was significant in the answer time model, but not in the answer error. The time estimate also includes additional interaction terms with the random effect of subject number. There are a total of 108 coefficients associated with the random effects and their interactions with the predictor variables. Trial number had no significant effect on selection answer time, so it does not show up in the regression model.

Selection Answer Time

$$\begin{aligned} \approx & \beta_0 + \beta_1 * Xalign + \beta_2 * XorientAid + \beta_3 * XinitAngle + \beta_{4m} * Ximage_m + \beta_{5m} \\ & * Xalign * Ximage_m + \beta_{6m} * XorientAid * Ximage_m + \beta_{7i} * Xsubject_i + \beta_{8i} \\ & * Xalign * Xsubject_i + \beta_{9i} * XorientAid * Xsubject_i \end{aligned}$$

$$i = 1: 12 \text{ subjects}, \quad m = 1: 24 \text{ images}$$

Equation 6: Imagery Rotation Test Selection Answer Time Regression Model

Table 10: Experiment 2 Selection Answer Time Predictor Variable Coefficients

These are the fixed effects coefficients from the regression model for selection answer time in experiment 2. The final numerical column represents the coefficient application to the median of the original distribution.

Predictor Variable	Term	Transformed Regression Estimate	Lower 95% Conf. Interval	Upper 95% Conf. Interval	t-stat	p-value	Reverse Transformed Estimate	units
Intercept	β_0	28.94	27.16	30.71	31.97	<1E-10	7.64	s
Xalign	β_1	-7.87	-10.02	-5.73	-7.20	<1E-10	-14.81	s
XorientAid	β_2	-2.16	-3.33	-0.98	-3.59	3.4E-04	-2.39	s
XinitAngle	β_3	0.02	0.01	0.03	6.19	9.5E-10	0.02	s/deg
Trial number, imagery feature categories and all interactions were tested, but they did not meet the 0.05 significance requirement for inclusion in this regression.								

Given the more controlled single task experiment, additional terms are included in the regression model compared to the similar effort in experiment 1 target acquisition time. The reference frame alignment technique was effective, but it includes an interaction with both random effects. This indicates that the benefit of aligning images depends on the image and subject involved in the test. This was also true of the orientation aid. These interactions with image were expected since some of the images, with fewer features or increased ambiguity would be more challenging to rotate without some sort of orientation from the display or orientation aid. However, other detailed images were easier to mentally rotate using features in the image. The basic subject, image, and initial angle effects were also expected.

The attempt to model the image effect with the image feature setting (featureless, ambiguous, or abundant as shown in Figure 67) was not effective. This value was not significant to the 0.05 level so it was not included in the regression. This could indicate a lack of an imagery feature effect or this result could be an indication of an inadequate categorization of imagery features. These feature variations provided a wide range of image characteristics, but were not uniformly influential on the results.

Although the alignment effect is more pronounced, both alignment and orientation aid reduced the median selection answer time. Reference frame alignment noticeably removed the tail of the skewed answer time distribution. This adjustment is shown in Figure 72. The orientation aid effect is shown in Figure 71. While both impacted the time required for the subject to find the target, alignment transformed the distribution by enabling more consistent and shorter selection answer times. Both of these are important contributions of this display technique.

Selection Answer Time vs. Orientation Aid (Observed Data)
Exp. 2, 12 Subjects, Aug - Nov 15

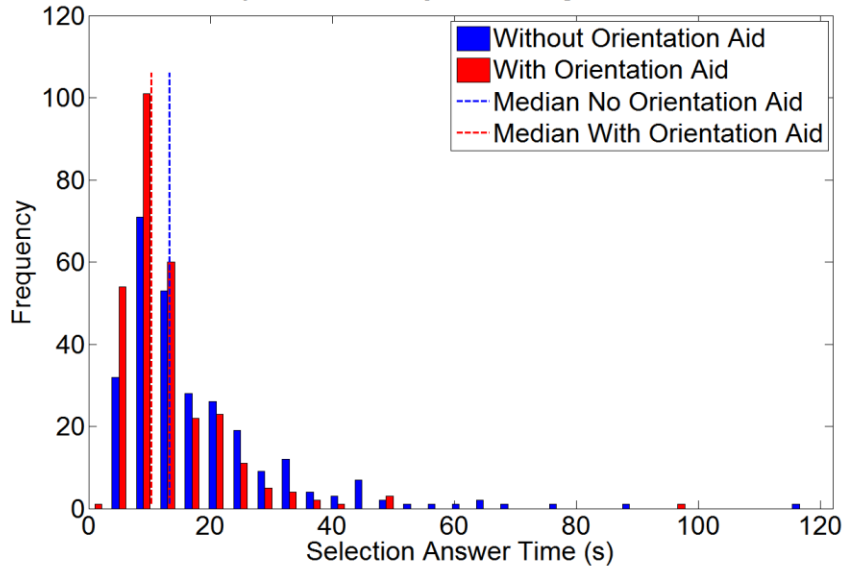


Figure 71: Selection Answer Time Orientation Aid Effect
Blue distribution is observed data without the orientation aid. Red distribution is observed data with the orientation aid and is shifted left of the blue data. (No Orientation Aid vs. Traditional)

Selection Answer Time vs. Alignment (Observed Data)
Exp. 2, 12 Subjects, Aug - Nov 15

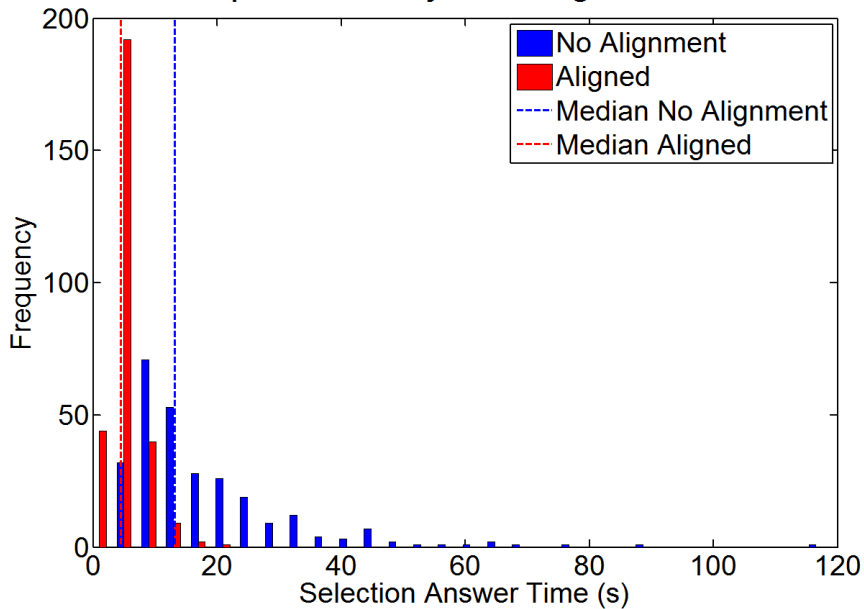


Figure 72: Selection Answer Time Alignment Effect
Blue distribution is observed data without alignment. Red distribution is observed data with aligned images. (No Orientation Aid vs. Aligned)

5.5.3. Experiment 2 Selection Answer Error Results

The selection answer error was the distance from the selected location and the actual target location, in % display width. The regression model shown in Equation 7 includes eight independent variables that were found significant to the p-value less than 0.05 level; however, given the categorical nature of the imagery and subject terms, this model results in 99 estimated coefficients. The first three of these, β_0, β_1 and β_2 account for the model intercept term and the fixed effects predictor variables: image alignment and orientation aid. The remaining 96 coefficients are associated with the random effects terms and interactions with subject number and image number. Initial angle and trial number had no significant effect on selection answer error, so they do not show up in the regression model.

$$\text{Selection Answer Error} \approx \beta_0 + \beta_1 * X_{\text{align}} + \beta_2 * X_{\text{orientAid}} + \beta_{3m} * X_{\text{image}_m} + \beta_{4m} * X_{\text{align}} * X_{\text{image}_m} + \beta_{5m} * X_{\text{orientAid}} * X_{\text{image}_m} + \beta_{6i} * X_{\text{subject}_i} + \beta_{7i} * X_{\text{align}} * X_{\text{subject}_i}$$

$$i = 1: 12 \text{ subjects}, \quad m = 1: 24 \text{ images}$$

Equation 7: Imagery Rotation Test Selection Answer Error Regression Model

Table 11: Experiment 2 Selection Answer Error Predictor Variable Coefficients

These are the fixed effects coefficients from the regression model for selection answer error in experiment 2. The final numerical column represents the coefficient application to the median of the original distribution.

Predictor Variable	Term	Regression Estimate	Lower 95% Conf. Interval	Upper 95% Conf. Interval	t-stat	p-value	Reverse Transformed Estimate	units
Intercept	β_0	0.74	0.29	1.19	3.23	1.29E-03	0.45	% display width
Xalign	β_1	-1.49	-1.87	-1.10	-7.62	<1E-10	-2.64	% display width
XorientAid	β_2	-0.30	-0.57	-0.03	-2.19	0.03	-0.28	% display width
Trial number, imagery feature categories and all interactions were tested, but they did not meet the 0.05 significance requirement for inclusion in this regression.								

This most closely parallels the qualitative error observations in experiment 1. However, no specific measure of error distance was recorded in experiment 1. Here, the selection answer error results fit a similar regression model to that of selection answer time. Both design variables were influential as expected. The image not only directly affected the results, but it also influenced how important the orientation aid and reference frame alignment were. This indicates that, even after mental rotation, some image qualities made the reference frame alignment and orientation aid more important for accuracy of target selection. Unlike the answer time results, the orientation aid impact on error was not influenced by a subject interaction. Perhaps the most significant difference between these models is that error distance was not significantly affected by the initial angle of rotation. While this increased the time required for the subject to find the target, it did not influence the error distance.

These data are reinforced with the evidence in Figure 73 and Figure 74. The small but significant effect of orientation aid demonstrates a decrease of about ¼% of the display width, while the alignment

reduces error by more than 2.6% of the display width. This difference is clearly visible in the two figures. The orientation aid effect is barely discernible with this grouped histogram, but the alignment effect virtually removes the tail of the distribution. This effect is much greater than the 2.6% demonstrated by the regression effect on the median % error distance. The removal of the distribution tail has an error reduction impact of nearly 60% on some data.

Selection Answer Error vs. Orientation Aid (Observed Data)
Exp. 2, 12 Subjects, Aug - Nov 15

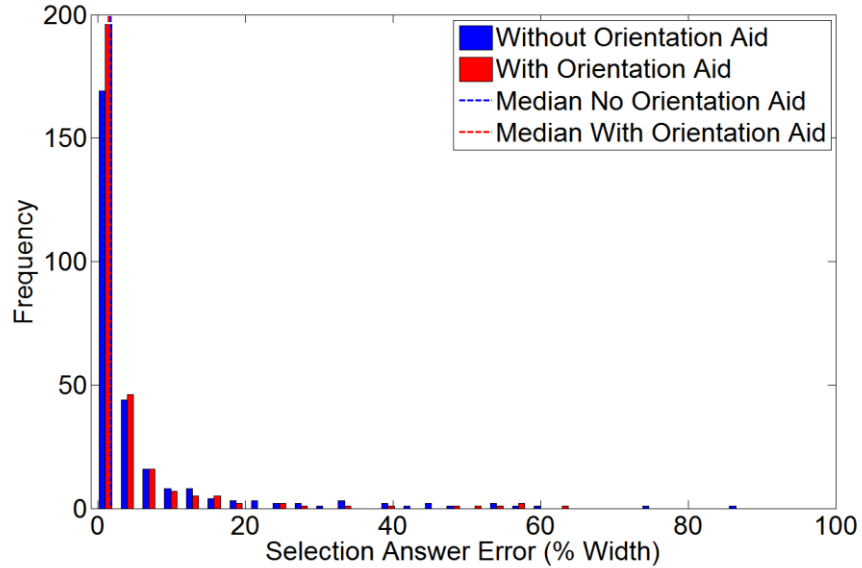


Figure 73: Selection Answer Error Orientation Aid Effect
Blue distribution is observed data without the orientation aid. Red distribution is observed data with the orientation aid and is shifted left of the blue data. (No Orientation Aid vs Traditional)

Selection Answer Error vs. Alignment (Observed Data) Exp. 2, 12 Subjects, Aug - Nov 15

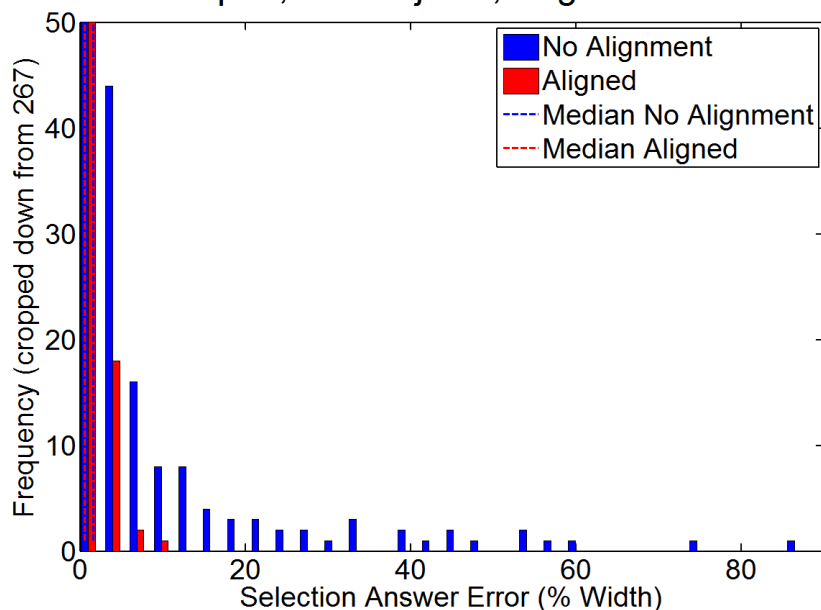


Figure 74: Selection Answer Error Alignment Effect

Blue distribution is observed data without alignment. Red distribution is observed data with aligned images. A slight shift in the median is observed, but the alignment virtually eliminates the tail of the distribution. (No Orientation Aid vs Aligned)

5.6. Experiment 2 Limitations

These conclusions are limited in scope to the types of images considered during this study. A wide range of images were included and are available for review in Appendix I: Imagery Feature Categories. The analysis of imagery features was limited by the subjective groupings developed for this experiment. Either these features did not affect response time or accuracy, or the images were inappropriately grouped. Likewise, the perfect symmetry of the synthetic images created an ambiguity which required the removal of several observations. This further hindered the feature category analysis because all of the removed data were images in the ambiguous feature category.

Additionally, these conclusions are limited to the mix of subjects who were included in this experiment. These consisted largely of MIT undergraduate or graduate students. For more information about subject experience and characteristics see Appendix B: Subject Characteristics. Finally, while subjects were instructed to consider this task as a weapon release, it is difficult to simulate the severity of consequences that would be associated with an incorrect target selection. Therefore, it is possible that these results represent faster selection answer times and higher selection answer errors than would be expected of personnel completing an actual weapon release.

5.7. Experiment 2 Conclusions

These results demonstrate a statistically significant impact of both image alignment and orientation aids on the selection answer time and selection answer error of a basic imagery rotation target location task. This supports the reference frame alignment hypothesis (#1) and the orientation aid hypothesis (#2). In both accuracy and time of target selection, the image alignment had a greater impact than orientation aid.

Since this imagery rotation task represents one portion of the larger and more complex unmanned aircraft operating tasks, both reference frame alignment and orientation aids could have a positive impact on unmanned aircraft operator performance. Of these, the alignment technique was much more impactful on the performance measures, which supports the findings of experiment 1. Here, with the reference frame alignment technique, the median time required to select the target location was reduced by 14.8 seconds and the median target selection error was reduced by 2.6% of the screen width. In contrast the orientation aid only reduced the median time required to select the target location by 2.4 seconds and the median target selection error by 0.3% of the screen width.

With the addition of a target-preview time, experiment 1 did not find an orientation aid effect on target acquisition time. The experiment 2 single-task study did not have a target-preview time, and that prevented the subject from choosing orientation features in the image before the simulation start time. The experiment 2 data revealed that the orientation aid might be impactful on the target acquisition task, with certain types of images and scenarios that were not observed in experiment 1. However, the difference in effect magnitude and distribution effect of the two techniques was pronounced in experiment 2.

The alignment technique was clearly more effective than the orientation aid. This is expected because the alignment technique virtually eliminates the orientation task, and the orientation aid merely provides assistance. In experiment 2, with targets that were not always discernible features like a building or car, the orientation task was repeated multiple times to find the target area and then fine tune the selected location. In this way, any differences between the techniques would have been magnified by each repetition of the basic orientation task.

The imagery feature hypothesis (#3) was not supported by these results because it was not significant to the 0.05 level; however, this could indicate a poor grouping of imagery features into categories, or it could indicate no imagery feature effect. Based on post-experiment questionnaires, subjects perceived an effect of the imagery features so it is possible that the lack of evidence is a function of the particular classification of images used during this research.

This page intentionally left blank.

6. Experiment 3: Display Integration and Reference Frame Alignment

6.1. Experiment 3 Overview

This experiment sought to provide additional information on the impact of multiple reference frames on the unmanned aircraft scenario. Following the significant results of experiment 1, the new display technique of display integration was evaluated along with the effects of reference frame alignment for their effectiveness in dealing with the sensor-view transformation and the aircraft-view transformation.

The aircraft-view transformation required the operator to imagine sitting in the aircraft, visible on the north-up map, and then determine the desired direction of bank control to maneuver the aircraft toward the desired flight path. The sensor-view transformation required the operator to observe motion on the sensor display and determine the cardinal direction of that movement with respect to the north-up reference frame.

Display integration was evaluated as a possible supplement to reference frame alignment since the aligned displays seemed to facilitate display integration. With current systems involving integrated displays of misaligned information, experiment 3 sought to characterize the impact of reference frame alignment on that architecture. This simulator experiment was conducted from November 2015 to December 2015 and involved 16 human subjects.

6.1.1. Experiment 3 Scenario and Tasks

This human subjects experiment followed a very similar scenario and task set to that of experiment 1, but moving targets were added to the scenario. Once again, the experiment was conducted in the unmanned aircraft simulator. The scenario required the subject to control an aircraft with an onboard video sensor. As previously described in 3.2.1, the scenario started with a 15 second target-preview time where the subject had the opportunity to read the target description and observe the target area satellite image. All of these scenarios included a description of a vehicle approaching an intersection, similar to the one shown in Figure 75. The right image is an example satellite image from experiment 3. To provide a sense of realism, the actual target is not visible in the satellite image. The left image represents the initial view as the simulator is initialized after the target-preview time. All textual descriptions in this experiment relied on a primary cardinal direction such as north, south, east, or west. This was realistic because missions are typically described in relation to these standardized directions. Furthermore, it prepared the subjects for future tasks which would be communicated to ground personnel in the north-up reference frame.

To prevent imagery effects, these images and associated vehicles were reused four times per subject. In each reuse, the entire simulator imagery and map were rotated to align a new direction to north. As reported in post-experiment interviews, only 1 of 24 subjects noticed large features on the map had rotated between trials, but that subject did not realize that the targets were reused. Every aspect of the moving vehicle scenario was then replicated on each of the display configurations.

Sensor Display

Mission Display

“Car approaching intersection from the WEST”



Figure 75: Example Target Description from Experiment 3

The right image represents an example satellite image with an associated textual description. The left image is the initial view provided by the sensor video with the vehicle visible at the bottom portion of the image to the west of the intersection. The vehicle is not visible in the right image. [Image ©Google]

Just as in experiment 1, after the initial target-preview time, the aircraft simulation began. The aircraft location was initialized along the desired circular flight path surrounding the target. The aircraft was initialized at zero bank angle so subjects were required to add left bank to maintain the aircraft on the circle. All orbits were flown to the left, to avoid any directional confusion from trial to trial.

Simultaneously, they were required to control the sensor video crosshairs to find and click on the target location. This click was accomplished with the trigger on the left control stick, as shown in Figure 29.

After this initial selection, the subject received graphical feedback in the form of a box around the target. If the subject selected the correct target, the box was green, otherwise the box was red and positioned on the correct target. This allowed collection of tracking data even if the subject initially selected the wrong target. Five seconds after the subject selected the target, or after the subject found the correct target, the box turned white and became the simulated vehicle.

After initial selection, the subject maintained the sensor display crosshairs on the target, and the aircraft on the flight path. Their tracking performance was recorded in both of these tasks.

Throughout the remainder of each trial, at 10-20 seconds intervals, subjects responded to a reaction time light which was said to inform them of activity in the target vehicle. They responded to this blinking light with the same trigger that was used to identify the target.

After each reaction time test, the subject knew to observe the vehicle for movement. A red asterisk symbol, representing a person exited the vehicle and ran off in a primary cardinal direction of north, south, east, or west. Subjects had to tell ground personnel which direction the suspect fled. They provided this input to ground personnel via the left control stick trim button, as shown in Figure 32. This

represented a basic orientation task where the subject had to mentally align the sensor-view reference frame to north-up in order to provide an answer for the direction of travel. This provided the most accurate measurement of the orientation time cost associated with different reference frames, and it was representative of actual mission requirements during unmanned aircraft surveillance.

Halfway through each trial, the white rectangular symbol, representing the vehicle, began to translate across the imagery. The subject was expected to track this vehicle as it moved throughout the rest of each trial. The vehicle followed roads in the imagery, but was always presented on top of any features. Actual surveillance imagery would include masking scenarios as the vehicle drove under trees or behind buildings, and this would add confounding measures to each subject's performance. In order to focus on the reference frame transformation problem, these realistic features of actual surveillance operations were removed to provide a more controlled data collection.

The subject continued with this scenario, and accompanying tasks, for 3 minutes and 12 seconds which is the time required to complete an entire orbit around the target area along the desired flight path. At the end of this time, the simulator froze and the subject was asked to provide one assessment of their mental workload during the initial portion of the trial, with a stationary target, and a second assessment of their mental workload during the latter portion of the trial, with a moving target. The Bedford Workload Scale, Figure 43, was used for these assessments.

The predictive aid (discussed in the display configuration) added to the experiment 3 displays could have allowed subjects to stabilize on a bank angle, but experiment 3 included a turbulence model and inflight winds for the aircraft flight path task to require subjects to continuously engage in the aircraft control task.

6.1.2. Experiment 3 Timeline

During experiment 3, after initially completing the consent form, subjects completed two basic spatial ability tests. The card rotations test and the Vandenberg MRT test, obtained from the MIT Man Vehicle Laboratory, were both administered before moving on to the simulator portion of the experiment. These tests were chosen because they provided the greatest correlation (out of four considered) with the imagery rotation study in experiment 2. A description of these tests and their results is available in Appendix H: Imagery Rotation Cognitive Process Examination.

Each subject underwent a training period with each of the possible display configurations. After reaching the required training performance on both static and dynamic targets, as described in section 3.4.1, each subject continued on to complete 17 experimental trials. Finally, the subject completed a post-experiment survey with specific questions administered to every subject and a period of open discussion with the researcher. The entire process, for a single subject, lasted 2.5 to 3 hours.

6.2. Experiment 3 Hypotheses

The objective of experiment 3 was to further characterize the impact of different reference frames on unmanned aircraft operations, and evaluate the possible mitigation techniques of reference frame alignment and display integration. This produced four overall experiment 3 hypotheses.

Hypothesis 1: Reference frame alignment reduces the orientation time required to interpret a display, and consequently increases performance across tasks that require coordination between information usually provided in multiple reference frames.

Hypothesis 4: Integration of displays reduces the orientation time required to interpret a display, and consequently increases performance across tasks that require coordination between information usually provided in multiple reference frames.¹

Hypothesis 5: Moving Target tasks increase the effect of reference frame alignment on the orientation time required to interpret a display.

Each of these hypotheses was investigated by modifying the display configurations that each subject used to control the simulator. These display configurations acted as the independent variables during this experiment and are discussed in the next section.

6.3. Experiment 3 Display Configurations (Independent Variables)

The four display configurations used in experiment 3 are described in Table 12 and shown in the following figures. For enlarged versions of these images see Appendix A: Display Configurations. Along with the moving target scenario change, experiment 3 included a predictive aid display enhancement on the navigation display of every configuration. This 10 second flight path predictor informed the subjects where the aircraft would be in 10 seconds if the winds and current bank angle remained constant.

Although there are slight differences between all the display configurations in experiment 3 and experiment 1, the naming convention is carried forward to provide consistency and identify the display features of interest. For this reason, two experiment 3 displays are named the same as experiment 1 displays (Traditional - A and Sensor and Aircraft Aligned - D) so the reader understands the commonality of the evaluated display features.

In experiment 3, display configuration A (Figure 76) presented the traditional display representation. Here, each display maintained its original reference frame, which required the subject to transform information for the aircraft control and sensor interpretation tasks. The aircraft transformation effect was only measured using flight path tracking performance, but the sensor transformation effect was directly measured via an orientation task within the sensor display.

Display configuration D added reference frame alignment to the sensor display and aircraft display. The sensor video was rotated to north-up, but the operator could still control the camera pointing in the same manner as the other display configurations. The aircraft display was also aligned to north-up. In this case, a control change was also required. As described in 3.2.3, with the north-up aircraft display, aircraft bank was controlled via control stick twist rather than tilt.

¹ Hypothesis 2, regarding the orientation aid, was only evaluated in experiments 1 and 2. Hypothesis 3 regarding imagery features and symmetry was only evaluated in experiment 2.

Performance differences between display configuration A (Traditional) and D (Sensor and Aircraft Aligned) were attributed directly to the orientation requirement associated with the sensor-view and aircraft-view reference frames. This offered one measurement of the reference frame alignment effect. Just like experiment 1, any measurable effect represented an effect of reference frame alignment which was greater than the currently used orientation aid because the orientation aid is present in both of these displays. A lack of measurable effect here would indicate that reference frame alignment offered no improvement over the orientation aid technique.

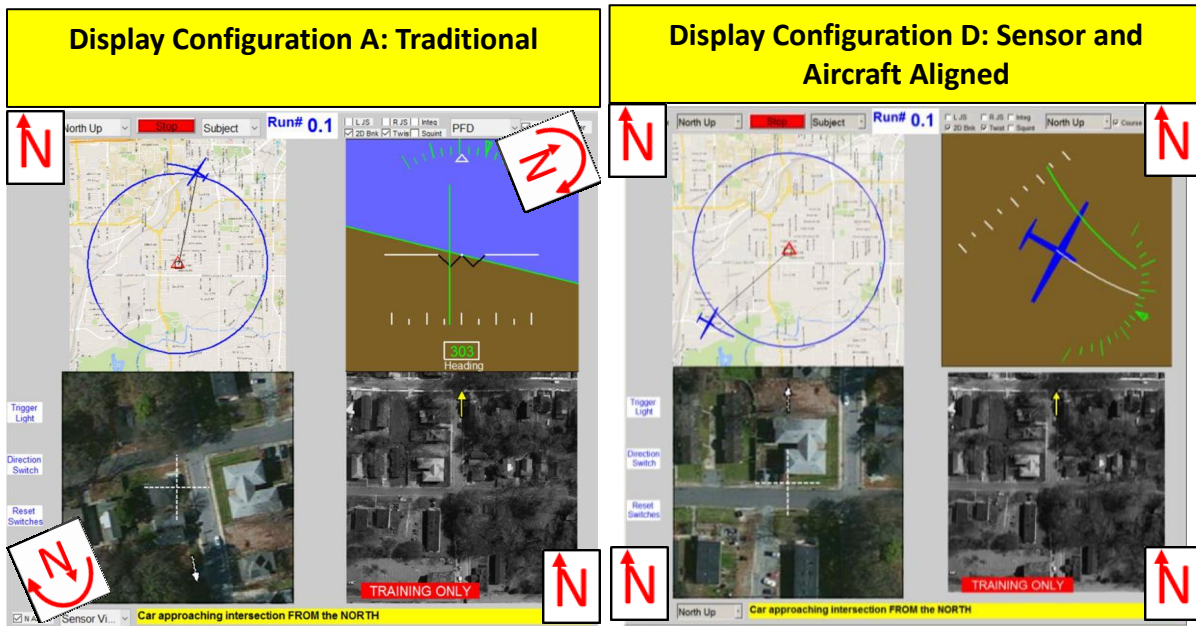


Figure 76: DISPLAY CONFIGURATION A: Traditional
N symbols are added to indicate fixed or rotating north direction. [Map Data and Image ©Google]

Figure 77: DISPLAY CONFIGURATION D: Sensor and Aircraft Aligned
N symbols are added to indicate fixed or rotating north direction. [Map Data and Image ©Google]

A second measure of reference frame alignment effectiveness, and the corresponding impact of multiple reference frames, was measured by comparing display configurations E (Integrated) and F (Aligned and Integrated), shown in Figure 78 and Figure 79 respectively. Display configuration E includes the traditional reference frames, but, unlike configuration A (Traditional), they are combined into one integrated display. Display configuration F has reference frame alignment applied to both the sensor and aircraft displays which brings all four displays to the north-up orientation, and they are also integrated onto one central display. While reference frame alignment corrected the orientation difference of displayed information, even the aligned and integrated display (F) still contained the scale difference associated with the sensor video and the navigation map.

Comparing these two configurations provided another measure of the multiple-reference-frame effect as mitigated by the predictive aid, orientation aid, and display integration. Here, with all three of these other display techniques, the benefit of reference frame alignment was evaluated for an additional effect. This also provided an opportunity to search for interaction effects between the reference frame alignment and integration effects. Although display configuration E is representative of

current systems, such as that shown in Figure 15, the operational display is not used for simultaneous control of both tasks.

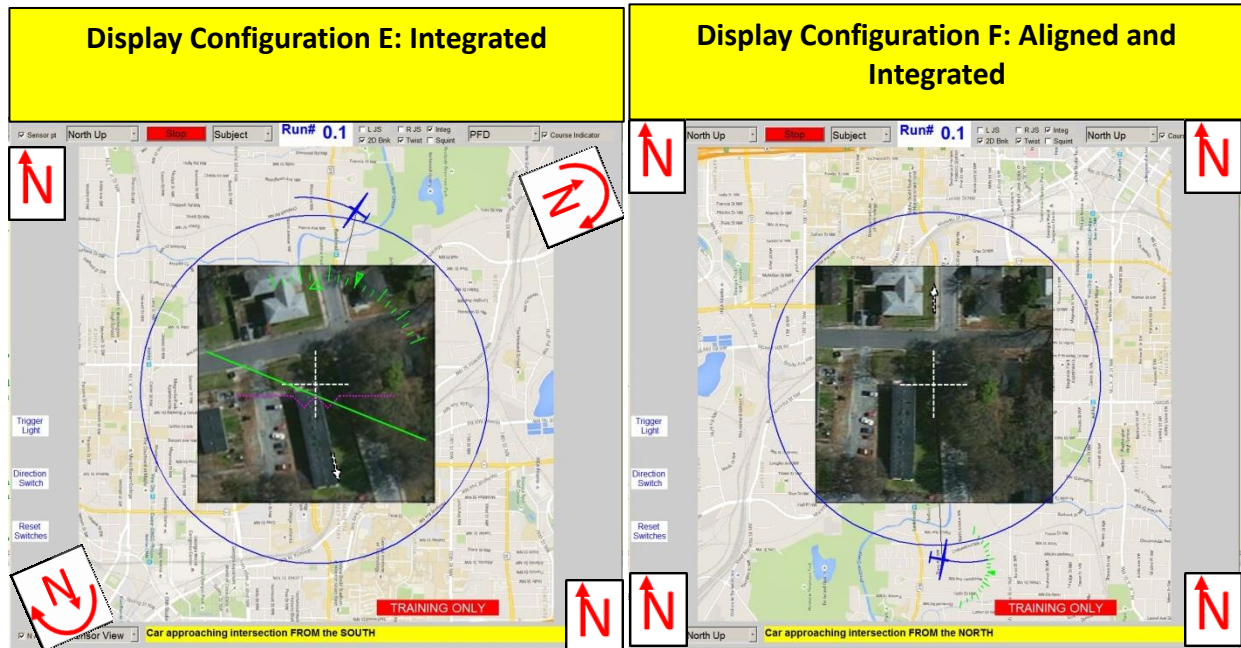


Figure 78: DISPLAY CONFIGURATION E: Integrated
N symbols are added to indicate fixed or rotating north direction for the information which originated on the formerly separate displays. [Map Data and Image ©Google]

Figure 79: DISPLAY CONFIGURATION F: Aligned and Integrated
N symbols are added to indicate fixed or rotating north direction for the information which originated on the formerly separate displays. [Map Data and Image ©Google]

As these display configurations are understood in light of the rest of this research, it should be noted that experiment 3 included a predictive aid on the navigation or aircraft displays. This is the blue line protruding from the front of each aircraft symbol and mirrored on the white line on the aircraft display of configuration D. The current aircraft position is shown along with a 10 second future projection. This also facilitated the integration of the north-up aircraft display overtop of the navigation display. The predictive aid acted as a bank indicator as well. This provided both an indication of controlled bank the corresponding flight path if that bank were maintained. An example of this dual-use predictive aid is shown in Figure 80. According to post-experiment questionnaires, no subject used the bank indicator during this experiment. Each subject reported that they relied solely on the curvature of the predictive aid for aircraft bank information.

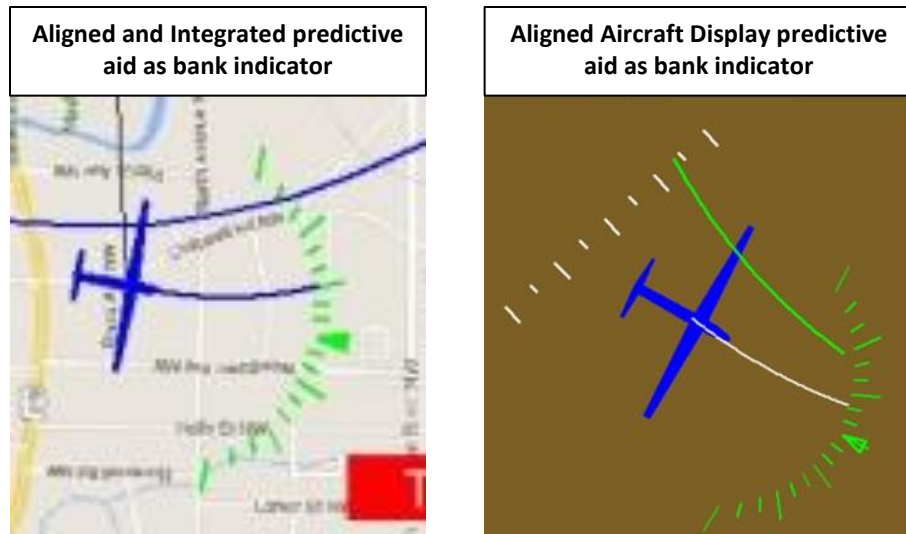


Figure 80: Predictive Aid as Bank Indicator

The left side of this figure shows the predictive on the aligned and integrated display configuration (F), and the right side shows the predictive aid as a bank indicator on the sensor and aircraft aligned display configuration (D).

Additionally, the target description (yellow bar across the bottom of each display configuration) and reaction time cue (top of the three white boxes on the left side of each display configuration) were relocated to the periphery to allow for these integrated display configurations. As this experiment is compared with experiment 1, it may be important to understand these differences in the simulator design.

Table 12: Experiment 3 Display Configurations
 Gray indicates design variables which were explored during this experiment.

Display	A Traditional	D Sensor and Aircraft Aligned	E Integrated	F Aligned and Integrated
Aircraft	Aircraft-View	North-up	Aircraft-View	North-up
Navigation	North-Up			
Sensor	Sensor-View	North-Up	Sensor-View	North-Up
Mission	North-Up			
# Reference Frames	3	1	3	1
Reference Frame Alignment	No	Yes	No	Yes
Display Integration	No	No	Yes	Yes

As shown in Table 12 and described earlier in this section, experiment 3 focused on reference frame alignment and display integration. These rows are highlighted to demonstrate the treatments across the four display configurations of experiment 3. Here, two levels of reference frame alignment and two levels of display integration were examined.

Rows 2 through 5 of this table describe the reference frame of each of the individual displays: aircraft, navigation, sensor, and mission. These orientations are described as north-up, aircraft-view, or sensor-view. Here, north-up indicates that the north direction is fixed at the top of the displayed information. A traditional map would usually be displayed in the north-up orientation. The aircraft-view label indicates that the information was displayed with respect to the direction of aircraft travel. Here, the current aircraft heading would always be into the display as if the display represented the frontal view out of the aircraft cockpit. Finally, the sensor-view description indicates that a display shows the representation which would be observed from the sensor location. Here the top of the display always represents the heading from the aircraft to the sensor pointing location. For instance, if the aircraft were north of the target area, then south would be the direction at the top of a sensor-view image.

The orientations identified in rows 2-5 demonstrate how the number of reference frames was determined. Experiment 3 adjusted the number of reference frames between 1 and 3 because reference frame alignment was now performed jointly on the sensor display and the aircraft display to support the development of a fully integrated and aligned display. This provided two levels of reference frame alignment treatment and two levels of display integration treatment.

With the understanding provided from experiment 1, all effects tested in experiment 3 were tested for their effectiveness beyond the orientation aid benefit. In this way, any effects shown here provide an indicator of potential improvements over the current reliance on orientation aids.

6.4. Experiment 3 Dependent Variables

The same performance and workload measurements were used during each simulator experiment. A short description of each is provided here. For a more in depth understanding of each measure, reference section 3.1. Each of these performance measurements evaluated the subject on one of the scenario-dependent tasks. The most direct measure of the transformation difficulty was the orientation time performance. This captured the difficulty of transforming from the sensor-view reference frame to the north-up reference frame. However, each of these metrics could be used to demonstrate a difference between the display configurations.

The eight performance and workload measurements collected during experiment 1:

1. **Orientation Time:** this is the time from the movement of the symbol on the sensor video (representing a fleeing suspect) to the subject's direction answer via the left control stick.
2. **Target Acquisition Time:** this is the time from the start of the simulation until the subject selected the target location via the control stick.
3. **Sensor Track Error:** this is the distance from the sensor crosshairs to the target location normalized by the diagonal distance across the sensor display and analyzed as a cumulative Root Mean Sum Squared Error.
4. **Flight Path Error:** this is the orthogonal distance from the orbit circle to the aircraft location normalized by the radius of the planned aircraft orbit and analyzed as a cumulative Root Mean Sum Squared Error.

5. **Bedford Workload Rating:** this is a subjective workload rating provided by the subject at the conclusion of each trial.
6. **Reaction Time:** this was the response time from the blinking of a light on the display to the subject's response via the control stick.
7. **Subjective Rankings:** this is a subjective ranking of the four displays, provided by the subject at the conclusion of his or her entire experimental period.

6.5. Experiment 3 Results

6.5.1. *Data Analysis Method*

Once again, each of the dependent variables measured during experiment 3 was analyzed independently of one another. When possible a linear regression analysis for the dependent variable as a function of reference frame alignment and display integration was conducted. This method accounted for several variables other than simply the display configuration. For each regression analysis, the following independent variables were considered.

Fixed Effects:

1. **Alignment (Xalign):** Categorical reference frame alignment setting describing whether or not the left image was aligned to north-up like the right image (yes or no)
2. **Display Integration (Xdisplnt) :** Categorical display integration setting describing whether or not the display was integrated (yes or no)
3. **Initial Angle (XinitAngle):** Angle of rotation, in degrees, between the sensor display and north-up reference frame at the start of an experiment trial
4. **Subject Trial Number (XtrialNum):** Counted up from 1 to 13 as the experiment progressed
5. **Target Movement (Xmove):** Categorical setting describing whether or not the target was moving.

Random Effects:

6. **Image (Ximage):** Categorical image number 1 to 4
7. **Subject (Xsubject):** Categorical subject number from 1 to 12

Similarly to experiment 1, the first five of these variables were considered as fixed effects, while the final two were considered as random effects. This required a mixed-effects linear regression analysis. The image and subject number were considered as random effects because no direct effect of any subject or image involved in this experiment was of interest to the objective. The experimental design minimized these random effects by controlling their presentation across the experimental trials, but it was still important to track the effects of these variables in order to build an appropriate model for the fixed effects. Each regression analysis considered the first five variables as potential predictor variables. With this approach a significant display design technique, such as reference frame alignment, would show up in multiple regression models to indicate its influence on the dependent variables measured during this experiment.

In addition to the regression analysis, pairwise comparisons were carried out between the specific displays. These were conducted for every dependent variable. For those suited to parametric analysis (1-4 and 6) a pairwise t-test comparison was conducted. Since the two subjective measures (5 and 7) collected during this experiment could not be analyzed with the regression method, they were compared with a Kruskal-Wallis rank test to determine if a difference was measured between the different displays. The regression analysis offered a more complete interpretation of the results, so when possible those are shown in this section and the pairwise comparisons are available in Appendix E: Experiment 3 Data Analysis

Each of the performance measurements and the secondary workload measurement (reaction time) were skewed distributions. This was an expected result since each of the measures represented a positive-only minimization for the subjects. For instance, while orientation time could never be negative, values as high as 9.2s (across all 3 experiments) were observed. Any attempt to directly fit these data using a regression analysis would be invalid. For this reason each of these variables were transformed using the Box-Cox transformation procedure. One example of the transformation's effect is shown in Figure 81. Here the top image shows the original skewed orientation time distribution for experiment 3, and the bottom image shows the distribution of the transformed orientation time. For details on any particular transformation used in experiment 3, see Appendix E: Experiment 3 Data Analysis.

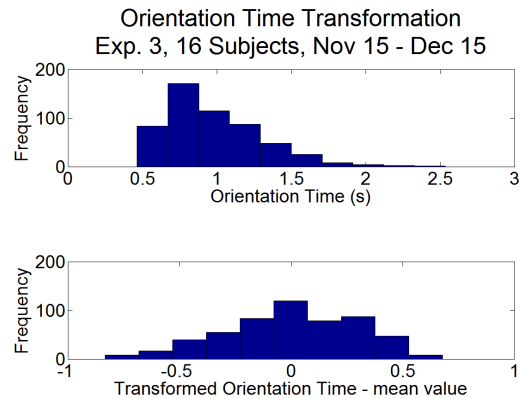


Figure 81: Orientation Time Data Transformation

Since transformation was required for every parametric measure, it is important to reiterate the limitation on interpretation of results. Resulting effects discovered in the regression analysis which are displayed in their original units should be interpreted as an effect on the median of the original distribution. For instance, if the reference frame alignment effect decreased orientation time by 0.5 seconds, this effect would increase on longer orientation times (those in the tail of the distribution), and decrease in magnitude on shorter orientation times (those close to zero). Although these transformations increase complexity at interpreting the results, they enable the detailed regression analyses which follow and provide a clear indication of whether or not a display technique impacted a particular dependent measure.

6.5.2. Experiment 3 Performance Measures

6.5.2.1. Experiment 3 Orientation Time Results

This dependent measure was the required time for a subject to determine a direction of movement in the sensor display. This was described as a suspect fleeing the target vehicle and represented as a red asterisk over the sensor video (see Figure 42). The regression model for orientation time, developed for this experiment 3, is shown in Equation 8. This was the basic measurement of the

increased performance of reference frame alignment over the orientation aid effect. Estimates of these effects are shown in Table 13. Display integration, initial angle, and image had no significant effect on orientation time, so they do not show up in the regression model.

$$OT'_{e3} \approx \beta_0 + \beta_1 * Xalign + \beta_2 * XtrialNum + \beta_3 * Xmove + \beta_{4i} * Xsubject + \beta_{5i} * Xalign * Xsubj_i$$

$$i = 1: 16 \text{ subjects}$$

Equation 8: Experiment 3 Orientation Time Regression Estimation

Table 13: Experiment 3 Orientation Time Predictor Variable Coefficients

Predictor Variable	Term	Transformed Regression Estimate	Lower 95% Conf. Interval	Upper 95% Conf. Interval	t-stat	p-value	Reverse Transformed Estimate (β')	units
(Intercept)	β_0	0.0063	-0.108	0.121	0.11	0.914	0.006	s
Xalign	β_1	-0.2321	-0.270	-0.194	-12.10	<1E-10	-0.274	s
XtrialNum	β_2	-0.0031	-0.006	-0.001	-2.45	0.0148	-0.003	s/#
Xmove	β_3	0.0795	0.057	0.102	6.95	<1E-10	0.069	s

Display integration, initial angle, image, and all interactions were tested, but they did not meet the 0.05 significance requirement for inclusion in this regression.

These results revealed several effects on orientation time; however, the display integration setting was not found to be significant so it was not included in this regression model. The reference frame alignment setting demonstrated an effect on this basic orientation time, but the model also showed an interaction between this display technique and the subject. The p-value associated with the alignment setting reveals a main effect of alignment, but this may have been reduced for some subjects based on the subject-alignment interaction. Although the entire table of random effect coefficients is not provided in this report, the highest subject-alignment interaction effect was 0.06 seconds. This would not eliminate the main alignment effect, but it demonstrates that alignment did not benefit each subject equally. The basic learning effect captured with trial number, and the human subject variation captured with the random subject effect, were both expected. Additionally, the movement effect was expected because this removed the subject's ability to rely on familiar imagery features for availability and it increased the overall complexity of the scenario. It was thought that this would induce an interaction effect with the alignment setting, but this was not observed here.

As designed this alignment effect represents a reference frame alignment impact beyond the orientation aid impact. Although orientation aids were not specifically evaluated through this experiment, their inclusion on every display configuration enabled this observation. Once again despite interactions with the subject effect, this experiment demonstrated that reference frame alignment was more effective than orientation aids at addressing the difficulty of a basic orientation task. Additionally, no measurable effect, positive or negative, of display integration was observed.

Although the subject effect makes it difficult to display the overall orientation time results, the overall distributions provide insight into these effects (larger versions are available in Appendix E: Experiment 3 Data Analysis). The data shown in Figure 82 and Figure 83 demonstrates the measurable effects of reference frame alignment and the moving target task. Figure 82 demonstrates a similar

compression of the distribution skew in response to reference frame alignment. The moving target effect, while measurable, does not invoke that same compression which matches its significance at less than 1/10 of a second in the regression model. Figure 84 shows the integration distributions. No measurable difference is observed between the cases with and without display integration.

Orientation Time vs. Alignment (Observed Data) Exp. 3, 16 Subjects, Nov 15 - Dec 15

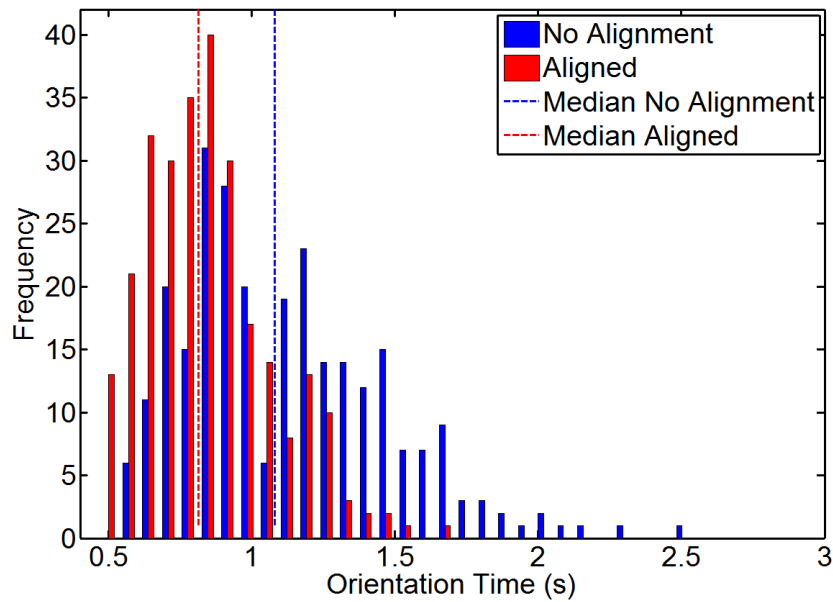


Figure 82: Orientation Time Alignment Effect

Blue distribution is observed data without alignment. Red distribution has alignment of both the sensor and aircraft displays and is shifted left of the blue data.

Orientation Time vs. Movement (Observed Data)
Exp. 3, 16 Subjects, Nov 15 - Dec 15

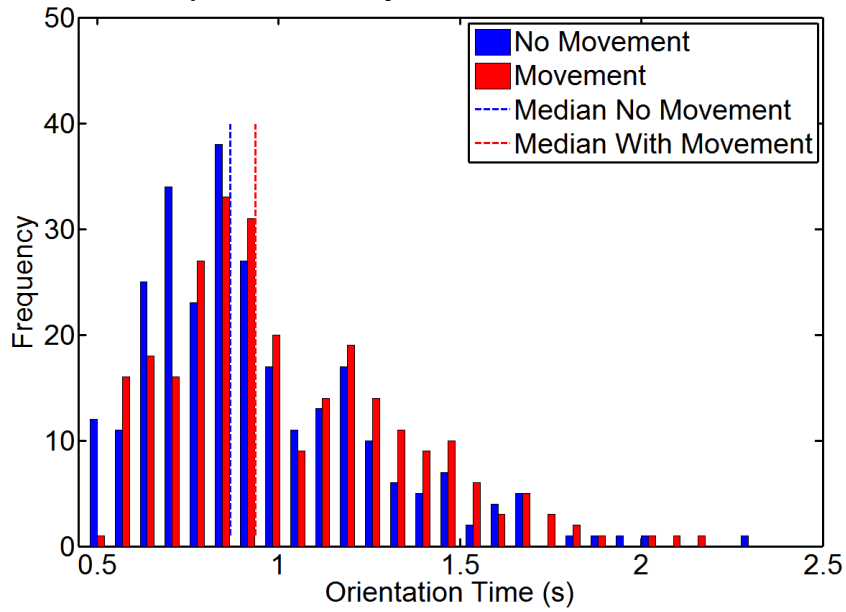


Figure 83: Orientation Time Moving Target Effect
Blue distribution is observed data with a stationary target. Red distribution is observed data with a moving target and is shifted right of the blue data.

Orientation Time vs. Integration (Observed Data)
Exp. 3, 16 Subjects, Nov 15 - Dec 15

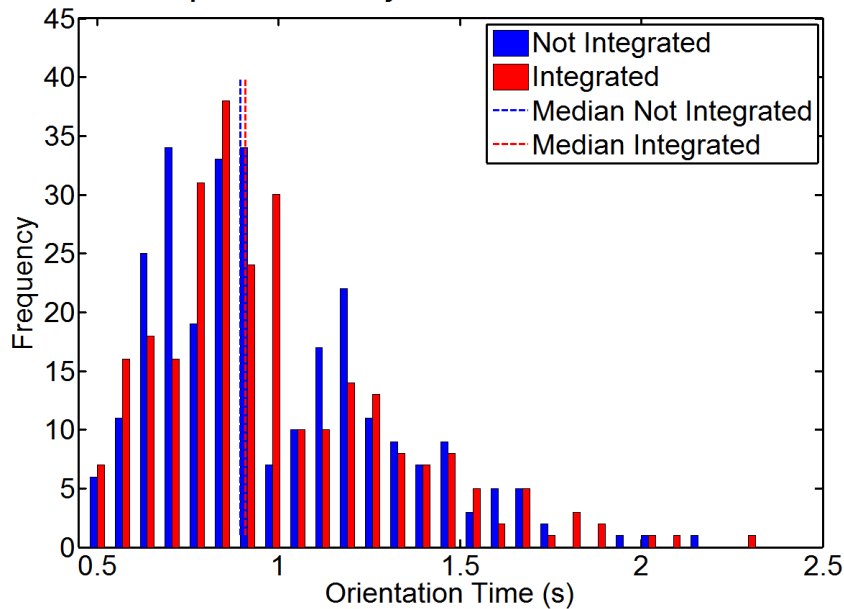


Figure 84: Orientation Time Integration Effect
Blue distribution is observed data with separate displays. Red distribution has a single integrated display. These distributions did not reveal a statistical difference.

Once again, these display techniques and the moving target scenario effects were inspected for their influence on error rates (percentage of orientation answers, for the entire experiment, which were wrong). Figure 85 shows a large decrease in error rates with the reference frame alignment technique and a smaller but noticeable increase with the moving target task; however, no decrease is evident with display integration. In fact, a small, but likely insignificant, increase in error was observed on integrated displays compared with separate displays.

These orientation time results continued to highlight the multiple reference frame challenge which was characterized in experiment 1 and they demonstrated a significant reference frame alignment effect mitigating that challenge, which supported the reference frame alignment hypothesis (#1). However, no integration effect or interaction was observed and no moving target interaction with reference frame alignment was observed, so the integration and moving target-alignment hypotheses were not supported here.

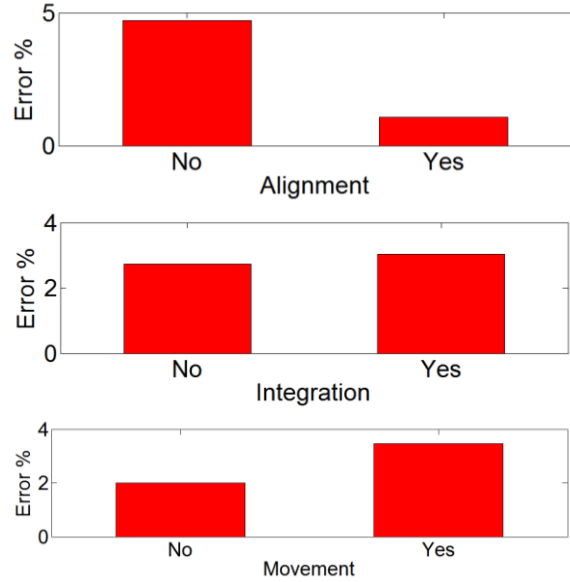


Figure 85: Orientation Errors vs. Alignment, Integration, and Moving Target Tasks

6.5.2.2. Experiment 3 Target Acquisition Time Results

As in all simulator experiments, this target acquisition time was measured from the start of the simulation until the subject identified the target location. If the subject misidentified the target, that time was not included in this regression analysis. This process was described as a weapon release to encourage the subject to take the accuracy requirement seriously. The regression model for target acquisition time, developed from experiment 3, is shown in Equation 9. Estimates of these effects are shown in Table 14. While orientation time represented a basic measurement of the multiple reference frame challenge, target acquisition time measured a broader impact of that challenge. Here, more than a simple orientation task was required. Subjects had to follow descriptions of the target area or complete imagery rotations between the target satellite image and the observed sensor video in order to locate a target in the sensor video scenery. The revealed orientation time effect from the previous section would likely be multiplied with the increased number of orientation tasks required to complete a target acquisition task. Furthermore, this was very representative of an actual unmanned aircraft surveillance task. Display integration and initial angle had no significant effect on target acquisition time, so they do not show up in the regression model.

$$TAT'_{e3} \approx \beta_0 + \beta_1 * X_{align} + \beta_2 * X_{trialNum} + \beta_{3i} * X_{subject_i} + \beta_{4m} * X_{image_m}$$

$$i = 1:16 \text{ subjects}, m = 1:4 \text{ images}$$

Equation 9: Target Acquisition Time Regression Estimation

Table 14: Experiment 3 Target Acquisition Time Predictor Variable Coefficients

Predictor Variable	Term	Transformed Regression Estimate	Lower 95% Conf. Interval	Upper 95% Conf. Interval	t-stat	p-value	Reverse Transformed Estimate (β')	units
(Intercept)	β_0	10.55	9.57	11.53	21.12	<1E-10	3.41	s
Xalign	β_1	-0.53	-0.81	-0.26	-3.80	1.77E-04	-0.55	s
XtrialNum	β_2	-0.043	-0.071	-0.015	-3.01	2.86E-03	-0.041	s/#
Display integration, initial angle, and all interactions were tested, but they did not meet the 0.05 significance requirement for inclusion in this regression.								

This regression model is much simpler than the orientation time model from the previous section. Here, only alignment and the learning effect (trial number) remain in the model as fixed effects. There is still a subject effect and now an image effect, but neither of these interact with the main effects. So once again, reference frame alignment demonstrates an increased effectiveness over the baseline orientation aid display. Here, aligning the reference frame allows the subject to locate the car faster by approximately ½ second at the median of the distribution.

Interestingly, initial angle (XinitAngle) is not a factor in the experiment 3 regression model even though it had a large impact in experiment 1. This could indicate that subjects in experiment 3 were not performing the same method of imagery rotation as that used in experiment 1. As a reminder, this initial angle was the rotation between the sensor display and the north-up reference frame. The targets in experiments 3 (and 4) were all along a single cardinal direction from a central intersection, while the experiment 1 targets often involved more complicated textual descriptions. In this way, experiment 1 may have encouraged a more involved imagery rotation to determine relationships between objects and experiments 3 and 4 only required the subject to complete one rotation on the image to determine the basic cardinal orientation.

The imagery effect revealed with this model could contradict this simplified understanding of the subject’s initial rotation task, because it indicates a difference in target acquisition time based on which of the four target scenarios were involved in any given trial. However, this effect on target acquisition time could also be a function of the varied distance from initial crosshair placement to the car’s location as demonstrated by Figure 86. This likely confound could not be corrected with a simple inclusion of this distance because some subjects used an accelerated crosshair movement for the more distant targets and others used a consistent pace of crosshair movement regardless. For this reason, the distance from crosshair to initial target location was not included in the model and this entire effect was included in the image effect coefficient.

“Car approaching intersection
from the NORTH”



“Car approaching intersection
from the WEST”



Figure 86: Example Target Images from Experiment 3

These images demonstrate the different relative location between the initial crosshair placement and the target vehicle. The right image has a longer distance between the crosshairs and vehicle. [Image ©Google]

These results show no interaction with the alignment effect; however, the learning effect does grow in significance to become more substantial than the alignment effect by the end of an experiment. With 17 trials, the regression model learning effect could grow to nearly 0.7 seconds ($17 \text{ trials} * 0.041 \text{ s/trial} = 0.7\text{s}$). However, the lack of interaction terms indicates that this did not measurably decrease the effectiveness of alignment. So, despite the fact that subjects were becoming increasingly capable at the target acquisition task, this did not decrease the measurable effect of alignment. This large learning effect is most likely due to the repeated nature of the target descriptions. Experiment 3 used a very repeatable target description with the target always identified as a car approaching an intersection from one direction. This consistency may have led subjects to develop new techniques as they realized the pattern of descriptions. This explanation of the learning effect is not reinforced with experiment 4 so further investigation is required to understand the rather large magnitude of the learning effect observed here.

The regression results are consistent with the observed distribution changes evident in Figure 87 and Figure 88 (larger versions are available in Appendix E: Experiment 3 Data Analysis). Figure 87 demonstrates the slight shift in the median target acquisition time when alignment is applied to the displays. The tail of the distribution is affected by the alignment effect; however, in this example one distant outlier is included with an aligned display. Despite this outlier, an overall alignment effect is still measured and advantageous in nature. The longer time period for this one particular data point should be understood in relation to the error rate effect.

Once again, the alignment effect decreased the observed error rate (percentage of target location answers, for the entire experiment, which were the wrong target) when subjects were searching for and selecting a target. These data are shown in Figure 89. The accuracy requirement of this task was intended to replicate that of a weapons employment task. None of the subjects had experience

operating unmanned aircraft, but it is still noteworthy that the alignment effect produced such a large decrease in error rate. With this in mind, the “outlier” in Figure 87 could represent an area of missing data from the answers without alignment. Since errors were not included in the regression analysis, or these plots of target acquisition time, correct but slow answers may appear as outliers. Since including this data point did not affect the conclusions of the regression analysis, it remains in the model.

Similarly to orientation aid, target acquisition time data did not show a significant effect of display integration. This is shown in Figure 88 with two very similar distributions. In fact, the median time required to find a target with an integrated display is actually higher than that of a non-integrated display. However, this too is not statistically significant, according to the regression analysis, so essentially integration demonstrated no measureable impact on target acquisition time. This does not directly support any of the hypotheses, but does imply that integration could be a viable display option for these separate tasks.

Tgt Acquisition Time vs. Alignment (Observed Data)
Exp. 3, 16 Subjects, Nov 15 - Dec 15

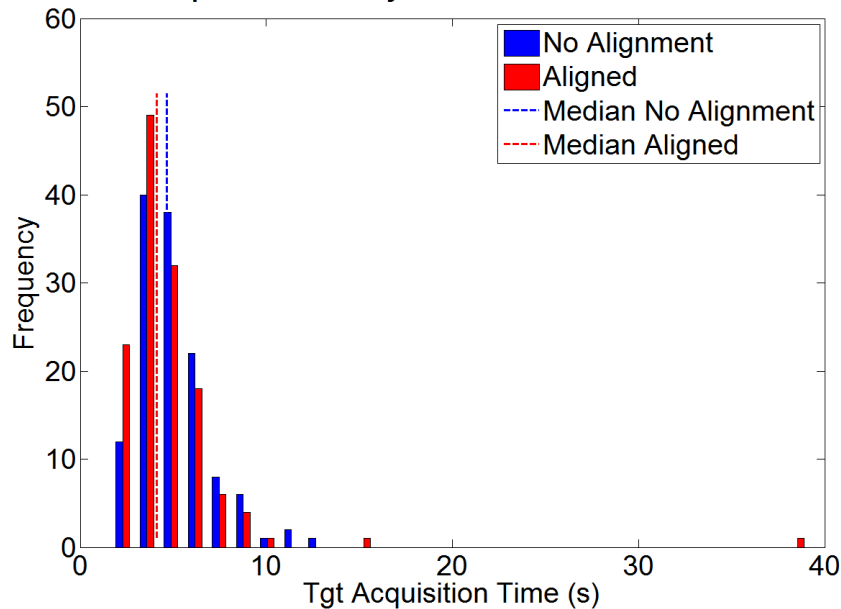


Figure 87: Target Acquisition Time Alignment Effect
Blue distribution is observed data without alignment. Red distribution is observed data with alignment of both the sensor and aircraft displays and includes the outlier out near 40 seconds. Despite this outlier the alignment effect is still evident with the shift in the distribution median.

Tgt Acquisition Time vs. Integration (Observed Data)
 Exp. 3, 16 Subjects, Nov 15 - Dec 15

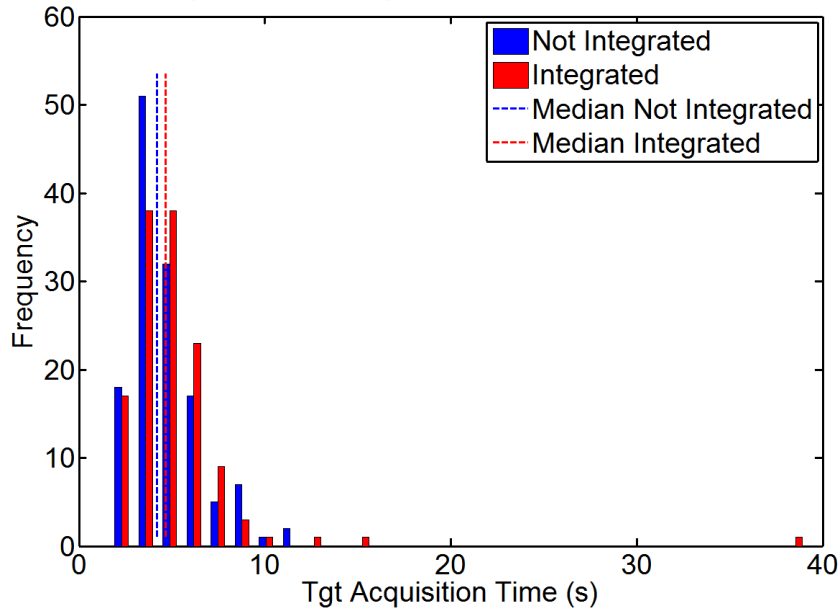


Figure 88: Target Acquisition Time Integration Effect
 Blue distribution is observed data with separate displays. Red distribution has a single integrated display. These distributions did not reveal a statistical difference.

Once again, both of the error rate comparisons are provided in Figure 89. As mentioned, the alignment technique decreased error rates while the integration technique actually increased error rate. This increase in target acquisition accuracy associated with reference frame alignment should also be considered a benefit of this display technique in addressing the multiple reference frame challenge.

These target acquisition time results demonstrated a significant impact of the multiple reference frames on the target acquisition task, and they demonstrated a reduction of that effect with the reference frame alignment. This supported the reference frame alignment hypothesis (#1). However, no effect was measured from the display integration technique; therefore, the display integration hypothesis (#4) was not supported with this work. The moving target-alignment hypothesis (#5) was not evaluated with the target acquisition task since all targets were stationary in the initial portion of each trial.

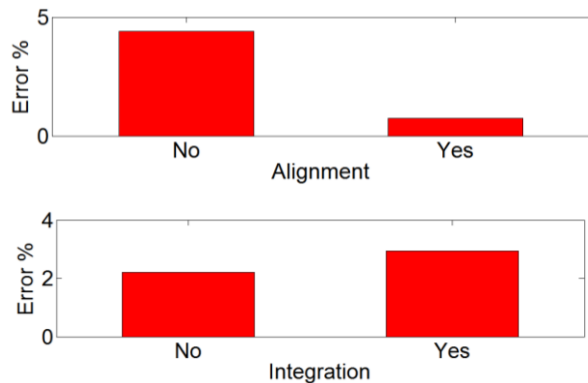


Figure 89: Target Acquisition Errors vs. Alignment and Integration

6.5.2.3. Experiment 3 Tracking Task Results

Since the experiment 3 results showed minimal effects of interest for flight path error or sensor track error, their results are combined in this section. These terms were both analyzed as a root mean squared error for each individual run. After transformation, the regression analyses resulted in the models shown in Equation 10 and Equation 11.

Neither of these measures revealed any direct impact of reference frame alignment or display integration on tracking performance. However, reference frame alignment indirectly affected flight path error through the initial alignment of the sensor video. This was manifest as an initial angle term in the regression estimation of flight path error. This is interesting because the initial angle was measured as the angle from the north-up reference frame to the sensor display reference frame. In this way, an aligned display would always have an initial angle of zero. While this has no direct influence on flight path guidance, since the angle was measured from the sensor video, the angle was directly related to initial aircraft heading. Since the aircraft always initialized on the predefined flight path in a counterclockwise orbit, an initial heading of west indicated that the aircraft initialized on the north side of the target. In this way the initial angle effect shown here is likely capturing the increased difficulty, without alignment, of controlling the aircraft when it is headed south. When the aircraft is headed south, error compensation is reversed when relying on the navigation display. This loss of display-control compatibility is restored if the display follows the reference frame alignment technique because the stick twist control input did not rely on a reference-frame-rotation task.

This seems reasonable given these data; however, a large number of subjects were observed rotating their heads to determine the left/right bank decision. Several clearly showed signs of maintaining a cognitive representation of the aircraft-view reference frame even though none was displayed on the screen. These observations cast doubt on the effect demonstrated in Equation 10 and Table 15.

It is clear, however, that target movement produced a significant effect on all three of these tracking error measurements. This was expected for the sensor track error, but somewhat surprising for the flight path error. The target movement changed the flight path task by adjusting the predefined flight path to keep the actual target centered at all times. Throughout an entire trial this was evident on the navigation display; however, the main impact is likely due to the increase in task difficulty for the sensor tracking task. As this task became more difficult it is likely that subjects diverted attention away from the flight path tracking task and concentrated more on the sensor tracking task.

$$FPE'_{e3} \approx \beta_0 + \beta_1 * Xmove + \beta_2 * XinitAngle$$

**Equation 10: Flight Path Error Regression Estimation
Only initial angle and target movement are included**

$$STE'_{e3} \approx \beta_0 + \beta_1 * Xmove$$

**Equation 11: Sensor Track Error Regression Estimation
No display design terms remained in the model**

Table 15: Experiment 3 Flight Path Error RMSE Predictor Variable Coefficients

Predictor Variable	Term	Transformed Regression Estimate	Lower 95% Conf. Interval	Upper 95% Conf. Interval	t-stat	p-value	Reverse Transformed Estimate (β')	units
(Intercept)	β_0	-0.04	-0.04	-0.04	-63.37	<1E-10	-3.19	RMSE
Xmove	β_1	1.17E-05	7.73E-07	2.27E-05	2.10	3.59E-02	1.08E-05	RMSE
XinitAngle	β_2	6.21E-03	4.55E-03	7.88E-03	7.33	<1E-10	4.57E-03	RMSE/deg

Alignment, display integration, trial number, subject, and all interactions were tested, but they did not meet the 0.05 significance requirement for inclusion in this regression.

The lack of display integration impact, once again, reinforces the opportunity to include this as a potential display design tool. This could be especially helpful in systems with smaller control stations and reduced display sizes. Although there was no demonstrated improvement, the ability to convey the same information on one single display rather than 4 separate displays could prove helpful in system design.

Since experiment 3 and experiment 1 both included the traditional display, these data also provided an opportunity to qualitatively examine the effectiveness of the predictive aid. These flight path errors are shown in Figure 90. This figure is a qualitative comparison of the flight path error data from experiment 1 and experiment 3. Despite the more complex tasks involved in experiment 3, such as moving targets and aircraft turbulence, the predictive aid increased the performance of the flight path control task. This provides a qualitative confirmation that the predictive aid assisted with the flight path tracking task.

**Flight Path Error vs. Predictive Aid(Observed Data)
Exp. 1 & 3 Display Configuration A**

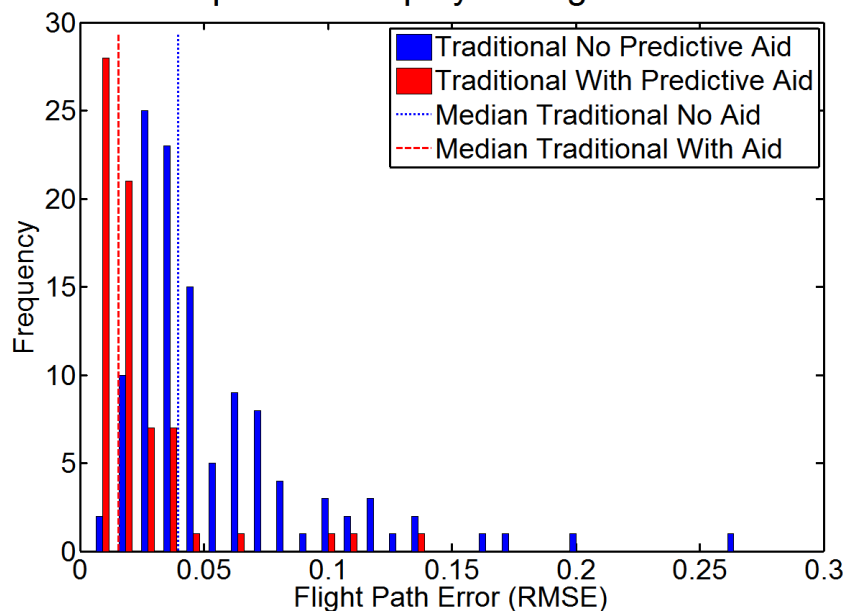


Figure 90: Predictive Aid Effect on Flight Path Error across Experiments 1 and 3
Blue distribution is observed data without predictive aid. Red distribution has the predictive aid and is shifted left of the blue data.

These tracking error results on the aircraft, sensor, and a combine measure fail to support any of the hypotheses for experiment 3. These results demonstrate a neutral effect of reference frame alignment and display integration on tracking performance. As stated, the initial angle effect on flight path error shows some potential of reference frame alignment, but this would need further investigation to ensure it represents a true alignment effect.

6.5.3. Experiment 3 Workload Measures

6.5.3.1. Experiment 3 Bedford Workload Rating Results

After each individual trial, subjects were asked to provide an assessment of the mental workload observed during that trial. The subjects provided a rating from 1-10 in accordance with the Bedford workload rating scale in Figure 43. This subjective workload was split into two measurements to account for the transition from static (stationary) to dynamic (moving) targets halfway through each trial. The static workload measurement included target acquisition, tracking, orientation, and reaction time tasks, but the dynamic workload measurement only included tracking, orientation, and reaction time tasks. These results were analyzed with a Kruskal-Wallis rank test to evaluate a difference in the distribution of these ordinal data. The raw data are plotted in Figure 91 and Figure 92 with respect to the two display techniques. Neither figure provides a clear indication of an effect of these display techniques: reference frame alignment and integration. Figure 91 shows a noticeable decrease in workload, but still includes some higher ratings for the aligned displays.

Bedford Workload vs. Alignment (Observed Data)
Exp. 3, 16 Subjects, Nov 15 - Dec 15

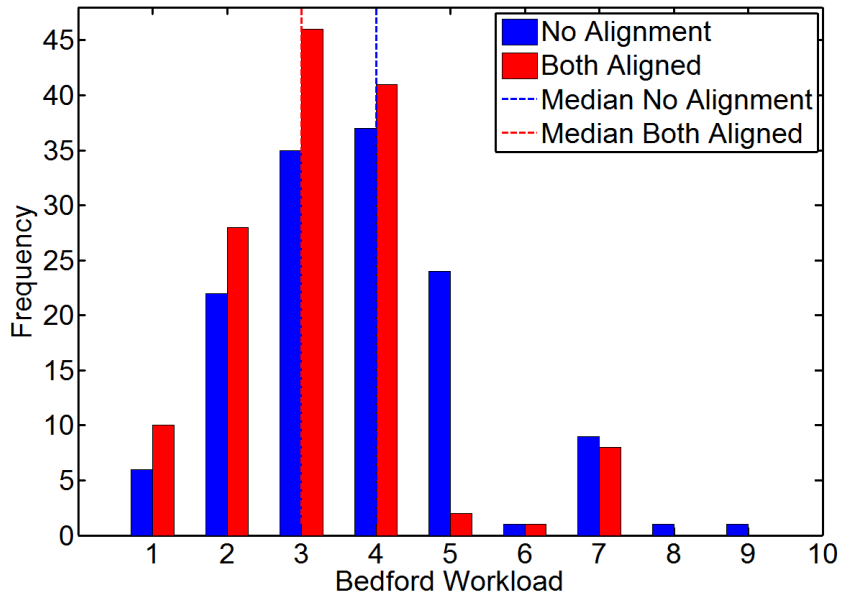


Figure 91: Reference Frame Alignment Effect on Bedford Workload
Blue distribution is observed data without alignment. Red distribution has alignment of both the sensor and aircraft displays and is shifted left of the blue data.

Bedford Workload vs. Integration (Observed Data)
Exp. 3, 16 Subjects, Nov 15 - Dec 15

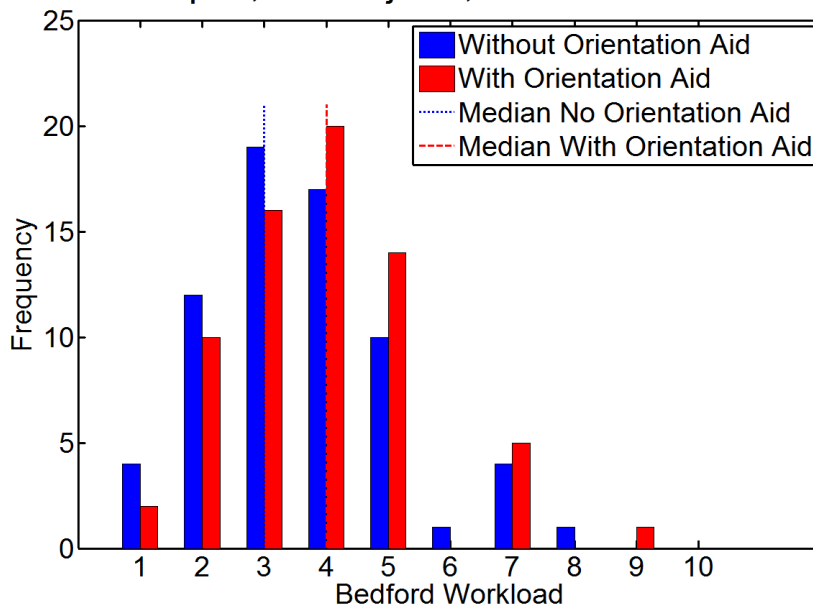


Figure 92: Integration effect on Bedford Workload Rating
Blue distribution is observed data with separate displays. Red distribution has a single integrated display.

A more interesting understanding is uncovered in the pairwise rank test comparisons presented in Table 16. These data show comparisons of every display configuration in experiment 3 (see 6.3). Here the first indication of an interaction between reference frame alignment and display integration is revealed. Contrary to hypothesis 4, this effect, as shown in Table 16, revealed a reduction in workload when reference frame alignment was applied and display integration was removed. This was the comparison between display configuration D (Sensor and Aircraft Aligned) and B (Sensor Aligned) with results shown in column 5 of the results. This effect was evident across both the moving and static target workload measures.

Additionally, these comparisons reveal information, for the first time, relevant to the moving target-alignment hypothesis (#5). This hypothesis anticipated an interaction effect between reference frame alignment and the moving target task. Here, in the subjective workload measure, a significant effect of reference frame alignment (without integration effects) is only evident when the moving target task is included. This is shown in the second column of results in the comparison between display configuration E (Integrated) and F (Aligned and Integrated). This could indicate a small reference frame alignment on workload which is only measurable as the task difficulty increases with the moving target requirement.

Table 16: Experiment 3 Subjective Workload Rating Results

These are the results of Kruskal-Wallis rank tests for pairwise comparisons of displays based on the subjective workload rating (Bedford Workload Scale shown in Figure 43). Green indicates a significant difference with a family significance of 0.05 Bonferroni corrected to 0.008.

A – misaligned / separate D – aligned / separate E – misaligned / integrated F – aligned / integrated		Adding Reference Frame Alignment		Adding Display Integration		Interaction Effects	
		Display	Display	Display	Display	Display	Display
		A ≠ D	E ≠ F	A ≠ E	D ≠ F	E ≠ D	A ≠ F
Bedford Workload Static Target (1-10)	Chi-sqr	2.90	6.92	1.35	0.30	8.68	1.64
	p-value	0.09	0.01	0.24	0.58	3.21E-03	0.20
Bedford Workload Dynamic Target (1-10)	Chi-sqr	5.82	12.37	0.88	1.48E-03	11.60	6.42
	p-value	0.02	4.36E-04	0.35	0.97	6.58E-04	0.01

The subjective workload ratings provide evidence of alternative effects than those discovered in the performance measures. However, they do not contradict any of the effects previously discussed. Although each of the hypotheses addresses performance, these workload results can indirectly support or oppose hypotheses based on the workload impact. With that in mind, the significant effect of reference frame alignment on subjective workload supports the reference frame alignment hypothesis (#1). Additionally, the moving target-alignment hypothesis (#5) is supported because the significant alignment effect on subjective workload is only measured with the moving target task.

The reference frame alignment hypothesis (#1) is supported because a reference frame alignment effect is observed when comparing integrated display configurations E (Integrated) and F (Aligned and Integrated). Some additional support is supplied when comparing display configurations E

(Integrated) and D (Sensor and Aircraft Aligned) because an improvement is noted with alignment even though integration is removed. The moving target interaction anticipated with hypothesis 5 is supported because a measurement is revealed during moving target tasks, but this was not apparent with the static task.

The opposition to a display integration effect (hypothesis 4) is more complicated. As shown in Table 16 the reference frame alignment had no measureable impact when applied to separate displays in display configuration A (Traditional) and D (Sensor and Aircraft Aligned). However, when the same effect was added in combination with removing display integration (going from display configuration E: Integrated to D: Sensor and Aircraft Aligned), a noticeable improvement was measured. This indicates that a decrease in workload from reference frame alignment was added to an increase in workload from display integration. Although both had minimum effects independently, when their effects were combined this experiment was able to measure the impact.

This section presented the subjective workload measures which could degrade into a measure of the subject’s frustration, so it is important to look for confirmation of these findings in the objective secondary workload measurement. These reaction time results are presented in the next section.

6.5.3.2. Experiment 3 Reaction Time Results

The reaction time test provided a secondary task objective workload measurement. Here subjects responded to a blinking visual light with a trigger squeeze.

$$RT'_{e3} \approx \beta_0 + \beta_1 * XdispInt + \beta_2 * Xalign + \beta_3 * XtrialNum + \beta_4 * Xmove + \beta_5 * XtrialNum * Xmove + \beta_{6i} * Xsubject + \beta_{7i} * XtrialNum * Xsubject_i + \beta_{8i} * Xmove * Xsubject_i$$

$$i = 1:16 \text{ subjects}$$

Equation 12: Reaction Time Regression Estimation

Table 17: Experiment 3 Reaction Time Predictor Variable Coefficients

Predictor Variable	Term	Transformed Regression Estimate	Lower 95% Conf. Interval	Upper 95% Conf. Interval	t-stat	p-value	Reverse Transformed Estimate (β')	units
(Intercept)	β_0	-0.21	-0.28	-0.15	-6.82	<1E-10	-0.30923	s
Xdisplnt	β_1	4.19E-02	2.86E-02	5.53E-02	6.18	1.27E-09	3.79E-02	s
Xalign	β_2	-2.37E-02	-3.70E-02	-1.04E-02	-3.49	5.19E-04	-2.37E-02	s
XtrialNum	β_3	-3.88E-03	-7.01E-03	-7.57E-04	-2.44	1.50E-02	-3.76E-03	s/#
Xmove	β_4	1.23E-02	-1.47E-02	3.94E-02	0.89	0.37	1.16E-02	s
XtrialNum*Xmove	β_5	2.57E-03	1.63E-04	4.98E-03	2.10	3.64E-02	2.46E-03	s/#
Initial angle, image, and other interactions were tested, but they did not meet the 0.05 significance requirement for inclusion in this regression.								

The reaction time regression model, shown in Table 17 and Equation 12, shows the effect of reference frame alignment, but also an impact of display integration. While the subjective ratings

discussed earlier showed signs of a negative display integration effect, the secondary task measurements confirm this with a measurable impact of display integration. This is contrary to display integration hypothesis (#4) because the display integration impact is increasing the reaction time, and therefore indicates an increased workload with an integrated display. Initial angle and image had no significant effect on reaction time, so they do not show up in the regression model.

Since these reaction time data are tightly grouped, it is difficult to observe either of these effects in Figure 93 or Figure 94, but the basic shift in median values is evident. The regression model is able to account for the subject effect, moving target effect, and trial number (learning) effect to reveal the underlying integration and reference frame alignment effects. Neither of these regression terms interacts with any of the other terms. All of the other terms included in this model can be thought of as nuisance terms with respect to display integration or alignment. In this way, the secondary measurement offers a much clearer understanding of the impact of these display techniques on workload. These results demonstrated a reference frame alignment benefit to secondary workload which indirectly supports the reference frame alignment hypothesis (#1). However, these data oppose the display integration hypothesis (#4) with the display integration effect.

Reaction Time vs. Alignment (Observed Data)
Exp. 3, 16 Subjects, Nov 15 - Dec 15

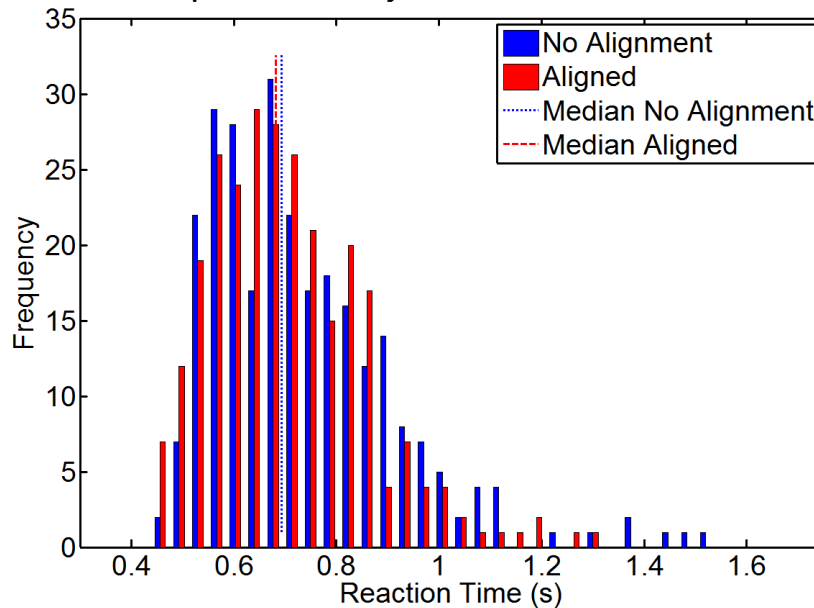


Figure 93: Reaction Time Alignment Effect
Blue distribution is observed data without alignment. Red distribution has alignment of both the sensor and aircraft displays and is shifted left of the blue data.

Reaction Time vs. Integration (Observed Data)
 Exp. 3, 16 Subjects, Nov 15 - Dec 15

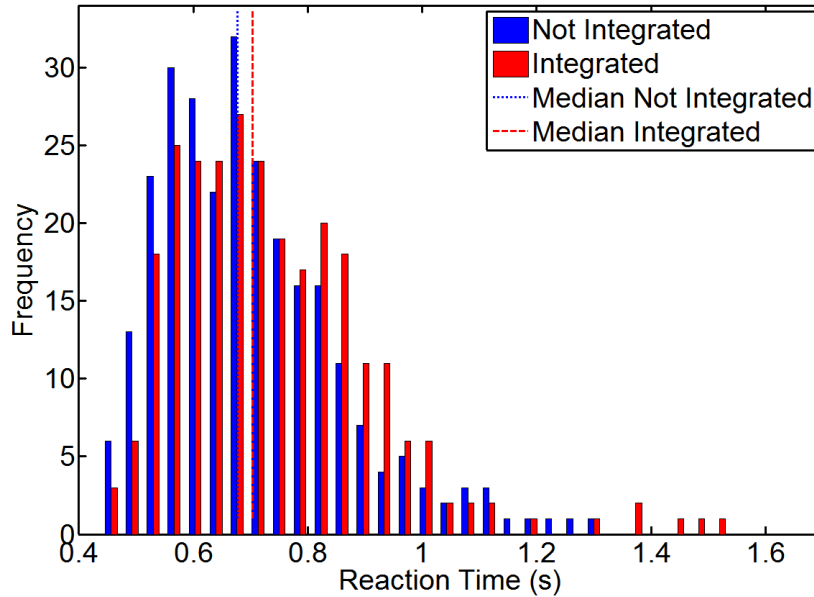
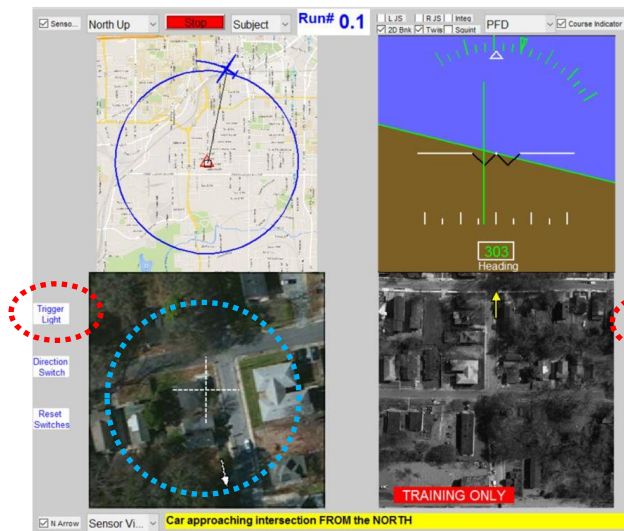


Figure 94: Reaction Time Integration Effect

Blue distribution is observed data with separate displays. Red distribution has a single integrated display.

While these results offer a powerful observation regarding display integration, they should only be considered in light of the specifics of this reaction time measurement. As shown in Figure 44 and more specifically here in Figure 95, the “trigger light” location may have played a role in this perceived impact. This light was used for the visual reaction time measurement. It was relocated to the periphery of the display for experiment 3 and 4 to allow for the integrated display configuration; however, this relocation put the indicator near the sensor display which may have decreased reaction time results with the separate display over those with the integrated display. Since the sensor display was the primary focus of most subjects (teal circles in Figure 95), especially with the moving target tasks, the displacement between the crosshairs on the sensor display and the “trigger light” could have influenced subject reaction time.

Display Configuration A



Display Configuration E

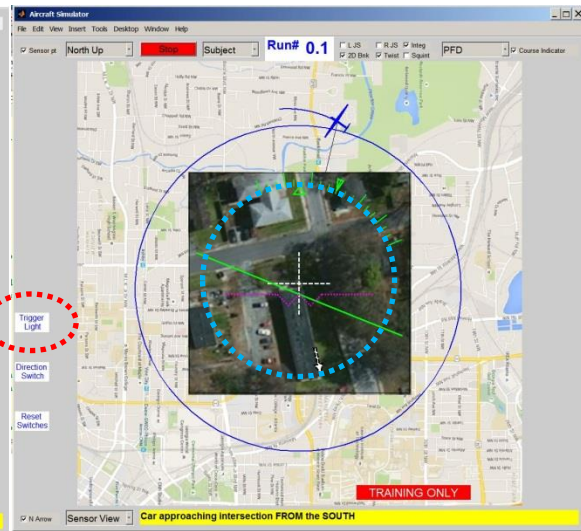


Figure 95: Trigger Light Location near Sensor Display
Red ovals highlight the location for the “trigger light” which would initiate a reaction time test during simulator experiments. The teal dashed circles indicate the central visual focus of a subject during each experiment. [Map Data and Image ©Google]

6.5.4. Experiment 3 User Preferences

6.5.4.1. Experiment 3 Subjective Ranking Results

After completion of the entire experiment, during the post-experiment questionnaire, each subject was asked to provide a ranking of the four displays from one to four, with one as the best and four as the worst. These results are all provided in Appendix G: Subjective Response Data.

These data were collected to capture the subject’s preference regarding the displays and does not necessarily represent a significant workload or performance benefit from any particular display. Here, as displayed in Table 18, they reinforce most of the findings from experiment 3. Based on these results, subjects clearly preferred reference frame alignment, but were indifferent to display integration. These user preferences support the reference frame alignment hypothesis (#1), but these 1-4 rankings did not allow subjects to provide any relative comparison between differences. If two displays nearly tied for first and another two tied for last, the subject still had to provide 1 to 4 rankings. In the final experiment another technique was added to allow subjects to better characterize their understanding of the difference between each display. However, with these available data, the reference frame alignment effect was certainly significant with regards to these subjects’ display preference.

Table 18: Experiment 3 Subjective Ranking Results

These are the results of Kruskal-Wallis rank tests for pairwise comparisons of displays. Green indicates a significant difference with a family significance of 0.05 Bonferroni corrected to 0.008.

A – misaligned / separate D – aligned / separate E – misaligned / integrated F – aligned / integrated		Adding Reference Frame Alignment		Adding Display Integration		Interaction Effects	
		Display	Display	Display	Display	Display	Display
		A ≠ D	E ≠ F	A ≠ E	D ≠ F	E ≠ D	A ≠ F
Rankings (1-4)	Chi-sqr	10.75	16.35	3.65E-03	2.02	10.15	15.89
Kruskal-Wallis	p-value	1.05E-03	5.26E-05	0.95	0.15	1.44E-03	6.70E-05

6.6. Experiment 3 Limitations

This experiment includes similar limitations to experiment 1. These results are limited based on the collection methods. The population of subjects for this experiment (characteristics available in Appendix B: Subject Characteristics) were mostly graduate and undergraduate MIT or Harvard students with no experience operating unmanned aircraft. This could influence the results toward displays that would not be easily managed by an experienced unmanned aircraft pilot or sensor operator, but rather tailored for a particular sort of college student.

Additionally, the short time associated with each individual run was not indicative of actual surveillance tasks which could span hours tracking the same target. This could mask potential vigilance issues with the display techniques. If a display included features which a subject could manage for minutes at a time but would prove challenging or impossible for long periods, this would not be discovered with this experiment.

Finally, only lateral navigation (aircraft bank angle) was controlled by the subject during these experiments. These results do not support sweeping changes to unmanned aircraft in general, but apply directly to the on-station surveillance time. It would be inappropriate, for instance, to advocate display changes for takeoff and landing based on these results alone. While not an exhaustive list these were evaluated as the most applicable limitations to these data and corresponding results and conclusions.

6.7. Experiment 3 Conclusions

Experiment 3 reinforced findings previously discovered in experiment 1, that reference frame alignment was more effective than basic orientation aids at addressing the multiple reference frame challenge. Since experiment 3 included orientation aids on every display configuration the multiple reference frame impact and the corresponding reference frame alignment technique effect were more difficult to measure; however, this allowed for a better understanding of this display technique’s influence on currently available systems. Since orientation aids are used throughout surveillance systems, this technique provides more informative results to guide future research efforts. This experiment included analysis of the display integration technique along with the reference frame alignment technique. It also included the more complex sensor tracking task of a moving target. Finally, the addition of a flight path predictive aid was included across all four experiment 3 display configurations.

In spite of the orientation aid limitation, reference frame alignment continued to produce a significant impact on nearly every performance and workload measure which supported the reference frame alignment hypothesis (#1). These results included a basic sensor video orientation task where median orientation time was reduced by 1/4 second, and a more complex sensor target acquisition task where median time was reduced by 1/2 second. This is a smaller impact than that observed in experiment 1, but here in experiment 3 the targets involved simplified descriptions that would have required fewer individual orientations. This resulted in a smaller additive effect of orientation time on target acquisition time.

Once again, and possibly more significant than the faster orientation or target acquisition times the reference frame alignment decreased the error rate (percentage of incorrect answers for the entire experiment) of both these tasks. Orientation time error rate was reduced from 4.7% to 1.1% despite the fact that orientation aids were included on each display, and target acquisition error rate was reduced from 4.4 to 0.7% with the reference frame alignment technique. These are important because errors at either of these tasks could have significant implications on operational effectiveness.

In this experiment the reference frame alignment effect was also observed on the aircraft flight path tracking task through the initial alignment angle of the sensor video. This could represent a workload effect because misalignment of the sensor video seemed to cause increased errors in flight path tracking; however, since the initial angle sensor angle was a function of initial aircraft position this could also represent the aircraft control transformation problem. Since the subject had to determine required bank angle from a north-up navigation display, the initial aircraft heading could have affected the difficulty of aircraft control. Both of these (workload and performance) effects likely combined to produce the small (<1% of orbit radius when initial angle was maximized at 180 degrees) but statistically significant increase in flight path error.

These results confirmed the reference frame alignment hypotheses (#1) because multiple reference frames had an impact on unmanned aircraft operations beyond that addressed by the orientation aid, and the reference frame alignment technique addressed some of this impact.

The display integration technique was less effective than anticipated. Both workload measures actually hinted at a potential increase in workload from the integration of display. This would be contrary to the display integration hypothesis (#4). However, some of the reaction time increase of 0.04 seconds with an integrated display could be explained by the location of the visual cue relative to the primary visual focus area for the subject. These results are also limited by the specific integrated display design used in these experiments. All of the performance measures showed a neutral display integration technique so they failed to support the integrated display hypothesis.

No performance measurement, revealed an interaction between the moving target task and the alignment effect. Only the subjective workload showed evidence of any impact between moving targets and the alignment display technique. These data supported the moving target-alignment hypothesis (#5); however, they were collected at the conclusion of each trial so they also have the memory latency confound embedded unequally in the static target responses. Since the first half of each run involved a static target and the second half involved a moving target, these post trial ratings were provided immediately after experiencing the moving target and almost 2 minutes after the static target experience. These data show that the moving target effect increased the preference for reference frame alignment, as measured by subjective workload (shown in Table 16). These data indicate an area for

additional exploration. Such an effect may be more evident if the moving target task is increased in complexity with a more realistic simulation.

Overall, this experiment reinforced findings from experiment 1 by demonstrating the presence of a multiple reference frame difficulty in unmanned aircraft operations, and the potential for reference frame alignment to address some of that difficulty. This effect was first evident in a basic sensor video orientation task where the subject had to observe movement in the sensor video and describe the direction in the north-up reference frame for communication to ground personnel. Additionally, this impact was also evident in the target acquisition task where subjects were told to find and identify a vehicle approaching an intersection from some cardinal direction. Subjects completing this task on an aligned display were faster than those on a misaligned display. Workload measures based on subjective rating and the secondary reaction time also showed benefits from reference frame alignment. In this experiment, unlike experiment 1, some reference frame alignment effect was even measured in the tracking task performance, specifically the flight path tracking task.

Finally, the predictive aid included on each display in experiment 3 demonstrated an effective improvement in flight path tracking, despite the increased difficulty of the experiment 3 moving target task, when it was compared to experiment 1. The predictive aid architecture included on display configuration F (Aligned and Integrated) highlighted a potential benefit of aligned integration that was carried forward to the following experiment (zoomed view available in Figure 96). Since the integrated and aligned display (display configuration F: Aligned and Integrated) presented the predictive aid as a bank indicator as well it highlighted a potential opportunity to control the aircraft without use of the aircraft display. In fact, all subjects reported that, after training, they ceased to rely on the aircraft display for bank control and relied completely on the curvature of the predictive aid instead. The other display configurations all included the predictive aid, but only display configuration F (Aligned and Integrated) included a bank indicator overlaid as that shown in Figure 96; however, with this knowledge and the subjects' observations of the task, each subject decided to sacrifice some of the precision of the aircraft display and rely solely on the navigation display for the aircraft control task, according to post-experiment questionnaires. This potential display redundancy was explored further in experiment 4 by eliminating the aircraft display in some of the display configurations.

While the reference frame alignment technique continues to show promise, these data do not support any particular benefit of the display integration technique, but they introduce the possibility that this technique could be added to unmanned aircraft displays without measurably decreasing performance. This experiment did hint at potential integration workload penalties which must be



Figure 96: Display Configuration F Predictive Aid
Red arrow highlights predictive aid which estimates aircraft location 10 seconds in the future and provides a direct indication of current bank angle.
[Map Data ©Google]

considered, but display integration could offer additional flexibility on future unmanned aircraft system designs.

This page intentionally left blank.

7. Experiment 4: Redundancy Reduction and Reference Frame Alignment

7.1. Experiment 4 Overview

This experiment sought to provide additional information on the impact of multiple reference frames on the unmanned aircraft scenario. Following the significant results of experiments 1 and 3, the new display technique of display redundancy reduction was evaluated along with the effects of reference frame alignment for their ability to deal with the sensor-view transformation and the aircraft-view transformation.

The aircraft-view transformation required the operator to imagine sitting in the aircraft, visible on the north-up map, and then determine the desired direction of bank control to maneuver the aircraft toward the desired flight path. The sensor-view transformation required the operator to observe motion on the sensor display and determine the cardinal direction of that movement with respect to the north-up reference frame. Experiments 1 and 3 found that these transformations produced significant effects on several performance and workload measures. These experiments also measured a benefit of reference frame alignment for addressing this multiple reference frame difficulty.

In experiment 4, display redundancy reduction was evaluated as a possible supplement to reference frame alignment since the navigation display predictive aid offered an alternative to the traditional aircraft display for controlling aircraft bank. With current systems only considering the predictive aid for basic navigation information and not as a form of bank control, and experiment 3 results highlighting that subjects relied on the predictive aid as a direct measurement for aircraft control, this experiment sought to characterize the impact of relying on the integrated predictive aid as a form of bank control and the continued impact of reference frame alignment on that architecture. This simulator experiment was conducted from December 2015 to January 2016 and involved 16 human subjects.

7.1.1. Experiment 4 Scenario and Tasks

This human subjects experiment followed the same scenario and task set to that of experiment 3, which was similar to experiment 1. For that reason, this section is virtually identical to 6.1.1 and is only included to provide a standalone description of experiment 4.

Once again, moving targets were included in the scenario from experiment 1. The experiment was conducted in the unmanned aircraft simulator with a scenario that required the subject to control an aircraft with an onboard video sensor. As previously described in 3.2.1, the scenario started with a 15 second target-preview time where the subject had the opportunity to read the target description and observe the target area satellite image. All of these scenarios included a description of a vehicle approaching an intersection, similar to the one shown in Figure 97. The right image is an example satellite image from experiment 4. In order to provide a sense of realism, the actual target is not visible in the satellite image. The left image represents the initial view as the simulator is initialized after the 15 second target-preview time. All textual descriptions in this experiment relied on a primary cardinal

selected the wrong target. Five seconds after the subject selected the target, or after the subject found the correct target, the box turned white and became the simulated vehicle.

After initial selection, the subject maintained the sensor display crosshairs on the target, and the aircraft on the flight path. Their tracking performance was recorded in both of these tasks.

Throughout the remainder of each trial, at 10-20 seconds intervals, subjects responded to a reaction time light which was said to inform them of activity in the target vehicle. They responded to this blinking light with the same trigger that was used to identify the target.

After each reaction time test, the subject knew to observe the vehicle for movement. A red asterisk symbol, representing a person exited the vehicle and ran off in a primary cardinal direction of north, south, east, or west. Subjects had to tell ground personnel which direction the suspect fled. They provided this input to ground personnel via the left control stick trim button, as shown in Figure 32. This represented a basic orientation task where the subject had to mentally align the sensor-view reference frame to north-up in order to provide an answer for the direction of travel. This provided the most accurate measurement of the orientation time cost associated with different reference frames, and it was representative of actual mission requirements during unmanned aircraft surveillance.

Halfway through each trial the white rectangular symbol, representing the vehicle, began to translate across the imagery. The subject was expected to track this vehicle as it moved throughout the rest of each trial. The vehicle followed roads in the imagery, but was always presented on top of any features. The vehicle was never masked or occluded in anyway. This was done to create a smooth measure of a subject's tracking performance. Actual surveillance imagery would include masking scenarios as the vehicle drove under trees or behind buildings, and this would add confounding measures to each subject's performance. In order to focus on the reference frame transformation problem, these realistic features of actual surveillance operations were removed to provide a more controlled data collection.

The subject continued with this scenario, and accompanying tasks, for a total of 3 minutes and 12 seconds in order to allow an entire orbit around the target area. At the end of this time, the simulator froze and the subject was asked to provide two assessments of their mental workload during that particular trial. The Bedford Workload Scale, Figure 43, was used for this assessment. One rating was provided for the portion of the mission with a stationary, static, target and another was provided for the moving, dynamic, target. It was possible to provide the same rating for both portions, but subjects were provided the opportunity to distinguish between the two portions.

Unlike experiment 1, experiments 3 and 4 included a turbulence model and inflight winds for the aircraft flight path task. This prevented subjects from stabilizing on a bank angle and abandoning the aircraft control task. Although this did not happen in experiment 1, the predictive aid (discussed in the display configuration) added to the experiment 3 and 4 displays could have provided subjects with this capability. For this reason turbulence and a constant wind were enabled in the simulation so that subjects could not abandon the flight path guidance task.

7.1.2. Experiment 4 Timeline

Experiment 4 followed the same timeline as experiment 3. After initially completing the consent form, subjects completed two basic spatial ability tests. The card rotations test and the Vandenberg

MRT test were both administered before moving on to the simulator portion of the experiment. These tests were chosen because they provided the greatest correlation (out of four considered) with the imagery rotation study in experiment 2. A description of these tests and their results is available in Appendix H: Imagery Rotation Cognitive Process Examination.

Each subject underwent a training period with each of the possible display configurations. After reaching the required training performance on both static and dynamic targets, as described in section 3.4.1, each subject continued on to complete 17 experimental trials. Finally, the subject completed a post-experiment survey with specific questions administered to every subject and a period of open discussion with the researcher. The entire process, for a single subject, lasted 2.5 to 3 hours.

7.2. Experiment 4 Hypotheses

The objective of experiment 4 was to characterize the impact of different reference frames on unmanned aircraft operations, and evaluate the possible mitigation techniques of reference frame alignment and orientation aids. This produced three overall experiment 4 hypotheses.

Hypothesis 1: Reference frame alignment reduces the orientation time required to interpret a display, and consequently increases performance across tasks that require coordination between information usually provided in multiple reference frames.

Hypothesis 5: Moving Target tasks increase the effect of reference frame alignment on the orientation time required to interpret a display.²

Hypothesis 6: Display redundancy reduction reduces the orientation time required to interpret a display, and consequently increases performance across tasks that require coordination between information usually provided in multiple reference frames.

Each of these hypotheses was investigated by modifying the display configurations that each subject used to control the simulator. These display configurations acted as the independent variables during this experiment and are discussed in the next section.

7.3. Experiment 4 Display Configurations (Independent Variables)

The four display configurations used in experiment 4 are described in Table 19 and shown in the following figures. For enlarged versions of these images see Appendix A: Display Configurations. Similarly to experiment 3, but contrary to experiment 1, experiment 4 included the moving target scenario, and predictive aid display enhancement on the navigation display of every configuration. This

² Hypothesis 2, regarding the orientation aid, was only evaluated in experiments 1 and 2. Hypothesis 3 regarding imagery features and symmetry was only evaluated in experiment 2. Hypothesis 4, regarding display integration, was only evaluated in experiment 3.

10 second flight path predictor informed the subjects where the aircraft would be in 10 seconds if the winds and current bank angle remained constant.

Although there are slight differences between all the display configurations in experiment 4 and experiment 1, the naming convention is carried forward to provide consistency and identify the display features of interest. For this reason, two experiment 4 displays are named the same as two experiment 1 displays (A and B) so the reader understands the commonality of the evaluated display features.

In experiment 4, display configuration A (Figure 98) presented the traditional display representation. Here, each display maintained its original reference frame, which required the subject to transform information for the aircraft control and sensor interpretation tasks. The aircraft transformation effect was only measured using flight path tracking performance, but the sensor transformation effect was directly measured via an orientation task within the sensor display. Display configuration B added reference frame alignment to the sensor display, but not the aircraft display. Since experiment 3 results showed a complete reliance on the flight path predictor for bank information, no aircraft display alignment was evaluated in experiment 4.

A degree of this alignment was always available since the predictive aid was displayed on the north-up navigation display; however, bank commands were always provided via tilt of the aircraft control stick during experiment 4. In this way, the subjects always had to consider the direction of the aircraft flight path when determining which way to command bank. The sensor video was rotated to north-up, but the operator could still control the camera pointing in the same manner as the other display configurations. Performance differences between display configuration A (Traditional) and B (Sensor Aligned) were attributed directly to the orientation requirement associated with the sensor-view reference frame. This offered one measurement of the reference frame alignment effect. Just like experiments 1 and 3, any measurable effect represented an effect of reference frame alignment which was greater than the currently used orientation aid because the orientation aid is present in both of these displays. A lack of measurable effect here would indicate that reference frame alignment offered no improvement over the orientation aid technique.

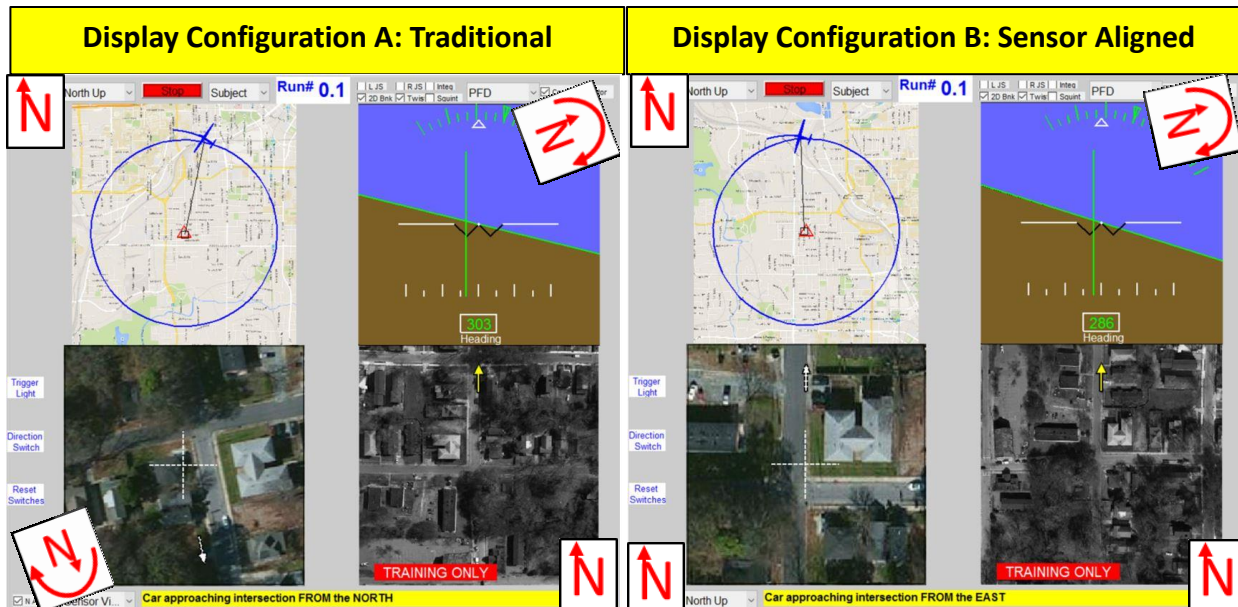


Figure 98: DISPLAY CONFIGURATION A: Traditional
N symbols indicate fixed or rotating north direction.
 [Map Data and Image ©Google]

Figure 99: DISPLAY CONFIGURATION B: Sensor Aligned
N symbols indicate fixed or rotating north direction.
 [Map Data and Image ©Google]

A second measure of reference frame alignment effectiveness, and the corresponding impact of multiple reference frames, was measured by comparing display configurations G (No Aircraft Display) and H (Sensor Aligned, No Aircraft Display), shown in Figure 100 and Figure 101 respectively. Both of these are identical to the first two display configurations, except the entire aircraft display has been removed. Since no altitude control was involved in this simulation, only bank and heading information was relevant on the navigation display with the predictive aid. Comparing these two configurations provided another measure of the multiple reference frame effect as mitigated by the predictive aid, orientation aid, and display redundancy reduction. Here, with all three of these other display techniques, the benefit of reference frame alignment was evaluated for an additional effect. This also provided an opportunity to search for interaction effects between the reference frame alignment and display redundancy effects. Neither of these is representative of an operational system, and many other factors would require consideration when completely eliminating the aircraft display; however, this evaluation measures the change in workload in performance from a simplified crosscheck when redundant information is eliminated from a display. There are other reasons which may require redundant information, but those are not under consideration during these control scenarios.

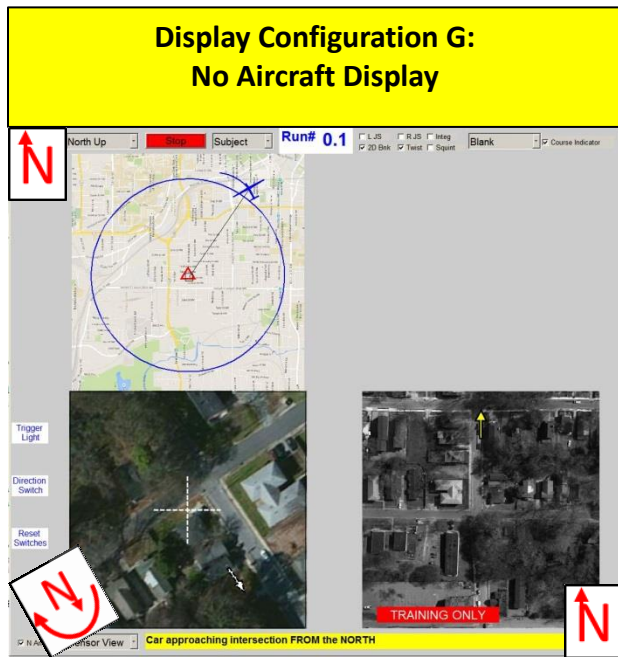


Figure 100: DISPLAY CONFIGURATION G: No Aircraft Display
N symbols indicate fixed or rotating north direction.
 [Map Data and Image ©Google]

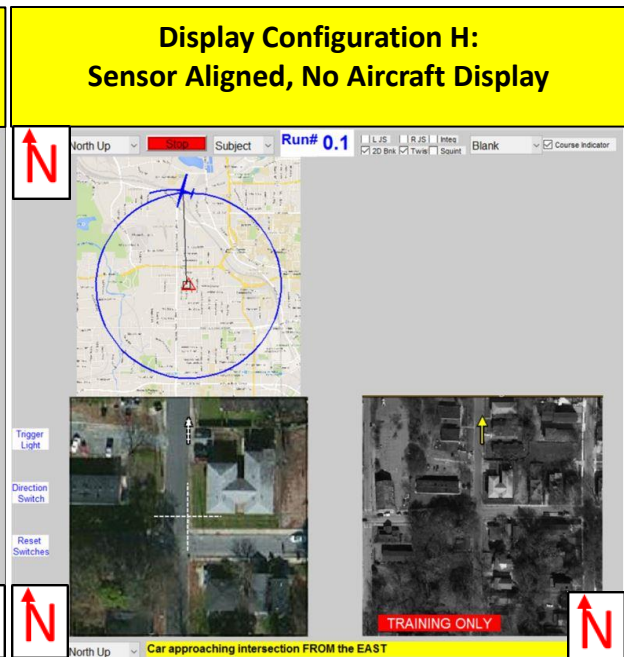


Figure 101: DISPLAY CONFIGURATION H: Sensor Aligned, No Aircraft Display
N symbols indicate fixed or rotating north direction.
 [Map Data and Image ©Google]

Once again, unlike experiment 1, experiment 4 included a predictive aid on the navigation display. This is the blue line protruding from the front of each aircraft symbol on the navigation displays. The current aircraft position is shown along with a 10 second future projection. Additionally, the target description (yellow bar across the bottom of each display configuration) and reaction time cue (top of the three white boxes on the left side of each display configuration) were relocated, compared to experiment 1, to the periphery to continue with the configuration from experiment 3 and allow for integrated display configurations. As this experiment is compared with experiment 1, it may be important to understand these differences in the simulator design.

Table 19: Experiment 4 Display Configurations
 Gray indicates design variables which were explored during this experiment.

Display	A Traditional	B Sensor Aligned	G No Aircraft Display	H Sensor Aligned, No Aircraft Display
Aircraft	Aircraft-View	Aircraft-View	None	None
Navigation	North-Up			
Sensor	Sensor-View	North-Up	Sensor-View	North-Up
Mission	North-Up			
# Reference Frames	3	2	3	2
Reference Frame Alignment	No	Yes	No	Yes
Display Redundancy	Yes	Yes	No	No

As shown in Table 19 and described earlier in this section, experiment 4 focused on reference frame alignment and display redundancy. These rows are highlighted to demonstrate the treatments across the four display configurations of experiment 4. Here, two levels of reference frame alignment and two levels of display redundancy were examined. Rows 2 through 5 of this table describe the reference frame of each of the individual displays: aircraft, navigation, sensor, and mission. These orientations are described as north-up, aircraft-view, sensor-view, or none.

Here, north-up indicates that the north direction is fixed at the top of the displayed information. A traditional map would usually be displayed in the north-up orientation.

The aircraft-view label indicates that the information was displayed with respect to the direction of aircraft travel. Here, the current aircraft heading would always be into the display as if the display represented the frontal view out of the aircraft cockpit.

The sensor-view description indicates that a display shows the representation which would be observed from the sensor location. Here, the top of the display always represents the heading from the aircraft to the sensor pointing location. For instance, if the aircraft were north of the target area, then south would be the direction at the top of a sensor-view image.

Finally, “none” indicates that the display was removed. However, this does not necessarily reduce the number of reference frames because the control inputs were still applied in the aircraft-view reference frame.

The orientations identified in rows 2-5 demonstrate how the number of reference frames was determined. Experiment 4 adjusted the number of reference frames between 2 and 3 because reference frame alignment was only performed on the sensor display. This provided two levels of reference frame alignment treatment and two levels of display redundancy treatment.

Once again, with the understanding provided from experiment 1 and the recurrence in experiment 3, all effects tested in experiment 4 were tested for their effectiveness beyond the orientation aid benefit. In this way, any effects shown here provide an indicator of potential improvements over the current reliance on orientation aids.

7.4. Experiment 4 Dependent Variables

The same performance and workload measurements were used during each simulator experiment. A short description of each is provided here. For a more in depth understanding of each measure, reference section 3.1. Each of these performance measurements evaluated the subject on one of the scenario-dependent tasks. The most direct measure of the transformation difficulty was the orientation time performance. This captured the difficulty of transforming from the sensor display reference frame to the north-up reference frame. However, each of these metrics could be used to demonstrate a difference between the display configurations.

The eight performance and workload measurements collected during experiment 1:

1. **Orientation Time:** this is the time from the movement of the symbol on the sensor video (representing a fleeing suspect), to the subject’s direction answer via the left control stick.

2. **Target Acquisition Time:** this is the time from the start of the simulation until the subject selected the target location via the control stick.
3. **Sensor Track Error:** this is the distance from the sensor crosshairs to the target location normalized by the diagonal distance across the sensor display and analyzed as a cumulative Root Mean Sum Squared Error.
4. **Flight Path Error:** this is the orthogonal distance from the orbit circle to the aircraft location normalized by the radius of the planned aircraft orbit and analyzed as a cumulative Root Mean Sum Squared Error.
5. **Bedford Workload Rating:** this is a subjective workload rating provided by the subject at the conclusion of each trial.
6. **Reaction Time:** this was the response time from the blinking of a light on the display, to the subject's response via the control stick.
7. **Subjective Rankings:** this is a subjective ranking of the four displays, provided by the subject at the conclusion of his or her entire experimental period.
8. **Subjective Ratings:** subjects provided a rating on a scale of 1-10 for each display. The scale was anchored so that a 1 represented the best display and a 10 represented the worst.

7.5. Experiment 4 Results

7.5.1. *Data Analysis Method*

Once again, each of the dependent variables measured during experiment 4 was analyzed independently of one another. When possible a linear regression analysis for the dependent variable as a function of reference frame alignment and display redundancy was conducted. This method accounted for several variables other than simply the display configuration. For each regression analysis, the following independent variables were considered.

Fixed Effects:

1. **Alignment (Xalign):** Categorical reference frame alignment setting describing whether or not the left image was aligned to north-up like the right image (yes or no)
2. **Display Redundancy (XdispRedun) :** Categorical display redundancy setting describing whether or not the display configuration included the aircraft display or not (yes or no)
3. **Initial Angle (XinitAngle):** Angle of rotation, in degrees, between the sensor display and north-up reference frame at the start of an experiment trial
4. **Subject Trial Number (XtrialNum):** Counted up from 1 to 13 as the experiment progressed
5. **Target Movement (Xmove):** Categorical setting describing whether or not the target was moving

Random Effects:

6. **Image (Ximage):** Categorical image number 1 to 4
7. **Subject (Xsubject):** Categorical subject number from 1 to 12

Similarly to experiments 1 and 3, the first five of these variables were considered as fixed effects, while the final two were considered as random effects. This required a mixed-effects linear regression analysis. The image and subject number were considered as random effects because no direct effect of any subject or image involved in this experiment was of interest to the objective. The experimental design minimized these random effects by controlling their presentation across the experimental trials, but it was still important to track the effects of these variables in order to build an appropriate model for the fixed effects. Each regression analysis considered the first four variables as potential predictor variables. With this approach, a significant display design technique, such as reference frame alignment, would show up in multiple regression models to indicate its influence on the dependent variables measured during this experiment.

In addition to the regression analysis, pairwise comparisons were carried out between the specific displays. These were conducted for every dependent variable. For those suited to parametric analysis (1-4 and 6) a pairwise t-test comparison was conducted. Since the three subjective measures (5, 7, and 8) collected during this experiment could not be analyzed with the regression method, they were compared with a Kruskal-Wallis rank test to determine if a difference was measured between the different displays. The regression analysis offered a more complete interpretation of the results, so when possible those are shown in this section and the pairwise comparisons are available in Appendix F: Experiment 4 Data Analysis. Since the subjective measures were not analyzed via a regression analysis, the Kruskal-Wallis rank test results are presented in this section. Each of the following sections discusses one of the dependent variables (1 through 9).

7.5.2. Experiment 4 Performance Measures

Similarly to experiments 1 and 3, each of the performance measurements and the secondary workload measurement (reaction time) were skewed distributions. This was an expected result since each of the measures represented a positive-only minimization for the subjects. For instance, while orientation time could never be negative, values as high as 9.2s (across all 3 experiments) were observed. Any attempt to directly fit these data using a regression analysis would be invalid. For this reason each of these variables were transformed using the Box-Cox transformation procedure. One example of the transformation's effect is shown in Figure 102. Here the top image shows the original skewed orientation time distribution for experiment 4, and the bottom image shows the distribution of the transformed orientation time. For details on any particular transformation used in experiment 4, see Appendix F: Experiment 4 Data Analysis. Since transformation was required for every parametric measure, it is important to reiterate the limitation on interpretation of results. Resulting effects discovered in the regression analysis, which are displayed in their original units, should be interpreted as

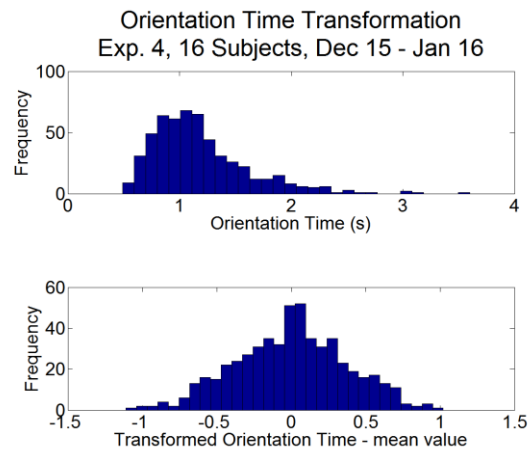


Figure 102: Experiment 4 Orientation Time Transformation Example

an effect on the median of the original distribution. For instance, if the reference frame alignment effect decreased orientation time by 0.5 seconds, this effect would increase on longer orientation times (those in the tail of the distribution), and decrease in magnitude on shorter orientation times (those close to zero). Although these transformations increase complexity at interpreting the results, they enable the detailed regression analyses which follow and provide a clear indication of whether or not a display technique impacted a particular dependent measure.

7.5.2.1. Experiment 4 Orientation Time Results

This dependent measure was the required time for a subject to determine a direction of movement in the sensor display. This was described as a suspect fleeing the target vehicle and represented as a red asterisk over the sensor video (see Figure 42). The regression model for orientation time, developed from experiment 4, is shown in Equation 13. This was the basic measurement of the increased performance of reference frame alignment over the orientation aid effect. Estimates of these effects are shown in Table 20. Initial angle and image had no significant effect on orientation time, so they do not show up in the regression model.

$$OT'_{e4} \approx \beta_0 + \beta_1 * XdispRedun + \beta_2 * Xalign + \beta_3 * XtrialNum + \beta_4 * Xmove + \beta_5 * Xalign * Xmove + \beta_6 * XtrialNum * Xmove + \beta_{7i} * Xsubject_i + \beta_{8i} * Xmove * Xsubject_i + \beta_{9i} * Xalign * Xsubject_i$$

$$i = 1: 16 \text{ subjects}$$

Equation 13: Orientation Time Regression Estimation

Table 20: Experiment 4 Orientation Time Predictor Variable Coefficients

Predictor Variable	Term	Transformed Regression Estimate	Lower 95% Conf. Interval	Upper 95% Conf. Interval	t-stat	p-value	Reverse Transformed Estimate (β')	units
(Intercept)	β_0	0.325	0.191	0.459	4.75	2.62E-06	0.259	s
XdispRedun ³	β_1	0.064	0.033	0.095	4.06	5.53E-05	0.060	s
Xalign	β_2	-0.420	-0.506	-0.333	-9.53	<1E-10	-0.560	s
XtrialNum	β_3	-0.013	-0.018	-0.008	-5.44	7.97E-08	-0.013	s/#
Xmove	β_4	0.019	-0.057	0.095	0.50	0.61	0.019	s
Xalign*Xmove	β_5	0.064	0.002	0.125	2.04	4.23E-02	0.060	s
XtrialNum*Xmove	β_6	0.010	0.003	0.016	3.01	2.73E-03	0.009	s/#
Initial angle, image, and other interactions were tested, but they did not meet the 0.05 significance requirement for inclusion in this regression.								

These results revealed several effects on orientation time. Both display redundancy and reference frame alignment produced significant effects on orientation time supporting both the reference frame alignment hypothesis (#1) and the display redundancy reduction hypothesis (#6). The

³ This regression analysis modeled display redundancy so a positive coefficient indicates that display redundancy reduction was effective because display redundancy increases orientation time.

reference frame alignment setting demonstrated an effect on this basic orientation time, but the model also revealed an interaction between this display technique and the subject. The p-value associated with the alignment setting reveals a main effect of alignment, but this effect was reduced for some subjects based on the subject-alignment interaction. Although the entire table of random effect coefficients is not provided in this report, the highest interaction effect between subject and alignment was 0.17 seconds. This would not completely eliminate the main alignment effect, but it demonstrates that alignment did not benefit each subject equally. This is a very similar observation to that of experiment 3.

Display redundancy showed an impact without any interaction with other effects. This improvement in orientation time resulted from the simple removal of the aircraft display. Despite every participant's claim that he or she did not use the aircraft display, removing it improved a subject's ability to determine the orientation of activity on the sensor display.

The basic learning effect captured with trial number, and the human subject variation captured with the random subject effect, were both expected. Additionally, the movement effect was expected because this removed the subject's ability to rely on familiar imagery features for orientation and it increased the overall complexity of the scenario. It was thought that this would induce an interaction effect with the alignment setting, and, unlike experiment 3, experiment 4 demonstrates this interaction. However, the interaction effect between alignment and movement is increasing orientation time. This is interesting because it was thought alignment would prove more important with the moving target task, and these data actually reveal that alignment was still beneficial with moving targets, but less so compared to stationary targets. The impact is an order of magnitude smaller than the alignment effect itself, but is still interesting.

Interestingly, the movement effect became larger as the subjects became more familiar with the task. This is counterintuitive as it was thought that any interaction here would improve the subject's ability to deal with the moving target difficulty. However, this could be related to a fixation on the moving target tracking and a corresponding increase in orientation time. If subjects were learning to track the moving target more effectively they might be devoting fewer attentional resources to orientation time; however, sensor tracking performance did not show a trial number effect. Another possibility is that the trial number impact is observed on error rate so that later trials had fewer errors and therefore better captured the difficulty associated with moving targets. If error rates decreased then more answers would be included in the analysis and if these previously incorrect answers were slower they would reveal a performance reduction. This too was not demonstrated with the data, since qualitatively error rates actually grew with trial number. Despite the lack of performance improvement in the sensor tracking task, the most likely explanation of the interaction effect between movement and trial number is that subjects were placing additional attention on this tracking task. As subjects became more familiar with the simulator they were likely focusing more on the challenging task of following the moving target. Although this did not result in improved tracking performance, it did result in increased orientation time.

As designed, these alignment and redundancy effects represent an impact beyond that of orientation aids. Although orientation aids were not specifically evaluated through this experiment, their inclusion on every display configuration enabled this observation. Once again despite the subject-alignment interaction, this experiment demonstrated that reference frame alignment and display

redundancy reduction were more effective than orientation aids at addressing the difficulty of a basic orientation task.

Although the basic subject effect makes it difficult to display the overall orientation time results, the overall distributions provide insight into these effects (larger versions are available in Appendix F: Experiment 4 Data Analysis). The data shown in Figure 103, Figure 104, and Figure 105 demonstrate the measurable effects of reference frame alignment, display redundancy and the moving target task. Figure 103 demonstrates the same compression of the orientation time distribution skew in response to reference frame alignment that was seen in experiment 1 and 3. The moving target effect and redundancy effect, shown in Figure 104 and Figure 105 respectively, show a more uniform and less significant adjustment to the distribution. These observations match the comparable significance shown in the regression model estimated effects.

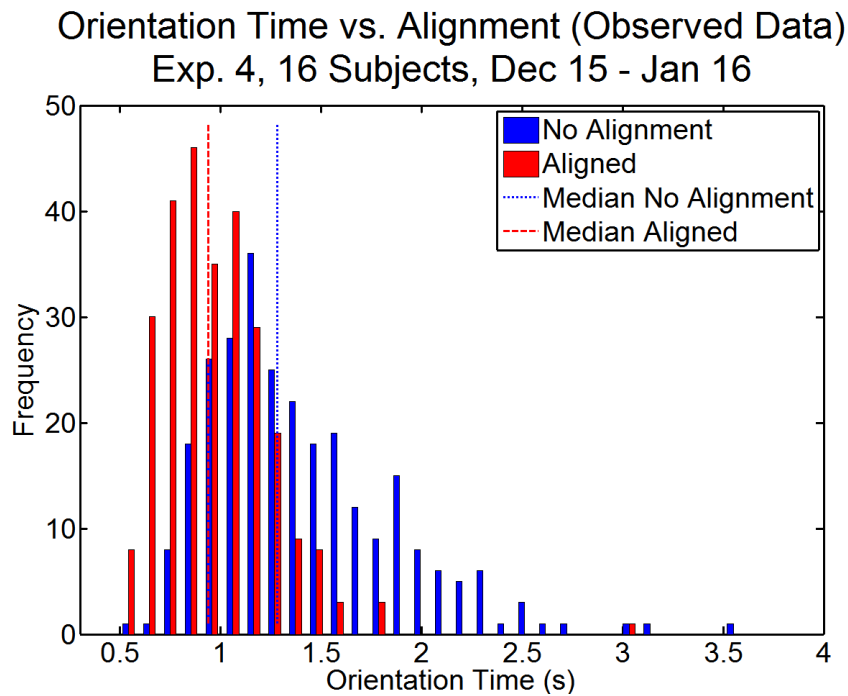


Figure 103: Orientation Time Alignment Effect

Blue distribution is observed data without alignment. Red distribution has alignment of the sensor display and is shifted left of the blue data.

Orientation Time vs. Movement (Observed Data)
Exp. 4, 16 Subjects, Dec 15 - Jan 16

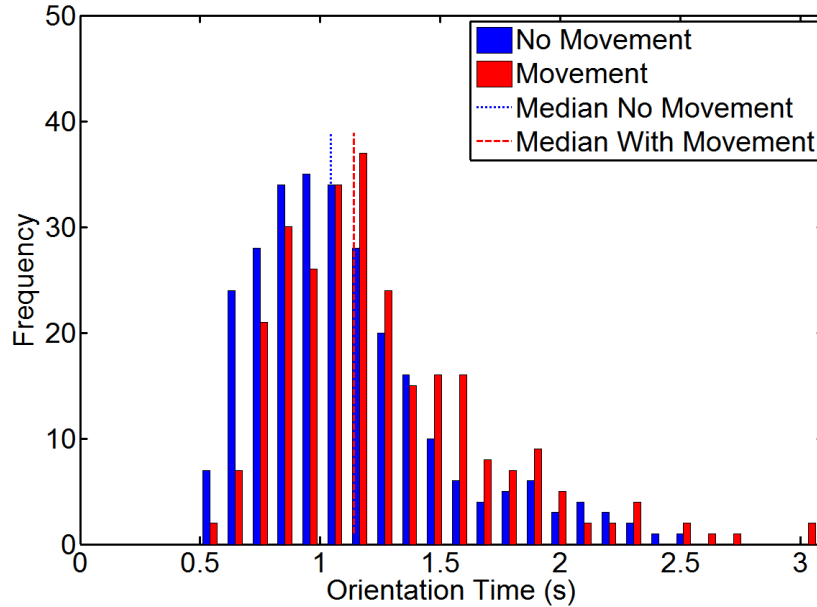


Figure 104: Orientation Time Moving Target Effect

Blue distribution is observed data with a stationary target. Red distribution is observed data with a moving target and is shifted right of the blue data.

Orientation Time vs. Display Redundancy (Observed Data)
Exp. 4, 16 Subjects, Dec 15 - Jan 16

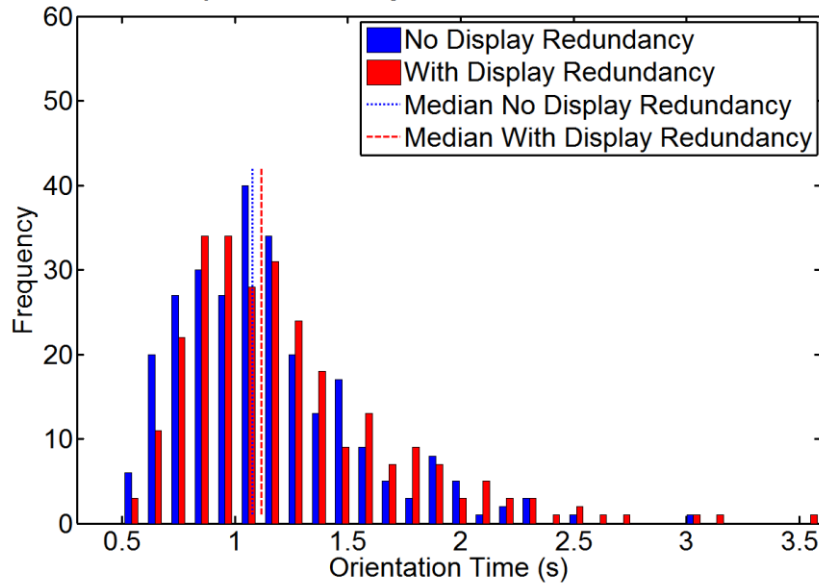


Figure 105: Orientation Time Display Redundancy Effect

Blue distribution is observed data with without the aircraft display. Red distribution includes the aircraft display.

Once again, these display techniques and the moving target scenario effects were inspected for their influence on error rates (percentage of incorrect orientation answers for the entire experiment). Figure 106 shows a similar change in error rates with the reference frame alignment technique and the moving target task; however, no decrease is evident with display redundancy. This is similar to experiment 3.

These orientation time results continued to highlight the multiple reference frame challenge which was characterized in experiments 1 and 3, and they demonstrated a significant reference frame alignment effect mitigating that challenge. This provided more support for the reference frame alignment hypothesis (#1). Furthermore, the reduced orientation times associated with display redundancy highlighted another potential display technique and supported the display redundancy reduction hypothesis (#6). However, the interaction between moving targets and the alignment actually decreased the alignment effect so this was contrary to the moving target-alignment hypothesis (#5).

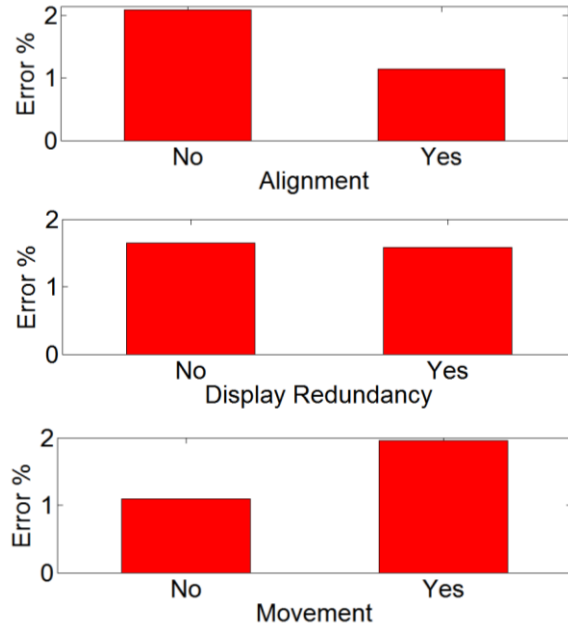


Figure 106: Orientation Errors vs. Alignment, Redundancy, and Moving Target Tasks

7.5.2.2. Experiment 4 Target Acquisition Time Results

As in all simulator experiments, this target acquisition time was measured from the start of the simulation until the subject identified the target location. If the subject misidentified the target, that time was not included in this regression analysis. This process was described as a weapon release to encourage the subject to take the accuracy requirement seriously. The regression model for target acquisition time, developed from experiment 4, is shown in Equation 14. Estimates of these effects are shown in Table 21. While orientation time represented a basic measurement of the multiple reference frame challenge, target acquisition time measured a broader impact of that challenge. Here, more than a simple orientation task was required. Subjects had to follow descriptions of the target area or complete imagery rotations between the target satellite image and the observed sensor video in order to locate a target in the sensor video scenery. The revealed orientation time effect from the previous section would likely be multiplied with the increased number of orientation tasks required to complete a target acquisition task. Furthermore, this was very representative of an actual unmanned aircraft surveillance task. Initial angle had no significant effect on target acquisition time, so it does not show up in the regression model.

$$TAT'_{e4} \approx \beta_0 + \beta_1 * XdispRedun + \beta_2 * Xalign + \beta_3 * XtrialNum + \beta_{4i} * Xsubject_i + \beta_{5i} * XtrialNum * Xsubject_i + \beta_{6m} * Ximage_m + \beta_{7m} * Xalign * Ximage_m$$

$$i = 1: 16 \text{ subjects, } m = 1:4 \text{ images}$$

Equation 14: Target Acquisition Time Regression Estimation

Table 21: Experiment 4 Target Acquisition Time Predictor Variable Coefficients

Predictor Variable	Term	Transformed Regression Estimate	Lower 95% Conf. Interval	Upper 95% Conf. Interval	t-stat	p-value	Reverse Transformed Estimate (β')	units
(Intercept)	β_0	8.80	8.11	9.50	24.96	<1E-10	3.21	s
XdispRedun	β_1	0.38	0.14	0.62	3.07	2.38E-03	0.35	s
Xalign	β_2	-0.74	-1.17	-0.32	-3.44	6.87E-04	-0.82	s
XtrialNum	β_3	-0.058	-0.084	-0.032	-4.37	1.76E-05	-0.057	s/#

Initial angle, and all interactions were tested, but they did not meet the 0.05 significance requirement for inclusion in this regression.

This regression model has all the predictor variables that were present in the orientation time model except the movement effect. This movement effect was not evaluated in the target acquisition task because the target movement did not begin until half way through each trial.

Two additions to this model which were not present in the orientation time model are the image random effect and a learning effect (trial number) interaction with subject. This indicates that the imagery scene had a basic impact on the target acquisition task and that subjects became more capable at the target acquisition task as the experiment progressed. Both of these were expected and accounted for in the experiment design; however, they are still captured in the regression model.

Once again, reference frame alignment demonstrated an increased effectiveness over the baseline orientation aid display. Here, aligning the reference frame allowed the subject to locate the car faster by approximately eight tenths of a second at the median of the distribution. Interestingly, initial angle was not a factor in the experiment 4 regression model even though it had a large impact in experiment 1. This was similar to experiment 3 and seemed to indicate that the subjects were not performing the same method of imagery rotation as that used in experiment 3. As a reminder, this initial angle was the rotation between the sensor display and the north-up reference frame. The targets in experiments 3 and 4 were all along a single cardinal direction from a central intersection, while the experiment 1 targets often involved more complicated textual descriptions. In this way, experiment 1 may have encouraged a more involved imagery rotation to determine relationships between objects, and experiments 3 and 4 only required the subject to complete one rotation on the image to determine the basic cardinal orientation.

The imagery effect revealed with this model could contradict this simplified understanding of the subject's initial rotation task, because it indicates a difference in target acquisition time based on which of the four target scenarios were involved in any given trial. However, this effect, on target acquisition time, could also be a function of the varied distance from initial crosshair placement to the car's location as demonstrated in Figure 107. This confound could not be corrected with a simple inclusion of this distance because some subjects used an accelerated crosshair movement for the more distant targets and others used a consistent, pace of crosshair movement regardless of the distance. For this reason, the distance from crosshair to initial target location was not included in the model and this distance effect was included in the image effect coefficient.

As the operators became more confident in their ability to find the target, as demonstrated by main trial number effect, they may have also adjusted their technique with crosshair movement and pursued the distant targets faster. The aligned display configuration could have allowed the subjects to predetermine their sensor control inputs since they would know to slew left for a car approaching from the west. The different starting locations would have unequally influenced the benefit of this technique. The shorter initial distances would have shown little improvement if the subject initiated an immediate crosshair movement, but the targets at longer distances would have resulted in faster acquisition times. This variation could be producing the alignment-image interaction effect in the regression model because the scenarios without alignment could not have benefited from any predetermination of slew direction. With the misaligned displays the subjects would have had to orient with the sensor-view imagery before determining which direction to slew the crosshairs. In this way, both the imagery effect and alignment-imagery interaction most likely include the initial target location confound. This influenced these data, but did not prevent the discovery of the main effects of interest.



Figure 107: Example Target Images from Experiment 4 (same as Experiment 3)
These images demonstrate the different relative location between the initial crosshair placement and the target vehicle. The right image has a longer distance between the crosshairs and vehicle.
[Image ©Google]

The learning effect in experiment 4 was similar to experiment 3. With 17 trials, the regression model learning effect could grow to nearly 1 second ($17 \text{ trials} * 0.057 \text{ s/trial} = 0.97\text{s}$). Also, the display redundancy added a significant impact of over three tenths of a second. This is a positive effect because a reduced redundancy (removing the aircraft display) would reverse this effect. This is significant because the aircraft display played virtually no role in the initial target acquisition portion of the experiment. Therefore, this represents a workload measurement with the target acquisition task, and highlights the impact of additional, unnecessary, display features.

Once again, subject effects make it difficult to display the overall target acquisition time results; however, these graphs provide some insight into these effects (larger versions are available in Appendix F: Experiment 4 Data Analysis). Figure 108 demonstrates the slight shift in the median target acquisition

time when alignment is applied to the sensor display. The tail of this distribution is affected by the alignment effect with a four second difference between the maximum target acquisition times of the two distributions. Display redundancy produced a similar shift in median target acquisition time, but no corresponding effect was seen on the tail of the distribution. These match the significance of these terms in the regression model.

Since incorrect target selections were not included in the target acquisition time analysis, the error rate effect (percentage of incorrect target location answers for the entire experiment) was not captured by the regression model. However, the alignment and redundancy effects, as shown in Figure 110, also adjusted the observed error rate when subjects were searching for and selecting a target. The accuracy requirement of this task was intended to replicate that of a weapons employment task. None of the subjects had experience operating unmanned aircraft, but it is still noteworthy that both the alignment effect and the redundancy effect produced such a large difference in error rate.

Tgt Acquisition Time vs. Alignment (Observed Data)
Exp. 4, 16 Subjects, Dec 15 - Jan 16

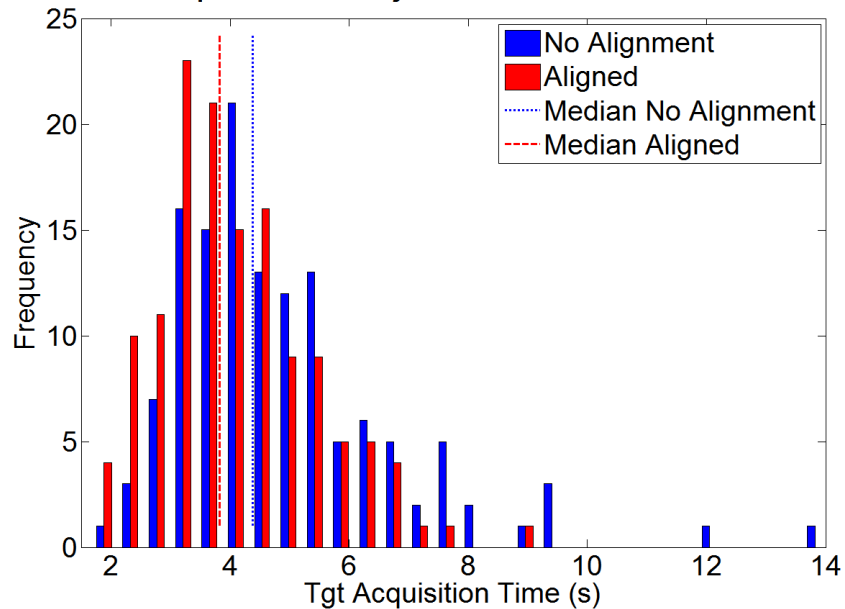


Figure 108: Target Acquisition Time Alignment Effect
Blue distribution is observed data without alignment. Red distribution has alignment of the sensor display and is shifted left of the blue data.

Tgt Acquisition Time vs. Display Redundancy (Observed)
Exp. 4, 16 Subjects, Dec 15 - Jan 16

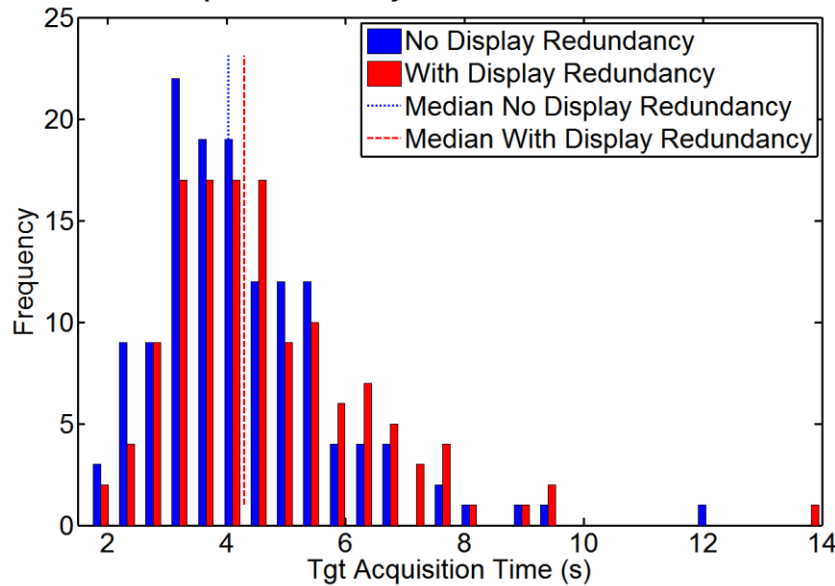


Figure 109: Target Acquisition Time Display Redundancy Effect
Blue distribution is observed data with without the aircraft display. Red distribution includes the aircraft display.

Once again, both of the error rate comparisons are provided in Figure 110. As mentioned, both the alignment technique and reducing the display redundancy decreased the error rates. This increase in target acquisition accuracy associated with reference frame alignment and redundancy reduction should also be considered a benefit of these display techniques in addressing the multiple reference frame challenge.

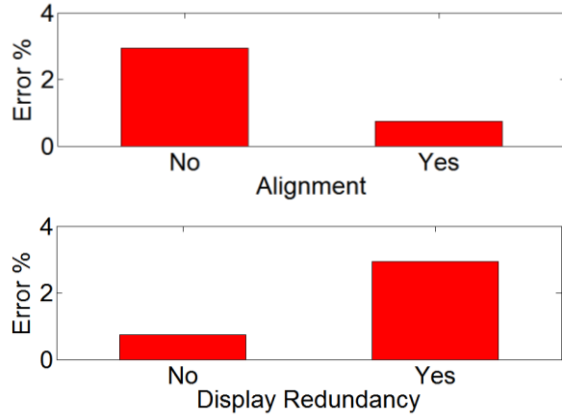


Figure 110: Target Acquisition Errors vs. Alignment and Display Redundancy

These target acquisition time results demonstrated a significant impact of the multiple reference frames on the target acquisition task, and they demonstrated a reduction of that effect with the reference frame alignment and redundancy reduction display techniques. This provided additional support for the reference frame alignment hypothesis (#1) and the display redundancy reduction hypothesis (#6). The moving target-alignment hypothesis (#5) was not evaluated with the target acquisition task since all targets were stationary in the initial portion of each trial.

7.5.2.3. Experiment 4 Tracking Task Results

Since, the experiment 4 tracking error (flight path error or sensor track error) results show minimal effects, their analyses are combined in this section. For separate descriptions of these analyses follow the provided charts in Appendix F: Experiment 4 Data Analysis. These terms were both analyzed as a root mean squared error for each individual run. After transformation, the regression analyses resulted in the models shown in Equation 15 and Equation 16. One of these measures revealed a direct impact of reference frame alignment on tracking performance, but neither revealed any direct or indirect influence of display redundancy. This reference frame alignment effect was observed in the flight path error. Even though the sensor display had the only use of reference frame alignment, the only effect was observed on the aircraft control task. This represents a workload benefit of the reference frame alignment technique.

Since the primary influence lies with the flight path error measurement, those results are discussed further. Here, as shown in Table 22, the alignment effect is barely discernible on the flight path error measurement. The -2.6E-3 RMSE effect, indicates that a single trial's average flight path error was decreased by less than 1% of the planned flight path orbit radius when the sensor display was aligned. Display redundancy, initial angle, trial number, and image had no significant effect on orientation time, so they do not show up in the regression model.

$$FPE'_{e4} \approx \beta_0 + \beta_1 * Xalign + \beta_2 * Xmove$$

Equation 15: Flight Path Error Regression Estimation

$$STE'_{e4} \approx \beta_0 + \beta_1 * Xmove$$

**Equation 16: Sensor Track Error Regression Estimation
No display design terms remained in the model**

Table 22: Experiment 4 Flight Path Error RMSE Predictor Variable Coefficients

Predictor Variable	Term	Transformed Regression Estimate	Lower 95% Conf. Interval	Upper 95% Conf. Interval	t-stat	p-value	Reverse Transformed Estimate (β')	units
(Intercept)	β_0	-0.08	-0.08	-0.07	-104.4	0	1.34	RMSE
Xalign	β_1	-2.44E-03	-4.07E-03	-7.99E-04	-2.92	3.62E-03	-2.6E-03	RMSE
Xmove	β_2	0.011	9.32E-03	0.013	13.15	1.86E-34	8.54E-03	RMSE

Display redundancy, Initial angle, trial number, image, subject, and other interactions were tested, but they did not meet the 0.05 significance requirement for inclusion in this regression.

Flight Path Error vs. Alignment (Observed Data) Exp. 4, 16 Subjects, Dec 15 - Jan 16

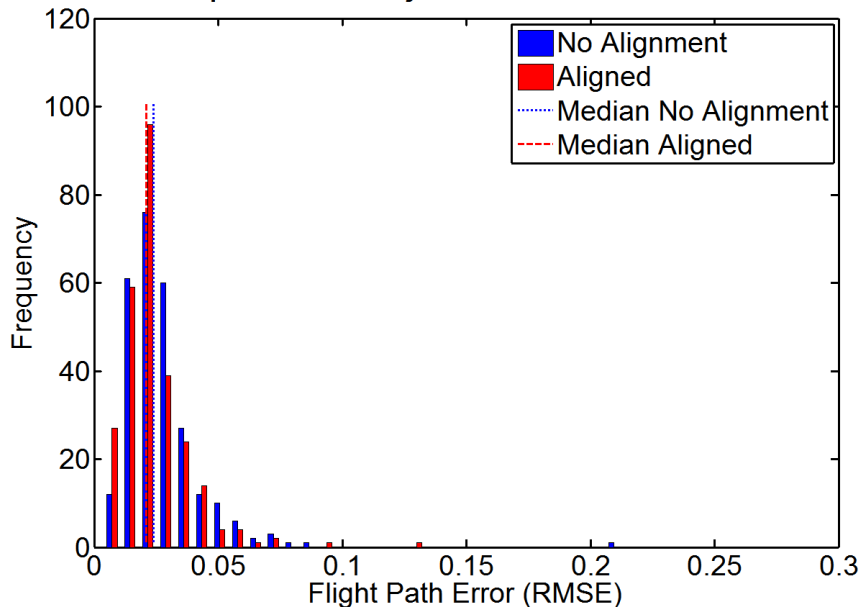


Figure 111: Flight Path Error Alignment Effect

Blue distribution is observed data without alignment. Red distribution has alignment of the sensor display and is shifted left of the blue data.

These results should be observed cautiously, however, because the demonstrated effect is influenced by one particular trial. This outlier is shown in Figure 111. Without alignment the greatest observed flight path error (RMSE over one trial) was approximately 22% of the orbit radius. This is a large error when compared to the next highest value of around 13% of the orbit radius. Qualitatively, this data point demonstrated the task saturation which can occur as an operator is confused by the orientation task; however, it is still important to understand its influence over this demonstrated effect.

Target movement produced a significant effect on both of these tracking error measurements, similarly to experiment 3. This was expected for the sensor track error, but somewhat surprising for the flight path error. The target movement changed the flight path tracking task because the predefined flight path moved to keep the actual target centered at all times. Throughout an entire trial this was evident on the navigation display; however, the main impact is likely due to the increase in task difficulty for the sensor tracking task. As this task became more difficult it is likely that subjects diverted attention away from the flight path tracking task and concentrated more on the sensor tracking task. This is similar to the reference frame alignment technique's effect. The seemingly insignificant improvement in error, of less than a percent of the planned orbit radius, represents roughly 1/3 of the moving target effect.

The lack of display redundancy impact still provides the opportunity to include this as a potential display design tool. Like display integration, this could be especially helpful in systems with smaller control stations and a reduced number of available displays. Although there was no demonstrated improvement, the ability to convey the same information on three displays rather than 4 could prove helpful in system design.

Since experiment 4 and experiment 1 both included the traditional display, these data also provided an opportunity to qualitatively examine the effectiveness of the predictive aid. These flight path errors are shown in Figure 113. This figure is a qualitative comparison of the flight path error data from experiment 1 and experiment 4. Despite the more complex moving target task involved in experiment 4 the predictive aid increased the performance of the flight path control task. Reinforcing the similar results in experiment 3, this provides a qualitative confirmation that the predictive aid assisted with the flight path tracking task.

**Flight Path Error vs. Predictive Aid(Observed Data)
Exp. 1 & 4 Display Configuration A**

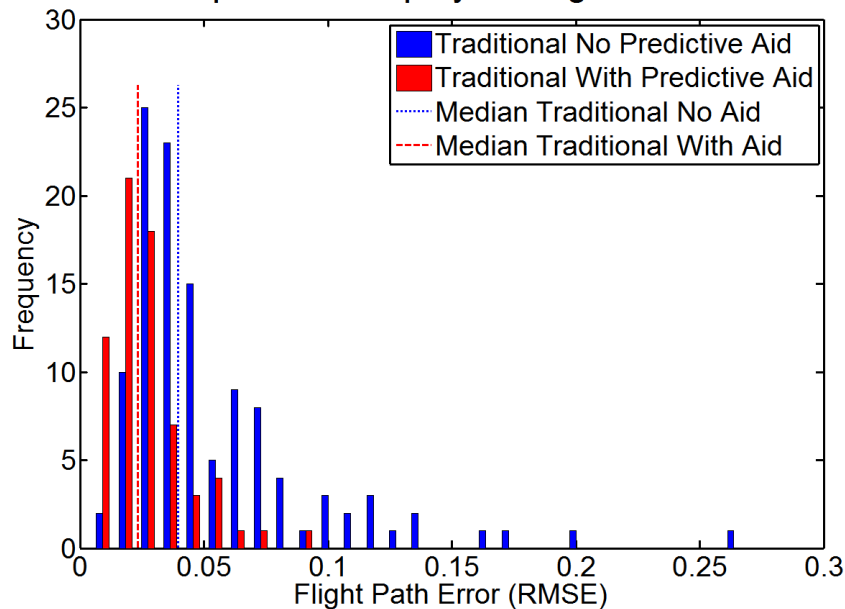


Figure 112: Predictive Aid Effect on Flight Path Error across Experiments 1 and 4
Blue distribution is observed data without predictive aid. Red distribution has the predictive aid and is shifted left of the blue data.

These data demonstrate an alignment effect which supports the reference frame alignment hypothesis (#1) and reinforces the angular effect demonstrated in the experiment 3 tracking error measures. These results fail to support the moving target-alignment hypothesis (#5) or the display redundancy reduction hypotheses (#6), but they do not significantly oppose those hypotheses either. This measure continues to support the significant effect of multiple reference frames and the possible benefit of the reference frame alignment technique, but no actionable information is produced regarding the removal of the aircraft display.

7.5.3. Experiment 4 Workload Measures

7.5.3.1. Experiment 4 Bedford Workload Rating Results

After each individual trial, subjects were asked to provide an assessment of the mental workload observed during that trial. The subjects provided a rating from 1-10 in accordance with the Bedford Workload rating scale in Figure 43. This subjective workload was split into two measurements to account for the transition from static (stationary) to dynamic (moving) targets half way through each trial. The static workload measurement included target acquisition, tracking, orientation, and reaction time tasks, but the dynamic workload measurement only included tracking, orientation, and reaction time tasks. These results were analyzed with a Kruskal-Wallis rank test to evaluate a difference in the distribution of these ordinal data. The raw data are plotted in Figure 113 and Figure 114 with respect to the two display techniques. Both of these figures show similar distributions for the two treatments, but Figure 113 demonstrates a slight shift in the median rating with reference frame alignment. Figure 114 shows virtually identical distributions and medians regardless of the display redundancy (aircraft display).

Bedford Workload vs. Alignment (Observed Data)
Exp. 4, 16 Subjects, Nov 14 - Feb 15

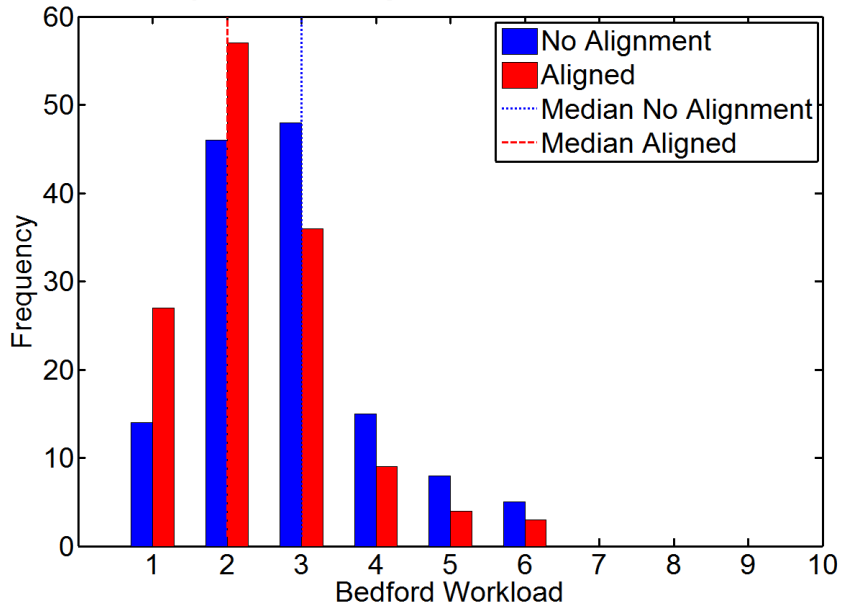


Figure 113: Reference Frame Alignment Effect on Bedford Workload
Blue distribution is observed data without alignment. Red distribution has alignment of the sensor display.

Bedford Workload vs. Display Redundancy (Observed)
Exp. 4, 16 Subjects, Nov 14 - Feb 15

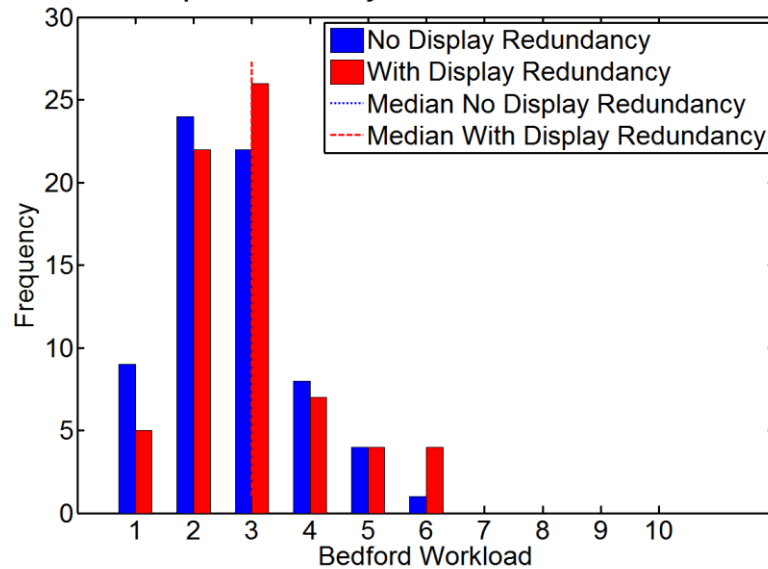


Figure 114: Display Redundancy effect on Bedford Workload
Blue distribution is observed data with without the aircraft display. Red distribution includes the aircraft display.

This is reinforced with the pairwise rank test comparisons presented in Table 23. These data show comparisons of every display configuration in experiment 4 (see 7.3). These demonstrate the reference frame alignment benefit only when the target was moving; however, there was always an observed difference among these displays was when both display redundancy reduction and reference frame alignment were applied. So, when the aircraft display was removed and the sensor display was aligned to north-up then a decrease in subjective workload was measured with or without target movement.

The basic significance of reference frame alignment, as measured with moving targets, also supports hypothesis 1 and 2 because it shows that multiple reference frames increased workload and reference frame alignment mitigated at least some of that increased workload. However, this was only shown with the moving target so this applies more directly to hypothesis 5.

Since reference frame alignment was significant with a moving target but not a stationary target, this supports hypothesis 5. The moving target increased task complexity which further highlighted the benefit of reference frame alignment. In this case it was the difference between a significant and insignificant benefit.

These results also lend a small measure of additional support to hypothesis 1, 2, and 6. It is possible that the impact on workload of display redundancy was too small to measure independently, but when combined with reference frame alignment (on the stationary targets) their combined effect was sufficiently large to observe with these experimental methods.

Table 23: Experiment 4 Subjective Workload Rating Results

These are the results of Kruskal-Wallis rank tests for pairwise comparisons of displays based on the subjective workload rating (Bedford Workload Scale shown in Figure 43). Green indicates a significant difference with a family significance of 0.05 Bonferroni corrected to 0.008.

A – misaligned / acft display B – aligned / aircraft display G – misaligned / no acft display H – aligned / no acft display		Adding Reference Frame Alignment		Adding Display Redundancy		Interaction Effects	
		Display	Display	Display	Display	Display	Display
		A ≠ B	G ≠ H	A ≠ G	B ≠ H	G ≠ B	A ≠ H
Bedford Workload Static Target (1-10)	Chi-sqr	6.37	3.38	1.75	0.26	1.52	10.10
	p-value	0.01	0.07	0.19	0.61	0.22	1.48E-03
Bedford Workload Dynamic Target (1-10)	Chi-sqr	9.22	6.62	0.87	0.39	4.02	13.18
	p-value	2.40E-03	0.01	0.35	0.53	0.04	2.83E-04

Once again, it is important to remember that the subjective workload measures presented here could degrade into a measure of the subject’s frustration so it is important to look for confirmation of these findings in the objective secondary workload measurement. These reaction time results are presented in the next section.

7.5.3.2. Experiment 4 Reaction Time Results

The reaction time test provided a secondary task objective workload measurement. Here, subjects responded to a blinking visual light with a trigger squeeze. This was not directly representative of any specific unmanned aircraft task, but it was explained as an activity sensor at the target area.

$$RT'_{e4} \approx \beta_0 + \beta_1 * XdispRedun + \beta_2 * Xalign + \beta_3 * XtrialNum + \beta_4 * Xmove + \beta_5 * XtrialNum * Xmove + \beta_{6i} * Xsubject_i + \beta_{7i} * Xmove * Xsubject_i + \beta_{8i} * Xalign * Xsubject_i$$

$$i = 1:16 \text{ subjects}$$

Equation 17: Reaction Time Regression Estimation

Table 24: Experiment 4 Reaction Time Predictor Variable Coefficients

Predictor Variable	Term	Transformed Regression Estimate	Lower 95% Conf. Interval	Upper 95% Conf. Interval	t-stat	p-value	Reverse Transformed Estimate (β')	units
(Intercept)	β_0	-0.293	-0.24	-0.15	-8.53	<1E-10	-0.29	s
XdispRedun	β_1	0.064	0.059	0.092	9.21	<1E-10	0.064	s
Xalign	β_2	-0.038	-0.049	-0.026	-6.29	6.71E-10	-0.038	s
XtrialNum	β_3	-3.85E-03	-5.76E-03	-2.28E-03	-4.55	6.68E-06	-3.85E-03	s/#
Xmove	β_4	0.032	4.49E-03	0.067	2.25	0.025	0.032	s
XtrialNum*Xmove	β_5	2.25E-03	6.89E-06	4.75E-03	1.97	0.049	2.25E-03	s/#
Initial angle, image, and other interactions were tested, but they did not meet the 0.05 significance requirement for inclusion in this regression.								

The reaction time regression model, shown in Table 24 and Equation 17, shows the effect of reference frame alignment, but even larger impact of display redundancy. In fact, this model closely parallels the results from experiment 3 with display redundancy replacing display integration in the model. Initial angle and image had no significant effect on orientation time, so they do not show up in the regression model.

The subjective ratings, discussed earlier, showed signs of a small reference frame alignment and display redundancy reduction effect which was only visible when both were combined; however, with the objective and parametric measure of reaction time, this finding is reinforced by the regression analysis. These effects are both observed in the reaction time regression model.

The model also includes an expected learning effect which shows a decrease in reaction time as subjects progressed through the experiment.

The expected moving target effect is also present. This increased reaction time during the period of each trial involving a moving target. However, the moving target effect interacted with the learning effect to actually decrease this effect. In other words the learning effect was decreased during the moving target portions of a trial. This is an unexpected interaction since it seems to indicate that subjects were getting worse at tracking the moving targets; however, this parallels the observations related to orientation time. Once again these could be related to a fixation on the moving target tracking and a corresponding increase in reaction time. If subjects were placing increased attention on

the moving target and not scanning for the “trigger light” as frequently, this could explain this observation. Sensor tracking performance did not show a trial number effect, but this does not exclude the possibility that subjects were placing more attentional resources on the sensor tracking task. As subjects became more familiar with the simulator they were likely focusing more on the challenging task of following the moving target. Although this did not result in improved tracking performance it did result in increased reaction time. These same indications were shown in the orientation time measurements.

This model also reveals an interaction of target movement and the alignment setting. Once again contrary to moving target-alignment hypothesis (#5), the presence of a moving target actually decreases the effectiveness of reference frame alignment. This was the same unexpected outcome that was observed in the orientation time results of experiment 4, but was not evident in either measurement during experiments 1 or 3.

The display redundancy reduction showed a marked decrease in reaction time (increase associated with including the aircraft display). This decrease in workload supported the display redundancy reduction hypothesis (#6), and makes sense because the display crosscheck was simplified from three to two displays, as shown in Figure 115. However, the placement of the “trigger light” may have played a role in this reaction time reduction. Since the light had been moved to the display periphery, it was right along the crosscheck of the reduced display (configuration E), but only along one side of the traditional display’s (configuration A) crosscheck. While these data still support a reduction in workload, this limitation should be considered.

Display Configuration A: Traditional

Display Configuration E:
Sensor Aligned and No Aircraft Display

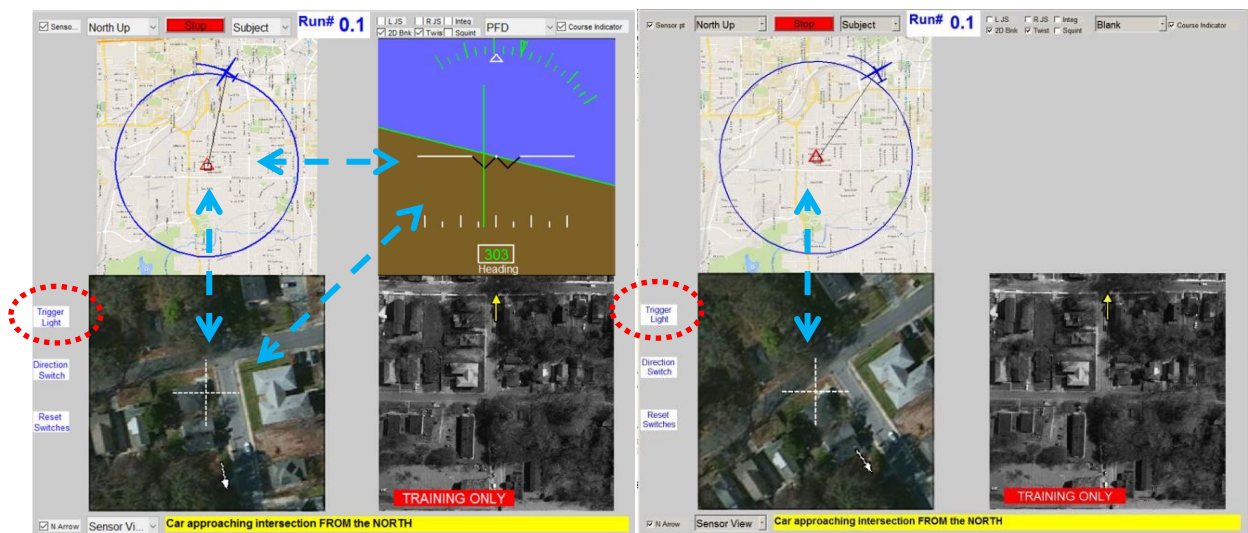


Figure 115: Simplified Crosscheck without Aircraft Display
Red ovals highlight the location for the “trigger light” which would initiate a reaction time test during simulator experiments. The teal dashed lines indicate the operator’s potential scan patterns and their proximity to the trigger light. [Map Data and Image ©Google]

These reaction time data also show evidence of these effects without all the factors accounted for in the regression model. Both Figure 116 and Figure 117 demonstrate the shift in median reaction

time associated with alignment of the sensor video and removal of the aircraft display respectively. Both of these show a limited reduction in distribution skew, with the more significant impact from display redundancy reduction. Overall, these data support hypothesis 1, 2, and 4, but they oppose hypothesis 5 because the alignment effect was decreased with the presence of a moving target.

Reaction Time vs. Alignment (Observed Data) Exp. 4, 16 Subjects, Dec 15 - Jan 16

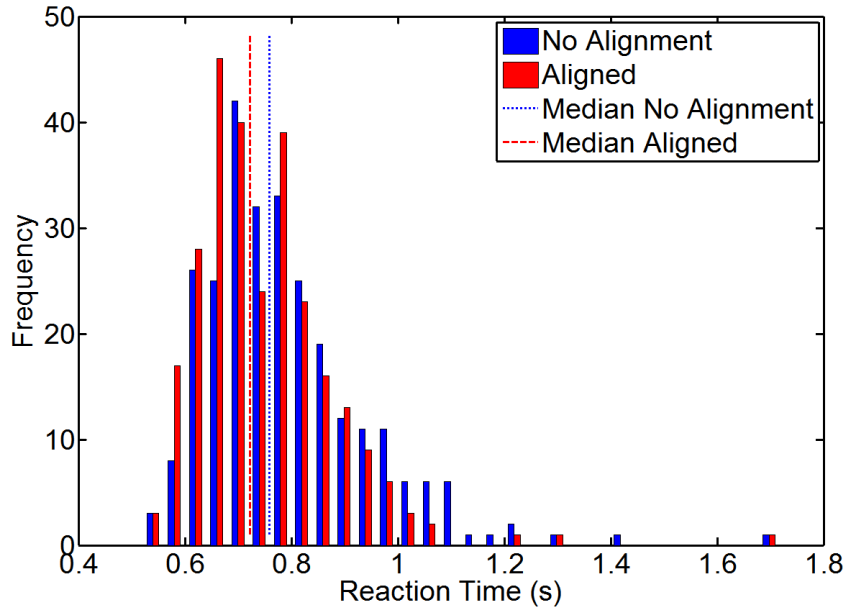


Figure 116: Reaction Time Alignment Effect
Blue distribution is observed data without alignment. Red distribution has alignment of the sensor display.

Reaction Time vs. Display Redundancy (Observed)
Exp. 4, 16 Subjects, Dec 15 - Jan 16

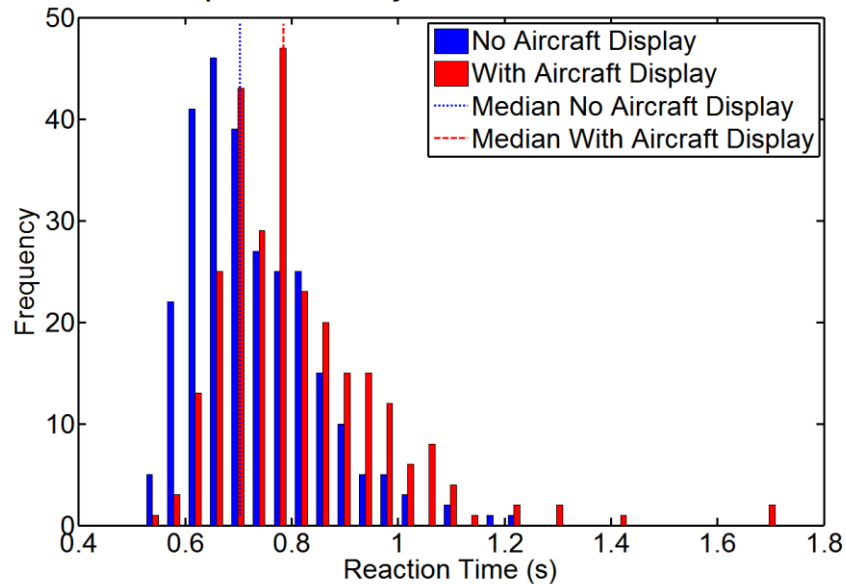


Figure 117: Reaction Time Display Redundancy Effect
Blue distribution is observed data with without the aircraft display. Red distribution includes the aircraft display.

7.5.4. Experiment 4 User Preferences

7.5.4.1. Experiment 4 Subjective Ranking Results

After subjects completed their entire experiment, during the post-experiment questionnaire, they were asked to provide a ranking of the four displays from one to four, with one as the best and four as the worst. These results are all provided in Appendix G: Subjective Response Data. These data were collected to capture the subject's preference regarding the displays and does not necessarily represent a significant workload or performance benefit from any particular display. Here, as displayed in Table 25, they reinforce some of the findings from experiment 4. Based on these results, subjects clearly preferred reference frame alignment, but were indifferent to display redundancy. These results support hypothesis 1 and 2 regarding the reference frame impact and benefit of alignment, but they do not support hypothesis 6 regarding display redundancy. These do not actually contradict other results of experiment 4, but they do not reveal the same impact of display redundancy as that shown with orientation time, target acquisition time, and reaction time measurements. As subjects verbalized their preferences it seemed that they did not place any significance on the aircraft display presence, and some of them could not rate it lower because it actually offered additional information. Their reasoning seemed to be that some information was better than no information even if they admitted that they did not use the display at all. This was an interesting observation.

Despite this limitation, these data clearly reveal a subjective preference in favor of the reference frame alignment technique for the set of tasks involved in this experiment.

Table 25: Experiment 4 Subjective Ranking Results

These are the results of Kruskal-Wallis rank tests for pairwise comparisons of displays. Green indicates a significant difference with a family significance of 0.05 Bonferroni corrected to 0.008.

		Adding Reference Frame Alignment		Adding Display Redundancy		Interaction Effects	
		Display	Display	Display	Display	Display	Display
		A ≠ B	G ≠ H	A ≠ G	A ≠ B	G ≠ H	A ≠ H
Rankings (1-4)	Chi-sqr	19.54	19.54	2.58	2.58	15.95	22.81
Kruskal-Wallis	p-value	9.87E-06	9.87E-06	0.11	0.11	6.51E-05	1.78E-06

7.5.4.1. Experiment 4 Subjective Rating Results

The 1-4 rankings, discussed in the previous section and in experiment 3, did not allow subjects to provide any relative comparison between differences. If two displays nearly tied for first and another two tied for last, the subject still had to provide 1 to 4 rankings. For this reason another subjective technique was added to allow subjects to better characterize their understanding of the difference between each display.

After subjects completed their entire experiment they were asked to provide a ranking of the four displays from one to four, with one as the best and four as the worst. With these rankings in mind, subjects were told to consider a scale of 1-10 where the display ranked 1 received a rating of 1 on the new scale and the display ranked 4 received a rating of 10 on the new scale. They were then asked to place the middle two displays on their new rating scale. This allowed them to provide a relative rating of the displays with some sense of magnitude for difference between any two displays. These results are all provided in Appendix G: Subjective Response Data.

Once again, these data were collected to capture the subject’s preference regarding the displays and do not necessarily represent a significant workload or performance benefit from any particular display. Here, as displayed in Table 26, they reinforce the same findings of the previous section, but with the increased sensitivity of ratings over rankings, the display redundancy effect is more pronounced. They are still not statistically significant with this experiment, but with p-values less than 0.009 these are trending towards significance.

Table 26: Experiment 4 Subjective Rating Results

These are the results of Kruskal-Wallis rank tests for pairwise comparisons of displays. Green indicates a significant difference with a family significance of 0.05 Bonferroni corrected to 0.008.

		Adding Reference Frame Alignment		Adding Display Redundancy		Interaction Effects	
		Display	Display	Display	Display	Display	Display
		A ≠ B	G ≠ H	A ≠ G	A ≠ B	G ≠ H	A ≠ H
Ratings (1-10)	Chi-sqr	21.27	21.06	2.99	3.79	15.50	25.22
Kruskal-Wallis	p-value	3.99E-06	4.46E-06	8.35E-02	5.15E-02	8.26E-05	5.12E-07

7.6. Experiment 4 Limitations

This experiment includes similar limitations to experiments 1 and 3. These results are limited based on the collection methods. The population of subjects for this experiment (characteristics available in Appendix B: Subject Characteristics) were mostly graduate and undergraduate MIT or Harvard students or engineering professionals at MIT Lincoln Laboratory with no experience operating unmanned surveillance aircraft. One subject in this experiment did have experience with remotely controlled fixed-wing aircraft and quadrotors, but this does not directly translate to experience with fixed-wing unmanned aircraft. This lack of experience could, once again, influence the results toward displays that would not be easily managed by an experienced unmanned aircraft pilot or sensor operator, but are rather tailored for a particular sort of college student or engineering professional.

Additionally, the short time associated with each individual run was not indicative of actual surveillance tasks which could span hours tracking the same target. This could mask potential vigilance issues with the display techniques. If a display included features which a subject could manage for minutes at a time but would prove challenging or impossible for long periods, this would not be discovered with this experiment.

Finally, the simulator design was simplified to focus on the multiple reference frame aspect of unmanned aircraft control, and the results and conclusions should stay limited in kind. It is important to understand that only lateral navigation (aircraft bank angle) was controlled by the subject during these experiments. These results do not support sweeping changes to unmanned aircraft in general, but apply directly to the on-station surveillance time. It would be inappropriate, for instance, to advocate removing the aircraft display for takeoff and landing based on these results alone. While not an exhaustive list these were evaluated as the most applicable limitations to these data and corresponding results and conclusions.

7.7. Experiment 4 Conclusions

Experiment 4 reinforced findings previously discovered in experiments 1 and 3. This experiment continued to explore the multiple reference frame impact on unmanned aircraft operations. After the findings of experiments 1 and 3, with confirmation that reference frame alignment was more significant than basic orientation aids at addressing the multiple reference frame challenge, experiment 4 once again included orientation aids on every display configuration (same as experiment 3). This decreased the ability to measure the multiple-reference-frame impact and the corresponding effect of the reference frame alignment technique; however, this allowed for a better understanding of this display technique's influence on currently available systems. Since orientation aids are used throughout surveillance systems, this experimental technique provides more useful information to future research efforts. This experiment included analysis of the display-redundancy-reduction technique along with the reference-frame-alignment technique. It also included the same moving target sensor tracking task as experiment 3. Finally, the continued use of a flight path predictive aid created the redundancy which allowed the removal of the aircraft display during this experiment.

Despite the presence of orientation aids on every display configuration, reference frame alignment continued to produce measurable effects across nearly every performance and workload measure. This provided additional support for the reference frame alignment hypothesis (#1).

The reference frame alignment effect appeared on a basic sensor video orientation task where median orientation time was reduced by more than 1/2 second, and a more complex sensor target acquisition task where median time was reduced by more than 0.8 seconds. This is similar to experiment 3 and once again a smaller impact than that observed in experiment 1, but here in experiment 4 the targets involved simplified descriptions (like experiment 3) that would have required fewer individual orientations. This resulted in a smaller additive effect of orientation time on target acquisition time.

Once again, and possibly more significant than the faster orientation or target acquisition times the reference frame alignment technique decreased the error rate of both these tasks. Orientation time error rate (percentage of all the orientation answers for this experiment) was reduced from 2% to 1.1% despite the fact that orientation aids were included on each display, and target acquisition error rate was reduced from 2.9 to 0.7% with the reference frame alignment technique. These are important because errors at either of these tasks could have significant implications on operational effectiveness.

In this experiment, like experiment 3, the reference frame alignment effect was also observed on the aircraft flight path tracking task. Contrary to experiment 3, these flight path tracking data in experiment 4 show a basic reference frame alignment effect not influenced by the degree of initial rotation. The alignment effect on flight path tracking demonstrates a workload measurement because experiment 4 only included reference frame alignment of the sensor video so alignment did not directly influence the flight path tracking task. However, this small but measurable effect (<1% of orbit radius) represents a blanket error increase in the presence of misaligned displays regardless of the angle of misalignment. However, this is a relatively small effect in magnitude (~25% of the moving target effect) and should not be overstated.

These results confirmed the reference frame alignment hypotheses (#1), that multiple reference frames have an impact on unmanned aircraft operations beyond that addressed by the orientation aid, and the reference frame alignment technique could potentially address some of this impact.

The display redundancy reduction technique also showed promising results across several measures. The median time required to determine the direction of movement on the sensor display (orientation time) was reduced by 0.06 seconds, and the median time required to find a particular target (target acquisition time) was also reduced as a function of display redundancy reduction by 0.35 seconds.

Interestingly, the mere presence of an aircraft display increased the likelihood of error in the target acquisition task. Orientation time error rate was not affected and remained at 1.6% with and without the aircraft display. However, despite the fact that subjects claimed to ignore the aircraft display target acquisition error rate was increased, almost identically to that of reference frame alignment, from 0.7 to 2.9% when the aircraft display was visible. This is important because target acquisition errors could have significant implications on operational effectiveness, and the aircraft display was not involved in the target acquisition task.

This effect was not measured in the tracking performance of either flight path or sensor tracking, but further evidence was revealed in the secondary workload reaction time measurement. However, the reaction time measurement could be explained by the location of the visual cue relative to

the path of a subject's visual scan between displays. Despite this uncertainty, the effectiveness of reducing display redundancy by removing the aircraft display was evident on two important measures: orientation time and target acquisition time. These results are limited by lateral only control task required in this experiment. As discussed, the subject did not have to control aircraft pitch. This lateral only control coupled with the predictive aid enabled the display redundancy reduction.

This experiment found no evidence to support the moving target-alignment hypothesis (#5). In fact, some indications were shown that moving targets actually have the opposite effect on the alignment benefit. This was demonstrated on the orientation time measurement. As mentioned, subjects were quicker to determine the direction of movement in the sensor video when this video was aligned to north-up. However, the magnitude of this benefit was reduced rather than increased when moving targets were present. Similar results were shown on workload with the secondary visual reaction time test. As measured in this experiment, the moving target impact on the alignment effect was directly contrary to the moving target-alignment hypothesis (#5).

Overall, this experiment reinforced findings from experiments 1 and 3, by demonstrating the presence of a multiple reference frame difficulty in unmanned aircraft operations, and the potential for reference frame alignment to address some of that difficulty. This effect was first evident in a basic sensor video orientation task where the subject had to observe movement in the sensor video and describe the direction in the north-up reference frame for communication to ground personnel. Additionally, this impact was also evident in the target acquisition task where subjects were told to find and identify a vehicle approaching an intersection from some cardinal direction. Subjects completing this task on an aligned display were faster than those on a traditional misaligned display. Workload measures based on subjective ratings and secondary reaction time tests also showed benefits from reference frame alignment. Unlike experiment 1, reference frame alignment, in experiment 4, also improved the flight path tracking task performance. This should be interpreted as an additional measure of workload because no aircraft display alignment was investigated in this experiment.

In addition to the continually demonstrated promise of the reference frame alignment technique, these data also revealed a benefit of display redundancy reduction. After removing the aircraft display, and placing complete reliance on the predictive aid for aircraft control, subjects demonstrated faster orientation times in the sensor video direction task, and faster target acquisition times when told to locate a vehicle approaching an intersection. The reason for this improved performance and decreased workload is unclear, but it is an important discovery for future designs.

This experiment included two potentially useful display design methods for unmanned aircraft surveillance tasks. Both reference frame alignment, which involved aligning all displayed information to a north-up reference frame, and display redundancy reduction, which involved removing the aircraft display, improved basic orientation and targeting task performance during this experiment.

This page intentionally left blank.

8. Conclusions

Current unmanned aircraft commonly require two operators for mission control. This architecture has developed to allow for one operator (pilot) to focus on the aircraft control portion of a mission, and the other operator (sensor operator) to focus on controlling the gimballed sensor. The dual-operator requirement has become a significant cost and personnel burden on the US Air Force. As the demand for these surveillance systems increases, the ability to field and fund new operations has proved challenging. In the past research efforts have sought to address this problem through flight path automation which enabled the pilot to control several vehicles at once. Unfortunately, this method retains the requirement for the continued attention and control of a sensor operator. An alternative approach is to redesign the system with a single-operator in mind. This shift from one operator controlling the flight path of multiple vehicles to one operator controlling all aspects of one vehicle retains the flexibility to adapt each aircraft's flight path to the needs of each surveillance mission, and it reduces the manpower burden further than the multi-vehicle control architectures. However, requiring a single-operator to perform sensor and aircraft control presents additional challenges.

One basic challenge of this new architecture is the requirement to transform information between the different reference frames currently associated with these tasks. The aircraft control task traditionally requires the operator to manage the bank of the aircraft via an aircraft-view (perspective out the front of the cockpit) reference frame. The operator (pilot) must transform information on the north-up navigation display into this aircraft-view before determining a direction of bank control. Meanwhile the sensor control task traditionally requires the operator to reference the sensor-view (orientation directly viewed by the sensor video camera) reference frame to determine control inputs and interpret information on the sensor display. He or she must then transform this information to the navigation display for communication with other personnel or to request potential flight path changes from the pilot. With this traditional architecture each operator must manage two reference frames and the corresponding transformation between them.

Any attempt to reorganize this into a single-operator design would require managing both of these tasks with both of these reference frame transformations. Reference frame transformations are not new to the unmanned aircraft mission, and several research programs have addressed them with respect to the pilot aircraft control task. However, these have always focused on optimizing the displays for the navigation task of primary concern to the pilot. In contrast, this research introduced the idea of a mission-focused design which sought to optimize the displays for all of the included tasks. This did not take a singular or primary focus on the aircraft control, but rather combined the requirements of both tasks and looked for a way to optimize the multiple-task environment. This thesis was particularly focused on investigating the difficulty presented by these multiple reference frames on traditional unmanned aircraft surveillance operations. However, this process of optimizing displays for the multiple required tasks rather than combining individual displays which have been optimized for separate tasks could be important as future systems, in any domain, often require the operator to control a greater variety of tasks.

To characterize the cognitive rotation challenges of these operations, this research included 4 human subject experiments with a total of 80 participants over more than a year of data collection. The focus of each of these experiments was to measure the reference frame rotation problem and

investigate how reference frame alignment may be used to deal with this difficulty. The currently accepted practice of including an orientation aid (e.g. north arrow) on the display was also examined. Furthermore, display techniques which might be enabled by the successful implementation of reference frame alignment, such as display integration and display redundancy reduction, were also examined. Each of these was implemented into a basic flight simulator in a manner which minimized additional display changes.

In a series of simulator experiments (experiments 1, 3, and 4), subjects were asked to perform several representative tasks of an unmanned aircraft mission. This simulator included an aircraft and sensor video simulation, both of which had to be controlled by the subject.

At the start of each experimental trial the subject was given a time period to preview a satellite image of a target area and read a description of the specific target location. After this preview time, the simulation began with the aircraft initialized on an orbit around that target area, and the sensor was initially pointing in the vicinity of, but not on, the target. The subject had to maneuver the sensor to the target and select the location with a control stick. Performance was measured by the time required to find the target (target acquisition time), and this was used to determine which display techniques assisted with the transformation between the targeting information in the north-up reference frame, and the sensor video information in the rotating sensor-view reference frame.

Simultaneously the subject had to control the aircraft bank in order to follow the predefined flight path, a circular orbit around the target. The subject then continued to track the target with the crosshairs in the sensor video, and control the aircraft to stay on the planned flight path. These two simultaneous tracking tasks continued throughout each experimental trial which lasted 3.2 minutes, which was the time required for a complete circular orbit around the target.

During this period of dual tracking, the subjects had to respond to periodic (10-20 second intervals) reaction time tests. They squeezed the control stick trigger in response to a blinking light on the display. The response time was a proxy measure of spare mental capacity which was used to estimate changes in their workload across the different display configurations. After each reaction time test, a symbol moved across the sensor video, simulating a person, and the subjects interpreted the direction of movement so that they could inform ground personnel about the activity. This traditionally required a transformation between the sensor-view reference frame and the north-up reference frame. This represented an orientation test in the sensor display which could estimate the basic difficulty of this reference frame transformation amidst the multitask environment of unmanned aircraft operations. This task was also representative of a regular requirement during unmanned aircraft surveillance. The planning and execution of an unmanned aircraft mission can often require interpretation of cardinal direction information in the sensor video. Any communication with ground personnel requires transformation to the north-up reference frame. The time required for the subject to respond to this orientation cue (orientation time) represented the most direct measure of the multiple-reference-frame cost.

After each experimental trial with experiments 1, 3, and 4, the subject provided a subjective assessment of mental workload via the Bedford Workload Rating scale. These measurements were observed for any patterns in the subjects' subjective interpretation of the different displays. After subjects finished with their entire experiment, between 13 and 17 trials depending on the experiment,

they were asked for their direct preferences regarding the four display choices tested during their time. These data were also analyzed for a subjective interpretation of displays.

Over the course of these four experiments, four different display design techniques were analyzed for their influence on the multiple reference frame difficulty of unmanned aircraft operations. These techniques, in order of their observed effectiveness were: reference frame alignment, display redundancy reduction, orientation aid, and display integration.

Reference frame alignment involved rotating displayed information so that every display had the same orientation. In the past, this technique has been applied to align the navigation display with the aircraft display in a track-up orientation. Because the surveillance mission is often described on a north-up reference frame, this study always aligned reference frames to a north-up orientation.

Display redundancy reduction involved removing duplicated information from the provided displays. During this research, this technique relied on a flight path predictive aid which identified the predicted aircraft location in ten seconds and the basic lateral only aircraft control required during these experiments. This tool was displayed on the navigation display as a line protruding from the front of the aircraft symbol. Since subjects could control aircraft bank by observing the curvature of the predictive aid, this enabled removal of the traditional aircraft display and bank indicator. In this research, display redundancy reduction indicates the removal of the aircraft display. It is important to understand that only lateral navigation (aircraft bank angle) was controlled by the subject during these experiments. This display technique (display redundancy reduction) removed any indication of pitch from the display. So if altitude or pitch control were required, this technique would not be appropriate.

The currently-accepted technique for transforming the sensor video information is the orientation aid. As tested here, this involved a north arrow on the sensor display to indicate the direction of north in the imagery. This facilitated the mental transformation between the sensor-view reference frame and the north-up reference frame to allow subjects to find target locations and to communicate the cardinal direction of observed movement in the sensor video. While this is common place in operational systems, no formal testing of its effectiveness was available. This research evaluated this common display technique to understand its benefits and limitations in the unmanned aircraft surveillance task.

Finally, display integration combined information from the previously separate displays in an overlaid manner onto one central display. Here, the sensor video was placed in the center of the display on top of the central portion of the map. The aircraft display information was overlaid on top of both of these other displays. With the integrated display the satellite imagery was available for the target-preview time and then only available via control stick switch selection. Similarly the central portion of the map was obscured by the sensor video but was also available via control stick switch selection. This configuration involved a mismatch of reference frame dimensions since the map and sensor video represented different geographic dimensions.

Each of these display techniques represented a potential improvement in dealing with the reference frame transformation problem. Some of them directly applied to the mental rotation task (reference frame alignment, and orientation aids) while others altered the physical crosscheck to gather information on multiple displays (display redundancy and display integration). Of these techniques, the most universally effective was reference frame alignment.

The reference frame alignment technique significantly increased performance in every experiment (experiments 1-4). This included the basic orientation time to transform information between reference frames, and the more involved process for finding a target location. The technique also reduced workload as measured by subjective ratings and the reaction time secondary task.

Display redundancy reduction also increased performance and decreased workload in the one experiment where it was examined (experiment 4). The mechanism for this technique is not certain. It was thought that removing this redundancy would simplify the subject's visual crosscheck, or scan pattern, but operators generally reported that they were not using the aircraft display even when it was available. However, this could be an important consideration when considering how much redundancy to provide to an operator in any system.

The orientation aid on the sensor video did help with the basic orientation task, as measured through orientation time; however, it did not assist with the more complex target acquisition task. Although this technique is regularly used in current operational systems, it was only minimally effective when compared to reference frame alignment and display redundancy reduction.

Finally, the display integration technique demonstrated a neutral or negative impact during the one experiment where it was examined (experiment 3). The integrated display increased workload as measured by the reaction time secondary task, and had no significant effect on any other performance and workload measurement. It was thought that this configuration would assist with the operator's visual scan of information in the display; however, this was not demonstrated in these experiments. This could be an indication that display integration is not helpful, or it could indicate that the simple display integration used in these experiments was suboptimal and therefore not effective.

The median orientation time, which measured the time between viewing movement in the sensor video and judging the direction of that movement, was reduced by approximately 0.5 seconds with reference frame alignment, 0.2 seconds with the orientation aid, and 0.06 seconds with display redundancy reduction. Reference frame alignment produced the greatest effect here, but these reductions are all significant because scenarios which require multiple transformations back and forth across reference frames, or high frequency task switching between displays, would amplify this effect. If each switch requires an orientation time to interpret a basic direction, the task performance could be greatly degraded with multiple reference frames.

During this orientation task, the reference frame alignment technique also repeatedly reduced error rates (percentage of incorrect orientation answers) during each experiment. The orientation aid also reduced error rates in the one experiment where it was examined (experiment 1), but to a lesser degree than reference frame alignment. Display redundancy reduction and display integration had no observed impact on error rates. These error rate reductions could be more important than the decreased orientation time because errors during these orientation tasks could lead operational problems in an actual unmanned aircraft mission. If the single operator were communicating misinformation to ground personnel, this could put those individuals at greater risk.

Besides orientation time, other factors also influenced the impact on more complex tasks such as target acquisition. Even though orientation aids were able to decrease the time required for an alignment transformation, they did not provide a measurable impact on the time required to find a target in the sensor video (target acquisition time). However, the larger impacts from reference frame alignment and display redundancy reduction were effective at reducing target acquisition time. The

target acquisition task which represented a realistic requirement to find a location in the sensor video, was improved (faster time to find the target) when the reference frame was aligned or when the aircraft display was removed. Both of these options offer a significant benefit to a regular and vital task of unmanned aircraft surveillance missions. Additionally, both of these techniques reduced the error rates of target acquisition (percentage of incorrect target location selections). Reference frame alignment and display redundancy reduction similarly reduced these error rates by more than half, but the orientation aid had no effect on the accuracy of target acquisition. Display integration actually decreased the accuracy of target acquisition. Since this task was representative of releasing a weapon on a target, these errors would be catastrophic in an actual unmanned aircraft mission. This reinforces the benefit of reference frame alignment and display redundancy reduction.

In order to assess these display techniques for the multi-task environment of unmanned aircraft surveillance, it was also important to observe performance of other unmanned aircraft tasks that are not directly related to the reference frame transformation. Any display technique which reduced the reference frame rotation difficulty but significantly increased difficulty in other surveillance related tasks would not be a valid solution to this problem. Performance of the aircraft flight path tracking which required reference frame transformation and sensor crosshair tracking tasks which did not were both monitored. None of these four techniques (reference frame alignment, display redundancy reduction, orientation aid, and display integration) degraded any measure of tracking performance, and only reference frame alignment actually improved one of these measures. Although a minor magnitude of improvement, reference frame alignment improved flight path tracking in experiments 3 and 4. This indicates that any of these four techniques are appropriate for the underlying sensor and flight path tracking tasks.

Ultimately, the reference frame alignment effect was demonstrated with every performance and workload measurement. In each experiment a significant effect on objective performance, workload and user preferences was measured. In contrast, the orientation aid technique (currently accepted practice) was only impactful in the basic orientation time performance during simulator experiments. The increased effectiveness of reference frame alignment is reinforced because an orientation aid was present in every display for experiments 3 and 4, and the reference frame alignment technique still produced a significant effect despite the continued presence of the orientation aid. These experiments demonstrated that reference frame alignment was much more effective than the orientation aid technique.

In addition to each of the parametric and non-parametric performance and workload differences that have been outlined in this document, the reference frame alignment technique also reduced error rates that could be crucial to the sorts of orientation tasks carried out by surveillance and targeting aircraft. One cannot exaggerate the significance of accuracy in the target acquisition task. In each experiment of this study, subjects were asked to consider the gravity of bombing the wrong target during the target acquisition task. Still, the error rates were much higher on the displays without reference frame alignment. Even if these results were explained as an effect of inexperienced subjects, correcting these mistakes would have undoubtedly led to increased target acquisition times for those trials and would have further increased the measurable effect of reference frame alignment on target acquisition time. Unmanned aircraft and other remotely operated system designers should consider incorporating some form of reference frame alignment to assist with time sensitive decision-making

which requires transformation of information across multiple reference frames and involves heavy penalties for errors. The central reference frame of this alignment should be selected to support the group of tasks associated with the given system rather than to support one specific task. In this research the effect was demonstrated using the north-up reference frame; however, other reference frames may be more appropriate for different systems.

These findings highlight a need for further research into the multiple reference frame problem, and the reference frame alignment technique to address that problem. Despite the current efforts to increase automation to replace the human, tools such as reference frame alignment, which could enable the human to more effectively complete the unmanned aircraft control task, should be explored in earnest for potential benefits throughout the research community. To reinforce or challenge the findings in this document, future research should explore more complex navigation requirements.

One specific area for exploration can evaluate the benefits of reference frame alignment compared with those of increasing the action implementation automation. Automation of the aircraft control problem has been heavily investigated, but only for simplified flight path requirements. Future efforts could investigate the tradeoff between the retained flexibility of manual flight path control as compared to an automated flight path guidance system. The aircraft guidance, during this research, followed basic orbits around the target; however, a greater benefit of reference frame alignment may be that it retains the operator's ability to control the aircraft for more complex and specific flight paths than autonomous alternatives. Including tasks which require two-dimensional aircraft control (pitch and bank) would challenge the aircraft display reference frame alignment because this display did not allow for pitch control; however, the sensor video alignment could still offer potential benefits in these scenarios.

In addition to the many positive observed effects of reference frame alignment, the display redundancy reduction technique was also promising. It did not have the same impact as reference frame alignment, but did highlight an important consideration for system designs that currently use multiple control screens and multiple controllers. Although the mechanism for the performance and workload impact in this research is uncertain, this is still an important consideration in display design. As modern cockpits (manned and unmanned) increase in complexity, the presence of redundant displays may impact the performance and workload of operations.

Although these experiments were not designed to evaluate the flight path predictive aid, a qualitative comparison across experiments revealed an effectiveness of the predictive aid at improving flight path tracking in both experiment 3 and experiment 4 when compared to a traditional display in experiment 1. These data relied on comparisons across subjects and with the experiment 3 and 4 moving target scenarios; however, despite the increased difficulty of the mission tasks, performance still increased on experiments 3 and 4 when compared with experiment 1. This is a powerful indicator of the predictive aid effectiveness. Many researchers have investigated the predictive aids for their potential benefit with latent flight controls, but this research shows the predictive aid benefit in the multitask environment without a control latency.

This understanding of reference frame alignment should not be considered complete, only one primary reference frame was considered during this research. This research highlighted the important consideration of designing displays for multitask requirements rather than combining displays which have been previously optimized for one task. With the specific multitask requirements of unmanned

aircraft surveillance operations in mind, the north-up reference frame was chosen as the central focus of reference frame alignment during this research. However, if another system includes a fundamental reference frame other than north-up then a different form of reference frame alignment may be more appropriate. Additionally, if the user has physical access to a reference frame, such as a manned pilot has access to the aircraft-view reference frame by looking out the cockpit window, then it may be impractical to remove that reference frame from the display design. However, when possible designers should consider the fundamental reference frame for a set of multiple tasks, and seek to align other tasks to that fundamental orientation. As demonstrated in this research, benefits and performance and workload are possible even if these new displays are not those traditionally used for certain tasks.

This research also introduced the idea of removing repetitive information from the available displays. Even though the aircraft display provided a higher resolution of aircraft bank, and the display design has been optimized for the aircraft control task, its removal actually increased performance and decreased workload. The simple predictive aid (“noodle”) on the navigation display was sufficient for this lateral only aircraft control task, and subjects were more effective when relying solely on the predictive aid for aircraft bank control. This effect could be based on the distraction offered by the aircraft display, but regardless of the reason, it is an important consideration for future designs which often include display redundancy. While system redundancy is often necessary for abnormal operations, this research highlighted the potential primary task benefits of a simplified display with a reduced level of redundancy. Future designers should consider the risk of overly redundant displays and examine the primary task effects when adding redundancy for abnormal operations.

Reference frame alignment, predictive aids, and display redundancy reduction effectively reduced the impact of multiple reference frames on tasks associated with the unmanned aircraft surveillance mission. These display techniques should be considered in future research and system development.

This page intentionally left blank.

Bibliography

- [1] J. A. Winnefeld and F. Kendall, "Unmanned Systems Integrated Roadmap," Department of Defense, Washington D.C., 2013.
- [2] R. Valerdi, "Cost Metrics for Unmanned Aerial Vehicles," in *Infotech@Aerospace AIAA*, Arlington, VA, 2005.
- [3] Press, "sUAS News," 14 Oct 2014. [Online]. Available: <http://www.suasnews.com/2014/10/predatorgray-eagle-series-surpasses-3-million-flight-hours/>. [Accessed 6 May 2016].
- [4] S. Kesselman, "AUVSI," 29 Oct 2014. [Online]. Available: <http://www.auvsi.org/browse/blogs/blogviewer?BlogKey=7dbc2cf2-b719-40df-bf80-285d3e3201a8>. [Accessed 5 May 2016].
- [5] J. Gordon, "Going the Distance: Globemaster III Hits Major Mileston, Flies 3,000,000 Hours," 8 May 2015. [Online]. Available: <http://www.robins.af.mil/news/story.asp?id=123447574>. [Accessed 6 May 2016].
- [6] B. Everstine, "Air Force Times," 4 Feb 2015. [Online]. Available: <http://www.airforcetimes.com/story/military/pentagon/2015/02/04/air-force-seeks-more-flight-hours-to-recover-from-2013-stand-down/22863401/>. [Accessed 6 May 2016].
- [7] M. Thompson, "Time," 2 April 2013. [Online]. Available: <http://nation.time.com/2013/04/02/costly-flight-hours/>. [Accessed 6 May 2016].
- [8] "MQ-9 Reaper USAF Fact Sheet," 23 September 2015. [Online]. Available: <http://www.af.mil/AboutUs/FactSheets/Display/tabid/224/Article/104470/mq-9-reaper.aspx>. [Accessed 3 May 2016].
- [9] "MQ-1B Predator USAF Fact Sheet," 23 September 2015. [Online]. Available: <http://www.af.mil/AboutUs/FactSheets/Display/tabid/224/Article/104469/mq-1b-predator.aspx>. [Accessed 3 May 2016].
- [10] "RQ-11B Raven USAF Fact Sheet," 31 October 2007. [Online]. Available: <http://www.af.mil/AboutUs/FactSheets/Display/tabid/224/Article/104533/rq-11b-raven.aspx>. [Accessed 3 May 2016].
- [11] "RQ-4 Global Hawk," 27 October 2014. [Online]. Available: <http://www.af.mil/AboutUs/FactSheets/Display/tabid/224/Article/104516/rq-4-global-hawk.aspx>. [Accessed 3 May 2016].
- [12] T. Scheve, "How the MQ-9 Reaper Works," 22 July 2008. [Online]. Available: <http://science.howstuffworks.com/reaper4.htm>. [Accessed 17 May 2015].
- [13] W. Wheeler, "The MQ-9's Cost and Performance," 28 February 2012. [Online]. Available: <http://nation.time.com/2012/02/28/2-the-mq-9s-cost-and-performance/>. [Accessed 3 May 2016].

- [14] J. Hasik, "James Hasik, Industrial Analysis for Global Security," 20 June 2012. [Online]. Available: <http://www.jameshasik.com/weblog/2012/06/affordably-unmanned-a-cost-comparison-of-the-mq-9-to-the-f-16-and-a-10-and-a-response-to-winslow-whe.html>. [Accessed 3 May 2016].
- [15] G. V. Jean, "Air Force Responding to Insatiable Demand for Surveillance Drones," *National Defense*, July 2009.
- [16] J. Rosamond, "DSEI: ONR Faces Uphill Struggle to Cut UAV Manpower Costs," 16 September 2015. [Online]. Available: <https://news.usni.org/2015/09/16/dsei-onr-faces-uphill-struggle-to-cut-uav-manpower-costs>. [Accessed 3 May 2016].
- [17] D. Majumdar, "Exclusive: U.S. Drone Fleet at 'Breaking Point', Air Force Says," *The Daily Beast*, 4 January 2015. [Online]. Available: <http://www.thedailybeast.com/articles/2015/01/04/exclusive-u-s-drone-fleet-at-breaking-point-air-force-says.html>. [Accessed 17 May 2016].
- [18] M. Pomerleau, "Air Force Takes Steps to Fix Drone Pilot Shortage," *Defense Systems: UAS & Robotics*, 20 May 2015. [Online]. Available: <https://defensesystems.com/articles/2015/05/20/air-force-addresses-drone-pilot-shortage.aspx>. [Accessed 5 May 2016].
- [19] M. Malenic, "USAF Enlisted Personnel to Operate Global Hawk UAVs," *IHS Jane's 360*, 21 January 2016. [Online]. Available: <http://www.janes.com/article/57360/usaf-enlisted-personnel-to-operate-global-hawk-uavs>. [Accessed 17 May 2016].
- [20] J. Schogol, "Air Force to Have Enlisted Pilots for First Time Since World War II," *Air Force Times*, 17 December 2015. [Online]. Available: <http://www.airforcetimes.com/story/military/2015/12/17/air-force-have-enlisted-pilots-first-time-since-world-war-ii/77490376/>. [Accessed 17 May 2016].
- [21] "AF Introduces Enlisted Global Hawk Pilots," *Secretary of the Air Force Public Affairs*, 17 December 2015. [Online]. Available: <http://www.af.mil/News/ArticleDisplay/tabid/223/Article/637192/af-introduces-enlisted-global-hawk-pilots.aspx>. [Accessed 147 May 2016].
- [22] B. Jordan, "Enlisted Airmen May Begin Flying Drones This Year, General Says," *Military.com*, 9 March 2016. [Online]. Available: <http://www.military.com/daily-news/2016/03/09/enlisted-airmen-may-begin-flying-drones-this-year-general-says.html>. [Accessed 17 May 2016].
- [23] S. Losey, "To Meet Anti-Terror Demand, Air Force Offers \$125K Bonuses to Keep Drone Pilots," *Air Force Times*, 15 December 2016. [Online]. Available: <http://www.airforcetimes.com/story/military/benefits/pay/2015/12/15/rpa-pilots-now-eligible-for-125k-retention-bonus/77370056/>. [Accessed 17 May 2016].
- [24] Y. Steinbuch, "Air Force so Desperate to Keep Drone Pilots, They're Offering Them \$125,000 Bonuses," *New York Post*, 15 December 2015. [Online]. Available: <http://nypost.com/2015/12/16/air-force-so-desperate-to-keep-drone-pilots-theyre-offering-them-125000-bonuses/>. [Accessed 17 May 2016].
- [25] P. D. Shinkman, "Air Force to Strengthen Drone Program by 3,000 Airmen, New Bases," *U.S. News*, 10 December 2015. [Online]. Available: <http://www.usnews.com/news/articles/2015/12/10/air-force-to-strengthen-drone-program-with-3-000-airmen-new-bases>. [Accessed 17 May 2016].

- [26] D. DeKunder, "Air Force RPA Training Pipeline Set to Expand," Joint Base San Antonio News, 20 August 2015. [Online]. Available: <http://www.jbsa.mil/News/News/tabid/11890/Article/613971/air-force-rpa-training-pipeline-set-to-expand.aspx>. [Accessed 17 May 2016].
- [27] A. J. Hebert, "Every Pilot in His Place," Air Force Magazine, October 2007. [Online]. Available: <http://www.airforcemag.com/MagazineArchive/Pages/2007/October%202007/1007pilot.aspx>. [Accessed 17 May 2016].
- [28] H. A. Ruff, G. L. Calhoun, M. H. Draper, J. V. Fontejon and B. J. Guilfoos, "Exploring Automation Issues in Supervisory Control of Multiple UAVs," in *Proceedings of the Human Performance, Situation Awareness, and Automation Technology Conference*, Wright Patterson AFB, OH, 2004.
- [29] B. Jacobs, E. de Visser, A. Freedy and P. Scerri, "Application of Intelligent Aiding to Enable Single Operator Multiple UAV Supervisory Control," Association for the Advancement of Artificial Intelligence, Palo Alto, CA, 2010.
- [30] H. A. Ruff, S. Narayanan and M. H. Draper, "Human Interaction with Levels of Automation and Decision-Aid Fidelity in the Supervisory Control of Multiple Simulated Unmanned Air Vehicles," *Presence*, vol. 11, no. 4, pp. 335-351, 2002.
- [31] D. Deptula, "Air Force Unmanned Aerial System (UAS) Flight Plan," US Air Force, Washington D.C., 2009.
- [32] J. Eggers and M. H. Draper, "Multi-UAV Control for Tactical Reconnaissance and Close Air Support Missions: Operator Perspectives and Design Challenges," in *Proceedings of the NATO RTO Human Factors and Medicine Panel Symposium*, 2006.
- [33] G. Calhoun, M. Draper, C. Miller, H. Ruff, C. Breeden and J. Hamell, "Adaptable Automation Interface for Multi-Unmanned Aerial Systems Control: Preliminary Usability Evaluation," in *Proceedings of the Human Factors and Ergonomics Society*, 2013.
- [34] J. Keller, "Air Force Asks General Atomics to Upgrade UAV Ground-Control Stations for Use with the Internet," 20 March 2014. [Online]. Available: <http://www.militaryaerospace.com/articles/2014/03/uav-control-upgrades.html>. [Accessed 6 May 2016].
- [35] I. General Atomics Aeronautical Systems, "Ground Control Stations," [Online]. Available: http://www.ga-asi.com/Websites/gaasi/images/products/ground_control/pdf/GCS021915.pdf. [Accessed 6 May 2016].
- [36] S. D. Scott, M. L. Cummings and F. B. da Silva, "Design Methodology for Unmanned Aerial Vehicle (UAV) Team Coordination," Massachusetts Institute of Technology, Cambridge, MA, 2007.
- [37] M. L. Cummings and P. J. Mitchell, "Predicting Controller Capacity in Supervisory Control of Multiple UAVs," *IEEE Transactions on Systems, Man, and Cybernetics-Part A: Systems and Humans*, vol. 116, no. 1, pp. 451-460, 2008.
- [38] T. Shaw, A. Emfield, A. Garcia, E. de Visser, C. Miller, R. Parasuraman and L. Fern, "Evaluating the Benefits and Potential Costs of Automation Delegation for Supervisory Control of Multiple UAVs," in *Proceedings of the Human Factors and Ergonomics Society*, 2010.

- [39] L. C. Robertson, S. E. Palmer and L. M. Gomez, "Reference Frames in Mental Rotation," *Journal of Experimental Psychology: Learning, Memory, and Cognition*, vol. 13, no. 3, pp. 368-379, 1987.
- [40] B. Tversky, "Cognitive Maps, Cognitive Collages, and Spatial Mental Models," in *Spatial Information Theory: A Theoretical Basis for GIS*, Berlin, 1993.
- [41] G. L. Beeker, "Equations of Motion I," in *Performance Flight Testing*, Edwards AFB, CA, USAF Test Pilot School, 1993, pp. 13.1-13.26.
- [42] J. J. Bertin and M. L. Smith, *Aerodynamics for Engineers*, Upper Saddle River, NJ: Simon & Schuster, 1998.
- [43] J. D. Anderson, *Fundamentals of Aerodynamics*, New York, NY: Mcgraw-Hill, 2011.
- [44] J. D. Anderson, *Introduction to Flight*, New York, NY: Mcgraw-Hill, 2008.
- [45] C. R. Kelley, "Manual Control," Office of Naval Research, Washington, D.C., 1964.
- [46] R. W. Proctor and T. Van Zandt, *Human Factors in Simple and Complex Systems*, 2d ed., New York: CRC Press, 2008.
- [47] A. J. Grunwald, "Tunnel Display for Four-Dimensional Fixed-Wing Aircraft Approaches," *Journal of Guidance, Control, and Dynamics*, vol. 7, no. 3, pp. 369-377, 1984.
- [48] M. Endsley, R. Sollenberger and E. Stein, "The Use of Predictive Displays for Aiding Controller Situation Awareness," *Proceedings of the Human Factors and Ergonomics Society*, vol. 43, no. 1, pp. 51-55, 1999.
- [49] S. N. Roscoe and R. S. Jensen, "Computer-Animated Predictive Displays for Microwave Landing Approaches," *IEEE Transactions on Systems, Man, and Cybernetics*, Vols. SMC-11, no. 11, pp. 760-764, 1981.
- [50] T. B. Sheridan, *Telerobotics, Automation, and Human Supervisory Control*, Cambridge, MA: Massachusetts Institute of Technology, 1992.
- [51] C. D. Wickens and E. Morphew, "Predictive Features of a Cockpit Traffic Display: A Workload Assessment," NASA Ames Research Center, Moffett Field, CA, 1997.
- [52] F. Bitton and R. Evans, "Report on Head-Up Display Symbology Standardization," USAF Instrument Flight Center, Randolph AFB, TX, 1990.
- [53] Lockheed Martin, "Sniper(R) Advanced Targeting Pod," 2015. [Online]. Available: www.lockheedmartin.com/content/dam/lockheed/data/mfc/photo/sniper-pod/feature/mfc-sniper-product-card.pdf. [Accessed 6 Jun 2016].
- [54] J. T. Richelson, "The National Security Archive," George Washington University, 16 October 2002. [Online]. Available: nsarchive.gwu.edu/NSAEBB/NSAEBB74/. [Accessed 6 June 2016].
- [55] N. Y. Barclay, "Air Force Photos," US Air Force, [Online]. Available: <http://www.af.mil/News/Photos.aspx?igphoto=2000578029>. [Accessed 6 May 2016].
- [56] R. Roughton and V. Young, "Daily Deployed," Airman Magazine, 6 July 2015. [Online]. Available: airman.dodlive.mil/2015/07/daily-deployed/. [Accessed 6 June 2016].
- [57] M. Reilly, "F18 Bombing Run in Iraq," YouTube, 10 August 2014. [Online]. Available: www.youtube.com/watch?v=P-jZmC2IzM8. [Accessed 6 June 2016].

- [58] L. Gugerty and J. Brooks, "Seeing Where You Are Heading: Integrating Environmental and Egocentric Reference Frames in Cardinal Direction Judgments," *Journal of Experimental Psychology: Applied*, vol. 7, no. 3, pp. 251-266, 2001.
- [59] L. Gugerty and J. Brooks, "Reference-Frame Misalignment and Cardinal Direction Judgments: Group Differences and Strategies," *Journal of Experimental Psychology: Applied*, vol. 10, no. 2, pp. 75-88, 2004.
- [60] A. J. Aretz and C. D. Wickens, "Cognitive Requirements for Aircraft Navigation," NASA Ames Research Center, Moffett Field, CA, 1990.
- [61] R. N. Shepard and S. Hurwitz, "Upward Direction, Mental Rotation, and Discrimination of Left and Right Turns in Maps," *Cognition*, vol. 18, pp. 161-193, 1984.
- [62] D. L. Hintzman, C. S. O'Dell and D. R. Arndt, "Orientation in Cognitive Maps," *Cognitive Psychology*, vol. 13, pp. 149-206, 1981.
- [63] G. Gunzelmann and J. Anderson, "Strategic Differences in the Coordination of Different Views of Space," in *Proceedings of the 24th Annual Conference of the Cognitive Science Society*, Cincinnati, OH, 2002.
- [64] W. Rodes and L. Gugerty, "Effects of Electronic Map Displays and Individual Differences in Ability on Navigation Performance," *Human Factors*, vol. 54, no. 4, pp. 589-599, 2012.
- [65] J. R. Helleberg and C. D. Wickens, "Effects of Data-Link Modality and Display Redundancy on Pilot Performance: an Attentional Perspective," *The International Journal of Aviation Psychology*, vol. 13, no. 3, pp. 189-210, 2003.
- [66] C. D. Wickens, J. Goh, J. Helleberg, W. J. Horrey and D. A. Talleur, "Attentional Models of Multitask Performance Using Advanced Display Technology," *Human Factors*, vol. 45, no. 3, pp. 360-380, 2003.
- [67] P. Michels, D. Ing, D. Gravenstein and D. R. Westenskow, "An Integrated Graphic Data Display Improves Detection and Identification of Critical Events During Anesthesia," *Journal of Clinical Monitoring*, vol. 13, no. 4, pp. 249-259, 1997.
- [68] D. C. Foyle, A. D. Andre, R. S. McCann, E. M. Wenzel, D. R. Begault and V. Battiste, "Taxiway Navigation and Situation Awareness (T-NASA) System: Problem, Design Philosophy, and Description of an Integrated Display Suite for Low-Visibility Airport Surface Operations," *SAE Transactions: Journal of Aerospace*, vol. 105, pp. 1411-1418, 1996.
- [69] J. V. O'Brien and C. D. Wickens, "Free Flight Cockpit Displays of Traffic and Weather: Effects of Dimensionality and Data Base Integration," *Proceedings of the Human Factors and Ergonomics Society*, vol. 41, pp. 18-22, 1997.
- [70] G. Calhoun, H. Ruff, A. Lefebvre, M. Draper, A. Ayala and , "'Picture-in-Picture" Augmentation of UAV Workstation Video Display," *Proceedings of the Human Factors and Ergonomics Society*, pp. 70-74, 2007.
- [71] C. M. Carswell and C. D. Wickens, "Comparative Graphics: History and Applications of Perceptual Integrality Theory and the Proximity Compatibility Hypothesis," U.S. Army Human Engineering Laboratory, Aberdeen Proving Ground, MD, 1988.

- [72] C. D. Wickens and J. G. Hollands, *Engineering Psychology and Human Performance*, Upper Saddle River, NJ: Prentice-Hall, 2000.
- [73] C. D. Wickens and A. D. Andre, "Proximity Compatibility and the Object Display," in *Proceedings of the Human Factors Society*, 1988.
- [74] T. S. Kam, G. K. Tharp, A. T. Tai, M. H. Draper, G. L. Calhoun and H. A. Ruff, "A Human Factors Testbed for Command and Control of Unmanned Air Vehicles," in *Digital Avionics Systems 22nd Conference*, 2003.
- [75] A. S. Clare, J. C. Ryan, K. F. Jackson and M. L. Cummings, "Innovative Systems for Human Supervisory Control of Unmanned Vehicles," *Proceedings of the Human Factors and Ergonomics Society*, vol. 56, pp. 531-535, 2012.
- [76] J. P. How, C. Fraser, K. C. Kulling, L. F. Bertuccelli, O. Toupet, L. Brunet, A. Bachrach and N. Roy, "Increasing Autonomy of UAVs," *IEEE Robotics & Automation Magazine*, vol. 16, no. 2, pp. 43-51, 2009.
- [77] V. Roberge, M. Tabouchi and G. Labonte, "Comparison of Parallel Genetic Algorithm and Particle Swarm Optimization for Real-Time UAV Path Planning," *IEEE Transactions on Industrial Informatics*, vol. 9, no. 1, pp. 132-141, 2013.
- [78] Defense Science Board, "The Role of Autonomy in DOD Systems," Department of Defense, Washington, D.C., 2012.
- [79] I. Maza, K. Kondak, M. Bernard and A. Ollero, "Mult-UAV Cooperation and Control for Load Transportation and Deployment," *J Intell Robot Syst*, vol. 57, pp. 417-449, 2010.
- [80] D. Liu, R. Wasson and D. A. Vincenzi, "Effects of System Automation Management Strategies and Multi-mission Operator-to-vehicle Ratio on Operator Performance in UAV Systems," *Journal of Intelligent and Robotic Systems*, vol. 54, pp. 795-810, 2009.
- [81] D. R. Olsen and S. B. Wood, "Fan-Out: Measuring Human Control of Multiple Robots," in *Proceedings of the SIGCHI Conference on Human Factors in Computing Systems*, Vienna, Austria, 2004.
- [82] F. B. da Silva, S. D. Scott and M. L. Cummings, "Design Methodology for Unmanned Aerial Vehicle (UAV) Team Coordination," Massachusetts Institute of Technology, Cambridge, MA, 2007.
- [83] R. Parasuraman, K. A. Cosenzo and E. D. Visser, "Adaptive Automation for Human Supervision of Multiple Uninhabited Vehicles: Effects on Change Detection, Situation Awareness, and Mental Workload," *Military Psychology*, vol. 21, pp. 270-297, 2009.
- [84] G. L. Calhoun, H. A. Ruff, M. H. Draper and E. J. Wright, "Automation-Level Transference Effects in Simulated Multiple Unmanned Aerial Vehicle Control," *Journal of Cognitive Engineering and Decision Making*, vol. 5, no. 1, pp. 55-82, 2011.
- [85] S. Fisher, "Replan Understanding for Heterogenous Unmanned Vehicle Teams," Massachusetts Institute of Technology, Cambridge, MA, 2007.
- [86] C. A. Miller and R. Parasuraman, "Designing for Flexible Interaction Between Humans and Automation: Delegation Interfaces for Supervisory Control," in *The Journal of the Human Factors and Ergonomics Society*, 2007.

- [87] K.-C. Lin, "Swarming UAVs Behavior Hierarchy," in *Multi-Robot Systems*, Netherlands, Springer, 2005, pp. 269-275.
- [88] J. Y. C. Chen, M. J. Barnes and M. Harper-Sciari, "Supervisory Control of Multiple Robots: Human-Performance Issues and User-Interface Design," *IEEE Transactions on Systems, Man, and Cybernetics - Part C: Applications and Reviews*, vol. 41, no. 4, pp. 435-454, 2011.
- [89] P. E. I. Pounds and S. P. N. Singh, "Integrated Electro-Aeromechanical Structures for Low-Cost, Self-Deploying Environment Sensors and Disposable UAVs," in *IEEE International Conference on Robotics and Automation (ICRA)*, Karlsruhe, Germany, 2013.
- [90] R. Beard, D. Kingston, M. Quigley, D. Snyder, R. Christiansen, W. Johnson, T. McLain and M. A. Goodrich, "Autonomous Vehicle Technologies for Small Fixed-Wing UAVs," *Journal of Aerospace Computing, Information, and Communication*, vol. 2, pp. 92-108, 2005.
- [91] E. P. Anderson and R. W. Beard, "An Algorithmic Implementation of Constrained Extremal Control for UAVs," in *AIAA Guidance, Navigation, and Control Conference and Exhibit*, Monterey, CA, 2002.
- [92] A. Ryan and J. K. Hedrick, "A Mode-Switching Path Planner for UAV-assisted Search and Rescue," in *IEEE Conference on Decision and Control, and the European Control Conference*, Seville, Spain, 2005.
- [93] S. R. Dixon, C. D. Wickens and D. Chang, "Comparing Quantitative Model Predictions to Experimental Data in Multiple-UAV Flight Control," *Proceedings of the Human Factors and Ergonomics Society*, vol. 47, pp. 104-108, 2003.
- [94] L. C. Thomas and C. D. Wickens, "Visual Displays and Cognitive Tunneling: Frames of Reference Effects on Spatial Judgments and Change Detection," *Proceedings of the Human Factors and Ergonomics Society Annual Meeting*, vol. 45, no. 4, pp. 336-340, 2001.
- [95] C. Ware and S. Osborne, "Exploration and Virtual Camera Control in Virtual Three Dimensional Environments," *Proceedings of the 1990 Symposium on Interactive 3D Graphics*, pp. 175-183, 1990.
- [96] C. D. Wickens, L. C. Thomas and R. Young, "Frames of Reference for the Display of Battlefield Information: Judgment-Display Dependencies.," *Human Factors*, vol. 42, no. 4, pp. 660-675, 2000.
- [97] C. D. Wickens and T. T. Preve, "Exploring the Dimensions of Egocentricity in Aircraft Navigation," *Journal of Experimental Psychology: Applied*, vol. 1, no. 2, pp. 110-135, 1995.
- [98] C. W. Nielsen, M. A. Goodrich and R. W. Ricks, "Ecological Interfaces for Improving Mobile Robot Teleoperation," *Transactions on Robotics*, vol. 23, no. 5, pp. 927-941, 2007.
- [99] S. L. Pazuchanics, "The Effects of Camera Perspective and Field of View on Performance in Teleoperated Navigation," *Proceedings of the Human Factors and Ergonomics Society Annual Meeting*, vol. 50, pp. 1528-1532, 2006.
- [100] K. Chintamani, A. Cao, R. D. Ellis and A. K. Pandya, "Improved Telemanipulator Navigation During Display-Control Misalignments Using Augmented Reality Cues," *IEEE Transactions on Systems, Man, and Cybernetics-Part A: Systems and Humans*, vol. 40, no. 1, pp. 29-39, 2010.

- [101] P. M. Fitts and C. W. Simon, "Some Relations Between Stimulus Patterns and Performance in a Continuous Dual-Pursuit Task," *Journal of Experimental Psychology*, vol. 43, no. 6, pp. 428-436, 1952.
- [102] P. M. Fitts and C. M. Seeger, "S-R Compatibility: Spatial Characteristics of Stimulus and Response Codes," *Journal of Experimental Psychology*, vol. 46, no. 3, pp. 199-210, 1953.
- [103] C. F. Michaels, "S-R Compatibility Between Response Position and Destination of Apparent Motion: Evidence of the Detection of Affordances," *Journal of Experimental Psychology: Human Perception and Performance*, vol. 14, no. 2, pp. 231-240, 1988.
- [104] R. W. Proctor and K.-P. L. Vu, *Stimulus-Response Compatibility Principles: Data, Theory, and Application*, New York, NY: CRC Press, 2006.
- [105] C. D. Wickens, "Attention in Aviation," *Proceedings of the Fourth International Symposium on Aviation Psychology*, pp. 602-608, 1987.
- [106] W. Hirst and D. Kalmar, "Characterizing Attentional Resources," *Journal of Experimental Psychology: General*, vol. 116, no. 1, pp. 68-81, 1987.
- [107] G. Sachs, "Flightpath predictor for minimum pilot compensation," *Aerospace Science and Technology*, vol. 4, pp. 247-257, 1999.
- [108] B. P. DeJong, E. Colgate and M. A. Peshkin, "Improving Teleoperation: Reducing Mental Rotations and Translations," *Conference on Robotics and Remote Systems - Proceedings*, vol. 8, no. 10, pp. 472-479, 2004.
- [109] M. J. Tarr and S. Pinker, "Mental Rotation and Orientation-Dependence in Shape Recognition," *Cognitive Psychology*, vol. 21, no. 2, pp. 233-282, 1989.
- [110] M. A. Just and P. A. Carpenter, "Cognitive Coordinate Systems: Accounts of Mental Rotation and Individual Differences in Spatial Ability," Carnegie-Mellon University, Pittsburgh, PA, 1984.
- [111] P. A. Kolers and D. N. Perkins, "Orientation of Letters and Their Speed of Recognition," *Perception & Psychophysics*, vol. 5, no. 5, pp. 275-280, 1969.
- [112] K. Gramann, J. Onton, D. Riccobon, H. J. Mueller, S. Bardins and S. Makeig, "Human Brain Dynamics Accompanying Use of Egocentric and Allocentric Reference Frames during Navigation," *Journal of Cognitive Neuroscience*, vol. 22, no. 12, pp. 2836-2849, 2010.
- [113] C. Quaiser-Pohl, "The Mental Cutting Test "Schnitte" and the Picture Rotation Test - Two New Measures to Assess Spatial Ability," *International Journal of Testing*, vol. 3, no. 3, pp. 219-231, 2003.
- [114] R. N. Shepard and J. Metzler, "Mental Rotation of Three-Dimensional Objects," *Science*, vol. 171, pp. 701-703, 1971.
- [115] S. G. Vandenberg and A. R. Kuse, "Mental Rotations, a Group Test of Three-Dimensional Spatial Visualization," *Perceptual and Motor Skills*, vol. 47, pp. 599-604, 1978.
- [116] L. A. Cooper, "Mental Rotation of Random Two-Dimensional Shapes," *Cognitive Psychology*, vol. 7, pp. 20-43, 1975.

- [117] M. S. Cohen, S. M. Kosslyn, H. C. Breiter, G. J. Digirolamo, W. L. Thompson, A. K. Anderson, S. Y. Bookheimer, B. R. Rosen and J. W. Belliveau, "Changes in Cortical Activity During Mental Rotation," *Brain*, vol. 119, pp. 89-100, 1996.
- [118] D. J. Bryant and B. Tversky, "Mental Representations of Perspective and Spatial Relations From Diagrams and Models," *Journal of Experimental Psychology*, vol. 25, no. 1, pp. 137-165, 1999.
- [119] M. Kozhevnikov, M. A. Motes, B. Rasch and O. Blajenkova, "Perspective-Taking vs. Mental Rotation Transformations and How They Predict Spatial Navigation Performance," *Applied Cognitive Psychology*, vol. 20, pp. 397-417, 2006.
- [120] R. D. Easton and M. J. Sholl, "Object-Array Structure, Frames of Reference, and Retrieval of Spatial Knowledge," *Journal of Experimental Psychology: Learning, Memory, and Cognition*, vol. 21, no. 2, pp. 483-500, 1995.
- [121] R. P. Darken and H. Cevik, "Map Usage in Virtual Environments: Orientation Issues," *Proceedings of IEEE Virtual Reality*, vol. 99, pp. 133-140, 1999.
- [122] C. D. Wickens, C.-C. Liang, T. Prevett and O. Olmos, "Electronic Maps for Terminal Area Navigation: Effects of Frame of Reference and Dimensionality," *The International Journal of Aviation Psychology*, vol. 6, no. 3, pp. 241-271, 1996.
- [123] H. P. Williams and C. D. Wickens, "A Comparison of Methods for Promoting Geographic Knowledge in Simulated Aircraft Navigation," NASA Ames Research Center, Moffett Field, CA, 1993.
- [124] D. A. Norman and D. G. Bobrow, "On the Analysis of Performance Operating Characteristics," *Psychological Review*, vol. 83, no. 6, pp. 508-510, 1976.
- [125] J. W. Crandall, M. A. Goodrich, D. R. Olsen and C. W. Nielsen, "Validating Human-Robot Interaction Schemes in Multitasking Environments," *IEEE Transactions on Systems, Man, and Cybernetics - Part A: Systems and Humans*, vol. 35, no. 4, pp. 438-449, 2005.
- [126] P. E. Dux, M. N. Tombu, S. Harrison, B. P. Rogers, F. Tong and R. Marois, "Training Improves Multitasking Performance by Increasing the Speed of Information Processing in Human Prefrontal Cortex," *Neuron*, vol. 63, pp. 127-138, 2009.
- [127] C. Rosen, "The Myth of Multitasking," *The New Atlantis*, pp. 105-110, 2008.
- [128] R. Parasuraman, T. B. Sheridan and C. D. Wickens, "A Model for Types and Levels of Human Interaction with Automation," *IEEE Transactions on Systems, Man, and Cybernetics - Part A: Systems and Humans*, vol. 30, no. 3, pp. 286-297, 2000.
- [129] P. M. Reeves, "A Non-Gaussian Turbulence Simulation," Air Force Flight Dynamics Laboratory, Wright-Patterson Air Force Base, OH, 1969.
- [130] A. H. Roscoe and G. A. Ellis, "A Subjective Rating Scale for Assessing Pilot Workload in Flight: A Decade of Practical Use," Royal Aerospace Establishment, Farnborough, Hampshire, 1990.
- [131] C. D. Wickens, "Multiple Resources and Mental Workload," *Human Factors*, vol. 50, no. 3, pp. 449-455, 2008.
- [132] Y. Takano, "Perception of Rotated Forms: A Theory of Information Types," *Cognitive Psychology*, vol. 21, pp. 1-59, 1989.

- [133] M. H. Kutner, J. Nachtsheim, J. Neter and W. Li, *Applied Linear Statistical Models*, 5th ed., Boston: McGraw-Hill, 2005.
- [134] S. W. Looney and T. R. Gullledge, "Use of the Correlation Coefficient with Normal Probability Plots," *American Statistical Association*, vol. 39, no. 1, pp. 75-79, 1985.
- [135] R. B. Ekstrom, J. W. French, H. H. Harman and D. Dermen, "Manual for Kit of Factor-Referenced Cognitive Tests," Education Testing Service, Princeton, NJ, 1976.
- [136] "Perspective Taking Ability Test (PTA-Test)," MM Virtual Design, [Online]. Available: http://www.mmvirtualdesign.com/html/pta_test.html. [Accessed 3 Mar 2016].
- [137] G. M. Bodner and R. B. Guay, "The Purdue Visualization of Rotations Test," *The Chemical Educator*, vol. 2, no. 4, pp. 1-17, 1997.
- [138] C. Ware, *Information Visualization*, 3rd ed., Waltham, MA: Elsevier, 2013.
- [139] B. Sachs, "Air Force Photos," [Online]. Available: <http://www.af.mil/News/Photos.aspx?igphoto=2001298256>. [Accessed 6 May 2016].
- [140] E. L. Duke, R. F. Antoniewicz and K. D. Krambeer, "Derivation and Definition of a Linear Aircraft Model," NASA, Edwards, CA, 1988.
- [141] N. Hall, "Banking Turn," NASA, 5 May 2015. [Online]. Available: <https://www.grc.nasa.gov/www/k-12/airplane/turns.html>. [Accessed 5 May 2016].
- [142] R. E. Maine and K. W. Iliff, "Application of Parameter Estimation to Aircraft Stability and Control: The Output-Error Approach," Ames Research Facility Dryden Flight Research Facility, Edwards, CA, 1986.

List of Figures

Figure 1: USAF MQ-1B Predator Aircraft [9].....	12
Figure 2: USAF MQ-9 Reaper Aircraft [8].....	12
Figure 3: USAF MQ-1B Predator Control Station [55].....	13
Figure 4: Single-Seat Reference Frame Requirements [55, 139].....	15
Figure 5: Aircraft Body Axis [140].....	16
Figure 6: Earth Axis System.....	16
Figure 7: Aircraft-View Reference Frame.....	17
Figure 8: North-up Reference Frame.....	17
Figure 9: Sensor-View Axis.....	18
Figure 10: Sensor-View Reference Frame.....	19
Figure 11: Multiple Reference Frames in Unmanned Aircraft Control.....	21
Figure 12: Predictive Aid.....	23
Figure 13: Course Deviation Indicator.....	24
Figure 14: Navigation Display Reference Frame Alignment.....	25
Figure 15: Enlarged Image of MQ-1B Predator Display [55].....	27
Figure 16: Target Acquisition Task Mental Process Differences.....	36
Figure 17: Performance Operating Characteristic [46].....	38
Figure 18: Multitasking Frequency Effect on Switch Cost.....	39
Figure 19: Bank Angle [141].....	44
Figure 20: Basic Simulator Display Configuration.....	45
Figure 21: The Navigation Display.....	46
Figure 22: The Aircraft Display.....	47
Figure 23: The Sensor Display.....	48
Figure 24: The Mission Display.....	49
Figure 25: Simulator Setup.....	50
Figure 26: Aircraft Display Reference Frame Alignment.....	51
Figure 27: Aircraft Control Stick Movement.....	51
Figure 28: Sensor Display Reference Frame Alignment.....	52
Figure 29: Sensor Control Stick.....	53
Figure 30: Target Preview Example.....	55
Figure 31: Displayed Orbit Example.....	56
Figure 32: Trim Switch.....	56
Figure 33: Reference Frame Alignment Example.....	58
Figure 34: Orientation Aid Example.....	60
Figure 35: Orientation Aid Example - Enlarged.....	60
Figure 36: Display Integration Example.....	61
Figure 37: Display Redundancy Reduction Example.....	62
Figure 38: Moving Target Example.....	63
Figure 39: Simulator Differences between Experiments.....	64
Figure 40: Sensor Track Error Example.....	66

Figure 41: Flight Path Error Examples.....	67
Figure 42: Moving Orientation Task Symbol Example.....	68
Figure 43: Bedford Workload Scale [130].....	69
Figure 44: Trigger Light Example.....	70
Figure 45: Training Performance Feedback Example.....	73
Figure 46: Example Target Images from Experiment 1.....	76
Figure 47: DISPLAY CONFIGURATION A: Traditional.....	78
Figure 48: DISPLAY CONFIGURATION B: Sensor Aligned.....	78
Figure 49: DISPLAY CONFIGURATION C: No Orientation Aid.....	79
Figure 50: DISPLAY CONFIGURATION D: Sensor and Aircraft Aligned.....	79
Figure 51: Experiment 1 Orientation Time Transformation Example.....	82
Figure 52: Orientation Time Alignment Effect.....	84
Figure 53: Orientation Time Orientation Aid Effect.....	85
Figure 54: Orientation Errors vs. Orientation Aid and Alignment Settings.....	85
Figure 55: Aircraft Display Reference Frame Alignment.....	87
Figure 56: Target Acquisition Time Alignment Effect.....	88
Figure 57: Target Acquisition Time Orientation Aid Effect.....	89
Figure 58: Target Acquisition Errors vs. Orientation Aid and Alignment Settings.....	89
Figure 59: Bedford Workload Rating Alignment Effect.....	91
Figure 60: Bedford Workload Rating Orientation Aid Effect.....	92
Figure 61: Reaction Time Alignment Effect.....	94
Figure 62: Reaction Time Orientation Aid Effect.....	94
Figure 63: Imagery Task Display Development.....	99
Figure 64: TRADITIONAL DISPLAY CONFIGURATION.....	100
Figure 65: ALIGNED DISPLAY CONFIGURATION.....	101
Figure 66: NO ORIENTATION AID DISPLAY CONFIGURATION.....	101
Figure 67: Image Feature Examples.....	102
Figure 68: Experiment 2 Selection Answer Time Transformation Example.....	103
Figure 69: Experiment 2 Target Ambiguity Example.....	104
Figure 70: Imagery Rotation Results Error vs. Time.....	105
Figure 71: Selection Answer Time Orientation Aid Effect.....	107
Figure 72: Selection Answer Time Alignment Effect.....	107
Figure 73: Selection Answer Error Orientation Aid Effect.....	109
Figure 74: Selection Answer Error Alignment Effect.....	110
Figure 75: Example Target Description from Experiment 3.....	114
Figure 76: DISPLAY CONFIGURATION A: Traditional.....	117
Figure 77: DISPLAY CONFIGURATION D: Sensor and Aircraft Aligned.....	117
Figure 78: DISPLAY CONFIGURATION E: Integrated.....	118
Figure 79: DISPLAY CONFIGURATION F: Aligned and Integrated.....	118
Figure 80: Predictive Aid as Bank Indicator.....	119
Figure 81: Orientation Time Data Transformation.....	122
Figure 82: Orientation Time Alignment Effect.....	124

Figure 83: Orientation Time Moving Target Effect	125
Figure 84: Orientation Time Integration Effect.....	125
Figure 85: Orientation Errors vs. Alignment, Integration, and Moving Target Tasks	126
Figure 86: Example Target Images from Experiment 3.....	128
Figure 87: Target Acquisition Time Alignment Effect	129
Figure 88: Target Acquisition Time Integration Effect.....	130
Figure 89: Target Acquisition Errors vs. Alignment and Integration.....	130
Figure 90: Predictive Aid Effect on Flight Path Error across Experiments 1 and 3	132
Figure 91: Reference Frame Alignment Effect on Bedford Workload	134
Figure 92: Integration effect on Bedford Workload Rating	134
Figure 93: Reaction Time Alignment Effect	137
Figure 94: Reaction Time Integration Effect	138
Figure 95: Trigger Light Location near Sensor Display.....	139
Figure 96: Display Configuration F Predictive Aid.....	142
Figure 97: Example Target Description from Experiment 4 (same as Experiment 3).....	146
Figure 98: DISPLAY CONFIGURATION A: Traditional.....	150
Figure 99: DISPLAY CONFIGURATION B: Sensor Aligned	150
Figure 100: DISPLAY CONFIGURATION G: No Aircraft Display.....	151
Figure 101: DISPLAY CONFIGURATION H: Sensor Aligned, No Aircraft Display.....	151
Figure 102: Experiment 4 Orientation Time Transformation Example.....	154
Figure 103: Orientation Time Alignment Effect.....	157
Figure 104: Orientation Time Moving Target Effect	158
Figure 105: Orientation Time Display Redundancy Effect	158
Figure 106: Orientation Errors vs. Alignment, Redundancy, and Moving Target Tasks	159
Figure 107: Example Target Images from Experiment 4 (same as Experiment 3).....	161
Figure 108: Target Acquisition Time Alignment Effect	162
Figure 109: Target Acquisition Time Display Redundancy Effect	163
Figure 110: Target Acquisition Errors vs. Alignment and Display Redundancy	163
Figure 111: Flight Path Error Alignment Effect	165
Figure 112: Predictive Aid Effect on Flight Path Error across Experiments 1 and 4	166
Figure 113: Reference Frame Alignment Effect on Bedford Workload	168
Figure 114: Display Redundancy effect on Bedford Workload.....	168
Figure 115: Simplified Crosscheck without Aircraft Display	171
Figure 116: Reaction Time Alignment Effect	172
Figure 117: Reaction Time Display Redundancy Effect	173
Figure 118: Display Symbology [Map Data and Image ©Google]	205
Figure 119: DISPLAY CONFIGURATION A: Traditional.....	207
Figure 120: DISPLAY CONFIGURATION B: Sensor Aligned	208
Figure 121: DISPLAY CONFIGURATION C: No Orientation Aid.....	209
Figure 122: DISPLAY CONFIGURATION D: Sensor and Aircraft Aligned	210
Figure 123: DISPLAY CONFIGURATION A: Traditional.....	212
Figure 124: DISPLAY CONFIGURATION D: Sensor and Aircraft Aligned	213

Figure 125: DISPLAY CONFIGURATION E: Integrated.....	214
Figure 126: DISPLAY CONFIGURATION F: Aligned and Integrated.....	215
Figure 127: DISPLAY CONFIGURATION B: Sensor Aligned	217
Figure 128: DISPLAY CONFIGURATION G: No Aircraft Display.....	218
Figure 129: DISPLAY CONFIGURATION H: Sensor Aligned, No Aircraft Display.....	219
Figure 130: Individual Target Acquisition Time vs. Rotation Angle	231
Figure 131: Target Acquisition Time Data Transformation.....	231
Figure 132: Target Acquisition Time Regression Residuals from Skewed Data.....	231
Figure 133: Target Acquisition Time Regression Residuals from Transformed Data	231
Figure 134: Box-Cox Transformation Parameter Estimation.....	232
Figure 135: Target Acquisition Time vs. Alignment	232
Figure 136: Target Acquisition Time Alignment Effect	233
Figure 137: Target Acquisition Time Orientation Aid Effect	233
Figure 138: Target Acquisition Time vs. Orientation Aid	234
Figure 139: Individual Orientation Time vs. Rotation Angle.....	238
Figure 140: Orientation Time Data Transformation	238
Figure 141: Orientation Time Regression Residuals from Skewed Data	239
Figure 142: Orientation Time Regression Residuals from Transformed Data	239
Figure 143: Orientation Time Box-Cox Transformation Parameter Estimation	239
Figure 144: Test of Randomness.....	240
Figure 145: Residuals vs. Xalign	240
Figure 146: Residuals vs. XtrialNum.....	240
Figure 147: Residuals vs. Ximage	240
Figure 148: Residuals vs Xsubject	240
Figure 149: Residuals vs Predicted Orientation Time	240
Figure 150: Residuals vs. XorientAid.....	241
Figure 151: Experiment 1 Orientation Time vs. Alignment	241
Figure 152: Experiment 1 Orientation Time Alignment Effect	242
Figure 153: Experiment 1 Orientation Time Orientation Aid Effect	242
Figure 154: Experiment 1 Orientation Time vs. Orientation Aid	243
Figure 155: Experiment 1 Bedford Workload Rating Orientation Aid Effect.....	244
Figure 156: Experiment 1 Bedford Workload Rating Alignment Effect.....	244
Figure 157: Individual Reaction Time vs. Rotation Angle	246
Figure 158: Reaction Time Data Transformation.....	246
Figure 159: Reaction Time Regression Residuals from Skewed Data	247
Figure 160: Reaction Time Regression Residuals from Transformed Data.....	247
Figure 161: Box-Cox Transformation Parameter Estimation	247
Figure 162: Test of Randomness.....	248
Figure 163: Residuals vs. Xalign	248
Figure 164: Residuals vs. XinitAngle.....	248
Figure 165: Residuals vs. XtrialNum.....	248
Figure 166: Residuals vs. Ximage	248

Figure 167: Residuals vs Xsubject	248
Figure 168: Residuals vs. Predicted Reaction Time	249
Figure 169: Reaction Time vs. Alignment	249
Figure 170: Reaction Time Alignment Effect	250
Figure 171: Reaction Time vs. Orientation Aid	250
Figure 172: Reaction Time Orientation Aid Effect	251
Figure 173: Selection Answer Time Orientation Aid Effect	254
Figure 174: Selection Answer Time Alignment Effect.....	254
Figure 175: Selection Answer Time Alignment Effect (Log Scale)	255
Figure 176: Selection Answer Error Orientation Aid Effect	257
Figure 177: Selection Answer Error Alignment Effect	257
Figure 178: Individual Target Acquisition Time vs. Rotation Angle	263
Figure 179: Target Acquisition Time Data Transformation.....	263
Figure 180: Target Acquisition Time Regression Residuals from Skewed Data.....	264
Figure 181: Target Acquisition Time Regression Residuals from Transformed Data	264
Figure 182: Target Acquisition Time Box-Cox Transformation Parameter Estimation.....	264
Figure 183: Test of Randomness.....	265
Figure 184: Residuals vs. Xalign	265
Figure 185: Residuals vs. XtrialNum.....	265
Figure 186: Residuals vs. Ximage	265
Figure 187: Residuals vs Xsubject	265
Figure 188: Residuals vs Predicted Target Acquisition Time	265
Figure 189: Residuals vs. Xdisplnt.....	266
Figure 190: Target Acquisition Time vs. Alignment	266
Figure 191: Experiment 3 Target Acquisition Time Alignment Effect.....	267
Figure 192: Target Acquisition Time vs. Display Integration	267
Figure 193: Experiment 3 Target Acquisition Time Integration Effect	268
Figure 194: Experiment 3 Flight Path Error Moving Target Effect.....	270
Figure 195: Experiment 3 Sensor Track Error Moving Target Effect	272
Figure 196: Individual Orientation Time vs. Rotation Angle.....	274
Figure 197: Orientation Time Data Transformation	274
Figure 198: Orientation Time Regression Residuals from Skewed Data	275
Figure 199: Orientation Time Regression Residuals from Transformed Data	275
Figure 200: Example Box-Cox Transformation Parameter Estimation	275
Figure 201: Orientation Time vs. Alignment.....	276
Figure 202: Experiment 3 Orientation Time Alignment Effect	277
Figure 203: Orientation Time vs. Display Integration	277
Figure 204: Experiment 3 Orientation Time Integration Effect	278
Figure 205: Orientation Time vs. Target Movement	278
Figure 206: Experiment 3 Orientation Time Moving Target Effect.....	279
Figure 207: Experiment 3 Bedford Workload Rating Display Integration Effect	280
Figure 208: Experiment 3 Bedford Workload Rating Alignment Effect	280



Figure 209: Individual Reaction Time vs. Rotation Angle	282
Figure 210: Reaction Time Data Transformation.....	282
Figure 211: Reaction Time Regression Residuals from Skewed Data.....	283
Figure 212: Reaction Time Regression Residuals from Transformed Data.....	283
Figure 213: Reaction Time Box-Cox Transformation Parameter Estimation	283
Figure 214: Reaction Time vs. Alignment	284
Figure 215: Experiment 3 Reaction Time Alignment Effect	284
Figure 216: Reaction Time vs. Display Integration	285
Figure 217: Experiment 3 Reaction Time Integration Effect.....	285
Figure 218: Reaction Time vs. Target Movement.....	286
Figure 219: Experiment 3 Reaction Time Moving Target Effect	286
Figure 220: Individual Target Acquisition Time vs. Rotation Angle	291
Figure 221: Target Acquisition Time Data Transformation.....	291
Figure 222: Target Acquisition Time Regression Residuals from Skewed Data.....	292
Figure 223: Target Acquisition Time Regression Residuals from Transformed Data	292
Figure 224: Experiment 4 Tgt Acq Time Box-Cox Transformation Parameter Estimation	292
Figure 225: Target Acquisition Time vs. Alignment	293
Figure 226: Experiment 4 Target Acquisition Time Alignment Effect.....	293
Figure 227: Target Acquisition Time vs. Display Redundancy	294
Figure 228: Experiment 4 Target Acquisition Time Display Redundancy Effect.....	294
Figure 229: Flight Path Error vs. Target Movement.....	296
Figure 230: Experiment 4 Flight Path Error Moving Target Effect.....	296
Figure 231: Flight Path Error vs. Alignment	297
Figure 232: Experiment 4 Flight Path Error Alignment Effect.....	297
Figure 233: Experiment 4 Flight Path Error Display Redundancy Effect.....	298
Figure 234: Sensor Track Error vs. Target Movement	300
Figure 235: Experiment 4 Sensor Track Error Moving Target Effect	300
Figure 236: Sensor Track Error vs. Alignment.....	301
Figure 237: Experiment 4 Sensor Track Error Alignment Effect	301
Figure 238: Experiment 4 Sensor Track Error Display Redundancy Effect	302
Figure 239: Experiment 4 Individual Orientation Time vs. Rotation Angle	304
Figure 240: Orientation Time Data Transformation	304
Figure 241: Orientation Time Regression Residuals from Skewed Data	305
Figure 242: Orientation Time Regression Residuals from Transformed Data	305
Figure 243: Exp 4 Orientation Time Box-Cox Transformation Parameter Estimation.....	305
Figure 244: Orientation Time vs. Alignment.....	306
Figure 245: Experiment 4 Orientation Time Alignment Effect	306
Figure 246: Orientation Time vs. Display Redundancy	307
Figure 247: Experiment 4 Orientation Time Display Redundancy Effect	307
Figure 248: Orientation Time vs. Target Movement	308
Figure 249: Experiment 4 Orientation Time Moving Target Effect.....	308
Figure 250: Experiment 4 Bedford Workload Rating Display Redundancy Effect	309

Figure 251: Experiment 4 Bedford Workload Rating Alignment Effect	309
Figure 252: Experiment 4 Individual Reaction Time vs. Rotation Angle	311
Figure 253: Reaction Time Data Transformation.....	311
Figure 254: Reaction Time Regression Residuals from Skewed Data	312
Figure 255: Reaction Time Regression Residuals from Transformed Data.....	312
Figure 256: Exp 4 Reaction Time Box-Cox Transformation Parameter Estimation	312
Figure 257: Test of Randomness.....	313
Figure 258: Residuals vs. Xalign	313
Figure 259: Residuals vs. XtrialNum.....	313
Figure 260: Residuals vs. Xmove	313
Figure 261: Residuals vs. Ximage	313
Figure 262: Residuals vs Xsubject	313
Figure 263: Residuals vs. Predicted Reaction Time	314
Figure 264: Reaction Time vs. Alignment	314
Figure 265: Experiment 4 Reaction Time Alignment Effect	315
Figure 266: Reaction Time vs. Display Redundancy.....	315
Figure 267: Experiment 4 Reaction Time Display Redundancy Effect	316
Figure 268: Reaction Time vs. Target Movement	316
Figure 269: Experiment 4 Reaction Time Moving Target Effect	317
Figure 270: Experiment 2 Cognitive Performance Comparisons by Subject	331
Figure 271: Experiments 3 and 4 Cognitive Performance Comparisons by Subject	332
Figure 272: Imagery Examples with Few Available Features.....	333
Figure 273: Imagery Examples with Ambiguous Features.....	334
Figure 274: Imagery Examples with Abundant and Discernible Features	334

This page intentionally left blank.

Appendix A: Display Configurations

A.1. Legend

	<p>This symbol indicates that a display was fixed north-up.</p>
	<p>This symbol indicates that a display would rotate with the physical environment.</p>

A.2. Display Symbology

Navigation Display

Red Triangle: Target
Black Square: Crosshairs

Course Indicator

Aircraft Location

Aircraft Display

Horizon

Bank Indicator

Aircraft Symbol

Course Deviation Indicator

056 Heading

Run # 0.11

Southwest Basketball Hoop

Crosshairs

North Arrow Orientation Aid

North Arrow Fixed Pointer

Sensor Display

Mission Display

TRAINING ONLY

Trigger Light

Direction Switch

Reset Switches

Sensor pt North Up Stop 4 L JS R JS 20 Bnk Twist PFD Course Indicator
 N Arrow Sensor View

Figure 118: Display Symbology [Map Data and Image ©Google]

A.3. Experiment 1

Table 27: Experiment 1 Display Configurations – gray indicates design variables which were explored during this experiment.

Display	A Traditional	B Sensor Aligned	C No Orientation Aid	D Sensor and Aircraft Aligned
Aircraft	Aircraft-View	Aircraft-View	Aircraft-View	North-up
Navigation	North-Up			
Sensor	Sensor-View	North-Up	Sensor-View	North-Up
Mission	North-Up			
# Reference Frames	3	2	3	1
Reference Frame Alignment	No	Yes	No	Yes
Orientation Aid	Yes	Yes	No	No
Display Integration	No	No	No	No
Display Redundancy	Yes	Yes	Yes	Yes

Display Configuration A: Traditional Experiment 1

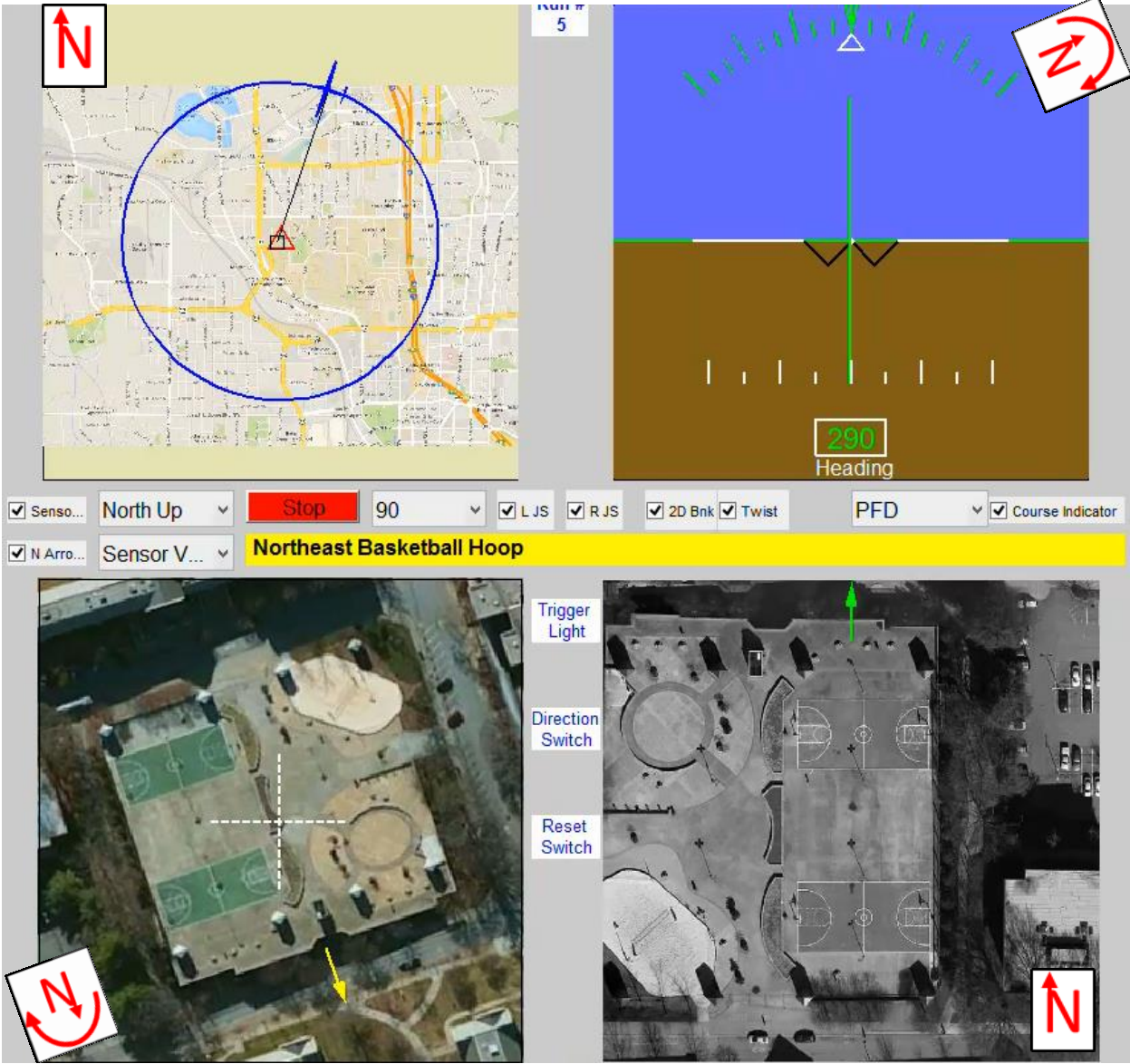


**Figure 119: DISPLAY CONFIGURATION A: Traditional
Experiment 1, Alignment = no, Orientation Aid = yes, Display Integration = no, Display Redundancy = yes
[Map Data and Image ©Google]**

Display Configuration B: Sensor Aligned Experiment 1

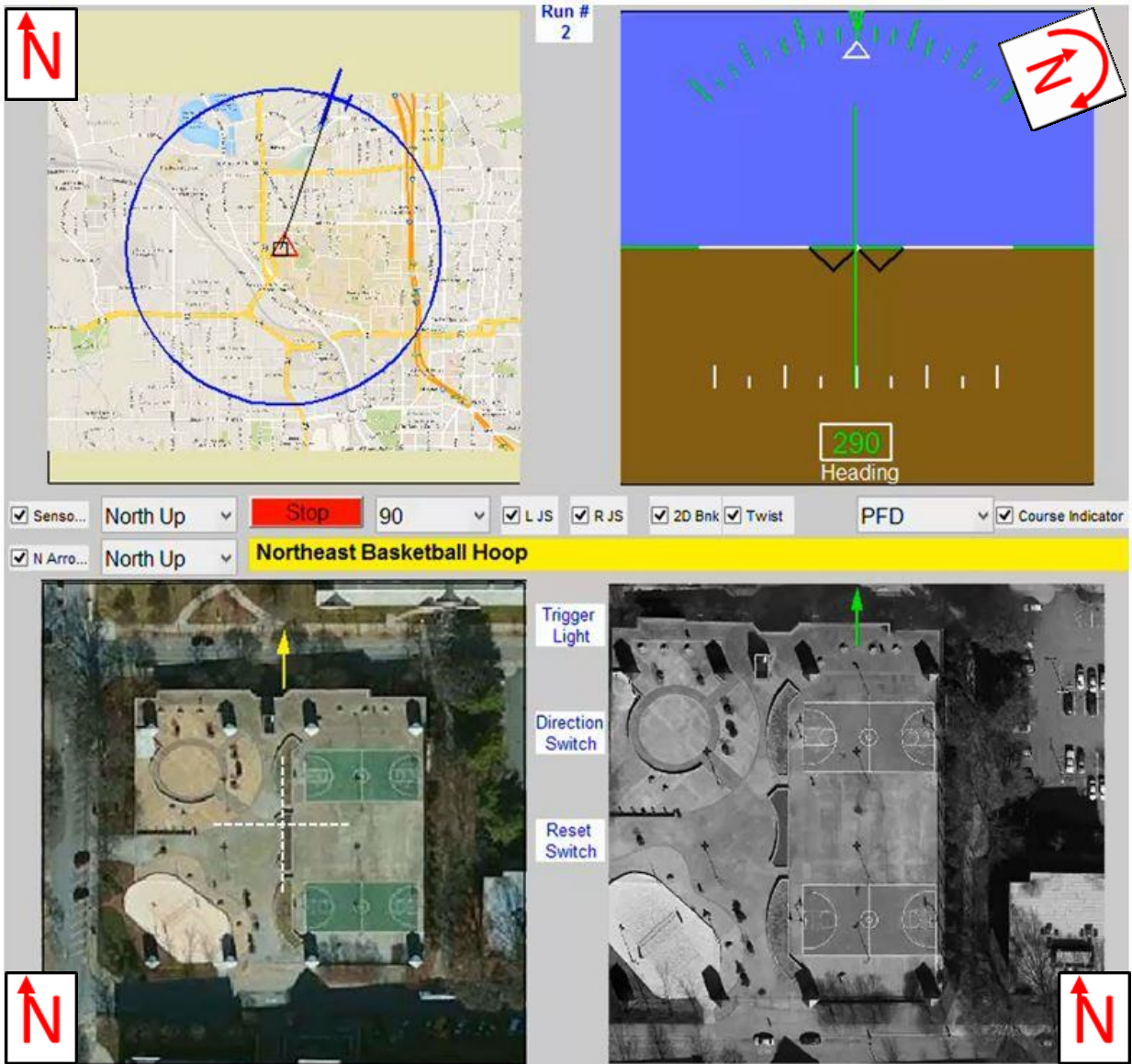


Figure 120: DISPLAY CONFIGURATION B: Sensor Aligned
Experiment 1, Alignment = yes, Orientation Aid = yes, Display Integration = no, Display Redundancy = yes
[Map Data and Image ©Google]

Display Configuration C: No Orientation Aid Experiment 1

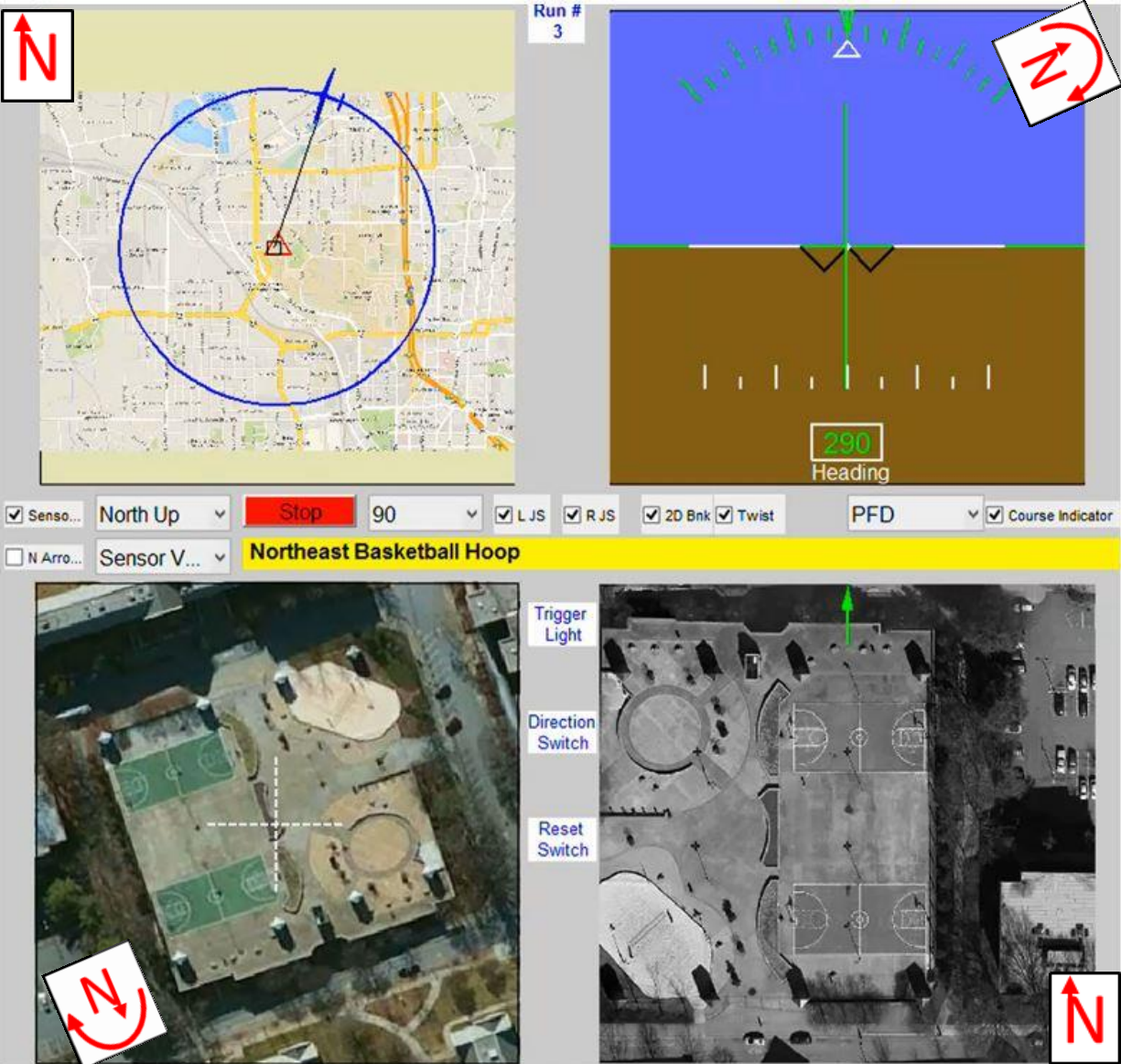


Figure 121: DISPLAY CONFIGURATION C: No Orientation Aid
 Experiment 1, Alignment = no, Orientation Aid = no, Display Integration = no, Display Redundancy = yes
 [Map Data and Image ©Google]

Display Configuration D: Sensor and Aircraft Aligned Experiment 1

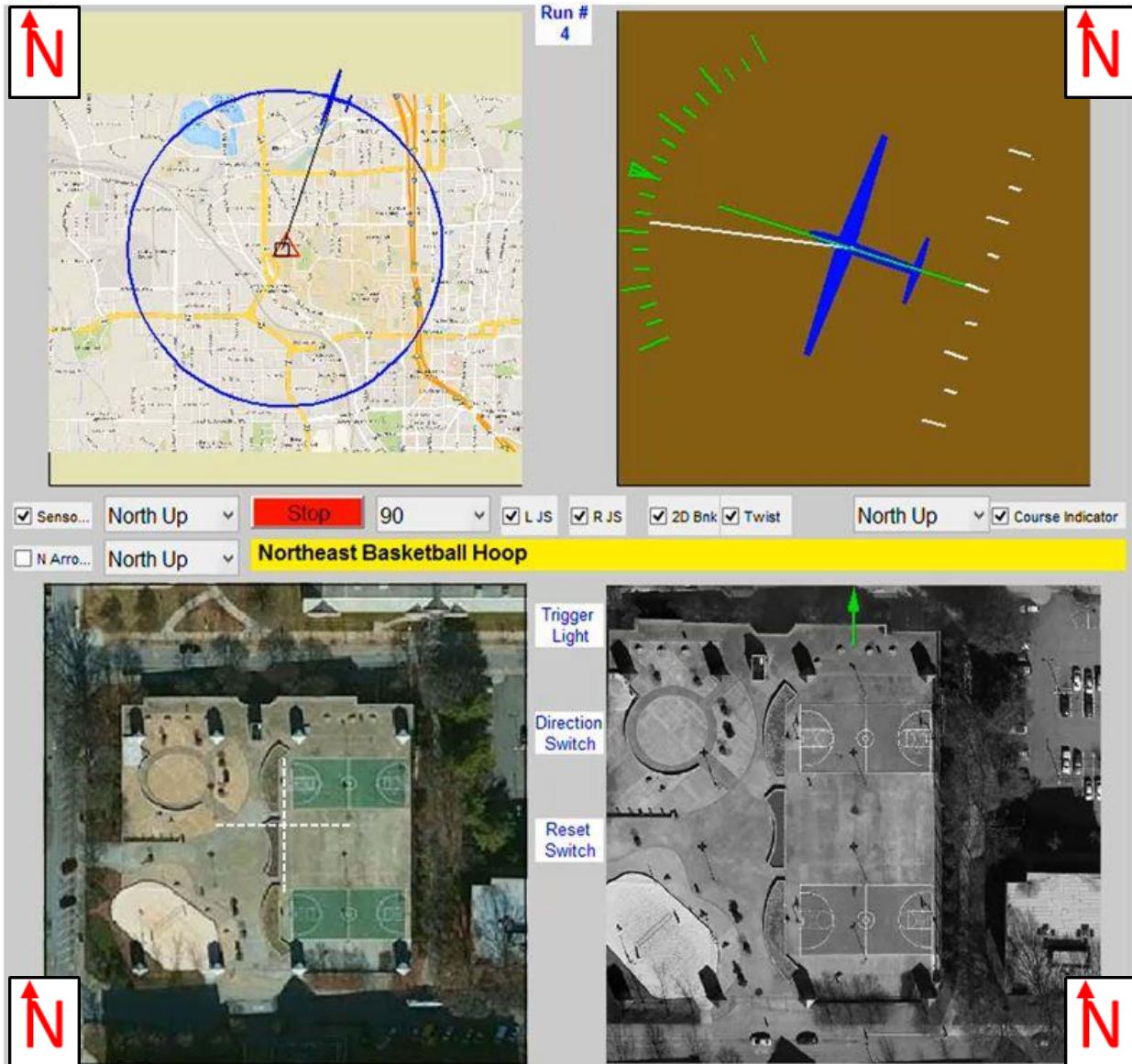


Figure 122: DISPLAY CONFIGURATION D: Sensor and Aircraft Aligned
Experiment 1, Alignment = yes, Orientation Aid = no, Display Integration = no, Display Redundancy = yes
[Map Data and Image ©Google]

A.4. Experiment 3

Table 28: Experiment 3 Display Configurations – gray indicates design variables which were explored during this experiment.

Display	A Traditional	D Sensor and Aircraft Aligned	E Integrated	F Aligned and Integrated
Aircraft	Aircraft-View	North-up	Aircraft-View	North-up
Navigation	North-Up			
Sensor	Sensor-View	North-Up	Sensor-View	North-Up
Mission	North-Up			
# Reference Frames	3	1	3	1
Reference Frame Alignment	No	Yes	No	Yes
Orientation Aid	Yes	Yes	Yes	Yes
Display Integration	No	No	Yes	Yes
Display Redundancy	Yes	Yes	Yes	Yes

Display Configuration A: Traditional Experiments 3 and 4



Figure 123: DISPLAY CONFIGURATION A: Traditional Experiment 3 and 4, Alignment = no, Orientation Aid = yes, Display Integration = no, Display Redundancy = yes [Map Data and Image ©Google]

Display Configuration D: Sensor and Aircraft Aligned Experiment 3

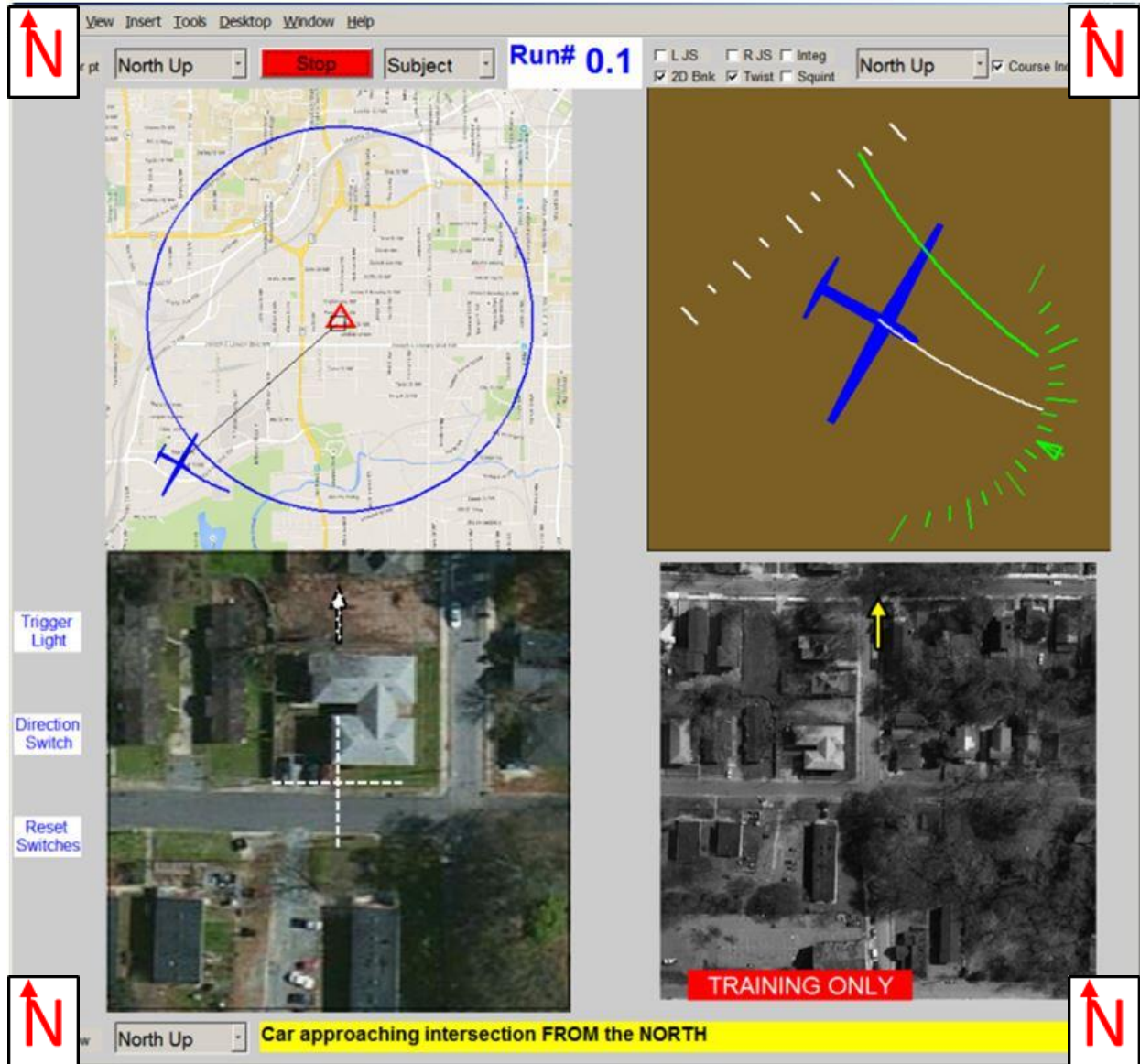


Figure 124: DISPLAY CONFIGURATION D: Sensor and Aircraft Aligned
Experiment 3, Alignment = yes, Orientation Aid = yes, Display Integration = no, Display Redundancy = yes
[Map Data and Image ©Google]

Display Configuration E: Integrated Experiments 3

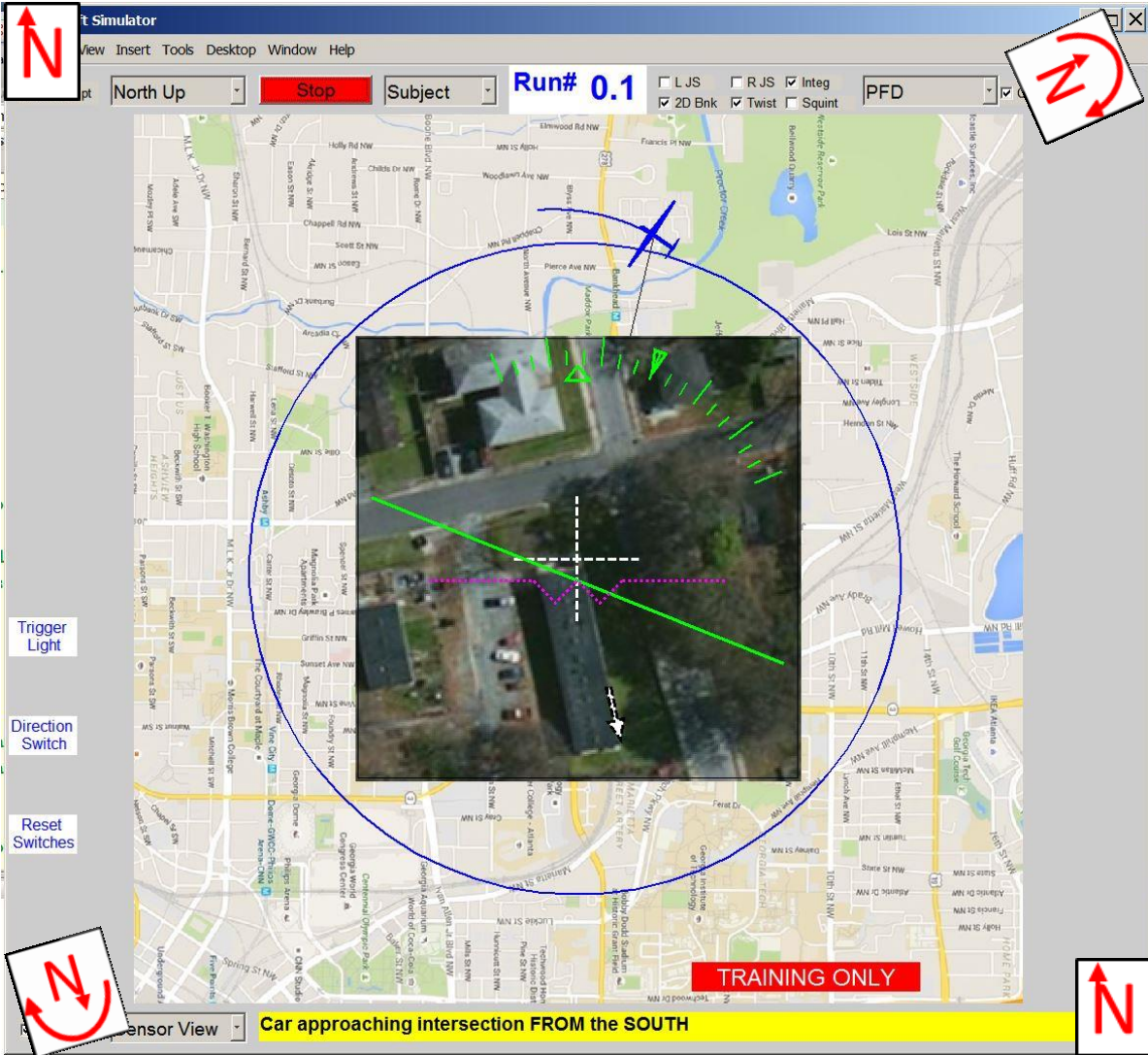


Figure 125: DISPLAY CONFIGURATION E: Integrated Experiment 3, Alignment = no, Orientation Aid = yes, Display Integration = yes, Display Redundancy = yes [Map Data and Image ©Google]

Display Configuration F: Aligned and Integrated Experiment 3

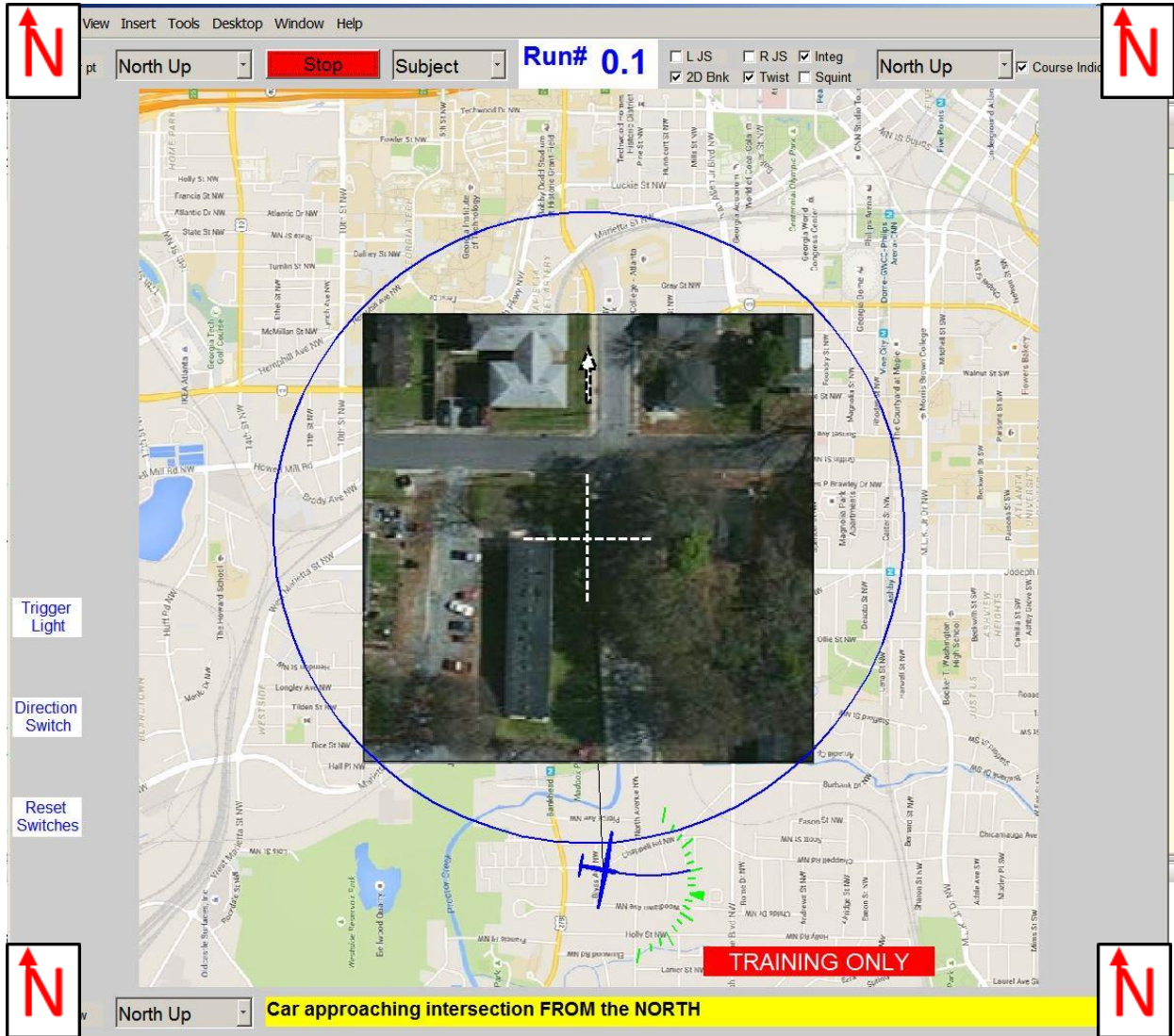


Figure 126: DISPLAY CONFIGURATION F: Aligned and Integrated Experiment 3, Alignment = yes, Orientation Aid = yes, Display Integration = yes, Display Redundancy = yes [Map Data and Image ©Google]

A.5. Experiment 4

Table 29: Experiment 4 Display Configurations – gray indicates design variables which were explored during this experiment.

Display	A Traditional	B Sensor Aligned	G No Aircraft Display	H Sensor Aligned and No Aircraft Display
Aircraft	Aircraft-View	Aircraft-View	None	None
Navigation	North-Up			
Sensor	Sensor-View	North-Up	Sensor-View	North-Up
Mission	North-Up			
# Reference Frames	3	2	3	2
Reference Frame Alignment	No	Yes	No	Yes
Orientation Aid	Yes	Yes	Yes	Yes
Display Integration	No	No	No	No
Display Redundancy	Yes	Yes	No	No

Display Configuration A (Traditional) is shown with Experiment 3 configurations in Figure 123.

Display Configuration B: Sensor Aligned Experiment 4

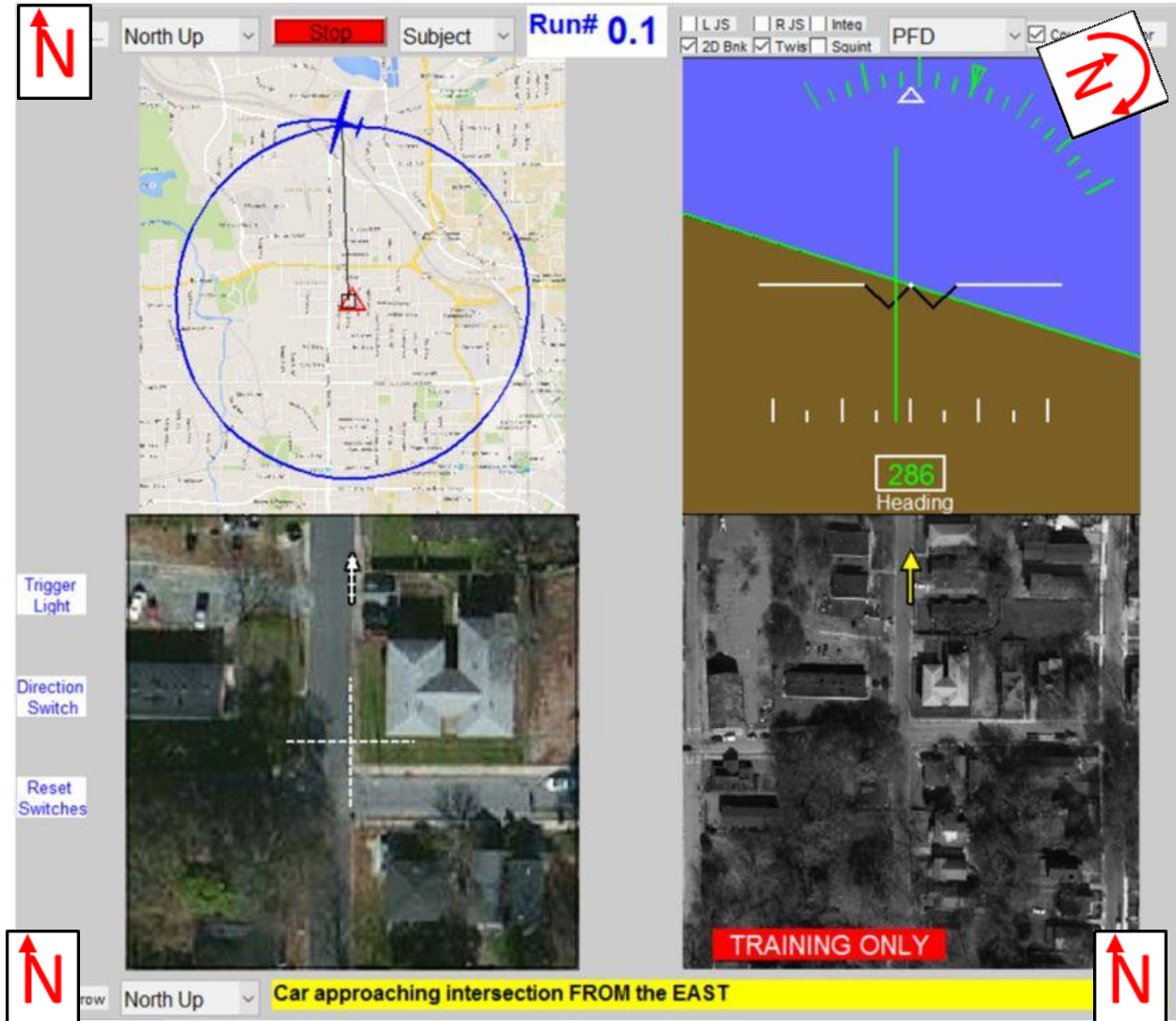


Figure 127: DISPLAY CONFIGURATION B: Sensor Aligned
Experiment 4, Alignment = yes, Orientation Aid = yes, Display Integration = no, Display Redundancy = yes
[Map Data and Image ©Google]

Display Configuration G: No Aircraft Display Experiments 4

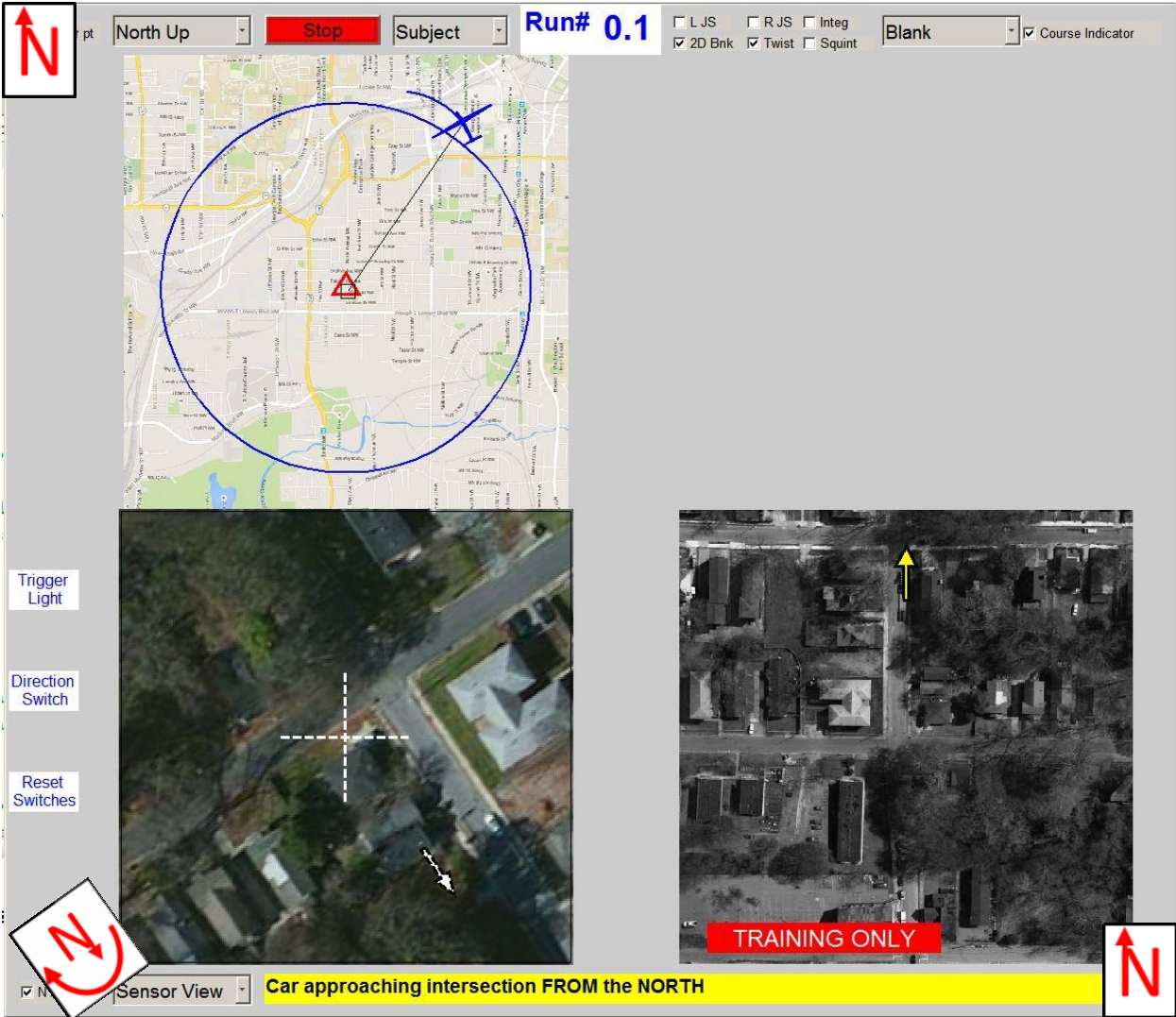


Figure 128: DISPLAY CONFIGURATION G: No Aircraft Display
Experiment 4, Alignment = no, Orientation Aid = yes, Display Integration = no, Display Redundancy = no
 [Map Data and Image ©Google]

Display Configuration H: Sensor Aligned, No Aircraft Display Experiment 4

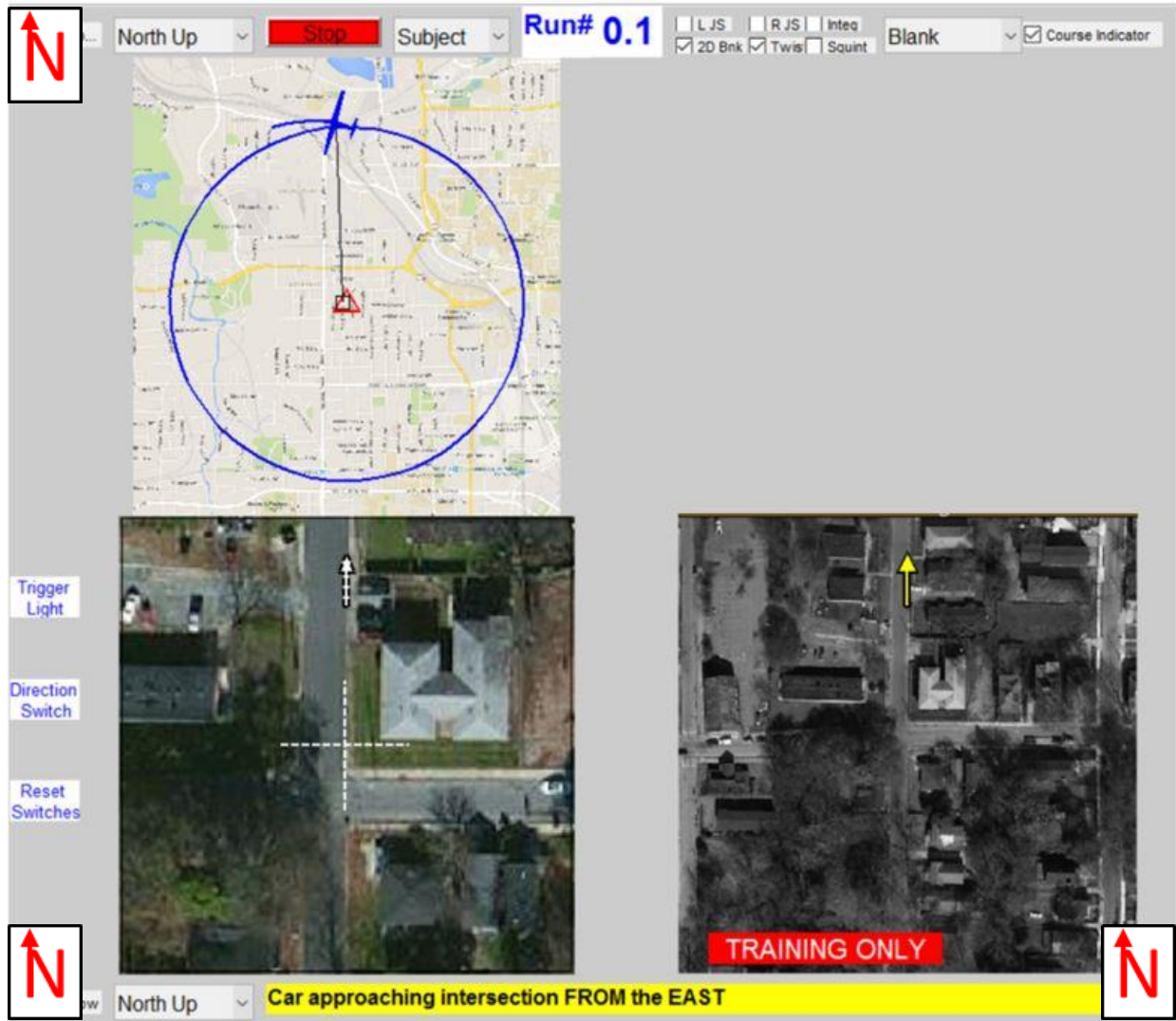


Figure 129: DISPLAY CONFIGURATION H: Sensor Aligned, No Aircraft Display
Experiment 4, Alignment = yes, Orientation Aid = yes, Display Integration = no, Display Redundancy = no
[Map Data and Image ©Google]

This page intentionally left blank.

Appendix B: Subject Characteristics

B.1. Legend

Before each simulator experiment, the subject was asked to rate their experience in a variety of categories. These responses, and the subject’s basic characteristics, are preserved in this appendix.

1-2	Little to no experience.
3-4	Familiar with the task, but limited exposure for increased proficiency. Someone who’s been flying a several times, but has not received a license yet.
5-6	Basic proficiency with the task. A private pilot’s license would represent this level of flight experience.
7-8	Fully comfortable and experienced at the task. Comfortable teaching the task to others. A recently qualified instructor pilot might be at this level for flight experience.
9-10	Extremely experienced at the task. Developed personal techniques beyond those learned from others. An experienced flight instructor who has learned and evaluated multiple techniques for various flight tasks would represent this level.

B.2. Experiment 1

During Experiment 1, control stick experience was considered as a measurement of video game experience, but future experiments separated these two metrics to get a separate measure of video game experience.

Table 30: Experiment 1 Subject Characteristics

This table describes the physical characteristics of each subject and also their self-reported experience levels. Once again, the legend described at the beginning of this appendix is used to highlight in red those with little or no experience in any given category.

Subject	Personal			Experience			
	Age	Dominant Hand	Gender	Flight	Remote Control	Video Control	Joystick
1	35	R	M	10	1	5	10
2	26	R	M	5	4	3	8
3	36	R	M	9	1	6	8
4	19	R	M	3	5	1	8
5	20	R	F	1	1	1	1
6	25	R	M	4	8	8	10
7	24	R	M	1	2	1	10
8	25	L	M	1	3	3	8
9	23	L	M	1	1	1	1
10	24	R	M	3	1	1	3

Table 30: Experiment 1 Subject Characteristics

This table describes the physical characteristics of each subject and also their self-reported experience levels. Once again, the legend described at the beginning of this appendix is used to highlight in red those with little or no experience in any given category.

Subject	Personal			Experience			
	Age	Dominant Hand	Gender	Flight	Remote Control	Video Control	Joystick
11	22	R	F	2	2	2	2
12	25	R	M	1	2	5	2
13	26	R	M	1	2	1	1
14	24	L	M	1	3	1	10
15	24	R	M	1	2	1	8
16	22	R	M	4	1	1	5
17	26	R	M	3	2	3	3
18	22	R	M	3	2	1	3
19	35	R	M	1	3	1	3
20	24	R	M	1	5	1	5
21	21	R	F	1	4	2	2
22	22	R	M	1	5	2	2
23	18	R	M	1	2	1	3
24	28	R	F	1	1	1	1
25	29	L	M	1	3	1	3
26	22	R	M	1	1	2	1
27	22	R	M	1	1	1	1
28	23	R	M	1	1	1	1
29	28	R	M	1	2	7	2
30	28	R	F	1	8	8	5
31	25	R	M	1	3	3	5
32	22	R	F	1	2	1	4
33	24	R	M	1	1	1	6
34	26	R	M	1	8	5	8
35	35	R	M	10	4	5	10
36	32	R	M	1	1	6	3

B.3. Experiment 2

The questionnaire in Experiment 2 did not request experience metrics.

Table 31: Experiment 2 Subject Characteristics – During experiment 2, only physical characteristics were recorded for each subject.

	Personal		
Subject	Age	Dominant Hand	Gender
1	35	1	1
2	22	1	1
3	20	1	1
4	22	1	1
5	23	2	1
6	23	1	1
7	18	1	2
8	20	1	2
9	24	2	1
10	22	1	2
11	37	1	1
12	34	1	2

B.4. Experiment 3

Experiment 3 and 4 both included a separate measure of video game experience.

Table 32: Experiment 3 Subject Characteristics - This table describes the physical characteristics of each subject and also their self-reported experience levels. Once again, the legend described at the beginning of this appendix is used to highlight in red those with little or no experience in any given category

Subject	Personal			Experience				
	Age	Dominant Hand	Gender	Flight	Remote Control	Video Control	Joystick	Video Game
1	23	R	F	1	1	1	1	1
2	23	R	M	4	1	1	3	4
3	18	R	F	1	1	1	1	1
4	23	L	M	5	2	1	2	5
5	22	R	M	5	5	1	10	9
6	23	R	M	2	1	4	3	6
7	25	R	F	1	1	1	2	1
8	24	R	M	1	1	1	5	4
9	23	R	M	3	2	1	2	3
10	25	R	M	1	2	1	3	5
11	26	R	M	1	1	1	2	6
12	27	R	M	4	3	1	5	2
13	23	R	M	1	1	1	1	3
14	30	R	M	1	1	1	2	4
15	32	R	M	1	2	1	1	1
16	23	R	M	1	1	1	1	5

B.5. Experiment 4

Experiment 3 and 4 both included a separate measure of video game experience.

Table 33: Experiment 4 Subject Characteristics – This table describes the physical characteristics of each subject and also their self-reported experience levels. Once again, the legend described at the beginning of this appendix is used to highlight in red those with little or no experience in any given category

Subject	Personal			Experience				
	Age	Dom Hand	Gender	Flight	Remote Control	Video Control	Joystick	Video Game
1	63	R	M	3	2	1	2	10
2	22	R	M	3	3	1	8	9
3	22	R	F	1	1	1	3	5
4	23	R	M	1	2	2	3	4
5	24	R	F	4	1	1	2	3
6	27	R	M	1	2	1	2	2
7	22	R	M	1	1	1	1	5
8	36	R	M	10	2	4	10	3
9	49	R	M	1	1	1	2	2
10	33	R	M	1	9	4	3	5
11	30	R	F	1	1	1	2	6
12	42	R	M	1	2	1	3	3
13	55	R	M	2	3	3	4	1
14	28	R	M	1	3	4	6	9
15	45	R	M	1	1	1	3	10
16	32	R	M	2	3	1	1	6

B.6. Experiment 3 and 4 Cognitive Test Results and Correlations

Table 34: Cognitive Study Results, the color scale highlights increasing performance from red to green, subjects are ordered based on their performance in Vandenberg MRT test since it had the highest correlation with experiment 3 and 4 performance.

Subject (Sorted by MRT score)	Card Rotation s	Vandenberg MRT	Average RT (s)	Average Orientation Time (s)	Average Target Acquisition Time (s)
Experiment 3: 62	81	0	0.80	1.29	4.83
59	72	8	0.68	1.14	3.86
55	72	10	1.24	1.30	4.68
51	83	13	0.96	1.02	4.28
58	117	18	0.90	1.38	5.11
53	142	23	0.53	0.62	4.15
52	135	25	0.61	0.70	2.99
54	137	25	0.55	0.85	6.44
60	123	25	0.73	0.91	3.92
57	109	26	0.58	0.79	3.66
61	128	26	0.84	1.17	5.74
63	112	26	0.69	0.96	6.53
49	153	27	0.72	0.86	4.23
56	125	35	0.60	1.16	4.52
50	152	36	0.77	0.99	5.90
64	84	37	0.62	0.63	7.37
Experiment 4: 70	74	10	0.67	1.31	5.52
67	116	11	0.75	1.38	5.34
65	104	12	0.96	1.73	5.16
78	153	17	0.66	0.98	3.77
69	114	18	0.88	1.30	4.75
80	93	18	0.67	0.93	4.72
79	107	21	0.76	1.22	4.85
73	152	24	0.84	1.59	4.86
76	137	24	0.83	0.94	4.32
71	95	25	0.81	1.18	4.21
75	120	25	0.80	1.33	5.18
77	106	25	0.82	1.25	3.58
68	148	31	0.92	1.43	4.03
66	147	32	0.66	0.88	4.55
72	152	37	0.67	0.94	3.28
74	144	38	0.66	0.77	3.39

Appendix C: Experiment 1 Data Analysis

C.1. Data Transformations

This research utilized the Box-Cox transformation to normalize data for parametric analysis [133]. This process analyzes both log transformation and a range of power functions. For example, Figure 131 shows the effect of the Box-Cox transformation on the Target Acquisition Time data.

$$W_i = \begin{cases} K_1 \left((Y + \lambda_2)_i^{\lambda_1} - 1 \right) & \lambda_1 \neq 0 \\ K_2 (\log_e Y_i) & \lambda_1 = 0 \end{cases}$$

Equation 18: Box-Cox Transformation

$$K_2 = \left(\prod_{i=1}^n (Y + \lambda_2)_i \right)^{1/n}$$

Equation 19: Box-Cox Standardization Coefficient 1

$$K_1 = \frac{1}{\lambda_1 K_2^{(\lambda_1 - 1)}}$$

Equation 20: Box-Cox Standardization Coefficient 2

The Box-Cox transformation is shown in Equation 18 through Equation 20. This shows the two parameter estimation procedure, where both λ_1 and λ_2 are estimated. None of these transformations required an estimate of λ_2 , but each measure required an estimation of λ_1 to allow for parametric analysis. Since the transformations are analyzed based on the Sum of Squared Error (SSE) of the resulting regression, the standardization parameters in Equation 19 and Equation 20 are used to prevent SSE fluctuations as a function of λ_1 . An example estimation of the λ_1 parameter is shown in Figure 134. The left vertical axis represents value of SSE which is minimized using this transformation. The right vertical axis represents the correlation coefficient between the residuals and their expected value under normality [134]. The horizontal green dashed line shows the correlation coefficient associated with an $\alpha = 0.005$ significance. Here in the Box-Cox transformation selects $\lambda_1 = -0.3$ to minimize SSE, and this also generates an acceptable correlation coefficient as shown by the green data in Figure 134. A similar process was used for every transformation and each figure is available throughout this appendix. The transformation equations are shown in the applicable figures and listed here:

$$TAT'_{e1} = -26.3 * (TAT^{-0.3} - 1)$$

Equation 21: Experiment 1 Transformed Target Acquisition Time

$$FPE'_{e1} = -0.0295 * (FPE^{-0.4} - 1)$$

Equation 22: Experiment 1 Transformed Flight Path Error

$$STE'_{e1} = -0.00509 * (STE^{-0.7} - 1)$$

Equation 23: Experiment 1 Transformed Sensor Track Error

$$OT'_{e1} = -2.02 * (OT^{-0.6} - 1)$$

Equation 24: Experiment 1 Transformed Orientation Time

$$RT'_{e1} = -0.587 * (RT^{-1.3} - 1)$$

Equation 25: Experiment 1 Transformed Reaction Time

C.2. Pairwise Display Comparisons

Table 35: Experiment 1 Pairwise Comparisons – These are the results of within-subjects 2-sided pairwise t-tests to the family significance of 0.05 (Bonferroni corrected to ~0.008 2-sided or ~0.004 1-sided). Green indicates a significant effect which improved performance, red indicates a significant effect which degraded performance. Black indicates that these data were not collected. P-values are indicative of the single tail probability, which would be less than 0.004 for significance.

				Adding Reference Frame Alignment		Including Orientation Aid		Interaction Effects	
				Display	Display	Display	Display	Display	Display
				A ≠ B	C ≠ D	A ≠ C	B ≠ D	C ≠ B	A ≠ D
PARAMETRIC ANALYSIS	Orientation Time ¹	t*	10.13	12.37	5.27	-0.74	12.77	8.90	
		p-value	3.00E-12	1.24E-14	3.53E-06	7.68E-01	4.88E-15	8.05E-11	
	Target Acquisition Time ¹	t*	3.13	6.37	0.85	2.08	5.75	4.51	
		p-value	1.77E-03	1.26E-07	2.00E-01	2.25E-02	8.29E-07	3.51E-05	
	Sensor Track Error ¹	t*	0.46	1.32	0.45	0.03	1.01	0.62	
		p-value	0.32	0.10	0.33	0.49	0.16	0.27	
	Flight Path Error ¹	t*	0.93	-1.49	-1.59	-0.84	-0.83	0.28	
		p-value	0.18	0.93	0.94	0.80	0.79	0.39	
	Reaction Time ¹	t*	2.59	3.75	1.61	0.08	4.00	2.26	
		p-value	0.01	3.24E-04	0.06	0.47	1.57E-04	1.49E-02	
	NON-PARAMETRIC ANALYSIS	Bedford Workload Static Target	Chi-sqr	1.24	12.87	6.38	0.36	15.54	0.29
			p-value	0.27	3.34E-04	1.16E-02	0.55	8.09E-05	0.59
Bedford Workload Dynamic Target		Chi-sqr							
		p-value							
Rankings (1-4) Kruskal-Wallis		Chi-sqr	43.50	43.46	18.33	1.47	53.03	25.50	
		p-value	4.24E-11	4.33E-11	1.86E-05	0.23	3.28E-13	4.42E-07	
Ratings (1-10) Kruskal-Wallis		Chi-sqr							
		p-value							

C.3. Target Acquisition Time

$$TAT'_{e1} \approx \beta_0 + \beta_1 * Xalign1 + \beta_2 * Xalign2 + \beta_3 * XinitAngle + \beta_4 * XtrialNum + \beta_5 * XinitAngle * XtrialNum + \beta_{6i} * Xsubject_i + \beta_{7m} * Ximage_m + \beta_{8m} * XinitAngle * Ximage_m$$

$$i = 1:36 \text{ subjects}, m = 1:3 \text{ images}$$

Equation 26: Experiment 1 Target Acquisition Time Regression Model – Yellow highlights terms of interest, which were discussed in the body of the document.

Table 36: Experiment 1 Target Acquisition Time Predictor Variable Coefficients – Yellow highlights that the first level of the alignment variable is not significant, but the second level is. The term stays in the regression model, but in itself is not significant.

Predictor Variable	Term	Transformed Regression Estimate	Lower 95% Conf. Interval	Upper 95% Conf. Interval	t-stat	p-value	Reverse Transformed Estimate (β')	units
(Intercept)	β_0	10.255	9.563	10.947	29.15	2.61E-98	3.753	s
Xalign1 Sensor Display Only	β_1	-0.333	-0.832	0.166	-1.31	0.190	-0.330	s
Xalign2 Sensor and Aircraft Displays	β_2	-0.688	-1.183	-0.192	-2.73	6.68E-03	-0.714	s
XinitAngle	β_3	0.018	0.009	0.026	3.86	1.34E-04	0.017	s
XtrialNum	β_4	-0.080	-0.131	-0.028	-3.03	2.60E-03	-0.076	s/#
XinitAngle*XtrialNum	β_5	-8.95E-04	-0.002	-6.78E-05	-2.13	3.40E-02	-0.001	s/#

Table 37: Experiment 1 Target Acquisition Time Tests for Error Variance Constancy of Regression Model – No color fill indicates that none of these results are significant, so the hypothesis holds that error variance is constant and regression analysis is suitable

Grouping	Bartlett F Statistic	Bartlett p-value	Levene F Statistic	Levene p-value	Brown-Forsythe F Statistic	Brown-Forsythe p-value
Xalign	1.241	0.265	1.764	0.185	1.831	0.177
XtrialNum	2.380	0.123	1.315	0.252	1.250	0.264
Xmove	0.039	0.844	1.088	0.298	1.192	0.276
Ximage	0.070	0.792	0.116	0.734	0.091	0.764
Xsubject	0.106	0.745	0.083	0.774	0.077	0.782
Predicted TAT'	0.000	0.984	0.003	0.959	0.003	0.959
Time Sequence	0.106	0.745	0.083	0.774	0.077	0.782

The residuals plots were removed from this appendix because none of the constancy tests were trending to significance.

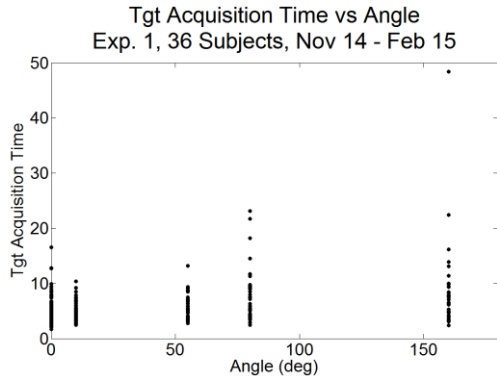


Figure 130: Individual Target Acquisition Time vs. Rotation Angle

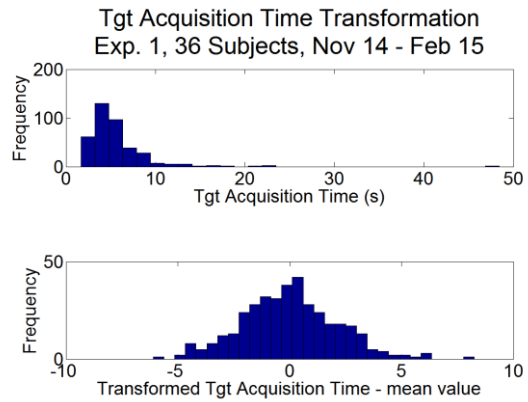


Figure 131: Target Acquisition Time Data Transformation

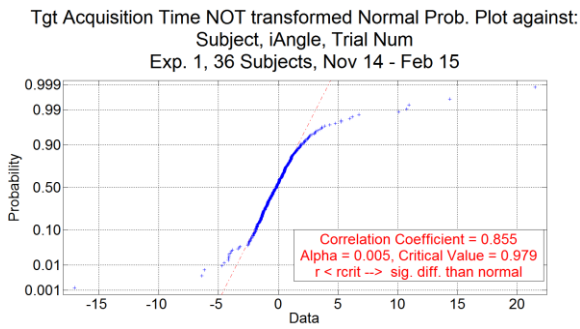


Figure 132: Target Acquisition Time Regression Residuals from Skewed Data

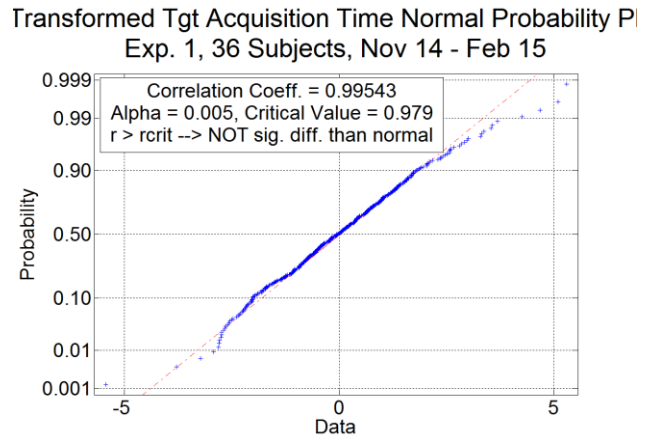


Figure 133: Target Acquisition Time Regression Residuals from Transformed Data

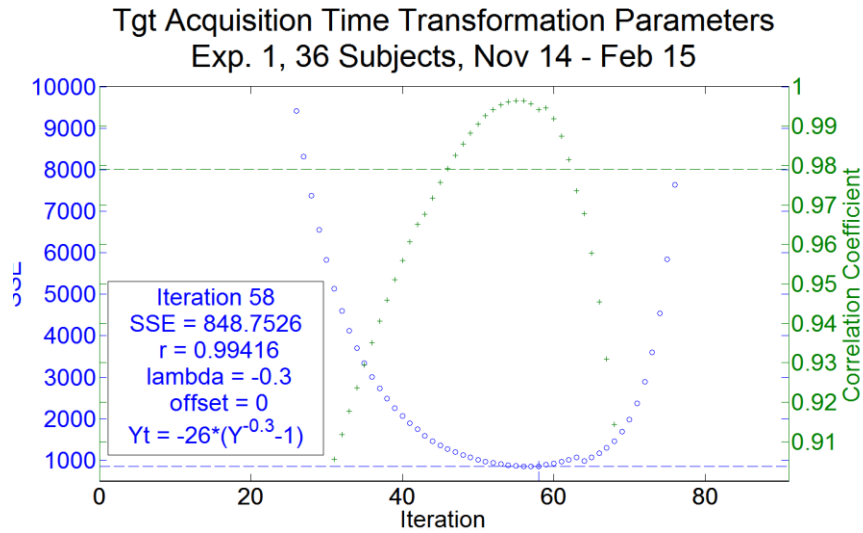


Figure 134: Box-Cox Transformation Parameter Estimation
 The blue data show how the regression Mean Squared Error was minimized with the Box-Cox Transformation. The green data show the corresponding effect on the correlation of the residuals with estimated values under normality.

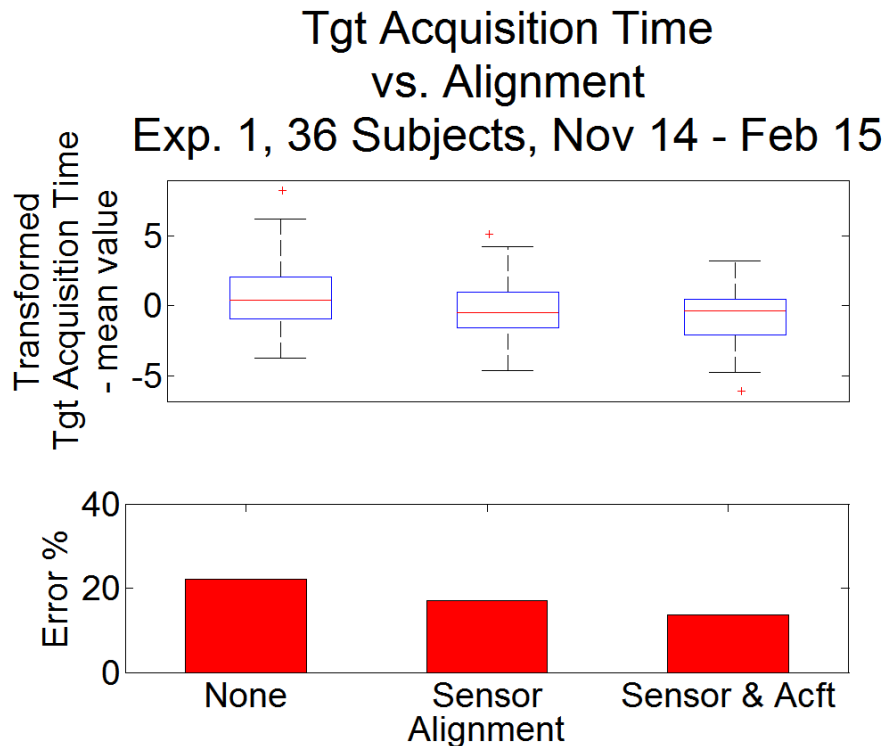


Figure 135: Target Acquisition Time vs. Alignment

Tgt Acquisition Time vs. Alignment (Observed Data)
Exp. 1, 36 Subjects, Nov 14 - Feb 15

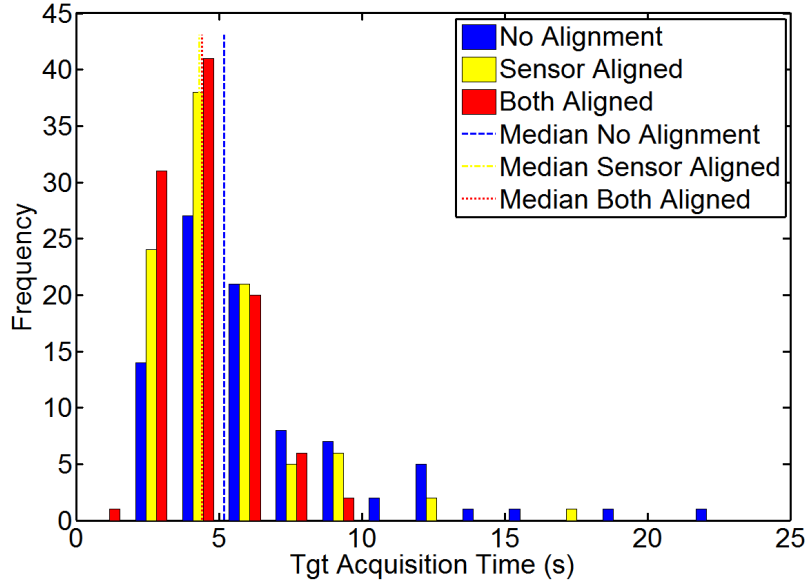


Figure 136: Target Acquisition Time Alignment Effect
Blue distribution is observed data without alignment. Yellow distribution is alignment of the sensor video only, and red has alignment of sensor and aircraft displays.

Tgt Acquisition Time Orientation Aid (Observed Data)
Exp. 1, 36 Subjects, Nov 14 - Feb 15

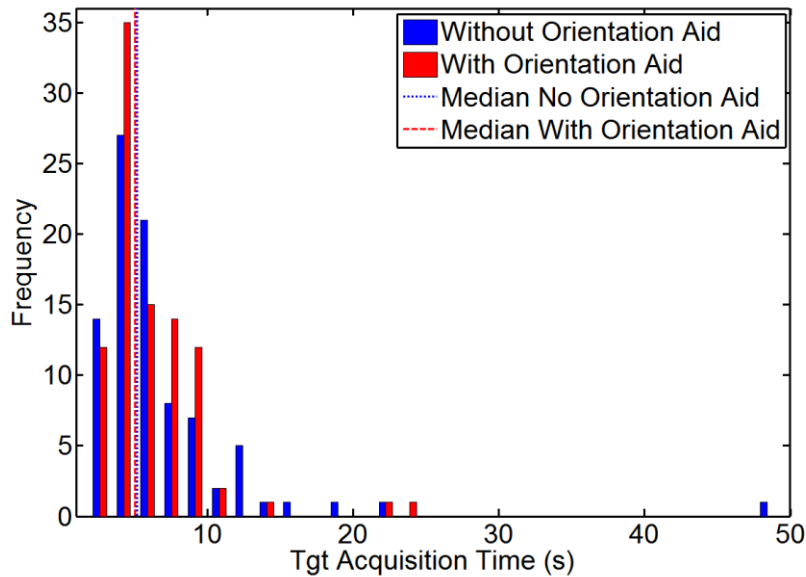


Figure 137: Target Acquisition Time Orientation Aid Effect
Blue distribution is observed data without the orientation aid. Red distribution is observed data with the orientation aid.

Tgt Acquisition Time vs. Orientation Aid Present

Exp. 1, 36 Subjects, Nov 14 - Feb 15

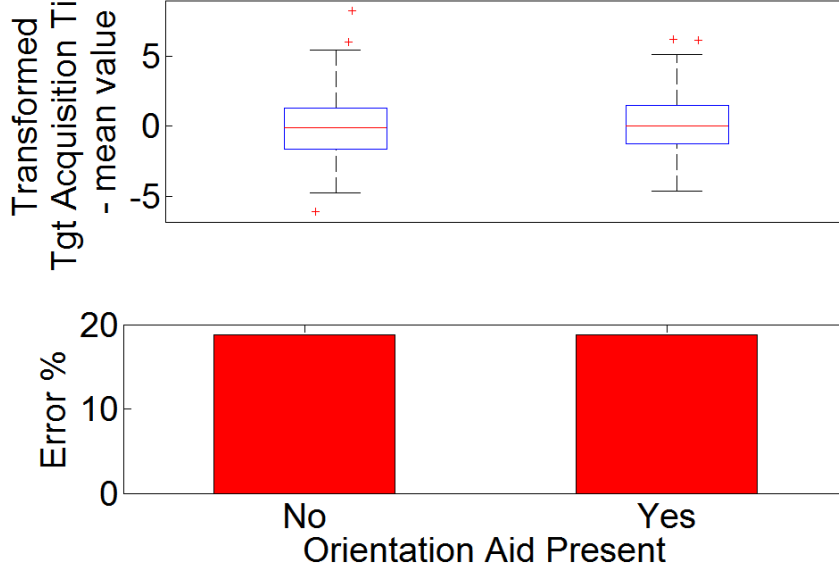


Figure 138: Target Acquisition Time vs. Orientation Aid

C.4. Flight Path Error

$$FPE'_{e1} \approx \beta_0$$

Equation 27: Flight Path Error Regression Estimation – No terms remained in the model

Table 38: Experiment 1 Flight Path Error RMSE Predictor Variable Coefficients

Predictor Variable	Term	Transformed Regression Estimate	Lower 95% Conf. Interval	Upper 95% Conf. Interval	t-stat	p-value	Reverse Transformed Estimate (β')	units
(Intercept)	β_0	-0.08	-0.08	-0.08	-75.16	5.51E-263	-0.86	RMSE

Table 39: Experiment 1 Flight Path Error Tests for Error Variance Constancy of Regression Model – No color fill indicates that none of these results are significant, so the hypothesis holds that error variance is constant and regression analysis is suitable

Grouping	Bartlett F Statistic	Bartlett p-value	Levene F Statistic	Levene p-value	Brown-Forsythe F Statistic	Brown-Forsythe p-value
XorientAid	0.10	0.75	0.79	0.37	0.79	0.37
Xalign	0.00	0.96	0.03	0.87	0.04	0.83
XtrialNum	0.02	0.89	0.18	0.67	0.20	0.66
Ximage	0.97	0.32	0.82	0.37	0.91	0.34
Xsubject	0.18	0.67	0.00	0.95	0.00	0.95
Predicted FPE'	0.18	0.67	0.00	0.95	0.00	0.95
Time Sequence	0.18	0.67	0.00	0.95	0.00	0.95

No figures are shown in this appendix because this model did not reveal any significant effects.

C.5. Sensor Track Error

$$STE'_{e1} \approx \beta_0 + \beta_1 * XtrialNum$$

Equation 28: Sensor Track Error Regression Estimation

Only the trial number was included in the model. This indicated that only a learning effect impacted the sensor track error.

Table 40: Experiment 1 Sensor Track Error RMSE Predictor Variable Coefficients

Predictor Variable	Term	Transformed Regression Estimate	Lower 95% Conf. Interval	Upper 95% Conf. Interval	t-stat	p-value	Reverse Transformed Estimate (β')	units
(Intercept)	β_0	-0.05	-0.05	-0.04	-34.70	3E-131	-0.64	RMSE
XtrialNum	β_1	-3.24E-04	-6.55E-04	6.13E-06	-1.93	0.05	-3.09E-04	RMSE/#

Table 41: Experiment 1 Flight Path Error Tests for Error Variance Constancy of Regression Model
 – No color fill indicates that none of these results are significant, so the hypothesis holds that error variance is constant and regression analysis is suitable

Grouping	Bartlett F Statistic	Bartlett p-value	Levene F Statistic	Levene p-value	Brown-Forsythe F Statistic	Brown-Forsythe p-value
XorientAid	0.08	0.77	0.18	0.67	0.19	0.66
Xalign	1.39	0.24	1.26	0.26	1.28	0.26
XtrialNum	2.31	0.13	2.62	0.11	2.67	0.10
Ximage	1.33	0.25	0.70	0.40	0.62	0.43
Xsubject	0.18	0.67	0.30	0.58	0.29	0.59
Predicted STE'	0.05	0.82	0.00	0.96	0.00	0.97
Time Sequence	0.18	0.67	0.30	0.58	0.29	0.59

No figures are shown in this appendix because this model did not reveal any significant effects.

C.6. Orientation Time

$$OT'_{e1} \approx \beta_0 + \beta_1 * XorientAid + \beta_2 * Xalign1 + \beta_3 * Xalign2 + \beta_4 * XtrialNum + \beta_{5i} * Xsubject_i + \beta_{6i} * XorientAid * Xsubject_i + \beta_{7i} * Xalign * Xsubject_i$$

$$i = 1:36 \text{ subjects}$$

Equation 29: Orientation Time Regression Estimation

Table 42: Experiment 1 Orientation Time Predictor Variable Coefficients

Predictor Variable	Term	Transformed Regression Estimate	Lower 95% Conf. Interval	Upper 95% Conf. Interval	t-stat	p-value	Reverse Transformed Estimate (β')	units
(Intercept)	β_0	0.45	0.35	0.55	8.91	1.15E-17	0.32	s
XorientAid	β_1	-0.15	-0.20	-0.10	-6.03	3.35E-09	-0.16	s
Xalign1 Sensor Display Only	β_2	-0.26	-0.31	-0.21	-9.94	3.17E-21	-0.30	s
Xalign2 Sensor and Aircraft Displays	β_3	-0.39	-0.46	-0.33	-11.97	6.04E-29	-0.51	s
XtrialNum	β_4	-0.01	-0.02	-0.01	-7.00	9.15E-12	-0.01	s/#

Table 43: Experiment 1 Orientation Time Tests for Error Variance Constancy of Regression Model

– Yellow indicates that some of these results are trending towards significance. The Bartlett test reveals non-constant variance with respect to orientation aid; however, the other two tests pass with 0.05 significance, so the hypothesis holds that error variance is constant and regression analysis is suitable. Still this is of interest in relying on this regression model.

Grouping	Bartlett F Statistic	Bartlett p-value	Levene F Statistic	Levene p-value	Brown-Forsythe F Statistic	Brown-Forsythe p-value
XorientAid	10.78	1.03E-03	4.47	0.03	4.18	0.04
Xalign	6.98	0.01	3.61	0.06	3.65	0.06
XtrialNum	3.61	0.06	4.18	0.04	4.20	0.04
Ximage	3.23	0.07	3.88	0.05	3.39	0.07
Xsubject	1.89	0.17	0.82	0.36	0.70	0.40
Predicted OT'	1.01	0.32	0.83	0.36	0.80	0.37
Time Sequence	3.23	0.07	3.61	0.06	3.49	0.06

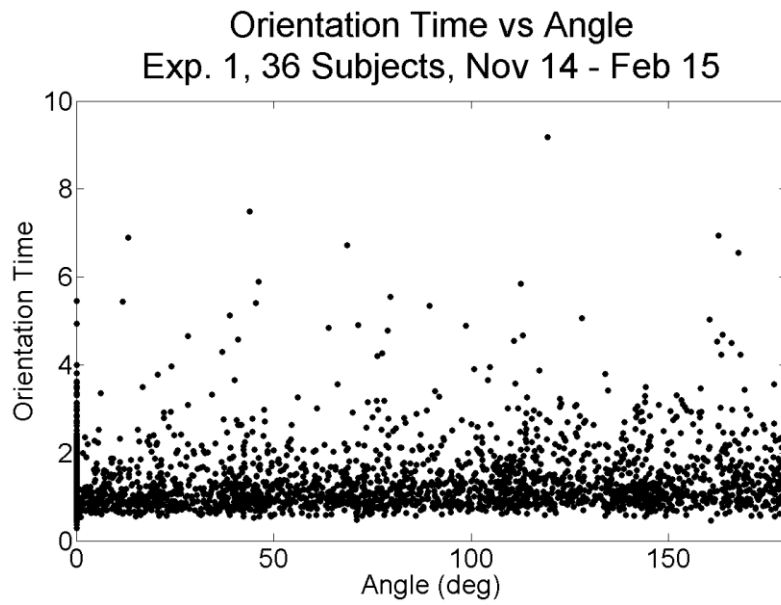


Figure 139: Individual Orientation Time vs. Rotation Angle

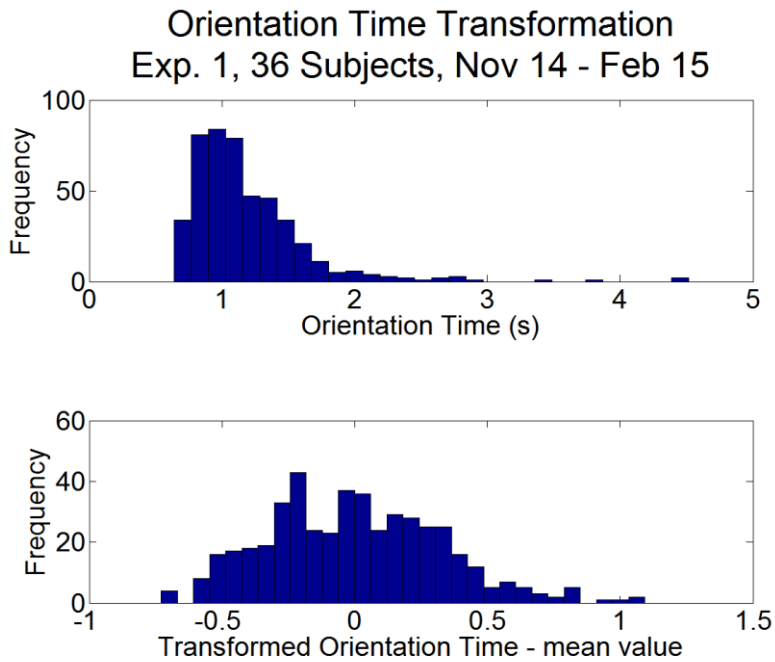


Figure 140: Orientation Time Data Transformation

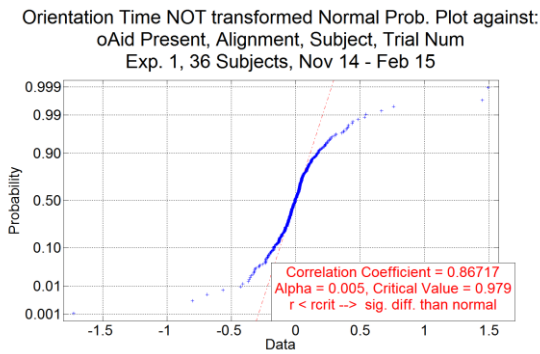


Figure 141: Orientation Time Regression Residuals from Skewed Data

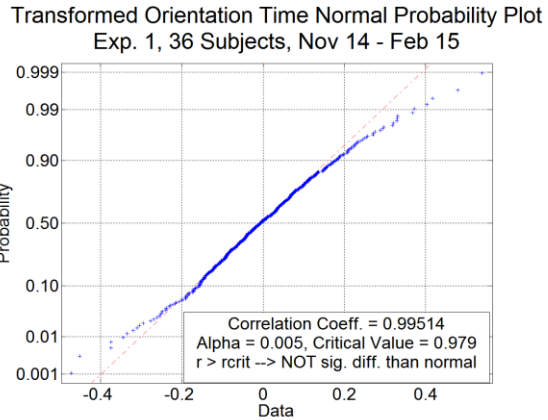


Figure 142: Orientation Time Regression Residuals from Transformed Data

Orientation Time Transformation Parameters Exp. 1, 36 Subjects, Nov 14 - Feb 15

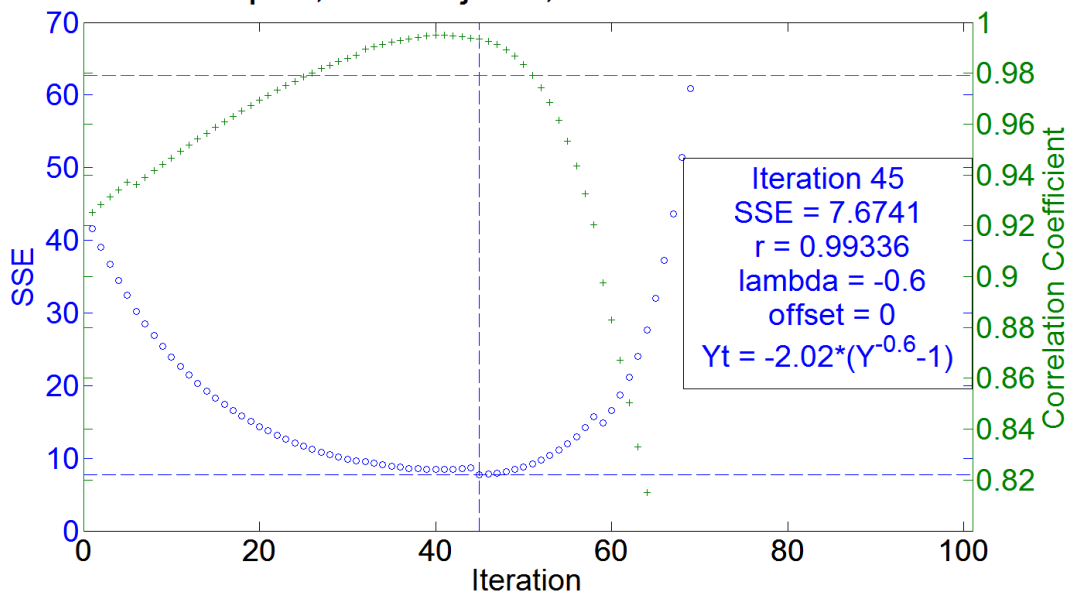


Figure 143: Orientation Time Box-Cox Transformation Parameter Estimation

The blue data show how the regression Mean Squared Error was minimized with the Box-Cox Transformation. The green data show the corresponding effect on the correlation of the residuals with estimated values under normality. The notches in these distributions occur when different terms are added to the model throughout the optimization process.

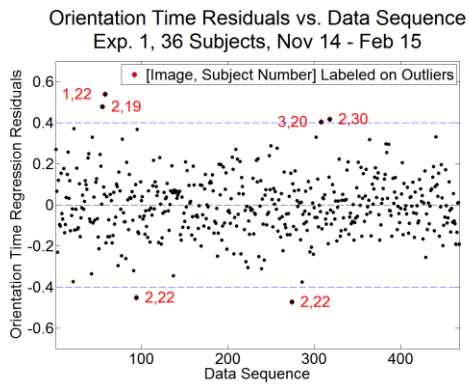


Figure 144: Test of Randomness

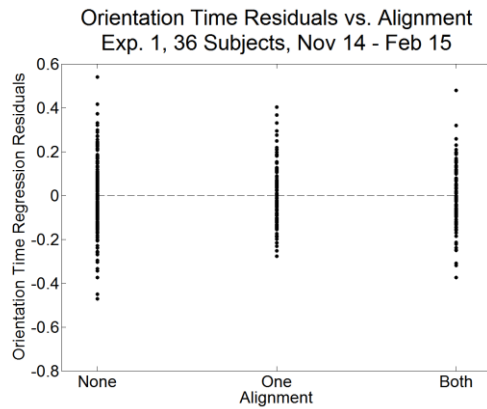


Figure 145: Residuals vs. Xalign

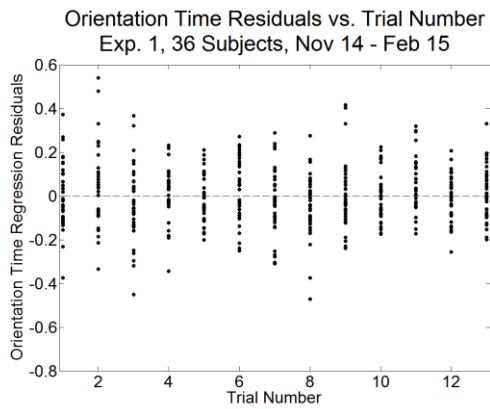


Figure 146: Residuals vs. XtrialNum

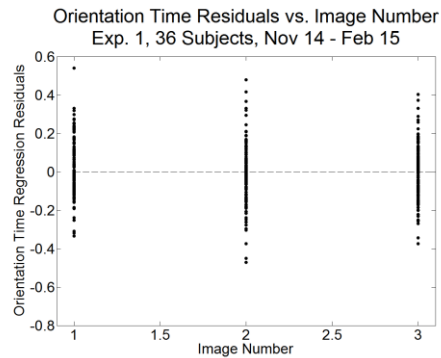


Figure 147: Residuals vs. Ximage

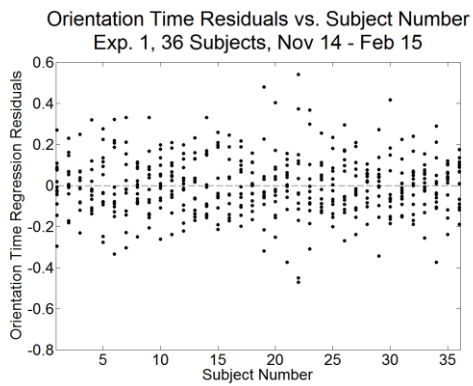


Figure 148: Residuals vs Xsubject

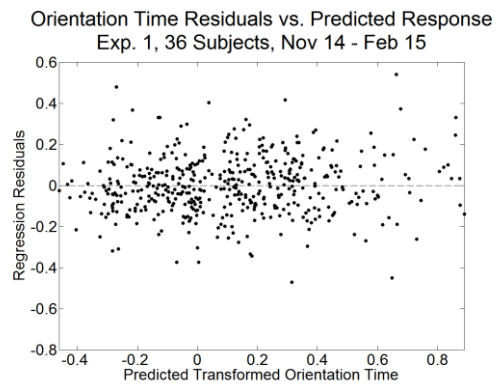


Figure 149: Residuals vs Predicted Orientation Time

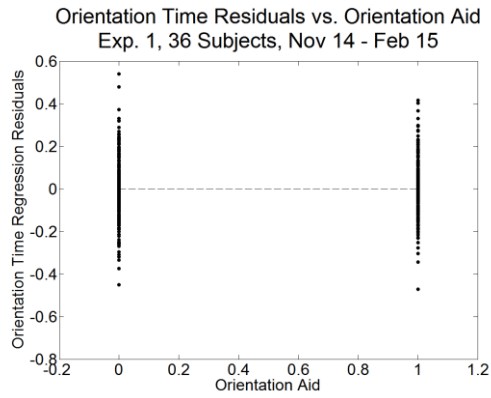


Figure 150: Residuals vs. XorientAid

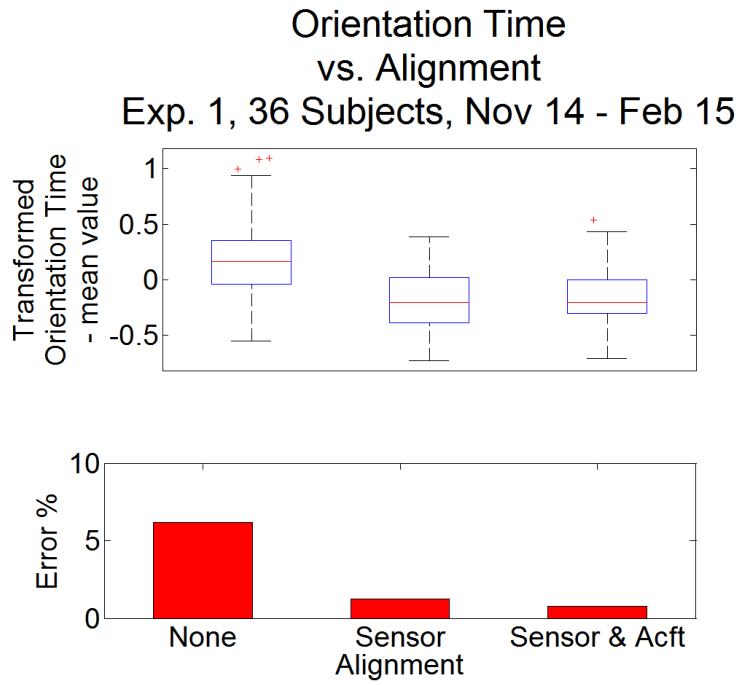


Figure 151: Experiment 1 Orientation Time vs. Alignment

Orientation Time vs. Alignment (Observed Data)
Exp. 1, 36 Subjects, Nov 14 - Feb 15

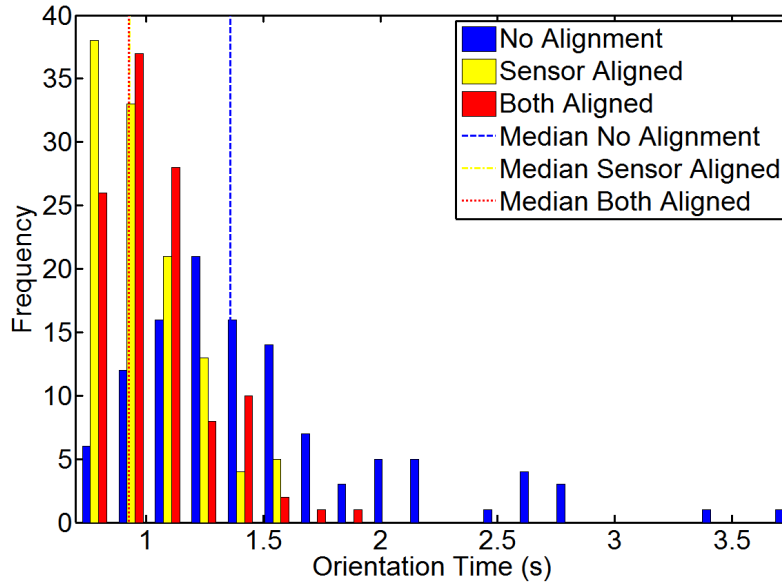


Figure 152: Experiment 1 Orientation Time Alignment Effect
Blue distribution is observed data without alignment. Yellow distribution is alignment of the sensor video only, and red has alignment of sensor and aircraft displays.

Orientation Time vs. Orientation Aid (Observed Data)
Exp. 1, 36 Subjects, Nov 14 - Feb 15

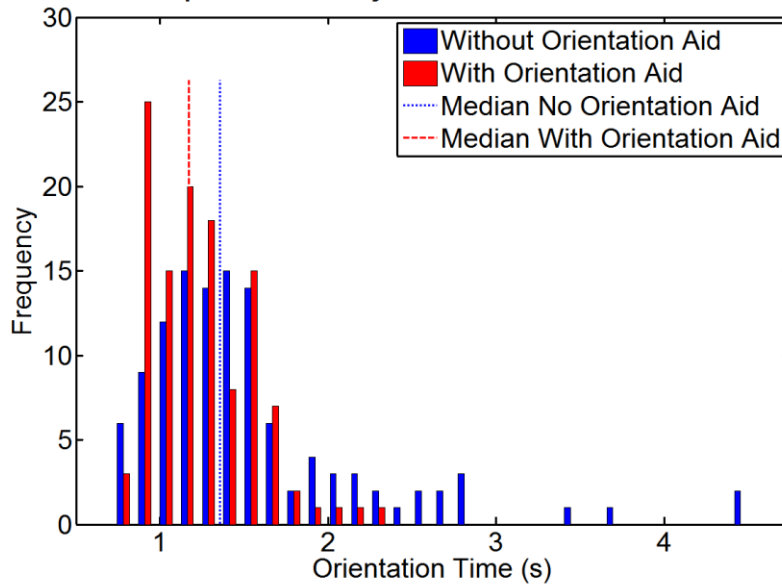


Figure 153: Experiment 1 Orientation Time Orientation Aid Effect
Blue distribution is observed data without the orientation aid. Red distribution is observed data with the orientation aid and is shifted left of the blue data.

Orientation Time
vs. Orientation Aid Present
Exp. 1, 36 Subjects, Nov 14 - Feb 15

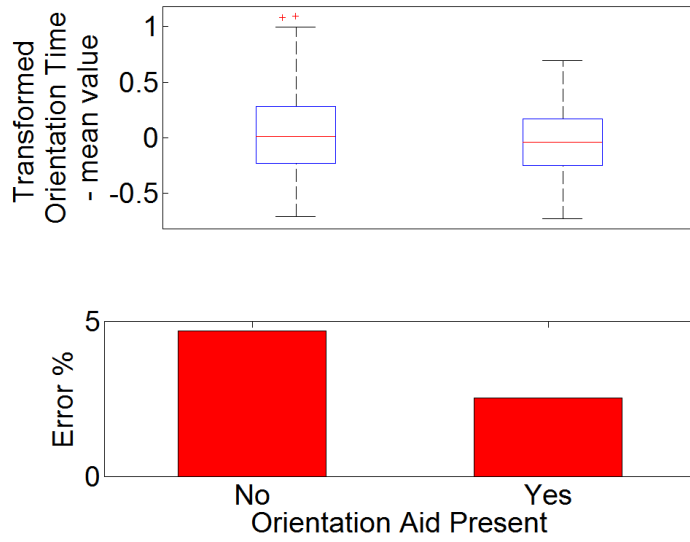


Figure 154: Experiment 1 Orientation Time vs. Orientation Aid

C.7. Bedford Workload Rating

Bedford Workload vs. Orientation Aid (Observed Data)
Exp. 1, 36 Subjects, Nov 14 - Feb 15

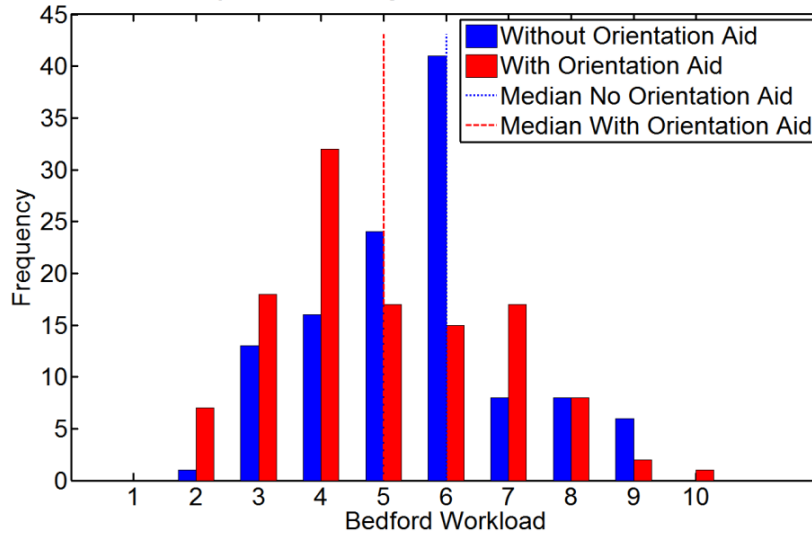


Figure 155: Experiment 1 Bedford Workload Rating Orientation Aid Effect
Blue distribution is observed data without the orientation aid. Red distribution is observed data with the orientation aid.

Bedford Workload vs. Alignment (Observed Data)
Exp. 1, 36 Subjects, Nov 14 - Feb 15

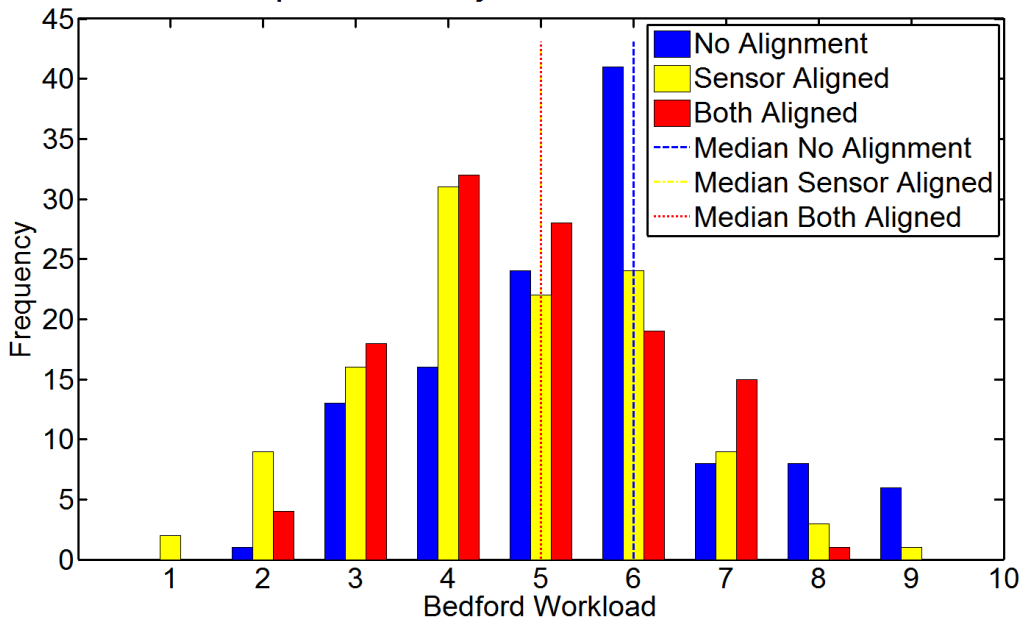


Figure 156: Experiment 1 Bedford Workload Rating Alignment Effect
Blue distribution is observed data without alignment. Yellow distribution is alignment of the sensor video only, and red has alignment of sensor and aircraft displays.

C.8. Reaction Time

$$RT'_{e1} \approx \beta_0 + \beta_1 * Xalign1 + \beta_2 * Xalign2 + \beta_3 * XtrialNum + \beta_{4i} * Xsubject + \beta_{5i} * XtrialNum * Xsubject_i$$

$i = 1:36$ subjects

Equation 30: Experiment 1 Reaction Time Regression Estimation

Table 44: Experiment 1 Reaction Time Predictor Variable Coefficients

Predictor Variable	Term	Transformed Regression Estimate	Lower 95% Conf. Interval	Upper 95% Conf. Interval	t-stat	p-value	Reverse Transformed Estimate (β')	units
(Intercept)	β_0	-0.07	-0.12	-0.02	-2.95	3.35E-03	-0.07	s
Xalign1 Sensor Display Only	β_1	-0.04	-0.06	-0.02	-3.72	2.21E-04	-0.04	s
Xalign2 Sensor and Aircraft Displays	β_2	-0.04	-0.06	-0.02	-3.83	1.44E-04	-0.04	s
XtrialNum	β_3	-3.73E-03	-0.01	-1.07E-03	-2.76	6.07E-03	-3.54E-03	s/#

Table 45: Experiment 1 Reaction Time Tests for Error Variance Constancy of Regression Model
Yellow indicates that some of these results are trending towards significance. However, the hypothesis holds that error variance is constant and regression analysis is suitable.

Grouping	Bartlett F Statistic	Bartlett p-value	Levene F Statistic	Levene p-value	Brown-Forsythe F Statistic	Brown-Forsythe p-value
XorientAid	3.23	0.07	2.94	0.09	2.90	0.09
Xalign	0.94	0.33	1.38	0.24	1.53	0.22
XtrialNum	0.57	0.45	0.27	0.60	0.35	0.55
Ximage	0.10	0.75	0.01	0.93	0.05	0.83
Xsubject	1.34	0.25	0.52	0.47	0.34	0.56
Predicted RT'	5.96	0.01	3.78	0.05	3.42	0.06
Time Sequence	1.53	0.22	0.75	0.39	0.84	0.36

Reaction Time vs Angle
Exp. 1, 36 Subjects, Nov 14 - Feb 15

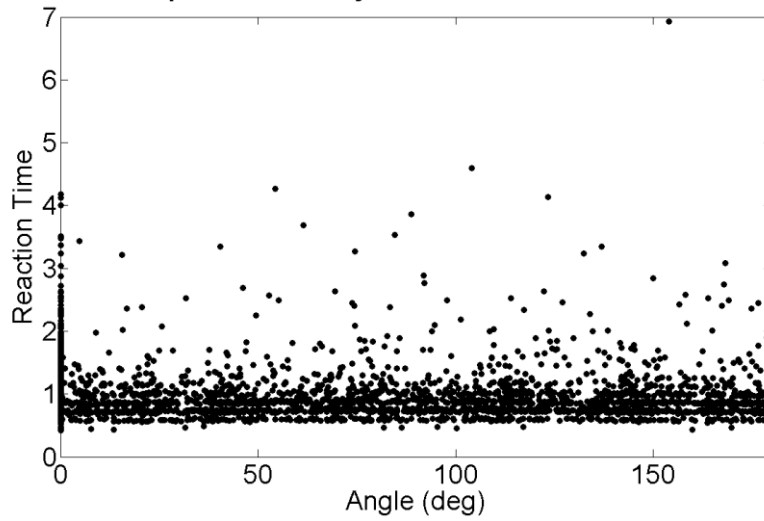


Figure 157: Individual Reaction Time vs. Rotation Angle

Reaction Time Transformation
Exp. 1, 36 Subjects, Nov 14 - Feb 15

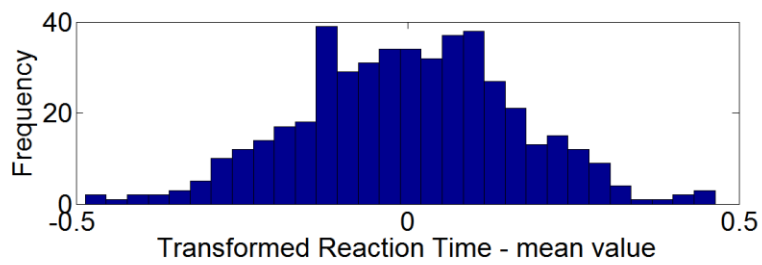
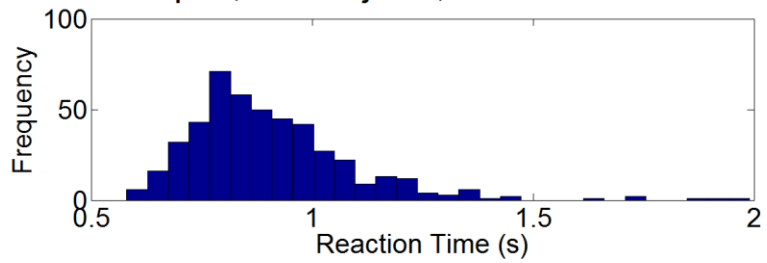


Figure 158: Reaction Time Data Transformation

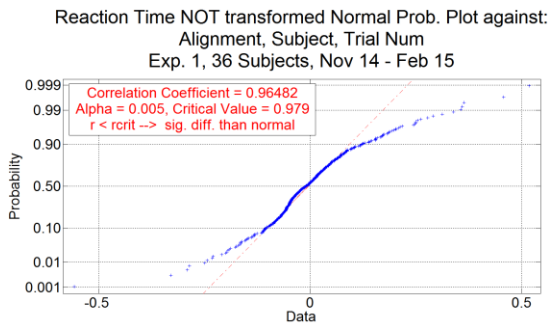


Figure 159: Reaction Time Regression Residuals from Skewed Data

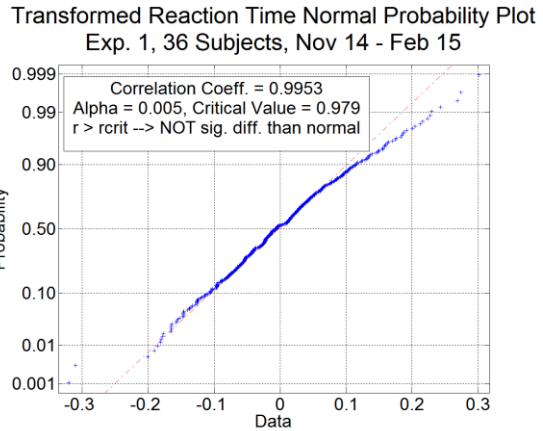


Figure 160: Reaction Time Regression Residuals from Transformed Data

Reaction Time Transformation Parameters Exp. 1, 36 Subjects, Nov 14 - Feb 15

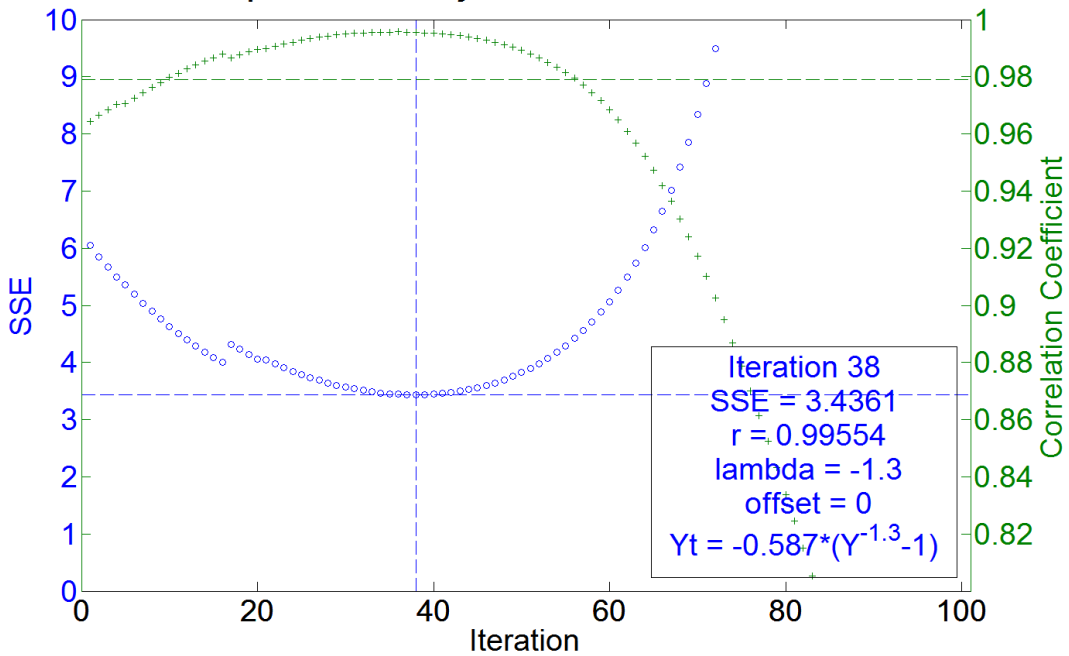


Figure 161: Box-Cox Transformation Parameter Estimation

The blue data show how the regression Mean Squared Error was minimized with the Box-Cox Transformation. The green data show the corresponding effect on the correlation of the residuals with estimated values under normality.

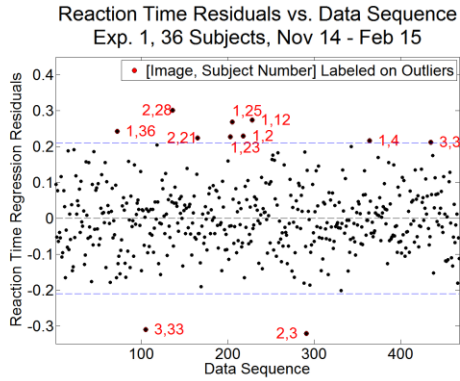


Figure 162: Test of Randomness

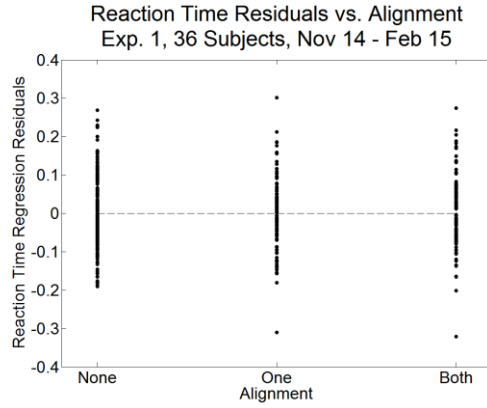


Figure 163: Residuals vs. Xalign

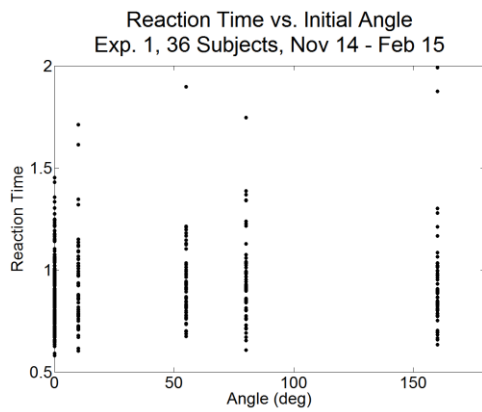


Figure 164: Residuals vs. XinitAngle

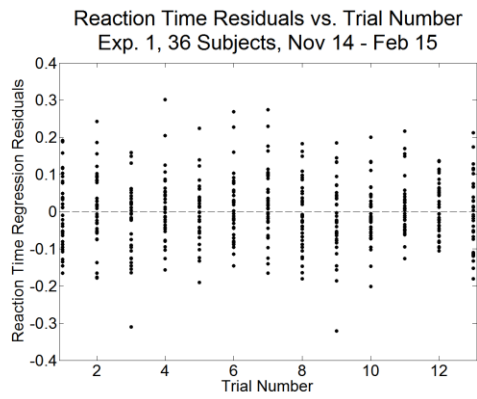


Figure 165: Residuals vs. XtrialNum

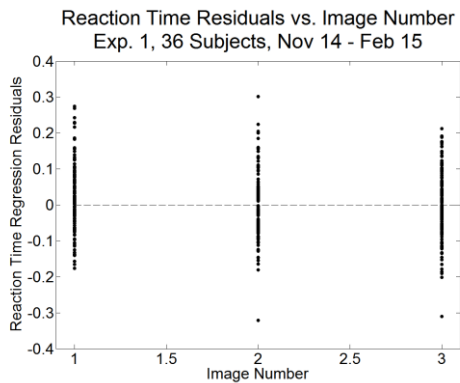


Figure 166: Residuals vs. Ximage

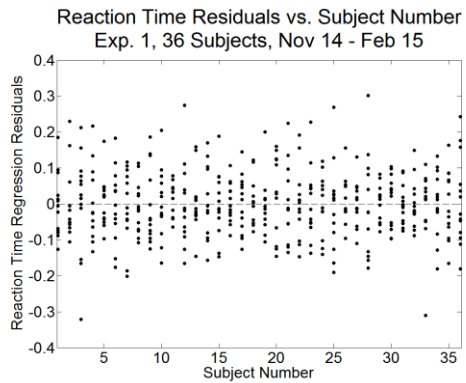


Figure 167: Residuals vs Xsubject

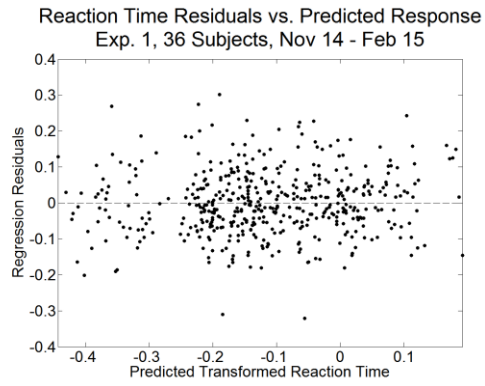


Figure 168: Residuals vs. Predicted Reaction Time

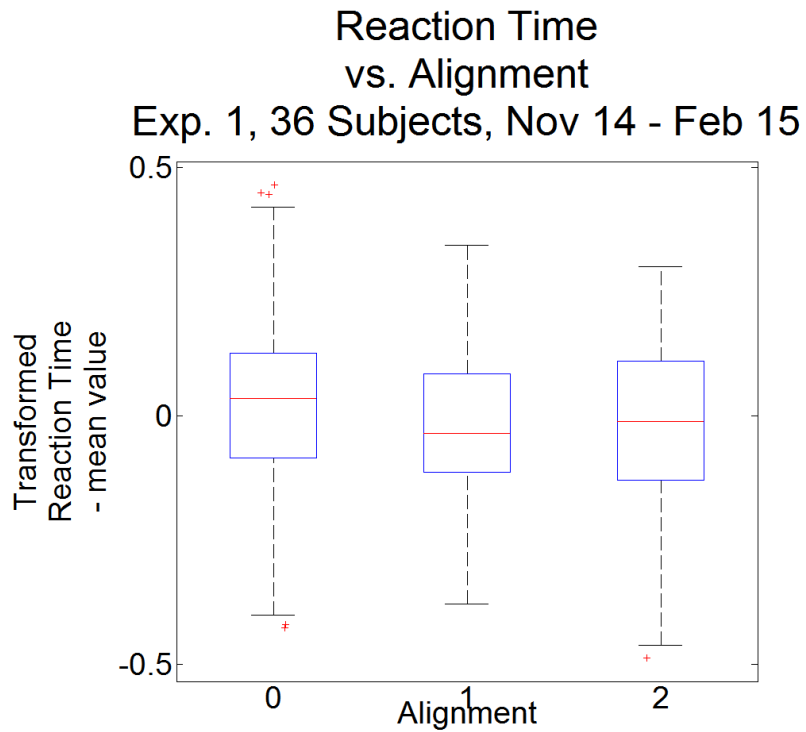


Figure 169: Reaction Time vs. Alignment

Reaction Time Alignment Effect(Observed Data)
Exp. 1, 36 Subjects, Nov 14 - Feb 15

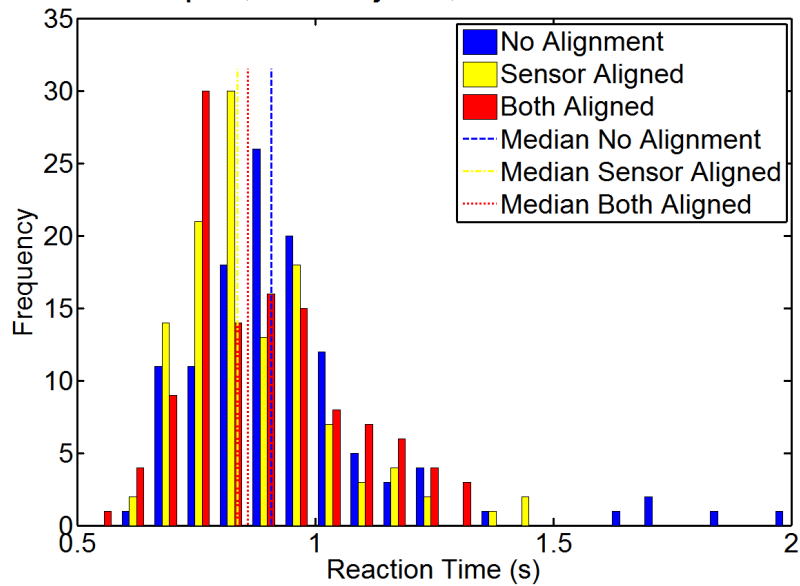


Figure 170: Reaction Time Alignment Effect
Blue distribution is observed data without alignment. Yellow distribution is alignment of the sensor video only, and red has alignment of sensor and aircraft displays

Reaction Time
vs. Orientation Aid Present
Exp. 1, 36 Subjects, Nov 14 - Feb 15

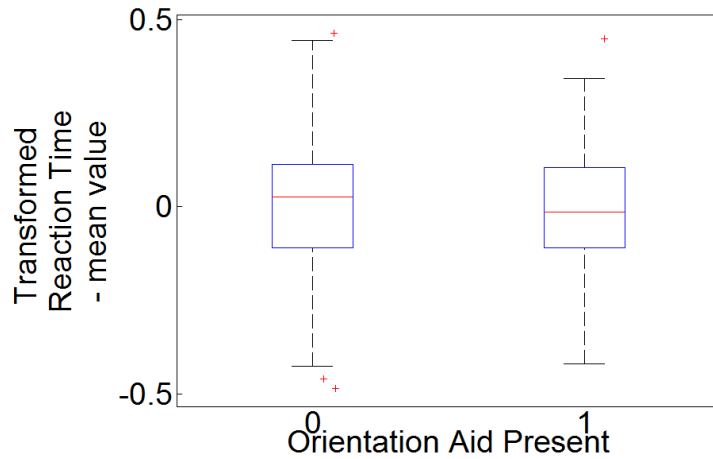


Figure 171: Reaction Time vs. Orientation Aid

Reaction Time Orientation Aid Effect (Observed)
Exp. 1, 36 Subjects, Nov 14 - Feb 15

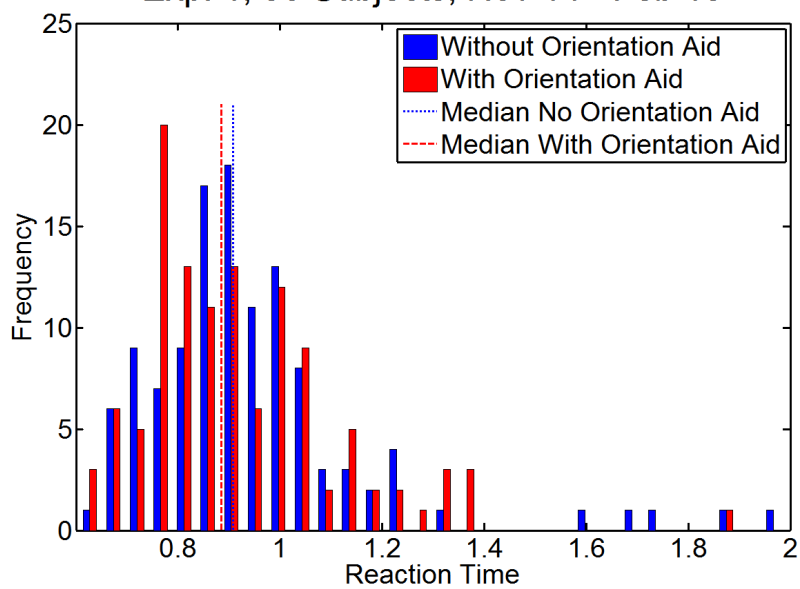


Figure 172: Reaction Time Orientation Aid Effect

Blue distribution is observed data without the orientation aid. Red distribution is observed data with the orientation aid and is shifted left of the blue data.

This page intentionally left blank.

Appendix D: Experiment 2 Data Analysis

D.1. Selection Answer Time

Selection Answer Time

$$\begin{aligned} \approx & \beta_0 + \beta_1 * Xalign + \beta_2 * XorientAid + \beta_3 * XinitAngle + \beta_{4m} * Ximage_m + \beta_{5m} \\ & * Xalign * Ximage_m + \beta_{6m} * XorientAid * Ximage_m + \beta_{7i} * Xsubject_i + \beta_{8i} \\ & * Xalign * Xsubject_i + \beta_{9i} * XorientAid * Xsubject_i \\ & i = 1: 12 \text{ subjects}, \quad m = 1: 24 \text{ images} \end{aligned}$$

Equation 31: Imagery Rotation Test Selection Answer Time Regression Model

Table 46: Experiment 2 Selection Answer Time Predictor Variable Coefficients

These are the fixed effects coefficients from the regression model for selection answer time in experiment 2. The final numerical column represents the coefficient application to the median of the original distribution.

Predictor Variable	Term	Transformed Regression Estimate	Lower 95% Conf. Interval	Upper 95% Conf. Interval	t-stat	p-value	Reverse Transformed Estimate	units
Intercept	β_0	28.94	27.16	30.71	31.97	9.4E-148	7.64	s
Xalign	β_1	-7.87	-10.02	-5.73	-7.20	1.3E-12	-14.81	s
XorientAid	β_2	-2.16	-3.33	-0.98	-3.59	3.4E-04	-2.39	s
XinitAngle	β_3	0.02	0.01	0.03	6.19	9.5E-10	0.02	s/deg

Table 47: Selection Answer Time Regression Including Cognitive Test Results, Significant correlations with cognitive tests are highlighted green

Term	SSE	DF	MSE	F	p-value
Trial Number	131.78	1	131.78	7.77	5.4E-03
Image Alignment	3282.65	1	3282.65	193.50	1.2E-39
Orientation Aid	551.16	1	551.16	32.49	1.7E-08
Initial Angle	428.44	1	428.44	25.26	6.2E-07
Image Number	4298.04	23	186.87	11.02	8.7E-35
Card Score	148.16	1	148.16	8.73	3.2E-03
MRT	103.47	1	103.47	6.10	1.4E-02
PTA	31.09	1	31.09	1.83	0.18
Purdue	21.79	1	21.79	1.28	0.26
	13893.80	819	16.96	1	

Selection Answer Time vs. Orientation Aid (Observed Data)
Exp. 2, 12 Subjects, Aug - Nov 15

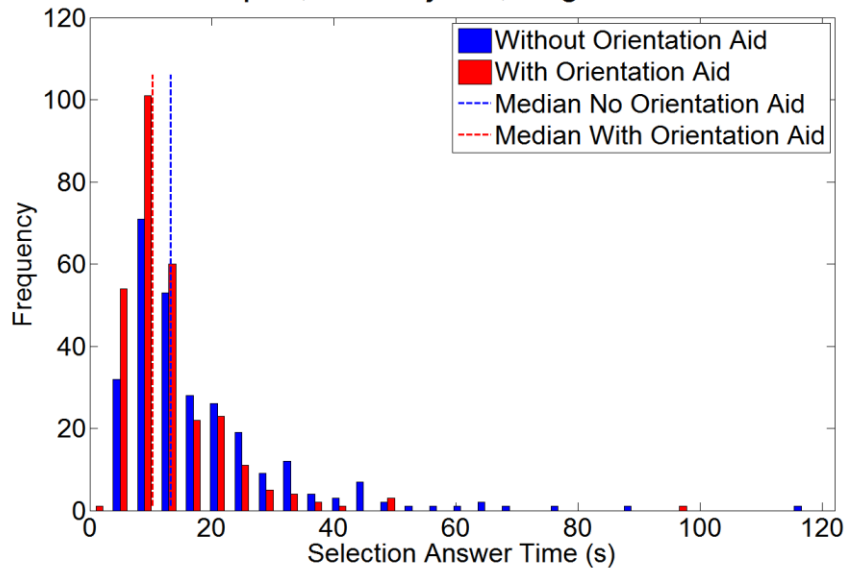


Figure 173: Selection Answer Time Orientation Aid Effect
Blue distribution is observed data without the orientation aid. Red distribution is observed data with the orientation aid and is shifted left of the blue data. (configuration Z vs X)

Selection Answer Time vs. Alignment (Observed Data)
Exp. 2, 12 Subjects, Aug - Nov 15

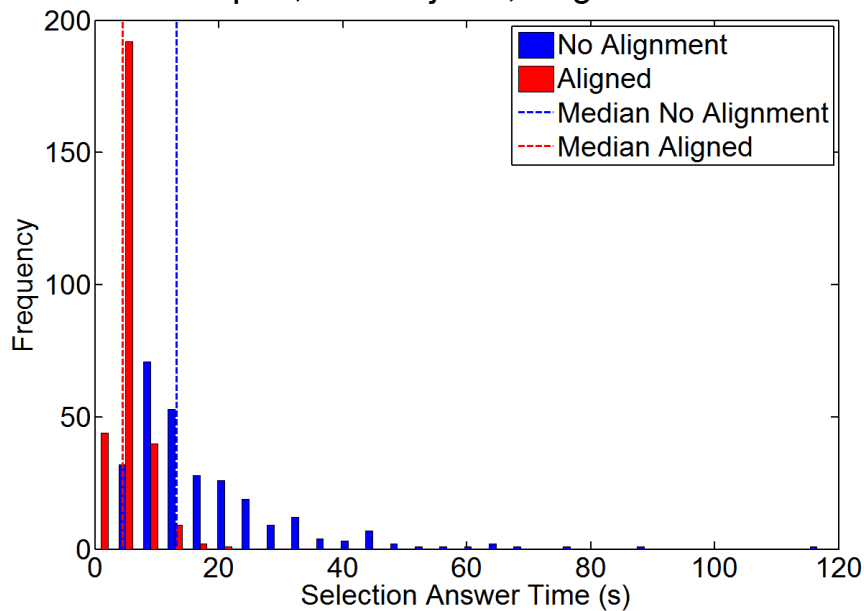


Figure 174: Selection Answer Time Alignment Effect
Blue distribution is observed data without alignment. Red distribution is observed data with alignment. (configuration Z vs Y)

Selection Answer Time vs. Alignment (Observed Data)
 Exp. 2, 12 Subjects, Aug - Nov 15

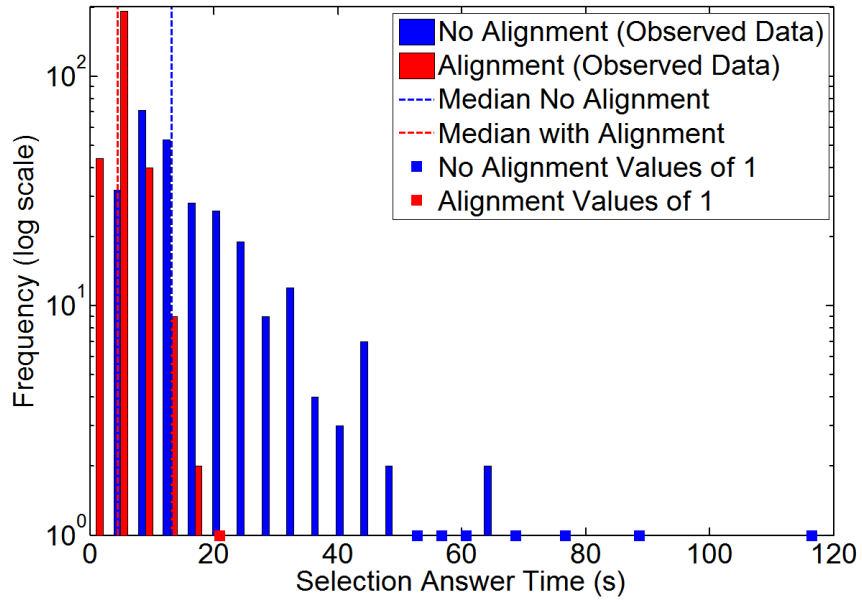


Figure 175: Selection Answer Time Alignment Effect (Log Scale)
 Blue distribution is observed data without alignment. Red distribution is observed data with alignment. (configuration Z vs Y)

D.2. Selection Answer Error

$$\text{Selection Answer Error} \approx \beta_0 + \beta_1 * X_{\text{align}} + \beta_2 * X_{\text{orientAid}} + \beta_{3m} * X_{\text{image}_m} + \beta_{4m} * X_{\text{align}} * X_{\text{image}_m} + \beta_{5m} * X_{\text{orientAid}} * X_{\text{image}_m} + \beta_{6i} * X_{\text{subject}_i} + \beta_{7i} * X_{\text{align}} * X_{\text{subject}_i}$$

$$i = 1:12 \text{ subjects}, \quad m = 1:24 \text{ images}$$

Equation 32: Imagery Rotation Test Selection Answer Error Regression Model

Table 48: Experiment 2 Selection Answer Error Predictor Variable Coefficients

These are the fixed effects coefficients from the regression model for selection answer error in experiment 2. The final numerical column represents the coefficient application to the median of the original distribution.

Predictor Variable	Term	Regression Estimate	Lower 95% Conf. Interval	Upper 95% Conf. Interval	t-stat	p-value	Reverse Transformed Estimate	units
Intercept	β_0	0.74	0.29	1.19	3.23	1.29E-03	0.45	% display width
Xalign	β_1	-1.49	-1.87	-1.10	-7.62	6.63E-14	-2.64	% display width
XorientAid	β_2	-0.30	-0.57	-0.03	-2.19	0.03	-0.28	% display width

Table 49: Selection Answer Error Regression Including Cognitive Test Results
Significant correlations with cognitive tests are highlighted green

Term	SSE	DF	MSE	F	p-value
Trial Number	0.95	1	0.95	0.03	0.86
Image Alignment	1313.39	1	1313.39	43.45	7.8E-11
Orientation Aid	197.94	1	197.94	6.55	0.011
Initial Angle	85.87	1	85.87	2.84	0.092
Image Number	2725.19	23	118.49	3.92	2.6E-09
Card Score	51.49	1	51.49	1.70	0.19
MRT	618.73	1	618.73	20.47	6.9E-06
PTA	18.01	1	18.01	0.60	0.44
Purdue	18.73	1	18.73	0.62	0.43
	24753.85	819	30.22	1	

Selection Answer Error vs. Orientation Aid (Observed Data)
Exp. 2, 12 Subjects, Aug - Nov 15

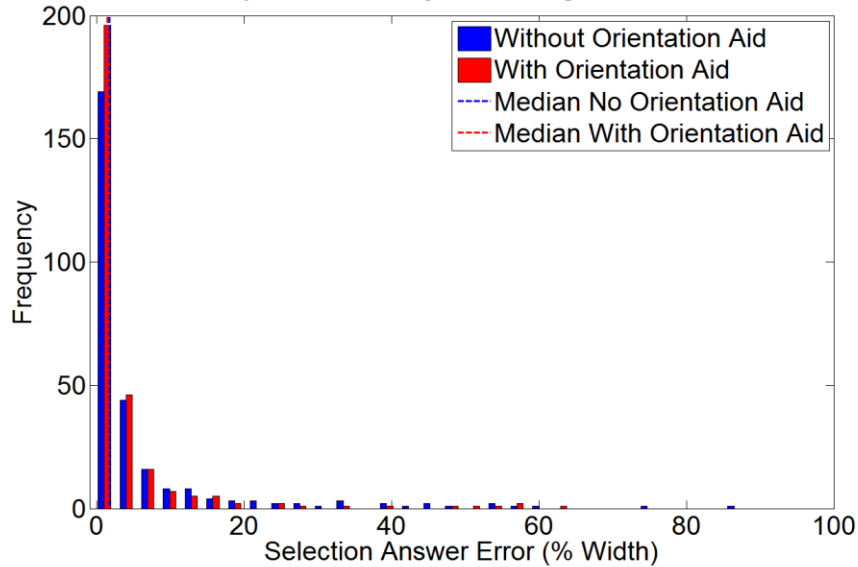


Figure 176: Selection Answer Error Orientation Aid Effect
Blue distribution is observed data without the orientation aid. Red distribution is observed data with the orientation aid and is shifted slightly left of the blue data.
(configuration Z vs X)

Selection Answer Error vs. Alignment (Observed Data)
Exp. 2, 12 Subjects, Aug - Nov 15

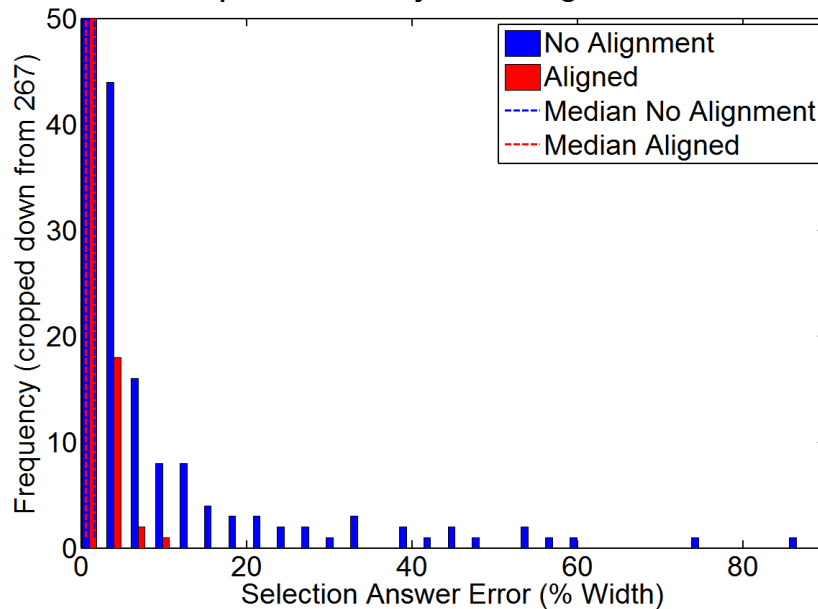


Figure 177: Selection Answer Error Alignment Effect
Blue distribution is observed data without alignment. Red distribution is observed data with alignment and is shifted slightly left. Also, the alignment virtually eliminates the tail of the distribution.
(configuration Z vs Y)

This page intentionally left blank.

Appendix E: Experiment 3 Data Analysis

E.1. Data Transformations

This research utilized the Box-Cox transformation to normalize data for parametric analysis [133]. This process analyzes both log transformation and a range of power functions. For example, Figure 179 shows the effect of the Box-Cox transformation on the Target Acquisition Time data.

$$W_i = \begin{cases} K_1 \left((Y + \lambda_2)_i^{\lambda_1} - 1 \right) & \lambda_1 \neq 0 \\ K_2 (\log_e Y_i) & \lambda_1 = 0 \end{cases}$$

Equation 33: Box-Cox Transformation

$$K_2 = \left(\prod_{i=1}^n (Y + \lambda_2)_i \right)^{1/n}$$

Equation 34: Box-Cox Standardization Coefficient 1

$$K_1 = \frac{1}{\lambda_1 K_2^{(\lambda_1 - 1)}}$$

Equation 35: Box-Cox Standardization Coefficient 2

The Box-Cox transformation is shown in Equation 18 through Equation 20. This shows the two parameter estimation procedure, where both λ_1 and λ_2 are estimated. None of these transformations required an estimate of λ_2 , but each measure required an estimation of λ_1 to allow for parametric analysis. Since the transformations are analyzed based on the Sum of Squared Error (SSE) of the resulting regression, the standardization parameters in Equation 19 and Equation 20 are used to prevent SSE fluctuations as a function of λ_1 . An example estimation of the λ_1 parameter is shown in Figure 182. The left vertical axis represents value of SSE which is minimized using this transformation. The right vertical axis represents the correlation coefficient between the residuals and their expected value under normality [134]. The horizontal green dashed line shows the correlation coefficient associated with an $\alpha = 0.005$ significance. Here in the Box-Cox transformation selects $\lambda_1 = -0.5$ to minimize SSE, and this also generates an acceptable correlation coefficient as shown by the green data in Figure 182. A similar process was used for every transformation and each figure is available throughout this appendix. The transformation equations are shown in the applicable figures and listed here:

$$TAT'_{e3} = -19.0 * (TAT^{-0.5} - 1)$$

Equation 36: Experiment 3 Transformed Target Acquisition Time

$$FPE'_{e3} = -0.0085 * (FPE^{-0.4} - 1)$$

Equation 37: Experiment 3 Transformed Flight Path Error

$$STE'_{e3} = -0.00115 * (STE^{-0.8} - 1)$$

Equation 38: Experiment 3 Transformed Sensor Track Error

$$OT'_{e3} = -1.10 * (OT^{-0.8} - 1)$$

Equation 39: Experiment 3 Transformed Orientation Time

$$RT'_{e3} = -0.381 * (RT^{-1.2} - 1)$$

Equation 40: Experiment 3 Transformed Reaction Time

E.2. Pairwise Comparisons

Table 50: Experiment 3 Pairwise Comparisons– These are the results of within-subjects 2-sided pairwise t-tests with the family significance of 0.05 (Bonferroni corrected to ~0.008 2-sided or ~0.004 1-sided). Green indicates a significant effect which improved performance, red indicates a significant effect which degraded performance. Black indicates that these data were not collected. P-values are indicative of the single tail probability, which would be less than 0.004 for significance.

		Adding Reference Frame Alignment		Including Orientation Aid		Interaction Effects			
		Display	Display	Display	Display	Display	Display		
		A ≠ D	E ≠ F	A ≠ E	D ≠ F	E ≠ D	A ≠ F		
PARAMETRIC ANALYSIS	Orientation Time ¹	t*	9.46	10.75	-1.16	0.02	8.18	10.93	
		p-value	5.17E-08	9.54E-09	0.87	0.49	3.28E-07	7.63E-09	
	Target Acquisition Time ¹	t*	1.65	4.03	-2.54	0.51	3.01	1.73	
		p-value	0.06	5.47E-04	0.99	0.31	4.37E-03	0.05	
	Sensor Track Error ¹	t*	0.38	-0.06	0.30	-0.08	0.02	0.28	
		p-value	0.35	0.52	0.38	0.53	0.49	0.39	
	Flight Path Error ¹	t*	-3.16E-03	-1.34	0.75	-0.43	-0.65	-0.65	
		p-value	0.50	0.90	0.23	0.66	0.74	0.74	
	Reaction Time ¹	t*	0.63	2.23	-4.37	-2.19	3.83	-1.77	
		p-value	0.27	0.02	1.00	0.98	8.28E-04	0.95	
	NON-PARAMETRIC ANALYSIS	Bedford Workload Static Target	Chi-sqr	2.90	6.92	1.35	0.30	8.68	1.64
			p-value	0.09	0.01	0.24	0.58	3.21E-03	0.20
Bedford Workload Dynamic Target		Chi-sqr	5.82	12.37	0.88	1.48E-03	11.60	6.42	
		p-value	0.02	4.36E-04	0.35	0.97	6.58E-04	0.01	
Rankings (1-4) Kruskal-Wallis		Chi-sqr	10.75	16.35	3.65E-03	2.02	10.15	15.89	
		p-value	1.05E-03	5.26E-05	0.95	0.15	1.44E-03	6.70E-05	
Ratings (1-10) Kruskal-Wallis		Chi-sqr							
		p-value							

E.3. Target Acquisition Time

$$TAT'_{e3} \approx \beta_0 + \beta_1 * Xalign + \beta_2 * XtrialNum + \beta_{3i} * Xsubject_i + \beta_{4m} * Ximage_m$$

$$i = 1:16 \text{ subjects}$$

Equation 41: Target Acquisition Time Regression Estimation

Yellow highlights terms of interest, which were discussed in the body of the document.

Table 51: Experiment 3 Target Acquisition Time Predictor Variable Coefficients

Predictor Variable	Term	Transformed Regression Estimate	Lower 95% Conf. Interval	Upper 95% Conf. Interval	t-stat	p-value	Reverse Transformed Estimate (β')	units
(Intercept)	β_0	10.55	9.57	11.53	21.12	1.68E-58	3.41	s
Xalign	β_1	-0.53	-0.81	-0.26	-3.80	1.77E-04	-0.55	s
XtrialNum	β_2	-0.043	-0.071	-0.015	-3.01	2.86E-03	-0.041	s/#

Table 52: Experiment 3 Target Acquisition Time Tests for Error Variance Constancy of Regression Model

– Yellow indicates that results are trending towards significance; however, each constancy test holds to the 0.005 significance level. The hypothesis holds that error variance is constant and regression analysis is suitable.

Grouping	Bartlett F Statistic	Bartlett p-value	Levene F Statistic	Levene P-value	Brown-Forsythe F Statistic	Brown-Forsythe p-value
Xdisplnt	0.91	0.34	1.32	0.25	1.19	0.28
Xalign	0.31	0.58	0.48	0.49	0.45	0.50
XtrialNum	6.55	0.01	2.32	0.13	2.06	0.15
Ximage	0.46	0.50	0.92	0.34	1.02	0.31
Xsubject	0.40	0.53	0.10	0.75	0.03	0.86
Predicted TAT'	0.81	0.37	0.00	0.94	0.00	0.94
Time Sequence	0.50	0.48	0.17	0.68	0.08	0.78

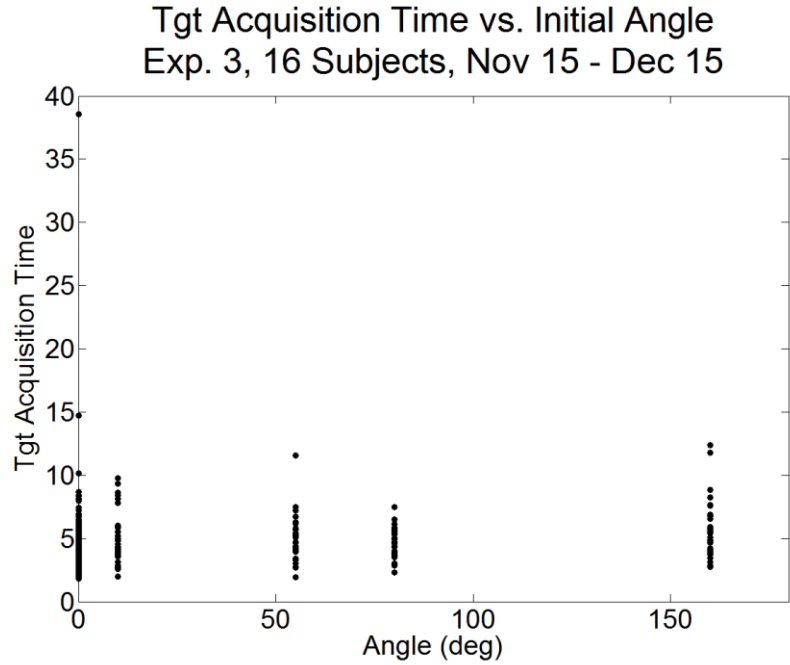


Figure 178: Individual Target Acquisition Time vs. Rotation Angle

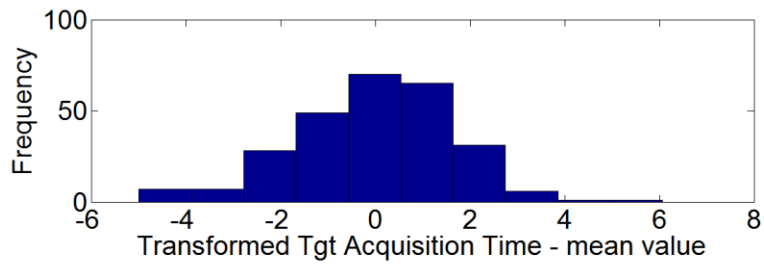
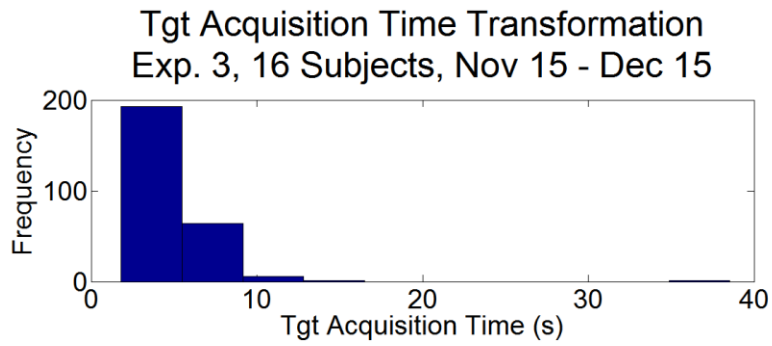


Figure 179: Target Acquisition Time Data Transformation

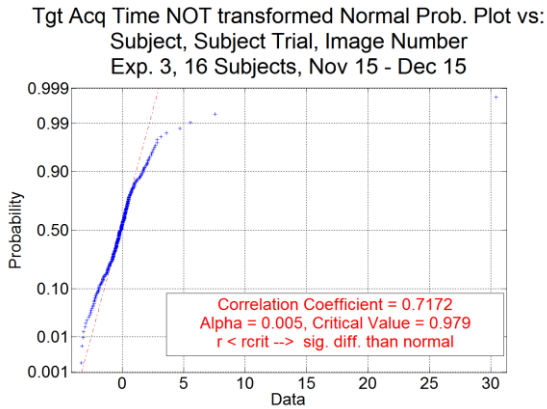


Figure 180: Target Acquisition Time Regression Residuals from Skewed Data

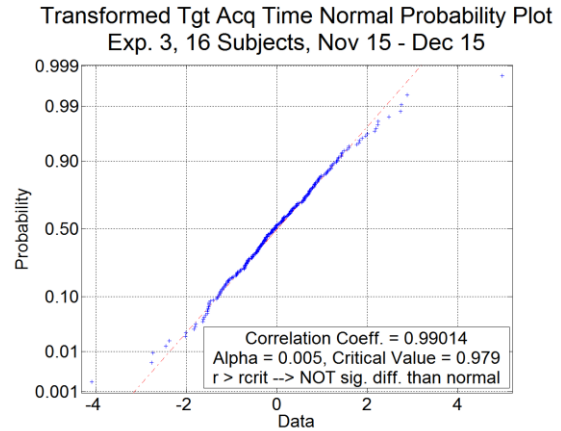


Figure 181: Target Acquisition Time Regression Residuals from Transformed Data

Tgt Acquisition Time Transformation Parameters Exp. 3, 16 Subjects, Nov 15 - Dec 15

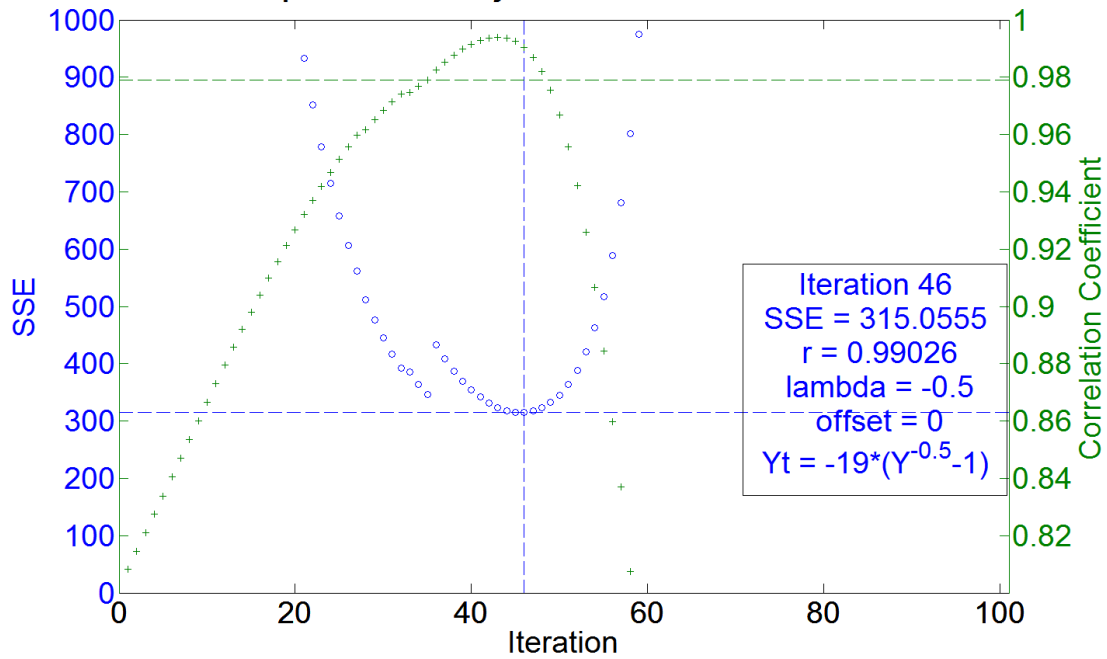


Figure 182: Target Acquisition Time Box-Cox Transformation Parameter Estimation

The blue data show how the regression Mean Squared Error was minimized with the Box-Cox Transformation. The green data show the corresponding effect on the correlation of the residuals with estimated values under normality. The notches in these distributions occur when different terms are added to the model throughout the optimization process.

Tgt Acquisition Time Residuals vs. Data Sequence
Exp. 3, 16 Subjects, Nov 15 - Dec 15

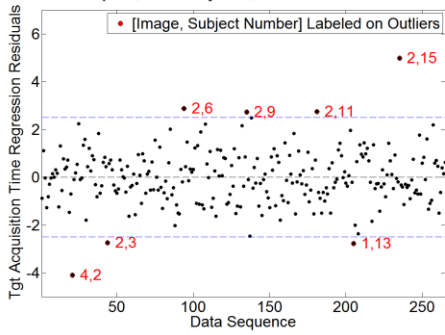


Figure 183: Test of Randomness

Tgt Acquisition Time Residuals vs. Alignment
Exp. 3, 16 Subjects, Nov 15 - Dec 15

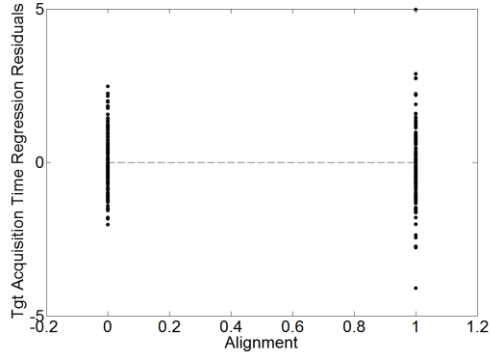


Figure 184: Residuals vs. Xalign

Tgt Acquisition Time Residuals vs. Trial Number
Exp. 3, 16 Subjects, Nov 15 - Dec 15

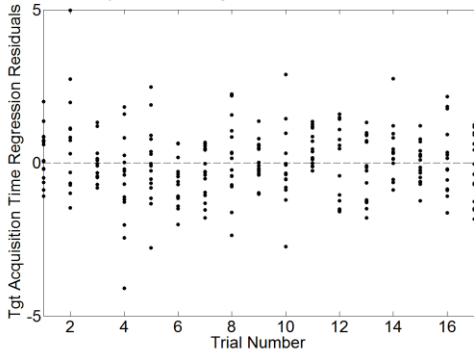


Figure 185: Residuals vs. XtrialNum

Tgt Acquisition Time Residuals vs. Image Number
Exp. 3, 16 Subjects, Nov 15 - Dec 15

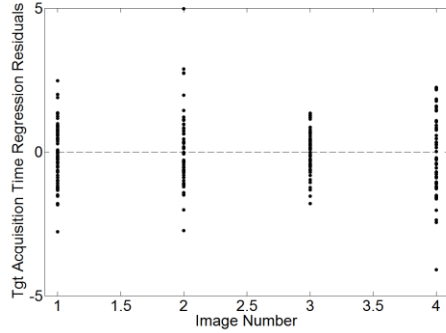


Figure 186: Residuals vs. Ximage

Tgt Acquisition Time Residuals vs. Subject Number
Exp. 3, 16 Subjects, Nov 15 - Dec 15

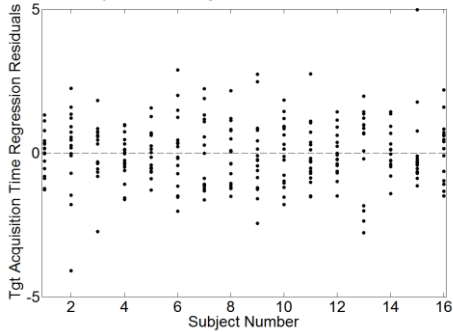


Figure 187: Residuals vs Xsubject

Tgt Acquisition Time Residuals vs. Predicted Response
Exp. 3, 16 Subjects, Nov 15 - Dec 15

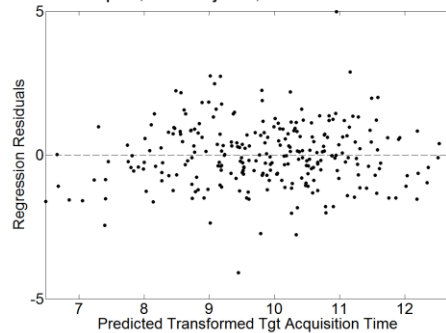


Figure 188: Residuals vs Predicted Target Acquisition Time

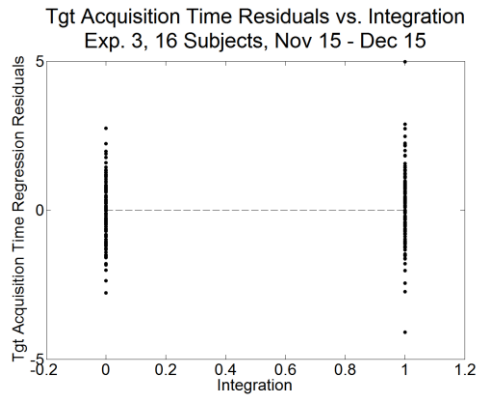


Figure 189: Residuals vs. Xdisplnt

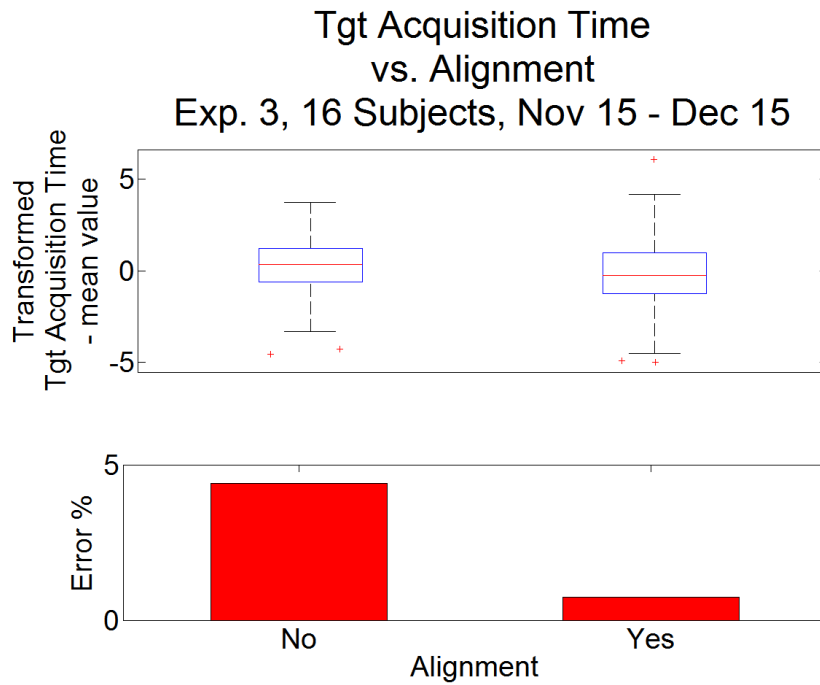


Figure 190: Target Acquisition Time vs. Alignment

Tgt Acquisition Time vs. Alignment (Observed Data) Exp. 3, 16 Subjects, Nov 15 - Dec 15

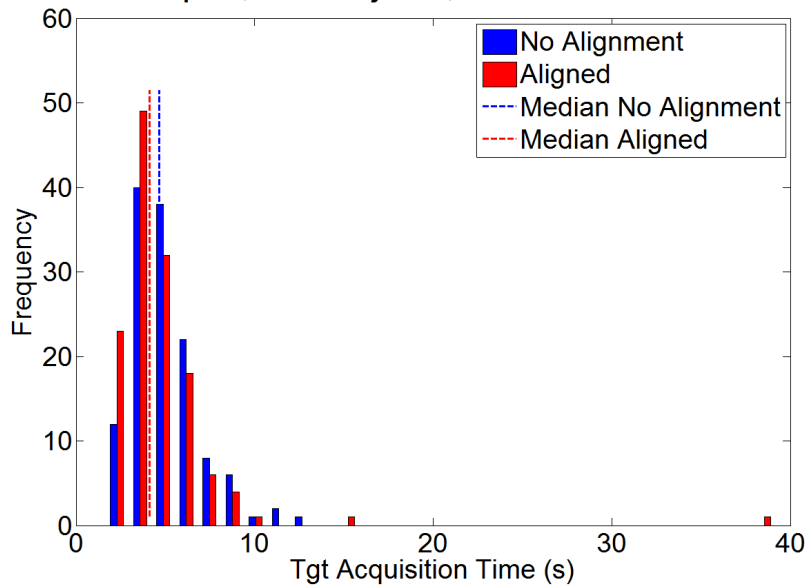


Figure 191: Experiment 3 Target Acquisition Time Alignment Effect
Blue distribution is observed data without alignment. Red distribution is observed data with alignment and includes the outlier out near 40 seconds. Despite this outlier the alignment effect is still evident with the shift in the distribution median.

Tgt Acquisition Time vs. Integration Exp. 3, 16 Subjects, Nov 15 - Dec 15

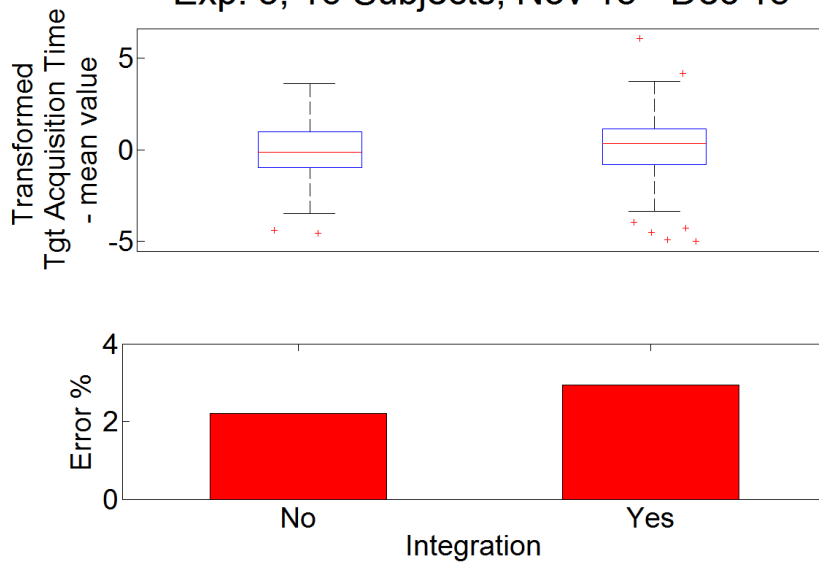


Figure 192: Target Acquisition Time vs. Display Integration

Tgt Acquisition Time vs. Integration (Observed Data)
Exp. 3, 16 Subjects, Nov 15 - Dec 15

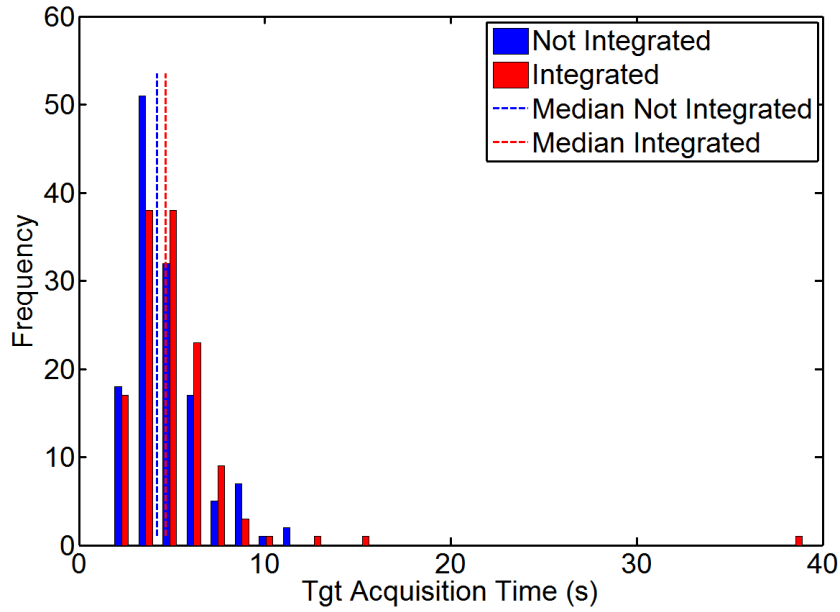


Figure 193: Experiment 3 Target Acquisition Time Integration Effect
Blue distribution is observed data without integration. Red distribution is observed data with integration.

E.4. Flight Path Error

$$FPE'_{e3} \approx \beta_0 + \beta_1 * Xmove + \beta_2 * XinitAngle$$

Equation 42: Flight Path Error Regression Estimation

Table 53: Experiment 3 Flight Path Error RMSE Predictor Variable Coefficients

Predictor Variable	Term	Transformed Regression Estimate	Lower 95% Conf. Interval	Upper 95% Conf. Interval	t-stat	p-value	Reverse Transformed Estimate (β')	units
(Intercept)	β_0	-0.04	-0.04	-0.04	-63.37	1.65E-252	-3.19	RMSE
Xmove	β_1	1.17E-05	7.73E-07	2.27E-05	2.10	3.59E-02	1.08E-05	RMSE
XinitAngle	β_2	6.21E-03	4.55E-03	7.88E-03	7.33	8.72E-13	4.57E-03	RMSE/deg

Table 54: Experiment 3 Flight Path Error Tests for Error Variance Constancy of Regression Model – Yellow indicates effects that are trending towards significance; however, these still pass the constancy test at a 0.005 level of significance.

Grouping	Bartlett F Statistic	Bartlett p-value	Levene F Statistic	Levene p-value	Brown-Forsythe F Statistic	Brown-Forsythe p-value
XdispInt	0.00	1.00	0.03	0.87	0.01	0.92
Xalign	0.00	1.00	0.03	0.87	0.01	0.92
XtrialNum	0.62	0.43	0.71	0.40	0.68	0.41
Xmove	0.00	1.00	0.03	0.87	0.01	0.92
Xmove*Xalign	4.88	0.03	7.13	0.01	6.94	0.01
Xmove*XtrialNum	0.04	0.85	0.01	0.93	0.03	0.86
Ximage	3.71	0.05	7.38	0.01	7.13	0.01
Xsubject	1.47	0.23	0.67	0.41	0.69	0.41
Predicted FPE'	4.83	0.03	7.10	0.01	7.15	0.01
Time Sequence	1.47	0.23	0.67	0.41	0.69	0.41

Flight Path Error vs. Movement (Observed Data) Exp. 3, 16 Subjects, Nov 15 - Dec 15

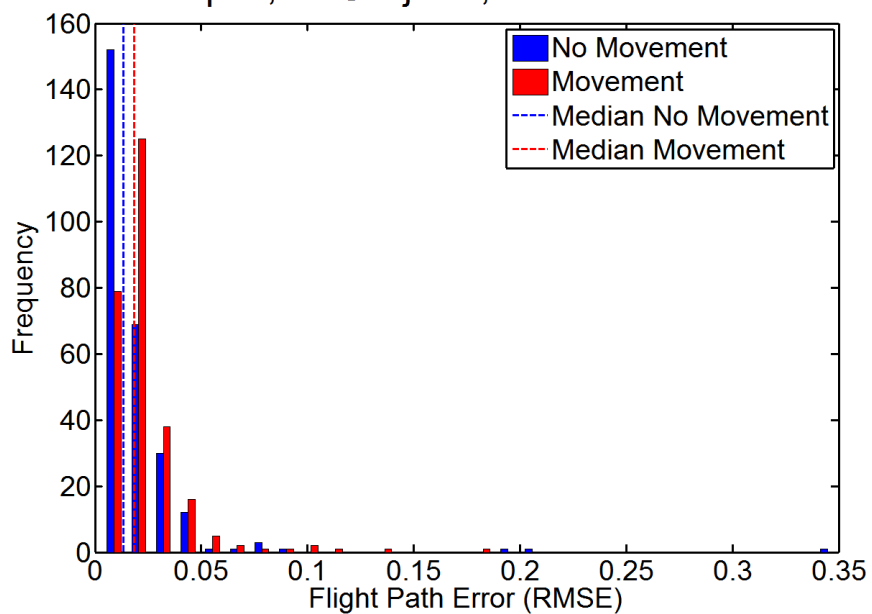


Figure 194: Experiment 3 Flight Path Error Moving Target Effect
Blue distribution is observed data with a stationary target. Red distribution is observed data with a moving target and is shifted left of the blue data.

E.5. Sensor Track Error

$$STE'_{e3} \approx \beta_0 + \beta_1 * Xmove$$

Equation 43: Sensor Track Error Regression Estimation

Table 55: Experiment 3 Sensor Track Error RMSE Predictor Variable Coefficients

Predictor Variable	Term	Transformed Regression Estimate	Lower 95% Conf. Interval	Upper 95% Conf. Interval	t-stat	p-value	Reverse Transformed Estimate (β')	units
(Intercept)	β_0	-0.03	-0.03	-0.03	-58.65	7.2E-237	0.66	RMSE
Xmove	β_1	0.01	4.32E-03	7.07E-03	8.16	2.42E-15	3.89E-03	RMSE

Table 56: Experiment 3 Sensor Track Error Tests for Error Variance Constancy of Regression Model – Yellow indicates effects that are trending towards significance; however, these still pass the constancy test at a **0.005 level of significance.**

Grouping	Bartlett F Statistic	Bartlett p-value	Levene F Statistic	Levene p-value	Brown-Forsythe F Statistic	Brown-Forsythe p-value
XdispInt	0.41	0.52	1.01	0.31	0.89	0.34
Xalign	0.41	0.52	1.01	0.31	0.89	0.34
XtrialNum	0.64	0.42	1.14	0.29	1.04	0.31
Xmove	0.41	0.52	1.01	0.31	0.89	0.34
Xmove*Xalign	0.03	0.86	0.22	0.64	0.17	0.68
Xmove*XtrialNum	7.63	0.01	6.53	0.01	5.88	0.02
Ximage	1.21	0.27	0.55	0.46	0.39	0.53
Xsubject	0.71	0.40	0.90	0.34	0.71	0.40
Predicted STE'	0.41	0.52	1.01	0.31	0.89	0.34
Time Sequence	0.71	0.40	0.90	0.34	0.71	0.40

Sensor Track Error vs. Movement (Observed Data)
Exp. 3, 16 Subjects, Nov 15 - Dec 15

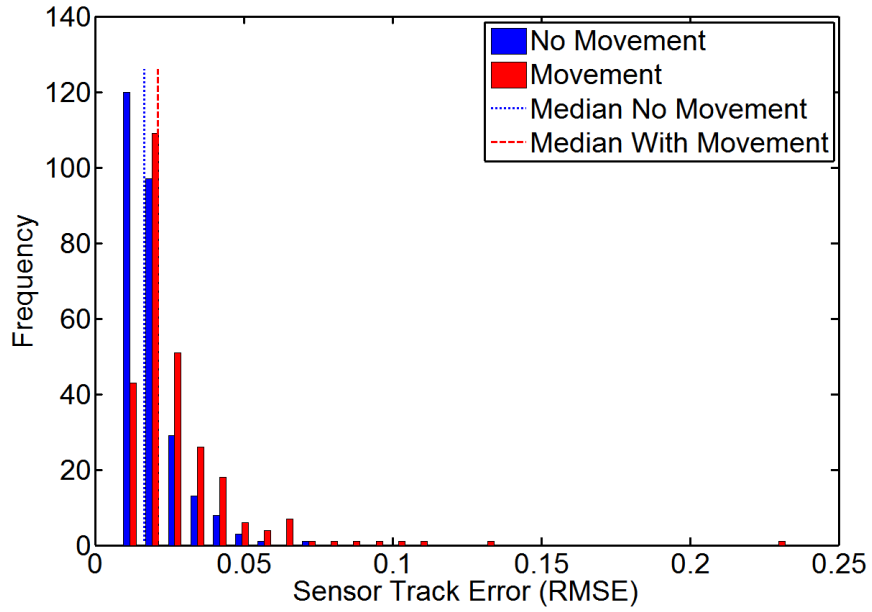


Figure 195: Experiment 3 Sensor Track Error Moving Target Effect
Blue distribution is observed data with a stationary target. Red distribution is observed data with a moving target and is shifted left of the blue data.

E.6. Orientation Time

$$OT'_{e3} \approx \beta_0 + \beta_1 * Xalign + \beta_2 * XtrialNum + \beta_3 * Xmove + \beta_{4i} * Xsubject + \beta_{5i} * Xalign * Xsubj_i$$

$$i = 1:16 \text{ subjects}$$

Equation 44: Orientation Time Regression Estimation

Table 57: Experiment 3 Orientation Time Predictor Variable Coefficients

Predictor Variable	Term	Transformed Regression Estimate	Lower 95% Conf. Interval	Upper 95% Conf. Interval	t-stat	p-value	Reverse Transformed Estimate (β')	units
(Intercept)	β_0	0.0063	-0.108	0.121	0.11	0.913756	0.006	s
Xalign	β_1	-0.2321	-0.270	-0.194	-12.10	5.26E-30	-0.274	s
XtrialNum	β_2	-0.0031	-0.006	-0.001	-2.45	0.014755	-0.003	s/#
Xmove	β_3	0.0795	0.057	0.102	6.95	1.02E-11	0.069	s

Table 58: Experiment 3 Orientation Time Tests for Error Variance Constancy of Regression Model
 – No color fill indicates that none of these results are significant, so the hypothesis holds that error variance is constant and regression analysis is suitable

Grouping	Bartlett F Statistic	Bartlett p-value	Levene F Statistic	Levene P-value	Brown-Forsythe F Statistic	Brown-Forsythe p-value
Xdisplnt	0.60	0.44	3.11	0.08	2.90	0.09
Xalign	0.60	0.44	3.11	0.08	2.90	0.09
XtrialNum	0.13	0.72	0.20	0.66	0.16	0.69
Xmove	0.60	0.44	3.11	0.08	2.90	0.09
Xmove*Xalign	0.58	0.45	0.34	0.56	0.29	0.59
Xmove*XtrialNum	0.60	0.44	3.11	0.08	2.90	0.09
Ximage	0.49	0.48	0.23	0.63	0.18	0.67
Xsubject	0.17	0.68	0.23	0.63	0.23	0.63
Predicted OT'	0.84	0.36	1.33	0.25	1.29	0.26
Time Sequence	0.00	0.98	0.00	0.97	0.00	1.00

Residuals analysis was removed from this appendix because the constancy tests did not reveal any trending towards significance.

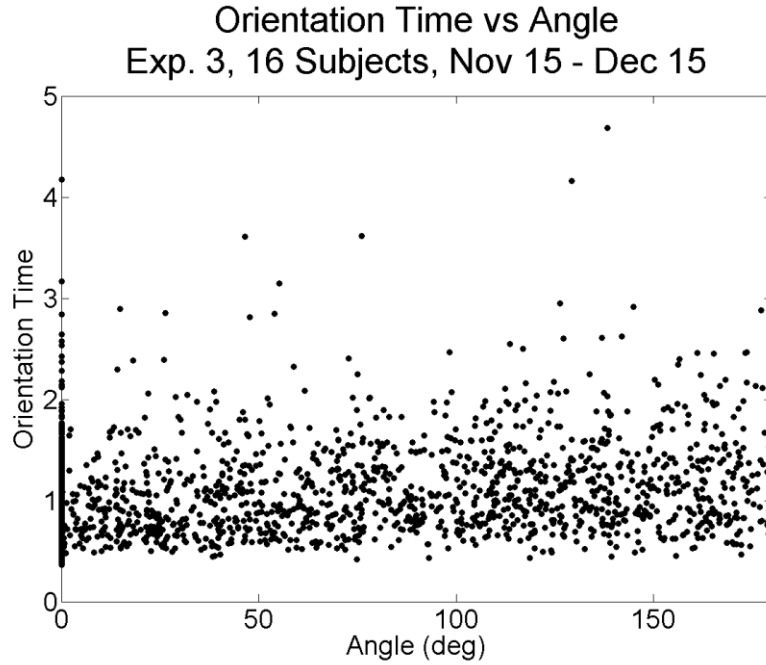


Figure 196: Individual Orientation Time vs. Rotation Angle

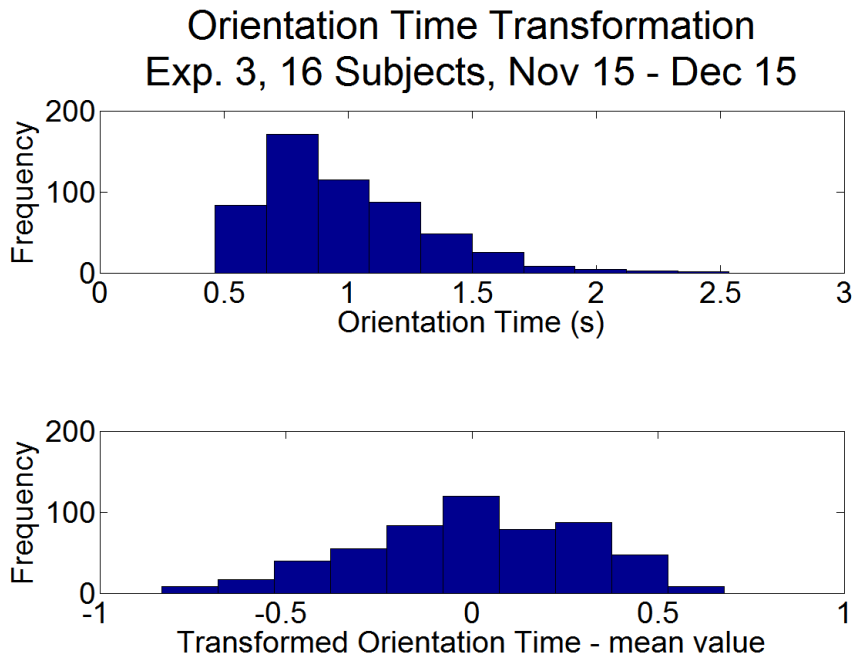


Figure 197: Orientation Time Data Transformation

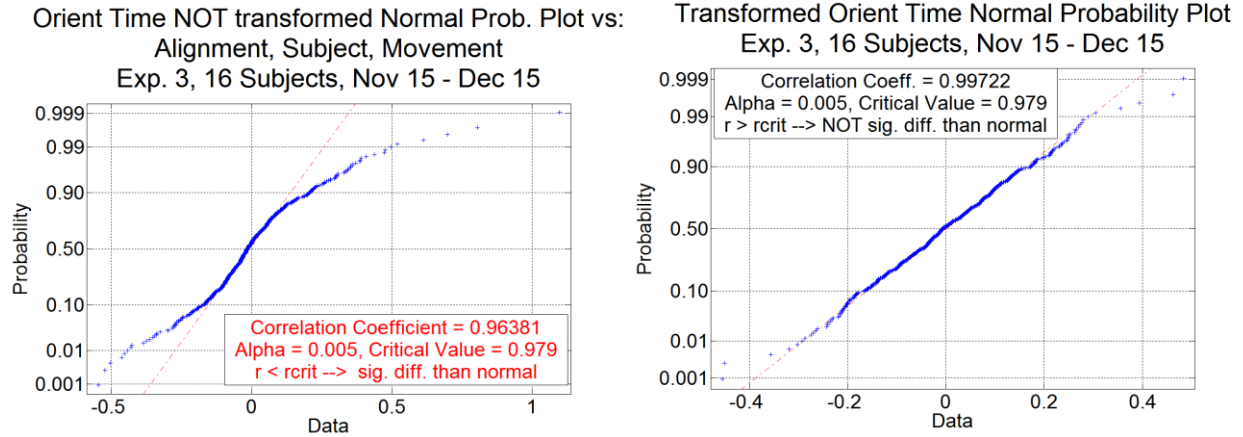


Figure 198: Orientation Time Regression Residuals from Skewed Data vs. Figure 199: Orientation Time Regression Residuals from Transformed Data

Orientation Time Transformation Parameters Exp. 3, 16 Subjects, Nov 15 - Dec 15

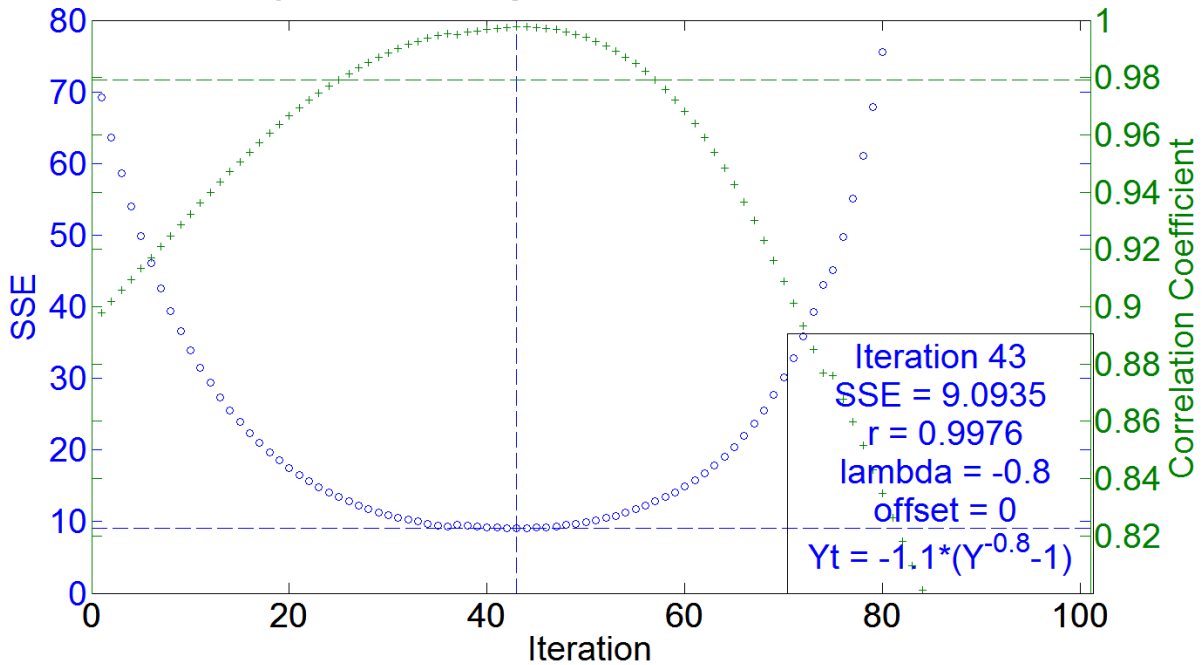


Figure 200: Example Box-Cox Transformation Parameter Estimation
The blue data show how the regression Mean Squared Error was minimized with the Box-Cox Transformation. The green data show the corresponding effect on the correlation of the residuals with estimated values under normality.

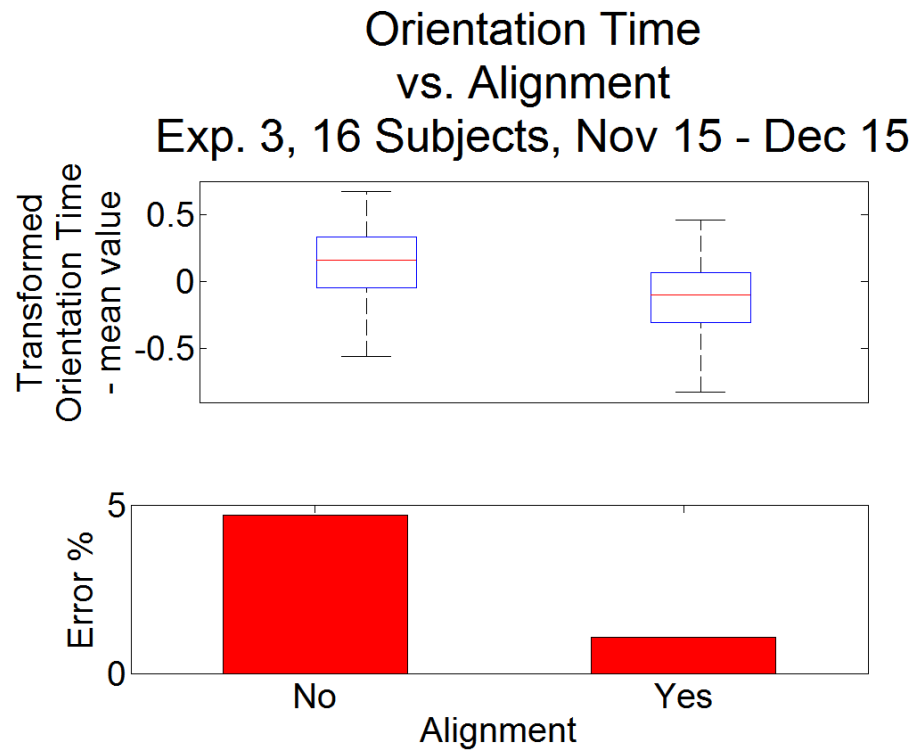


Figure 201: Orientation Time vs. Alignment

Orientation Time vs. Alignment (Observed Data) Exp. 3, 16 Subjects, Nov 15 - Dec 15

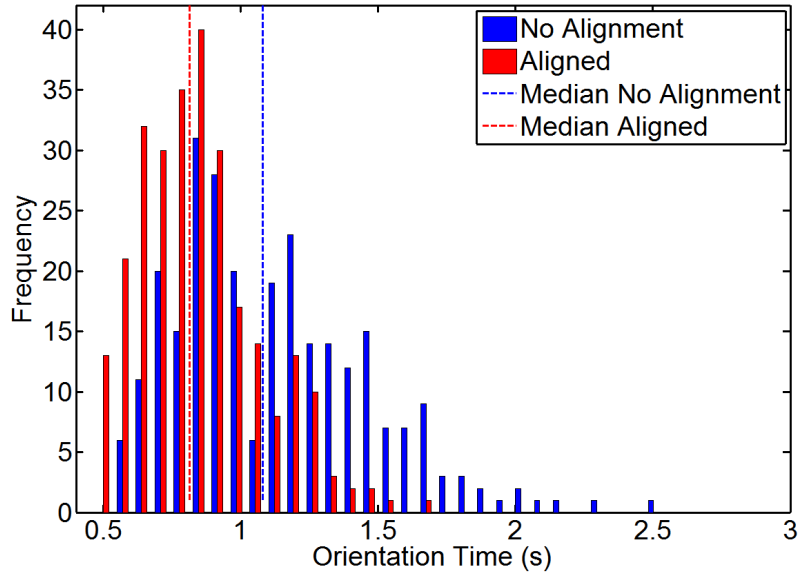


Figure 202: Experiment 3 Orientation Time Alignment Effect
Blue distribution is observed data without alignment. Red distribution has alignment of both the sensor and aircraft displays and is shifted left of the blue data.

Orientation Time vs. Integration

Exp. 3, 16 Subjects, Nov 15 - Dec 15

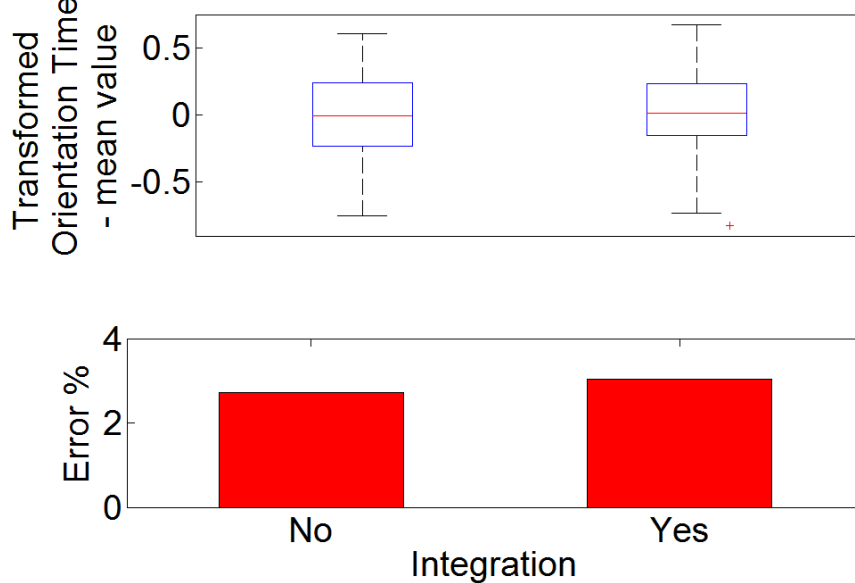


Figure 203: Orientation Time vs. Display Integration

Orientation Time vs. Integration (Observed Data)
Exp. 3, 16 Subjects, Nov 15 - Dec 15

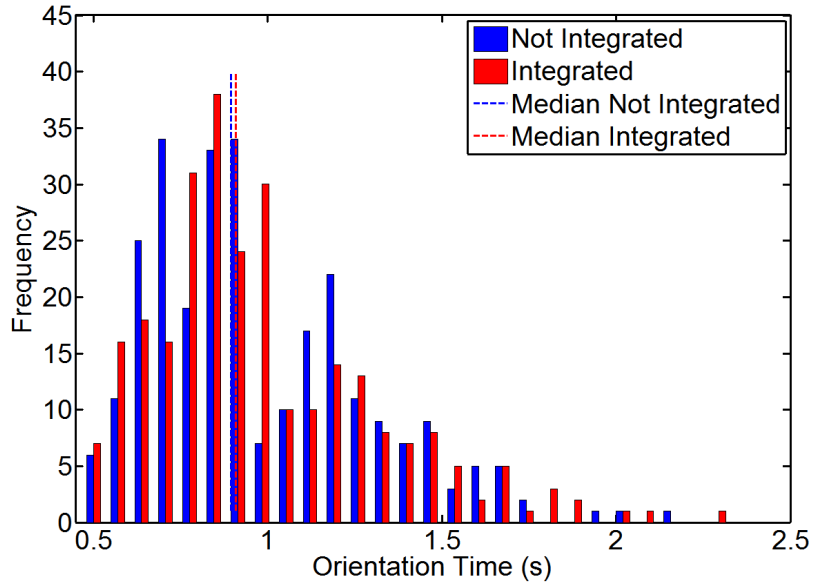


Figure 204: Experiment 3 Orientation Time Integration Effect
Blue distribution is observed data with separate displays. Red distribution has a single integrated display. These distributions did not reveal a statistical difference.

Orientation Time
vs. Target Movement
Exp. 3, 16 Subjects, Nov 15 - Dec 15

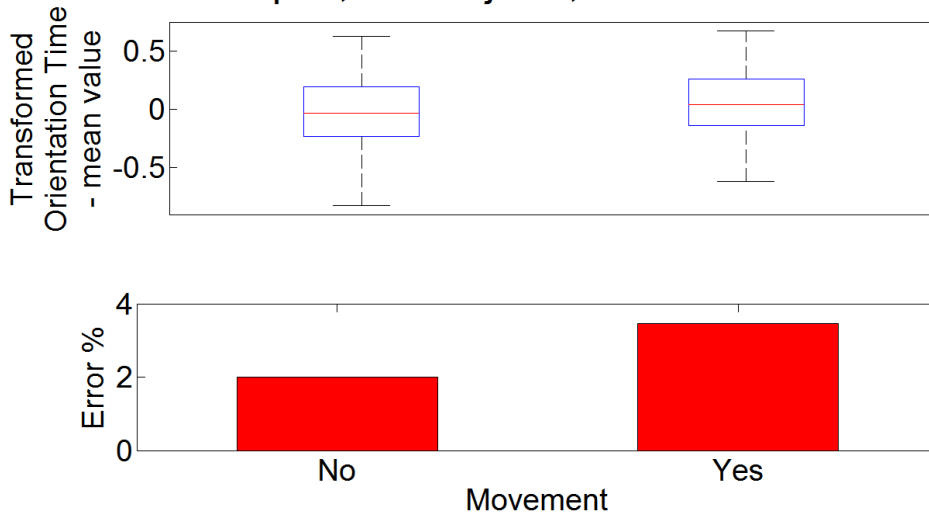


Figure 205: Orientation Time vs. Target Movement

Orientation Time vs. Movement (Observed Data)
Exp. 3, 16 Subjects, Nov 15 - Dec 15

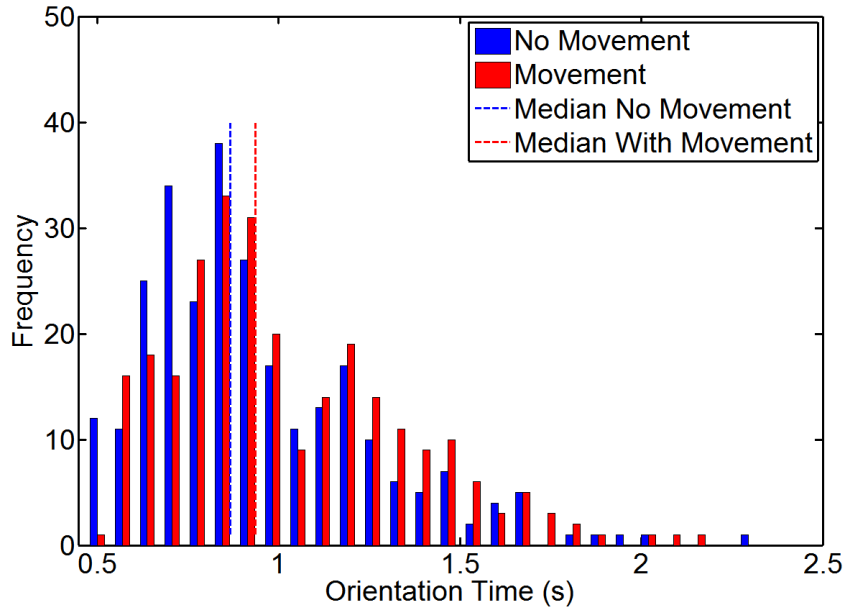


Figure 206: Experiment 3 Orientation Time Moving Target Effect
Blue distribution is observed data with a stationary target. Red distribution is observed data with a moving target and is shifted left of the blue data.

E.7. Bedford Workload Rating

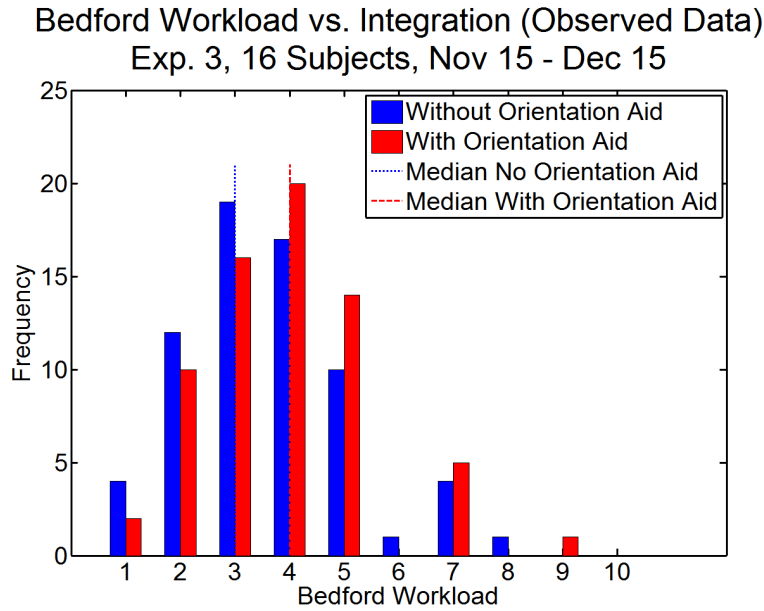


Figure 207: Experiment 3 Bedford Workload Rating Display Integration Effect
Blue distribution is observed data with separate displays. Red distribution has a single integrated display.

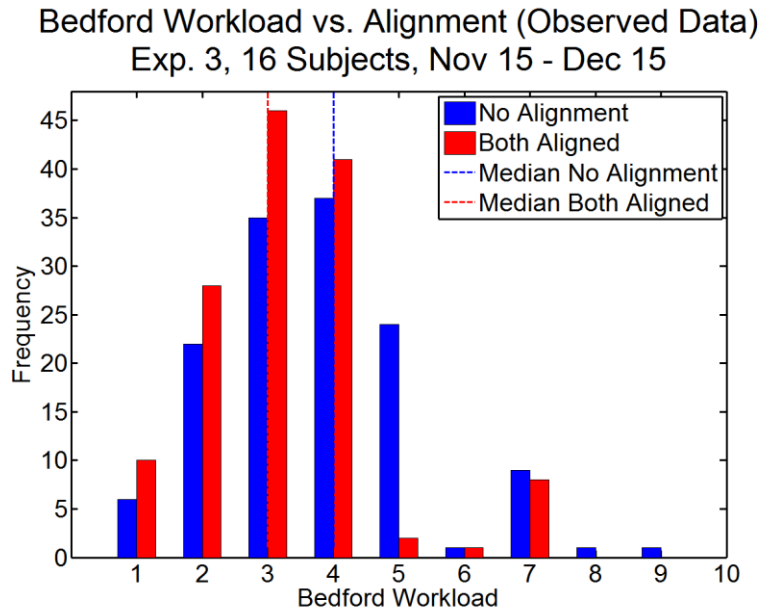


Figure 208: Experiment 3 Bedford Workload Rating Alignment Effect
Blue distribution is observed data without alignment. Red distribution has alignment of both the sensor and aircraft displays and is shifted left of the blue data.

E.8. Reaction Time

$$RT'_{e3} \approx \beta_0 + \beta_1 * XdispInt + \beta_2 * Xalign + \beta_3 * XtrialNum + \beta_4 * Xmove + \beta_5 * XtrialNum * Xmove + \beta_{6i} * Xsubject + \beta_{7i} * XtrialNum * Xsubject_i + \beta_{8i} * Xmove * Xsubject_i$$

$$i = 1:16 \text{ subjects}$$

Equation 45: Reaction Time Regression Estimation

Table 59: Experiment 3 Reaction Time Predictor Variable Coefficients – Yellow indicates that this coefficient was not significant and was only included in the model because a reaction term with this variable was significant.

Predictor Variable	Term	Transformed Regression Estimate	Lower 95% Conf. Interval	Upper 95% Conf. Interval	t-stat	p-value	Reverse Transformed Estimate (β')	units
(Intercept)	β_0	-0.21	-0.28	-0.15	-6.82	2.45E-11	-0.30923	s
XdispInt	β_1	4.19E-02	2.86E-02	5.53E-02	6.18	1.27E-09	3.79E-02	s
Xalign	β_2	-2.37E-02	-3.70E-02	-1.04E-02	-3.49	5.19E-04	-2.37E-02	s/#
XtrialNum	β_3	-3.88E-03	-7.01E-03	-7.57E-04	-2.44	1.50E-02	-3.76E-03	s
Xmove	β_4	1.23E-02	-1.47E-02	3.94E-02	0.89	0.37	1.16E-02	s
XtrialNum*Xmove	β_5	2.57E-03	1.63E-04	4.98E-03	2.10	3.64E-02	2.46E-03	s/#

Table 60: Experiment 3 Reaction Time Tests for Error Variance Constancy of Regression Model – No color fill indicates that none of these results are significant, so the hypothesis holds that error variance is constant and regression analysis is suitable

Grouping	Bartlett F Statistic	Bartlett p-value	Levene F Statistic	Levene P-value	Brown-Forsythe F Statistic	Brown-Forsythe p-value
XdispInt	0.48	0.49	0.12	0.73	0.21	0.65
Xalign	0.48	0.49	0.12	0.73	0.21	0.65
XtrialNum	0.12	0.73	0.00	0.95	0.03	0.85
Xmove	0.48	0.49	0.12	0.73	0.21	0.65
Xmove*Xalign	0.01	0.94	0.16	0.69	0.15	0.70
Xmove*XtrialNum	0.48	0.49	0.12	0.73	0.21	0.65
Ximage	0.75	0.39	0.87	0.35	0.77	0.38
Xsubject	0.63	0.43	0.28	0.60	0.24	0.63
Predicted RT'	0.29	0.59	0.28	0.60	0.30	0.58
Time Sequence	0.49	0.49	0.06	0.81	0.14	0.71

Residuals analysis was removed from this appendix since no constancy trends were noted.

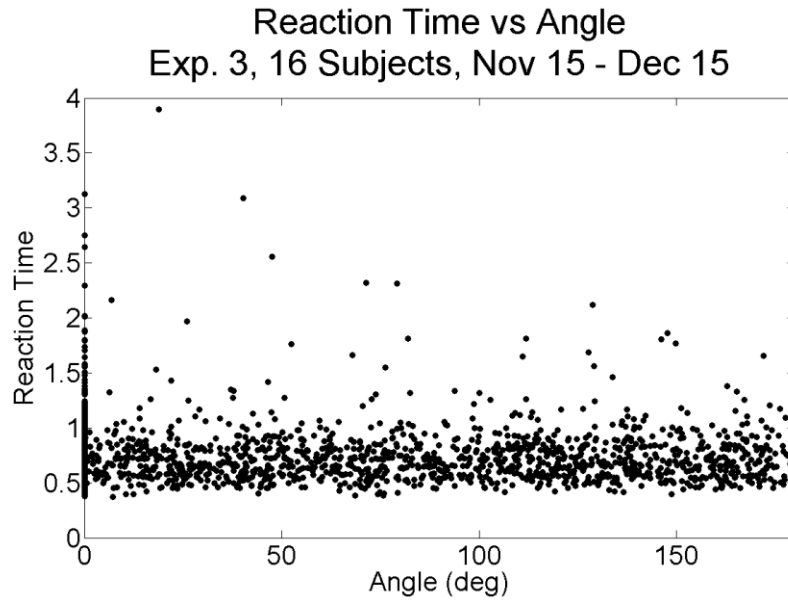


Figure 209: Individual Reaction Time vs. Rotation Angle

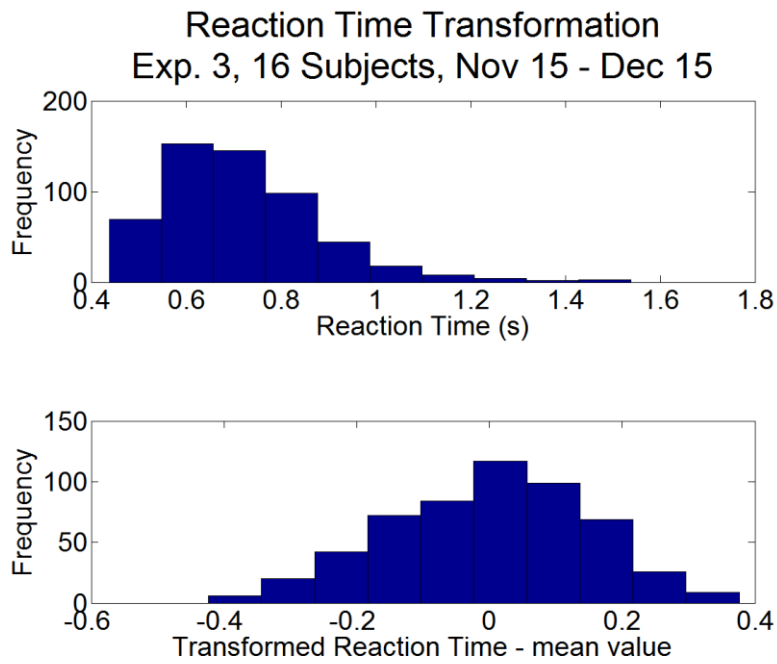


Figure 210: Reaction Time Data Transformation

React Time NOT Transformed Normal Prob. Plot vs:
Integration, Alignment, Subject, Subject Trial, Movemer
Exp. 3, 16 Subjects, Nov 15 - Dec 15

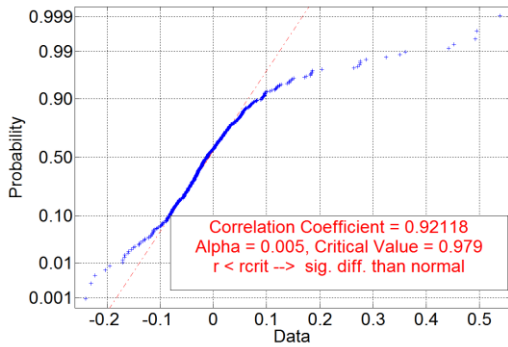


Figure 211: Reaction Time Regression Residuals from Skewed Data

Transformed React Time Normal Probability Plot
Exp. 3, 16 Subjects, Nov 15 - Dec 15

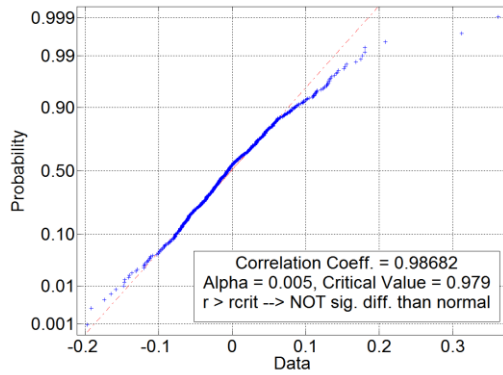


Figure 212: Reaction Time Regression Residuals from Transformed Data

Reaction Time Transformation Parameters
Exp. 4, 16 Subjects, Dec 15 - Jan 16

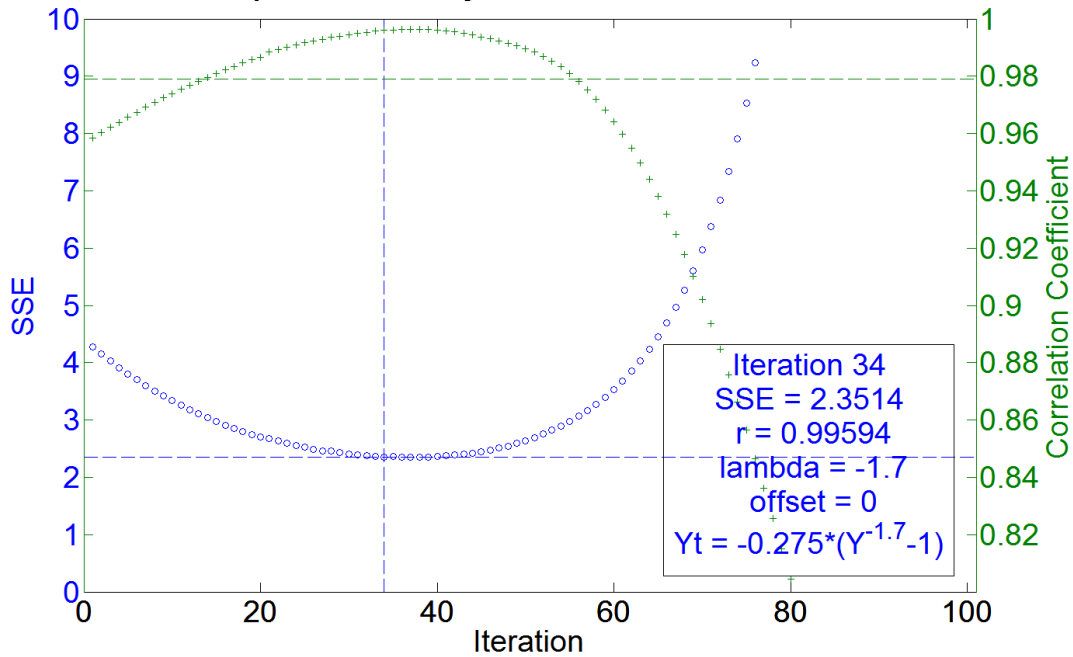


Figure 213: Reaction Time Box-Cox Transformation Parameter Estimation
The blue data show how the regression Mean Squared Error was minimized with the Box-Cox Transformation. The green data show the corresponding effect on the correlation of the residuals with estimated values under normality.

Reaction Time vs. Alignment Exp. 3, 16 Subjects, Nov 15 - Dec 15

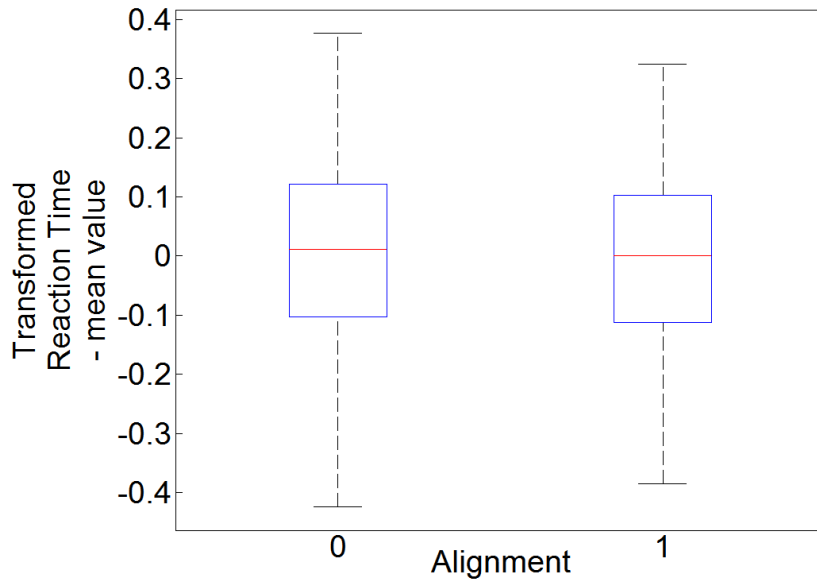


Figure 214: Reaction Time vs. Alignment

Reaction Time vs. Alignment (Observed Data) Exp. 3, 16 Subjects, Nov 15 - Dec 15

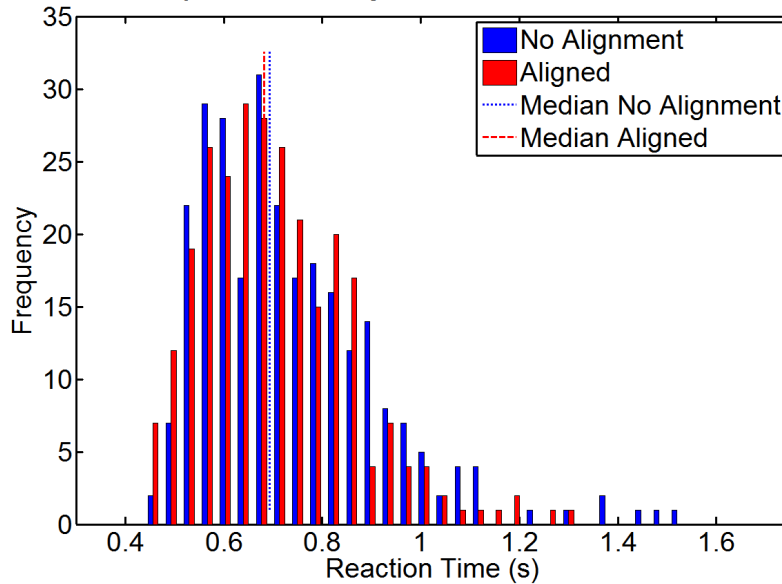


Figure 215: Experiment 3 Reaction Time Alignment Effect
Blue distribution is observed data without alignment. Red distribution has alignment of both the sensor and aircraft displays and is shifted left of the blue data.

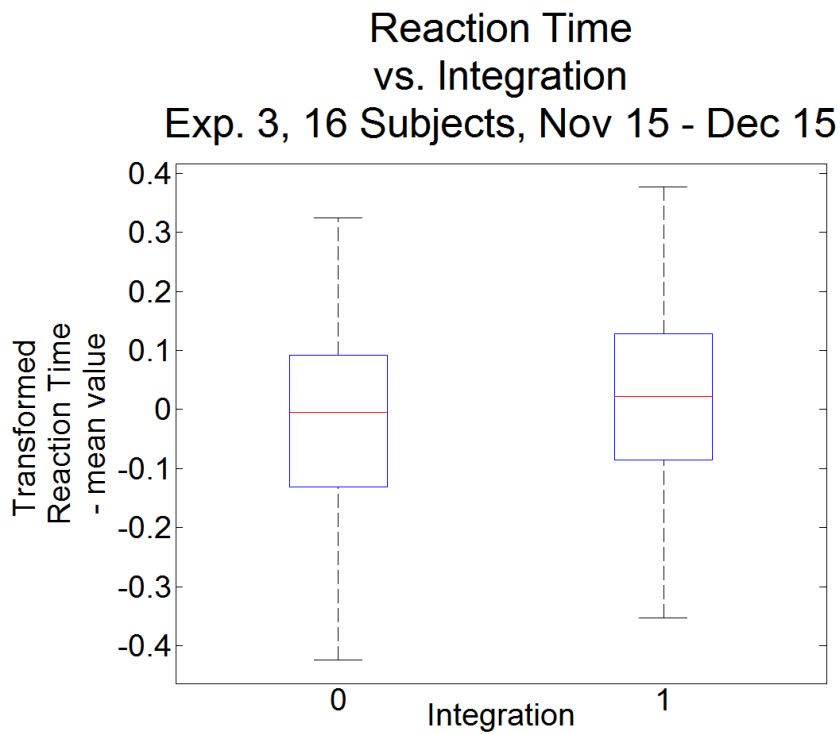


Figure 216: Reaction Time vs. Display Integration

Reaction Time vs. Integration (Observed Data)

Exp. 3, 16 Subjects, Nov 15 - Dec 15

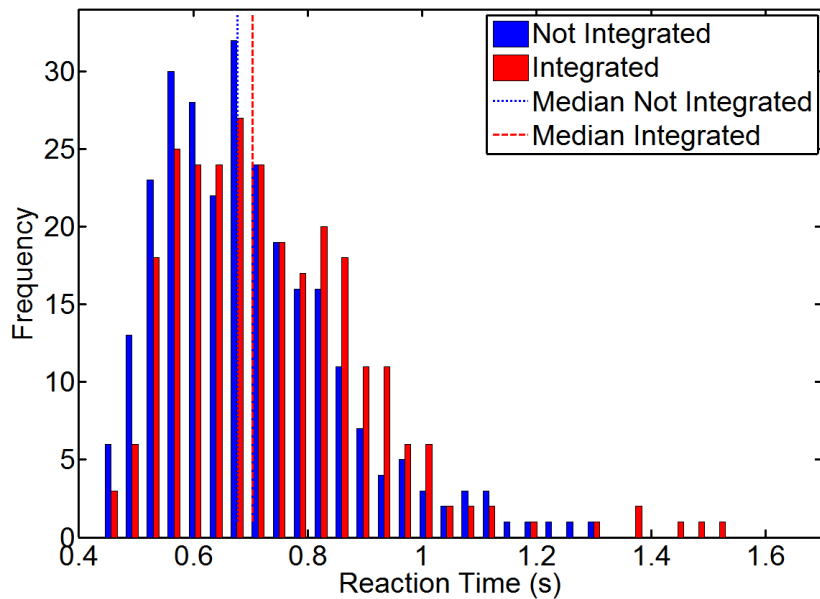


Figure 217: Experiment 3 Reaction Time Integration Effect
 Blue distribution is observed data with separate displays. Red distribution has a single integrated display.

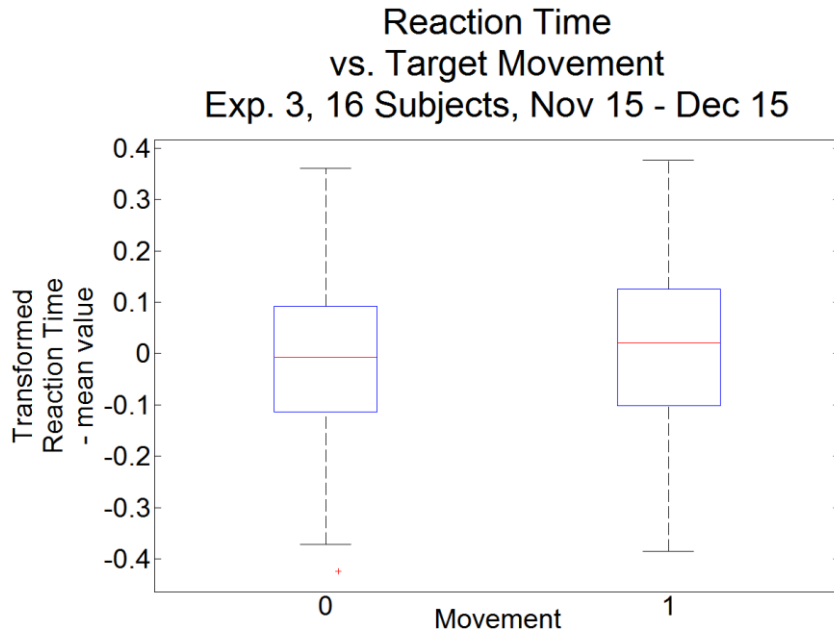


Figure 218: Reaction Time vs. Target Movement

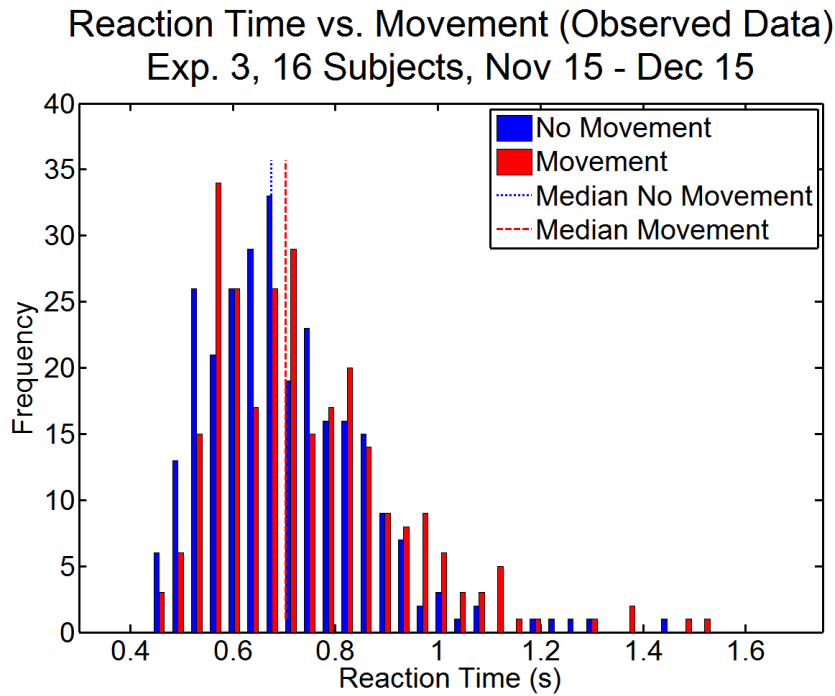


Figure 219: Experiment 3 Reaction Time Moving Target Effect
Blue distribution is observed data with a stationary target. Red distribution is observed data with a moving target and is shifted right of the blue data.

Appendix F: Experiment 4 Data Analysis

F.1. Data Transformations

This research utilized the Box-Cox transformation to normalize data for parametric analysis [133]. This process analyzes both log transformation and a range of power functions. For example, Figure 221 shows the effect of the Box-Cox transformation on the Target Acquisition Time data.

$$W_i = \begin{cases} K_1 \left((Y + \lambda_2)_i^{\lambda_1} - 1 \right) & \lambda_1 \neq 0 \\ K_2 (\log_e Y_i) & \lambda_1 = 0 \end{cases}$$

Equation 46: Box-Cox Transformation

$$K_2 = \left(\prod_{i=1}^n (Y + \lambda_2)_i \right)^{1/n}$$

Equation 47: Box-Cox Standardization Coefficient 1

$$K_1 = \frac{1}{\lambda_1 K_2^{(\lambda_1-1)}}$$

Equation 48: Box-Cox Standardization Coefficient 2

The Box-Cox transformation is shown in Equation 18 through Equation 20. This shows the two parameter estimation procedure, where both λ_1 and λ_2 are estimated. None of these transformations required an estimate of λ_2 , but each measure required an estimation of λ_1 to allow for parametric analysis. Since the transformations are analyzed based on the Sum of Squared Error (SSE) of the resulting regression, the standardization parameters in Equation 19 and Equation 20 are used to prevent SSE fluctuations as a function of λ_1 . An example estimation of the λ_1 parameter is shown in Figure 224. The left vertical axis represents value of SSE which is minimized using this transformation. The right vertical axis represents the correlation coefficient between the residuals and their expected value under normality [134]. The horizontal green dashed line shows the correlation coefficient associated with an $\alpha = 0.005$ significance. Here in the Box-Cox transformation selects $\lambda_1 = -0.4$ to minimize SSE, and this also generates an acceptable correlation coefficient as shown by the green data in Figure 224. A similar process was used for every transformation and each figure is available throughout this appendix. The transformation equations are shown in the applicable figures and listed here:

$$TAT'_{e4} = -18.7 * (TAT^{-0.4} - 1)$$

Equation 49: Experiment 4 Transformed Target Acquisition Time

$$FPE'_{e4} = -0.153 * (FPE^{-0.1} - 1)$$

Equation 50: Experiment 4 Transformed Flight Path Error

$$STE'_{e4} = -0.00135 * (STE^{-0.8} - 1)$$

Equation 51: Experiment 4 Transformed Sensor Track Error

$$OT'_{e4} = -2.36 * (OT^{-0.5} - 1)$$

Equation 52: Experiment 4 Transformed Orientation Time

$$RT'_{e4} = -0.275 * (RT^{-1.7} - 1)$$

Equation 53: Experiment 4 Transformed Reaction Time

F.2. Pairwise Display Comparisons

Table 61: Experiment 4 Pairwise Comparisons – These are the results of within-subjects 2-sided pairwise t-tests to the family significance of 0.05 (Bonferroni corrected to ~0.008 2-sided or ~0.004 1-sided). Green indicates a significant effect which improved performance, red indicates a significant effect which degraded performance.

P-values are indicative of the single tail probability, which would be less than 0.004 for significance. Other pairwise test results are available in Appendices E-H.

		Reference Frame Alignment		Display Redundancy Reduction		Interaction Effects			
		Display	Display	Display	Display	Display	Display		
		A ≠ B	G ≠ H	A ≠ G	B ≠ H	G ≠ B	A ≠ H		
PARAMETRIC ANALYSIS	Orientation Time ¹	t*	7.43	9.62	1.97	2.53	7.07	8.70	
		p-value	1.05E-06	4.13E-08	0.03	0.01	1.92E-06	1.52E-07	
	Target Acquisition Time ¹	t*	3.99	3.63	1.98	2.04	1.91	5.26	
		p-value	5.88E-04	1.24E-03	0.03	0.03	0.04	4.78E-05	
	Sensor Track Error ¹	t*	-0.90	0.47	-1.07	0.25	0.20	-1.12	
		p-value	0.81	0.32	0.85	0.40	0.42	0.86	
	Flight Path Error ¹	t*	1.86	2.37	-0.42	0.73	1.66	1.93	
		p-value	0.04	0.02	0.66	0.24	0.06	0.04	
	Reaction Time ¹	t*	5.31	3.04	7.45	6.84	-4.27	9.04	
		p-value	4.35E-05	4.12E-03	1.02E-06	2.78E-06	1.00	9.26E-08	
	NON-PARAMETRIC ANALYSIS	Bedford Workload Static Target	Chi-sqr	6.37	3.38	1.75	0.26	1.52	10.10
			p-value	0.01	0.07	0.19	0.61	0.22	1.48E-03
Bedford Workload Dynamic Target		Chi-sqr	9.22	6.62	0.87	0.39	4.02	13.18	
		p-value	2.40E-03	0.01	0.35	0.53	0.04	2.83E-04	
Rankings (1-4) Kruskal-Wallis		Chi-sqr	19.54	19.54	2.58	2.58	15.95	22.81	
		p-value	9.87E-06	9.87E-06	0.11	0.11	6.51E-05	1.78E-06	
Ratings (1-10) Kruskal-Wallis		Chi-sqr	21.27	21.06	2.99	3.79	15.50	25.22	
		p-value	3.99E-06	4.46E-06	8.35E-02	5.15E-02	8.26E-05	5.12E-07	

F.3. Target Acquisition Time

$$TAT'_{e4} \approx \beta_0 + \beta_1 * XdispRedun + \beta_2 * Xalign + \beta_3 * XtrialNum + \beta_{4i} * Xsubject_i + \beta_{5i} * XtrialNum * Xsubject_i + \beta_{6m} * Ximage_m + \beta_{7m} * Xalign * Ximage_m$$

$i = 1: 16$ subjects, $m = 1:4$ images

Equation 54: Target Acquisition Time Regression Estimation – Yellow highlights terms of interest, which were discussed in the body of the document.

Table 62: Experiment 4 Target Acquisition Time Predictor Variable Coefficients

Predictor Variable	Term	Transformed Regression Estimate	Lower 95% Conf. Interval	Upper 95% Conf. Interval	t-stat	p-value	Reverse Transformed Estimate (β')	units
(Intercept)	β_0	8.80E+00	8.11	9.50	24.96	2.60E-71	3.21	s
XdispRedun	β_1	3.80E-01	0.14	0.62	3.07	2.38E-03	0.35	s
Xalign	β_2	-7.41E-01	-1.17	-0.32	-3.44	6.87E-04	-0.82	s
XtrialNum	β_3	-5.82E-02	-8.44E-02	-3.20E-02	-4.37	1.76E-05	-5.72E-02	s/#

Table 63: Experiment 4 Target Acquisition Time Tests for Error Variance Constancy of Regression Model – No colors indicate that the hypothesis holds that error variance is constant and regression analysis is suitable.

Grouping	Bartlett F Statistic	Bartlett p-value	Levene F Statistic	Levene P-value	Brown-Forsythe F Statistic	Brown-Forsythe p-value
XdispRedun	2.60	0.11	0.26	0.61	0.26	0.61
Xalign	3.55	0.06	0.67	0.41	0.67	0.41
XtrialNum	0.02	0.89	0.00	1.00	0.00	1.00
Ximage	1.31	0.25	1.38	0.24	1.39	0.24
Xsubject	0.18	0.67	0.01	0.92	0.01	0.91
Predicted TAT'	0.53	0.47	0.01	0.93	0.00	0.96
Time Sequence	0.21	0.64	0.01	0.92	0.01	0.91

Residuals analysis was removed from this appendix since no constancy trends were noted.

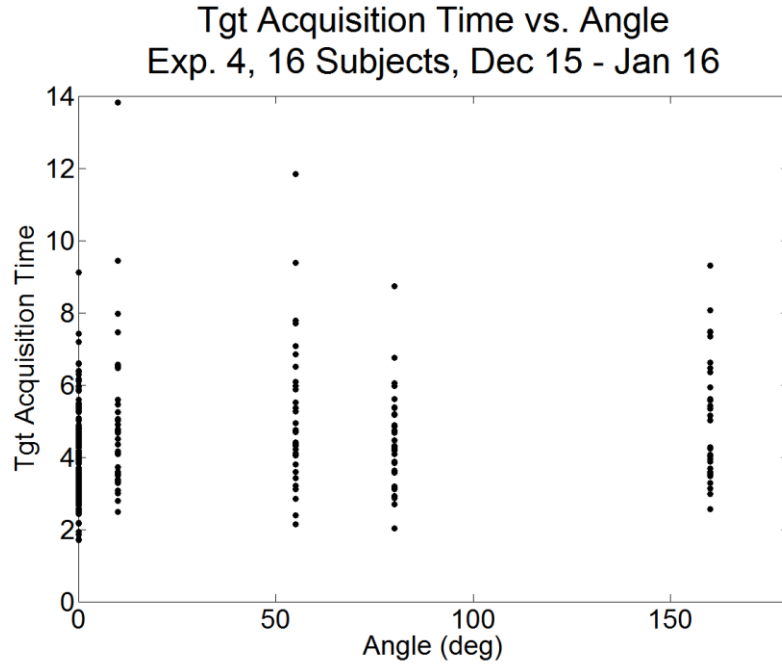


Figure 220: Individual Target Acquisition Time vs. Rotation Angle

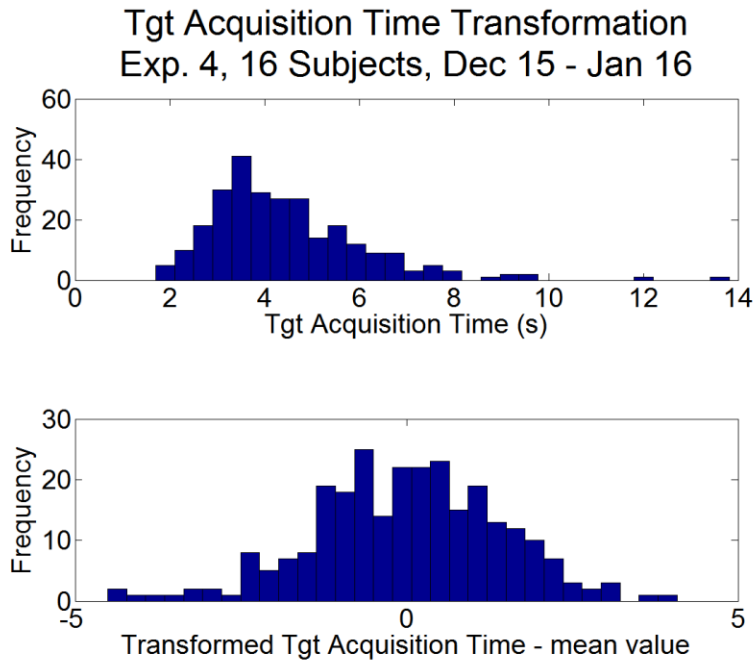


Figure 221: Target Acquisition Time Data Transformation

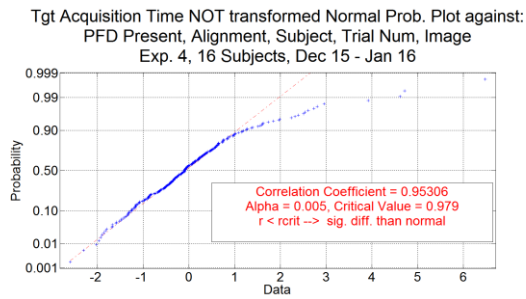


Figure 222: Target Acquisition Time Regression Residuals from Skewed Data

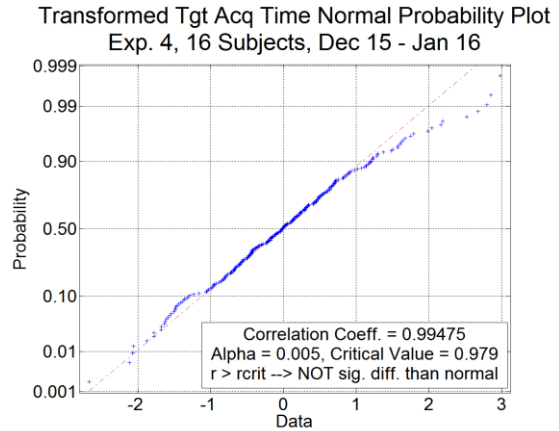


Figure 223: Target Acquisition Time Regression Residuals from Transformed Data

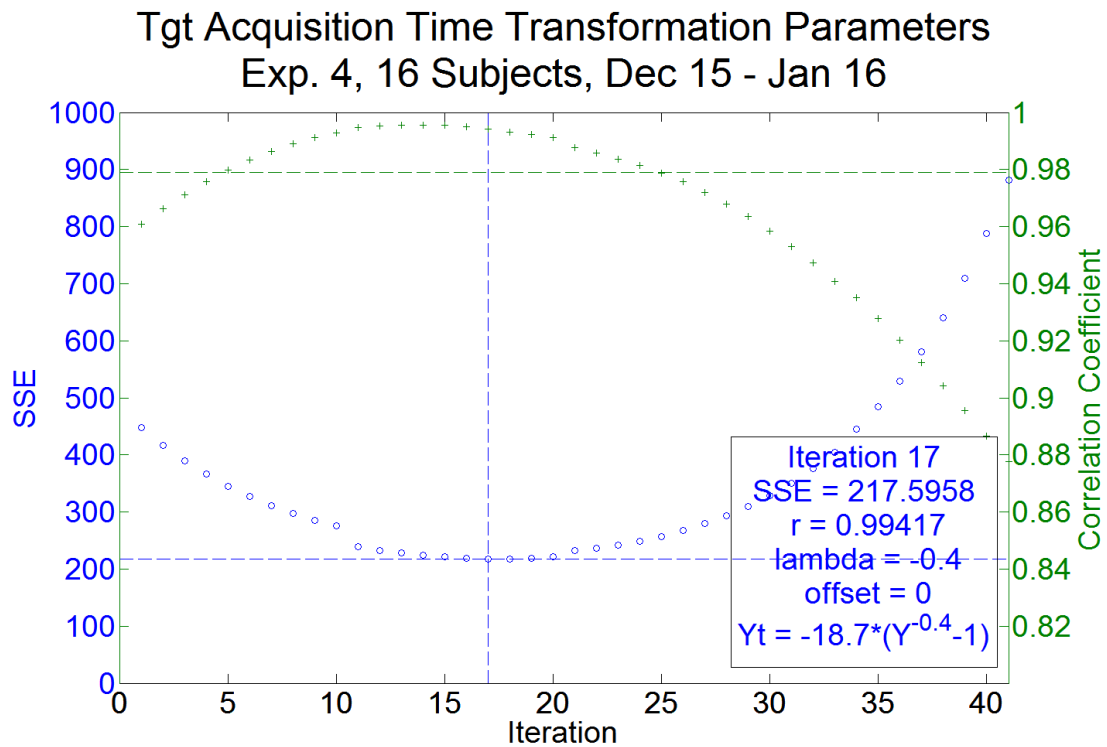


Figure 224: Experiment 4 Tgt Acq Time Box-Cox Transformation Parameter Estimation
The blue data show how the regression Mean Squared Error was minimized with the Box-Cox Transformation. The green data show the corresponding effect on the correlation of the residuals with estimated values under normality. The notch in these distributions occurs when different terms are added to the model throughout the optimization process.

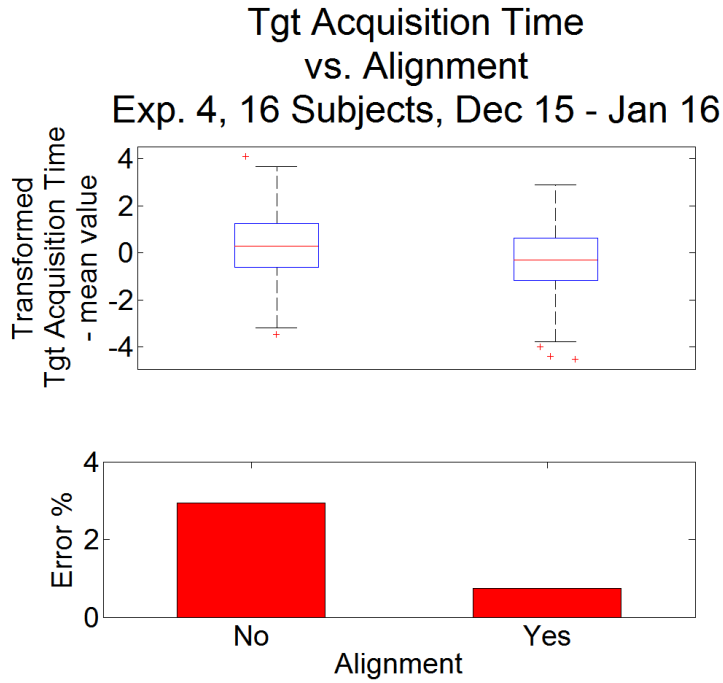


Figure 225: Target Acquisition Time vs. Alignment

Tgt Acquisition Time vs. Alignment (Observed Data)

Exp. 4, 16 Subjects, Dec 15 - Jan 16

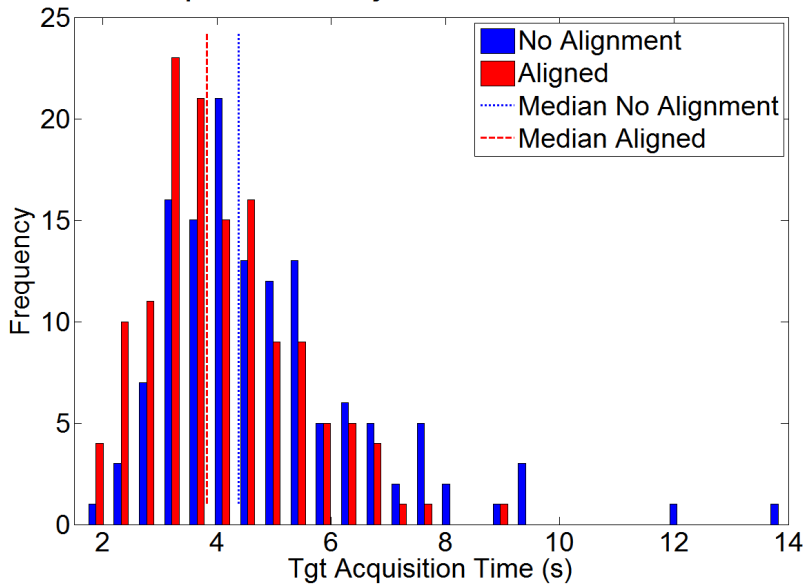


Figure 226: Experiment 4 Target Acquisition Time Alignment Effect
 Blue distribution is observed data without alignment. Red distribution has alignment of the sensor display and is shifted left of the blue data.

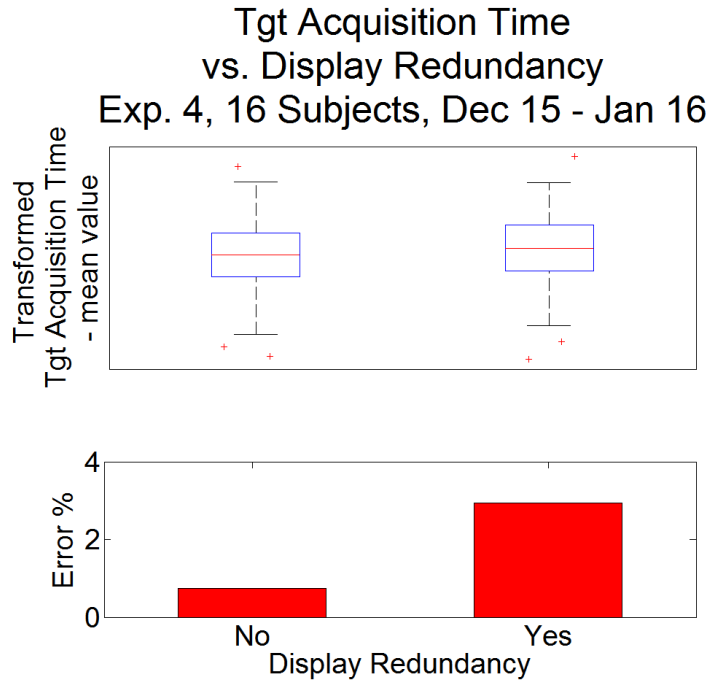


Figure 227: Target Acquisition Time vs. Display Redundancy

Print Figure
Tgt Acquisition Time vs. Display Redundancy (Observed)
Exp. 4, 16 Subjects, Dec 15 - Jan 16

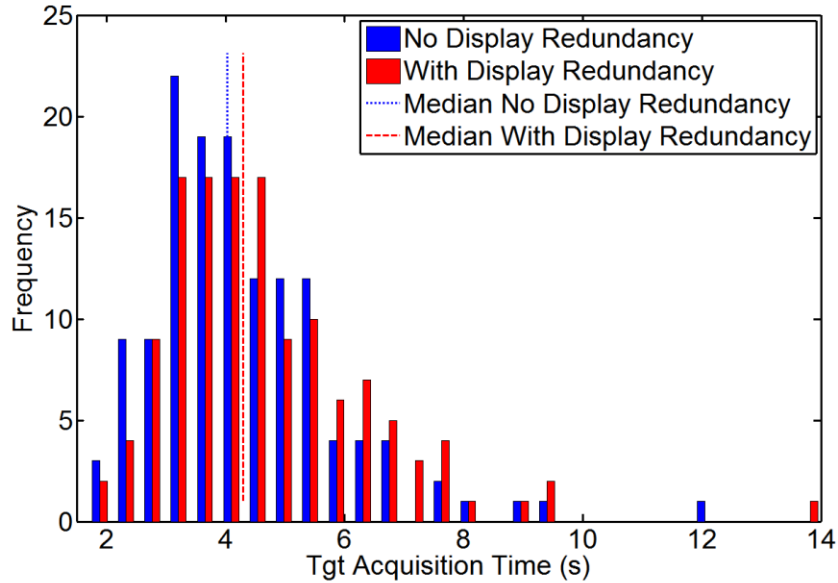


Figure 228: Experiment 4 Target Acquisition Time Display Redundancy Effect
Blue distribution is observed data with without the aircraft display. Red distribution includes the aircraft display.

F.4. Flight Path Error

$$FPE'_{e4} \approx \beta_0 + \beta_1 * Xalign + \beta_2 * Xmove$$

Equation 55: Flight Path Error Regression Estimation

Table 64: Experiment 4 Flight Path Error RMSE Predictor Variable Coefficients

Predictor Variable	Term	Transformed Regression Estimate	Lower 95% Conf. Interval	Upper 95% Conf. Interval	t-stat	p-value	Reverse Transformed Estimate (β')	units
(Intercept)	β_0	-0.08	-0.08	-0.07	-104.4	0	1.34	RMSE
Xalign	β_1	-2.44E-03	-4.07E-03	-7.99E-04	-2.92	3.62E-03	-2.6E-03	RMSE
Xmove	β_2	0.011	9.32E-03	0.013	13.15	1.86E-34	8.54E-03	RMSE

Table 65: Experiment 4 Flight Path Error Tests for Error Variance Constancy of Regression Model
 – Yellow indicates effects that are trending towards significance; however, these still pass the constancy test at a **0.005 level of significance.**

Grouping	Bartlett F Statistic	Bartlett p-value	Levene F Statistic	Levene p-value	Brown-Forsythe F Statistic	Brown-Forsythe p-value
XdispRedun	2.72	0.10	3.31	0.07	2.69	0.10
Xalign	2.72	0.10	3.31	0.07	2.69	0.10
XtrialNum	1.69	0.19	0.60	0.44	0.38	0.54
Xmove	2.72	0.10	3.31	0.07	2.69	0.10
Xmove*Xalign	6.41	0.01	5.33	0.02	5.21	0.02
Xmove*XtrialNum	0.36	0.55	0.54	0.46	0.34	0.56
Ximage	8.29	0.00	5.33	0.02	5.17	0.02
Xsubject	7.03	0.01	5.39	0.02	5.62	0.02
Predicted FPE'	5.87	0.02	3.84	0.05	3.67	0.06
Time Sequence	7.03	0.01	5.39	0.02	5.62	0.02

Flight Path Error
vs. Target Movement
Exp. 4, 16 Subjects, Dec 15 - Jan 16

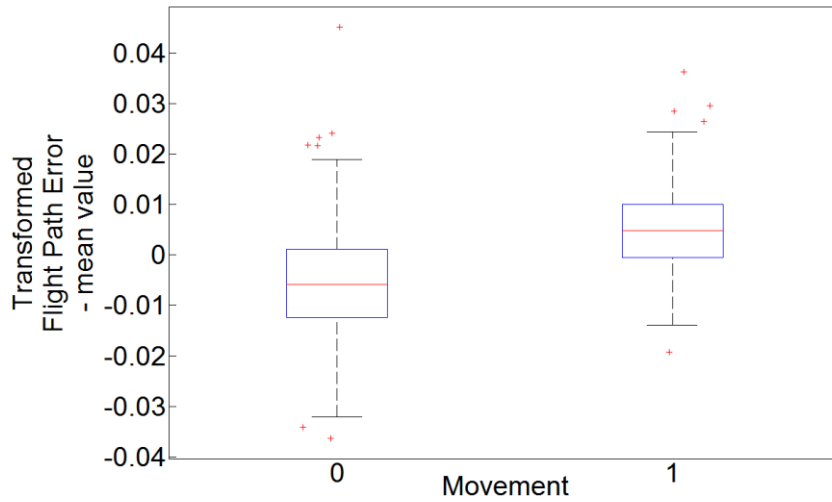


Figure 229: Flight Path Error vs. Target Movement

Flight Path Error vs. Movement (Observed Data)
Exp. 4, 16 Subjects, Dec 15 - Jan 16

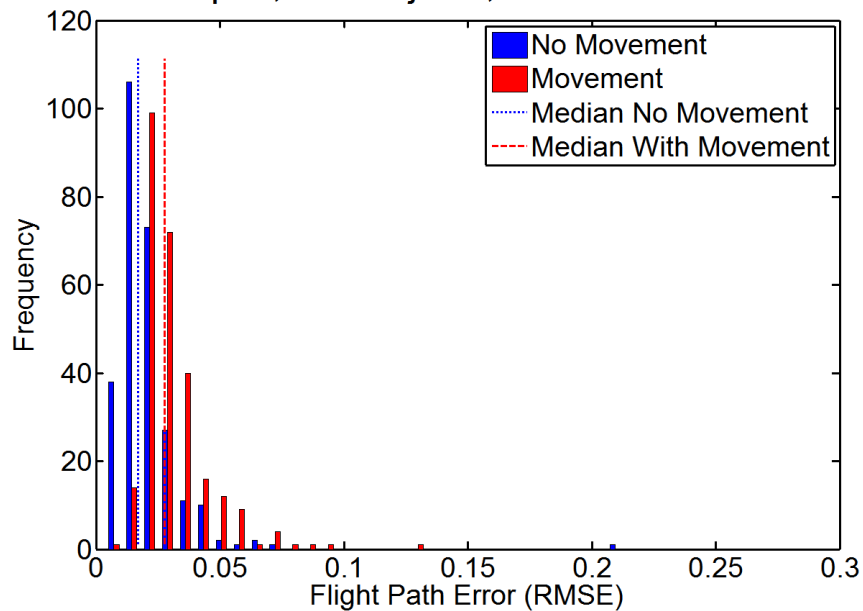


Figure 230: Experiment 4 Flight Path Error Moving Target Effect
Blue distribution is observed data with a stationary target. Red distribution is observed data with a moving target and is shifted right of the blue data.

Flight Path Error vs. Alignment Exp. 4, 16 Subjects, Dec 15 - Jan 16

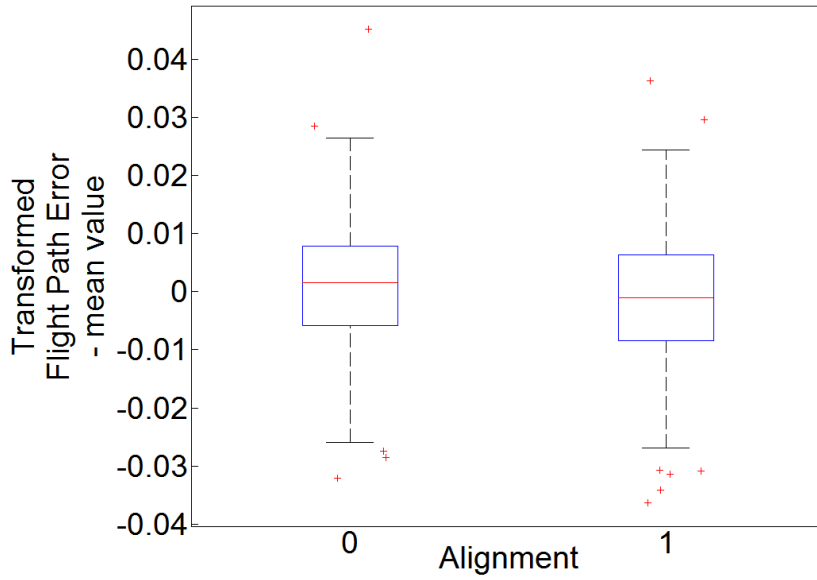


Figure 231: Flight Path Error vs. Alignment

Flight Path Error vs. Alignment (Observed Data) Exp. 4, 16 Subjects, Dec 15 - Jan 16

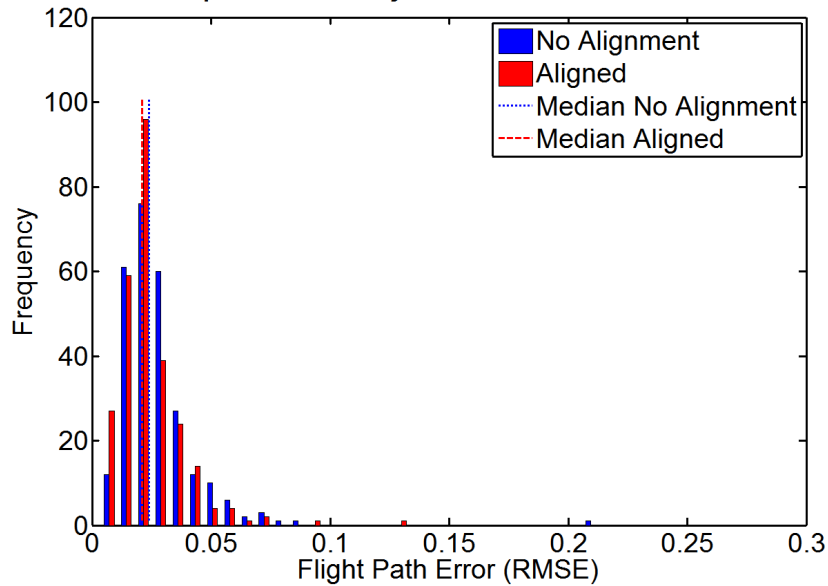


Figure 232: Experiment 4 Flight Path Error Alignment Effect
Blue distribution is observed data without alignment. Red distribution has alignment of the sensor display and is shifted left of the blue data.

Flight Path Error vs. Display Redundancy (Observed)
Exp. 4, 16 Subjects, Dec 15 - Jan 16

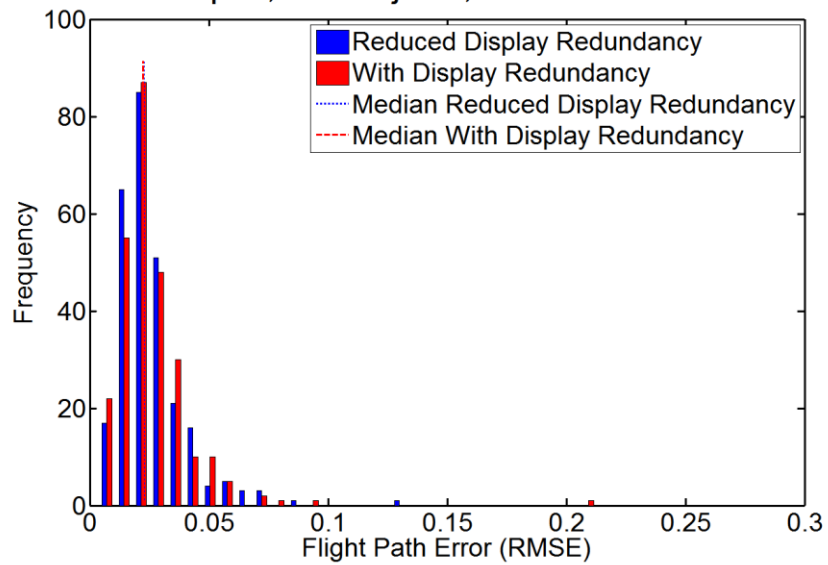


Figure 233: Experiment 4 Flight Path Error Display Redundancy Effect
Blue distribution is observed data with without the aircraft display. Red distribution includes the aircraft display. Note that this does not represent a significant difference.

F.5. Sensor Track Error

$$STE'_{e4} \approx \beta_0 + \beta_1 * Xmove$$

Equation 56: Sensor Track Error Regression Estimation

Table 66: Experiment 4 Sensor Track Error RMSE Predictor Variable Coefficients

Predictor Variable	Term	Transformed Regression Estimate	Lower 95% Conf. Interval	Upper 95% Conf. Interval	t-stat	p-value	Reverse Transformed Estimate (β')	units
(Intercept)	β_0	-3.41E-02	-3.50E-02	-3.31E-02	-69.26	2.22E-271	0.17	RMSE
Xalign	β_1	1.09E-02	9.50E-03	1.22E-02	15.63	9.95E-46	6.98E-03	RMSE

Table 67: Experiment 4 Sensor Track Error Tests for Error Variance Constancy of Regression Model
 – No color indicates that all pass the constancy test at a 0.005 level of significance.

Grouping	Bartlett F Statistic	Bartlett p-value	Levene F Statistic	Levene p-value	Brown-Forsythe F Statistic	Brown-Forsythe p-value
Grouping	0.00	0.95	0.01	0.93	0.00	0.95
XdispRedun	0.00	0.95	0.01	0.93	0.00	0.95
Xalign	0.80	0.37	0.42	0.52	0.49	0.48
XtrialNum	0.00	0.95	0.01	0.93	0.00	0.95
Xmove	0.06	0.81	0.01	0.92	0.00	0.98
Xmove*Xalign	1.11	0.29	0.92	0.34	0.79	0.37
Xmove*XtrialNum	0.21	0.65	0.00	0.95	0.01	0.90
Ximage	0.25	0.62	0.10	0.76	0.13	0.72
Xsubject	0.00	0.95	0.01	0.93	0.00	0.95
Predicted STE'	0.25	0.62	0.10	0.76	0.13	0.72

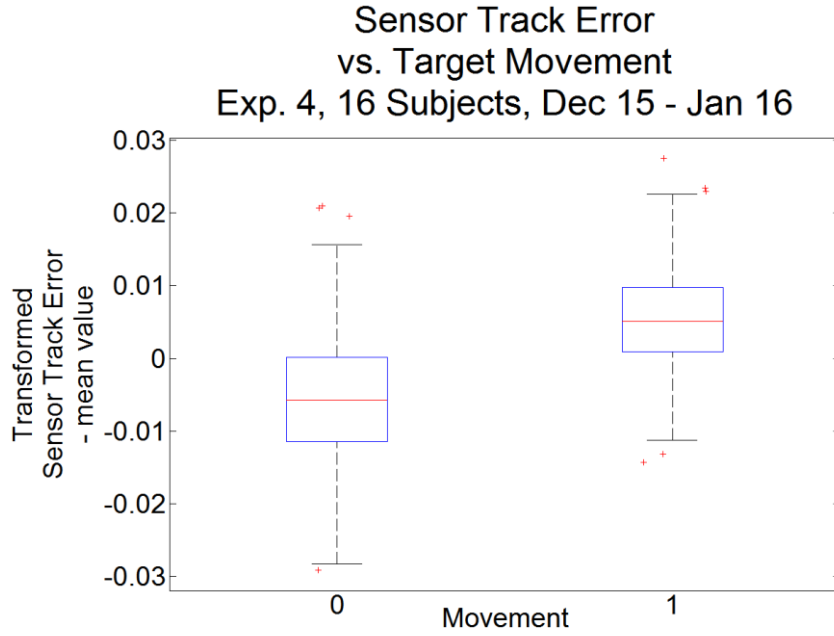


Figure 234: Sensor Track Error vs. Target Movement

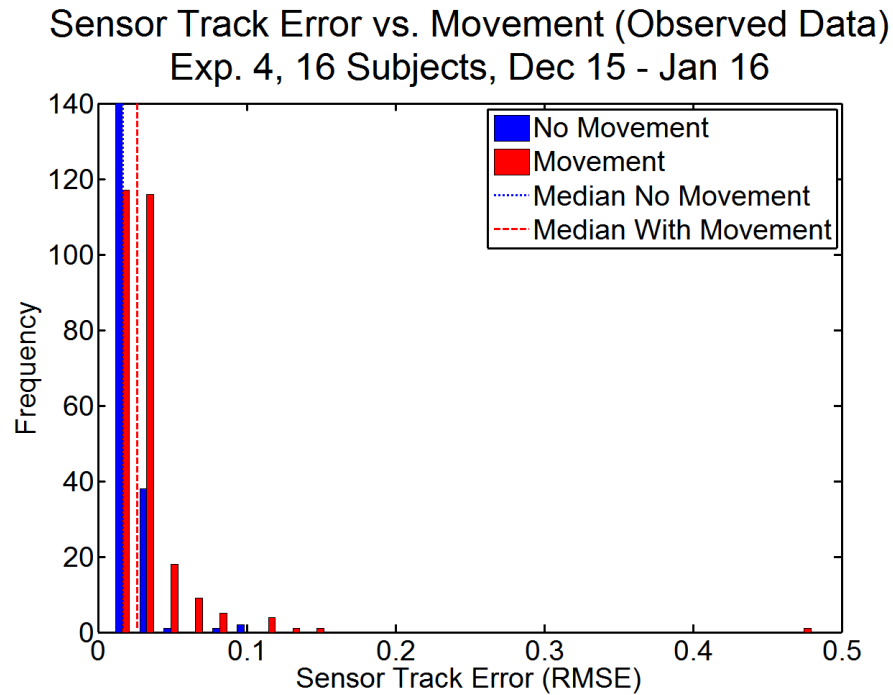


Figure 235: Experiment 4 Sensor Track Error Moving Target Effect
 Blue distribution is observed data with a stationary target. Red distribution is observed data with a moving target and is shifted right of the blue data.

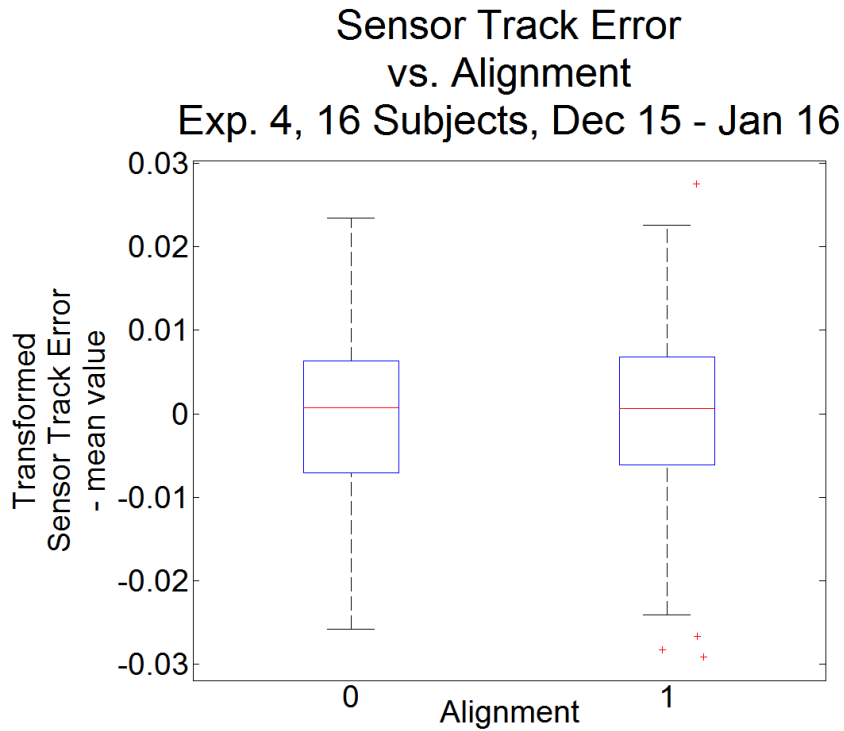


Figure 236: Sensor Track Error vs. Alignment

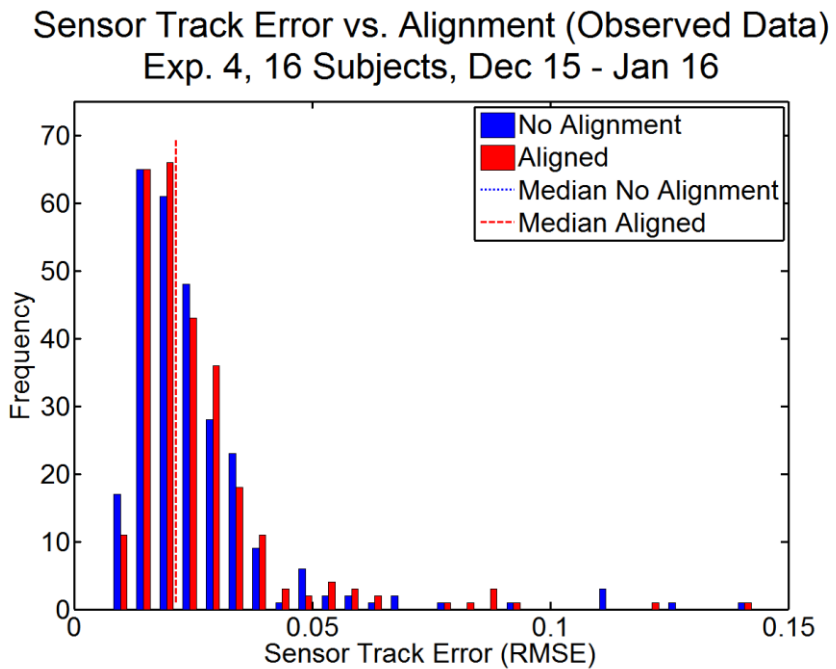


Figure 237: Experiment 4 Sensor Track Error Alignment Effect
Blue distribution is observed data without alignment. Red distribution has alignment of the sensor display. Note that this does not represent a significant difference.

Sensor Track Error vs. Display Redundancy (Observed)
Exp. 4, 16 Subjects, Dec 15 - Jan 16

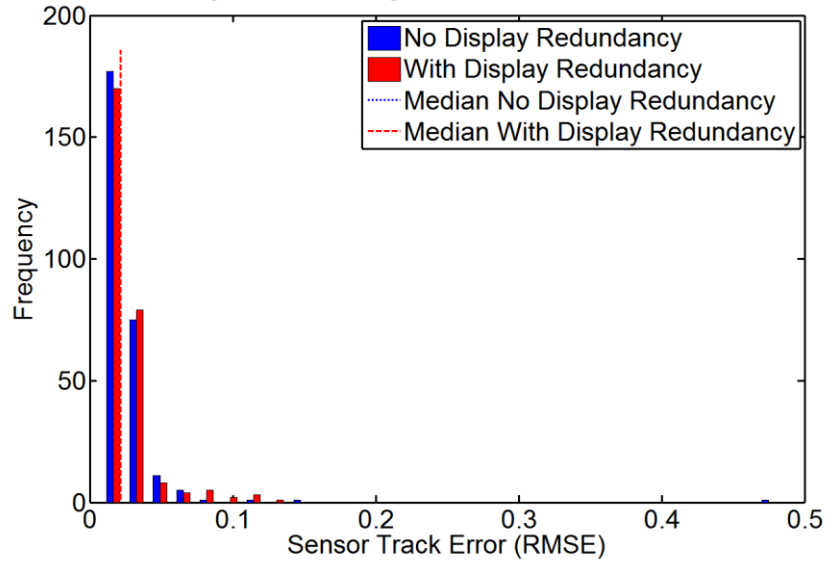


Figure 238: Experiment 4 Sensor Track Error Display Redundancy Effect
Blue distribution is observed data with without the aircraft display. Red distribution includes the aircraft display. Note that this does not represent a significant difference.

F.6. Orientation Time

$$OT'_{e4} \approx \beta_0 + \beta_1 * XdispRedun + \beta_2 * Xalign + \beta_3 * XtrialNum + \beta_4 * Xmove + \beta_5 * Xalign * Xmove + \beta_6 * XtrialNum * Xmove + \beta_{7i} * Xsubject_i + \beta_{8i} * Xmove * Xsubject_i + \beta_{9i} * Xalign * Xsubject_i$$

$i = 1:16$ subjects

Equation 57: Orientation Time Regression Estimation

Table 68: Experiment 4 Orientation Time Predictor Variable Coefficients

Predictor Variable	Term	Transformed Regression Estimate	Lower 95% Conf. Interval	Upper 95% Conf. Interval	t-stat	p-value	Reverse Transformed Estimate (β')	units
(Intercept)	β_0	0.325	0.191	0.459	4.75	2.62E-06	0.259	s
XdispRedun	β_1	0.064	0.033	0.095	4.06	5.53E-05	0.060	s
Xalign	β_2	-0.420	-0.506	-0.333	-9.53	5.38E-20	-0.560	s
XtrialNum	β_3	-0.013	-0.018	-0.008	-5.44	7.97E-08	-0.013	s/#
Xmove	β_4	0.019	-0.057	0.095	0.50	0.61	0.019	s
Xalign*Xmove	β_5	0.064	0.002	0.125	2.04	4.23E-02	0.060	s
XtrialNum*Xmove	β_6	0.010	0.003	0.016	3.01	2.73E-03	0.009	s/#

Table 69: Experiment 4 Orientation Time Tests for Error Variance Constancy of Regression Model
 – No color fill indicates that none of these results are significant, so the hypothesis holds that error variance is constant and regression analysis is suitable

Grouping	Bartlett F Statistic	Bartlett p-value	Levene F Statistic	Levene P-value	Brown-Forsythe F Statistic	Brown-Forsythe p-value
XdispRedun	0.16	0.69	0.35	0.55	0.36	0.55
Xalign	0.16	0.69	0.35	0.55	0.36	0.55
XtrialNum	0.29	0.59	0.48	0.49	0.47	0.49
Xmove	0.16	0.69	0.35	0.55	0.36	0.55
Xmove*Xalign	1.86	0.17	1.60	0.21	1.58	0.21
Xmove*XtrialNum	0.16	0.69	0.35	0.55	0.36	0.55
Ximage	0.51	0.47	0.001	0.98	0.001	0.98
Xsubject	1.97	0.16	0.02	0.88	0.02	0.88
Predicted OT'	0.83	0.36	0.92	0.34	0.93	0.34
Time Sequence	1.07	0.30	1.05	0.31	1.05	0.31

Residual plots were removed because no trends were noted.

Orientation Time vs Angle Exp. 4, 16 Subjects, Dec 15 - Jan 16

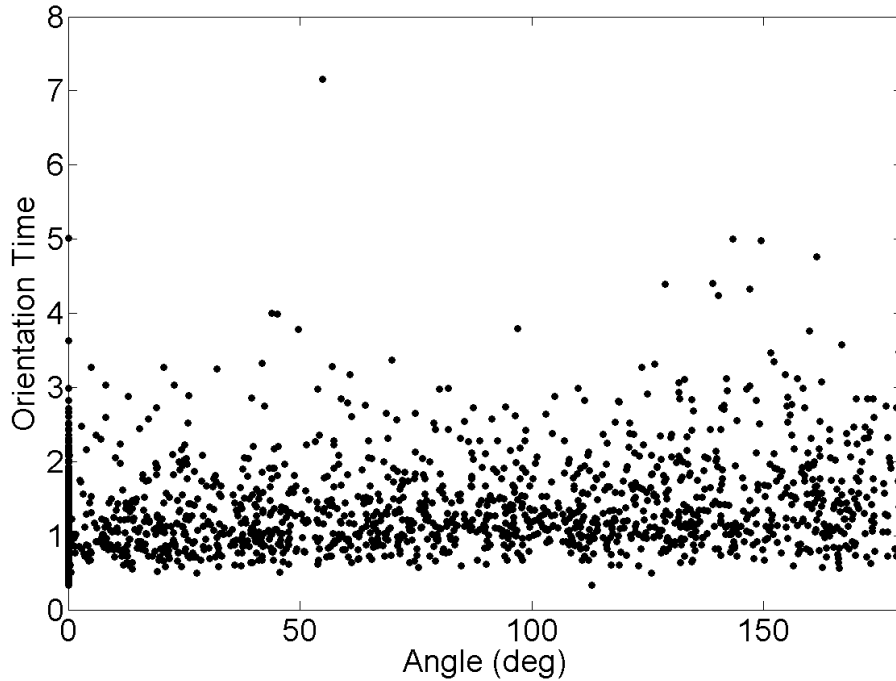


Figure 239: Experiment 4 Individual Orientation Time vs. Rotation Angle
 Since the orientation time analysis was conducted on mean orientation times for each run, this chart examines the individual rotation angles associate with each answer to look for missed trends on rotation angle effects.

Orientation Time Transformation Exp. 4, 16 Subjects, Dec 15 - Jan 16

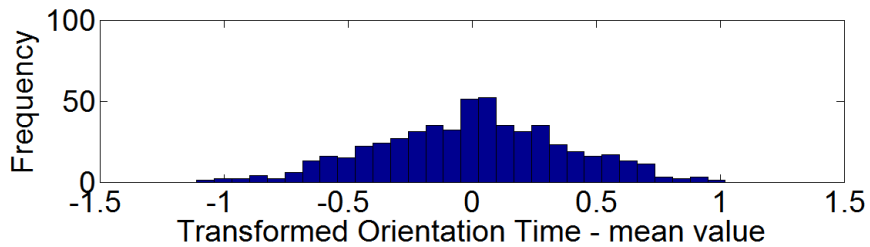
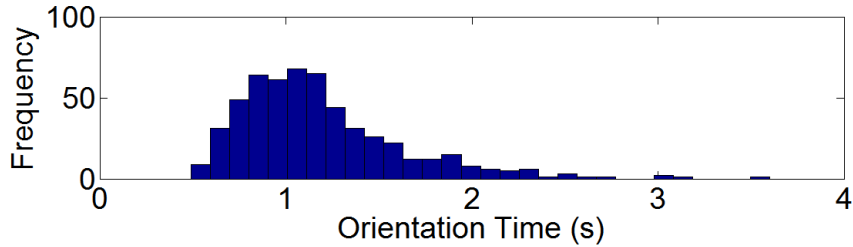


Figure 240: Orientation Time Data Transformation

Orientation Time NOT transformed Normal Prob. Plot against:
 PFD Present, Alignment, Subject, Trial Num, Movement
 Exp. 4, 16 Subjects, Dec 15 - Jan 16

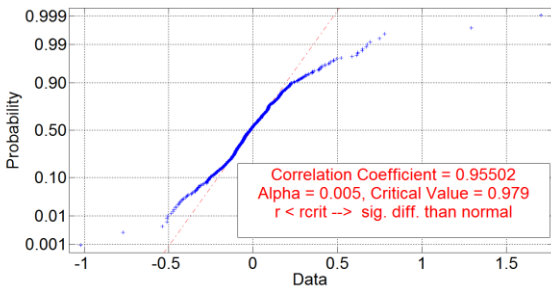


Figure 241: Orientation Time Regression Residuals from Skewed Data

Transformed Orientation Time Normal Probability Plot
 Exp. 4, 16 Subjects, Dec 15 - Jan 16

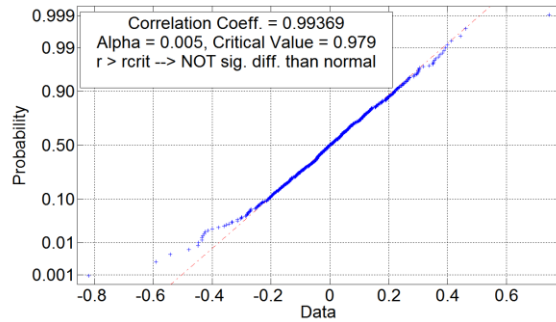


Figure 242: Orientation Time Regression Residuals from Transformed Data

Orientation Time Transformation Parameters Exp. 4, 16 Subjects, Dec 15 - Jan 16

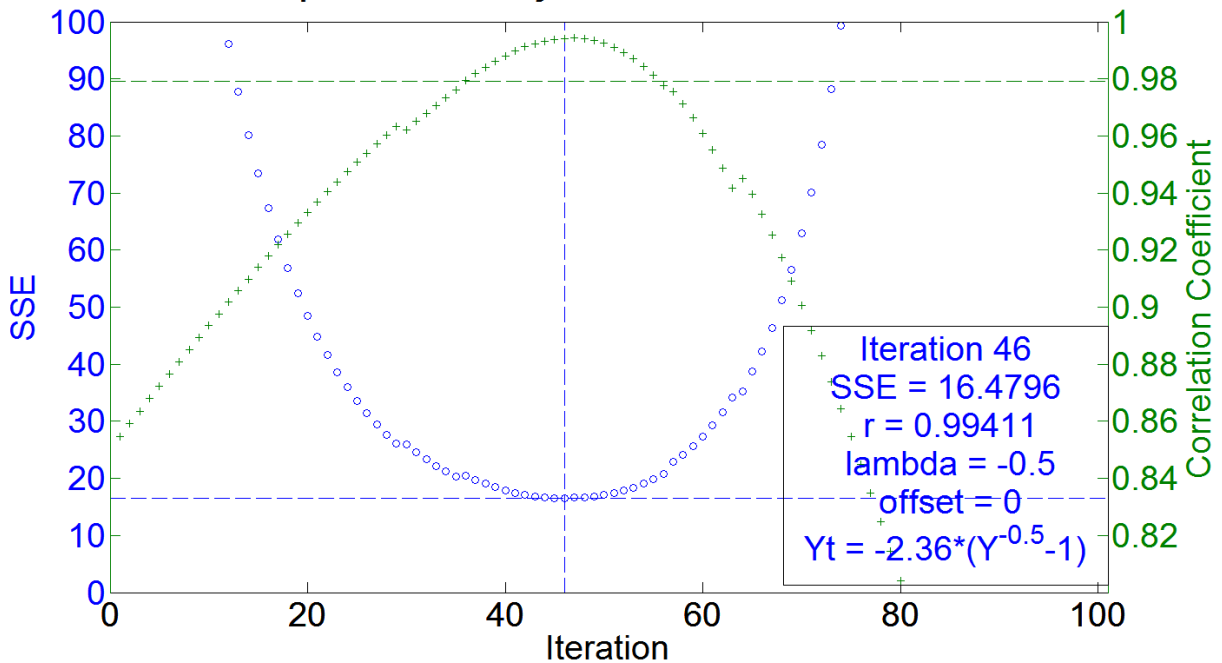


Figure 243: Exp 4 Orientation Time Box-Cox Transformation Parameter Estimation
 The blue data show how the regression Mean Squared Error was minimized with the Box-Cox Transformation. The green data show the corresponding effect on the correlation of the residuals with estimated values under normality.

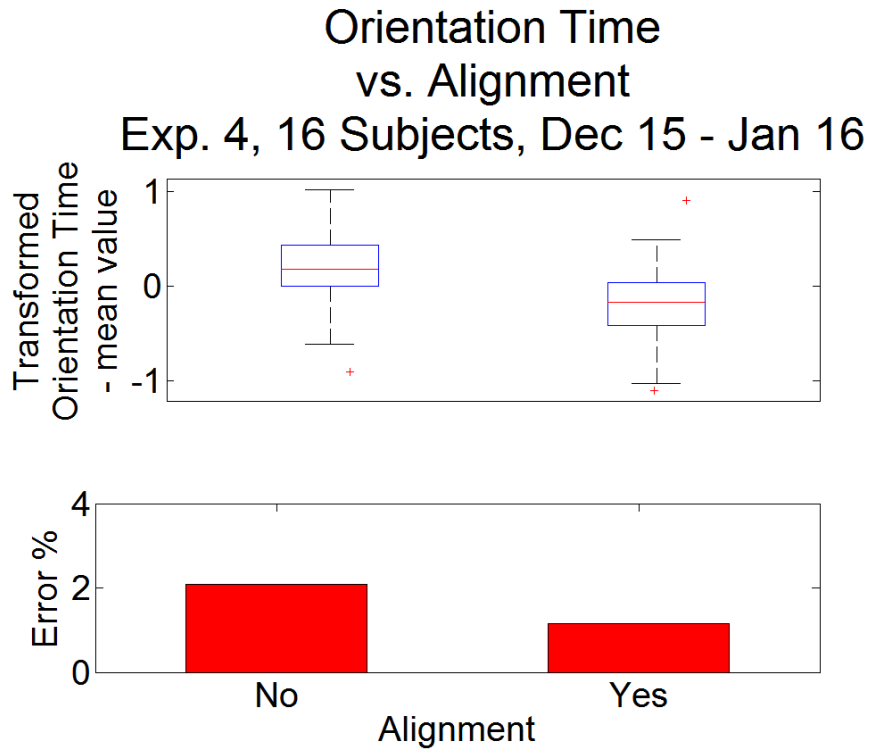


Figure 244: Orientation Time vs. Alignment

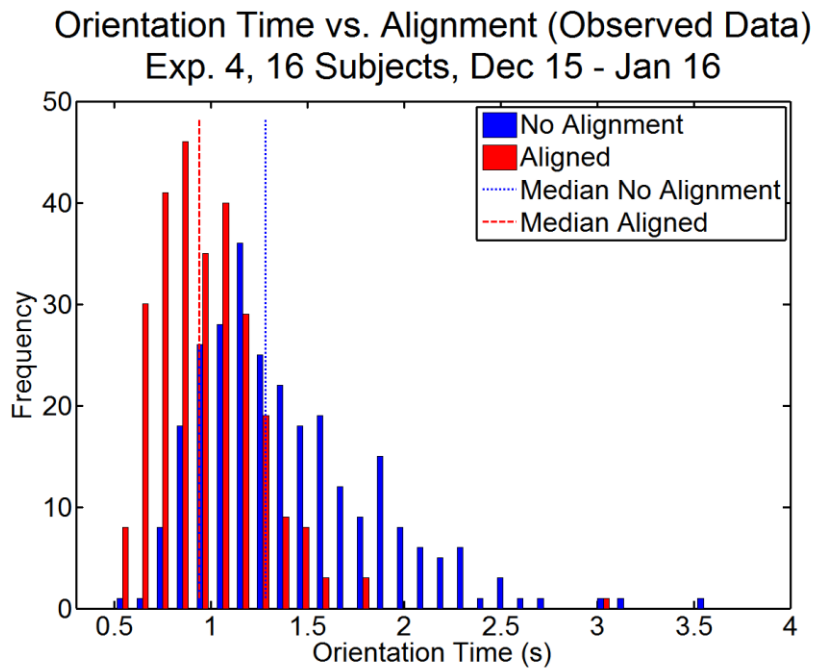


Figure 245: Experiment 4 Orientation Time Alignment Effect
Blue distribution is observed data without alignment. Red distribution has alignment of the sensor display and is shifted left of the blue data.

Tgt Acquisition Time vs. Display Redundancy Exp. 4, 16 Subjects, Dec 15 - Jan 16

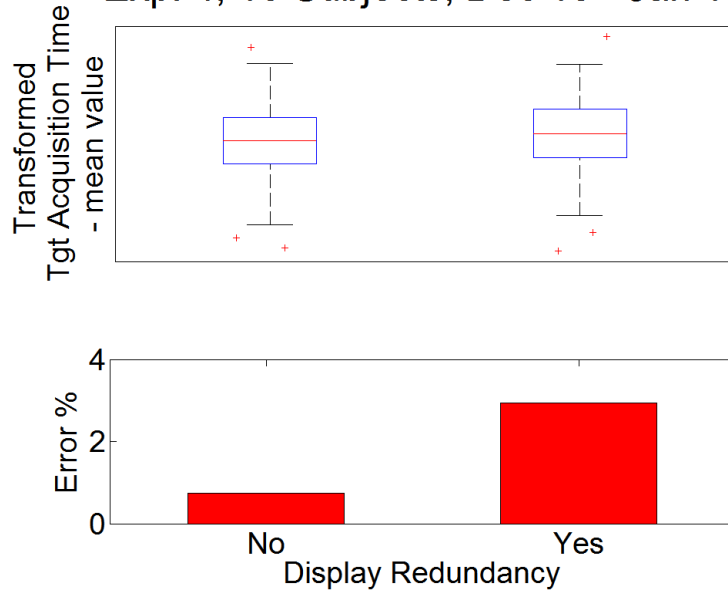


Figure 246: Orientation Time vs. Display Redundancy

Orientation Time vs. Display Redundancy (Observed Data) Exp. 4, 16 Subjects, Dec 15 - Jan 16

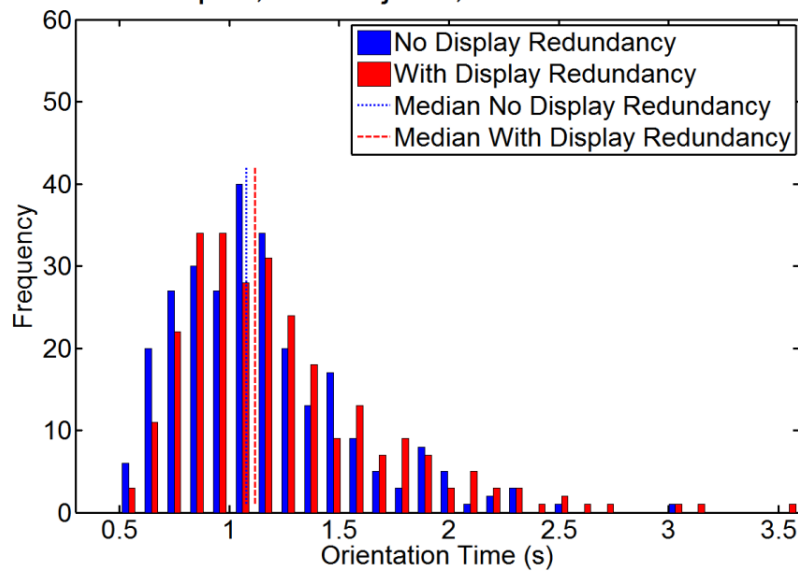


Figure 247: Experiment 4 Orientation Time Display Redundancy Effect
Blue distribution is observed data with without the aircraft display. Red distribution includes the aircraft display. Here, the aircraft display was detrimental to performance because it increased orientation time.

Orientation Time vs. Target Movement Exp. 4, 16 Subjects, Dec 15 - Jan 16

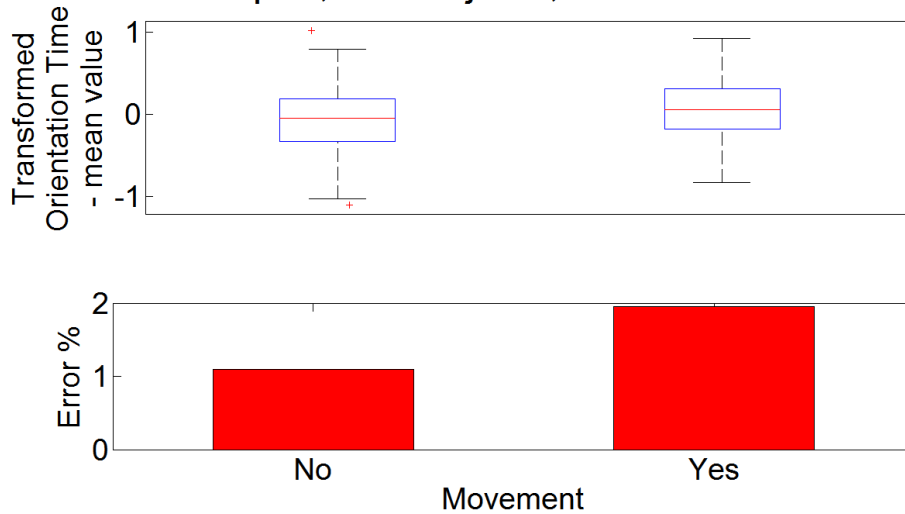


Figure 248: Orientation Time vs. Target Movement

Orientation Time vs. Movement (Observed Data) Exp. 4, 16 Subjects, Dec 15 - Jan 16

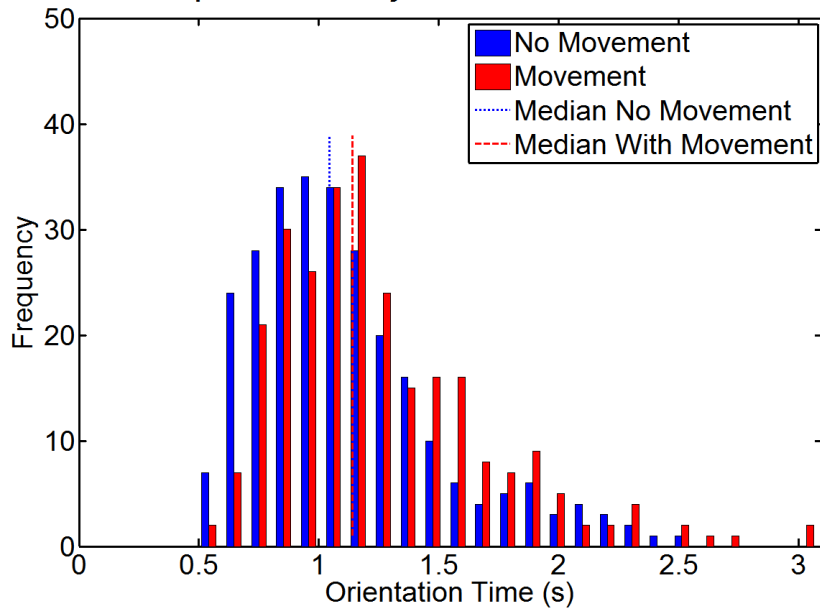


Figure 249: Experiment 4 Orientation Time Moving Target Effect
Blue distribution is observed data with a stationary target. Red distribution is observed data with a moving target and is shifted right of the blue data.

F.7. Bedford Workload Rating

Bedford Workload vs. Display Redundancy (Observed)
Exp. 4, 16 Subjects, Nov 14 - Feb 15

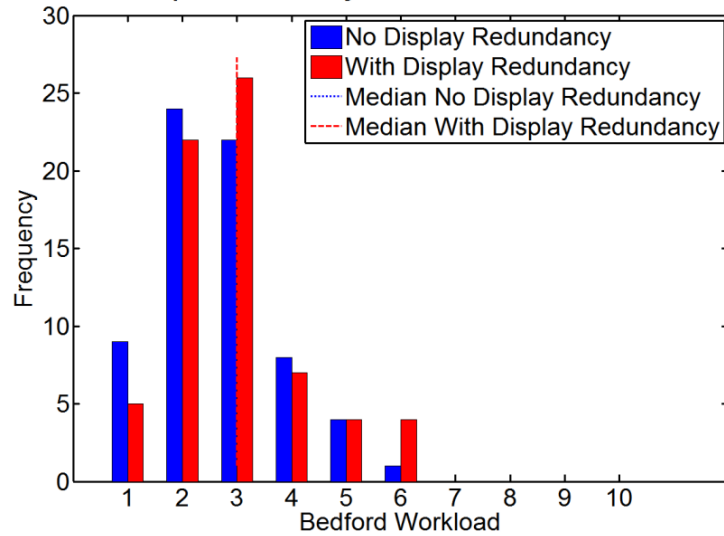


Figure 250: Experiment 4 Bedford Workload Rating Display Redundancy Effect
Blue distribution is observed data with without the aircraft display. Red distribution includes the aircraft display.

Bedford Workload vs. Alignment (Observed Data)
Exp. 4, 16 Subjects, Nov 14 - Feb 15

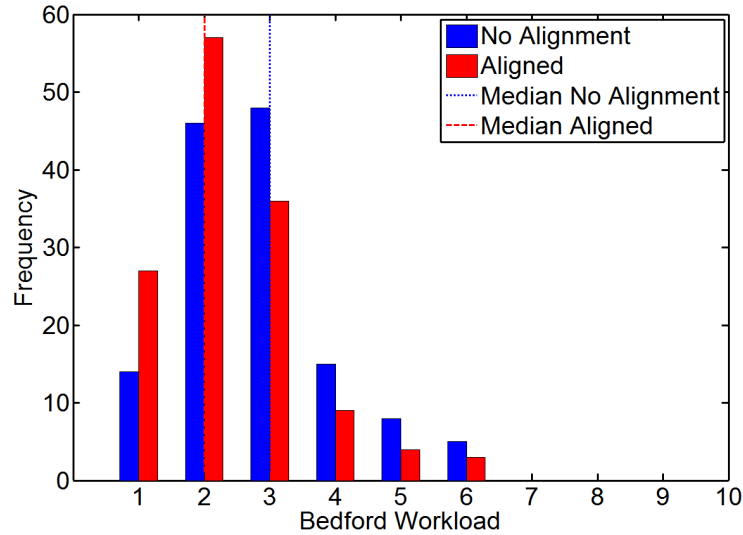


Figure 251: Experiment 4 Bedford Workload Rating Alignment Effect
Blue distribution is observed data without alignment. Red distribution has alignment of the sensor display.

F.8. Reaction Time

$$RT'_{e4} \approx \beta_0 + \beta_1 * XdispRedun + \beta_2 * Xalign + \beta_3 * XtrialNum + \beta_4 * Xmove + \beta_5 * XtrialNum * Xmove + \beta_{6i} * Xsubject_i + \beta_{7i} * Xmove * Xsubject_i + \beta_{8i} * Xalign * Xsubject_i$$

$i = 1: 16 \text{ subjects}$

Equation 58: Reaction Time Regression Estimation

Table 70: Experiment 4 Reaction Time Predictor Variable Coefficients

Predictor Variable	Term	Transformed Regression Estimate	Lower 95% Conf. Interval	Upper 95% Conf. Interval	t-stat	p-value	Reverse Transformed Estimate (β')	units
(Intercept)	β_0	-2.93E-01	-2.44E-01	-1.53E-01	-8.53	1.49E-16	-2.93E-01	s
XdispRedun	β_1	6.36E-02	5.94E-02	9.16E-02	9.21	6.99E-19	6.36E-02	s
Xalign	β_2	-3.79E-02	-4.89E-02	-2.56E-02	-6.29	6.71E-10	-3.79E-02	s
XtrialNum	β_3	-3.85E-03	-5.76E-03	-2.28E-03	-4.55	6.68E-06	-3.85E-03	s/#
Xmove	β_4	3.20E-02	4.49E-03	6.71E-02	2.25	2.51E-02	3.20E-02	s
XtrialNum*Xmove	β_5	2.25E-03	6.89E-06	4.75E-03	1.97	4.93E-02	2.25E-03	s/#

Table 71: Experiment 4 Reaction Time Tests for Error Variance Constancy of Regression Model
Yellow indicates results which are trending towards significance; however, none of these are significant to the 0.05 level, so the hypothesis holds that error variance is constant and regression analysis is suitable

Grouping	Bartlett F Statistic	Bartlett p-value	Levene F Statistic	Levene P-value	Brown-Forsythe F Statistic	Brown-Forsythe p-value
XdispRedun	0.78	0.38	0.89	0.35	0.91	0.34
Xalign	0.78	0.38	0.89	0.35	0.91	0.34
XtrialNum	6.84	0.0089	3.88	0.049	3.80	0.052
Xmove	0.78	0.38	0.89	0.35	0.91	0.34
Xmove*Xalign	4.42	0.036	1.75	0.19	1.70	0.19
Xmove*XtrialNum	0.78	0.38	0.89	0.35	0.91	0.34
Ximage	2.60	0.11	4.36	0.037	4.40	0.037
Xsubject	2.57	0.11	2.64	0.10	2.61	0.11
Predicted RT'	0.26	0.61	0.26	0.61	0.24	0.62
Time Sequence	3.50	0.061	1.85	0.17	1.80	0.18

Reaction Time vs Angle Exp. 4, 16 Subjects, Dec 15 - Jan 16

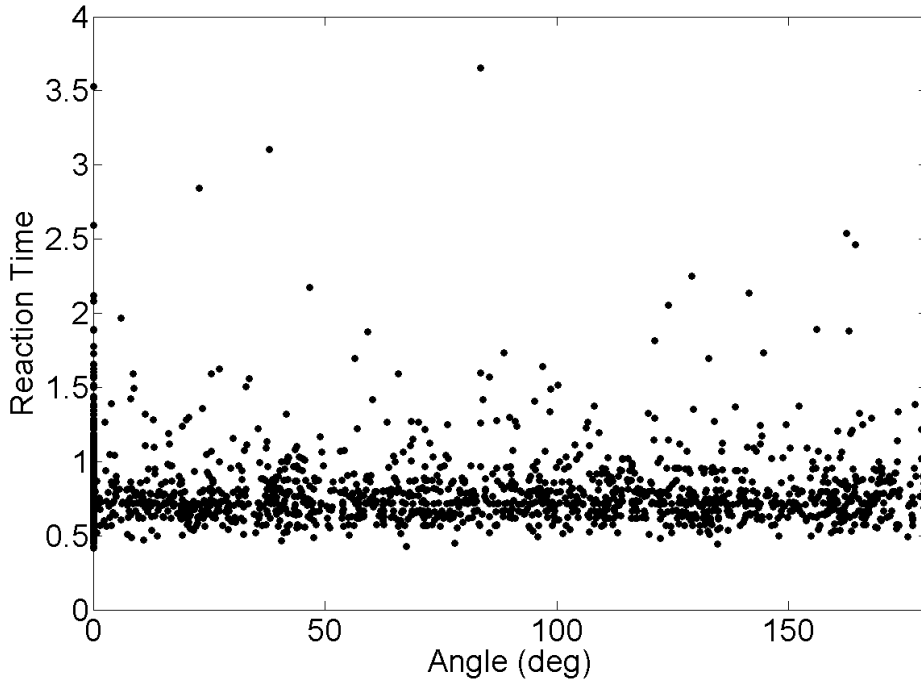


Figure 252: Experiment 4 Individual Reaction Time vs. Rotation Angle
Since the reaction time analysis was conducted on mean reaction times for each run, this chart examines how the individual rotation angles associate with each answer to look for missed trends on rotation angle effects.

Reaction Time Transformation Exp. 4, 16 Subjects, Dec 15 - Jan 16

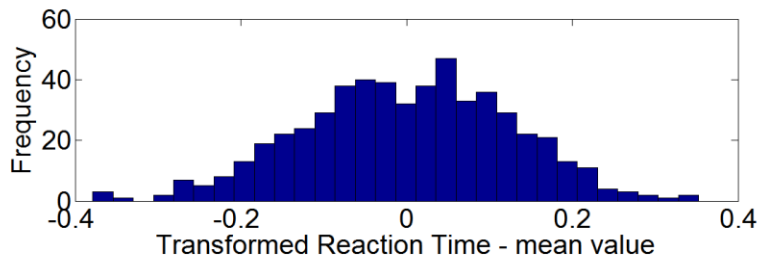
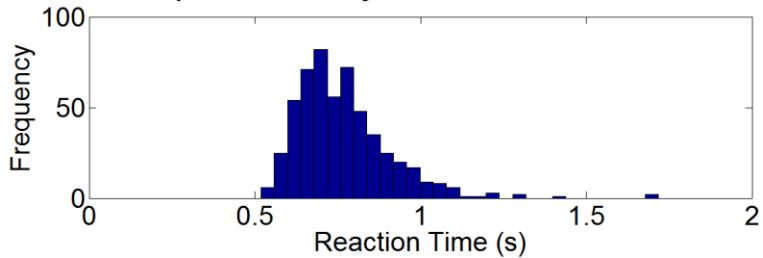


Figure 253: Reaction Time Data Transformation

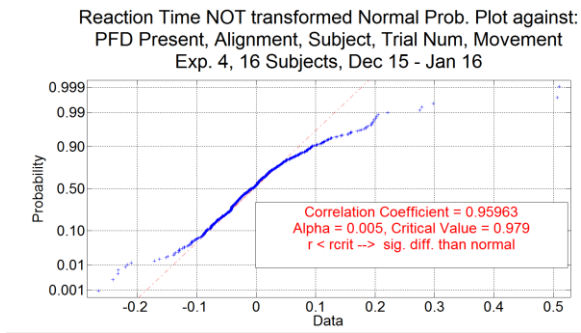


Figure 254: Reaction Time Regression Residuals from Skewed Data

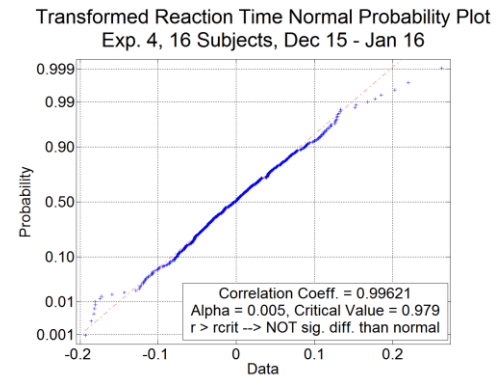


Figure 255: Reaction Time Regression Residuals from Transformed Data

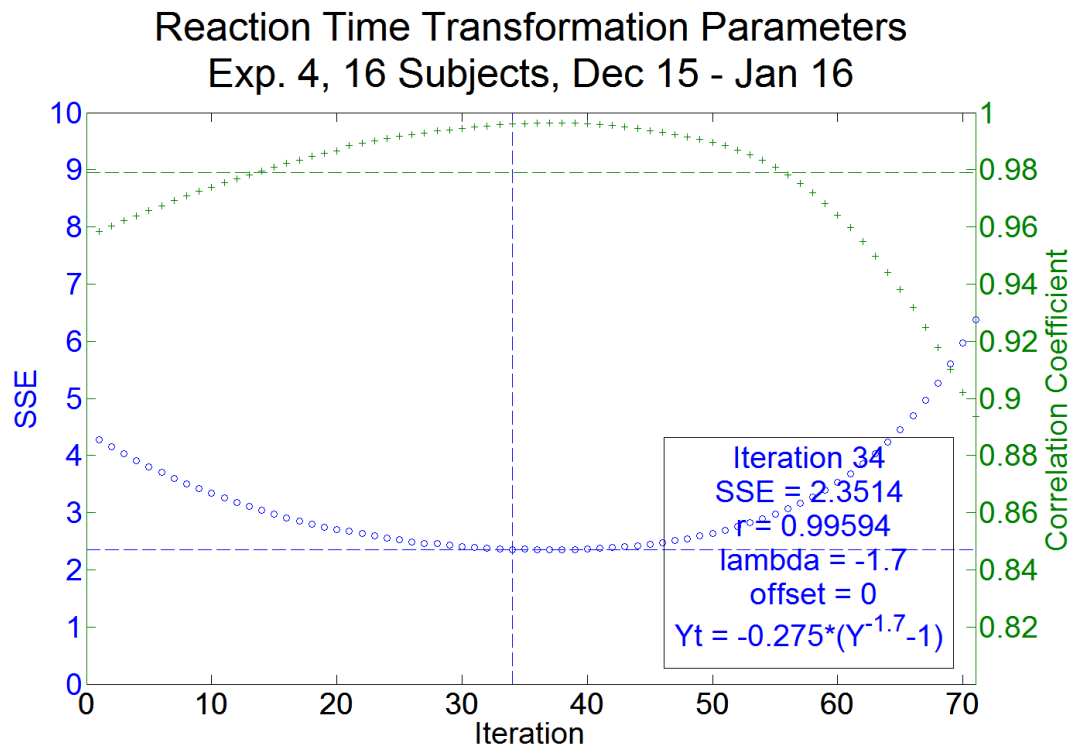


Figure 256: Exp 4 Reaction Time Box-Cox Transformation Parameter Estimation
 The blue data show how the regression Mean Squared Error was minimized with the Box-Cox Transformation. The green data show the corresponding effect on the correlation of the residuals with estimated values under normality.

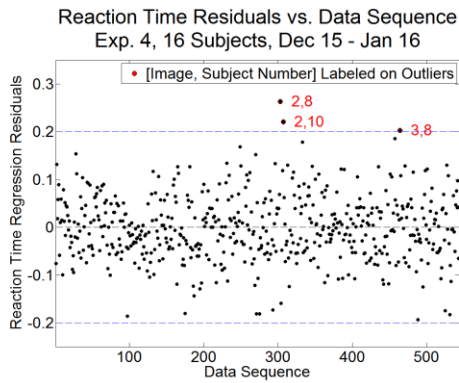


Figure 257: Test of Randomness

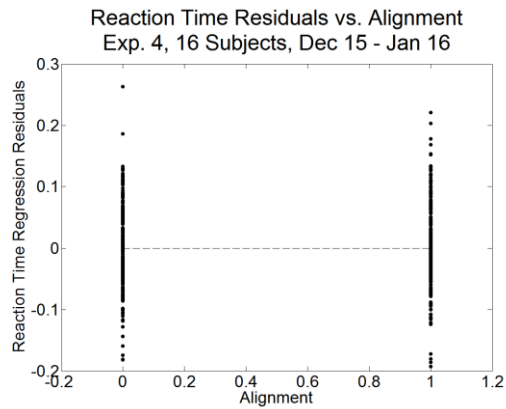


Figure 258: Residuals vs. Xalign

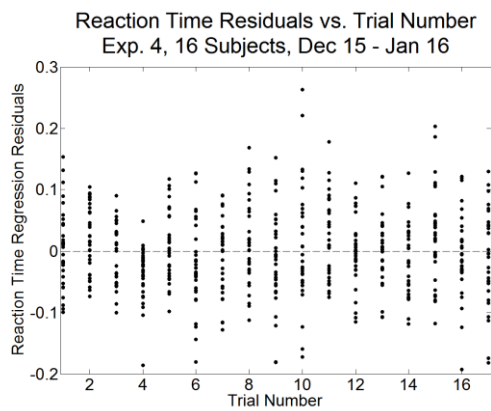


Figure 259: Residuals vs. XtrialNum

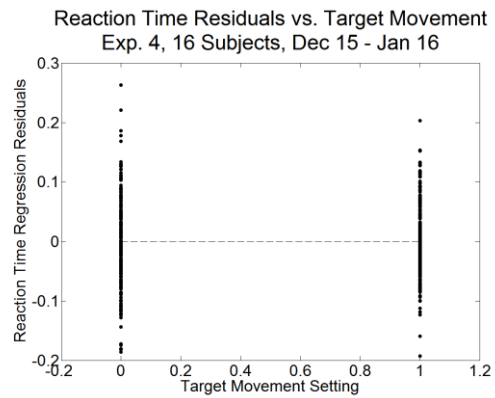


Figure 260: Residuals vs. Xmove

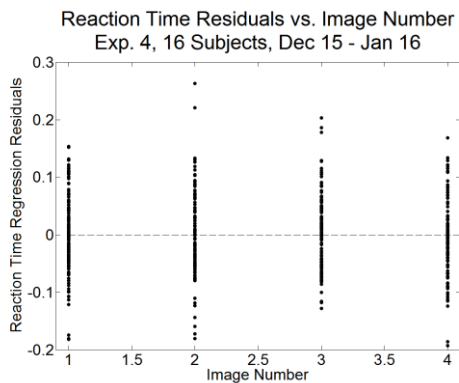


Figure 261: Residuals vs. Ximage

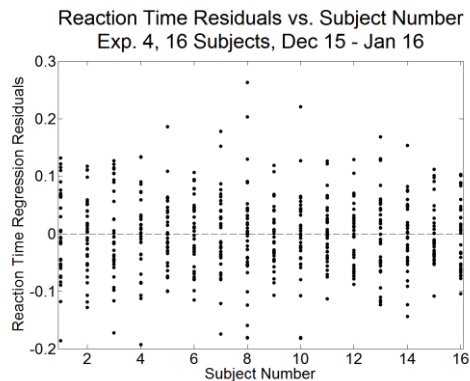


Figure 262: Residuals vs Xsubject

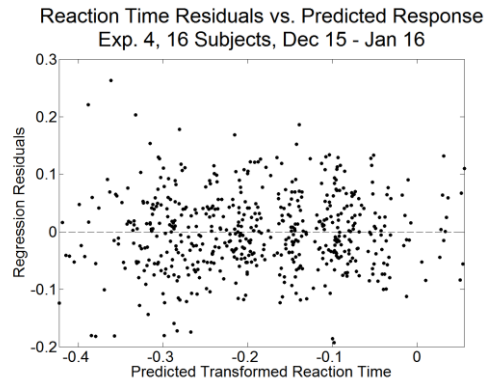


Figure 263: Residuals vs. Predicted Reaction Time

Reaction Time
vs. Alignment
Exp. 4, 16 Subjects, Dec 15 - Jan 16

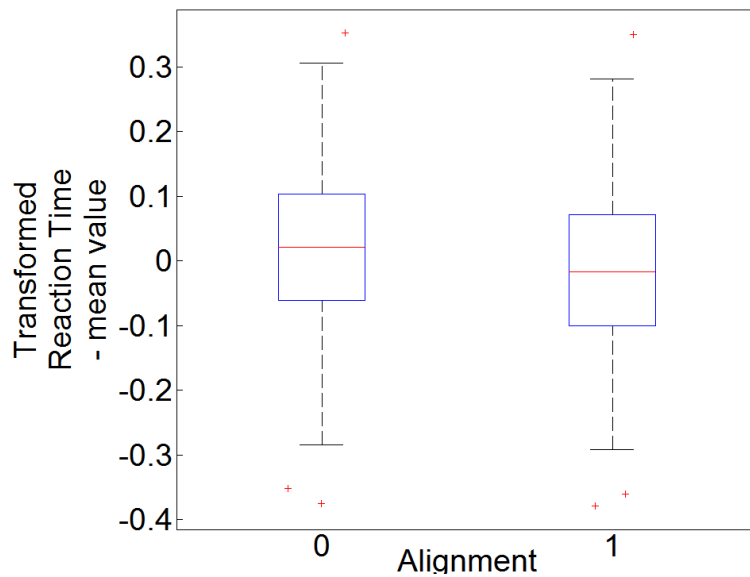


Figure 264: Reaction Time vs. Alignment

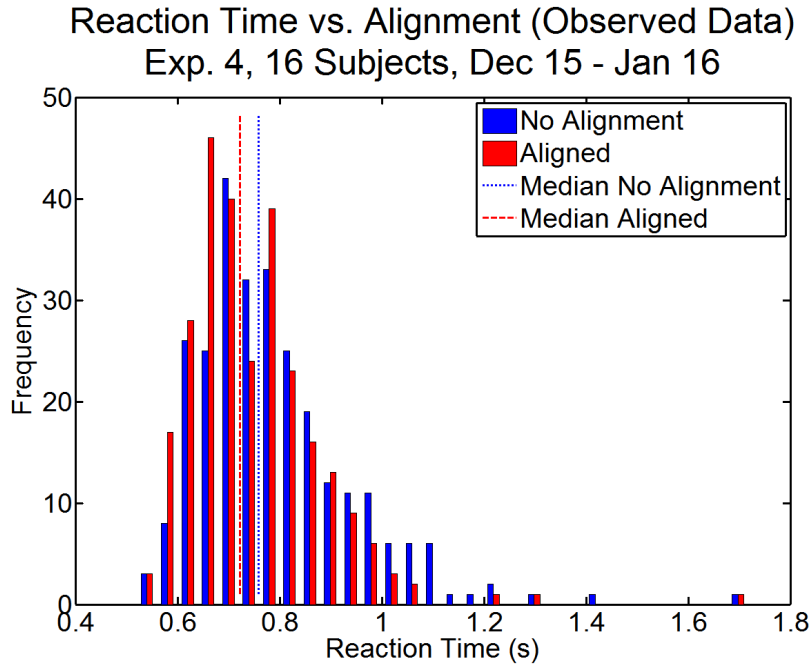


Figure 265: Experiment 4 Reaction Time Alignment Effect
Blue distribution is observed data without alignment. Red distribution has alignment of the sensor display.

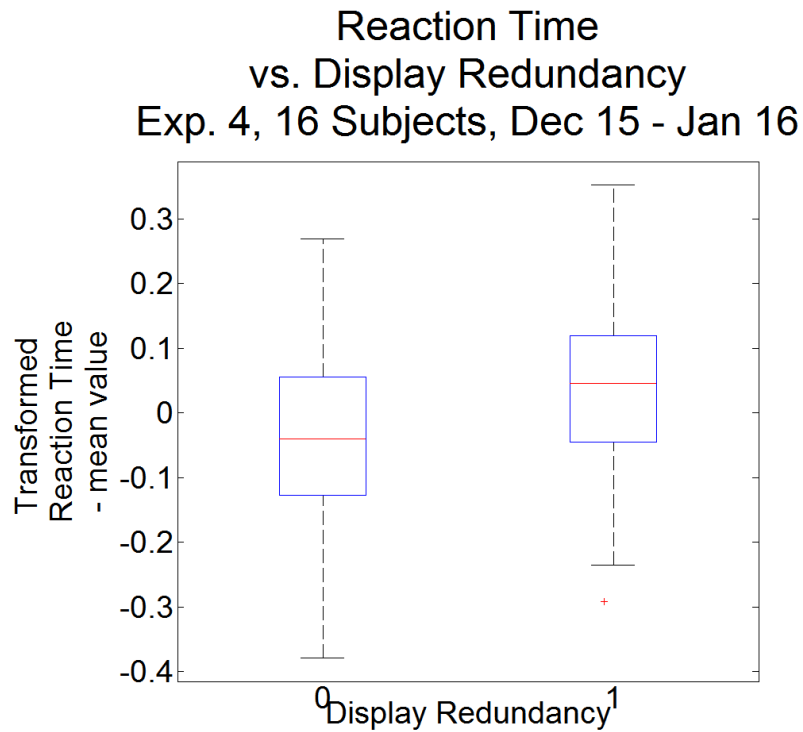


Figure 266: Reaction Time vs. Display Redundancy

Reaction Time vs. Display Redundancy (Observed)
Exp. 4, 16 Subjects, Dec 15 - Jan 16

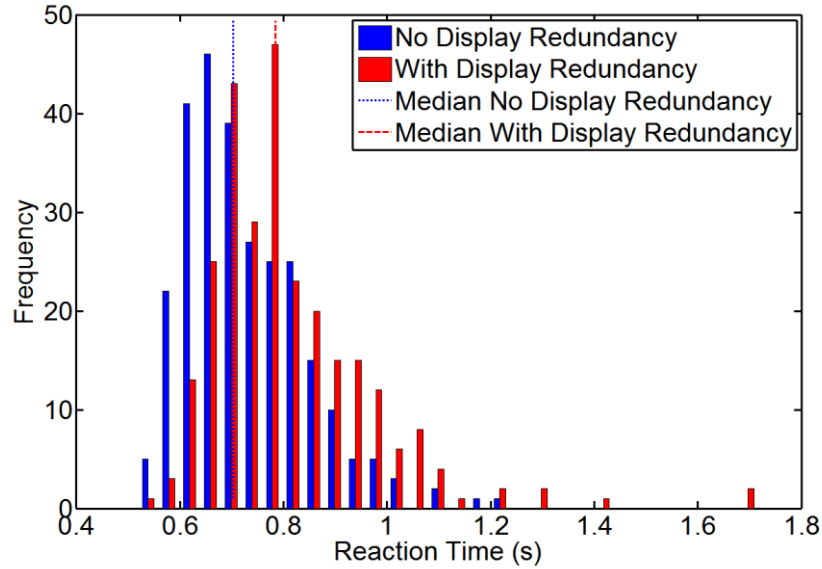


Figure 267: Experiment 4 Reaction Time Display Redundancy Effect
Blue distribution is observed data with without the aircraft display. Red distribution includes the aircraft display.

Reaction Time
vs. Target Movement
Exp. 4, 16 Subjects, Dec 15 - Jan 16

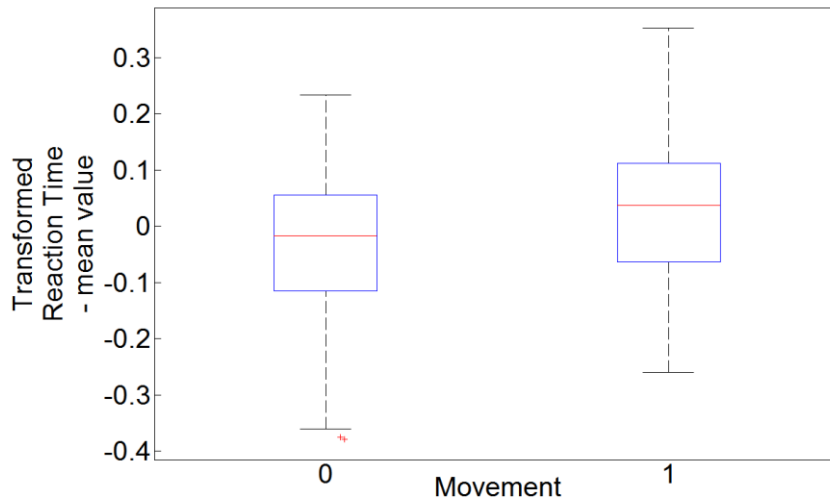


Figure 268: Reaction Time vs. Target Movement

Reaction Time vs. Movement (Observed Data)
Exp. 4, 16 Subjects, Dec 15 - Jan 16

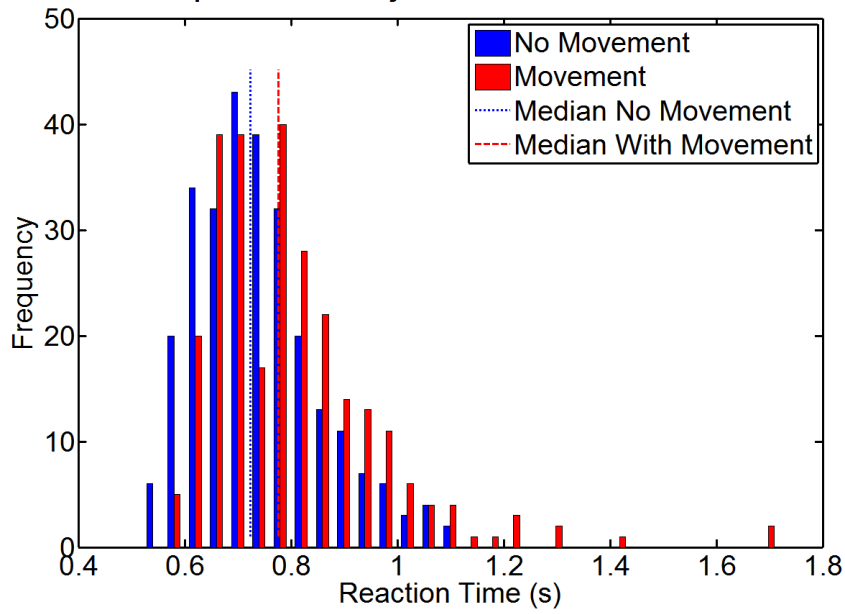


Figure 269: Experiment 4 Reaction Time Moving Target Effect
Blue distribution is observed data with a stationary target. Red distribution is observed data with a moving target

This page intentionally left blank.

Appendix G: Subjective Response Data

Experiments 1 through 3 collected a subjective ranking of the displays from each participant. These results are displayed here and color-coded according to the following table.

Table 72: Subjective Responses' Color Code, this color coding was applied to subjective responses for display ranking after each simulator experiment (1, 3, and 4)

0-1	1-2	2-3	3-4
-----	-----	-----	-----

Table 73: Experiment 1 Subjective Display Rankings

Subject Number	Disp. A Not Aligned, Orientation Aid	Disp. B Aligned Sensor Display, Orientation Aid	Disp. C Not Aligned, No Orientation Aid	Disp. D Aligned Sensor and Aircraft Displays, No Orientation Aid
1	3	1	4	2
2	3.5	1	3.5	2
3	3.5	2	3.5	1
4	1	2	3.5	3.5
5	3	1	3	3
6	3	1	3	3
7	3	1	3	3
8	3	3	3	1
9	3	2	4	1
10	3	1	4	2
11	3	1	3	3
12	3	2	4	1
13	2	1	4	3
14	3	2	4	1
15	3	1	3	3
16	3.5	2	3.5	1
17	3.5	1.5	3.5	1.5

Table 73: Experiment 1 Subjective Display Rankings

Subject Number	Disp. A Not Aligned, Orientation Aid	Disp. B Aligned Sensor Display, Orientation Aid	Disp. C Not Aligned, No Orientation Aid	Disp. D Aligned Sensor and Aircraft Displays, No Orientation Aid
18	3.5	1.5	3.5	1.5
19	2.5	1	4	2.5
20	3.5	2	3.5	1
21	3.5	2	3.5	1
22	3	1	4	2
23	3.5	2	3.5	1
24	3	2	4	1
25	3	1	3	3
26	3.5	1.5	3.5	1.5
27	3	2	4	1
28	3.5	2	3.5	1
29	3	2	4	1
30	2.5	1	4	2.5
31	3.5	2	3.5	1
32	3	1	3	3
33	3.5	2	3.5	1
34	1.5	1.5	3.5	3.5
35	3.5	1	3.5	2
36	3	1	4	2

Table 74: Experiment 3 Subjective Display Rankings

Subject Number	Disp. A Not Aligned Not Integrated	Disp. D Aligned Sensor and Aircraft Displays, Not Integrated	Disp. E Not Aligned Integrated	Disp. F Aligned Sensor and Aircraft Displays, Integrated
49	2	1	4	3
50	3	1	4	2
51	3	1	4	2
52	3	1	4	2
53	1	3	4	2
54	3.5	2	3.5	1
55	4	3	2	1
56	4	3	2	1
57	4	2	3	1
58	3	1	4	2
59	4	3	2	1
60	3	2	4	1
61	4	2	3	1
62	4	3	2	1
63	4	3	2	1
64	2	1	4	3

Table 75: Experiment 4 Subjective Display Rankings

Subject Number	Disp. A Not Aligned With Aircraft Display	Disp. B Aligned Sensor Display, With Aircraft Display	Disp. G Not Aligned No Aircraft Display	Disp. H Aligned Sensor Display No Aircraft Display
65	3	1	4	2
66	4	2	3	1
67	3	1	4	2
68	4	2	3	1
69	4	2	3	1
70	4	2	3	1
71	4	2	3	1
72	3	1	4	2
73	3	1	4	2
74	4	2	3	1
75	4	2	3	1
76	4	2	3	1
77	2	4	1	3
78	3	1	4	2
79	4	2	3	1
80	4	2	3	1

Table 76: Subjective Responses' Color Code, this color coding was applied to subjective responses for display rating after experiment 4

0-2	>2-4	>4-6	>6-8	>8-10
------------	----------------	----------------	----------------	-----------------

Table 77: Experiment 4 Subjective Display Ratings

Subject Number	Disp. A Not Aligned With Aircraft Display	Disp. B Aligned Sensor Display, With Aircraft Display	Disp. G Not Aligned No Aircraft Display	Disp. H Aligned Sensor Display No Aircraft Display
65	10	1	10	1
66	10	3	8	1
67	7	1	10	3
68	10	2	9	1
69	10	3	7	1
70	10	2	9	1
71	10	3	8	1
72	10	1	10	1
73	9	1	10	2
74	10	3	7	1
75	10	2	9	1
76	10	4	8	1
77	4	10	1	7
78	7	1	10	3
79	10	1	10	1
80	10	3	8	1

This page intentionally left blank.

Appendix H: Imagery Rotation Cognitive Process Examination

Much of this research effort was focused on human subject experiments using an unmanned aircraft simulator; however, several specific spatial ability tests were also performed. This section describes the targeted examinations of subjects' ability to perform a single cognitive rotation task. These tasks examined the object rotation and perspective-taking differences and were also compared with the imagery-rotation task results from experiment 2. This investigation sought to understand the mental process associated with the sensor display imagery transformation associated with unmanned aircraft operations. To this end, these results were used to select two tests for comparison with the experiment 3 and experiment 4 results from this research. These results did not significantly affect the main purpose for this research so they have been moved to this appendix.

H.1. Additional Spatial Ability Tests

During experiment 2, four established techniques to measure a subject's ability to perform mental object rotation or perspective-taking were conducted. These results were used to examine correlations with the imagery rotation task required by an unmanned aircraft operator. This comparison was made using the single imagery rotation task performed during experiment 2. The experiment 2 evaluation was performed without all of the other unmanned aircraft simulator tasks. This is not the only rotation task required of an unmanned aircraft operator, but it was the most significant, according to subjective feedback, in experiment 1. In experiment 2, subjects were tested on their ability to find a location within an image. They were provided two images with the target location identified on one of the images. This paralleled the coordination task faced by an unmanned aircraft operator when a target is indicated on a provided satellite or overhead image and the operator must find this same target on the sensor video screen. For more information about experiment 2 see Experiment 2: Imagery Rotation Subtask.

The following sections describe the four different spatial ability tests that were performed along with experiment 2 and considered for inclusion on experiments 3 and 4. Each of these was obtained from the MIT Manned Vehicle Laboratory.

H.1.1. Card Rotations Test

The card rotations test was developed by the Educational Testing Service to determine two-dimensional (2D) object rotation capability [135]. Here the subject is shown a reference image, and several test images which have been rotated and possibly reflected (flipped over). In each row the subject must determine whether the test image is simply a rotation of the target image or if it is a reflection. If the test image is a rotation the image is marked "s" for same, but if it is a reflection, the image is marked "d" for different. A reflection would require picking up the test image and turning it over while a rotation would only require sliding the test image around on the paper to see if it could line up with the reference image. As designed by ETS, and to match past experiments, this test was administered in two parts. In both cases the subject had three minutes to complete as many questions as possible out of a total of 80 test images. The test was scored with one point for each correct answer

minus one point for each incorrect answer for a highest possible score of 160. This score was not shared with the subject until the conclusion of the entire experiment time.

H.1.2. *Vandenberg Mental Rotation Test*

The Vandenberg Mental Rotation Test (MRT) was first developed in 1978 by Steven G. Vandenberg and Allan R. Kuse [115]. They based their 3-D object mental rotation test on a simpler 1971 study conducted by Shepard and Metzler [114]. Here, both groups were trying to understand a subject's ability to compare 3-D objects that had been rotated about some axis. Since 1978 many have used the Vandenberg format to examine this capability. In this experiment subjects were tested in two phases, similarly to the card rotations test described above. For each phase the subject was asked to examine different target images, and compare them each to four test images. Each of the test and target images were different perspectives of a series of cubes assembled to form 3-D shapes. In this format, two of the test images are 3-D rotations of the target image and 2 are not. The subject was told to select the two images that were mere rotations of the test image. The two incorrect images were meant to distract the subject. For this experiment, the two phases were each 3 minutes in length and included 10 test images each. Once again, incorrect answers were penalized to discourage guessing. The total score was recorded as the number correct minus the number incorrect. In this manner, the highest possible score was 40, two per test image, if all answers were provided and correct. As with all of these cognitive tests, no score was shared with the participant until the conclusion of their entire experiment.

H.1.3. *Perspective-Taking Ability Test*

The Perspective-Taking Ability (PTA) Test was designed to measure a subject's ability to perform a perspective-taking task rather than an object rotation task. This test was developed by MM Virtual Design for 2-dimensional perspective-taking and was run using a computer program [136]. It relies on a landmark-based scene where the subject was required to imagine themselves within the scene. The landmarks were prominent features in a town or city such as a school or factory. The specific location of each landmark was labeled with a black dot. The subject was told to imagine themselves at a location in the scene depicted by a face. The subject imaged facing the same direction as the symbolic face, and this direction was reinforced with a textual description at the top of the window. The subject was given approximately five seconds to become familiar with this landscape and then, accompanied by an aural tone, one of the landmark indicators would blink red. At this time the subject was to indicate which direction the indicated landmark was in relationship to the direction the subject was "facing". The subject was presented with 58 of these landmark scenes during one continuous trial.

For each of these scenes the only available answers were one of eight arrows (each 45 degree increment from and including straight forward); however, answers were rarely presented at these discrete angles. This left the subject with the difficult task of deciding between two possible answers. The subject could quickly determine that a landmark was to the left and slightly forward, but then he or she would have to decide whether to hit the left arrow or the forward/left arrow on the answer key. With the 8 possible answers every 45 degrees around the 2-D continuous space, the subject had to determine if angular differences were greater or less than 22.5 degrees from the available answer. At

times, this angle was as high as 21 degrees which made it difficult for many subjects to choose the correct answer.

The subject's performance with each scene was scored based on a combination of answer time and angular error. The subject was rewarded for a fast answer, and penalized for incorrect answers. Finally, these scores were averaged to provide a total subject score.

H.1.4. Purdue Spatial Visualization Test

Just as the PTA test examined 2-D perspective-taking, the Purdue Spatial Visualization Test examined 3-D perspective-taking ability of the subject [137]. Here the subject was shown a 2-D view of a 3-D object with a see-through cube outlined around the object. One of the corners of the cube was marked with a dot and the subject was told to imagine themselves at the dot looking toward the 3-D object. Subjects were also presented with 5 test views and told to choose the view that would be seen from the indicated corner of the see-through cube. Each of the five test images represents the view from a different corner of the see-through cube so, unlike the PTA Test, subjects were not required to make determinations between fine angular differences.

Each subject was given a single six minute period to work through 30 of these visualization problems. Guessing was again discouraged and scores were calculated by number correct minus number incorrect. This could have resulted with a maximum score of 30.

H.2. Spatial Ability Test Results

The four cognitive studies conducted during experiment 2 and described throughout this section were examined for their correlation to the imagery rotation test. This section describes the results of those five studies and the correlations between them. These are only the results of the studies conducted during experiment 2. Two of these tests were also included in experiments 3 and 4, but those results are discussed later in this section.

H.2.1. Cognitive Test Results

The results from the four previously-developed spatial-ability tests are shown in Table 78. A color scale is available to distinguish patterns in the table. None of the subjects were able to earn a perfect score on any of the four tests, and several subjects had high scores on one test, but lower scores on another. This gives some credence to the idea that separate mental methods are used during these exams. However, some of the subjects showed increased performance across all tests, which indicates a general capability for mental rotation tasks independent of the object rotation or perspective-taking divide.

Table 78: Cognitive Study Results, the color scale highlights increasing performance from red to green, as compared to fellow subjects in this study. Subjects are ordered based on

their performance in the card rotations test.

Subject	Card Rotations	Vandenberg MRT	PTA	Purdue
8	66	13	19.7	11
9	92	14	23.2	18
6	104	19	22	19.75
7	107	16	11.9	15
4	112	20	20.9	24
3	125	17	19.9	23.75
2	128	26	18.9	14.25
12	133	14	15.6	6.75
5	136	30	20.4	19
10	141	32	26	12
1	152	37	26.1	25.25
11	154	30	23.6	14.75

One goal of this experiment was to determine if the imagery rotation task involved in unmanned aircraft operations required an object rotation or perspective-taking mental task. Each subject's performance on these four basic cognitive tests was compared to their performance on the imagery rotation task.

H.3. Image Rotation and Spatial Ability Correlation Results

The image rotation test provided an opportunity to directly examine the image rotation or orientation aid effects, but it also provided a correlation to other cognitive tests of a subject's mental rotation capability. This section describes how a subject's performance on those four cognitive tests correlated with their performance on the imagery rotation test.

Each of the cognitive tests was analyzed for its linear correlation with the transformed performance parameters from the imagery rotation test. These results are shown in columns 6 and 7 of Table 79. The highest correlations are highlighted gray. Additionally a final combination of selection answer time and error was tested for correlation with each of these cognitive tests. This result is shown in the furthest right column of Table 79. As shown in the table, the card rotation test had one of the strongest correlations with imagery rotation test results in each of the three categories. The Virtual Mental Rotation Test (vMRT) had the strongest correlation for the error and normalized combined response variables. However, the Purdue Spatial Visualization Test held the strongest correlation on the selection answer time response variable.

Table 79: Cognitive Test Correlations with Imagery Rotation Test – Gray indicates the top two correlations in any given category.

	Card	vMRT	PTA	Purdue	Transformed Selection Answer Time	Transformed Selection Answer Error	Combined Normalized Time + Error
Card	1	0.785	0.321	0.136	-0.039	-0.139	-0.111
vMRT	0.785	1	0.624	0.285	-0.007	-0.201	-0.129
PTA	0.321	0.624	1	0.370	-0.019	-0.113	-0.083
Purdue	0.136	0.285	0.370	1	-0.029	-0.035	-0.040

These correlations were also examined within the linear regression models of the imagery rotation test. For simplicity of presentations, fixed effect procedures were followed for each of the independent variables: Subject Trial Number, Image Alignment, Orientation Aid, Initial Angle, Image Number, Card Rotation Test Score, Vandenberg MRT Score, PTA Score, and Purdue SVT Score. This simplified regression analysis reinforces the correlation observations in Table 79. The regression ANOVA for the combined metric is shown in Table 80. The individual metrics are available in Appendix D: Experiment 2 Data Analysis. In all three cases, the Card Rotation Test and the Vandenberg MRT have the highest statistical significance. These models were developed without discarding insignificant terms, which allows for a simple presentation of each term’s significance. Rows in each table with a higher p-value in the last column would be discarded while developing a more appropriate model of the given response variable: time, error, or the combination. All of these models remove subject as an independent variable and attempt to replace the subject effect with the subject’s performance on the four cognitive tests. The two most significant cognitive tests, card and MRT, produce a significant effect on selection answer time, but only MRT produces significant effects on the error and combined measures (Table 80). The individual regression analyses are shown in Appendix D: Experiment 2 Data Analysis.

Table 80: Combined Selection Performance Regression with Cognitive Test Results, the highest probability effects are highlighted gray and a green border is added to the only significant cognitive test results effect.

Term	SSE	DF	MSE	F	p-value
Trial Number	0.03	1	0.03	3.76	0.053
Image Alignment	1.79	1	1.79	210.41	1.3E-42
Orientation Aid	0.29	1	0.29	33.91	8.3E-09
Initial Angle	0.18	1	0.18	21.63	3.8E-06
Image Number	2.24	23	0.10	11.47	2.3E-36
Card Score	0.01	1	0.01	0.62	0.43
MRT	0.04	1	0.04	5.05	0.025
PTA	3.9E-04	1	3.9E-04	0.05	0.83
Purdue	3.1E-05	1	3.1E-05	3.6E-03	0.95
	6.96	819	8.5E-03	1	

H.4. Imagery Rotation and Spatial Ability Correlation Conclusions

The four cognitive tests were compared for their ability to predict performance on the imagery rotation task in answer time and answer error. As shown in Figure 270, there was a good deal of variability in subject performance across each of the tests, including differences between answer error and answer time on the imagery rotation test. This bar graph depicts the median normalized answer time and answer error from the imagery rotation test along with normalized results from each of the four cognitive tests. Since the imagery rotation test was a simplified portion of the greater mix of unmanned aircraft operational tasks, this variability was expected to increase with results from the unmanned aircraft simulator studies. Therefore, it seemed unlikely that any of these cognitive tests would be adequate to represent the subject variability in the greater studies. Since the final two simulator studies were planned to include two of these cognitive tests, the card rotation and Vandenberg MRT were chosen due to their increased correlation with the imagery rotation results. Although it was expected that performance on these tests would not account for enough of the variability associated with a given subject, they would still offer a standardized means to characterize each subject's mental rotation capability.

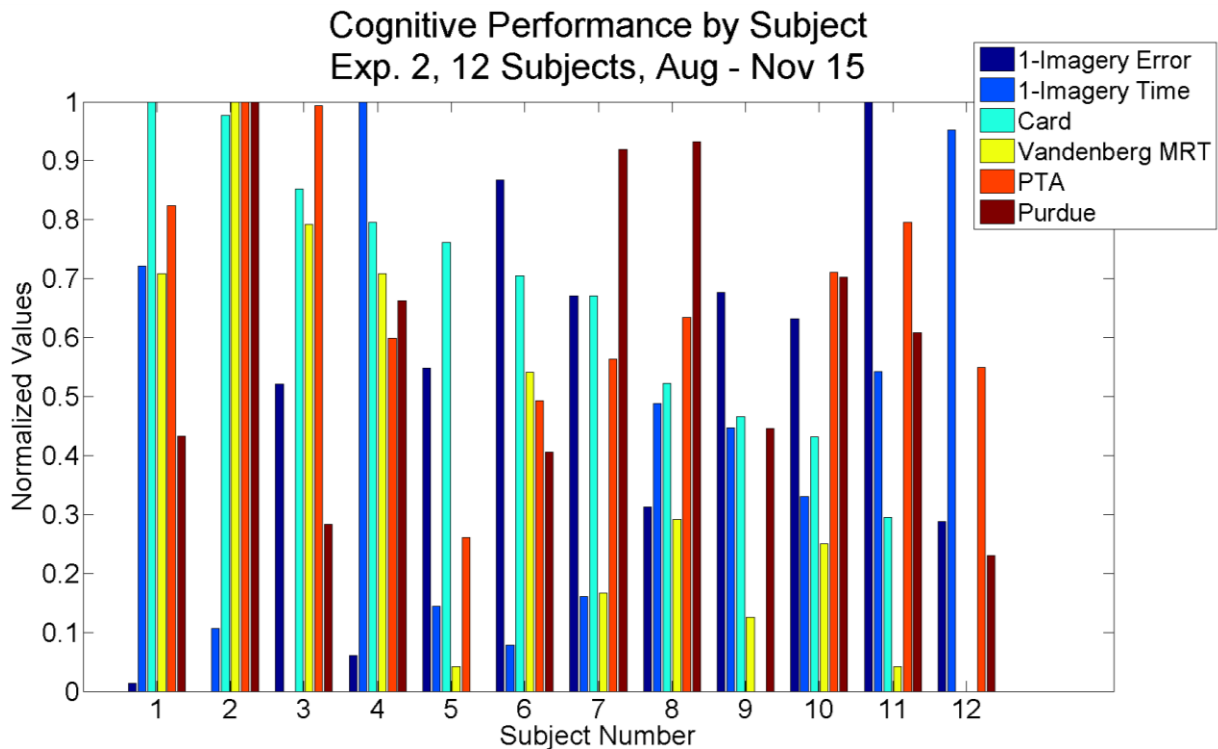


Figure 270: Experiment 2 Cognitive Performance Comparisons by Subject

This chart displays results for both of the selection performance measures (1-normalized error or 1-time), and the four cognitive studies. Results are sorted from best to worst by the teal colored card rotation results.

These four cognitive tests and the imagery rotation test provided a more concentrated examination of the mental rotation challenge associated with unmanned aircraft operational tasks. However, they represented individual single task studies where the subject was able to fully concentrate on one task at a time. In order to examine how the multiple reference frame environment affects the unmanned aircraft operator, a more representative experiment was required.

H.5. Spatial Ability Correlation with Simulator Performance

Subjects in experiments 3 and 4 completed the Vandenberg Mental Rotation Test and the card rotations test before their simulator experiment trials. These scores are compared to each subject’s average performance scores across each simulator performance measure. This comparison is provided in Table 34 of Appendix B: Subject Characteristics. The correlation results are shown here in Table 81. The results show that the 3-D object rotation task examined in the Vandenberg MRT was more representative of subject performance throughout most unmanned aircraft simulator tasks. This is an interesting result because this unmanned aircraft simulator relied on 2-D imagery rotation for video recreation, and yet the greater performance correlation is shown with the 3-D object rotation task.

Table 81: Experiment 3 and 4 Cognitive Test Correlations, green indicates the highest correlation for each simulator performance measure Reaction Time (RT), Orientation Time (OT), and Target Acquisition Time (TAT)

	Card	vMRT	RT	OT	TAT
Card	1.00	0.63	-0.30	-0.23	-0.23
vMRT	0.63	1.00	-0.39	-0.47	-0.01
RT	-0.30	-0.39	1.00	0.66	0.03
OT	-0.23	-0.47	0.66	1.00	0.11
TAT	-0.23	-0.01	0.03	0.11	1.00

These data only support the comparison between 2-D and 3-D object rotation and do not add significant information regarding the object rotation vs. perspective-taking mental process. Recall that the decision was made to proceed with the card rotation and Vandenberg MRT tests based on their correlation with the image rotation task in experiment 2 where the card rotation test had the highest correlation. However, now that cognitive tests results are compared with more realistic unmanned aircraft operator performance, the Vandenberg MRT test shows a higher correlation in every category except the target acquisition time. This aligns with the experiment 2 data, but also indicates that the mental process involved with target acquisition may differ from that required for the rest of the simulator tasks. These results should be investigated in future experiments to gain a greater understanding of the mental process associated with realistic unmanned aircraft operations.

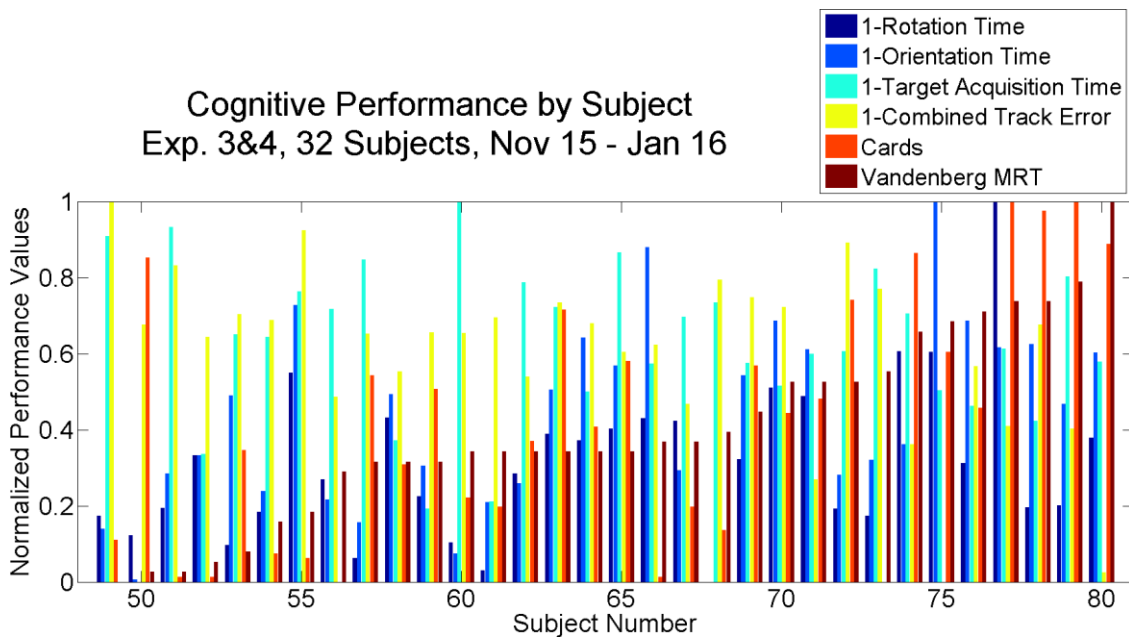


Figure 271: Experiments 3 and 4 Cognitive Performance Comparisons by Subject

This graph shows results for both of the selection performance measures (1 - normalized error or time), and the four cognitive studies. Results are sorted from worst to best by the dark red Vandenberg MRT 3-D object rotation results.

Appendix I: Imagery Feature Categories

These are all the image samples that were used during the experiment 2 image rotation study.

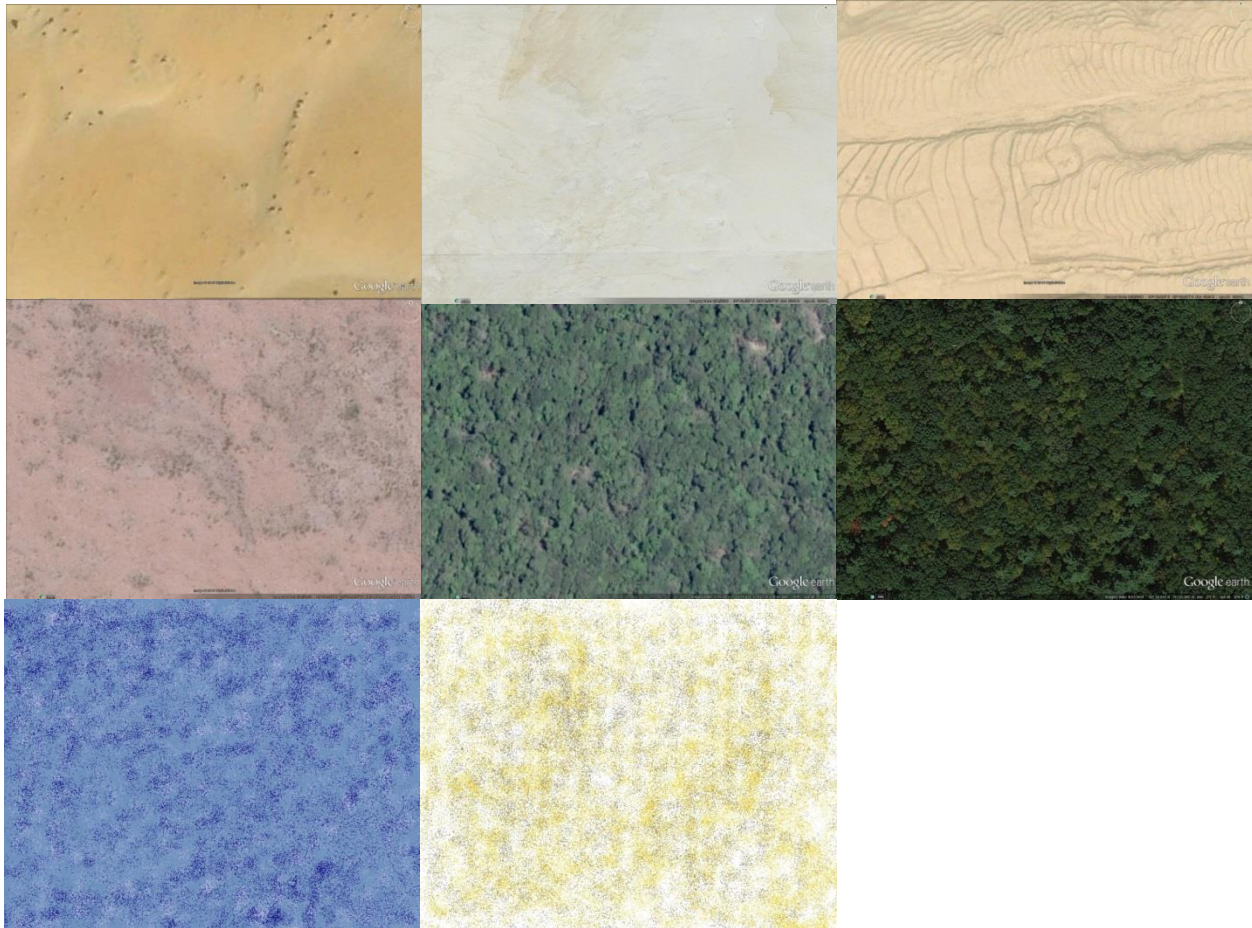


Figure 272: Imagery Examples with Few Available Features

None of these images have clear and discernible features that could be used as a substitution for an orientation aid. [Image ©Google]

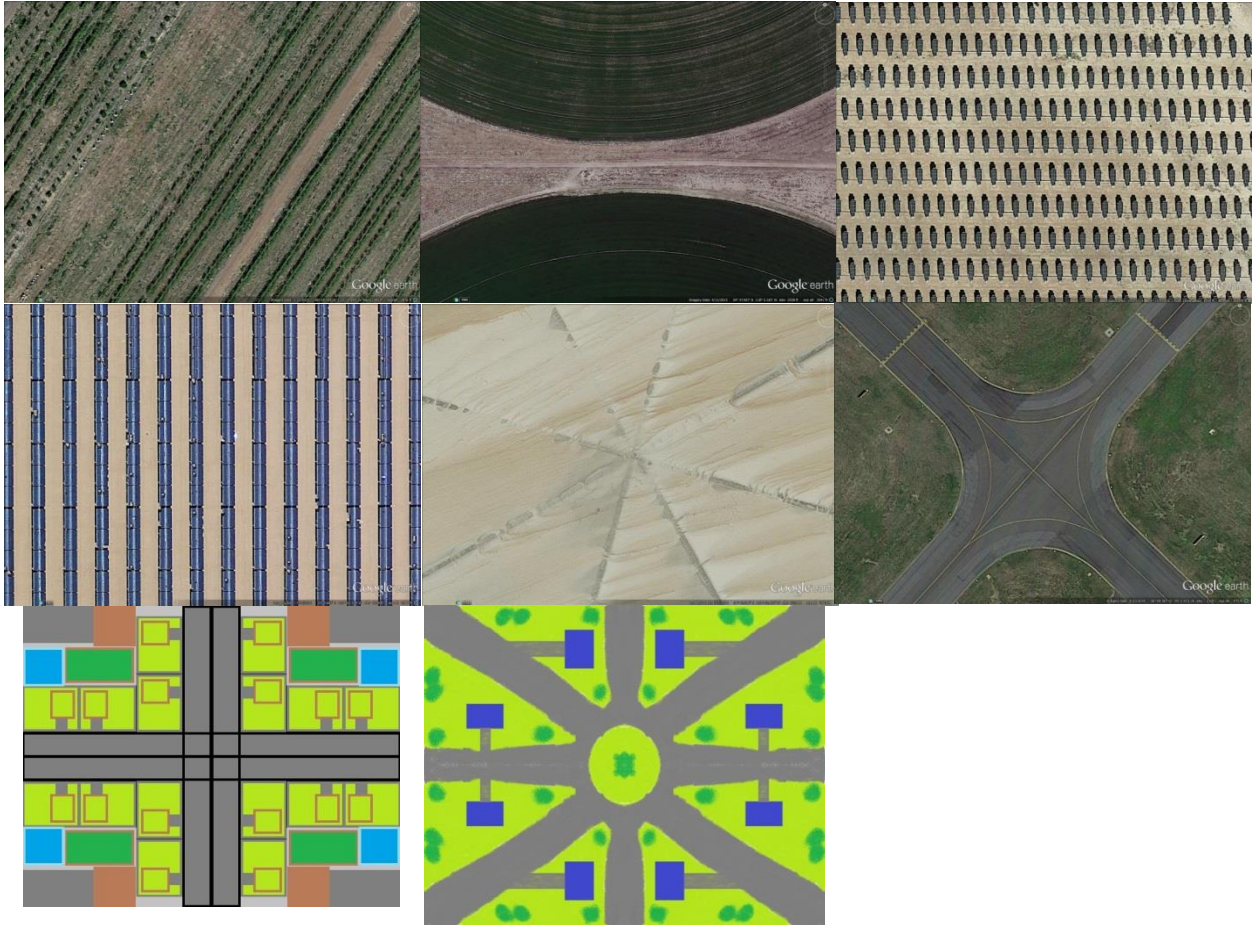


Figure 273: Imagery Examples with Ambiguous Features

Each one of these images has some level of dual axis symmetry, which could create confusion when orienting and finding a target. [Image ©Google]

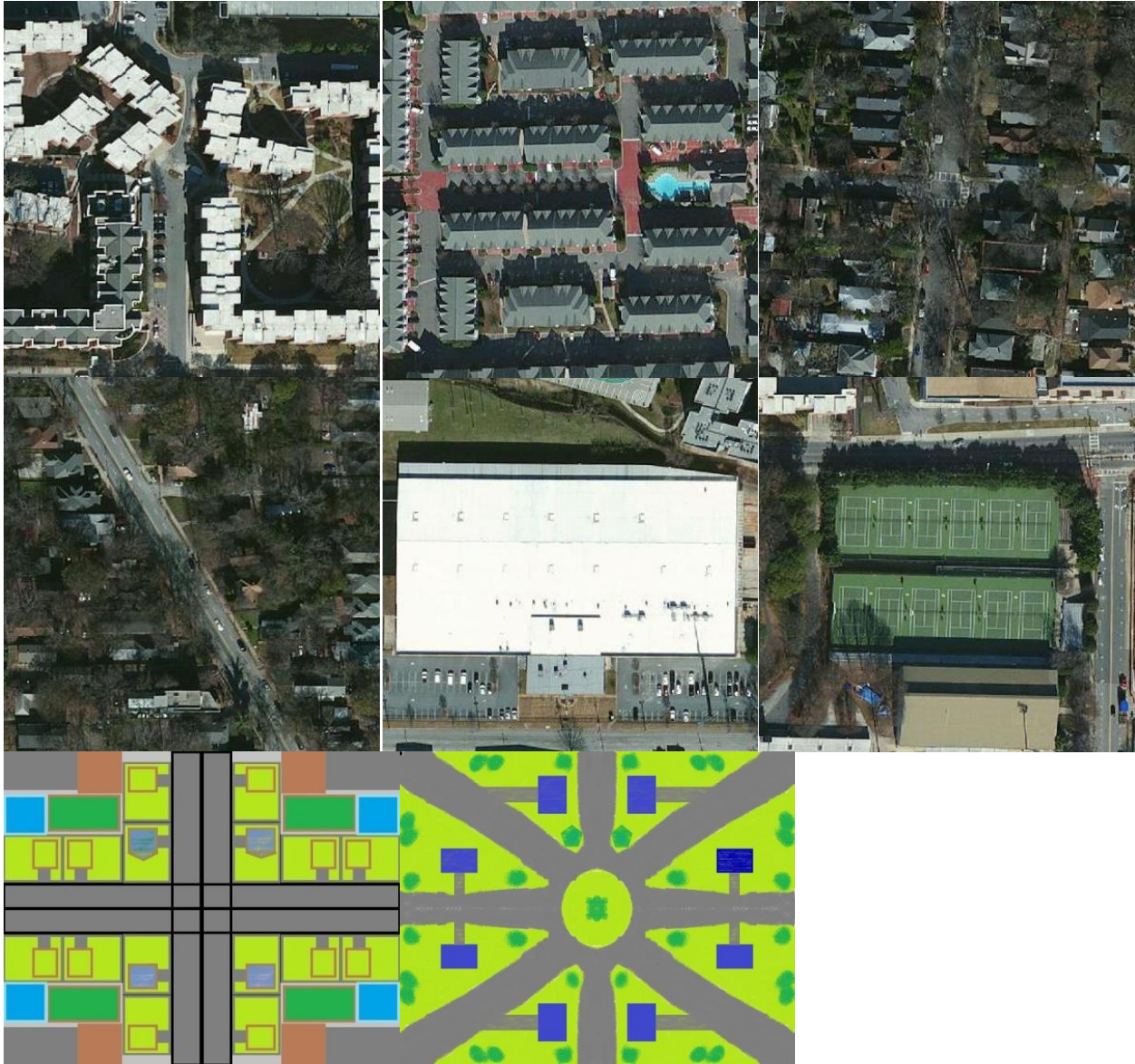


Figure 274: Imagery Examples with Abundant and Discernible Features

Each of these images has obvious features that could be used as a substitution for an orientation aid. [Image ©Google]